

B. ATLANTIC SEA SCALLOP STOCK ASSESSMENT FOR 2010

Invertebrate Subcommittee¹

Terms of Reference

1. Characterize the commercial catch including landings, effort, LPUE and discards. Describe the uncertainty in these sources of data.
2. Characterize the survey data that are being used in the assessment (e.g., regional indices of abundance, recruitment, state surveys, length data, etc.). Describe the uncertainty in these sources of data. Document the transition between the survey vessels and their calibration. If other survey data are used in the assessment, describe those data as they relate to the current assessment (Exclude consideration of future survey designs and methods).
3. Estimate annual fishing mortality, recruitment and stock biomass (both total and spawning stock) for the time series, and characterize the uncertainty of those estimates.
4. Update or redefine biological reference points (BRPs; estimates or proxies for B_{MSY} , $B_{THRESHOLD}$, and F_{MSY} ; and estimates of their uncertainty). Comment on the scientific adequacy of existing and redefined BRPs.
5. Evaluate stock status with respect to the existing BRPs, as well as with respect to updated or redefined BRPs (from TOR 4).
6. Develop and apply analytical approaches and data that can be used for conducting single and multi-year stock projections and for computing candidate ABCs (Acceptable Biological Catch; see Appendix to the TORs).
 - a. Provide numerical short-term projections (through 2014). Each projection should estimate and report annual probabilities of exceeding threshold BRPs for F, and probabilities of falling below threshold BRPs for biomass. In carrying out projections, consider a range of assumptions to examine important sources of uncertainty in the assessment.
 - b. Comment on which projections seem most realistic, taking into consideration uncertainties in the assessment.
 - c. Describe this stock's vulnerability to becoming overfished, and how this could affect the choice of ABC.
7. Review, evaluate and report on the status of the SARC and Working Group research recommendations listed in recent SARC reviewed assessments and review panel reports. Identify new research recommendations.

¹ Meetings and members of the Invertebrate Subcommittee who helped prepare this assessment are listed in Appendix 1.

Executive Summary

TOR 1. *Characterize the commercial catch, effort and CPUE, including descriptions of landings and discards of that species.* (Section 4 and Appendix II)

U.S. sea scallop landings averaged about 26,000 mt meats during 2002-2009, about twice their long-term average. Landings have been particularly high in the Mid-Atlantic Bight region. Fishing effort reached its maximum in 1991, and then declined during the 1990s so that effort in 1999 was less than half that in 1991. Effort in the most recent period has been fairly stable. Landings per unit effort (LPUE) showed general declines from the mid-1960s through the mid-1990s, with brief occasional increases due to strong recruitment. LPUE more than quadrupled between 1998 and 2001, and remained high during 2001-2009. LPUE has been especially high in the Mid-Atlantic and in the Georges Bank access areas (areas that had been closed and are now under special management). Discards of sea scallops were unusually high during 2002-2004, averaging about 10% of landings (by weight), but declined since then, probably due to changes in gear regulations that reduced catches of small individuals.

TOR 2. *Characterize the survey data that are being used in the assessment (e.g., regional indices of abundance, recruitment, state surveys, length data, etc.). Describe the uncertainty in these sources of data. Document the transition between the survey vessels and their calibration. If other survey data are used in the assessment, describe those data as they relate to the current assessment (Exclude consideration of future survey designs and methods).* (Section 5 and Appendices III, IV, V, VI, IX, X, XIV).

Direct and indirect comparisons between the *R/V Albatross IV*, which conducted the NEFSC sea scallop surveys until 2007, and the *R/V Hugh Sharp*, which conducted the 2008-2009 surveys, indicated no statistically significant differences in the catch rates of the two vessels (Appendix IV). However, dredge sensor data indicated that the tow path of the *R/V Hugh Sharp* was about 5% longer than that of the *R/V Albatross IV*, so catches in the time-series were reduced by that amount during 2008-2009.

Comparison of about 140 paired stations between catches of the lined survey dredge and underwater towed camera images (HabCam) gave estimates of survey dredge efficiency of 0.38 in survey strata containing substantial amounts of coarse sediment (gravel, cobble, rock), and 0.44 in all other strata, containing mostly sandy sediments (Appendices IX and X). Edge effects were examined for the SMAST drop camera survey which led to a re-estimation of scallop densities for this survey (Appendix III).

NEFSC sea scallop dredge survey indices were generally low from 1979-1995, and size-frequencies indicated a truncated size distribution with few large scallops. On Georges Bank, abundance and biomass rose substantially in the late 1990s, and then leveled off. After a decline between 2005-2007, indices increased again after strong recruitment was observed during 2007-2009. In the Mid-Atlantic, NEFSC survey indices increased substantially between 1997 and 2003, and have been stable or increased slightly since then. Substantial broadening of the size-structure was observed in both regions starting in the mid-to-late 1990s. SMAST drop video camera survey indices were fairly steady on Georges Bank during 2003-2009. In the Mid-Atlantic, the video estimates declined sharply between 2003 and 2004, and have declined slowly since then. Declines in abundance between 2003 and 2004 were also observed in the lined dredge and the NEFSC winter bottom trawl surveys. These declines are either due to overestimation of the large year class in the 2003 survey indices or high natural or fishing induced mortality of this

year class or some combination of these effects.

TOR 3. Estimate fishing mortality, spawning stock biomass, and total stock biomass for the current year and characterize the uncertainty of those estimates. If possible, also include estimates for earlier years. (Section 6 and Appendix XI).

A dynamic size-based stock assessment model (CASA) was used to estimate biomass, abundance and fishing mortality. This model was introduced in a preliminary version in NEFSC (2004) and used as the primary assessment model in NEFSC (2007). Data used in CASA included commercial catch, LPUE, and fishery shell height compositions, the NEFSC sea scallop and winter trawl surveys, the SMAST large camera video survey, growth increment data from scallop shells, and shell height/meat weight data adjusted to take into account commercial practices and seasonality. Because both the video and lined dredge survey (via the paired dredge/camera experiment) give estimates of scale (absolute abundances), prior estimates for efficiencies of these two surveys were used in the CASA model.

The sea scallop stock was assessed in two components (Georges Bank and Mid-Atlantic) separately and then combined. Estimates of fishing mortality were made from 1975-2009 for both regions. The models generally gave good fits to survey and commercial data, but there was tension in the Mid-Atlantic Bight model between the efficiency priors (especially for the video survey) and the recent stable or declining trends observed in surveys. Possible mild retrospective patterns were observed in the model, especially in the Mid-Atlantic Bight.

Model output and fishery size composition data indicate a substantial shift in selectivity towards larger scallops. Fishing mortality rates in 2009 are comparable to revised reference points but they are not comparable among fishery selectivity periods except as measures of fishing mortality on the fully selected individuals because of the shifts in selectivity. Whole stock fully recruited fishing mortality increased from 1975-1992, reaching a peak of 1.47 in 1992, rapidly declined during the late 1990s, and has been fairly stable since 2002. Estimated fishing mortality in 2009 was 0.18 (Georges Bank), 0.60 (Mid-Atlantic) and 0.378 for the whole stock.

Combined model estimated abundances and biomass increased rapidly in the decade starting in 1994, and have been stable or slightly increasing since then. July 1, 2009 estimated biomasses were 62,470 mt meats for Georges Bank and 67,233 mt meats in the Mid-Atlantic. Whole stock abundance and biomass estimates for July 1 2009 were 4,446 billion scallops and 129,703 mt meats. Both abundance and biomass for 2009 were at the maximum of the 1975-2009 time series.

TOR 4. Update or redefine biological reference points (BRPs; estimates or proxies for B_{MSY} , $B_{THRESHOLD}$, and F_{MSY} ; and estimates of their uncertainty). Comment on the scientific adequacy of existing and redefined BRPs. (Section 7).

The per recruit reference points F_{MAX} and B_{MAX} had been used as proxies for F_{MSY} and B_{MSY} in previous assessments. NEFSC (2007) estimated $F_{MAX} = 0.29$ and $B_{MAX} = 109,000$ mt meats (January 1 biomass). These estimates were updated in this assessment using new data and the current CASA model: $F_{MAX} = 0.30$ and $B_{MAX} = 125,000$ mt meats, based on January 1 biomass as was used in NEFSC (2007).

During the last benchmark assessment (NEFSC 2007), it was recommended that alternative reference points be explored because the changes in selectivity have made yield per recruit curves increasingly flat, which makes F_{MAX} more difficult to estimate and sensitive to small changes in assumed parameters.

A new method for estimating reference points is proposed in this assessment (SYM – Stochastic Yield Model) which explicitly takes into account uncertainties in per recruit and stock-recruit relationships to estimate F_{MSY} and B_{MSY} using Monte-Carlo simulations. This model estimated whole-stock $F_{MSY} = 0.38$, $B_{MSY} = 125,358$ mt meats (July 1 biomass), and $MSY = 24,975$ mt meats. This assessment used July 1 model biomass since it is a more representative of the actual biomass in the population. July 1 model abundance and biomass are always lower than those on January 1 because all growth and recruitment in the model occur on January 1.

TOR 5. Evaluate stock status with respect to the existing BRPs, as well as with respect to updated or redefined BRPs (from TOR 4). (Section 8).

According to the Amendment 10 overfishing definition (NEFMC 2003), sea scallops are overfished when the survey biomass index for the whole stock falls below $1/2 B_{TARGET}$. The target biomass estimated in NEFSC (2007), $B_{TARGET} = 109,000$ mt on January 1, was calculated as the median recruitment in the survey time series times BPR_{MAX} , the biomass per recruit obtained when fishing at F_{MAX} . NEFSC (2007) estimated $F_{MAX} = 0.29$, which has been used since then as the overfishing threshold. The updated values in this assessment are $F_{MAX} = 0.30$ and $B_{MAX} = 85,000$ mt (July 1 biomass). The new proposed stochastic MSY reference points are $F_{MSY} = 0.38$ and $B_{MSY} = 125,358$ mt (July 1).

Estimated whole-stock biomass in for January 1, 2009 was 158,610 mt meats, and 129,703 mt for July 1. These estimates are above the biomass target of 109,000 mt meats from NEFSC (2007) as well as the new biomass targets (85,000 mt meats July 1 using per recruit analysis, 125,358 mt meats using the stochastic yield approach). Thus, the current estimated biomass is more than twice the biomass threshold of $1/2 B_{TARGET}$, regardless of which reference point approach is used. The sea scallop stock was therefore not overfished in 2009.

Estimated whole stock fishing mortality was 0.38 for the whole stock (to three decimal places 0.378), which is above the NEFSC (2007) overfishing threshold of 0.29 and its updated value of 0.30, but equal to the proposed estimate of $F_{MSY} = 0.38$. Therefore, overfishing was not occurring in 2009 based on the new recommended overfishing definition; however, overfishing would be occurring if the previous definition or its updated value had been used.

TOR 6. Develop and apply analytical approaches and data that can be used for conducting single and multi-year stock projections and for computing candidate ABCs (Acceptable Biological Catch; see Appendix to the TORs).

a. Provide numerical short-term projections (through 2014). Each projection should estimate and report annual probabilities of exceeding threshold BRPs for F , and probabilities of falling below threshold BRPs for biomass. In carrying out projections, consider a range of assumptions to examine important sources of uncertainty in the assessment.

b. Comment on which projections seem most realistic, taking into consideration uncertainties in the assessment.

c. Describe this stock's vulnerability to becoming overfished, and how this could affect the choice of ABC. (Section 8)

The recommended projection model is spatially explicit and accommodates differences among regions in recruitment, growth, initial size structure, shell height/meat weight relationships, management approach (open vs. closed areas and catch quota vs. limits on fishing effort), intensity of fishing effort, and other factors. Projections done assuming status-quo management but varying initial conditions, natural mortality and recruitment indicate that

biomass and landings are expected to increase modestly until 2012, and then level off. There is less than a 0.1% chance of the stock becoming overfished by 2014. The stock has low vulnerability to becoming overfished.

TOR 7. *Review, evaluate and report on the status of the SARC/Working Group Research Recommendations offered in recent SARC reviewed assessments.* Completed (Section 9)

Progress has been made on some of the recommendations, such as estimation of natural mortality and seasonal growth models. But no progress has been made on others, such as obtaining better estimates of discard and incidental mortality.

Introduction

Life History

The Atlantic sea scallop, *Placopecten magellanicus*, is a bivalve mollusk that occurs on the eastern North American continental shelf north of Cape Hatteras. Major aggregations in US waters occur in the Mid-Atlantic from Virginia to Long Island, on Georges Bank, in the Great South Channel, and in the Gulf of Maine (Hart and Chute 2004). In Georges Bank and the Mid-Atlantic, sea scallops are harvested primarily at depths of 30 to 100 m, whereas the bulk of landings from the Gulf of Maine are from near-shore waters. This assessment focuses on the two main portions of the sea scallop stock and fishery, Georges Bank in the north and the Mid-Atlantic in the south (Figure B-1). Results for Georges Bank and the Mid-Atlantic are combined to evaluate the stock as a whole. Assessments of the Gulf of Maine populations can be found in Appendices V and VI.

US landings during 2003-2009 exceeded 24,000 mt (meats) each year, roughly twice the long-term mean.² US ex-vessel sea scallop revenues during 2005-2009 averaged \$389 million, making it the most valuable US fishery during this time. Unusually strong recruitment in the Mid-Atlantic Bight area and increased yield per recruit due to effort reduction and fishing gear modification measures are the key reasons for high recent landings. The mean meat weight of a landed scallop during 2005-2009 was over 25 g, compared to less than 14 g during the early to mid 1990s.

Area closures and reopenings have a strong influence on sea scallop population dynamics (Figure B-1). Roughly one-half of the productive scallop grounds on Georges Bank and Nantucket Shoals were closed to both groundfish and scallop gear during most of the time since December 1994. Limited openings to allow scallop fishing in closed areas contributed more than half of Georges Bank landings during 1999-2000 and since 2004.

In the Mid-Atlantic, there have been five rotational scallop closures. Two areas (Hudson Canyon South and Virginia Beach) were closed in 1998 and then reopened in 2001. Although the small Virginia Beach closure was unsuccessful, scallop biomass built up in Hudson Canyon Closed Area while it was closed, and substantial landings were obtained from Hudson Canyon during 2001-2007. This area was again closed in 2008, and will likely reopen in 2011. A third rotational closure, the Elephant Trunk area east of Delaware Bay, was closed in 2004, after extremely high densities of small scallops were observed in surveys during 2002 and 2003. About 30,000 mt of scallops have been landed from that area since it reopened in 2007. A fourth closed area (Delmarva), directly south of the Elephant Trunk area, was closed in 2007 and was reopened in 2009.

² In this assessment, landings and biomass figures are metric tons (mt) of scallop meats, unless otherwise indicated.

Early attempts to model sea scallop population dynamics (NEFSC 1992, 1995, 1997, 1999) were not successful because biomass estimates were less than the minimum swept area biomass obtained from the NEFSC scallop survey (NEFSC 1999). In lieu of model based estimates, fishing mortality was estimated in NEFSC (1999, 2001 and 2004) using a simple rescaled F method which relies heavily on survey and landings data. A size-structured forward projecting model (CASA, based on Sullivan et al. 1990) was used in the last sea scallop benchmark assessment in 2007 as the primary methodology. A slightly refined version of this model is used in this assessment as well (Table B-1).

Life History and Distribution

Sea scallops are found in the Northwest Atlantic Ocean from North Carolina to Newfoundland along the continental shelf, typically on sand and gravel bottoms (Hart and Chute 2004). Sea scallops feed by filtering phytoplankton, microzooplankton, and detritus particles. Sexes are separate and fertilization is external. Sea scallops typically become mature at age 2, but gamete production is limited until age 4. Larvae are planktonic for 4-7 weeks before settling to the bottom. Scallops fully recruit to the NEFSC survey at 40 mm SH, and to the current commercial fishery at around 90-105 mm SH, although sea scallops between 70-90 mm were common in landings prior to 2000.³

According to Amendment 10 of the Atlantic Sea Scallop Fishery Management Plan, all sea scallops in the US EEZ belong to a single stock. However, the US sea scallop stock can be divided into Georges Bank, Mid-Atlantic, Southern New England, and Gulf of Maine regional components based on survey data, fishery patterns, and other information (NEFSC 2004, Figure B-1). For assessment modeling purposes, Southern New England is considered to be part of the Georges Bank region.

Age and growth

Sea scallop assessments prior to 2007 estimated growth using the von Bertalanffy growth parameters from Serchuk et al. (1979). During the 2007 assessment, new analysis of shells collected during the 2001-2006 NEFSC scallop surveys was introduced (NEFSC 2007). This approach was based on growth increments inferred by successive rings on shells. The shell rings have been confirmed as annual marks (NEFSC 2007, Hart and Chute 2009a). Von Bertalanffy growth parameters were estimated in NEFSC (2007) using data from surveys from 2001 to 2006 using a mixed-effects model. Hart and Chute (2009b) gave a slightly refined version of this model that also included shells collected in 2007. Here we updated these estimates to include shells collected in 2008, using the same methodology as Hart and Chute (2009b). The current growth curves have lower mean L_{∞} and higher mean K values than Serchuk et al. (1979). Differences between the current estimates and that of NEFSC (2007) are minor, and that between current estimates and Hart and Chute (2009b) are almost negligible (Figure B-2). Note that growth parameter t_0 cannot be estimated using growth increments, but it is not used in this assessment.

³ Scallop body size is measured as shell height (SH, the maximum distance between the umbo and shell margin).

Mean growth parameters for sea scallops

Source	Region	L_{∞}	SE	K	SE
New (NEFSC 2010)	Mid-Atlantic	132.1	0.3	0.527	0.004
	Georges Bank	144.0	0.3	0.429	0.002
Hart & Chute (2009)	Mid-Atlantic	133.3	0.4	0.508	0.004
	Georges Bank	143.9	0.3	0.427	0.002
NEFSC (2007)	Mid-Atlantic	131.6	0.4	0.495	0.004
	Georges Bank	146.5	0.3	0.375	0.002
Serchuk et al. (1979)	Mid-Atlantic	151.84		0.2997	
	Georges Bank	152.46		0.3374	

Maturity and fecundity

Sexual maturity commences at age 2; sea scallops > 40 mm that are reliably detected in the surveys used in this assessment are all considered mature individuals. Although sea scallops reach sexual maturity at a relatively young age, individuals younger than 4 years may contribute little to total egg production (MacDonald and Thompson 1985; NEFSC 1993).

According to MacDonald and Thompson (1985) and McGarvey et al. (1992), annual fecundity (reproductive output, including maturity, spawning frequency, oocyte production, etc.) increases quickly with shell height in sea scallops

($Eggs=0.00000034 SH^{4.07}$). Spawning generally occurs in late summer or early autumn. DuPaul et al. (1989) found evidence of spring, as well as autumn, spawning in the Mid-Atlantic Bight area. Almeida et al. (1994) and Dibacco et al. (1995) found evidence of limited winter-spring spawning on Georges Bank.

Shell height/meat weight relationships

Shell height-meat weight relationships allow conversion from numbers of scallops at a given size to equivalent meat weights. They are expressed in the form $W=\exp(\alpha+\beta\ln(H))$, where W is meat weight in grams and H is shell height in mm. NEFSC (2001) combined the shell height/meat weight relationships from Serchuk and Rak (1983) with relationships from NEFSC (1999; later published as Lai and Helser 2004) to obtain “blended” estimates that were used in NEFSC (2001) and NEFSC (2004).

New shell height/meat weight data was collected during annual NEFSC sea scallop surveys during 2001-2009. Unlike previous studies, where meats were either frozen or brought in live and then weighed on land, meats were weighted at sea just after they were shucked. Estimates based on the 2001-2006 data were used in NEFSC (2007). This assessment updates these estimates by adding 2007-2008 data (see table below, Figure B-3 and Appendix VII). Due to the change in timing of the survey, 2009 data were not used.

Meat weights also depend on covariates such as depth and latitude. Meat weights decreasing with depth, probably because of reduced food (phytoplankton) supply. Analysis of the new data indicated that depth and (at least in some cases) latitude had a significant effect on the shell height/meat weight relationship (Appendix VII). Estimated coefficients for the relationship $W=\exp(\alpha+[\beta+\rho\ln(D)]\ln(H) + \gamma\ln(D)+\delta\ln(L))$, where D is depth in meters and L is latitude, are given below. In this assessment, depth-adjusted shell height/meat weight

relationships were used to calculate survey biomass information, and traditional relationships were used in the models (CASA and SAMS), where depth is not explicit.

	α	β	γ	δ	ρ
Mid-Atlantic Bight					
Haynes (1966)	-11.09	3.04			
Serchuk and Rak (1983)	-12.16	3.25			
NEFSC (2001)	-12.25	3.26			
Lai and Helser (2004)	-12.34	3.28			
NEFSC (2007)	-12.01	3.22			
NEFSC (2007) with Depth effect	-9.18	3.18	-0.65		
NEFSC (2010)	-10.80	2.97			
NEFSC (2010) with Depth effect	-8.94	2.94	-0.43		
NEFSC (2010) with Depth effect and interaction	-16.88	4.64	1.57	-	-0.43
Georges Bank					
Haynes (1966)	-10.84	2.95			
Serchuk and Rak (1983)	-11.77	3.17			
NEFSC (2001)	-11.60	3.12			
Lai and Helser (2004)	-11.44	3.07			
NEFSC (2007)	-10.70	2.94			
NEFSC (2007) with Depth effect	-8.62	2.95	-0.51		
NEFSC (2010)	-10.25	2.85			
NEFSC (2010) with Depth effect	-8.05	2.84	-0.51		
NEFSC (2010) with Depth, Latitude and subarea effect	14.380	2.826	0.529	5.980	0.051 ^b

Meat weights for scallops in the commercial fishery may differ from those predicted based on research survey data for a number of reasons. First, the shell height-meat weight relationship varies seasonally, in part due to the reproductive cycle, so that meat weights collected during the NEFSC survey in July and August may differ from those in the rest of year. Additionally, commercial fishers concentrate on speed, and often leave some meat on the shell during shucking (Naidu 1987, Kirkley and DuPaul 1989). On the other hand, meats may gain weight due to water uptake during storage on ice (DuPaul et al. 1990). Finally, fishers may target areas with relatively large meat weight at shell height, and thus may increase commercial meat weights compared to that collected on the research vessel.

Observer data was used to adjust meat weights for seasonal variation and for commercial practices (Appendix VIII). Annual commercial meat weight anomalies were computed based on the seasonal patterns of landings together with the mean monthly commercial meat weight at shell height (Figure B-4).

Natural mortality

Previous assessments assumed a natural mortality of $M = 0.1$ based on Merrill and Posgay (1964), who estimated M based on ratios of clappers to live scallops in survey data. Clappers are shells from dead scallops that are still intact (i.e., both halves still connected by the hinge ligament). The basis of the estimate (Dickie 1955) is an assumed balance between the rate at which new clappers are produced ($M \cdot L$, where L is the number of live scallops) and the rate at which clappers separate ($S \cdot C$, where S is the rate at which shell ligaments degrade, and C is the number of clappers). At equilibrium, the rates of production and loss must be equal, so that $M \cdot L = S \cdot C$ and:

$$M = C / (L \cdot S).$$

Merrill and Posgay estimated $S=33$ weeks from the amount of fouling on the interior of clappers. The observed ratio C/L was about 0.066 and M was thus estimated to be $0.104 \approx 0.1 \text{ y}^{-1}$. However, the estimate of S is highly uncertain; for example Dickie (1955) estimated S to be 14.3 weeks based on tank experiments. The high level of uncertainty in the denominator implies that the estimator for M using the point estimated of S is biased low. If the standard error in the estimate of S is 12 weeks, an unbiased estimate of M is slightly more than 0.12. For this assessment, we use an estimate of $M = 0.12$ for Georges Bank. As shown below, this new assumption is supported by a number of modeling results.

No direct estimate of M is available for Mid-Atlantic sea scallops. The ratio of the growth coefficient K to M is generally regarded as a life history invariant that should be approximately constant for similar organisms (Beverton and Holt 1959, Chernov 1993). Applying this idea indicates that sea scallop natural mortality in the Mid-Atlantic should be about $0.527/0.429$ that of Georges Bank (see the estimates of growth coefficients above). Using $M = 0.12$ in Georges Bank implies that natural mortality in the Mid-Atlantic is $0.12 \cdot 0.527/0.429$, or about 0.15. This is the estimate used in this assessment.

TOR 1: Commercial and Recreational Catch

The US sea scallop fishery is currently conducted mainly by about 350 vessels with limited access permits. Two types of allocation are given to each vessel. The first are trips (with a trip limit, typically of 18,000 lbs meats) to rotational access areas that had been closed to scallop fishing in the past. The second are days at sea, which can be used in areas outside the closed and access areas. Vessels fishing under days at sea are restricted to a 7 man crew in order to limit their processing power. The percentage of landings from the access trips have increased since the access area programs began in 1999; in recent years, about 60% of landings are from the access areas. Landings from 1964-2009 are given in Table B-2.

The remainder of landings come from vessels operating under "General Category" permits that are restricted to 400 lbs per trip, with a maximum of one trip per day. Landings from these vessels were less than 1% of total landings in the late 1990s, but increased to 10% or more of landings during 2007-2009. This type of permit had been open access, but was converted to an individual transferable quota (ITQ) fishery in March 2010.

Principal ports in the sea scallop fishery are New Bedford, MA, Cape May, NJ, and Hampton Roads, VA. New Bedford style scallop dredges are the main gear type in all regions, although some scallop vessels use otter trawls in the Mid-Atlantic. Recreational catch is negligible; a small amount of catch in the Gulf of Maine may be due to recreational divers.

Management history

The sea scallop fishery in the US EEZ is managed under the Atlantic Sea Scallop Fishery Management Plan (FMP), implemented on May 15, 1982. From 1982 to 1994, the primary management control was a minimum average meat weight requirement for landings.

FMP Amendment 4 (NEFMC 1993), implemented in 1994, changed the management strategy from meat count regulation to limited access, effort control and gear regulations for the entire US EEZ. Incremental restrictions were made on days-at-sea (DAS), minimum ring size, and crew limits (Table B-3). In addition, three large areas on Georges Bank and Nantucket Shoals were closed to groundfish and scallop fishing in December 1994 (Figure B-1). Scallop biomass rapidly increased in these areas. Two areas in the Mid-Atlantic were closed to scallop fishing in April 1998 for three years in order to similarly increase scallop biomass and mean weight.

Sea scallops were formally declared overfished in 1997, and Amendment 7 was implemented during 1998 with more stringent days-at-sea limitations and a mortality schedule intended to rebuild the stocks within ten years. Subsequent analyses considering effects of closed areas indicated that the stocks would rebuild with less severe effort reductions than called for in Amendment 7, and this days at sea schedule was thus modified. A combination of the closures, effort reduction, gear and crew restrictions led to a rapid increase in biomass (Hart and Rago 2006), and sea scallops were rebuilt by 2001. Prior to 2004, there were a number of ad hoc area management measures, including the Georges Bank and Mid-Atlantic closures in 1994 and 1998, limited reopenings of portions of the Georges Bank areas between June 1999 and January 2001, and reopening of the first Mid-Atlantic rotational areas in 2001.

A new set of regulations was implemented as Amendment 10 during 2004. This amendment formalized an area based management system, with provisions and criteria for new rotational closures, and separate allocations (in days-at-sea or TACs) for reopened closed areas and general open areas. Amendment 10 closed an area offshore of Delaware Bay (the Elephant Trunk area) where high numbers of small scallops were observed in the 2002 and 2003 surveys. This area reopened in 2007, when an area directly to the south was closed (Delmarva closure). One of the original Mid-Atlantic rotational closures, Hudson Canyon South, which had been closed in 1998 and reopened in 2001, was closed again in 2008, and is scheduled to reopen in 2011.

Amendment 10 also increased the minimum ring size to 4" and, together with subsequent frameworks, allowed limited reopening of portions of the groundfish closed areas.

Landings

Sea scallop landings in the US increased substantially after the mid-1940's (Figure B-5), with peaks occurring around 1960, 1978, 1990, and 2004. Maximum US landings were 29,109 mt meats in 2004.

Proration of total commercial sea scallop landings into Georges Bank, Mid-Atlantic, Southern New England, and the Gulf of Maine regions used the standard allocation procedures of the NEFSC (Wigley et al. 2008). Landings from the Georges Bank and the Mid-Atlantic regions have dominated the fishery since 1964 (Table B-2 and Figure B-6). US Georges Bank landings had peaks during the early 1960's, around 1980 and 1990, but declined precipitously during 1993 and remained low through 1998 (Table B-2 and Figure B-6). Landings in Georges Bank during 1999-2004 were fairly steady, averaging almost 5000 mt annually, and then

increased in 2005-2006, primarily due to reopening of portions of the groundfish closed areas to scallop fishing. Poor recruitment in the middle of the decade and the reduction of biomass in the Georges Bank access areas have led to reductions in landings in the most recent years.

Until recently, the Mid-Atlantic landings were lower than those on Georges Bank. Mid-Atlantic landings during 1962-1982 averaged less than 1800 mt per year. An upward trend in both recruitment and landings has been evident in the Mid-Atlantic since the mid-eighties. Landings peaked in 2004 at 24,494 mt.

Landings from other areas (Gulf of Maine and Southern New England) are minor in comparison (Table B-2). Most of the Gulf of Maine scallop population is assessed and managed by the State of Maine because it is primarily in state waters (see Appendices V and VI). Gulf of Maine landings in 2009 were less than 1% of the total US sea scallop landings. Maximum landings in the Gulf of Maine were 1,614 mt during 1980.

Fishing effort and LPUE

Prior to 1994, landings and effort data were collected during port interviews by port agents and based on dealer data. Since 1994, commercial data are available as dealer reports (DR) and in vessel trip report (VTR) logbooks. DR data are total landings, and, since 1998, landings by market category. VTR data contain information about area fished, fishing effort, and retained catches of sea scallops. Ability to link DR and VTR reports in data processing is reduced by incomplete data reports and other problems, although there have been significant improvements recently. A standardized method (Wigley et al. 2008) for matching DR to VTRs and assigning areas to landings was used to allocate landings to region for 1994-2008. The method used in previous assessments (e.g., NEFSC 2007) that stratified landings and VTR by state was used for 2009, since the allocation tables for 2009 have not yet been completed.

Landings per unit effort (LPUE, computed as landings per day fished) (Figure B-7) shows a general downward trend from the beginning of the time series to around 1998, with occasional spikes upward probably due to strong recruitment events. LPUE increased considerably from 1999-2003 as the stock recovered; further increases in LPUE have been seen in recent years in the Mid-Atlantic, likely due to strong recruitment. Note the close correspondence in most years between the LPUE in the Mid-Atlantic and Georges Bank, probably reflecting the mobility of the fleet; if one area has higher catch rates, it is fished harder until the rates are equalized. Although comparisons of LPUE before and after the change in data collection procedures during 1994 need to be made cautiously, there is no clear break in the LPUE trend in 1994.

Fishing effort (days fished) in the US sea scallop fishery generally increased from the mid-1960s to about 1991, and then decreased during the 1990s, first because of low catch rates, and later as a result of effort reduction measures (Figure B-8). Effort increased in the Mid-Atlantic during 2000-2005, initially due to reactivation of latent effort among limited access vessels, and then due to increases in general category effort. Total effort since 2005 has remained fairly stable, though there have been shifts between regions.

Discards and discard mortality

Sea scallops are sometimes discarded on directed scallop trips because they are too small to be economically profitable to shuck, or because of high-grading, particularly during access area trips. Ratios of discard to total catch (by weight) were recorded by sea samplers aboard

commercial vessels since 1992, though sampling intensity on non-access area trips was low until 2003; see Appendix II for detailed estimates.

Discarded sea scallops may suffer mortality on deck due to crushing, high temperatures, or desiccation. There may also be mortality after they are thrown back into the water from physiological stress and shock, or from increased predation due to shock and inability to swim or shell damage (Veale et al. 2000, Jenkins and Brand 2001). Murawski and Serchuk (1989) estimated that about 90% of tagged scallops were still living several days after being tagged and placed back in the water. Total discard mortality (including mortality on deck) is uncertain but has been estimated as 20% in previous assessments (e.g., NEFSC 2007); this assessment also makes this assumption. However, discard mortality may be higher during the Mid-Atlantic during the summer due to high water and deck temperatures.

Incidental mortality

Scallop dredges likely kill and injure some scallops that are contacted but not caught, primarily due to damage (e.g., crushing) caused to the shells by the dredge. Caddy (1973) estimated that 15-20% of the scallops remaining in the track of a dredge were killed. Murawski and Serchuk (1989) estimated that less than 5% of the scallops remaining in the track of a dredge suffered non-landed mortality. Caddy's study was done in a relatively hard bottom area in Canada, while the Murawski and Serchuk study was in sandy bottom off the coast of New Jersey. It is possible that the difference in indirect mortality estimated in these two studies was due to different bottom types (Murawski and Serchuk 1989).

In order to use the above estimates to relate landed and non-landed fishing mortality in stock assessment calculations, it is necessary to know the efficiency e of the dredge (the probability that a fully recruited scallop in the path of a dredge is captured). Denote by c the fraction of scallops that suffer mortality among sea scallops in the path of the dredge but not caught. The best available information indicates that $c = 0.15-0.2$ (Caddy 1973), and $c < 0.05$ (Murawski and Serchuk 1989). The ratio R of scallops in the path of the dredge that were caught, to those killed but not caught is:

$$R = e/[c(1-e)]$$

If scallops suffer direct (i.e., landed) fishing mortality at rate F_L , then the rate of indirect (non-landed) fishing mortality will be (Hart 2003):

$$F_I = F_L / R = F_L c (1-e)/e.$$

If, for example, the commercial dredge efficiency e is 50%, then $F_I = F_L c$, where F_L is the fully recruited fishing mortality rate for sea scallops. Assuming $c = 0.15$ to 0.2 (Caddy 1973) gives $F_I = 0.15 F_L$ to $0.2 F_L$. With $c < 0.05$ (Murawski and Serchuk 1989) $F_I < 0.05 F_L$. Because there may be unobserved damage, actual incidental mortality may be higher than that observed in these studies. For this assessment, incidental mortality was assumed to be $0.2 F_L$ in Georges Bank and $0.1 F_L$ in the Mid-Atlantic.

Commercial shell height data

Since most sea scallops are shucked at sea, it has often been difficult to obtain reliable commercial size compositions. Port samples of shells brought in by scallopers have been

collected, but there are questions about whether the samples were representative of the landings and catch. Port samples taken during the meat count era often appear to be selected for their size rather than being randomly sampled, and the size composition of port samples from 1992-1994 differed considerably from those collected by at-sea observers during this same period. For this reason, size compositions from port samples after 1984 when meat count regulations were in force are not used in this assessment.

Sea samplers (observers) have collected shell heights of kept scallops from commercial vessels since 1992, and discarded scallops since 1994. Although these data are likely more reliable than that from port sampling, they still must be interpreted cautiously for years prior to 2003 (except for the access area fisheries) due to limited observer coverage.

Shell heights from port and sea sampling data indicate that sea scallops between 70-90 mm often made up a considerable portion of the landings during 1975-1998, but sizes selected by the fishery have increased since then, so that scallops less than 90 mm were rarely taken during 2002-2009 (Figure B-9).

Dealer data (landings) have been reported by market categories (under 10 meats per pound, 10-20 meats per pound, 20-30 meats per pound etc) since 1998 (Figure B-10). These data also indicate a trend towards larger sea scallops in landings. While nearly half the landings in 1998 were in the smaller market categories (more than 30 meats per pound), about 75% of the 2009 landings were below 20 count and about 99% were below 30 count.

Economic trends in the U.S. sea scallop fishery

This section describes the trends in landings, revenues, prices, producer surplus and profits for the sea scallop fishery since 1994.

Trends in landings, prices and revenues

In the fishing years 2002-2008, the landings from the northeast sea scallop fishery stayed above 50 million pounds, surpassing the levels observed historically (Figure B-11). The recovery of the scallop resource and consequent increase in landings and revenues was striking given that average scallop landings per year were below 16 million pounds during the 1994-1998 fishing years, less than one-third of the present level of landings. The increase in the abundance of scallops coupled with higher scallop prices increased the profitability of fishing for scallops by the general category vessels. As a result, general category landings increased from less than 0.4 million pounds during the 1994-1998 fishing years to more than 4 million pounds during the last four fishing years (2005-2008), peaking at 7 million pounds in 2005 or 13.5% of the total scallop landings.

Figure B-12 shows that total fleet revenues tripled from about \$100 million in 1994 to over \$350 million in 2008 (in inflation-adjusted 2008 dollars). Scallop ex-vessel prices increased after 2001 as the composition of landings changed to larger scallops that in general command a higher price than smaller scallops. However, the rise in prices was not the main factor that led to the increase in revenue in the recent years compared to 1994-1998 and in fact, the inflation adjusted ex-vessel price of scallops in 2008 was lower than the price in 1994 (Figure B-12). The increase in total fleet revenue was mainly due to the increase in scallop landings and the increase in the number of active limited access vessels during the same period. Fig B6-9 shows that average landings and revenue per limited access vessel more than doubled in recent years compared to the period 1994 -1998. The number of active limited access vessels increased

by 50 % (from about 220 in 1994 to 345 in fishing year 2008) resulting in tripling of total fleet scallop landings and revenue in 2008 compared to 1994 (Figure B-12 and Figure B-13).

Figure B-13 shows that average scallop revenue per limited access vessel more than doubled from about \$400,000 in 1994 to about \$950,000 despite the fact that inflation adjusted ex-vessel price per pound of scallops was slightly higher in 1994 (\$7.15 per pound) compared to the ex-vessel price in 2008 (\$6.92 per pound). In other words, the doubling of revenue was the result of the doubling of the average scallop landings per vessel in 2008 (over 136,000 pounds) from its level in 1994 (over 57,000 pounds). The total fleet revenue for all the limited access vessels more than tripled during the same years as new vessels became active. Average scallop revenue per full-time vessel peaked in the 2005 fishing year to over \$1.1 million as a result of higher landings combined with an increase in ex-vessel price to about \$8.50 per pound of scallops (in terms inflation adjusted 2008 prices).

Trends in the meat count and size composition of scallops

Average scallop meat count has declined continuously since 1999 as a result of effort-reduction measures, area closures, and an increase in ring sizes implemented by the Sea Scallop FMP. The share of larger scallops increased with the share of U10 scallops rising to over 20% since 2006. The share of 11-20 count scallops increased from 12% in 1999 to 53% in 2008. On the other hand, the share of 30 or more count scallops declined from 30% in 1999 to 1% in 2008 (Figure B-10 and tables below). Larger scallops priced higher than the smaller scallops contributed to the increase in average scallop prices in recent years despite larger landings (Figure B-12 and tables below).

Size composition of scallops

YEAR	Under 10 count	11-20 count	21-30 count	30 count and over	Unclassified
1999	17%	12%	25%	35%	12%
2000	7%	18%	44%	20%	11%
2001	3%	24%	49%	11%	13%
2002	5%	15%	65%	5%	11%
2003	6%	21%	56%	3%	13%
2004	7%	41%	42%	2%	8%
2005	13%	57%	21%	2%	7%
2006	23%	52%	18%	1%	6%
2007	24%	52%	13%	4%	8%
2008	23%	53%	18%	1%	4%

Price of scallop by market category (in 2008 inflation adjusted prices)

YEAR	<=10 count	11-20 count	21-30 count	>30 count
1999	7.8	7.9	7.3	6.4
2000	8.7	6.8	5.9	6.1
2001	7.2	4.7	4.4	4.7
2002	6.7	4.8	4.5	5.1
2003	5.7	4.8	4.8	5.3
2004	6.8	5.8	5.5	5.7
2005	8.8	8.6	8.5	8.3
2006	6.6	7.3	7.6	7.6
2007	7.2	6.9	6.8	6.2
2008	7.2	6.9	6.8	6.4

Trends in Foreign Trade

One of most significant change in the trend for foreign trade for scallops after 1999 was the striking increase in scallop exports. The increase in landings especially of larger scallops led to a tripling of U.S. exports of scallops from about 5 million lb. in 1999 to over 20 million lb. per year since 2005 (Figure B-14). Figure B-14 shows exports from New England and Mid-Atlantic ports combined including fresh, frozen and processed scallops. Although exports include exports of bay, calico or weathervane scallops, it mainly consists of sea scallops. France and other European countries were the main importers of US scallops. The exports from all other states and areas totaled only about \$1 million in 2006 and 2007, and thus were not considered significant. Imports of scallops fluctuated between 45 million lb. and 60 million lb. during the same period.

TOR 2: Survey Data

Sea scallop surveys were conducted by NEFSC in 1975 and annually after 1977 to measure abundance and size composition of sea scallops in the Georges Bank and Mid-Atlantic regions (Figure B-1). The 1975-1978 surveys used a 3.08 m (10') unlined dredge with 50 mm rings. A 2.44 m (8') survey dredge with 50 mm rings and a 38 mm plastic liner has been used consistently since 1979. The lined survey dredge was judged to be unselective for scallops greater than 40 mm by comparing its catches to observations from sea floor video (NEFSC 2007). The northern edge of Georges Bank was not surveyed until 1982, so survey data for this area are incomplete for this area during 1975-1981. The 1979-1981 data were supplemented with Canadian survey data that covered much of the unsurveyed area (see Appendix XIII), allowing an extension of the lined survey dredge time series back to 1979.

The *R/V Albatross IV* was used for all NEFSC scallop surveys from 1975-2007, except during 1990-1993, when the *R/V Oregon II* was used instead. Surveys by the *R/V Albatross IV* during 1989 and 1999 were incomplete on Georges Bank. In 1989, the *R/V Oregon II* and *R/V Chapman* were used to sample the South Channel and a section of the Southeast Part. Serchuk and Wigley (1989) found no significant differences in catch rates between the *R/V Albatross IV*, *R/V Oregon II* and *R/V Chapman*.

The *F/V Tradition* was used to complete the 1999 survey on Georges Bank. NEFSC (2001) found no statistically significant differences in catch rates between the *F/V Tradition* and *R/V Albatross IV* from 21 comparison stations after adjustments were made for tow path length. Therefore, as in previous assessments (e.g., NEFSC 2004), survey indices for the period 1990-93 based on data from the *R/V Oregon II* were used without adjustment, and survey dredge tows from the *F/V Tradition* in 1999 were used after adjusting for tow distance.

In 2008-2009, the NEFSC scallop survey was conducted on the *R/V Hugh Sharp*. Direct and indirect comparisons between the catches of these vessels showed no significant differences (Appendix IV). However, examination of tow path length from dredge sensor data indicates that the tow path of the dredge on the *R/V Sharp* is about 5% longer than the *R/V Albatross*. Thus, survey catches in 2008-9 were reduced by 5%. Rock excluder chains have been used on the NEFSC sea scallop survey dredge since 2004 in certain hard bottom strata to enhance safety at sea and increase reliability (NEFSC 2004). Based on pair tows with and without the excluders, the best overall estimate was that rock chains increased survey catches on hard grounds by a factor of 1.31 ($cv = 0.196$). To accommodate rock chain effects in hard bottom areas, survey data collected prior to 2004 from strata 49-52 were multiplied by 1.31 prior to calculating stratified random means for larger areas; variance calculations in these strata include a term to account for the uncertainty in the adjustment factor (NEFSC 2007).

Calculation of mean numbers of scallops per tow, mean meat weight per tow and variances in this assessment were standard calculations for stratified random surveys (Serchuk and Wigley 1989; Wigley and Serchuk 1996; Smith 1997) with some extensions described below.

Relatively high abundance of sea scallops in closed areas makes it necessary to post-stratify survey data by splitting NEFSC shellfish strata that cross open/closed area boundaries. After post-stratification, adjacent strata were grouped into regions corresponding to the various open and closed areas. Finally, in cases where the closed or open portion of an NEFSC survey stratum was very small, it was necessary to combine the small portion with an adjacent stratum to form a new slightly larger stratum (NEFSC 1999).

Survey abundance and biomass trends

Biomass and abundance trends for the Mid-Atlantic Bight and Georges Bank are presented in Table B-4 and Figure B-15 and Figure B-16. Variances for strata with zero means were assumed to be zero.

In the Mid-Atlantic Bight, abundance and biomass were at low levels during 1979-1997, and then increased rapidly during 1998-2003, due to area closures, reduced fishing mortality, changes in fishery selectivity, and strong recruitment. Biomass was relatively stable since 2003. In Georges Bank, biomass and abundance increased during 1995-2000 after implementation of closures and effort reduction measures. Abundance and biomass declined from 2004-2007 because poor recruitment and reopening of portions of the groundfish closed areas. Abundances, and to a lesser extent, biomasses, increased since 2007 due to strong recruitment. Survey shell height frequencies show a trend to larger shell heights in both regions in recent years (Figure B-17).

Video survey data collected by the School for Marine Sciences and Technology (SMAST), University of Massachusetts, Dartmouth between 2003-2009 (Table B-5, Table B-6 and Figure B-18). SMAST survey data are counts and shell height measurements from images that were recorded by two video cameras. The “large” camera was mounted 1.575 m above the bottom in the center of the sampling frame while the “small” camera was mounted 0.7 m above the bottom. Adjustments have been made in this assessment to the estimated observed area of a quadrat, which is the area viewed by the large camera and to the number of sea scallops actually counted (Appendix III).

The SMAST survey is based on a systematic sampling pattern with stations centered on a 5.6 x 5.6 km grid pattern (Stokesbury et al. 2004). Four quadrats (drops) are sampled at each

station and one image taken with each camera is analyzed from each quadrat. The sampling frame and cameras are placed on the bottom at the center of the grid where video footage from the first quadrat is collected. The sampling frame is then raised until the sea floor is no longer visible and the ship is allowed to drift approximately 50 m in the current before the sampling frame is lowered and video footage from the second quadrat image is collected. The third and fourth images are collected in the same manner. All scallops with any portion of their shell lying within the sample area are counted. Measurements are taken from images projected on a digitizing tablet from all specimens where the umbo and shell margins are clearly visible. The precision of measurements must be considered in interpreting video shell height data. Based on Jacobson et al. (2010) and NEFSC (2004), video shell height measurements from the large camera have a standard deviation of 6.1 mm across a wide range of sea scallop shell heights.

Video survey data in this assessment are expressed as densities (number m^{-2}). Variances for estimated densities are approximated using the estimator for a simple random survey applied to station means. There was some variability in the areas covered during each year (Table B-5 and Table B-6).

Dredge efficiency calibration

During 2007-2009, approximately 140 NEFSC scallop survey tows were also sampled using the HabCam towed digital camera system (Appendices IX and X). Analysis of these tows indicates that the lined survey dredge has an efficiency of about 0.44 in sandy areas and 0.38 in survey strata with a substantial fraction of gravel/cobble/rock substrate (Appendix X). These estimates are reasonably consistent with previous efficiency estimates (Table B-7).

TOR 3: Fishing Mortality, Biomass, and Recruitment Estimates

A catch at size analysis (CASA, Sullivan et al 1990) was used as the primary assessment model. CASA models growth using a stochastic growth matrix, which can be estimated using shell growth increment data. A CASA model for sea scallops was presented for preliminary review in (NEFSC 2004) and was used as the primary assessment model in the last assessment (NEFSC 2007). Simulation testing generally indicated good model performance (NEFSC 2007). CASA models for both stocks were run between 1975-2009. Shell heights were modeled with 5mm shell height bins starting at 20mm, but only scallops larger than 40mm were used in tuning to the data. The final (plus) group were the bins that included L_{∞} ; this bin were given special plus group weights based on the mean observed weight in the NEFSC survey in that year for scallops in the plus group (Figure B-19). Transition matrices were derived directly from shell increment data, as in the last assessment. Population shell height/meat weight conversions were based on 2001-2008 research vessel derived parameters, and fishery meat weights were adjusted based on estimated seasonal anomalies and the seasonal distribution of landings in that year (see Appendix VIII). Commercial shell heights data was obtained from 1975-1984 from port samples, and from 1992-2009 from sea samples (observers). Asymptotic delta method variances calculated in CASA with AD-Model Builder software were used to compute variances and coefficients of variation (cvs).

CASA model for Georges Bank

The model time-series for this assessment was 1975-2009, compared to 1982-2009 in NEFSC (2007). Three surveys were used for both trends and shell heights: the NEFSC lined dredge survey (1979-2009), the SMAST large video camera survey (2003-2009) and the NEFSC

unlined dredge survey (1975-1978). The selectivity of the lined dredge survey was assumed flat (NEFSC 2007), and the selectivity of the video and unlined dredge survey was fixed on the basis of experimental evidence (NEFSC 2007, Serchuk and Smolowitz 1980). Priors with a cv of 0.15 were assumed for the NEFSC dredge (assuming a mean dredge efficiency of 0.41, see Appendix X), and for the large camera video survey (assuming 100% detectability of fully selected scallops). The prior distributions were implemented using symmetrical beta distributions. Fishery selectivity periods were 1975-1995, 1996-1998, 1999-2000, 2001-2003, and 2003-2009. Domed (double logistic) selectivity was assumed for the 1996-1998 and 2001-2003 periods, when there was no fishing access in the closed areas, so that large scallops were not fully selected to the fishery. LPUE was not used as an index of abundance. Natural mortality was set at $M = 0.12$ and incidental fishing mortality at 0.2 times fully recruited fishing mortality.

Model predicted trends and shell heights generally fit observations well (Figure B-20 to Figure B-23). This is also reflected in the relatively high implied effective sample sizes for the shell height data (Figure B-24). Mean posterior estimated efficiency for the lined dredge was 0.464, slightly higher than the 0.41 efficiency prior (Figure B-25). The large camera posterior mean was 1.5, indicating that the model estimates were lower than the camera data.

Fishery selectivity was strongly domed during the period that the closed areas were unavailable to the fishery (Figure B-26). Otherwise, selectivity has shifted over time toward larger shell heights. Biomass and abundance generally declined from 1975-1994 and then increased rapidly and reaching a peak in 2005 (Table B-8, Figure B-27). Biomass then fell through 2008, but increased from 2008 to 2009. Biomass in 2009 was 62470 mt. Recruitment appears to be cyclic, with several years of strong recruitment followed by several years of weaker recruitment. Fully recruited fishing mortality increased from 1975 to a peak of over 1.7 in 1992 and then declined. Fully recruited fishing mortality in 2009 was 0.18. As a result of the changes in selectivity and fully recruited fishing mortality, survival to large shell heights has increased substantially in recent years (Figure B-28). During 1975-1995, 100mm scallops were nearly fully selected, and 80 mm scallops were about 80% selected (Figure B-29). By contrast, 100 mm scallops were only about 40% selected during 2004-2009, whereas 80 mm scallops were essentially not selected at all.

Model abundance and biomass estimates correspond well to the expanded estimates from the lined dredge survey, but in most years are modestly below the large camera survey (Figure B-30). Model estimates of fishing mortality are consistent with the Beverton-Holt (1956) length-based equilibrium estimator (Figure B-31). The model 80+mm exploitation index (numbers caught/population numbers > 80mm), is similar to an empirical estimate of the same quantity, estimated directly from fishery and lined dredge survey data, expanded using a dredge efficiency of 0.41 (Figure B-31).

CASA Model for Mid-Atlantic

The Mid-Atlantic CASA model uses the same three survey time series as in Georges Bank, plus the NEFSC winter bottom trawl survey, conducted between 1992-2007. This survey uses "flat net" trawl gear similar to that used by commercial flounder and scallopers and should fairly reliably catch scallops. Preliminary runs with domed selectivity for this survey could not obtain reliable estimates for the declining portion of the dome, so selectivity was modeled by a logistic curve with estimated parameters. However, residuals and direct comparisons between dredges and trawls (Rudders et al. 2000) suggest the possibility that some doming exists. Priors and selectivity assumptions for the other three surveys was as in Georges Bank. Selectivity

periods were 1975-1979, 1980-1997, 1998-2001, 2002-2004, 2005-2009. The first period was modeled as domed (double logistic) selectivity due to the predominance of small scallops in fishery length data, whereas all the other periods were assumed to have logistic selectivity.

The model trend fit the lined dredge survey well, but was contrary to the large camera survey, which decreased while the model trend generally increased during 2003-2009 (Figure B-32). Predicted shell heights usually fit the data well, except for incoming strong year classes, which tended to be overestimated in the surveys relative to the model (Figure B-33, Figure B-34, Figure B-35, Figure B-36). Mean posterior efficiency for the dredge was 0.68, somewhat higher than the 0.44 estimated by the paired dredge/habcam experiment. Mean posterior efficiency for the large camera was 1.41, again indicating the model estimated abundances were generally less than those from the camera (Figure B-37). One cause of this is the downward trend in the large camera survey, which tends to pull the model estimate lower.

Selectivity was strongly domed during 1975-1979; selectivity moved father to the right during subsequent periods so that in the 2005-2009 period, only the plus group was fully selected (Figure B-38). Model estimated abundance and biomass were relatively low during 1975-1998, and then rapidly increased from 1998-2003 and has been steady to slightly increasing since then (Table B-8; Figure B-39). Recruitment has been much greater since 1998 than before this year. Fully recruited fishing mortality was between 0.5 and 1.2 in most years between 1975-1996. Since then, fishing mortality has ranged between 0.35 and 0.87. However, the force of fishing mortality is much less than this on most scallops because of the selectivity patterns. This is illustrated by the dramatic increase in survival since 1998 (Figure B-40), and the reductions in fishing mortality on 80 and 100 mm SH scallops (Figure B-41).

Model abundance and biomass estimates generally agree well with those of the lined dredge survey (expanded using a dredge efficiency of 0.44) except in the most recent period, when the dredge survey is modestly higher (Figure B-42). Model estimates were well below the large camera survey for 2003-2005, but well above them for 2009, again reflecting the conflicting trend. Model estimates of fishing mortality and exploitation agree reasonably well with simple empirical based estimates of these quantities, especially in the most recent years (Figure B-43).

Whole stock biomass, abundance and mortality

Biomass, egg production, abundance, recruitment and fishable mean abundance were estimated for the whole stock by adding estimates for the Mid-Atlantic Bight and Georges Bank. Whole stock fishing mortality rates for each year were calculated $F = (C_M + C_G) / (\bar{N}_M + \bar{N}_G)$ where C_M and C_G are catch numbers for the Mid-Atlantic Bight and Georges Bank. Terms in the denominator are average fishable abundances during each year calculated in the original CASA model $\bar{N} = \sum_L \frac{N_L(1 - e^{-Z_L})}{Z_L}$ with the mortality rate for each size group (L) adjusted for fishery selectivity. The simple ratio formula used to calculate whole stock F is an “exact” solution because the catch equation implies that $C = F\bar{N}$.

Whole stock variances and coefficients of variation were calculated assuming that estimation errors for Georges Bank and the Mid-Atlantic Bight were independent. In particular, variances for biomass, abundance and catch estimates were the sum of the variances for Georges Bank and the Mid-Atlantic Bight. CVs for the ratios estimating whole stock F were approximated $CV_F = \sqrt{CV_C^2 + CV_{\bar{N}}^2}$, which is exact if catch number C_N and average abundance

\bar{N} are independent and lognormally distributed (Deming 1960). The CV for measurement errors in catch for each region was 0.05, the same as assumed in fitting the CASA model.

Like the individual populations, whole-stock fishing mortality generally increased from 1975-1992 and then declined (Table B-8 and Figure B-44). Whole stock biomass, abundance and fishing mortality in 2009 were respectively 129,703 mt meats, 7446 billion (both on July 1) and 0.38. The biomass and abundance in 2009 were the highest in the 1975-2009 time series.

Variances for the stock as a whole depend on the assumption that model errors in Georges Bank and the Mid-Atlantic are independent; these variance would be higher if a positive correlation between model errors exists, and lower if they are negatively correlated.

The apparent precision of the estimates for sea scallops may be surprising and the cvs calculated in this assessment certainly do not capture all of the underlying uncertainties. Estimates were relatively precise because of the long time series of relatively precise dredge survey data and recent video survey data, together with the assumptions of known survey selectivities and prior information on survey efficiencies probably contributed to the small cvs. Retrospective and sensitivity analyses as well as likelihood profiles can help elucidate the uncertainties in the assessment.

Retrospective patterns

CASA model runs for Georges Bank and the Mid-Atlantic show moderate retrospective patterns, with biomass tending to decrease and fishing mortality tending to increase, with the additional years of data (Figure B-45 and Figure B-46). The pattern is stronger in the Mid-Atlantic, likely because of the downward re-estimation of the large year class observed in 2003 and the steep drop in the large camera survey in 2009.

Historical retrospective

Comparisons between the current estimates of fishing mortality and biomass and ones made in previous assessments indicate that estimates on Georges Bank have been fairly stable but there is a tendency in the Mid-Atlantic for estimates fishing mortality to increase and biomass to decrease over time (Figure B-47 and Figure B-48).

Likelihood profile analysis

Likelihood profiles were constructed for natural mortality (M) and mean of large camera survey q (Figure B-49 and Figure B-50). On Georges Bank, minimum $-\log$ -likelihoods for natural mortality occur at about the estimated $M = 0.12$ for survey length compositions, and only slightly higher for survey trends, whereas the priors and commercial catches suggest a higher natural mortality. Most data sources tend to suggest a higher than estimated prior for the large camera survey.

In the Mid-Atlantic, survey trends and shell heights suggest the best estimate of natural mortality slightly below the estimated value (0.15), but the priors and commercial landings show minimums at larger values of M . Most sources of data tend to suggest a higher mean value for dredge efficiency than assumed in the prior, again demonstrating the tension between the survey priors and the other data sources.

Sensitivity analysis

The fact that survey estimated abundances tend to be somewhat higher than model estimates, especially in the Mid-Atlantic, suggest the possibility that there is some source of

mortality, such as unreported landings, discard or incidental fishing mortality or natural mortality, the is greater than that assumed in the model. Alternatively, growth curves are based on data from the most recent period only (2001-2008); there would be model misspecification if growth was different in previous periods (e.g., because the heavy fishing affected growth, see the discussion in Hart and Chute 2009b). Violation of the assumption of spatial uniformity may also play a role in the conflict. Finally, it is possible that some systematic error in camera surveys could also explain at least part of the conflict (e.g., see Appendix III).

To estimate the uncertainty surrounding two key model inputs, sensitivity analyses were performed on input natural mortality and the assumed mean prior efficiencies of the lined dredge and large camera surveys (Figure B-51 and Figure B-52). For natural mortality, runs were conducting using the 5th, 25th, 75th, and 95th percentiles of the natural mortality distribution used in the stochastic reference point models.

Changing natural mortality modestly altered estimates, especially during the 1995-2005 period, but had little effect on the estimates of 2009 biomasses or fishing mortalities. Relaxing the assumptions on priors had almost no effect on 1975-1999 estimates, but did affect estimates in the most recent years, largely because that is when the large camera data occurs. Relaxing the priors gave lower biomasses and higher fishing mortalities than the basecase.

TOR 4: Biological Reference Points

In previous assessments, per recruit reference points F_{MAX} and B_{MAX} were used as proxies for F_{MSY} and B_{MSY} . F_{MAX} is the fishing mortality rate for fully recruited scallops that generates maximum yield-per-recruit. B_{MAX} was defined as the product of BPR_{MAX} (biomass per recruit at $F = F_{MAX}$, from yield-per-recruit analysis) and median numbers of recruits. NEFSC (2007) reported January 1 biomass units, and estimated $F_{MAX} = 0.29$ and $B_{MAX} = 109,000$ mt meats as overall reference points, estimated from the CASA model.

Using the same methods but with updated data and CASA model, the estimates are $F_{MAX} = 0.30$ and $B_{MAX} = 127,000$ mt (Figure B-53). The increase in B_{MAX} is mostly due to the inclusion of special weights for the plus groups in the model; this feature was not in the 2007 model. The value of B_{MAX} is based on January 1 biomass, which was used to report biomass in NEFSC (2007). This assessment mainly reports model biomasses on July 1, which are less than those on January 1, because all growth and recruitment occur on that date in the model. The B_{MAX} corresponding to July 1 biomass is 85,000 mt. This value is somewhat less than the sum of the biomasses that maximize surplus production curves (Figure B-54).

As selectivity has shifted to larger scallops, yield per recruit curves have become increasingly flat, particularly in the Mid-Atlantic, making yield per recruit reference points both difficult to estimate and sensitive to small changes in parameters. Additionally, recruitment has been much stronger during the most recent period in the Mid-Atlantic when biomass has been high, suggesting that spawner-recruit relationships should be included in reference points.

This assessment introduces a stochastic model (SYM – Stochastic Yield Model) for calculating reference points and their uncertainty. It uses Monte-Carlo simulations to propagate the uncertainty of inputs to per recruit and stock-recruit calculations to the estimation of yield per recruit and yield curves. Besides its use in calculating limit reference points, a version of this model was employed to perform a risk assessment that was used to estimate Allowable Biological Catch (ABC) for the sea scallop fishery in 2010.

Description of stochastic yield model

Although the SYM model is separate from CASA, efforts were made to make the two models as compatible as possible. Recruits are initially spread out over 10 size bins (20-70 mm), and growth is modeled using a stochastic growth matrix, as in the CASA model.

Per recruit calculations depend on a number of parameters that each carry a level of uncertainty:

- (1) Von Bertalanffy growth parameters K and L_{∞}
- (2) Shell height/meat weight parameters a and b
- (3) Natural mortality rate M
- (4) Fishery selectivity parameters α and β
- (5) The cull size of the catch and the fraction of discards that survive
- (6) The level of incidental fishing mortality, i.e., non-catch mortality caused by fishing.

The mean, standard error and correlation (when applicable) for each of the parameters is given in Table B-9. Details on each of these parameters is given below.

Growth parameters K and L_{∞} .

These were simulated as negatively correlated normals, using the mean and covariance from shell growth increment data, as estimated by a linear mixed-effects model (Hart and Chute 2009b), updated by including 2008 data. The level of individual variability in these two parameters was taken as estimated in the mixed-effects model without error.

Shell height/meat weight relationships.

Meat weight W at shell height H is calculated using a formula of the form:

$$W = \exp(a + b \ln(H)) \quad (1)$$

The means, variances and covariance of parameters a and b were taken from the analysis described in Appendix VII. Similar to the growth parameters, the estimates of a and b have a strong negative correlation. This means that the predicted meat weight at a given shell height carries less uncertainty than it would appear from the variances of the individual parameters. Meat weights vary seasonally, with the greatest meat weights during the late spring and early summer (NEFSC 2007). Haynes (1966) constructed a number of monthly shell height/meat weight relationships, and did not find any significant trend in the slopes. If this is the case, seasonality would not affect the F_{MAX} or F_{MSY} reference point. For this reason, seasonal variability was not considered a source of uncertainty for this analysis.

Natural mortality M .

As discussed in Section B3, natural mortality for sea scallops was estimated by Merrill and Posgay (1964) as

$$M = \frac{1}{S} \frac{C}{L} \quad (2)$$

where L is the number of live scallops, S is the mean clapper separation time and C is the number of clappers. Probably the greatest uncertainty in this calculation is the mean separation time S . For example, Dickie (1955) estimated S to be 100 days (14.3 weeks), less than half that estimated by Merrill and Posgay. Reflecting this uncertainty, it was assumed S was distributed

as a gamma random variable, with mean 33 weeks and standard deviation 12 weeks. The resulting distribution of M has the desirable characteristic of being skewed to the right (Figure B-55). This makes sense since, for example, a natural mortality of $M = 0.2$ is possible, but an $M = 0$, or even close to zero, is not. Note that because S appears in the denominator of (2), the expected value of M is not equal to applying equation (2) with the mean value of S .

Fishery selectivity.

Fishery selectivity s was estimated using an ascending logistic curve of the form:

$$s = \frac{1}{1 + \exp(\alpha - \beta H)} \quad (3)$$

where H is shell height. The means and covariances of the α and β parameters were taken as estimated by the CASA stock assessment model during the most recent selectivity period. Note that fishery selectivity reflects targeting as well as gear selectivity.

Discard mortality .

Sea scallops that are caught but are less than 90 mm are assumed to be discarded, based on observer data. Sea scallops likely tolerate discarding fairly well, provided they are returned to the water relatively promptly and they are not damaged by the capture process or their time on deck. Here, discard mortality was simulated as a gamma distribution, with a mean of 0.2 and a standard deviation of 0.15, reflecting the high uncertainty in this parameter. This feature is not included in the CASA model, but makes little difference as few scallops below 90 mm are selected in the most recent selectivity period.

Incidental fishing mortality

Incidental fishing mortality occurs when scallops are killed but not captured by the gear. Consistent with the assumptions of the CASA model, incidental mortality was estimated as 0.2 that of landed fishing mortality on Georges Bank and 0.1 in the Mid-Atlantic. Because of the considerable uncertainty in these numbers, incidental mortality was simulated here with a gamma distribution with these means and coefficients of variation of 0.75.

Stock-recruit relationships

Stock-recruit relationships were based on the basecase CASA runs and fitted to Beverton-Holt stock-recruit curves of the form:

$$R = \frac{sB}{\gamma + B}, \quad (4)$$

assuming log-normal errors (Figure B-56). Here R is recruitment, B is spawning stock biomass (or egg production), and s and γ are parameters, representing the asymptotic recruitment when B is large, and the spawning stock biomass where recruitment is half its asymptotic value, respectively. Standard errors of the stock-recruit parameters and their correlation were also estimated using the delta method.

Calculation of equilibrium yield per recruit and yield

Per recruit and stock-recruit parameters were assigned probability distributions reflecting their level of uncertainty, as discussed above. For each iteration, parameters were drawn from their distributions, and then per recruit and yield curves were calculated. This was repeated for

$n = 50000$ iterations and the results collected. The stock-recruit parameters were simulated as correlated log-normals

For each run, equilibrium recruitment at fishing mortality F is given by

$$R = s - \gamma/b(F) \quad (5)$$

where b is biomass per recruit. Total yield is therefore

$$Y(F) = y(F)R = y(F)[(s - \gamma)/b(F)] \quad (6)$$

where y is yield per recruit.

Median (and mean) per recruit and yield curves were calculated as the median (mean) of these quantities as a function of fishing mortality. The probabilistic F_{MSY} (and F_{MAX} were taken as the fishing mortality that maximizes the median yield curve. The median was preferred because it avoided strong influence by likely unrealistic model outliers. The probabilistic MSY and B_{MSY} are the median yield and biomass at F_{MSY} over all runs.

Results

Simulated yield per recruit curves on Georges Bank generally showed a distinct peak between 0.2 and 0.3, but the simulated stock-recruit curves were almost completely flat (Figure B-57). By contrast, simulated yield per recruit curves from the Mid-Atlantic were flat, with F_{MAX} highly variable among runs, which induced a high F_{MAX} (0.835) for the median yield curve (Figure B-58). The correlation between biomass and recruitment induced a much lower F_{MSY} estimate (0.43) for the median yield curve for the Mid-Atlantic. The SYM model gives overall estimates of $F_{MSY} = 0.38$, $B_{MSY} = 125,358$ mt and MSY = 24,975 mt (Table B-9, Figure B-59).

Estimation of Allowable Biological Catch (ABC)

Probabilistic methods such as those employed here are ideal for quantifying risk and precaution, such as that used for deriving ABCs. For the purposes of setting the 2010 sea scallop ABC, the fishing mortality corresponding to the ABC was set by the NEFMC Science and Statistical Committee at the 25th percentile of the distribution of the overall F_{MSY} (i.e., the 25th of the distribution of F_{MSY} values from the individual simulations) which at the time was estimated at 0.28. Using the current simulations, the 25th percentile of F_{MSY} is at 0.31 (Figure B-59 (b)). Equilibrium yield at 0.31 is about 0.8% less than that at F_{MSY} (Figure B-60).

Special considerations for sedentary resources under area management

The above reference point calculations are based on the assumption that fishing mortality risk does not vary among individuals. For sedentary organisms such as sea scallops, these assumptions are never even approximately true; area management such as closed areas means that the assumption of uniform fishing mortality is strongly violated (Hart 2001, 2003; Smith and Rago 2004). In such situations, mean yield-per-recruit, averaged over all recruits, may be different than yield-per-recruit obtained by a conventional per-recruit calculation performed on a recruit that suffers the mean fishing mortality risk (Hart 2001). This condition is exaggerated, as in the case of the scallop fishery, with use of rotational or long-term closures. Moreover, estimates of fishing mortality may be biased low, because individuals with low mortality risk are overrepresented in the population (Hart 2001, 2003).

TOR 5: Status Determination

According to the Amendment 10 overfishing definition (NEFMC 2003), sea scallops are overfished when the survey biomass index for the whole stock falls below $1/2 B_{TARGET}$. The target biomass estimated in NEFSC (2007) is $B_{TARGET} = 109,000$ mt (January 1) was calculated as the median recruitment in the survey time series times BPR_{MAX} , the biomass per recruit obtained when fishing at F_{MAX} . NEFSC (2007) estimated $F_{MAX} = 0.29$, which has been used since then as the overfishing threshold. The updated values are $F_{MAX} = 0.30$ and $B_{MAX} = 85,000$ mt (July 1 biomass). The new recommended stochastic MSY reference points are $F_{MSY} = 0.38$ and $B_{MSY} = 125,358$ mt.

According to the basecase CASA run, total biomass in 2009 was 129,703 mt meats, which is above the estimated B_{MSY} or its proxy, regardless of whether the previous, updated or proposed biomass target is used. Therefore, the sea scallop fishery was not overfished in 2009. The probability the stock was below the $1/2 B_{MSY}$ biomass threshold is < 0.0001 , regardless of which biomass reference point is used.

Overall fishing mortality was 0.38 (to three decimal places 0.378), which is above the previous (NEFSC 2007) overfishing threshold of 0.29 and its updated value of 0.30, but equal to the newly recommended (in 2010) $F_{MSY} = 0.38$. Therefore, overfishing was not occurring in 2009 based on the new recommended overfishing definition; however, overfishing would be occurring if the previous definition or its updated value were to be used. Using the new recommended overfishing definition, the probability that overfishing was occurring in 2009 was just under 0.50.

TOR 6: Stock Projections

Because of the sedentary nature of sea scallops, fishing mortality can vary considerably in space even in the absence of area specific management (Hart 2001). Area management such as rotational and long-term closures can make variation even more extreme. Projections that ignore such variation might be unrealistic and misleading. For example, suppose 80% of the stock biomass is in areas closed to fishing (as occurred in some years in Georges Bank). A stock projection that ignored the closure and assumed a whole-stock F of 0.2 would forecast landings nearly equal to the entire stock biomass of the areas remaining open to fishing. Thus, using a non-spatial forecasting model can lead to setting a level of landings that appears sustainable if all areas were fished uniformly, but is in fact unsustainable for a given area management policy.

For this reason, a spatial forecasting model (the Scallop Area Management Simulator, SAMS) was developed for use in sea scallop management (Appendix XII). Various versions of SAMS have been used since 1999 and the model was discussed at length in the last assessment (NEFSC 2007). Growth is modeled in SAMS and CASA in a similar manner, except that each subarea of Georges Bank and the Mid-Atlantic in SAMS has its own stochastic growth transition matrix derived from the shell increments collected in that area. Mortality and recruitment are also area-specific. In example calculations, natural mortality was chosen from a gamma distribution with means 0.12 (Georges Bank) and 0.15 (Mid-Atlantic), to be compatible with reference point calculations in the SYM model (see Section B7). Fishing mortality can either be explicitly specified in each area, calculated using a simple fleet dynamics model which assumes fishing effort is proportional to fishable biomass, or a combination of the two.

Projected recruitment is modeled stochastically with the log-transformed mean and covariance for recruitment in each area matching that observed in NEFSC dredge survey time

series. Initial conditions were based on the 2009 NEFSC and SMAST sea scallop surveys with uncertainty measured by bootstrapping as described by Smith (1997). Survey dredge efficiencies were set in SAMS so that the mean 2009 biomass matched estimates from the CASA model. Further details regarding the SAMS model are given in Appendix XII.

Example calculations

Only example calculations can be given here but the model has and will be used by the NEFMC Scallop Plan and Development Team to evaluate possible management alternatives, which are complex for sea scallops. For the example simulations, the stock area was split into 16 subareas (Figure B-61), six in the Mid-Atlantic (Virginia Beach, Delmarva, Elephant Trunk, Hudson Canyon South, New York Bight, and Long Island) and ten on Georges Bank (Closed Area I, II and Nantucket Lightship EFH closures, Closed Area I, II and Nantucket Lightship access areas, Great South Channel proposed closure and the remainder of the Great South Channel, Northern Edge and Peak, and Southeast Part).

The EFH (Essential Fish Habitat) closures on Georges Bank were assumed to be closed for the duration of the simulations. One of the Georges Bank access areas were assumed to be fished on a rotating basis (Closed Area II in 2009 and 2012, Nantucket Lightship in 2010 and 2013, and Closed Area I in 2011 and 2014). Landings in these areas (as actually has occurred or is planned) were set at 1400 mt in 2009, and 2700 mt in 2010-2014. The Hudson Canyon South rotational closure area was assumed to be closed to fishing in 2009-2010, and then reopened with a TAC of 5400 mt in 2011-2013. It is assumed to revert to a general open area in 2014. The Elephant Trunk rotational area was assumed to have landings of 8100 mt in 2009, 5400 mt in 2010 and 2700 mt in 2011, and then reverts to be part of the open areas. Landings in the Delmarva rotational area are assumed to be 2700 mt in 2009 and 2010, 5400 mt in 2011 and 2012 and then it reverts to the open pool. All other areas (Virginia Beach, New York Bight, Long Island, South Channel areas, Northern Edge and Peak, Southeast Part). In projections, fishing effort was allocated to areas so that the overall fishing mortality rate was 0.24 in all years, consistent with current policy, and somewhat lower than the 2009 recommend ABC fishing mortality of 0.28. Fishing effort was distributed among the open areas according to a simple fleet dynamics model, where fishing mortality in each area was assumed to be proportional to fishable biomass.

A total of $n=5000$ projection runs were performed, with stochastically varying initial conditions, recruitment, and natural mortality. Projected mean biomass is expected to increase modestly from 2009-2012, mainly on Georges Bank due to the large year classes observed during 2007-2009, and then level off (Figure B-62). Landings are expected to be lower in 2010 than 2009, then increase somewhat, with a peak in 2012 at about 27,000 mt, and then level off to about 24,000 mt. Fishing mortality is expected to be greater in the Mid-Atlantic than in Georges Bank. Not surprisingly, uncertainty regarding biomass and landings increases over time (Figure B-63). Nonetheless, the 25th percentile of biomass is over 130,000 mt in all years, and thus over the target biomass. The minimum biomass of the 5000 runs stayed above the overfishing threshold through 2012, but dropped below it for 2013 and 2014. However, even the 0.1th percentile of the runs remained over the overfishing threshold in all years. Thus, the forecasts indicate that there is little chance of the stock becoming overfished under status quo management.

In summary, the projections indicate that the stock is stable, and biomass and landings may increase modestly from 2009 levels assuming status quo management. Especially given the recent selectivity patterns, the stock's vulnerability to being overfished is low.

TOR 7: Research Recommendations

Research Recommendations from NEFSC 2007

1) Refine estimates of natural mortality focusing on variation among regions, size groups and over time. Abundance trends in closed areas where no fishing occurs may provide important information about the overall level of natural mortality and time trends. Survey clapper catches may provide information about spatial, temporal and size related patterns in natural mortality.

This assessment contains a re-evaluation of natural mortality in sea scallops. Further work on natural mortality using the closed areas is ongoing.

2) Evaluate the within and between reader error rates in identification and measurement of growth increments on scallop shells.

This has not been done since there is at this time only a single reader.

3) Improve estimates of incidental and discard mortality rates.

This has not been done, but the results of this assessment indicate its importance, especially for the Mid-Atlantic.

4) Consider using autocorrelated recruitment in SAMS projection model runs. CASA model estimates indicate that sea scallop recruitment may be autocorrelated.

SAMS has the ability to model autocorrelated recruitment, but this was not done in the simulations presented here because of the difficulties in estimating the autocorrelation on the small scale that SAMS operates.

5) Consider modeling the spatial dynamics of the fishing fleet in the SAMS projection model based on catch rates, rather than exploitable abundance, of scallops in each area.

Not done

6) Evaluate assumptions about the spatial dynamics of the fishing fleet in the SAMS model by comparing predicted distributions to VMS data.

Work with VMS data is ongoing, but has been slowed due to problems obtaining the data.

7) Investigate the feasibility and benefits of using information about the size composition of sea scallops in predicting the spatial distribution of the fishing fleet in the SAMS projection model.

Not done.

8) Evaluate the accuracy of the SAMS projection model retrospectively by comparison to historical survey abundance trends.

This has been done in other venues. The SAMS model had a tendency to overestimate projected biomass and landings. The changes in the assumptions of growth, natural mortality and incidental mortality may make the forecasts more realistic.

9) Consider implementing discard mortality calculations in the CASA model that are more detailed and involve discarded shell height composition data from at sea observers.

This was considered, but not done due to lack of time. Discard mortality may be important during some periods, especially in the Mid-Atlantic. Additionally, empirical studies estimating discard mortality will be needed to make the modeling useful.

10) Consider implementing a two or more "morph" formulation in the CASA model to accommodate scallops that grow at different rates.

Not done.

11) Consider approaches to implementing seasonal growth patterns in the CASA model to improve fit to shell height composition data. Scallops grow quickly at small sizes and growth rates vary by season.

Considerable time was spent on implementing a CASA model with seasonal growth, but the model did not perform well with seasonal growth. Thus, this assessment still uses an annual growth model.

New Research Recommendations

1. Look into a way to fit discarded scallops, which have a different length frequency from the rest of the population, into the model.
2. Evaluate the effect of the four-inch rings on incidental mortality. Now that a larger fraction of small scallops are traveling through the mesh, has incidental mortality increased or are the scallops relatively unscathed?
3. Consider finding a better way to express the variation in the HABCAM abundance data (the data were kriged for this assessment, and the variance was calculated by summing the variance of each of the kriged grids).
4. Look at the historical patterns of the “whole stock”; how the spatial patterns of scallops and the fishery have changed over time.
5. Estimate incidental mortality by running Habcam or an AUV along dredge tracks
6. Effort should be made to make sure the survey dredge is fitted with a camera at some point during the survey to record the movements of the dredge. This will help answer some questions about when the dredge starts and stops fishing, and the determination of tow times.
7. Seasonal patterns in scallop shell growth need to be analyzed and this data incorporated into the model.
8. Stock-recruit relationships should be calculated for various sub-sections of the stock, smaller areas than just MAB and GBK to look for possible patterns or relationships.
9. Further refine the estimate of the extent of scallop habitat relative to that of the survey
10. Age archived scallop shells from the 1980s and 1990s.
11. Continue to look at patterns of seasonality in weight of the meats and gonads, and timing of spawning.

References:

(including references cited in Scallop Appendixes)

- Almeida F, Sheehan T, Smolowitz R. 1994. Atlantic sea scallop, *Placopecten magellanicus*, maturation on Georges Bank during 1993. NEFSC Ref Doc. 94-13.
- Beverton RJH, Holt SJ. 1956. A review of methods for estimating mortality rates in fish populations, with special reference to sources of bias in catch sampling. Rapp. P.-v. Reun Cons Int Explor Mer. 140:67-83.
- Beverton RJH, Holt SJ. 1959. A review of the lifespans and mortality rates of fish in nature and the relation to growth and other physiological characteristics. Pgs 142-177 in: Ciba Foundation colloquia in ageing. V. The lifespan of animals. Churchill, London.
- Caddy JF. 1971. Efficiency and selectivity of the Canadian offshore scallop dredge. ICES CM 1971/K:25.
- Caddy JF. 1973. Underwater observations on tracks of dredges and trawls and some effects of dredging on a scallop ground. J Fish Res Bd Can. 30:173-180.
- Caddy JF, Radley-Walters C. 1972. Estimating count per pound of scallop meats by volumetric measurement. Fish Res Brd Can Man Rep Ser. 1202.
- Charnov EL. 1993. Life history invariants: Some explorations of symmetry in evolutionary ecology. Oxford Press, Oxford.
- Deming WE. 1960. Sample design in business research. Wiley & Sons, Inc. New York. 517 p.
- Dibacco C, Robert G, Grant J. 1995. Reproductive cycle of the sea scallop, *Placopecten magellanicus* (Gmelin, 1791), on northeastern Georges Bank. J Shellfish Res. 14:59-69.
- Dickie LM. 1955. Fluctuations in abundance of the giant scallop, *Placopecten magellanicus* (Gmelin), in the Digby Area of the Bay of Fundy. J Fish Res Bd Can 12:797-857.
- DuPaul WD, Fisher RA, Kirkley JE. 1990. An evaluation of at-sea handling practices: Effects on sea scallop meat quality, volume and integrity. Contract report to Gulf and South Atlantic Fisheries.
- DuPaul WD, Kirkley JE, Schmitzer AC. 1989. Evidence of a semiannual reproductive cycle for the sea scallop, *Placopecten magellanicus* (Gmelin, 1791), in the Mid-Atlantic region. J Shellfish Res. 8:173-178.
- Fournier D, Archibald CP. 1982. General theory for analyzing catch at age data. Can J Fish Aquat Sci. 39: 1195-1207.
- Gedamke T, DuPaul WD, Hoenig JM. 2004. A spatially explicit open-ocean DeLury analysis to estimate commercial scallop dredge efficiency. N Amer J Fish Manage. 24: 335-351.
- Gedamke T, DuPaul WD, Hoenig JM. 2005. Index-removal estimates of dredge efficiency for sea scallops on Georges Bank. N Amer J Fish Manage. 25:1122-1129.
- Hart DR. 2001. Individual-based yield-per-recruit analysis, with an application to the Atlantic sea scallop, *Placopecten magellanicus*. Can J Fish Aquat Sci. 58: 2351-2358.
- Hart DR. 2003. Yield- and biomass-per-recruit analysis for rotational fisheries, with an application to the Atlantic sea scallop (*Placopecten magellanicus*). Fish Bull. 101: 44-57.
- Hart DR, Chute AS. 2004. Essential fish habitat source document: Sea scallop, *Placopecten magellanicus*, life history and habitat characteristics, 2nd ed. NOAA Tech Memo NMFS NE-189.
- Hart DR, Chute AS. 2009a. Verification of Atlantic sea scallop, *Placopecten magellanicus*, shell growth rings by tracking cohorts in fishery closed areas. Can J Fish Aquat Sci. 66:751-758.

- Hart DR, Chute AS. 2009b. Estimating von Bertalanffy growth parameters from growth increment data using a linear mixed-effects model, with an application to the sea scallop *Placopecten magellanicus*. ICES J Mar Sci. 66: 2165-2175.
- Hart DR, Rago PJ. 2006. Long-term dynamics of US Atlantic sea scallop *Placopecten magellanicus* populations. N Amer J Fish Manage. 26:490-501.
- Haynes EB. 1966. Length-weight relationship of the sea scallop *Placopecten magellanicus* (Gmelin). Res Bull Int Comm Northw Atl Fish. 3: 32-48.
- Holling CS. 1959. Some characteristics of simple types of predation and parasitism. Can Entomologist, 91: 385-398.
- Jacobson LD, Stokesbury KDE, Allard M, Chute A, Harris BP, Hart D, Jaffarian T, Marino MC II, Nogueira JI, Rago PR. 2010. Quantification, effects and stock assessment modeling approaches for measurement errors in body size data from sea scallops (*Placopecten magellanicus*). Fish. Bull. 108:233-247.
- Jenkins SR, Brand AR. 2001. The effect of dredge capture on the escape response of the great scallop, *Pecten maximus* (L.): implications for the survival of undersized discards. J Exp Mar Biol Ecol. 266: 33-50.
- Kirkley JE, DuPaul WD. 1989. Commercial practices and fishery regulations: The United States northwest Atlantic sea scallop, *Placopecten magellanicus* (Gmelin, 1791), fishery. J Shellfish Res. 8: 139-149.
- Lai HL, Helser T. 2004. Linear mixed-effects models for weight-length relationships. Fish Res. 70: 377-387.
- MacDonald BA, Thompson RJ. 1985. Influence of temperature and food availability on the ecological energetics of the giant scallop *Placopecten magellanicus*. II. Reproductive output and total production. Mar Ecol Prog Ser. 25: 295-303.
- MacDonald BA, Thompson RJ. 1986. Production, dynamics and energy partitioning in two populations of the giant scallop *Placopecten magellanicus* (Gmelin). J Exp Mar Biol Ecol. 101: 285-299.
- McCullagh P, Nelder JA. 1989. Generalized linear models, 2nd ed. Chapman & Hall.
- McGarvey R, Serchuk FM, McLaren IA. 1992. Statistics of reproduction and early life history survival of the Georges Bank sea scallop (*Placopecten magellanicus*) population. J Northw Atl Fish Sci. 13:83-89.
- Merrill AS, Posgay JA. 1964. Estimating the natural mortality rate of sea scallop. Res Bull Int Comm NW Atl Fish. 1:88-106.
- Merrill AS, Posgay JA, Nichy F. 1966. Annual marks on shell and ligament of sea scallop (*Placopecten magellanicus*). Fish Bull. 65: 299-311.
- Methot RD. 2000. Technical description of the stock synthesis assessment program. NOAA Tech Memo. NMFS-NWFSC-43: 1-46.
- Millar RB. 1992. Estimating the size-selectivity of fishing gear by conditioning on the total catch. J Am Stat Assoc. 87: 962-968.
- Millar RB, Fryer RJ. 1999. Estimating the size-selection curves of towed gears, traps, nets and hooks. Reviews in Fish Biology and Fisheries 9(1):86-116
- Millar RB, Broadhurst MK, Macbeth WG. 2004. Modeling between-haul variability in the size selectivity of trawls. Fish Res. 67: 171-181.

- Murawski SA, Serchuk FM. 1989. Environmental effects of offshore dredge fisheries for bivalves. ICES C.M. 1989/K:27
- Naidu KS. 1987. Efficiency of meat recovery from Iceland scallops (*Chlamys islandica*) and sea scallops (*Placopecten magellanicus*) in the Canadian offshore fishery. J Northw Atl Fish Sci. 7:131-136.
- NEFMC [New England Fisheries Management Council]. 1993. Amendment #4 and supplemental environmental impact statement to the sea scallop fishery management plan. New England Fisheries Management Council, Saugus, MA.
- NEFMC. 2003. Final Amendment 10 to the Atlantic sea scallop fishery management plan with a supplemental environmental impact statement, regulatory impact review, and regulatory flexibility analysis. New England Fisheries Management Council, Newburyport, MA.
- NEFMC. 2010. Framework adjustment 21 to the Atlantic sea scallop FMP, including an environmental assessment, regulatory impact review, regulatory flexibility analysis and stock assessment and fishery evaluation (SAFE) report. New England Fisheries Management Council, Newburyport, MA.
- NEFSC [Northeast Fisheries Science Center]. 1992. Report of the 14th Northeast Regional Stock Assessment Workshop (14th SAW). [By Northeast Regional Stock Assessment Workshop No. 14.] NEFSC Ref Doc. 92-07.
- NEFSC. 1995. [Report of the] 20th Northeast Regional Stock Assessment Workshop (20th SAW), Stock Assessment Review Committee (SARC) Consensus Summary of Assessment. NEFSC Ref Doc. 95-18.
- NEFSC. 1997. [Report of the] 23rd Northeast Regional Stock Assessment Workshop (23rd SAW), Stock Assessment Review Committee (SARC) Consensus Summary of Assessment. NEFSC Ref. Doc. 97-05, Woods Hole, MA.
- NEFSC 1999. [Report of the] 29th Northeast Regional Stock Assessment Workshop (29th SAW). Stock Assessment Review Committee (SARC) consensus summary of assessments. NEFSC Ref Doc. 99-14.
- NEFSC. 2001. [Report of the] 32nd Northeast Regional Stock Assessment Workshop (32nd SAW). Stock Assessment Review Committee (SARC) consensus summary of assessments. NEFSC Ref Doc. 01-05.
- NEFSC. 2004. 39th Northeast Regional Stock Assessment Workshop (39th SAW) Assessment Summary Report & Assessment Report. NEFSC Ref Doc. 04-10.
- NEFSC. 2007. 45th Northeast Regional Stock Assessment Workshop (45th SAW): 45th SAW assessment report. NEFSC Ref Doc. 07-16.
- Pennington M, Burmeister L-M, Hjellvik V. 2002. Assessing the precision of frequency distributions estimated from trawl-survey samples. Fish Bull. 100: 74-80.
- Rudders DB, DuPaul WD, Kirkley JE. 2000. A comparison of size selectivity and relative efficiency of sea scallop *Placopecten magellanicus* (Gmelin, 1791), trawls and dredges. J Shellfish Res. 19: 757-764.
- Serchuk FM, Rak RS. 1983. Biological characteristics of offshore Gulf of Maine scallop populations: size distributions, shell height-meat weight relationships and relative fecundity patterns. NMFS, Woods Hole Lab Ref Doc. 83-07: 42 p.
- Serchuk FM, Smolowitz RJ. 1980. Size selection of sea scallops by an offshore scallop survey dredge. ICES CM. 1980/K: 24.
- Serchuk FM, Smolowitz RJ. 1989. Seasonality in sea scallop somatic growth and reproductive cycles. J Shellfish Res. 8: 435.

- Serchuk FM, Wigley SE. 1989. Current resource conditions in USA Georges Bank and Mid-Atlantic sea scallop populations: Results of the 1989 NMFS sea scallop research vessel survey. NEFSC SAW-9, Working Paper No 9: 52p.
- Serchuk FM, Wood PW, Posgay JA, Brown BE. 1979. Assessment and status of sea scallop (*Placopecten magellanicus*) populations of the northeast coast of the United States. Proc Natl Shellfish Assoc. 69: 161-191.
- Smith SJ. 1997. Bootstrap confidence limits for groundfish trawl survey estimates of mean abundance. Can J Fish Aquat Sci. 54: 616-630.
- Smith SJ, Rago PJ. 2004. Biological reference points for sea scallops (*Placopecten magellanicus*): the benefits and costs of being nearly sessile. Can J Fish Aquat Sci. 61: 1338-1354.
- Smolowitz RJ, Serchuk FM, Reidman RJ. 1989. The use of a volumetric measure for determining sea scallop meat count. NOAA Tech Memo. F/NER-1.
- Stokesbury KDE, Harris BP, Marino MC, II, Nogueira JI. 2004. Estimation of sea scallop abundance using a video survey in off-shore U.S. waters. J Shellfish Res. 23: 33-40.
- Sullivan PJ, Lai H-L, Gallucci VF. 1990. A catch-at-length analysis that incorporates a stochastic model of growth. Can J Fish Aquat Sci. 47: 184-198.
- Thouzeau G, Robert G, Smith SJ. 1991. Spatial variability in distribution and growth of juvenile and adult sea scallops *Placopecten magellanicus* (Gmelin) on eastern Georges Bank (Northwest Atlantic). Mar Ecol Prog Ser. 74: 205-218.
- Veale LO, Hill AS, Brand AR. 2000. An in situ study of predator aggregations on scallop (*Pecten maximus* (L.)) dredge discards using a static time-lapse camera system. J Exp Mar Biol Ecol. 255: 111-129.
- Wigley SE, Serchuk FM. 1996. Current resource conditions in Georges Bank and Mid-Atlantic sea scallop populations: Results of the 1994 NEFSC sea scallop research vessel survey. NEFSC Ref Doc. 96-03.
- Wigley SE, Hersey P, Palmer JE. 2008. A Description of the Allocation Procedure Applied to the 1994 to 2007 Commercial Landings Data. NEFSC Ref Doc. 08-18.

Tables

Table B-1. List of changes made to CASA models for the 2010 sea scallop assessment.

- 1) Updated growth increments -plus groups changed to match new L_{∞} estimates
- 2) Updated shell height meat weight relationships
- 3) Updated commercial meat weight anomalies (substantial changes)
- 4) Empirical plus group weights for fishery and population (new code and input data)
- 5) $M=0.12$ (GBK) and 0.15 (MAB) instead of 0.1
- 6) Incidental fishing mortality estimates increased (0.15 to 0.2 on GB; 0.04 to 0.1 in MAB)
- 7) NEFSC survey
 - Adjustments for R/V Sharp in 2008-2009
 - Canadian tows on GBK during 1979-1981
 - Efficiency estimates from paired HabCam tows used as prior
 - Used unlined dredge survey (1975+1977) on Georges Bank
- 8) GBK starts in 1975 (instead of 1982)
- 9) LPUE no longer used in model
- 10) SMAST large camera survey (2003-2009) in place of small camera
- 11) Prior $cv(s)$ set at 0.15 rather than 0.20
- 12) Primarily report July 1 rather than January 1 abundance/biomass
- 13) Assumed CV for surveys tuned to residual variance

Table B-2. US sea scallop landings (mt meats) 1964-2009.

Year	Gulf of Maine				Georges Bank				S. New England				Mid Atlantic Bight				Total			
	dredge	trawl	other	sum	dredge	trawl	other	sum	dredge	trawl	other	sum	dredge	trawl	other	sum	dredge	trawl	other	sum
1964		0	208	208		0	6,241	6,241		52	3	55		0	137	137		52	6,590	6,642
1965		0	117	117		3	1,478	1,481		2	24	26		0	3,974	3,974		5	5,592	5,598
1966		0	102	102		0	883	884		0	8	8		0	4,061	4,061		1	5,055	5,056
1967		0	80	80		4	1,217	1,221		0	8	8		0	1,873	1,873		4	3,178	3,182
1968		0	113	113		0	993	994		0	56	56		0	2,437	2,437		0	3,599	3,599
1969		1	122	123		8	1,316	1,324		8	18	19		5	846	851		14	2,302	2,317
1970		0	132	132		5	1,410	1,415		0	6	6		14	459	473		19	2,006	2,026
1971		4	358	362		18	1,311	1,329		0	7	7		0	274	274		22	1,949	1,971
1972		1	524	525		5	816	821		0	2	2		5	653	658		11	1,995	2,006
1973		0	460	460		15	1,065	1,080		0	3	3		4	245	249		19	1,773	1,792
1974		0	223	223		15	911	926		0	4	5		0	937	938		16	2,076	2,091
1975		6	741	746		13	844	857		8	42	50		52	1,506	1,558		80	3,132	3,212
1976		3	364	366		38	1,723	1,761		4	3	7		819	2,972	3,791		361	5,061	5,422
1977		4	254	258		27	4,709	4,736		1	10	11		255	2,564	2,819		58	7,536	7,595
1978	242	1	0	243	5,532	37	0	5,569	25	2	0	27	4,435	207	0	4,642	10,234	247	0	10,481
1979	401	5	1	407	6,253	25	7	6,285	61	5	0	66	2,857	29	1	2,888	9,572	64	9	9,645
1980	1,489	122	3	1,614	5,382	34	2	5,419	130	3	0	133	2,202	85	79	2,366	9,204	245	83	9,532
1981	1,225	73	7	1,305	7,787	56	0	7,843	68	1	0	69	772	14	2	788	9,852	144	9	10,005
1982	631	28	5	664	6,204	119	0	6,322	126	0	0	126	1,602	6	2	1,610	8,562	153	7	8,723
1983	815	72	7	895	4,247	32	4	4,284	243	1	0	243	3,092	19	10	3,121	8,398	124	21	8,542
1984	651	18	10	678	3,011	29	3	3,043	161	3	0	164	3,695	53	2	3,750	7,518	103	14	7,635
1985	408	3	10	421	2,860	34	0	2,894	77	4	0	82	3,230	49	2	3,281	6,575	90	12	6,677
1986	308	2	6	316	4,428	10	0	4,438	76	2	0	78	3,407	386	6	3,799	8,218	400	12	8,631
1987	373	0	9	382	4,821	30	0	4,851	67	1	0	68	7,639	1,168	1	8,808	12,900	1,199	10	14,109
1988	506	7	13	526	6,036	18	0	6,054	65	4	0	68	6,071	938	8	7,017	12,678	966	21	13,666
1989	600	0	44	644	5,637	25	0	5,661	127	11	0	138	7,894	534	5	8,433	14,258	570	49	14,876
1990	545	0	28	574	9,972	10	0	9,982	110	6	0	116	6,364	541	10	6,915	16,991	558	38	17,587
1991	527	3	75	605	9,235	77	0	9,311	55	16	0	71	6,408	878	14	7,300	16,225	973	89	17,288
1992	676	2	45	722	8,230	7	0	8,238	119	5	0	124	4,562	570	5	5,137	13,587	584	50	14,221
1993	763	2	32	797	3,637	18	0	3,655	65	1	0	66	2,412	393	3	2,808	6,878	413	36	7,327
1994	410	6	9	425	1,182	7	0	1,189	29	1	0	30	5,211	754	0	5,965	6,832	768	9	7,609
1995	342	6	13	361	992	4	1	997	41	2	0	43	5,786	798	7	6,591	7,161	810	21	7,992
1996	544	5	12	561	2,126	7	4	2,137	59	5	0	64	4,467	653	4	5,124	7,196	670	20	7,886
1997	673	5	21	699	2,347	9	1	2,357	81	11	3	95	2,703	378	1	3,082	5,804	403	26	6,233
1998	392	5	15	412	2,045	19	1	2,065	103	3	0	106	2,411	564	6	2,981	4,951	591	22	5,564
1999	267	2	2	271	5,172	6	1	5,179	78	1	0	79	3,629	959	1	4,589	9,146	968	4	10,118
2000	162	21	43	226	4,910	40	5	4,955	85	3	1	89	8,139	1,210	2	9,351	13,296	1,274	51	14,621
2001	335	7	1	343	4,879	58	6	4,943	28	37	0	65	14,144	1,543	16	15,703	19,386	1,645	23	21,054
2002	386	18	1	405	5,967	33	11	6,011	20	12	0	32	15,981	1,426	36	17,443	22,354	1,489	48	23,891
2003	197	3	1	201	4,859	22	2	4,883	53	4	0	57	19,040	1,226	10	20,276	24,149	1,255	13	25,417
2004	165	12	0	177	4,249	146	11	4,406	830	151	11	992	22,313	1,194	26	23,533	27,557	1,503	48	29,108
2005	163	12	12	187	8,958	69	15	9,042	845	13	40	898	14,361	1,096	109	15,566	24,327	1,190	176	25,693
2006	147	3	5	155	15,688	51	21	15,760	2,029	10	8	2,047	7,944	782	46	8,772	25,808	846	80	26,734
2007	97	8	12	117	9,419	45	18	9,482	335	18	7	360	16,234	345	55	16,634	26,085	416	92	26,593
2008	103	12	5	120	6,405	24	11	6,440	303	6	16	325	16,819	556	13	17,388	23,630	598	45	24,273
2009	81	0	3	84	6,451	8	16	6,475	216	1	3	220	17,487	12	1,851	19,350	24,235	21	1,873	26,129

Table B-3. Summary of sea scallop management history.

Period	Days at sea#	Minimum Ring Size	Minimum Twine Top	Maximum Crew Size	GB Closures	GB Access Areas	MA Closures	MA Access Areas
1982-1993	N/A	N/A	N/A	N/A	0	0	0	0
1994	204	3"-3.25"	5.5"	9	3	0	0	0
1995	182	3.25"	5.5"	7	3	0	0	0
1996	182	3.5"	5.5"	7	3	0	0	0
1997	164	3.5"	5.5"	7	3	0	0	0
1998	142	3.5"	5.5"	7	3	0	2	0
1999	120	3.5"	5.5"	7	3	1	2	0
2000	120	3.5"	8"	7	3	3	2	0
2001	120	3.5"	8"	7	3	1	0	2
2002	120	3.5"	8"	7	3	0	0	2
2003	120	3.5"	8"	7	3	0	0	2
2004	42*	3.5"	8"	7	3	2	1	1
2005	40*	4"	10"	7	3	2	1	1
2006	52*	4"	10"	7	3	2	1	1
2007	51*	4"	10"	7	3	2	1	2
2008	35*	4"	10"	7	3	1	2	1
2009	37*	4"	10"	7	3	1	1	2

Full-time permit

*Does not include access area trips; for each year between 2005-2009, full-time vessels were allocated 5 access area trips, with trip limits of 18,000 lbs meats.

Table B-4. NEFSC sea scallop lined survey stratified mean indices for (a) Georges Bank, (b) Mid-Atlantic, and (c) combined for shell heights greater than 40 mm. The expanded abundance and biomass figures were calculated using an assumed efficiency of 0.41 for Georges Bank and 0.44 for the Mid-Atlantic.

(a) Georges Bank

year	Abundance index (mean N/tow)	CV	Biomass index (kg/tow)	CV	N tows	Proportion positive tows	mean weight (g/scallop)	Expanded abundance (millions)	Expanded biomass (mt)
1979	82.9	0.57	1.650	0.35	121	0.90	19.9	1042	20740
1980	70.2	0.32	0.785	0.16	155	0.78	11.2	883	9861
1981	46.4	0.20	0.957	0.18	86	0.80	20.6	583	12022
1982	133.3	0.56	0.837	0.31	129	0.80	6.3	1675	10517
1983	50.8	0.30	0.607	0.24	138	0.85	12.0	638	7626
1984	28.8	0.12	0.421	0.10	138	0.83	14.6	362	5294
1985	52.1	0.18	0.554	0.17	170	0.85	10.6	655	6967
1986	90.8	0.18	0.715	0.11	194	0.85	7.9	1141	8983
1987	107.0	0.21	0.907	0.17	190	0.82	8.5	1345	11402
1988	81.9	0.17	0.709	0.14	192	0.78	8.7	1029	8908
1989	85.0	0.35	0.702	0.16	254	0.82	8.3	1068	8818
1990	166.7	0.30	1.036	0.23	194	0.80	6.2	2095	13025
1991	242.2	0.49	1.116	0.26	194	0.88	4.6	3044	14031
1992	236.8	0.53	1.605	0.46	191	0.86	6.8	2976	20166
1993	57.5	0.29	0.400	0.17	182	0.82	7.0	722	5026
1994	38.4	0.18	0.367	0.13	194	0.80	9.6	482	4618
1995	109.2	0.25	0.649	0.17	193	0.85	5.9	1372	8159
1996	111.8	0.18	1.114	0.16	189	0.87	10.0	1406	14000
1997	78.7	0.14	1.292	0.15	206	0.85	16.4	989	16239
1998	265.6	0.26	3.728	0.33	230	0.86	14.0	3338	46850
1999	156.0	0.15	2.527	0.16	198	0.94	16.2	1961	31756
2000	681.2	0.30	6.118	0.21	188	0.89	9.0	8562	76893
2001	372.0	0.14	5.724	0.14	225	0.94	15.4	4676	71934
2002	294.8	0.15	6.158	0.14	229	0.90	20.9	3705	77398
2003	226.0	0.12	5.796	0.14	225	0.92	25.6	2840	72844
2004	264.2	0.11	7.606	0.13	230	0.92	28.8	3321	95596
2005	210.0	0.12	6.048	0.11	227	0.93	28.8	2640	76010
2006	153.5	0.11	5.013	0.14	237	0.91	32.6	1930	62999
2007	183.2	0.09	4.373	0.09	232	0.94	23.9	2303	54955
2008	292.9	0.13	6.242	0.10	182	0.90	21.3	3681	78448
2009	380.6	0.19	6.186	0.18	179	0.94	16.3	4784	77748

(b) Mid-Atlantic Bight

year	Abundance index (mean N/tow)	CV	Biomass index (kg/tow)	CV	N tows	Proportion positive tows	mean weight (g/scallop)	Expanded abundance (millions)	Expanded biomass (mt)
1979	32.3	0.09	0.580	0.10	166	0.92	17.9	466	8364
1980	41.2	0.12	0.497	0.08	167	0.94	12.1	595	7173
1981	30.7	0.16	0.386	0.12	167	0.91	12.6	443	5574
1982	31.2	0.11	0.406	0.08	185	0.91	13.0	451	5864
1983	29.1	0.09	0.365	0.08	193	0.89	12.5	420	5269
1984	29.4	0.10	0.351	0.08	204	0.91	12.0	424	5069
1985	69.9	0.12	0.558	0.08	201	0.94	8.0	1008	8048
1986	119.6	0.09	0.956	0.08	226	0.93	8.0	1726	13787
1987	119.9	0.09	0.829	0.06	226	0.93	6.9	1731	11962
1988	134.9	0.10	1.300	0.07	227	0.91	9.6	1946	18763
1989	171.1	0.09	1.190	0.07	244	0.93	7.0	2469	17175
1990	205.4	0.22	1.275	0.17	216	0.89	6.2	2964	18402
1991	77.0	0.10	0.738	0.11	228	0.92	9.6	1110	10647
1992	40.9	0.11	0.418	0.07	229	0.87	10.2	590	6037
1993	130.7	0.10	0.591	0.08	214	0.96	4.5	1886	8527
1994	128.0	0.11	0.787	0.09	227	0.94	6.1	1847	11351
1995	164.4	0.13	1.149	0.10	227	0.96	7.0	2372	16574
1996	55.8	0.08	0.568	0.07	211	0.89	10.2	806	8197
1997	42.5	0.13	0.423	0.06	225	0.93	10.0	613	6106
1998	151.8	0.17	0.841	0.14	227	0.92	5.5	2190	12132
1999	241.4	0.24	1.768	0.19	226	0.92	7.3	3483	25508
2000	294.1	0.15	3.060	0.13	229	0.88	10.4	4243	44156
2001	305.3	0.12	3.386	0.13	227	0.90	11.1	4405	48852
2002	295.0	0.10	3.721	0.11	206	0.89	12.6	4256	53694
2003	655.4	0.16	5.780	0.09	201	0.90	8.8	9456	83400
2004	494.5	0.12	5.332	0.07	248	0.89	10.8	7135	76938
2005	379.0	0.09	5.973	0.08	241	0.93	15.8	5469	86185
2006	380.1	0.09	5.926	0.07	230	0.93	15.6	5485	85505
2007	308.3	0.07	5.440	0.07	240	0.92	17.6	4449	78491
2008	435.5	0.10	6.229	0.09	207	0.96	14.3	6283	89884
2009	401.9	0.13	6.731	0.12	196	0.92	16.8	5798	97125

(c) Whole Stock									
year	Abundance index (mean N/tow)	CV	Biomass index (kg/tow)	CV	N tows	Proportion positive tows	mean weight (g/scallop)	Expanded abundance	Expanded biomass
1979	55.9	0.40	1.1	0.25	287	0.91	19.3	1508	29104
1980	54.7	0.20	0.6	0.10	322	0.86	11.5	1477	17033
1981	38.0	0.13	0.7	0.13	253	0.87	17.1	1026	17596
1982	78.7	0.44	0.6	0.20	314	0.86	7.7	2126	16381
1983	39.2	0.18	0.5	0.15	331	0.87	12.2	1058	12895
1984	29.1	0.08	0.4	0.07	342	0.88	13.2	786	10363
1985	61.6	0.10	0.6	0.09	371	0.89	9.0	1663	15015
1986	106.2	0.09	0.8	0.06	420	0.89	7.9	2867	22770
1987	113.9	0.11	0.9	0.09	416	0.88	7.6	3076	23363
1988	110.2	0.09	1.0	0.07	419	0.85	9.3	2975	27671
1989	131.0	0.12	1.0	0.07	498	0.87	7.3	3537	25993
1990	187.4	0.18	1.2	0.14	410	0.85	6.2	5060	31427
1991	153.9	0.36	0.9	0.16	422	0.90	5.9	4154	24677
1992	132.1	0.44	1.0	0.36	420	0.87	7.3	3566	26203
1993	96.6	0.11	0.5	0.08	396	0.90	5.2	2608	13553
1994	86.3	0.10	0.6	0.07	421	0.88	6.9	2330	15969
1995	138.7	0.12	0.9	0.09	420	0.91	6.6	3744	24733
1996	81.9	0.12	0.8	0.10	400	0.88	10.0	2212	22198
1997	59.3	0.10	0.8	0.11	431	0.89	14.0	1602	22345
1998	204.7	0.17	2.2	0.26	457	0.89	10.7	5527	58981
1999	201.7	0.16	2.1	0.12	424	0.93	10.5	5444	57265
2000	474.3	0.21	4.5	0.14	417	0.88	9.5	12805	121048
2001	336.4	0.09	4.5	0.10	452	0.92	13.3	9080	120786
2002	294.9	0.09	4.9	0.10	435	0.90	16.5	7961	131092
2003	455.5	0.12	5.8	0.08	426	0.91	12.7	12296	156244
2004	387.3	0.09	6.4	0.08	478	0.90	16.5	10456	172534
2005	300.4	0.07	6.0	0.07	468	0.93	20.0	8109	162195
2006	274.7	0.08	5.5	0.07	467	0.92	20.0	7415	148504
2007	250.1	0.06	4.9	0.06	472	0.93	19.8	6752	133446
2008	369.1	0.08	6.2	0.07	389	0.93	16.9	9964	168332
2009	392.0	0.11	6.5	0.10	375	0.93	16.5	10582	174873

Table B-5. SMAST large camera video survey mean densities for sea scallops 40+ mm SH.

Georges Bank							
Year	Stations	Area Surveyed km ²	Mean SH mm	SH Adj Area m ²	SH Adj Density sc/m ²	SE	95% CI
2003	929	27906	102.1	3.199	0.149	0.0117	0.0230
2004	935	28430	107.5	3.219	0.122	0.0145	0.0284
2005	902	27844	106.6	3.215	0.117	0.0127	0.0248
2006	939	28276	114.6	3.245	0.109	0.0116	0.0227
2007	912	27813	99.0	3.188	0.144	0.0160	0.0313
2008	910	27227	93.3	3.167	0.100	0.0087	0.0170
2009	899	29079	92.2	3.164	0.160	0.0175	0.0344
Mid Atlantic Bight							
Year	Stations	Area Surveyed km ²	Mean SH mm	SH Adj Area m ²	SH Adj Density sc/m ²	SE	95% CI
2003	804	24664	73.9	3.098	0.505	0.0835	0.1636
2004	840	25591	90.4	3.157	0.229	0.0224	0.0439
2005	864	26547	91.6	3.161	0.215	0.0254	0.0499
2006	897	26918	92.0	3.163	0.195	0.0193	0.0379
2007	941	28739	94.5	3.172	0.183	0.0163	0.0320
2008	931	28184	91.4	3.161	0.188	0.0187	0.0367
2009	928	28647	96.4	3.179	0.137	0.0085	0.0166

Table B-6. SMAST small camera video survey mean densities for sea scallops 40+ mm SH.

Georges Bank									
Year	Stations	Area Surveyed km ²	Mean SH mm	SH Adj Area m ²	SH Adj Density sc/m ²	Abundance	Biomass (mt)	SE	95% CI
2003	904	27906	88.3	0.738	0.1698	4737032049	66669	0.0174	0.03
2004	921	28430	101.4	0.761	0.1256	3569624137	74432	0.0142	0.03
2005	902	27844	111.2	0.778	0.1001	2787348077	77929	0.0128	0.03
2006	916	28276	109.1	0.775	0.1412	3993072108	108805	0.0143	0.03
2007	901	27813	80.0	0.724	0.1974	5489504503	77729	0.022	0.04
2008	882	27227	99.4	0.758	0.1526	4153894290	102842	0.0189	0.04
2009	942	29079	96.1	0.752	0.1556	4525694473	94067	0.0186	0.04
Mid-Atlantic Bight									
Year	Stations	Area Surveyed km ²	Mean SH mm	SH Adj Area m ²	SH Adj Density sc/m ²	Abundance	Biomass (mt)	SE	95% CI
2003	799	24664	58.6	0.688	0.7063	17419973913	81353	0.1427	0.28
2004	829	25591	84.7	0.732	0.2319	5935561328	69252	0.0263	0.05
2005	860	26547	87.2	0.737	0.2181	5790580803	81756	0.0267	0.05
2006	872	26918	93.4	0.747	0.2049	5516773301	88323	0.0216	0.04
2007	931	28739	90.4	0.742	0.2204	6333997245	88941	0.0213	0.04
2008	913	28184	90.7	0.743	0.2160	6086579306	103164	0.0207	0.04
2009	928	28647	98.1	0.755	0.1260	3608213579	71936	0.0091	0.02

Table B-7. Comparison of various estimates of New Bedford scallop dredge efficiencies.

Source		Area	Gear	Method	Estimates	cv
NEFSC(2010)		MA + GB sand	Lined survey	Paired camera/dredge comparisons	0.44	0.01
NEFSC(2010)		GB gravel/cobble	Lined survey	Paired camera/dredge comparisons	0.38	0.03
NEFSC(2007)		ALL	Lined survey	Comparison of video,dredge surveys	0.38	0.10
NEFSC(2007)		Georges Bank	Lined survey	Comparison of video,dredge surveys	0.37	0.18
NEFSC(2007)		Mid-Atlantic	Lined survey	Comparison of video,dredge surveys	0.4	0.07
NEFSC(2004)		Georges Bank	Lined survey	Comparison of video,dredge surveys	0.33	
NEFSC(2004)		Mid-Atlantic	Lined survey	Comparison of video,dredge surveys	0.46	
NEFSC(2001)		Georges Bank	Commercial	Depletion	0.38-0.81	0.19-0.98
NEFSC(2001)		Mid-Atlantic	Commercial	Depletion	0.59-0.75	0.1-0.72
Gedamke et al. 2005		Georges Bank CAII	Commercial	Index removal	0.41-0.54	
Gedamke et al. 2004		Georges Bank CAII	Commercial	Depletion	0.35-0.525	
Caddy 1971		Canada	Commercial	Dredge mounted camera	0.17	

Table B-8. CASA model estimates and standard errors for fully recruited sea scallop fishing mortality, July 1 abundance 40+mm SH, and July 1 biomass 40+ mm SH.

Year	Georges Bank						MidAtlantic						Total			
	Full_F	SE	Abundance (millions)	SE	Biomass (mt meats)	SE	Full_F	SE	Abundance (millions)	SE	Biomass (mt meats)	SE	Full_F	SE	Abundance (millions)	SE
1975	0.11	0.02	1148	56	20780	1038	0.59	0.09	591	34	6503	386	0.21	0.09	1739	66
1976	0.20	0.04	1419	60	24705	1112	1.00	0.16	787	33	7931	491	0.38	0.16	2205	69
1977	0.33	0.05	1115	52	24522	1056	0.53	0.07	772	30	9933	487	0.39	0.23	1886	60
1978	0.39	0.06	1260	51	21973	920	1.05	0.15	567	21	9690	443	0.57	0.3	1827	55
1979	0.53	0.08	878	40	17822	762	1.07	0.20	364	15	7678	364	0.63	0.44	1242	43
1980	0.47	0.08	1060	43	14970	628	0.35	0.05	343	16	6365	347	0.44	0.34	1403	45
1981	0.62	0.09	747	34	12579	533	0.13	0.03	403	18	6754	364	0.48	0.44	1151	38
1982	0.83	0.13	808	35	9505	425	0.25	0.04	442	21	7401	386	0.58	0.46	1250	41
1983	0.71	0.11	573	30	7680	393	0.53	0.07	497	25	6987	417	0.64	0.41	1070	39
1984	0.42	0.08	565	34	7364	442	0.80	0.12	536	31	6062	459	0.58	0.25	1101	46
1985	0.51	0.10	610	42	7840	528	0.75	0.13	744	40	6346	506	0.61	0.3	1354	58
1986	0.88	0.21	984	60	8481	542	0.57	0.09	977	47	8704	556	0.72	0.41	1962	76
1987	0.76	0.16	1096	66	9988	596	1.20	0.17	1171	49	9340	585	0.96	0.43	2267	82
1988	0.83	0.18	1251	77	11321	686	0.90	0.12		49	10365	558	0.86	0.44	2399	91
1989	0.64	0.13	1415	81	13453	736	1.14	0.15	1147	42	9852	534	0.85	0.39	2562	91
1990	1.11	0.21	1369	74	12791	678	0.96	0.11	1018	36	9747	418	1.05	0.63	2387	82
1991	1.53	0.28	1486	68	10725	475	1.07	0.10	705	26	8026	327	1.32	0.8	2191	73
1992	1.72	0.25	783	36	7056	303	1.10	0.12	468	24	5426	298	1.47	1.01	1251	43
1993	1.19	0.21	553	32	4868	279	0.86	0.14	894	38	5634	319	1.05	0.66	1448	49
1994	0.31	0.07	531	36	5719	394	1.37	0.18	1137	40	8027	360	0.87	0.18	1668	53
1995	0.16	0.03	1003	48	9878	553	1.08	0.11	965	34	8785	361	0.62	0.1	1968	59
1996	0.33	0.07	1201	53	15406	727	0.74	0.08	647	31	8167	411	0.53	0.18	1849	62
1997	0.28	0.07	1305	62	20141	885	0.47	0.06	690	44	7850	528	0.35	0.18	1995	76
1998	0.22	0.06	1924	82	27276	1022	0.53	0.10	1695	82	11858	716	0.31	0.16	3619	116
1999	0.54	0.13	2008	87	33163	1211	0.49	0.09	2872	106	23689	1043	0.51	0.23	4881	137
2000	0.48	0.12	3129	99	41066	1410	0.48	0.08	3523	112	37324	1326	0.48	0.14	6652	149
2001	0.26	0.05	3294	95	53064	1704	0.54	0.07	3766	107	45795	1433	0.43	0.11	7061	143
2002	0.23	0.05	2819	88	62370	1994	0.61	0.08	3427	100	48798	1449	0.41	0.12	6246	133
2003	0.17	0.04	2945	96	69416	2294	0.68	0.08	4174	115	48756	1397	0.42	0.1	7119	150
2004	0.10	0.02	2708	96	74629	2603	0.87	0.09	3703	112	50029	1468	0.38	0.07	6411	147
2005	0.18	0.03	2571	103	73828	2862	0.84	0.14	3609	131	49027	1728	0.37	0.13	6180	167
2006	0.38	0.06	2128	108	62768	3090	0.35	0.06	3805	166	56405	2377	0.37	0.23	5933	198
2007	0.25	0.05	2364	151	53650	3472	0.55	0.09	3853	209	61784	3260	0.40	0.14	6217	258
2008	0.19	0.04	2769	204	55508	4234	0.54	0.10	4509	313	63983	4518	0.37	0.11	7278	374
2009	0.18	0.05	3453	294	62470	5341	0.60	0.13	3993	352	67233	6460	0.38	0.11	7446	458

Table B-9. Biological reference points from the previous and current sea scallop assessments.

Reference point	SARC-45, whole Stock	Updated		
		GBK	MAB	Whole stock
F_{MSY}	--	0.21	0.47	0.38
B_{MSY} (July 1, 40+ mm SH)	--	41,468	86,330	125,358
$B_{Threshold=1/2 B_{MSY}}$	--	20,734	43,165	62,679
MSY	--	6,410	19,040	24,975
F_{MAX} (SYM)		0.295	0.835	0.48
F_{MAX} (CASA)	0.29	0.23	0.375	0.30
B_{MSY} proxy (CASA) (Jan. 1, 40+ mm)	108,628	--	--	127,000
$B_{Threshold=1/2 B_{MSY}}$ proxy	54,314	--	--	63,500

Figures

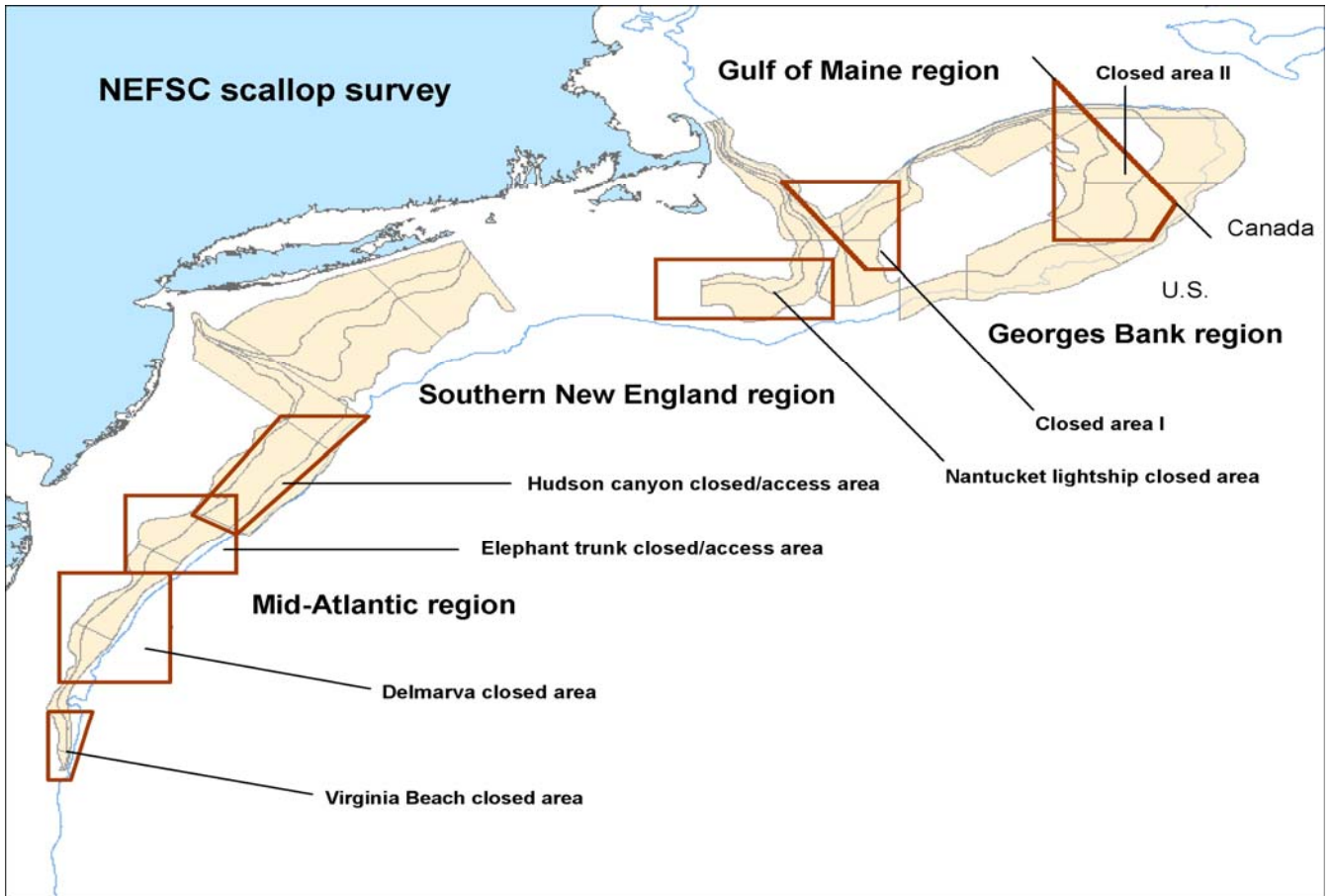


Figure B-1. Map of NEFSC sea scallop survey areas (yellow, with stratum boundaries shown) and the closed or rotational access areas (bounded by dark red lines).

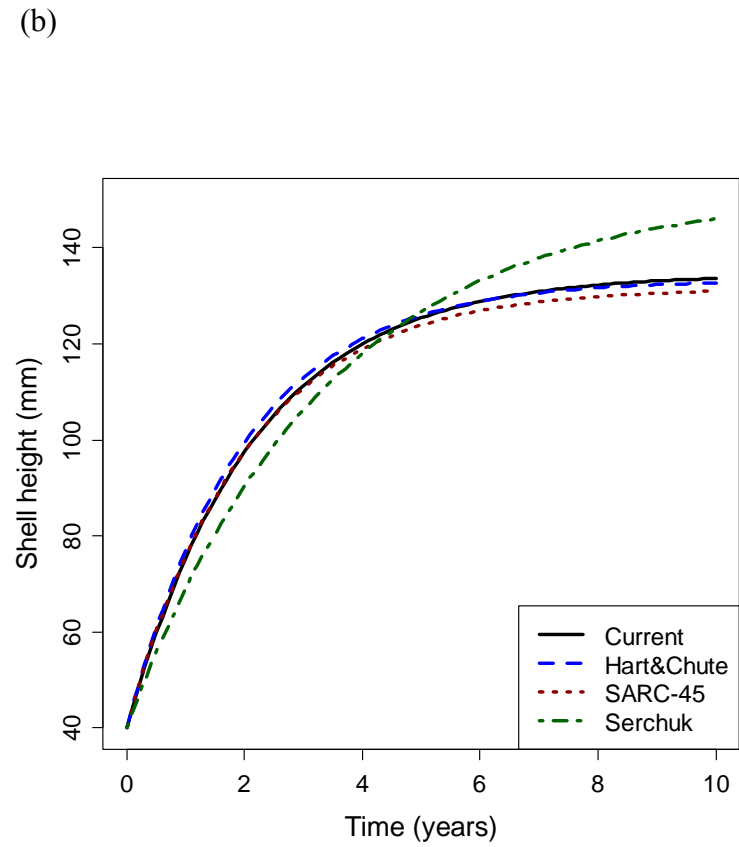
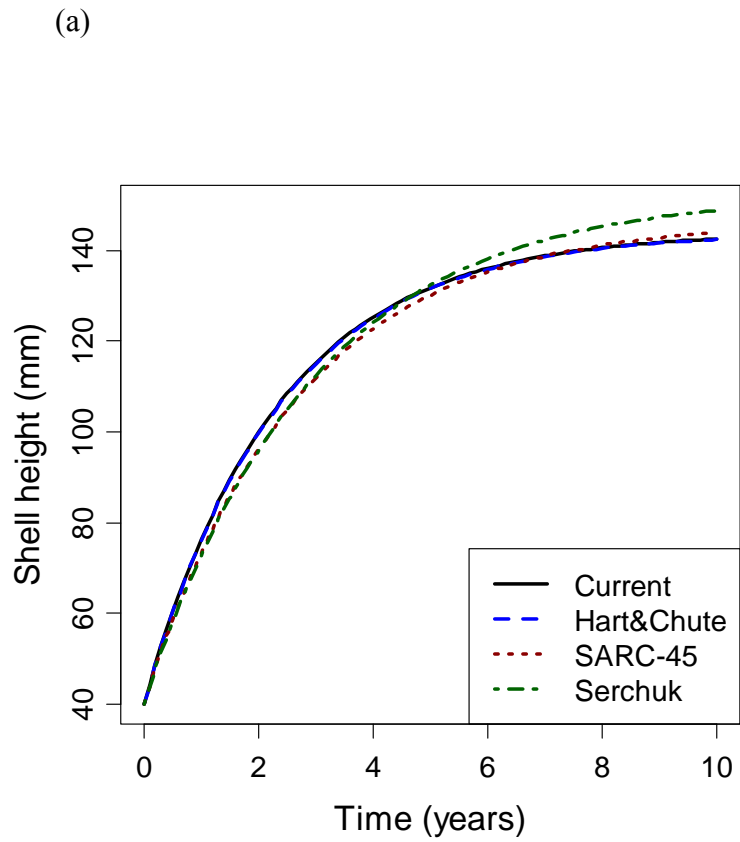
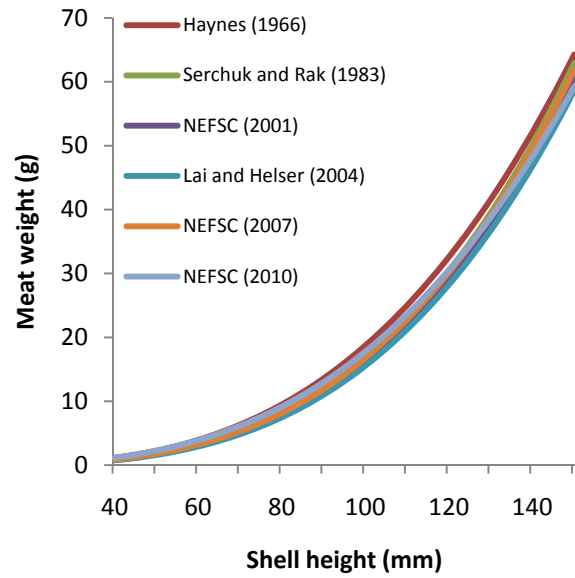


Figure B-2. Comparison of growth curves for a scallop with starting shell height of 40 mm in (a) Georges Bank and (b) Mid-Atlantic.

(a)



(b)

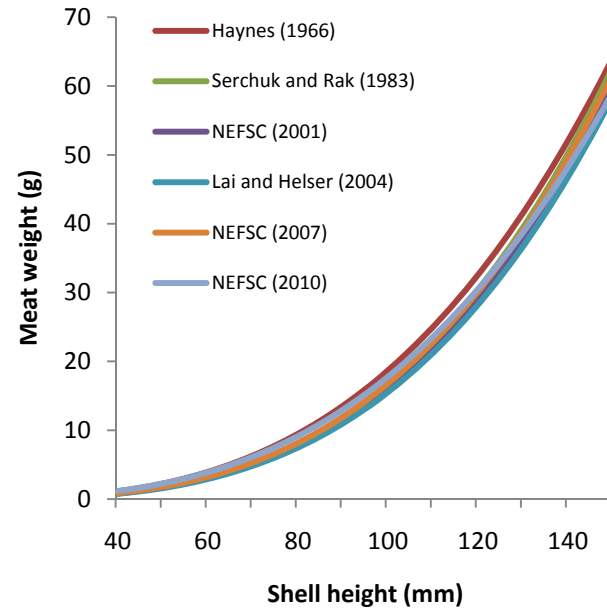
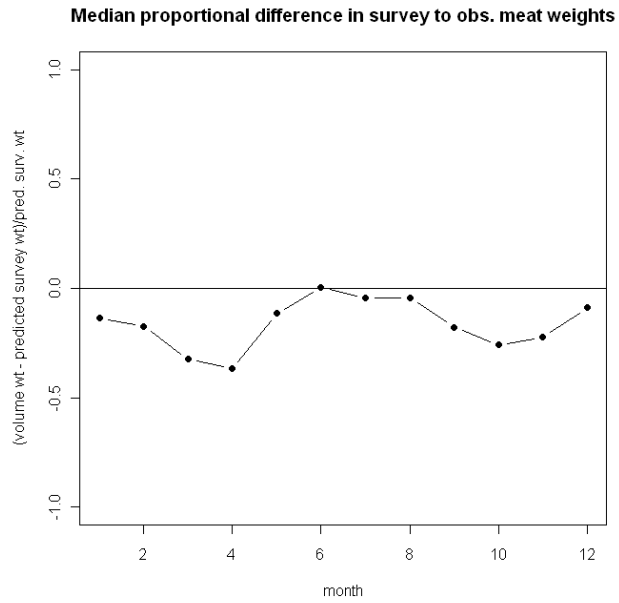


Figure B-3. Comparison of new shell height/meat weight relationships (calculated ignoring depth effects) for (a) Georges Bank and (b) Mid-Atlantic with other shell height/meat weight curves.

(a)



(b)

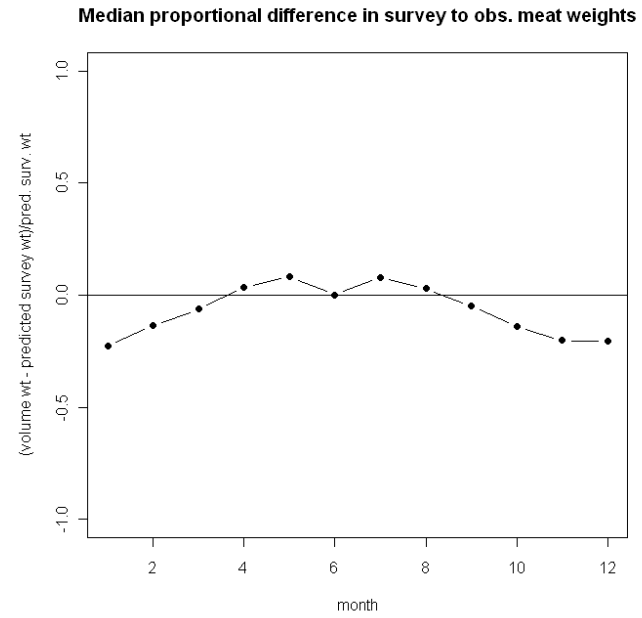


Figure B-4. Seasonal anomalies in shell height/meat weight relationships relative to that estimated from R/V data for (a) Georges Bank and (b) Mid-Atlantic Bight.

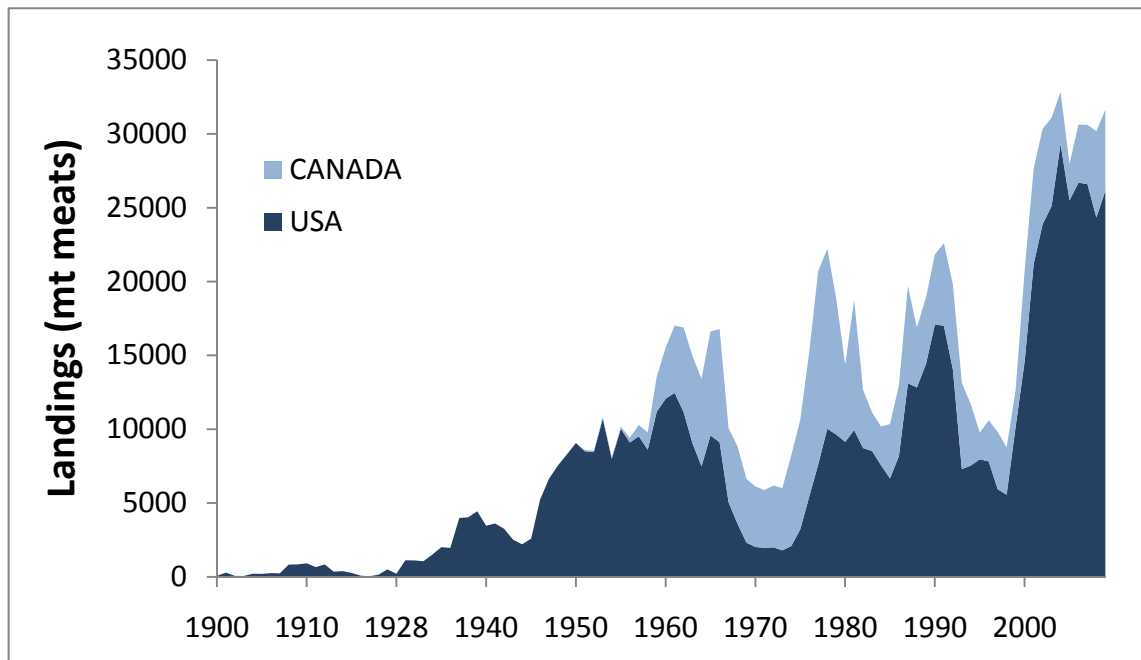


Figure B-5. Long-term sea scallop landings in NAFO areas 5 and 6 (U.S. and Canadian Georges Bank).

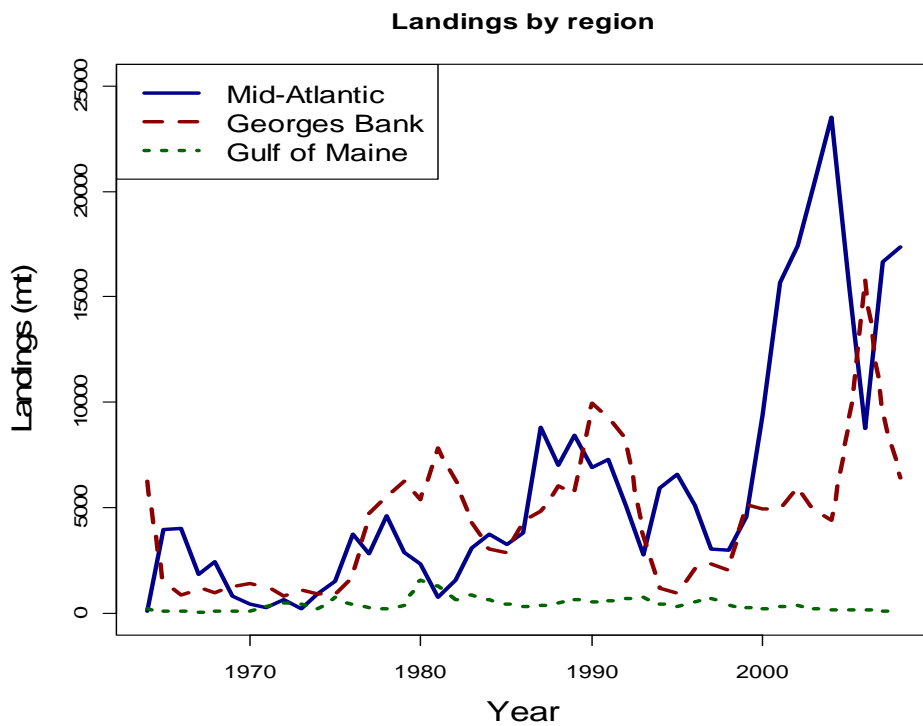
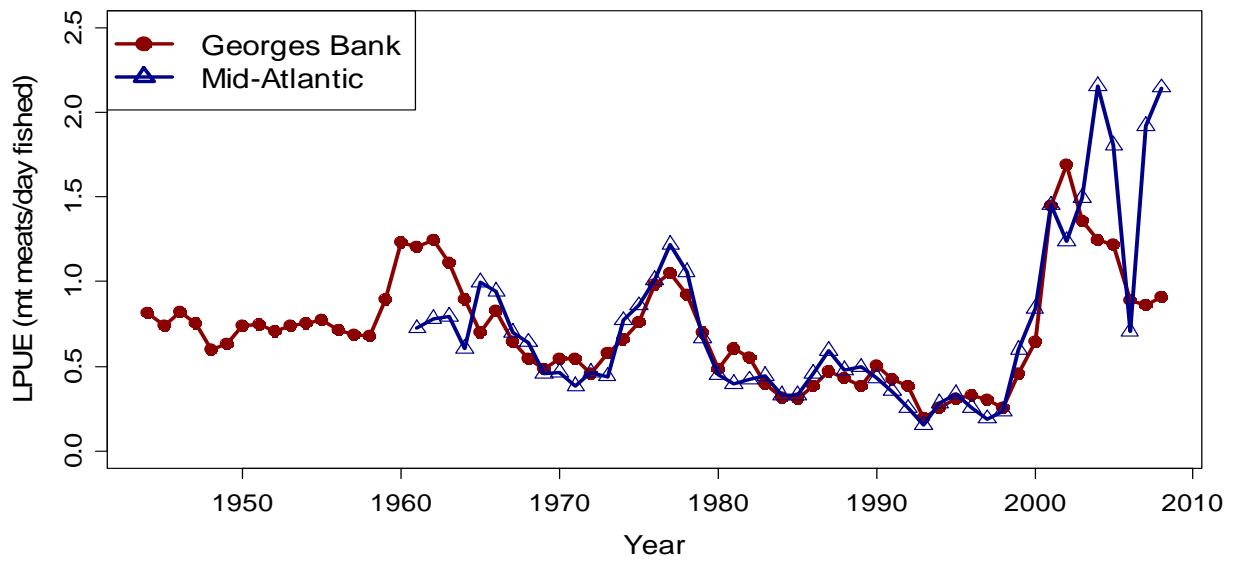


Figure B-6. U.S. sea scallop landings (mt meats) by region.

(a)



(b)

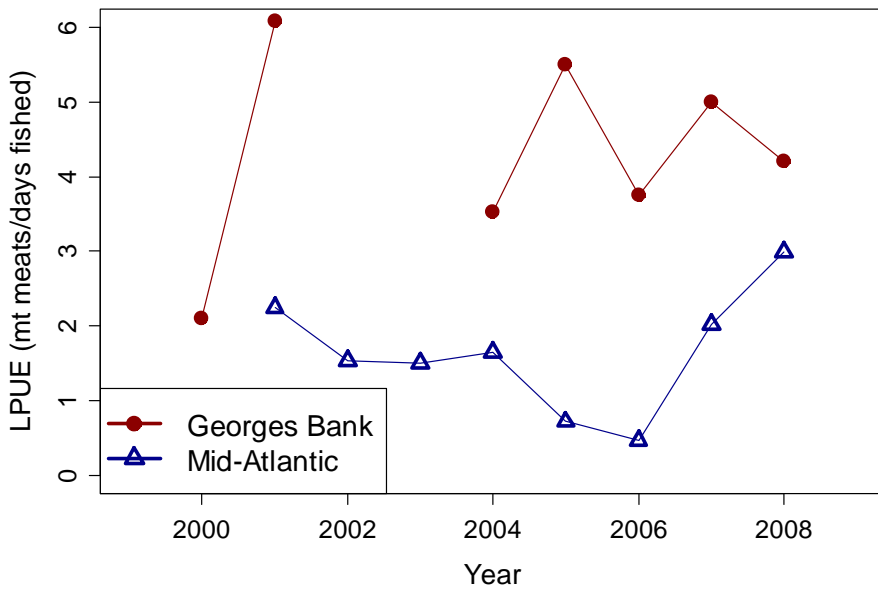
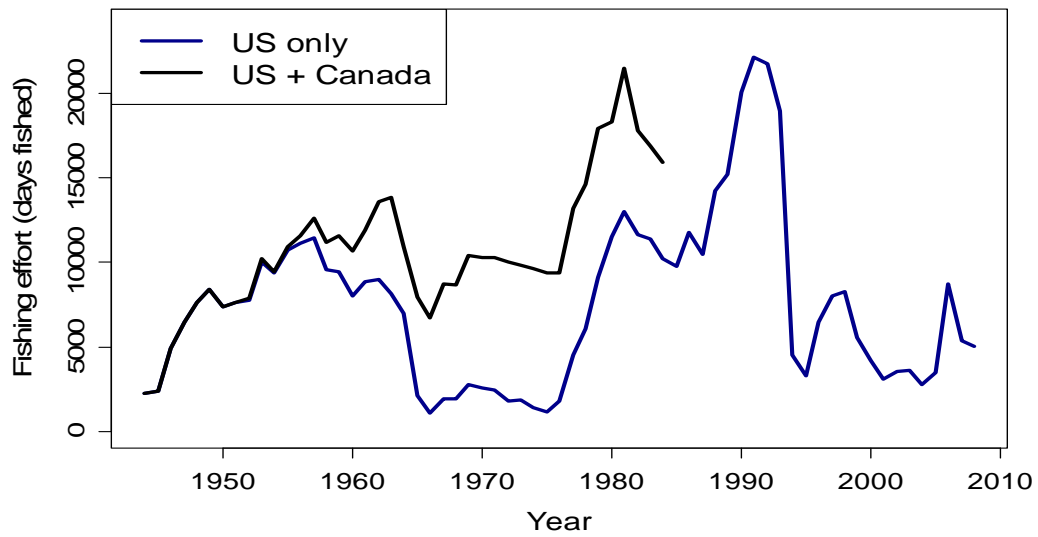


Figure B-7. Landings per day fished in (a) “open” areas, and (b) special access areas.

(a)



(b)

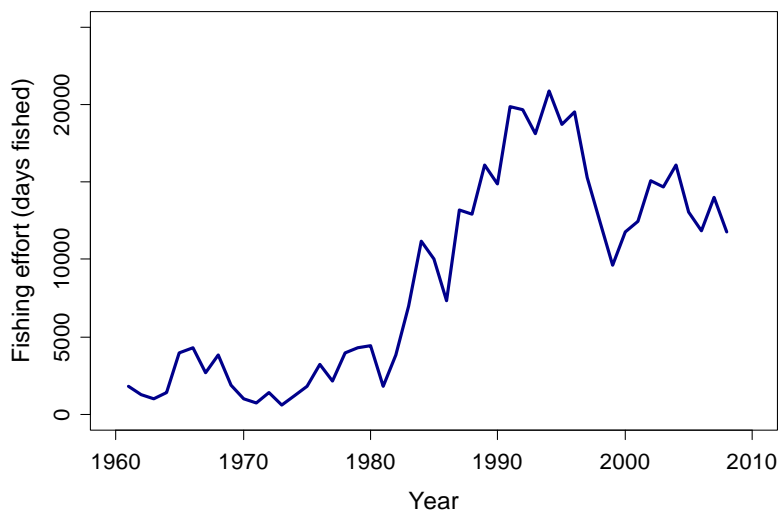


Figure B-8. Days fished in the sea scallop fishery in (a) Georges Bank and (b) Mid-Atlantic

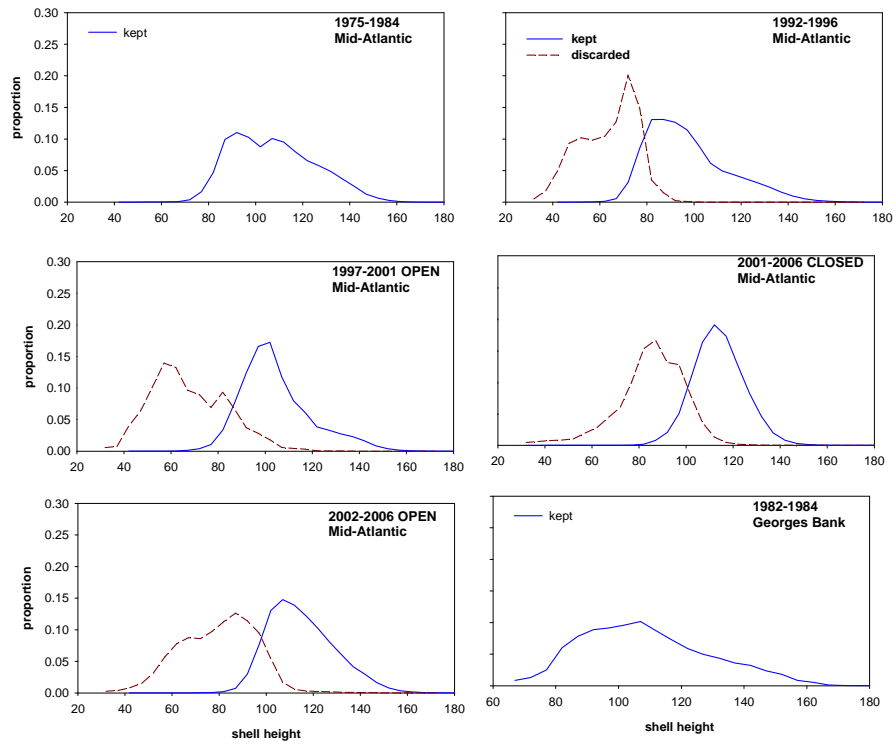


Figure B-9. Shell heights of commercial kept (solid line) and discarded (dashed line) sea scallops, from port sampling (1975-1984) and sea sampling (1992-2009).

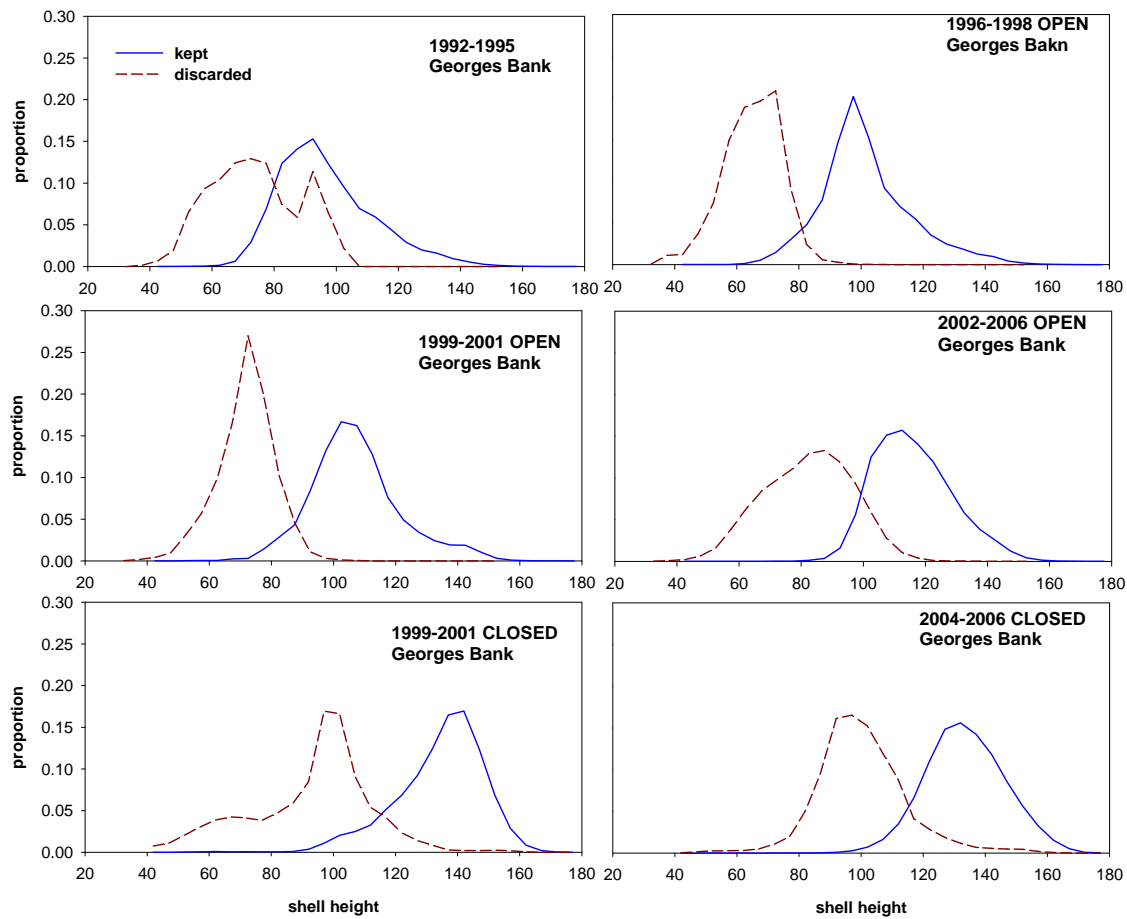


Figure B-9 continued

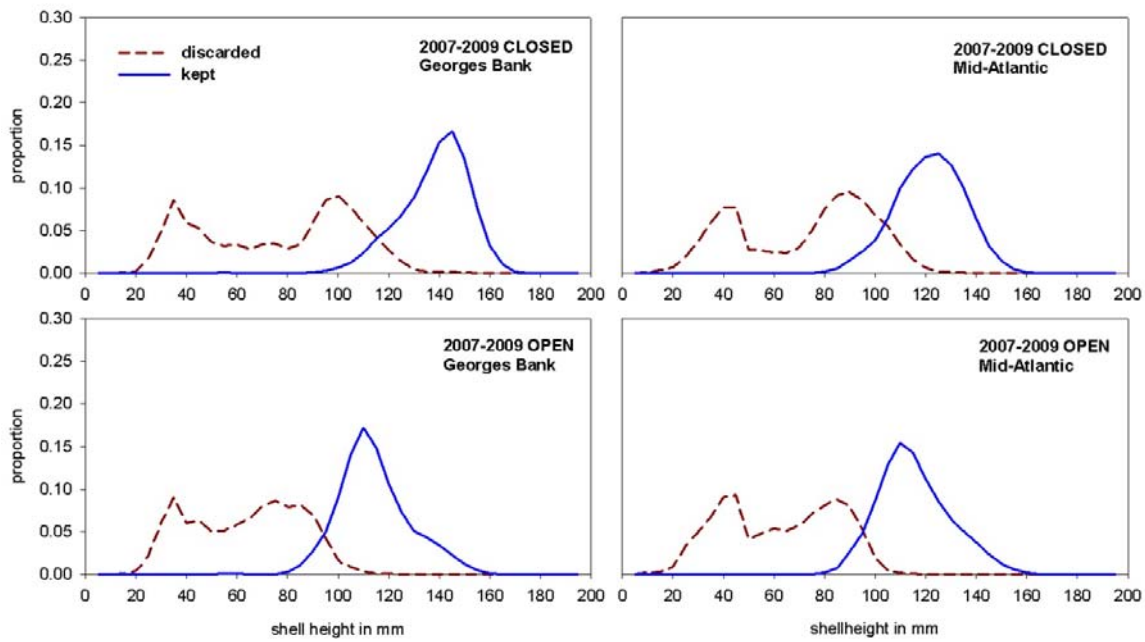


Figure B-9 continued

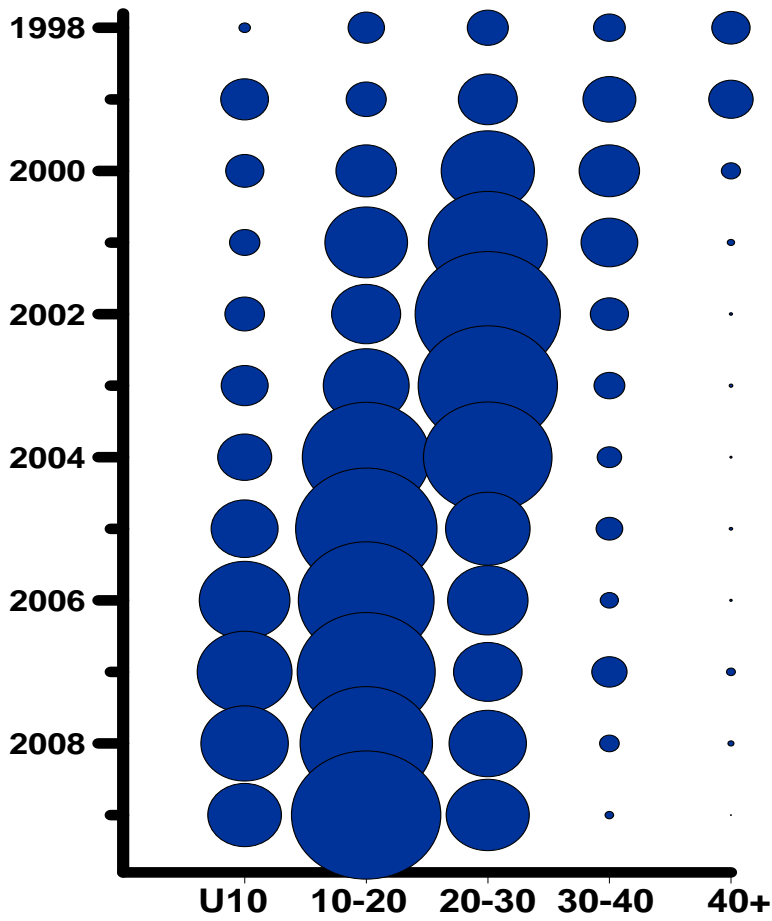


Figure B-10. Commercial landings by meat count category (number of meats per pound, U10 = less than 10 meats per pound).

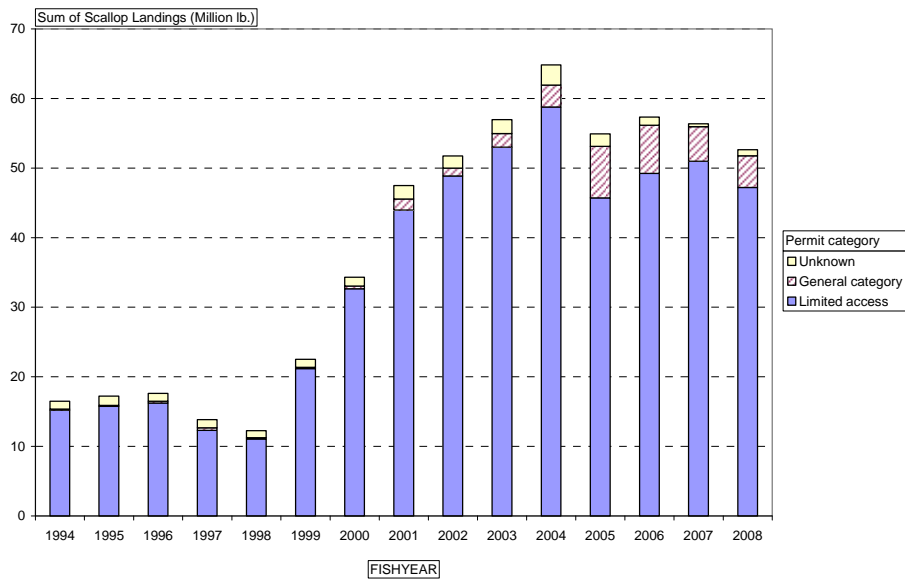


Figure B-11. Landings by permit category and fishing year (fishing year starts March 1).

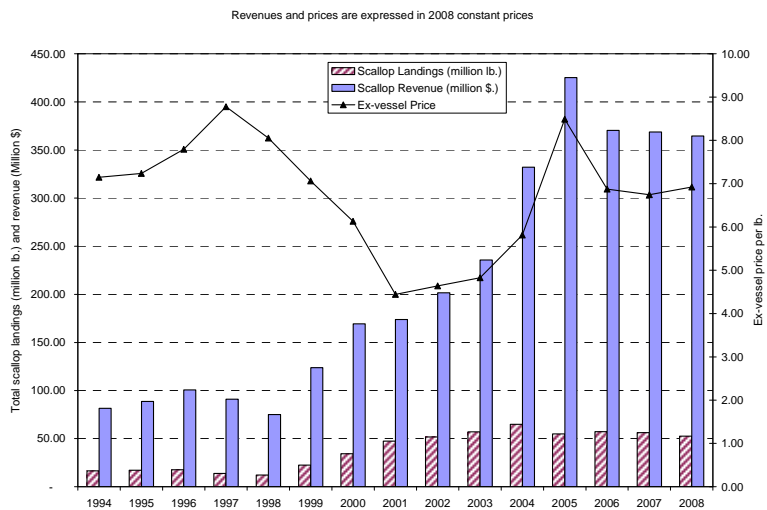


Figure B-12. Trends in scallop landings, revenue and ex-vessel prices by fishing year.

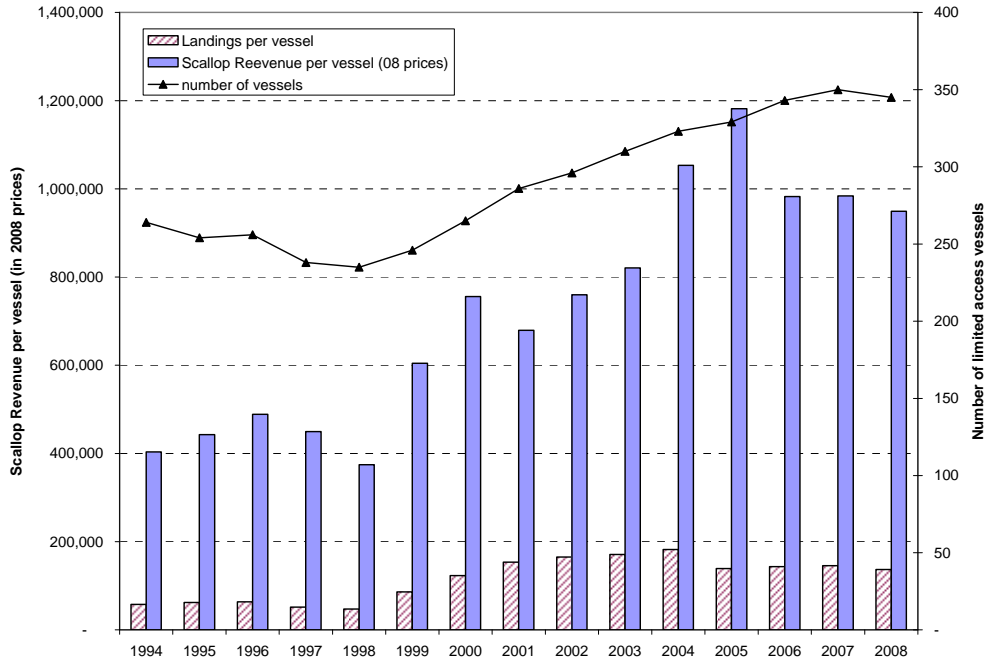


Figure B-13. Trends in average scallop landings and revenue per full time vessel and number of active limited access vessels.

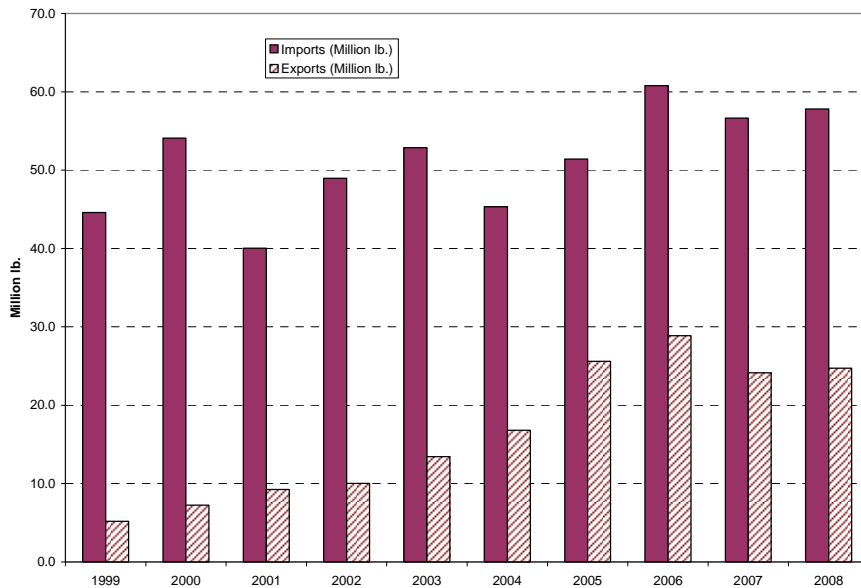
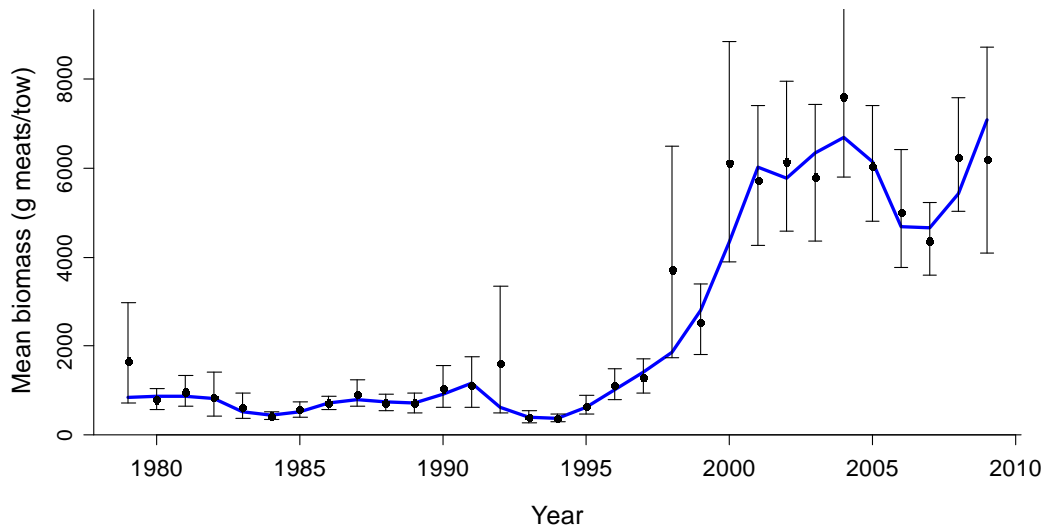


Figure B-14. Scallop exports and imports (includes other scallop species).

(a)



(b)

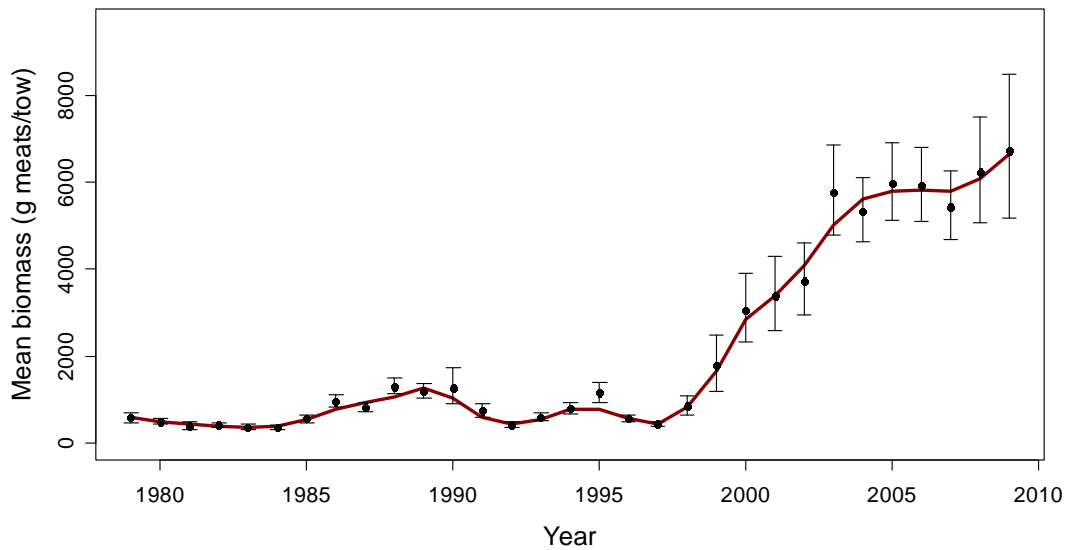
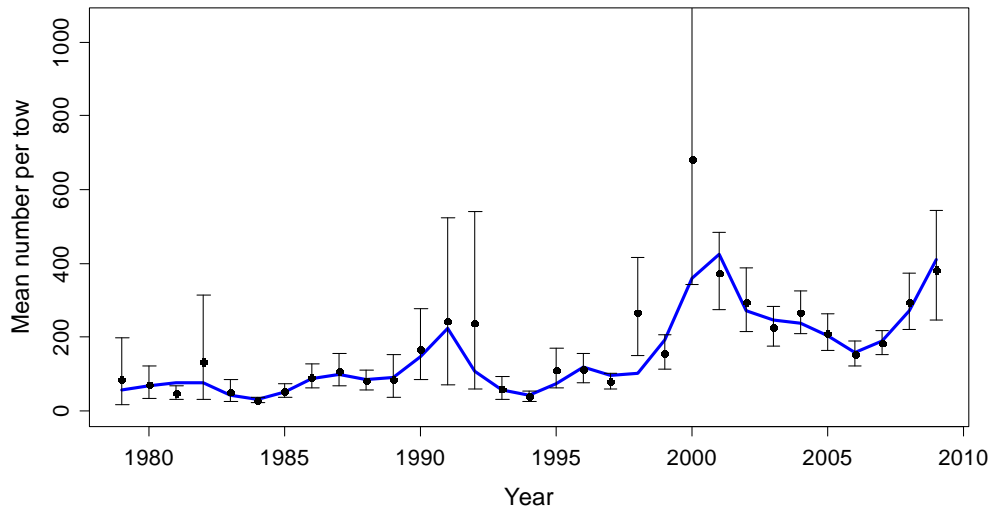


Figure B-15. NEFSC lined dredge sea scallop survey biomass indices in (a) Georges Bank and (b) Mid-Atlantic. 95% confidence intervals and inverse variance weighted lowest smoothers (lines, span = 0.25) are also shown.

(a)



(b)

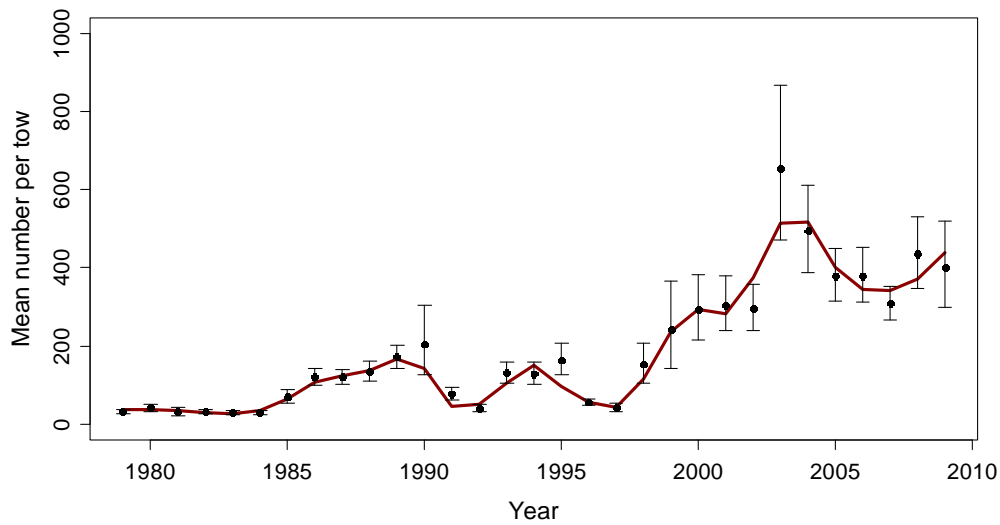
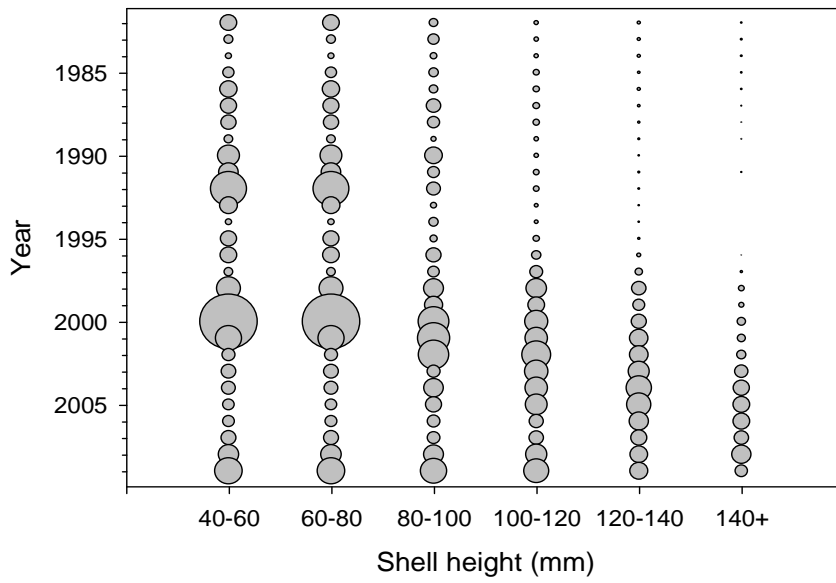


Figure B-16. NEFSC lined dredge sea scallop survey abundance indices in (a) Georges Bank and (b) Mid-Atlantic. 95% confidence intervals and inverse variance weighted lowest smoothers (lines, span = 0.25) are also shown.

(a)



(b)

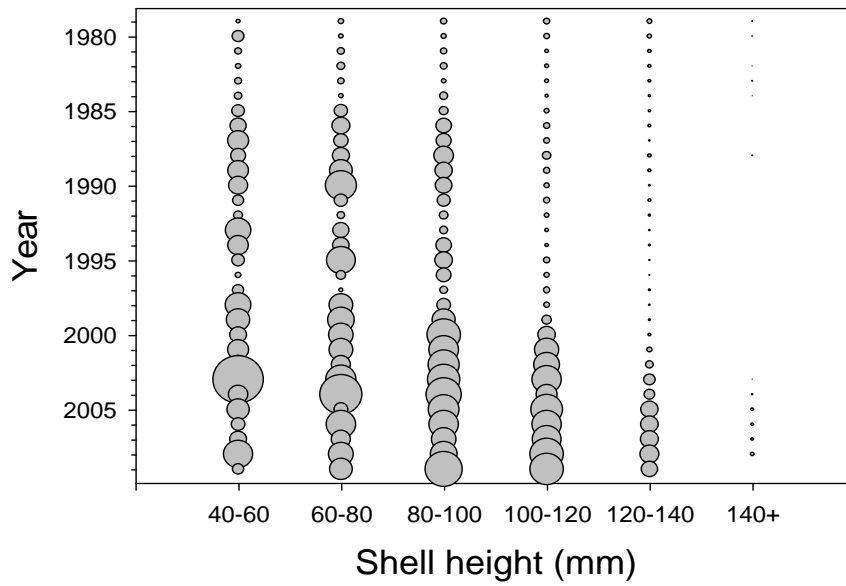


Figure B-17. Numbers of scallops by shell height group for (a) Georges Bank and (b) Mid-Atlantic, based on the NEFSC lined dredge survey.

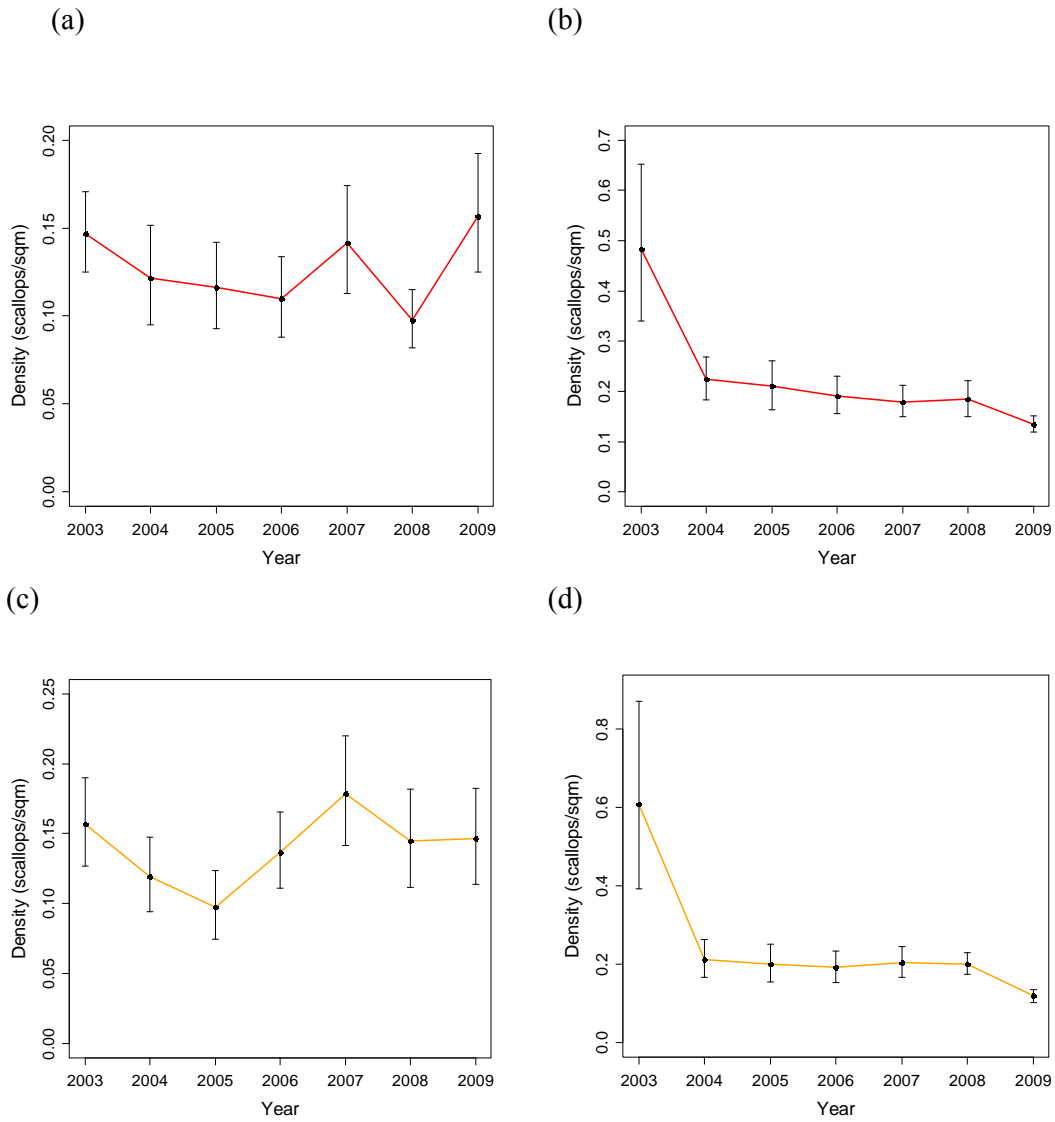
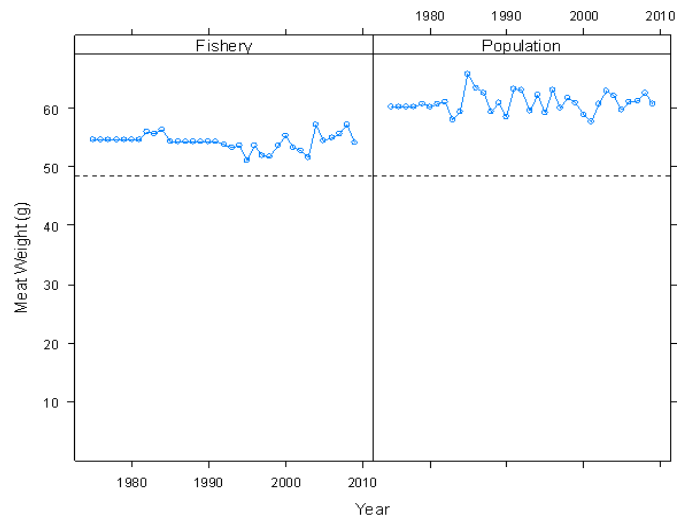


Figure B-18. Sea scallop density estimates from (a-b) the large video camera, and (c-d) the small video camera, in (a) and (c) Georges Bank and (b) and (d) the Mid-Atlantic. 95% confidence intervals are also shown.

(a)



(b)

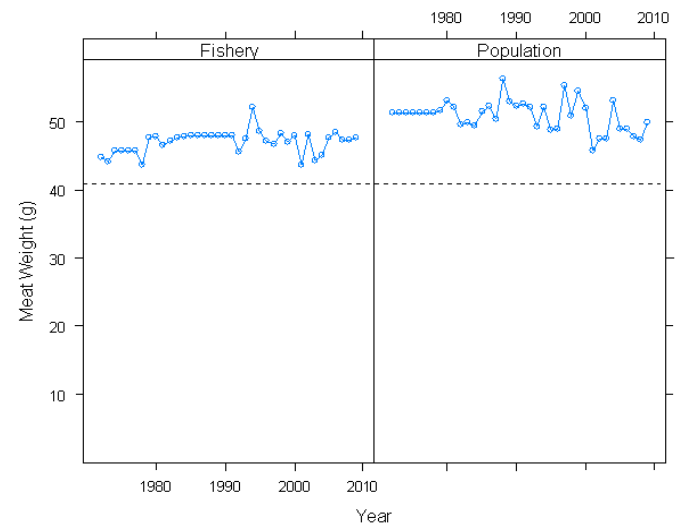


Figure B-19. Plus group meat weights for the population and the fishery in (a) Georges Bank and (b) Mid-Atlantic. Plus groups represent >140 mm SH in Geroges Bank and >130mm SH in the Mid-Atlantic.

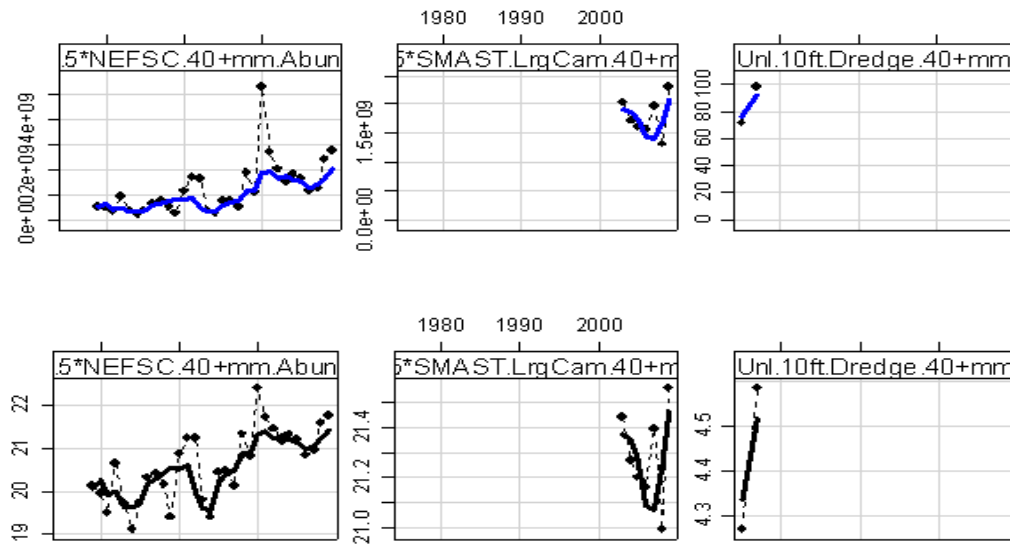


Figure B-20. Comparison between survey trend data (solid circles) and corresponding model estimates (lines) for the NEFSC lined dredge survey, the SMAST large camera survey and the NEFSC unlined dredge survey. Results are shown on a linear scale (top) and a log scale (bottom).

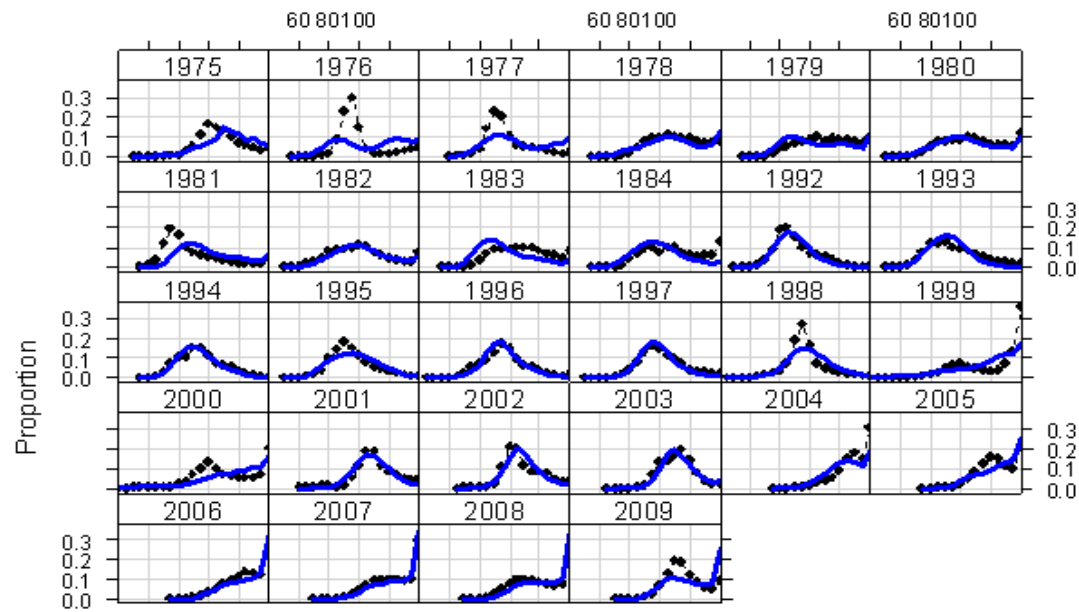


Figure B-21. Comparison of fishery shell height proportions (solid circles) and model estimated fishery shell height proportions (lines) for Georges Bank.

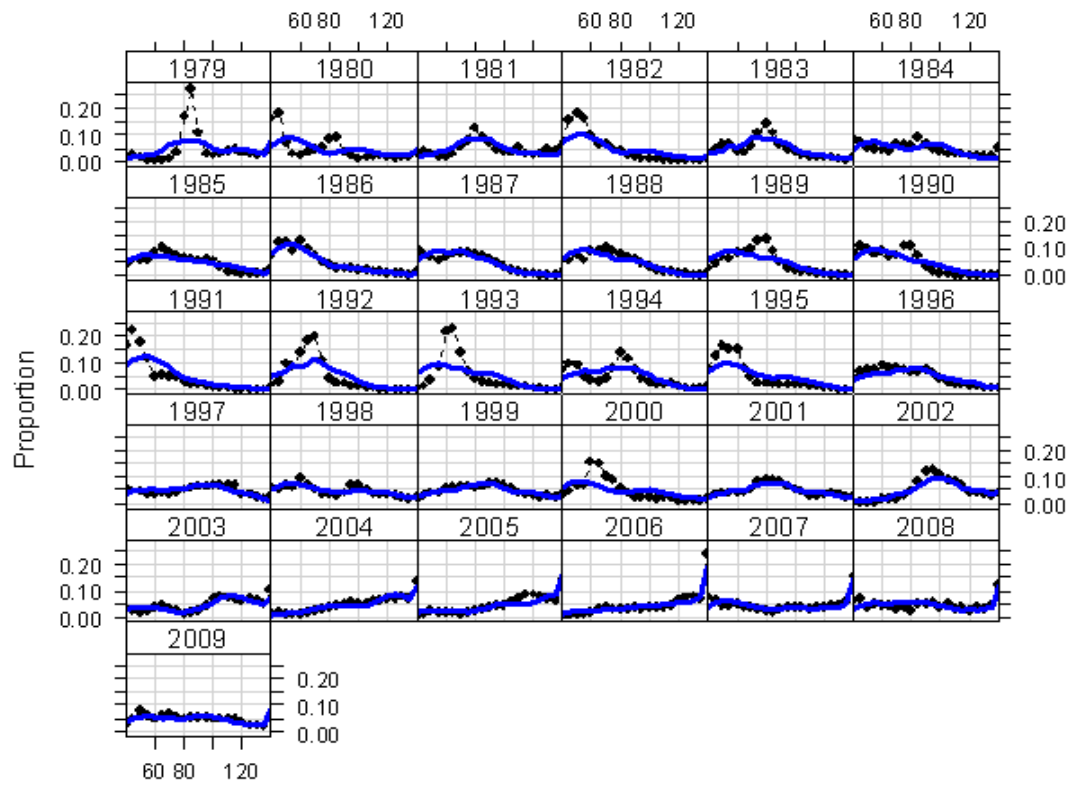


Figure B-22. NEFSC lined dredge survey shell height proportions (solid circles) and model estimated shell height proportions (line) for Georges Bank.

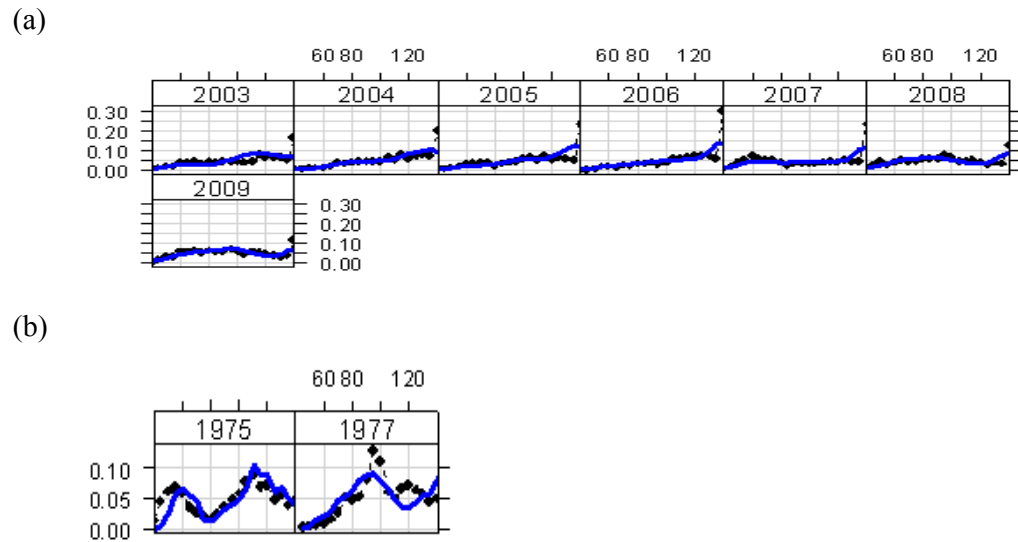


Figure B-23. Shell height proportions for (a) the S Mast large camera survey and (b) the NEFSC unlined dredge survey together with model predicted proportions (lines).

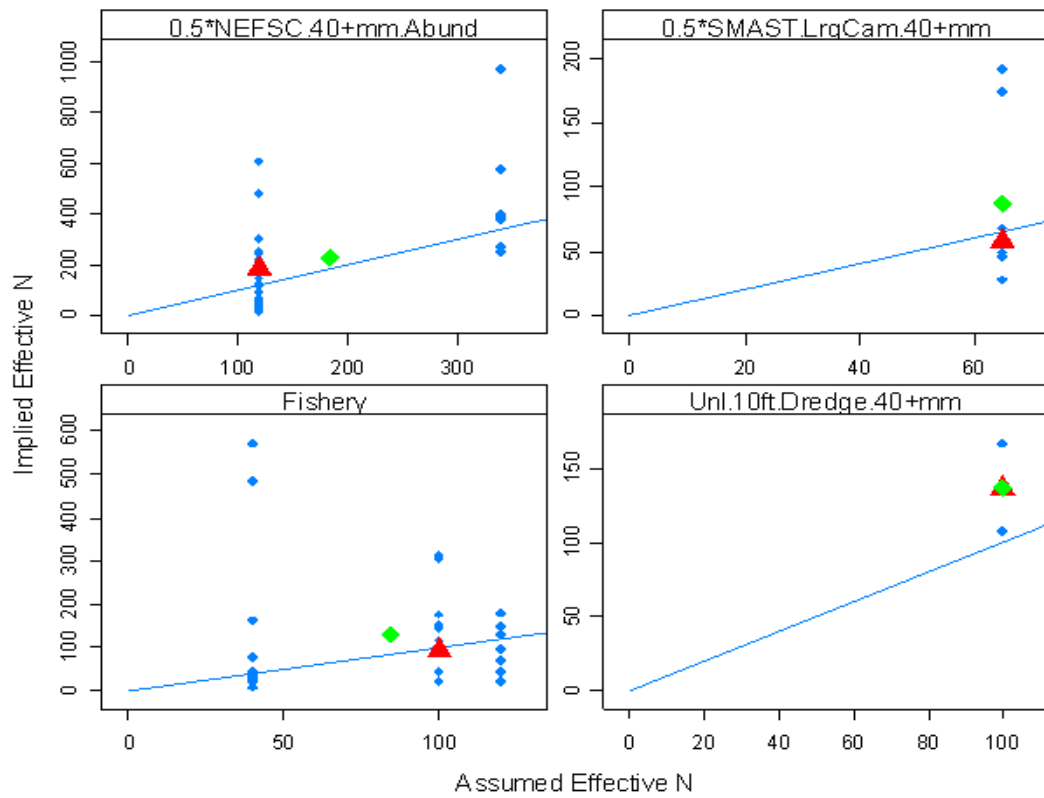


Figure B-24. Assumed and model implied effective sample sizes for the three surveys (NEFSC unlined dredge, SMAST large camera, NEFSC unlined dredge) and the fishery shell height compositions for Georges Bank.

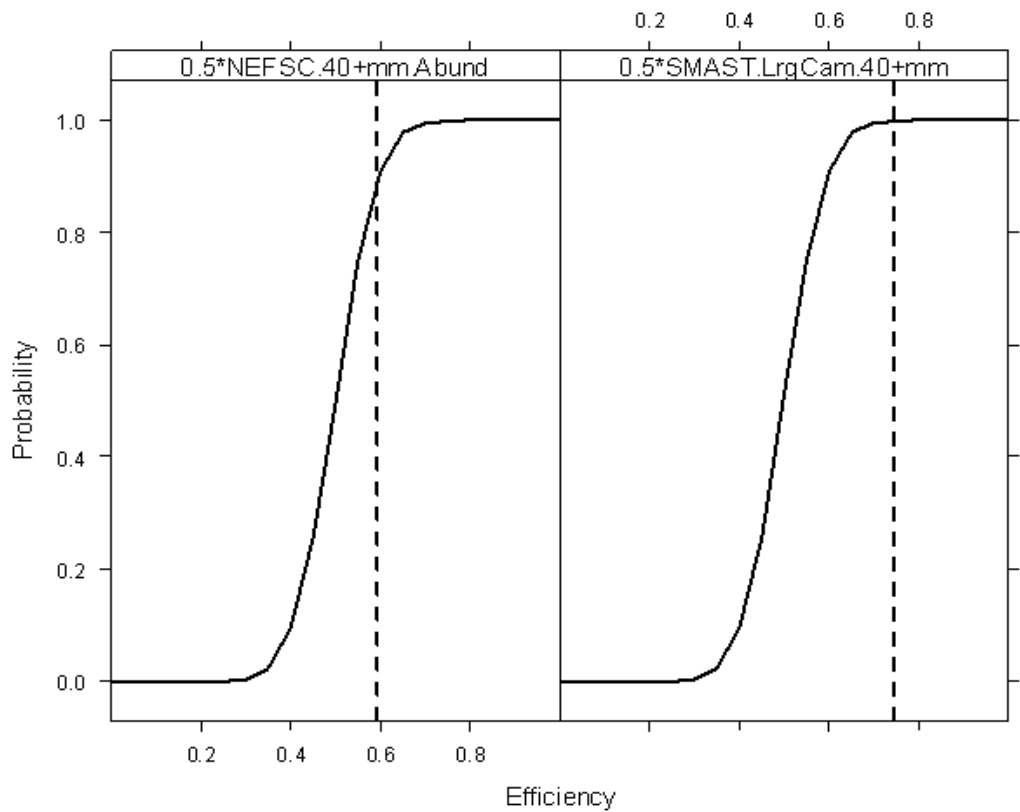
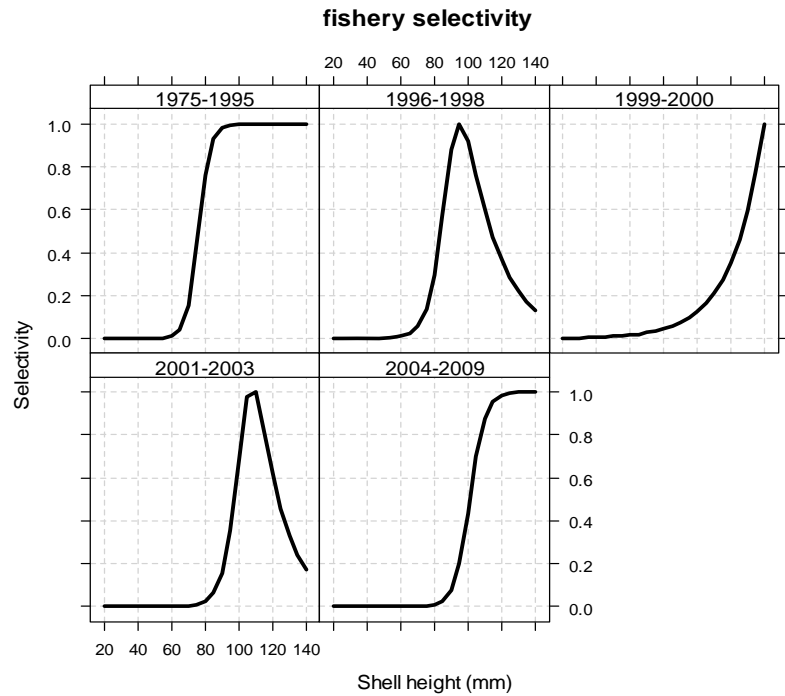


Figure B-25. Prior cumulative distributions for efficiency of the lined dredge survey (left) and large camera video survey (right) for Georges Bank. The dashed lines are the mean posterior estimate for survey efficiency.

(a)



(b)

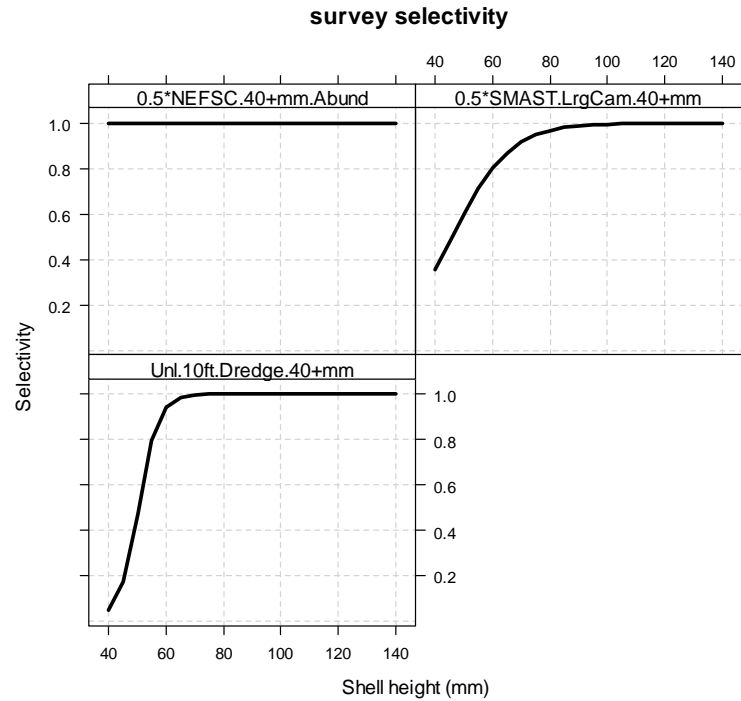


Figure B-26. (a) Estimated fishery selectivities and (b) assumed survey selectivities (lined dredge top right, large camera top left, unlined dredge bottom left) for Georges Bank.

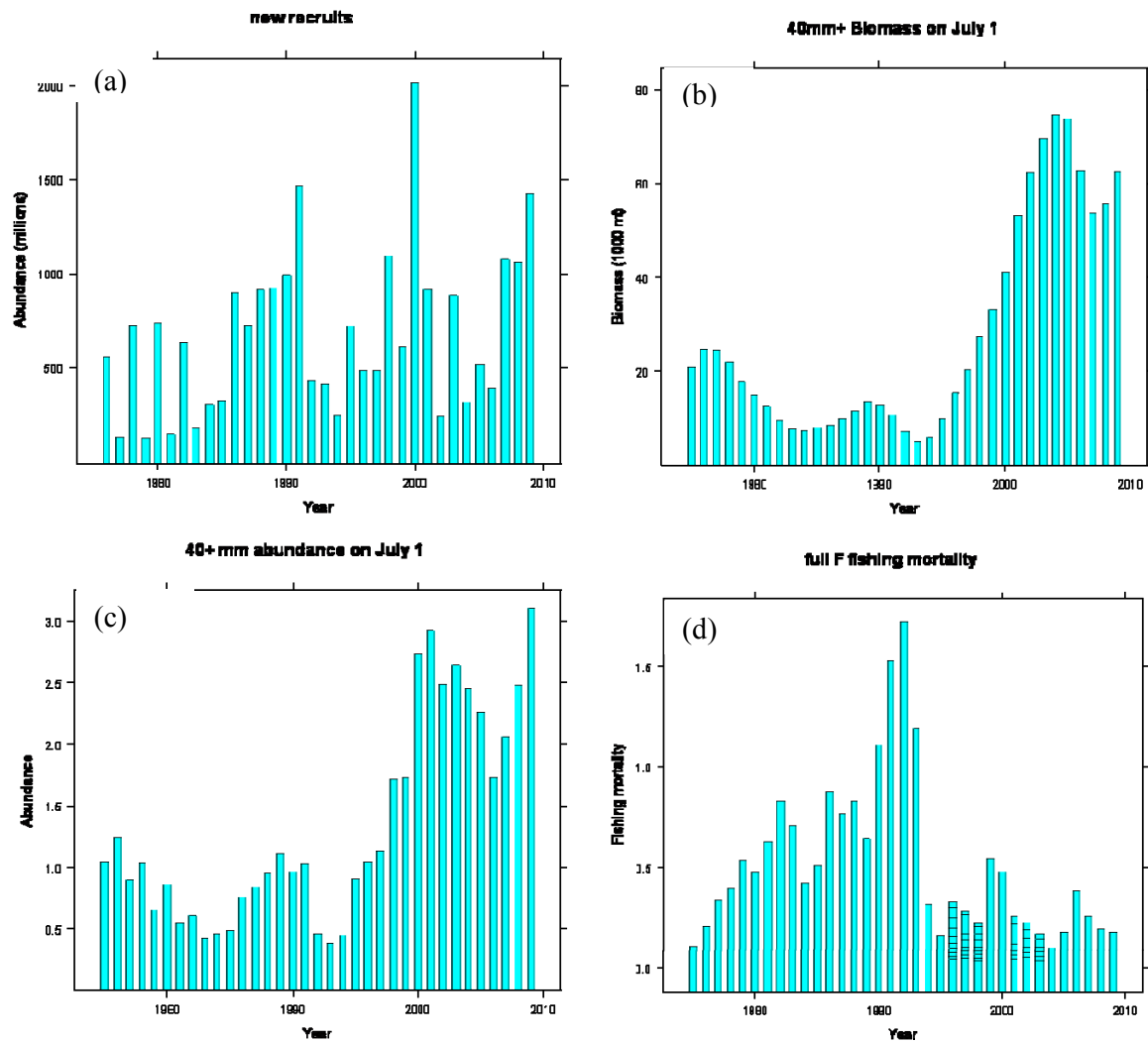


Figure B-27. CASA model estimated (a) recruitment, (b) July 1 biomass, (c) July 1 abundance and (d) fully recruited fishing mortality for Georges Bank.

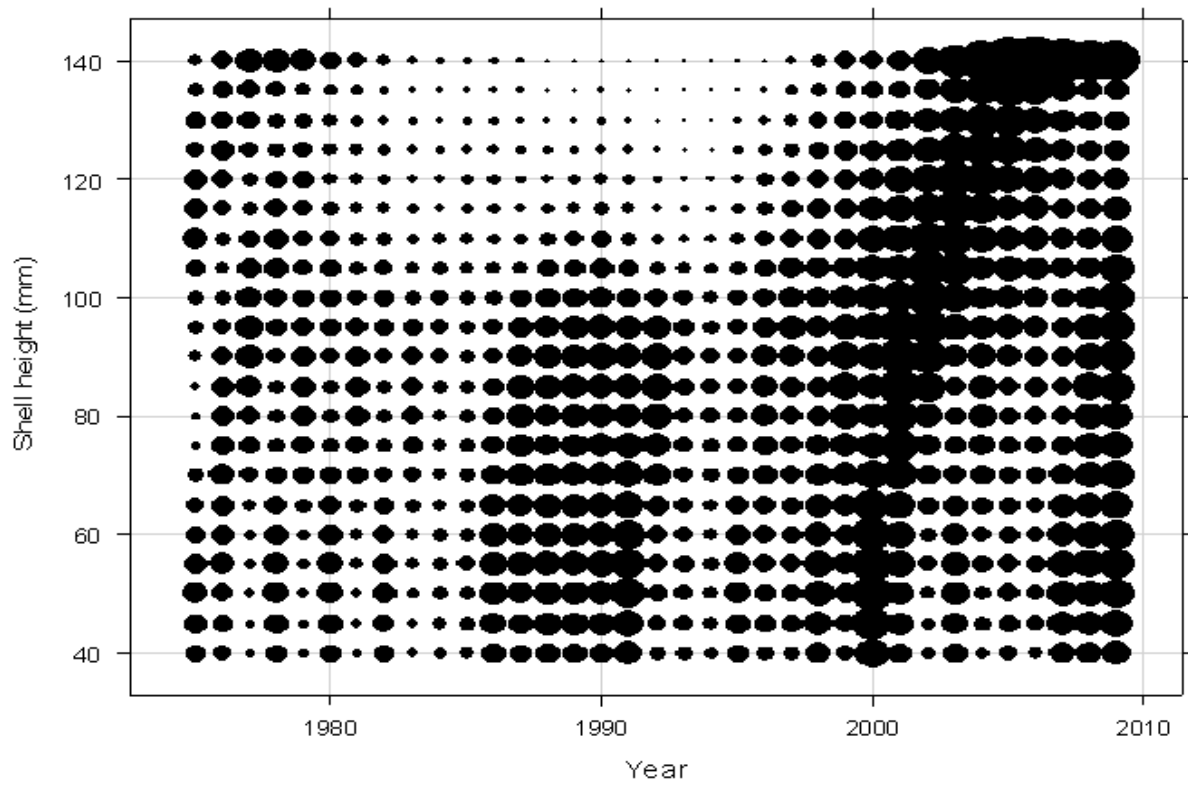


Figure B-28. Model estimated abundances at shell height for Georges Bank. Disk areas are proportional to abundance.

Fishing Mortality at Shell Height

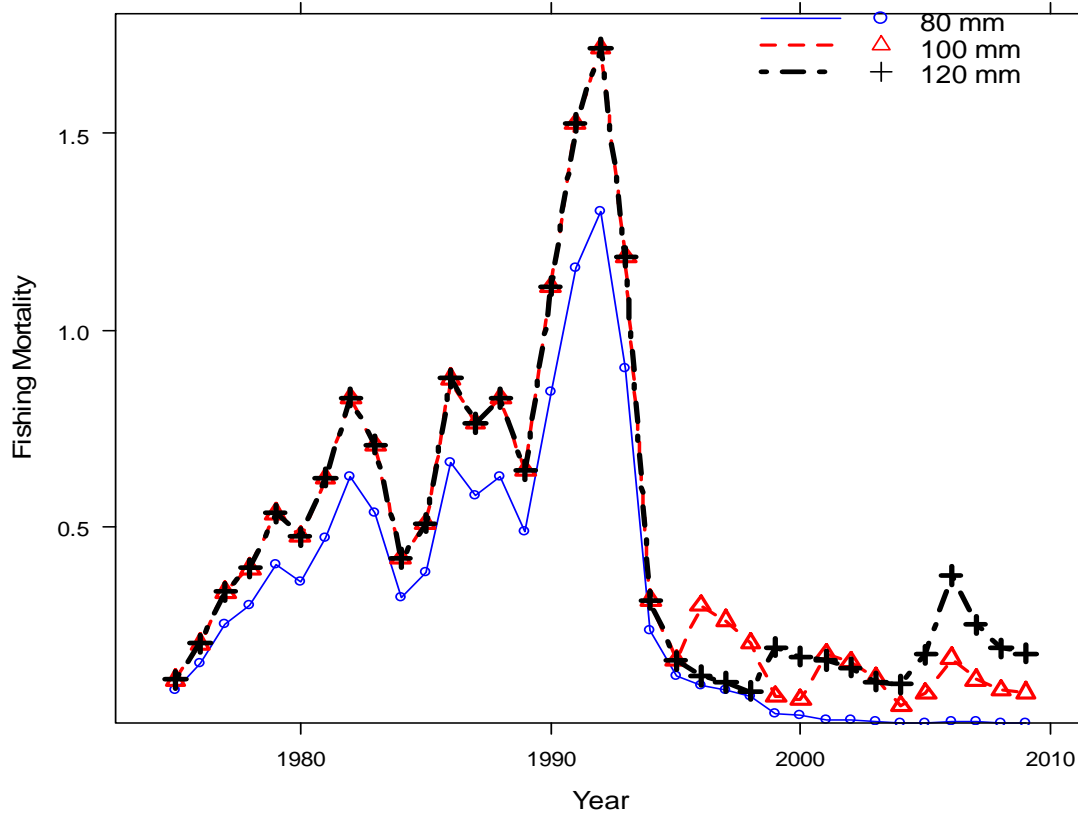
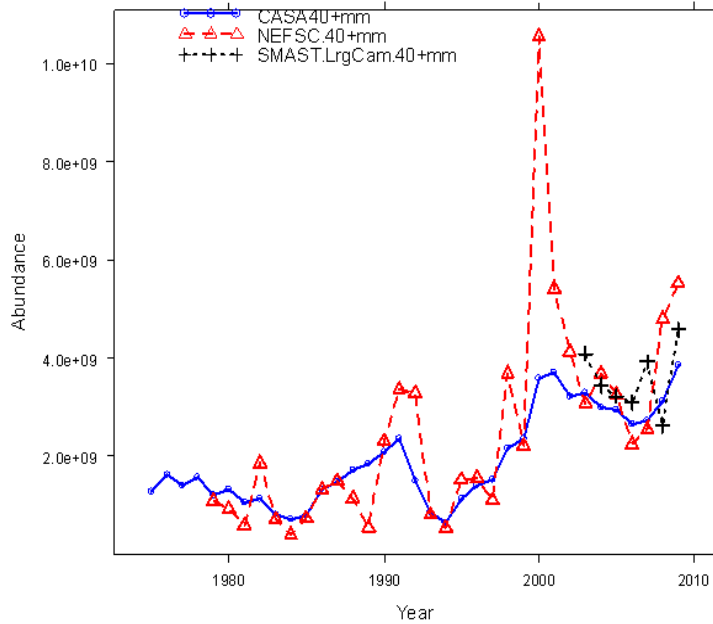


Figure B-29. CASA model estimated fishing mortality at 80 mm (blue line with circles), 100 mm (red dashed line with triangles) and 120 mm SH (black dot-dashed line with pluses) for Georges Bank.

(a)



(b)

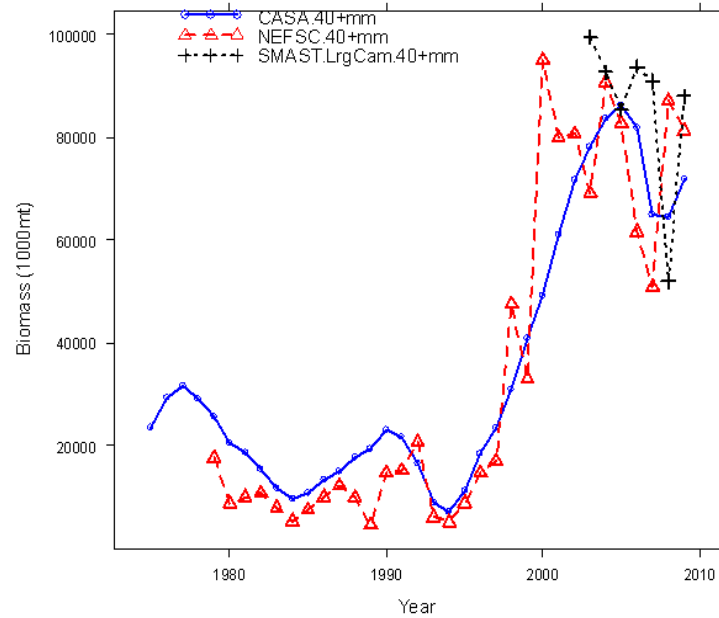
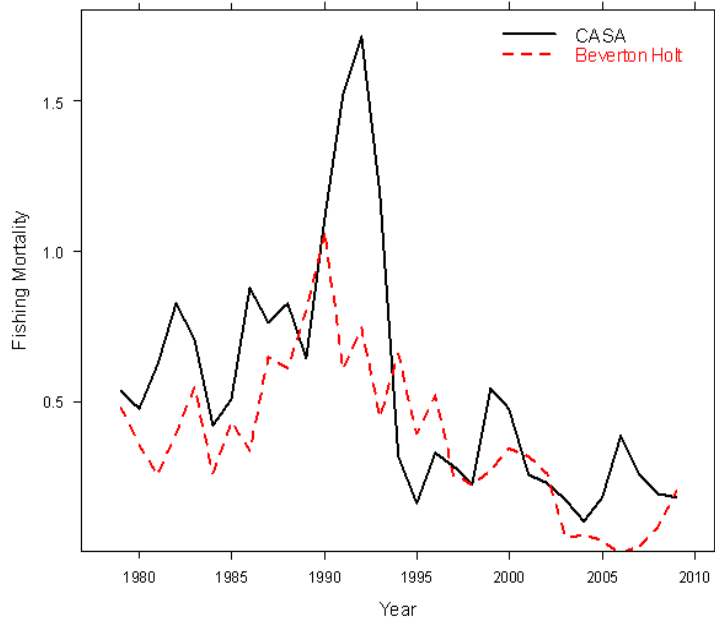


Figure B-30. Comparison of CASA model estimated (a) abundance and (b) biomass with estimates from the lined dredge survey (dashed red line with triangles) and large camera survey (dotted line with pluses) for Georges Bank. The dredge survey was expanded assuming an efficiency of 0.41.

(a)



(b)

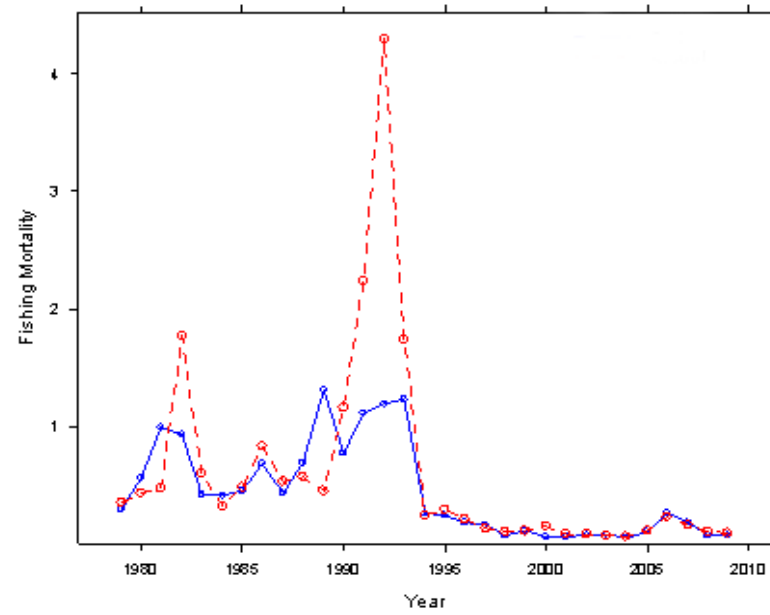


Figure B-31. (a) Comparison of fully recruited CASA fishing mortality with those calculated from the Beverton-Holt equilibrium estimator ($L_c=100\text{mm}$) for Georges Bank. (b) Comparison of an exploitation index (number landed/population abundance $> 80\text{mm}$) based on the fishery and lined dredge survey data (red dotted line), and CASA model (blue solid line) for Georges Bank.

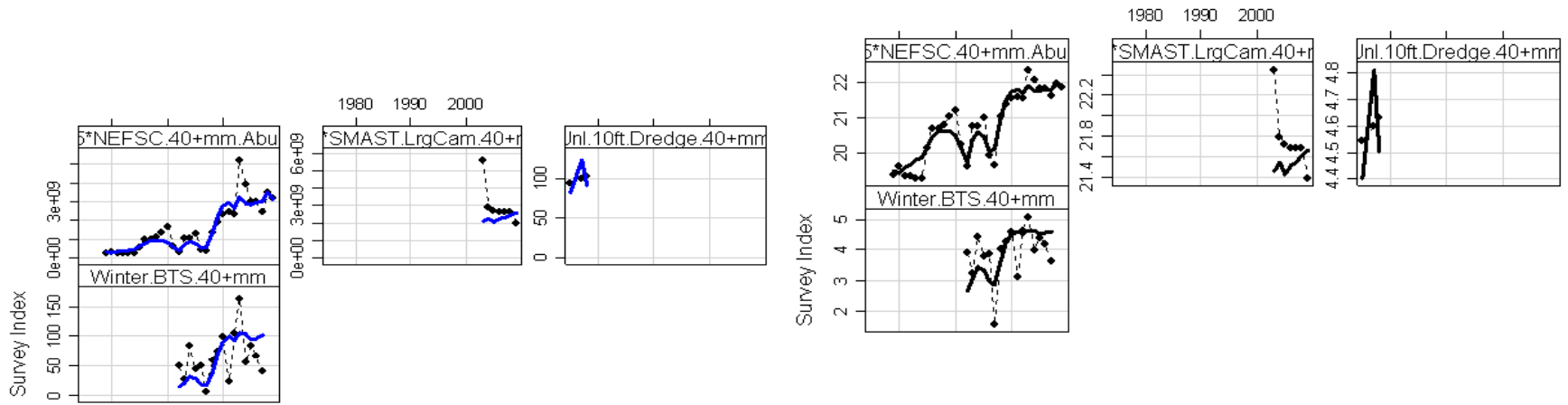


Figure B-32. Comparison between survey trend data (solid circles) and corresponding model estimates (lines) for the NEFSC lined dredge survey, the SMAST large camera survey, the NEFSC unlined dredge and winter trawl surveys for the Mid-Atlantic. Results are shown on a linear scale (left) and a log scale (right).

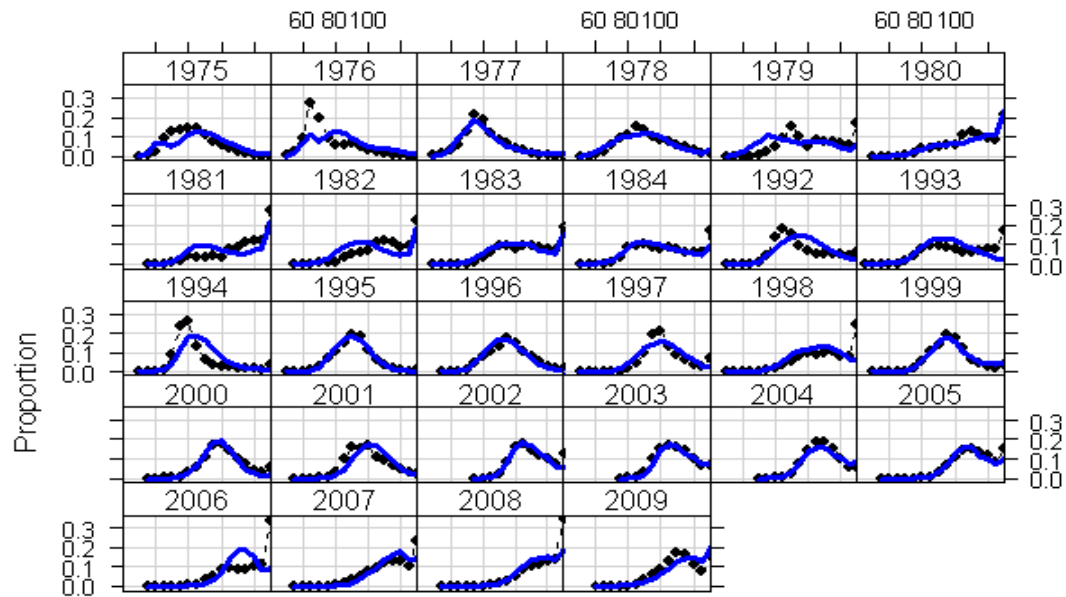


Figure B-33. Comparison of fishery shell height proportions (solid circles) and model estimated fishery shell height proportions (lines) for the Mid-Atlantic.

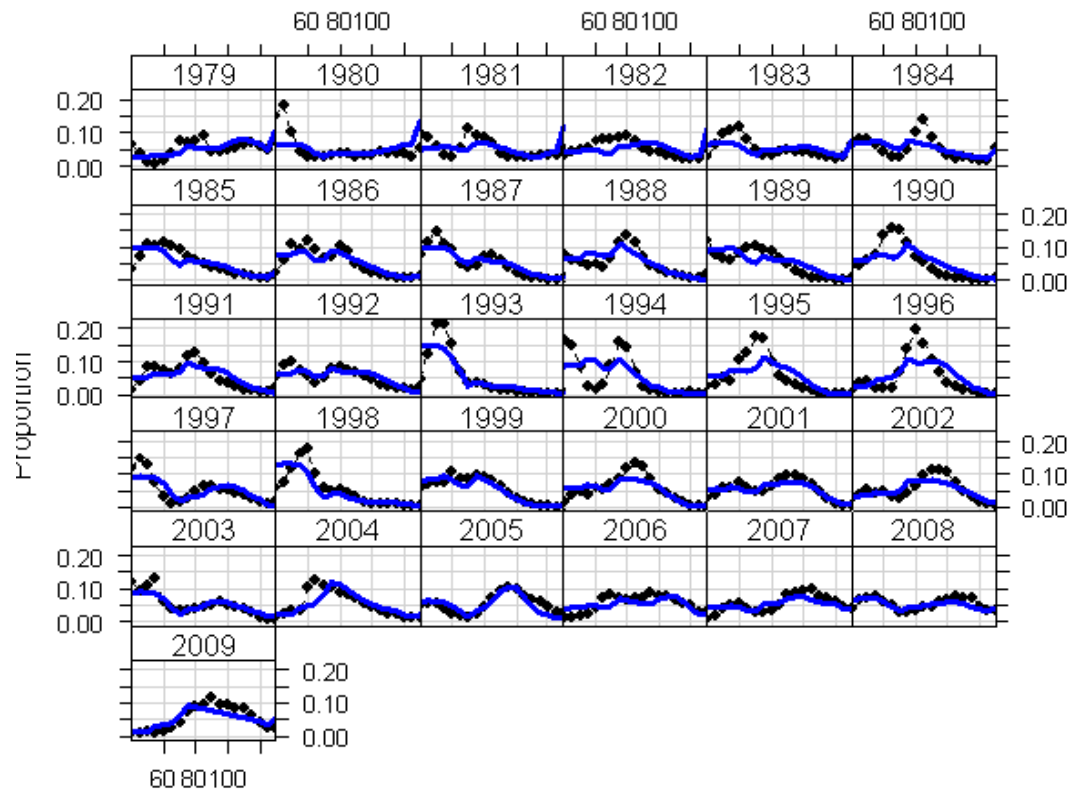


Figure B-34. NEFSC lined dredge survey shell height proportions (solid circles) and model estimated shell height proportions (line) for the Mid-Atlantic.

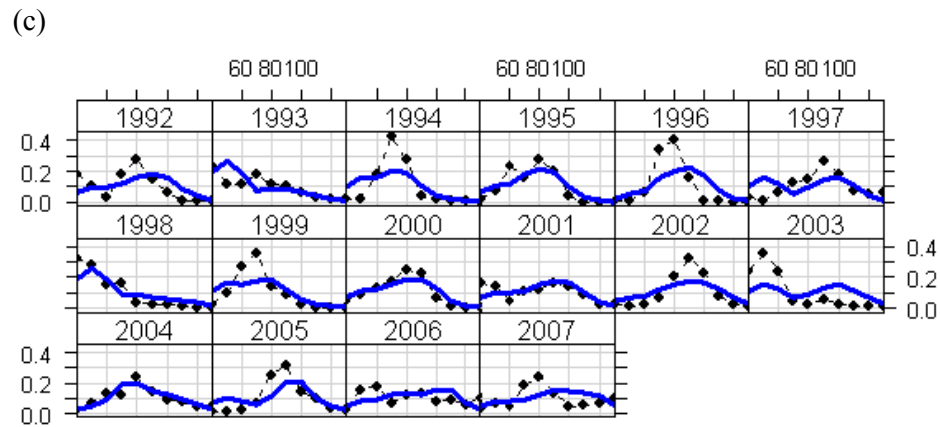
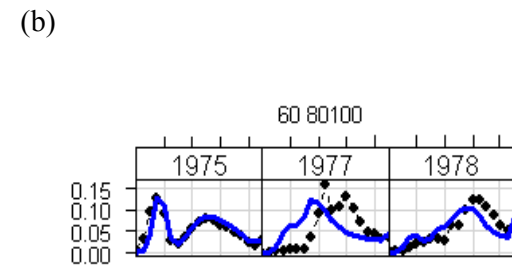
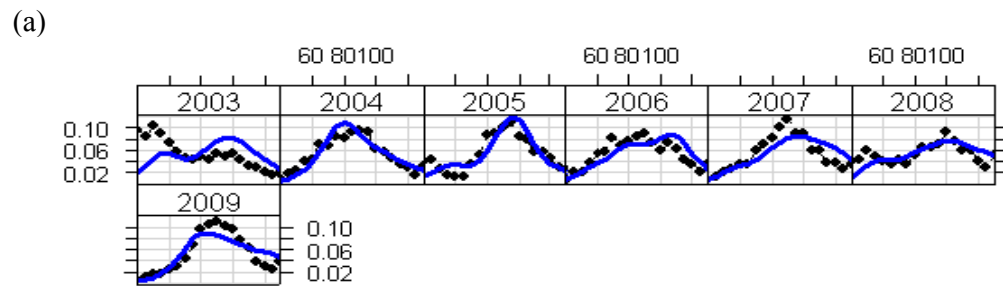


Figure B-35. Shell height proportions for (a) the SMAST large camera survey (b) the NEFSC unlined dredge survey and (c) the NEFSC winter trawl survey together with model predicted proportions (lines) in the Mid-Atlantic.

SH effective sample size diagnostics

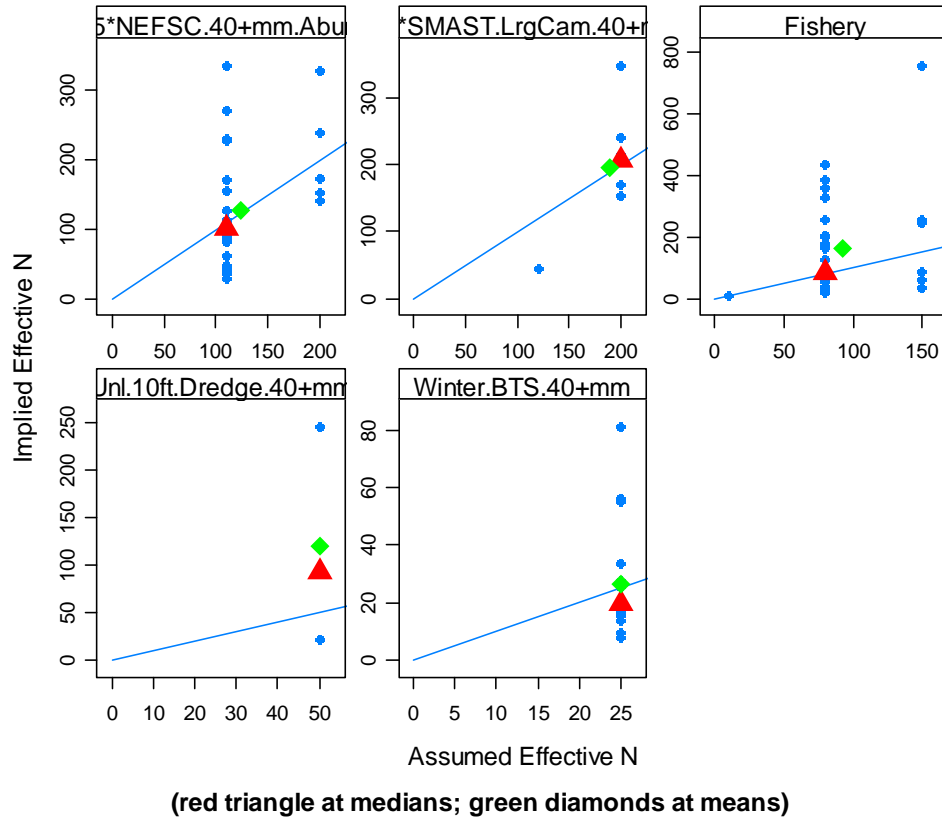


Figure B-36. Assumed and model implied effective sample sizes for the four surveys (NEFSC unlined dredge, SMAST large camera, NEFSC unlined dredge, winter bottom trawl) and the fishery shell height compositions for the Mid-Atlantic.

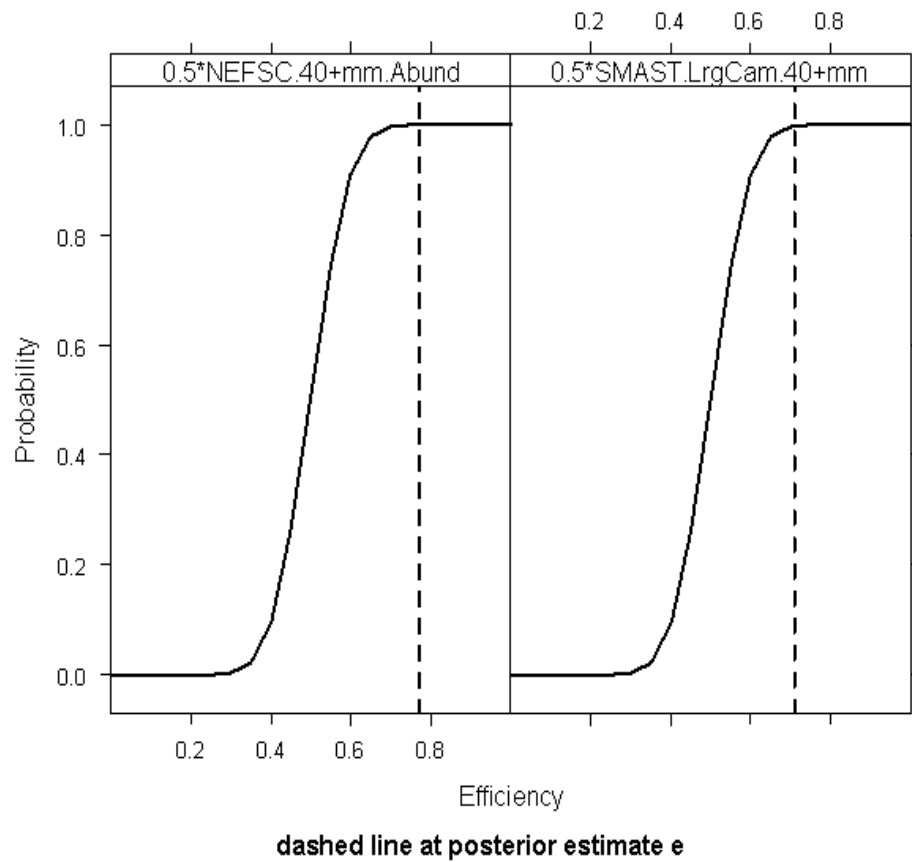
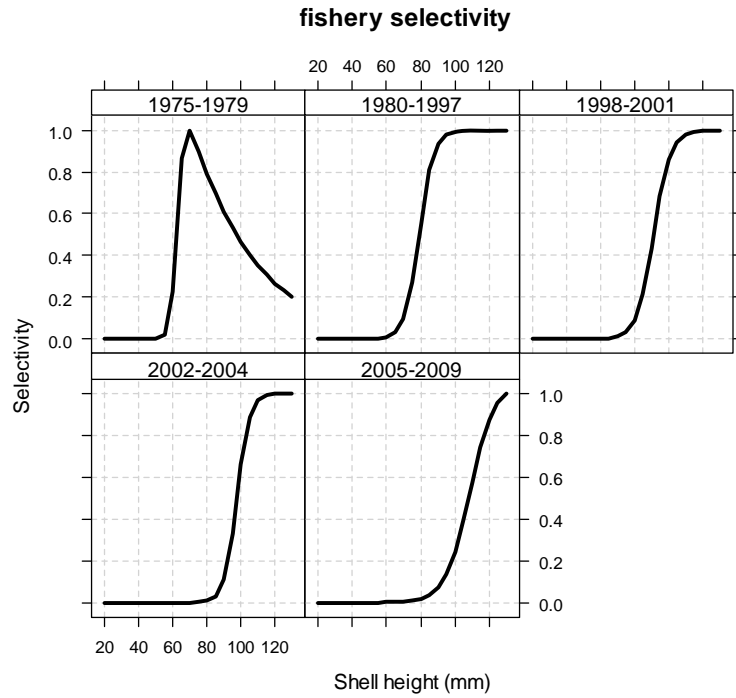


Figure B-37. Prior cumulative distributions for efficiency of the lined dredge survey (left) and large camera video survey (right) for the Mid-Atlantic. The dashed lines are the mean posterior estimate for survey efficiency.

(a)



(b)

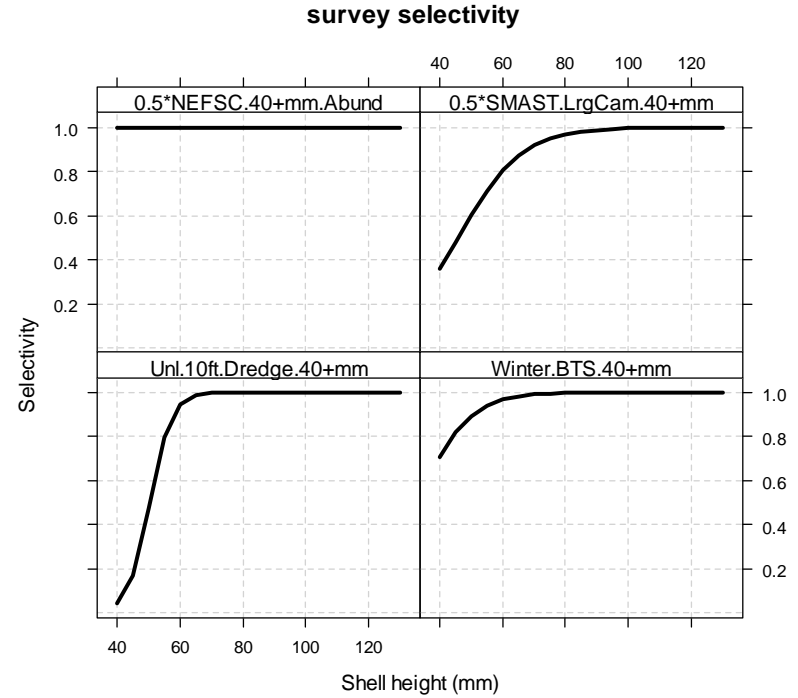


Figure B-38. (a) Estimated fishery selectivities and (b) survey selectivities (lined dredge top left, large camera top right, unlined dredge bottom left, winter trawl bottom right) for the Mid-Atlantic. The trawl survey selectivity was estimated; the other survey selectivities were fixed.

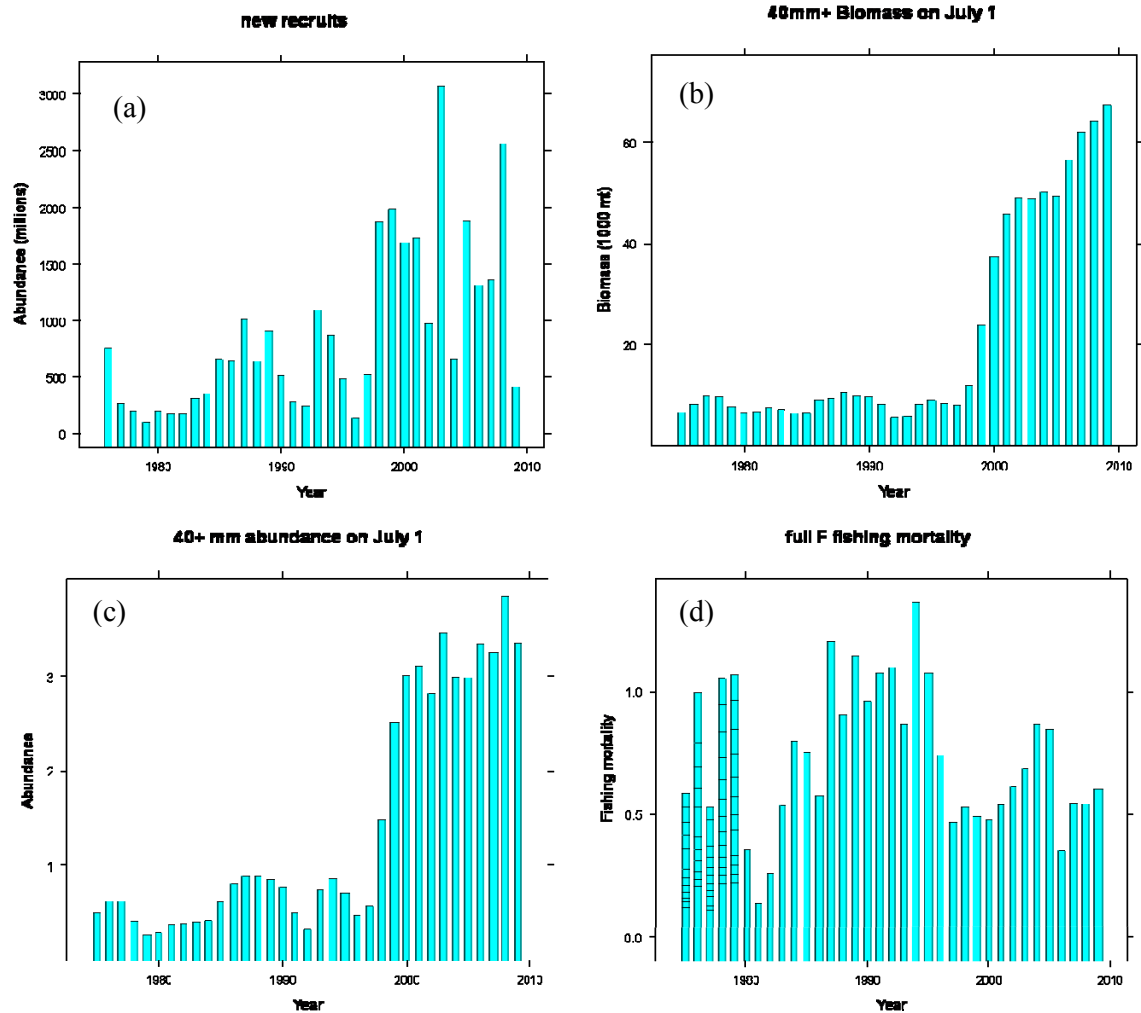


Figure B-39. CASA model estimated (a) recruitment, (b) July 1 biomass, (c) July 1 abundance and (d) fully recruited fishing mortality for the Mid-Atlantic.

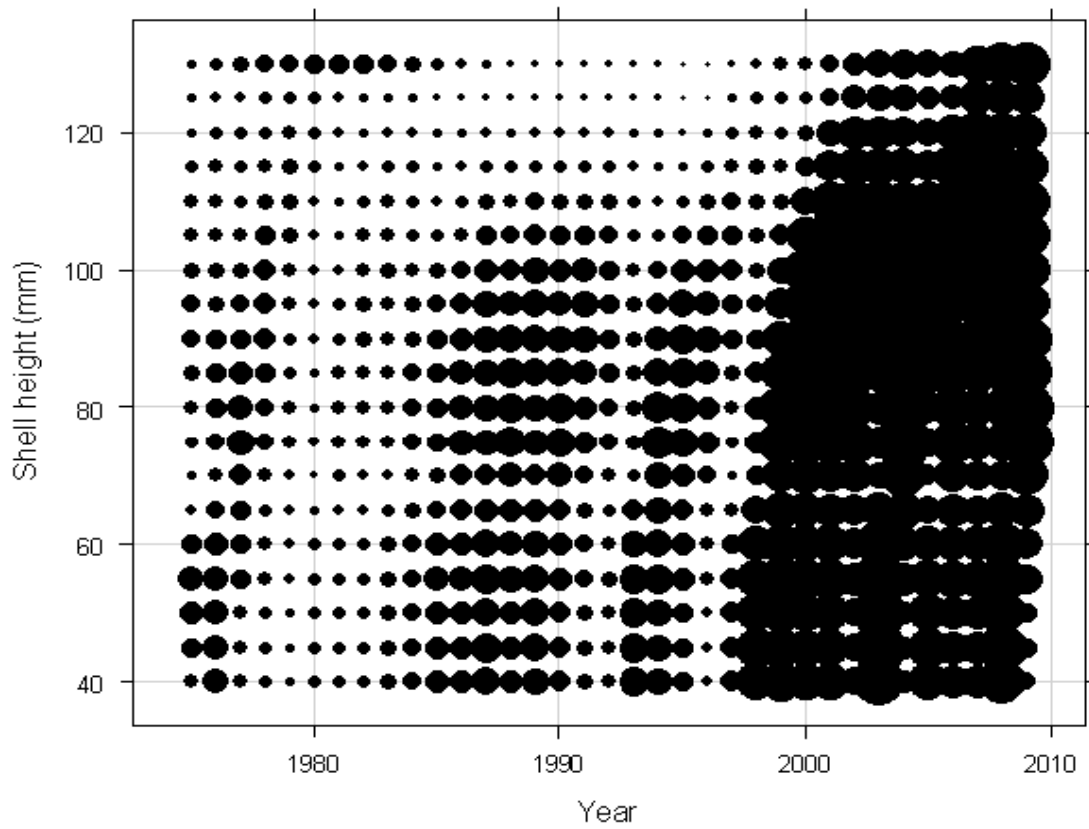


Figure B-40. Model estimated abundances at shell height for the Mid-Atlantic. Disk areas are proportional to abundance.

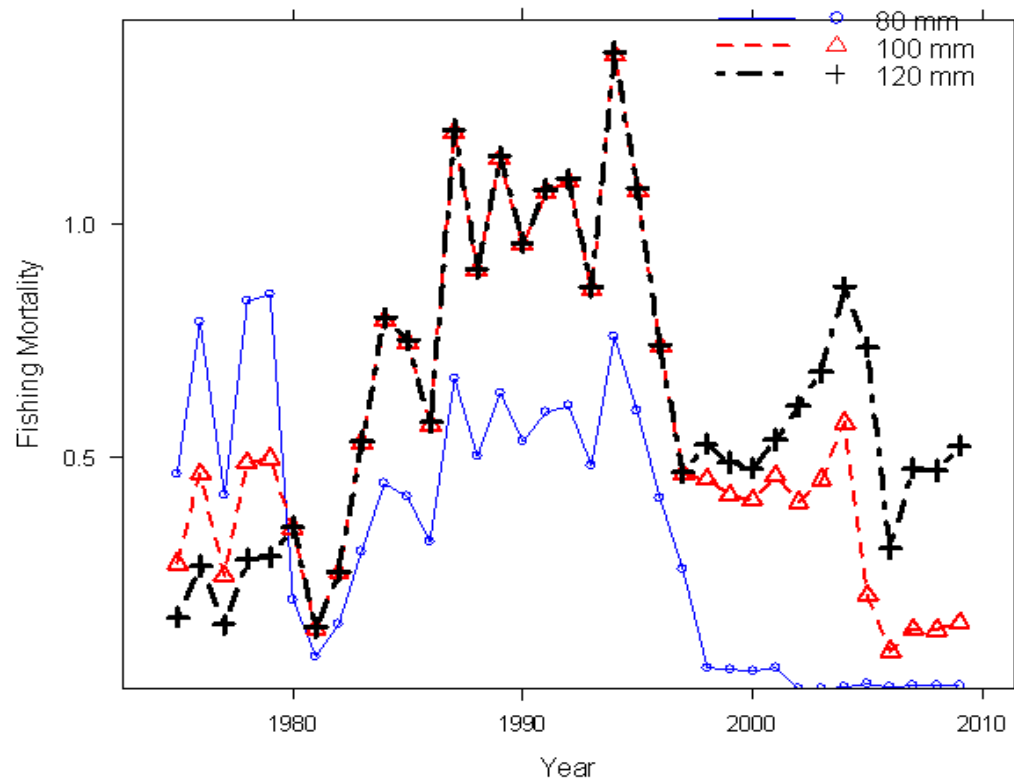


Figure B-41. CASA model estimated fishing mortality at 80 mm (blue line with circles), 100 mm (red dashed line with triangles) and 120 mm SH (black dot-dashed line with pluses) for the Mid-Atlantic.

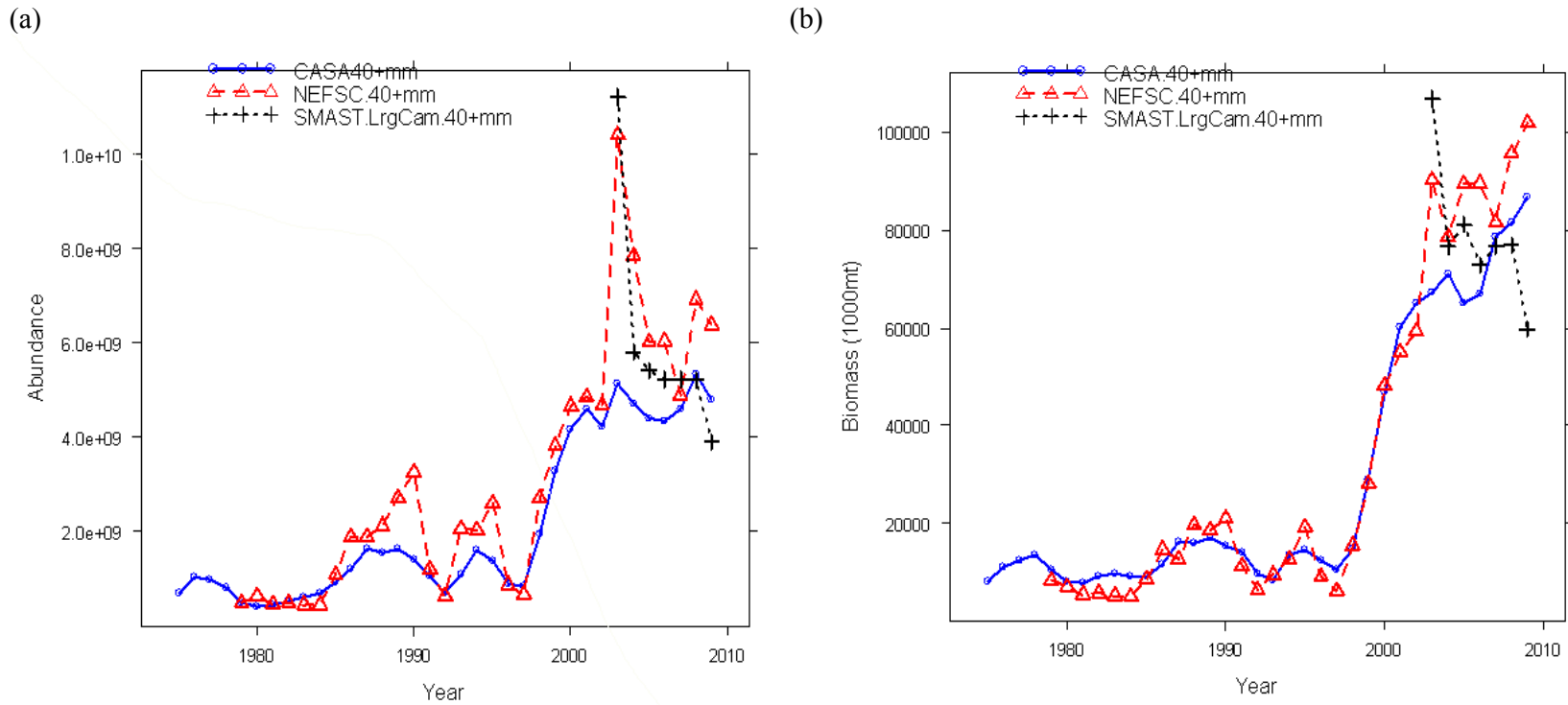
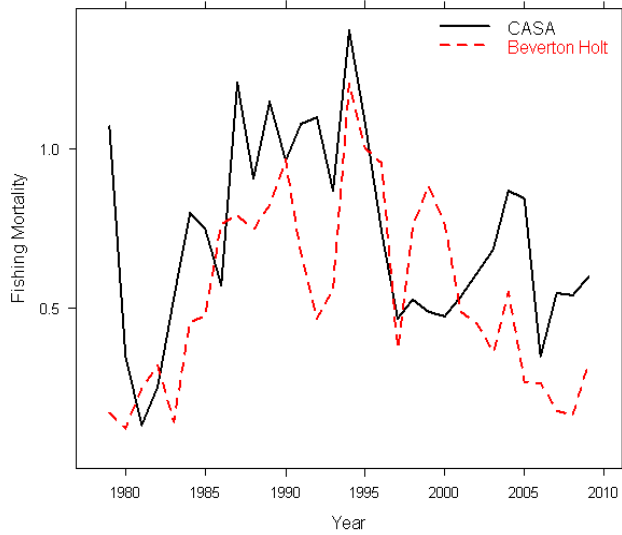


Figure B-42. Comparison of CASA model estimated (a) abundance and (b) biomass with estimates from the lined dredge survey (dashed red line with triangles) and large camera survey (dotted line with pluses) for the Mid-Atlantic. The dredge survey was expanded assuming an efficiency of 0.44.

(a)



(b)

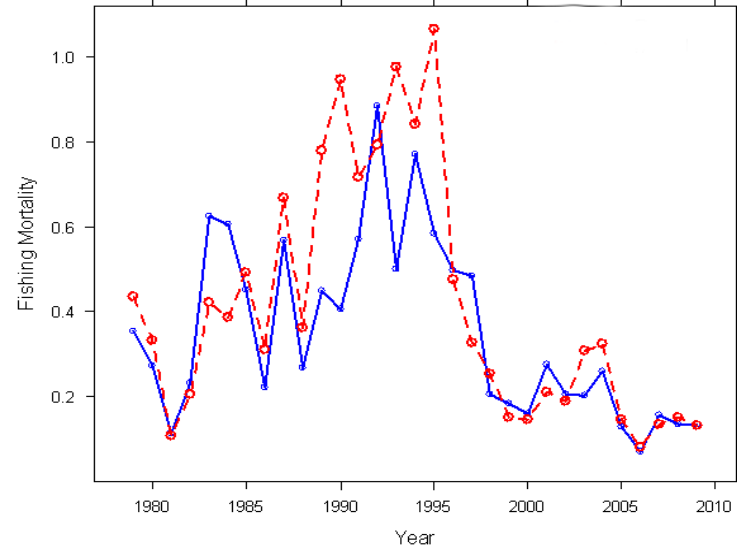


Figure B-43. (a) Comparison of fully recruited CASA fishing mortality with those calculated from the Beverton-Holt equilibrium estimator ($L_c=100\text{mm}$) for the Mid-Atlantic. (b) Comparison of an exploitation index (number landed/population abundance $> 80\text{mm}$) based on the fishery and lined dredge survey data (red dashed line), and CASA model (blue solid line) for the Mid-Atlantic.

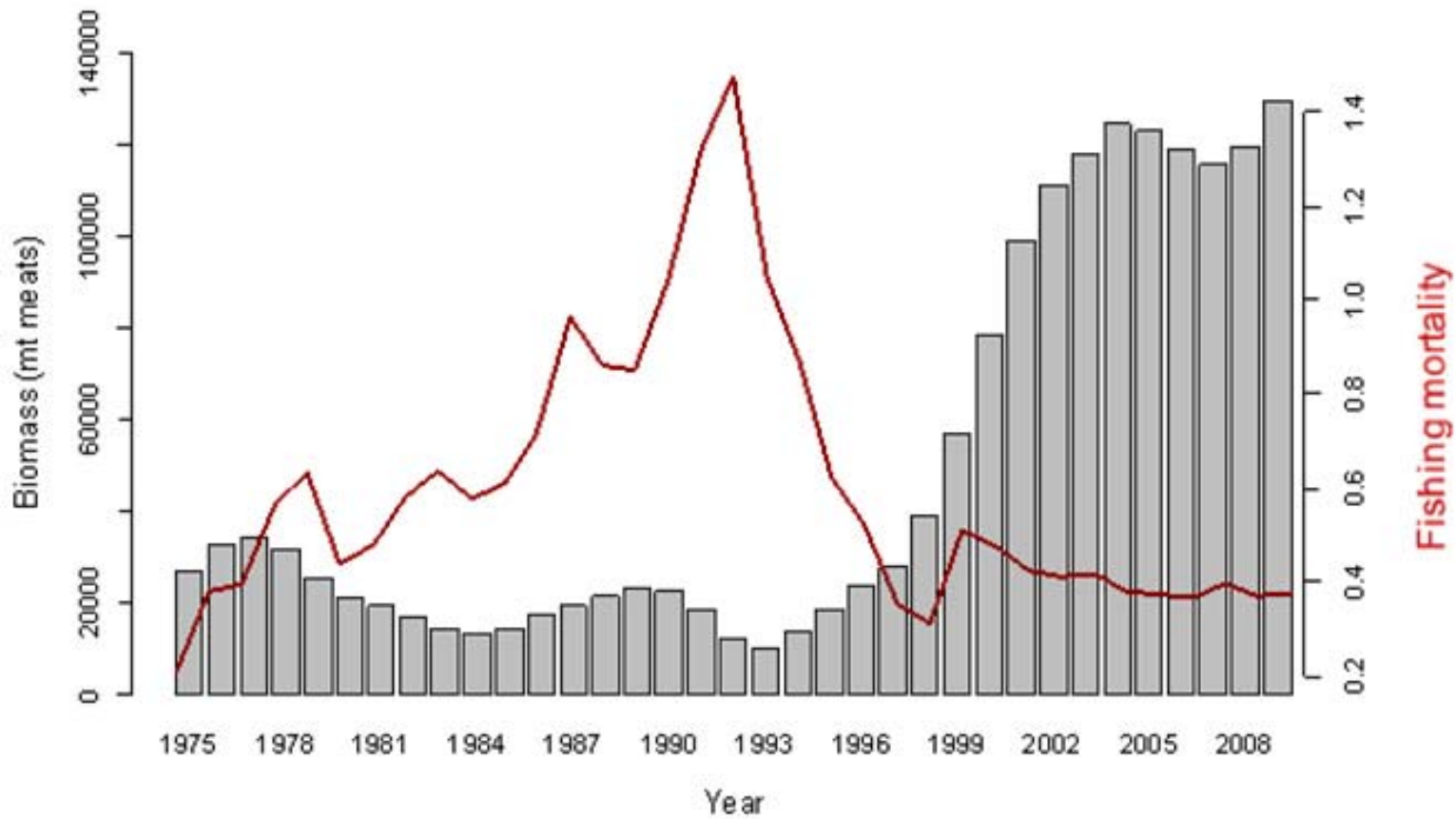


Figure B-44. Whole-stock CASA model estimates of biomass (bars) and fully recruited fishing mortality (line).

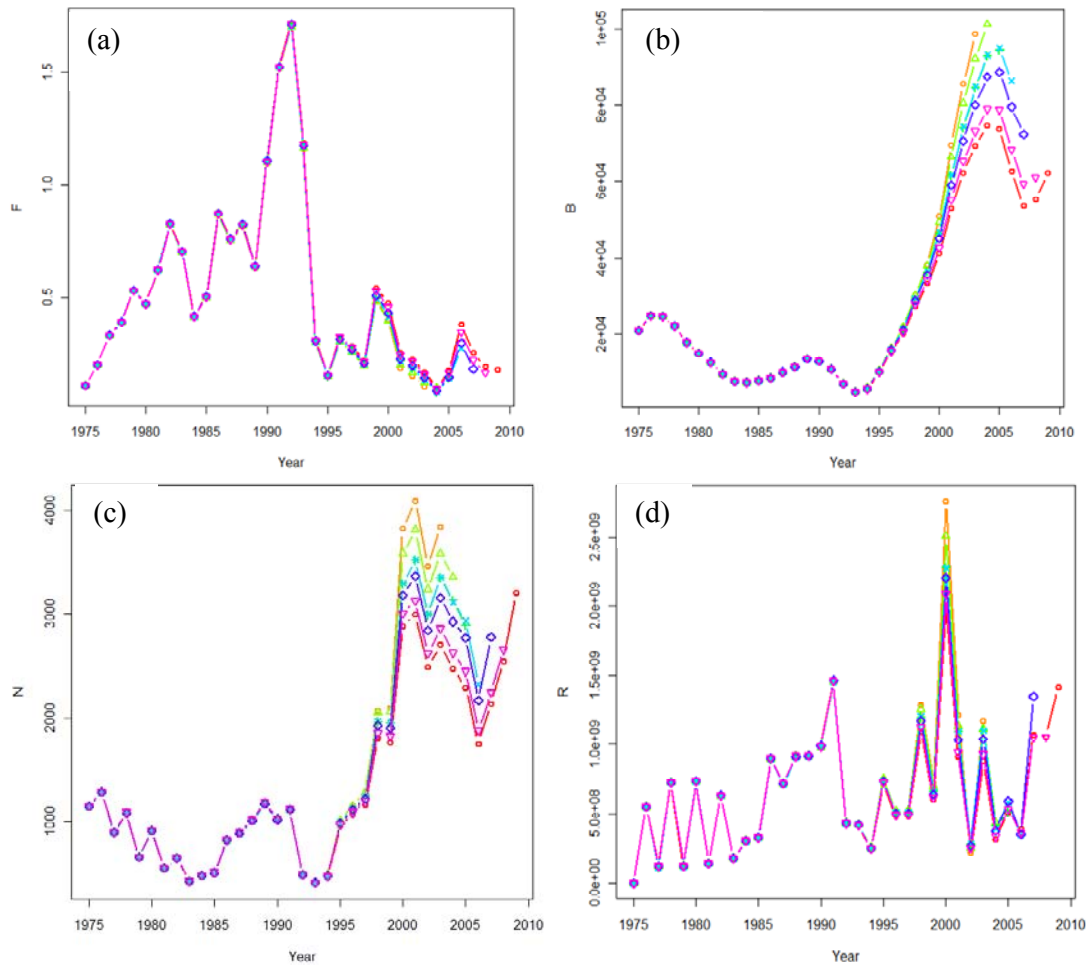


Figure B-45. Plots of retrospective analysis of the Georges Bank CASA model: (a) fishing mortality, (b) biomass, (c) abundance, and (d) recruitment. The CASA model was run with terminal year 2004 (orange), 2005 (green), 2006 (cyan), 2007 (blue), 2008 (magenta) and 2009 (red).

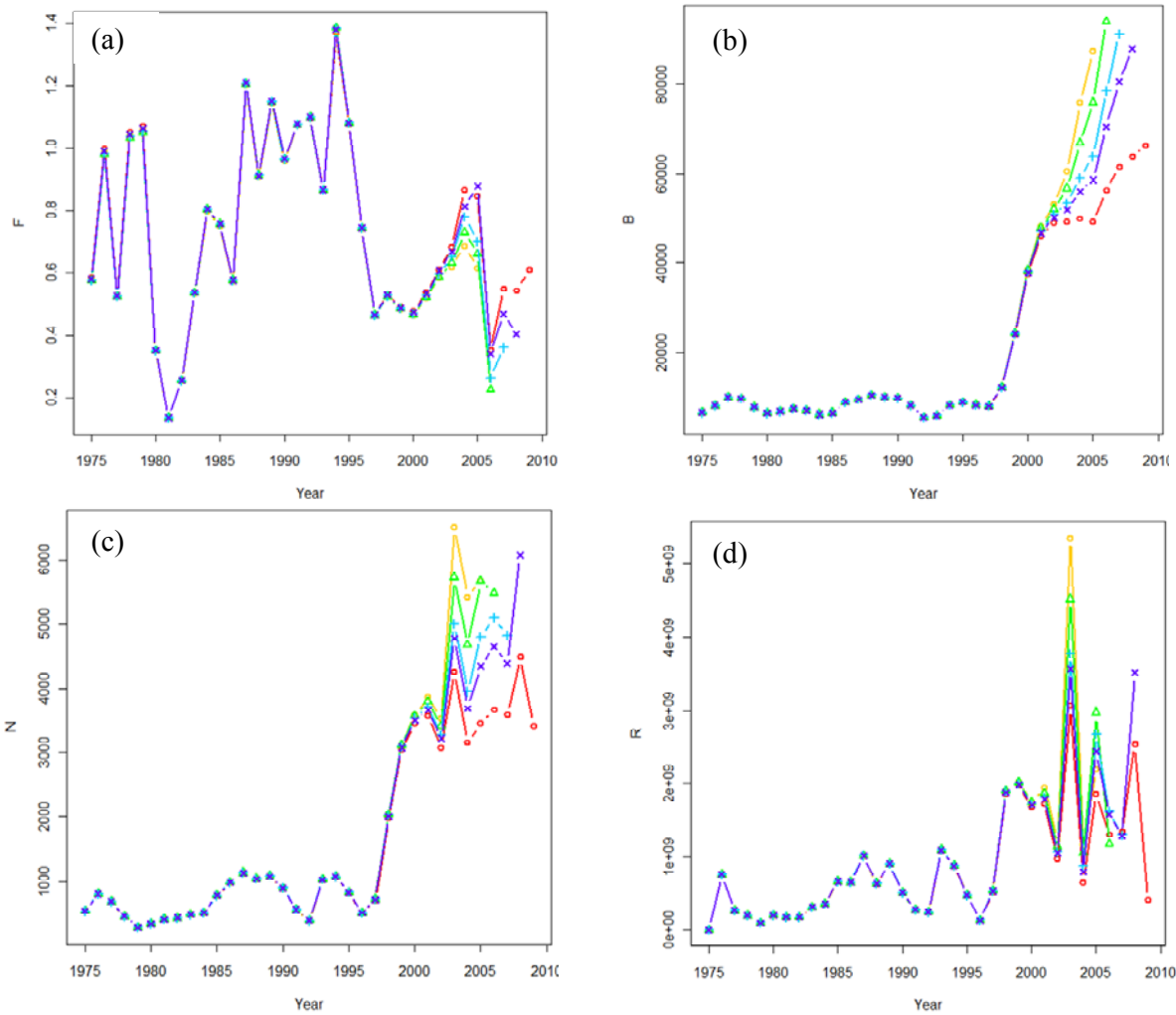


Figure B-46. Plots of retrospective analysis of the Mid-Atlantic CASA model: (a) fishing mortality, (b) biomass, (c) abundance, and (d) recruitment. The CASA model was run with terminal years 2004 (orange), 2005 (green), 2006 (cyan), 2007 (blue), 2008 (purple) and 2009 (red).

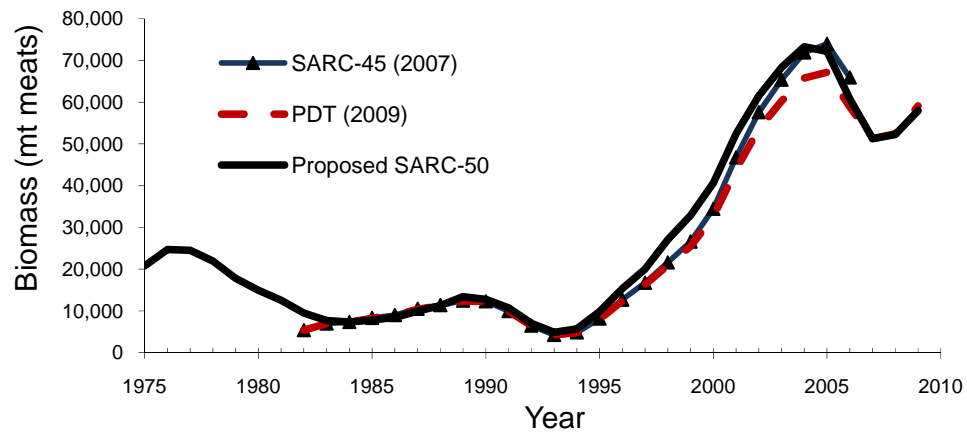
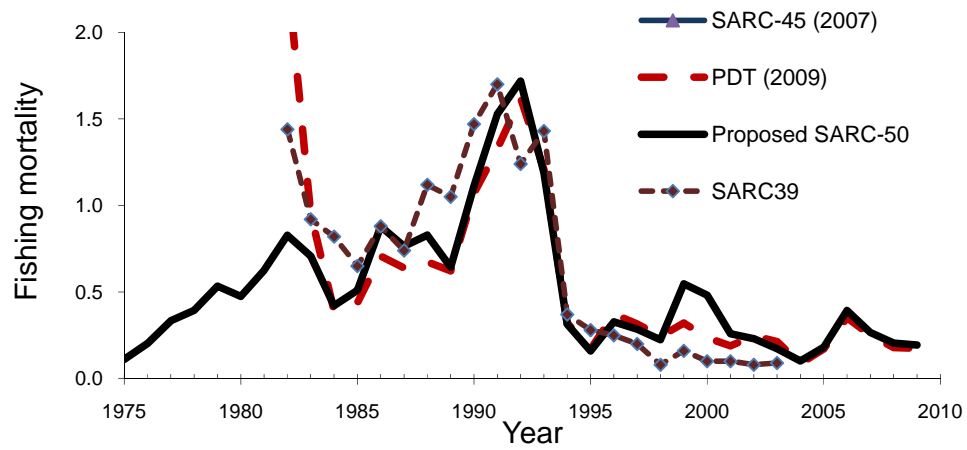


Figure B-47. Comparison of current estimates (black line) of fully recruited fishing mortality (above) and July 1 biomass (below) on Georges Bank with that of previous assessments (SARC-39/NEFSC 2004 short dashed line (fishing mortality only), SARC-45/NEFSC 2007, blue line with triangles, update assessment by the scallop PDT in 2009 (NEFMC 2010), long red dashed line).

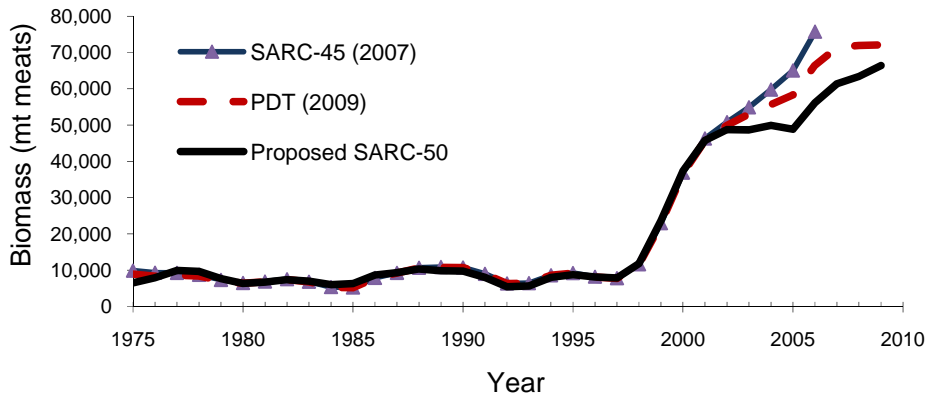
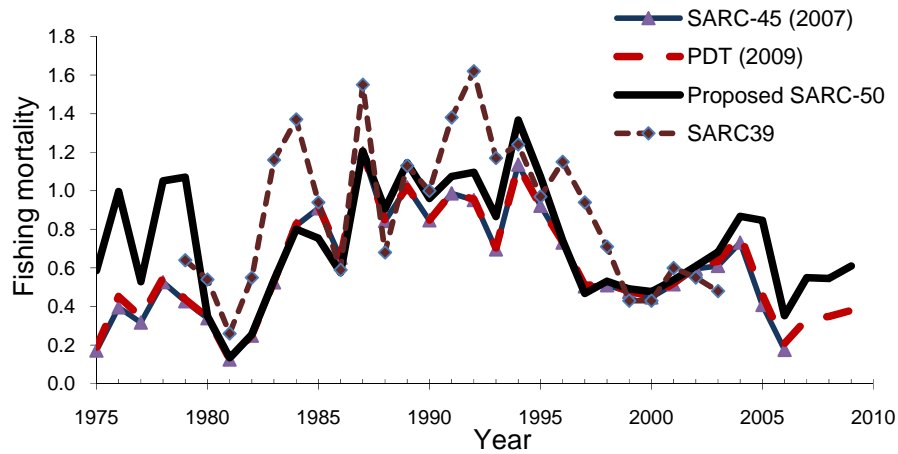


Figure B-48. Comparison of current estimates (black line) of fishing mortality (above) and biomass (below) in the Mid-Atlantic with that of previous assessments (SARC-39/NEFSC 2004 short dashed line (fishing mortality only), SARC-45/NEFSC 2007, blue line with triangles, update assessment by the scallop PDT in 2009 (NEFMC 2010), long red dashed line).

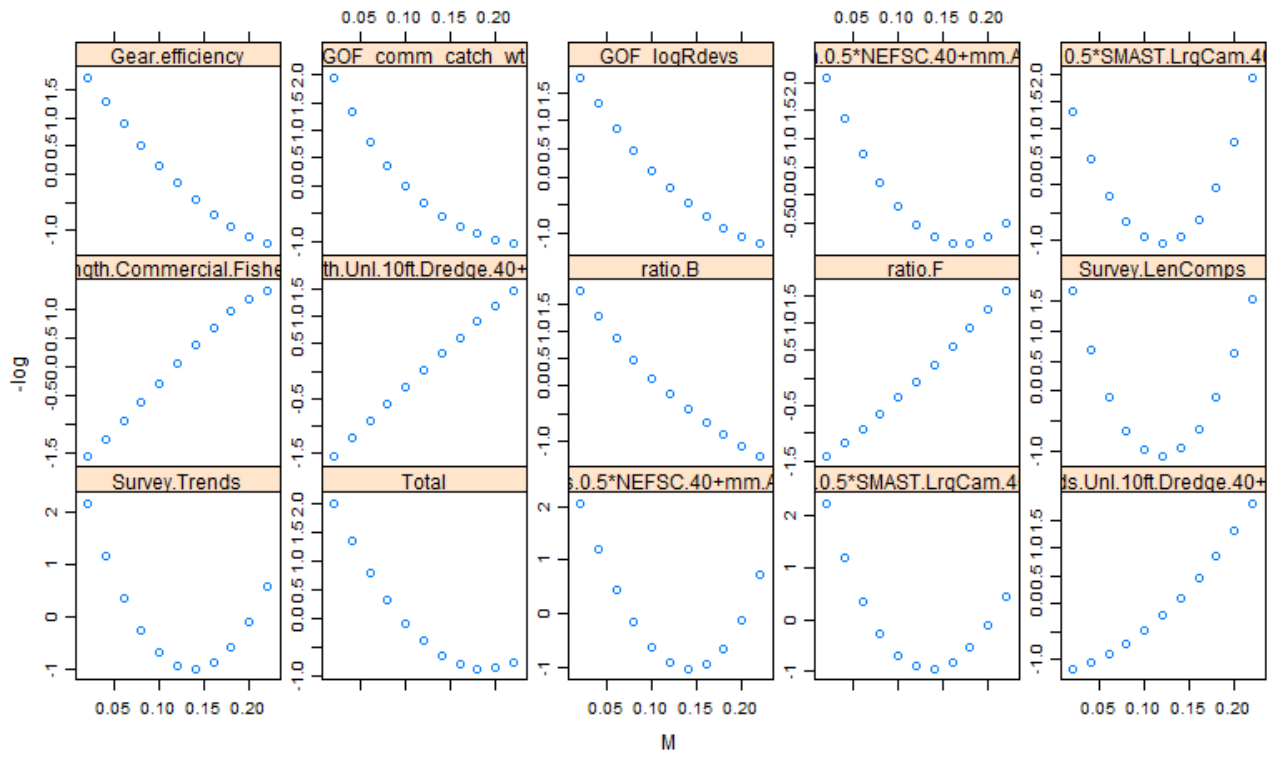


Figure B-49 Likelihood profile for (a) natural mortality and (b) large camera efficiency (q) on Georges Bank.

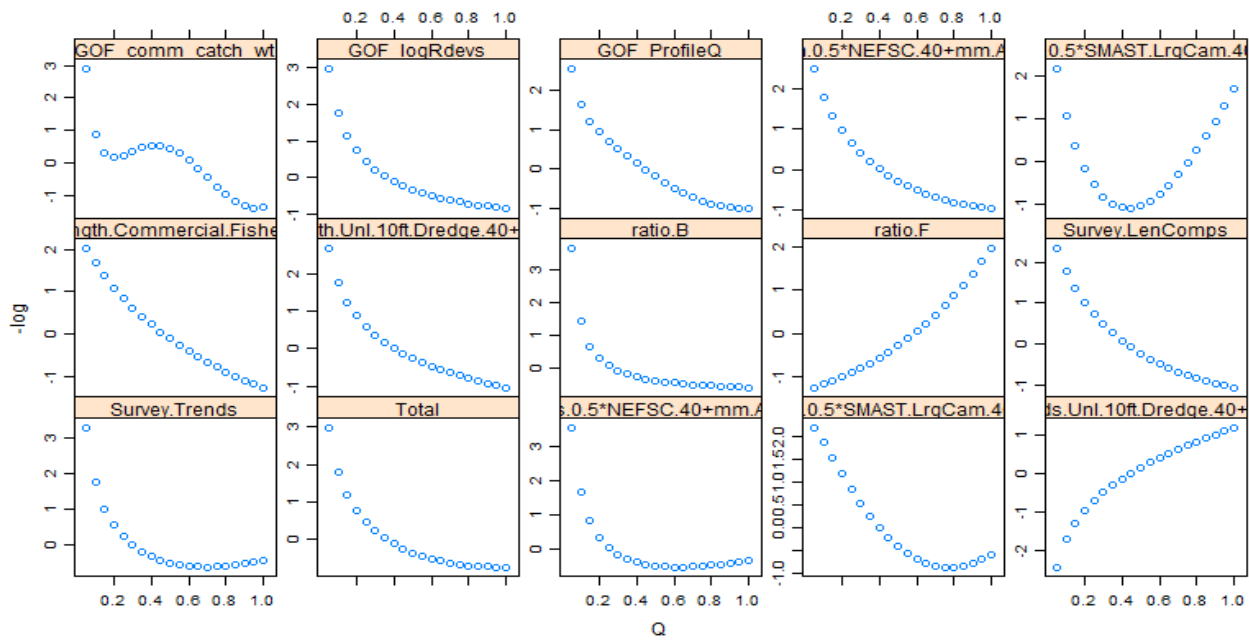


Figure B-49(b)

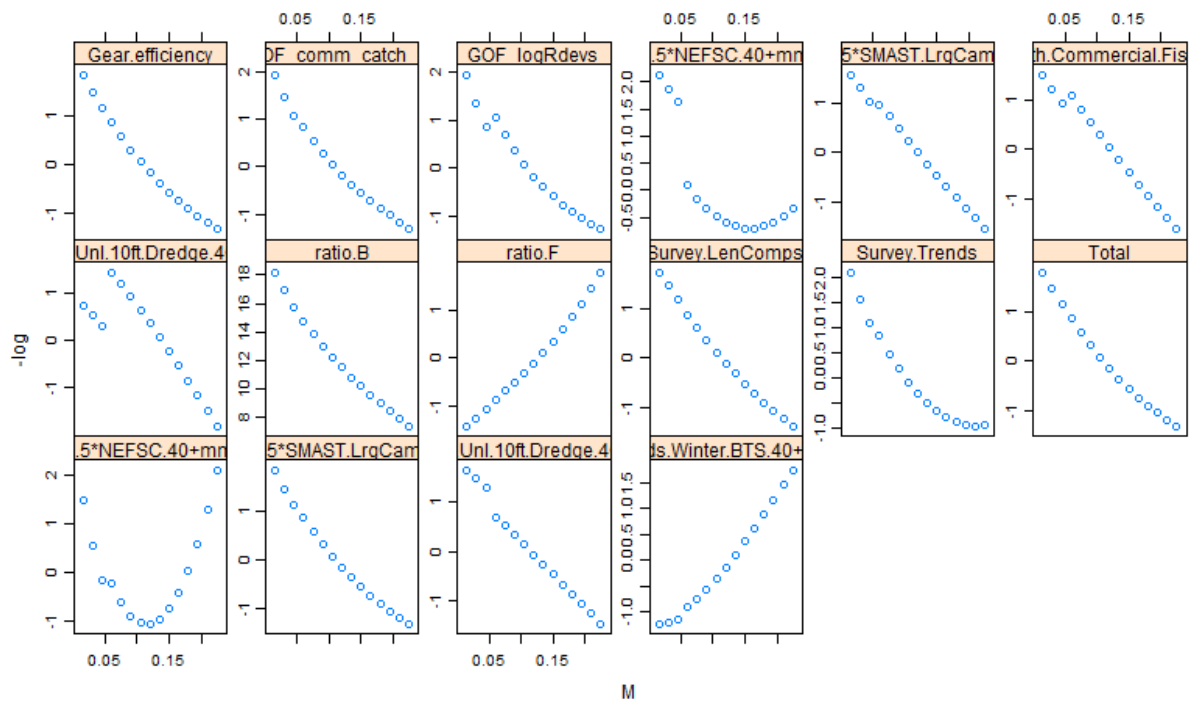


Figure B-50. Likelihood profiles for (a) natural mortality and (b) large camera survey q for the Mid-Atlantic.

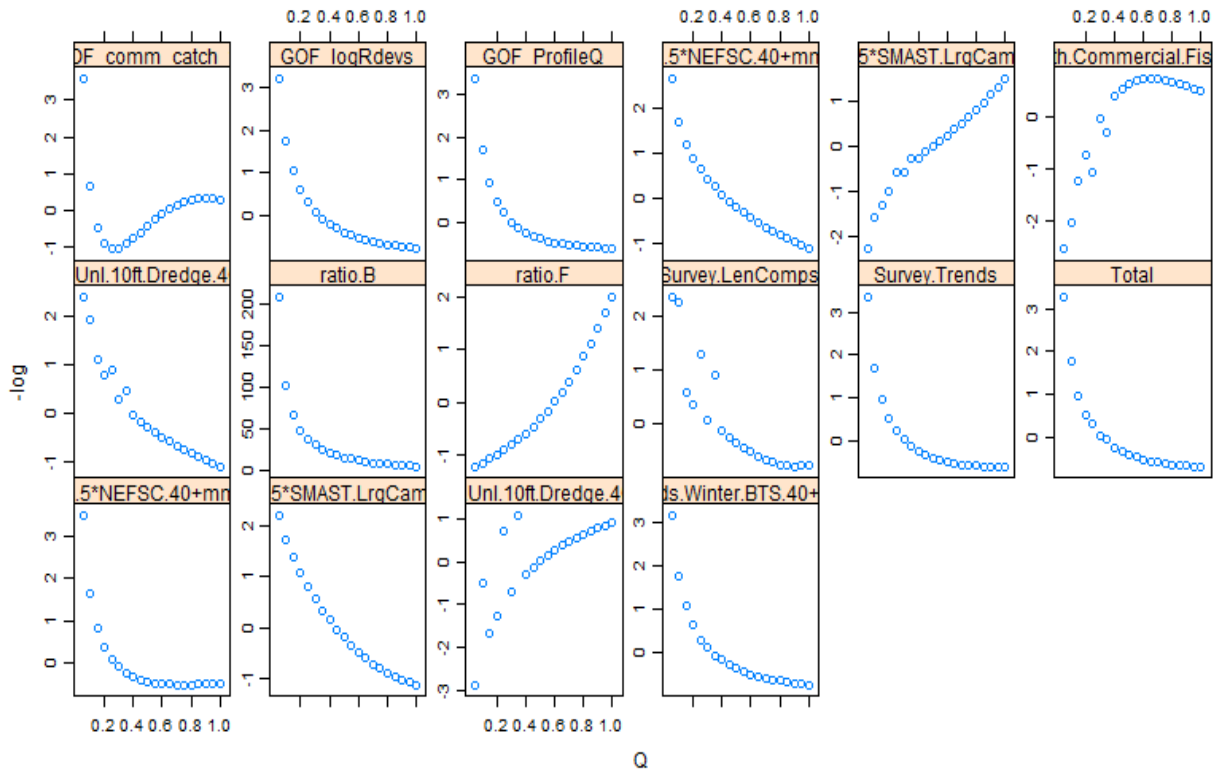


Figure B-50 (b)

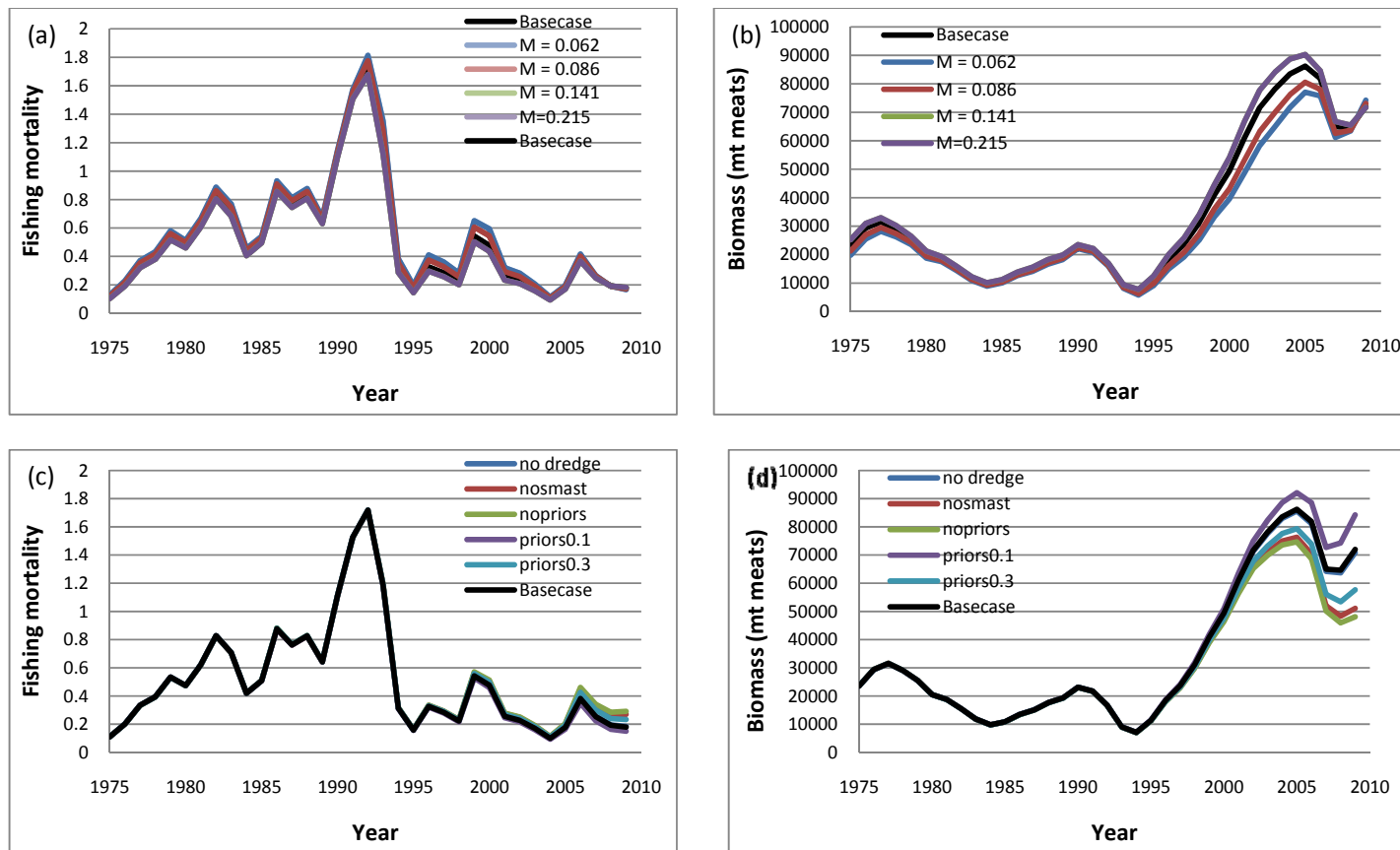


Figure B-51. Sensitivity analysis to the assumed value of (a-b) natural mortality and (c-d) priors on estimated values of fully recruited fishing mortality (a) and (c), and biomass (b) and (d) on Georges Bank. The values of natural mortality represent the assumed value (0.12, basecase) and the 5th, 25th, 75th and 95th percentile of the distribution of M used in the stochastic reference point model (Section 7). The assumptions on the priors are dredge and large camera $cv = 0.15$ (basecase), no dredge prior, no camera prior, no priors, $cv = 0.1$ for both priors and $cv = 0.3$ for both priors.

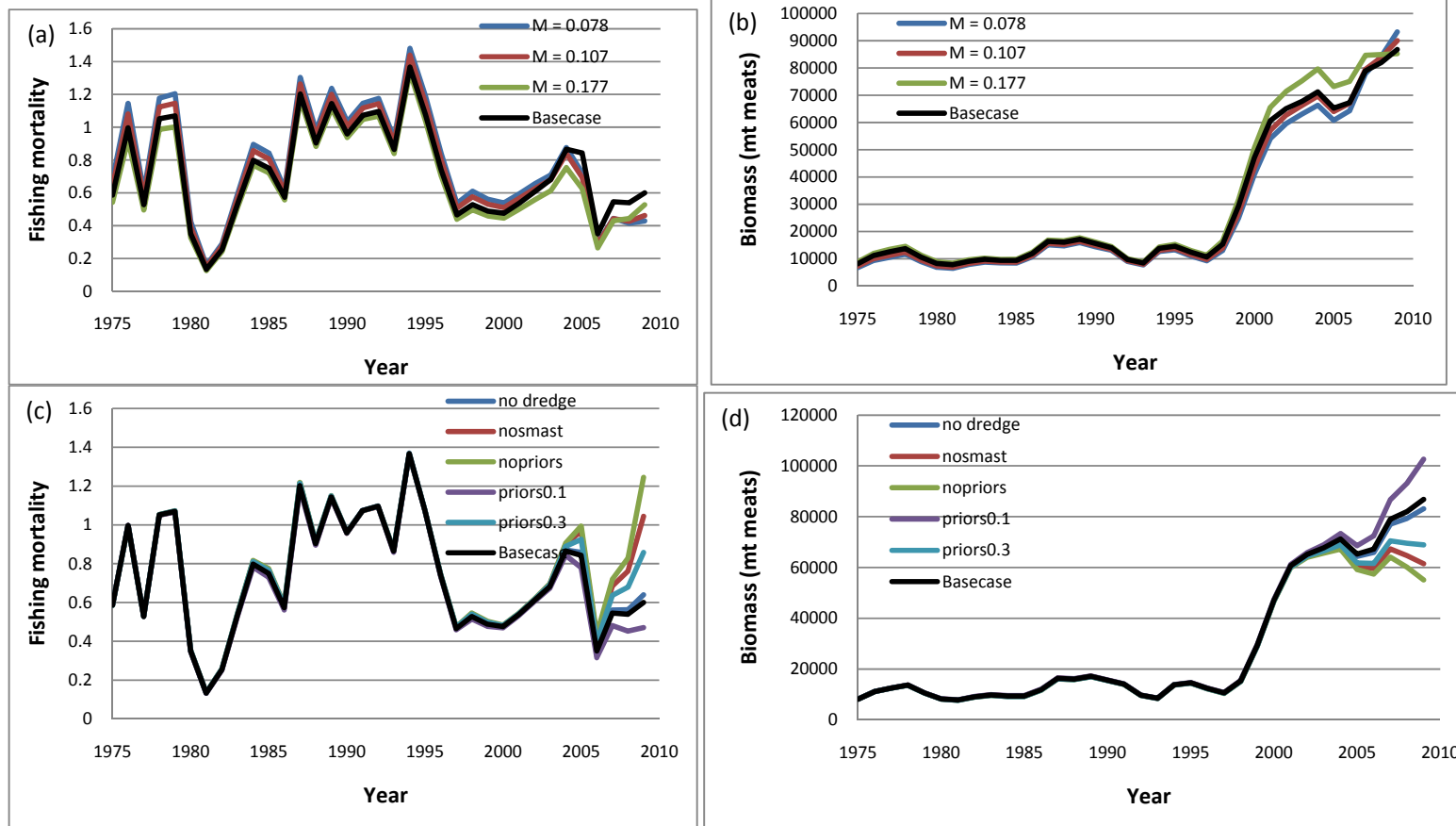


Figure B-52. Sensitivity analysis to the assumed value of (a-b) natural mortality and (c-d) large camera efficiency on estimated values of fully recruited fishing mortality (a) and (c), and biomass (b) and (d) on Georges Bank. The values of natural mortality represent the assumed value (0.12, basecase) and the 5th, 25th and 75th of the distribution of M used in the stochastic reference point model (Section 7; the model did not converge for the 95th percentile of M). The assumptions on the priors are dredge and large camera $cv = 0.15$ (basecase), no dredge prior, no camera prior, no priors, $cv = 0.1$ for both priors and $cv = 0.3$ for both priors.

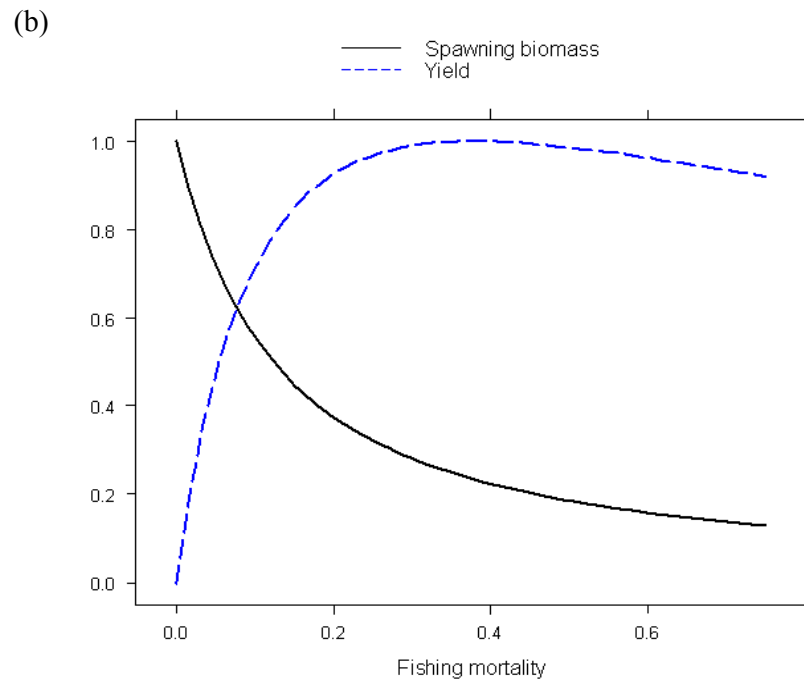
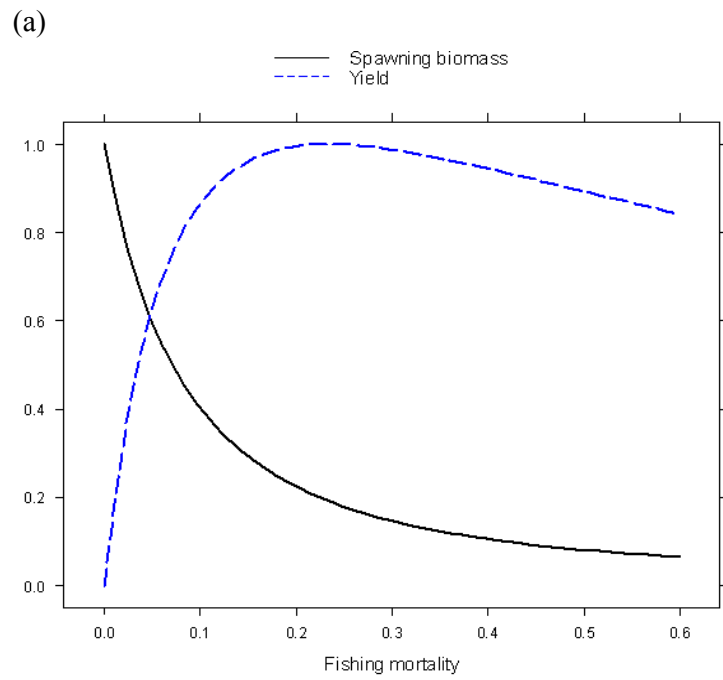
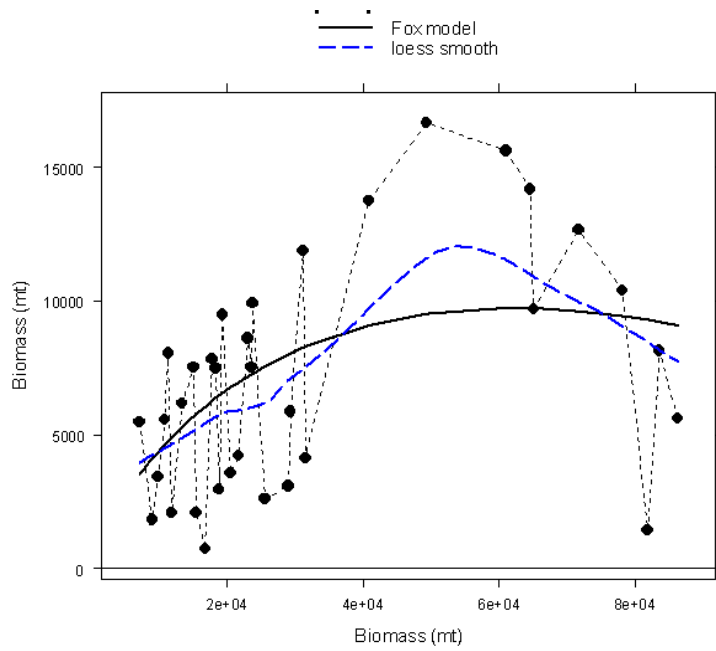


Figure B-53. Yield per recruit (blue dashed line) and spawning biomass per recruit (black solid line) for (a) Georges Bank and (b) Mid-Atlantic from the CASA model.

(a)



(b)

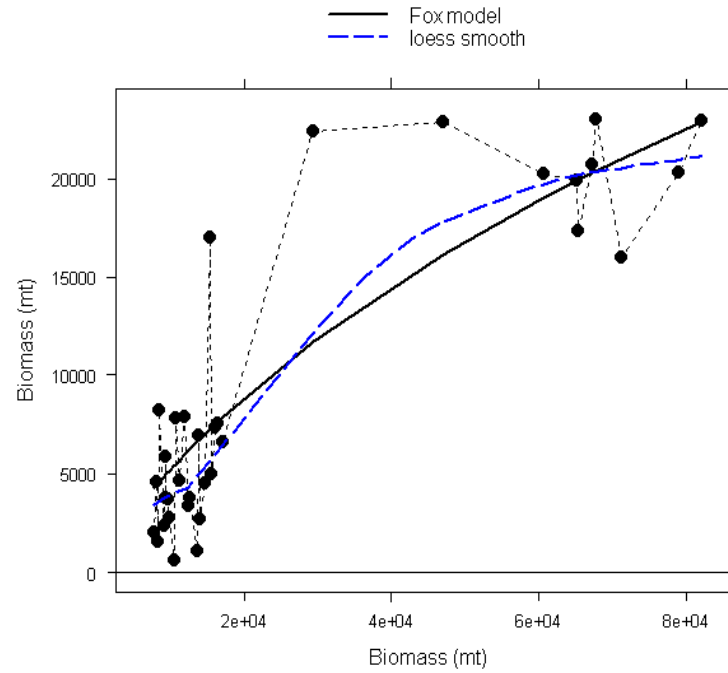
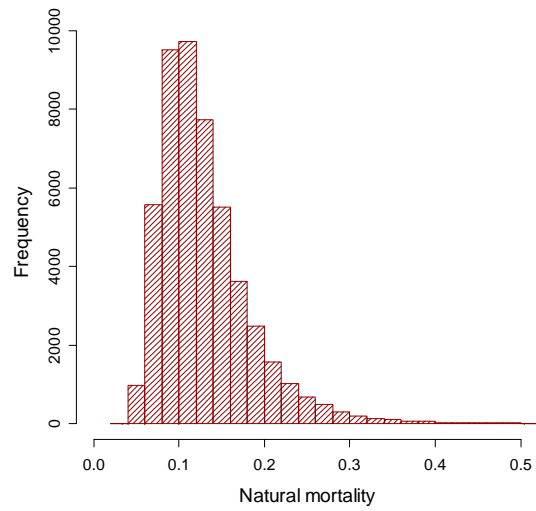


Figure B-54. Annual surplus production (solid circles) vs. biomass for (a) Georges Bank and (b) Mid-Atlantic. Fits to the Fox surplus production model (solid lines) and a loess smoother are also shown.

(a)



(b)

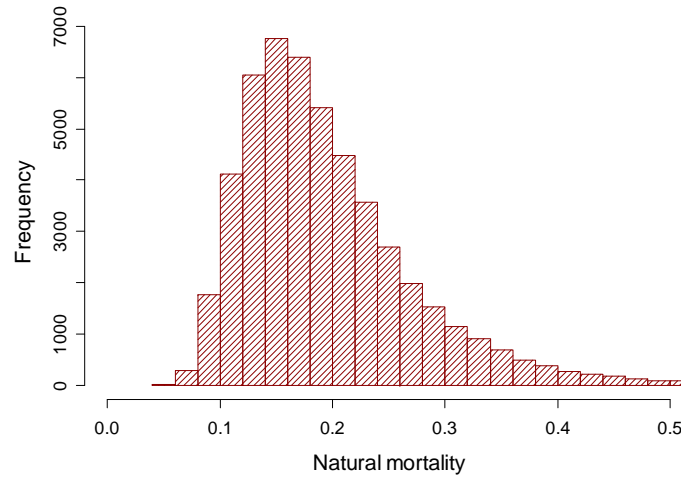
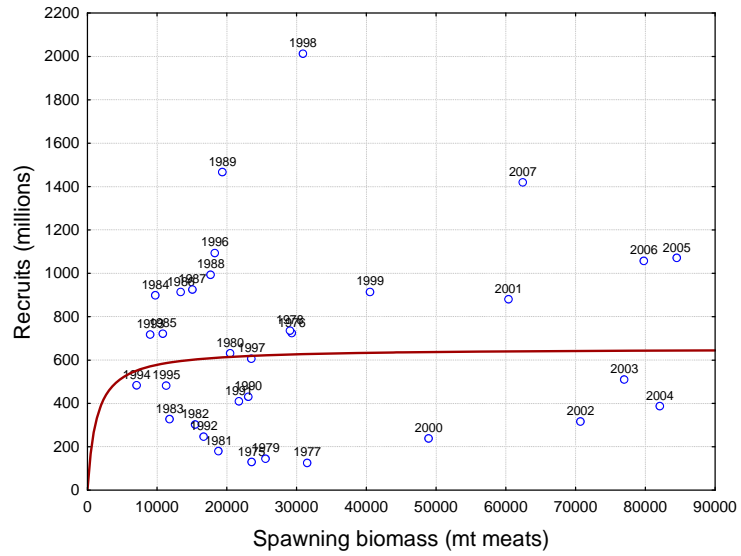


Figure B-55. Histograms of the assumed distributions of natural mortality in (a) Georges Bank and (b) the Mid-Atlantic.

(a)



(b)

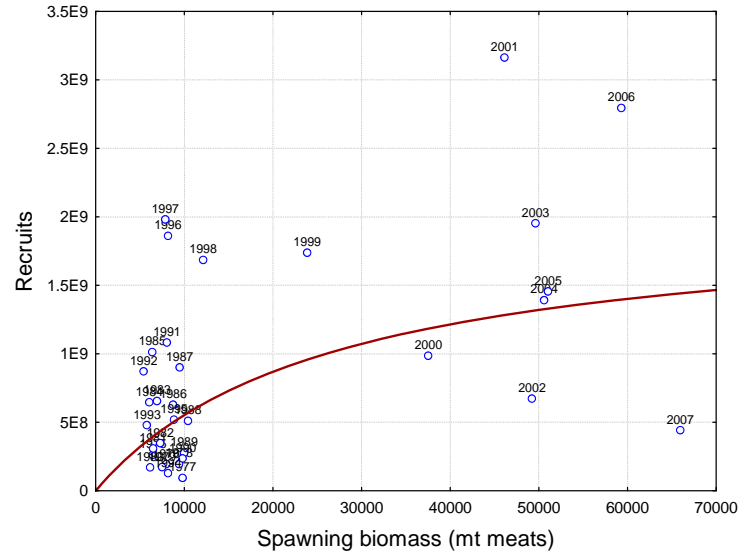
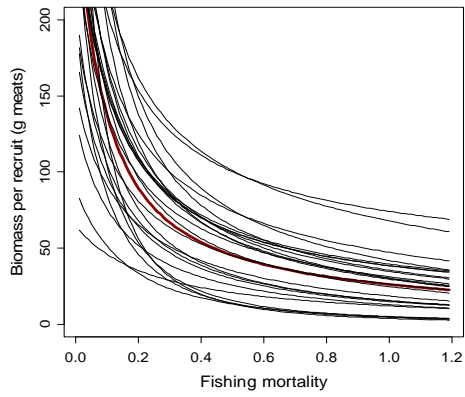
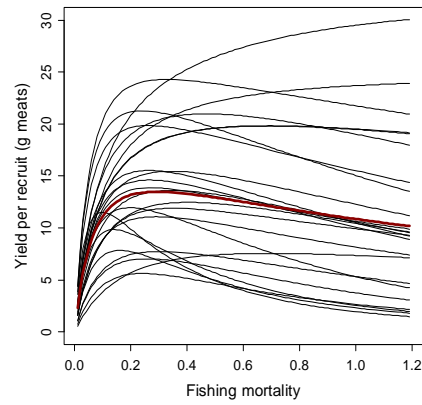


Figure B-56. Plots of stock-recruit relationships together with fits to Beverton-Holt stock-recruit curves for (a) Georges Bank and (b) Mid-Atlantic.

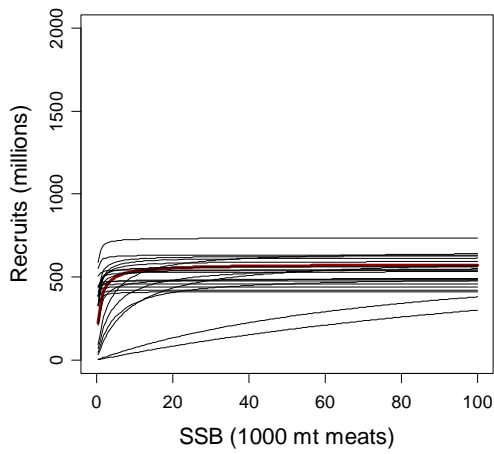
(a)



(b)



(c)



(d)

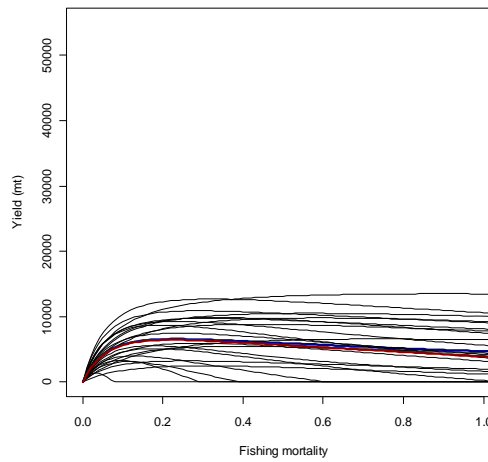


Figure B-57. Plots of (a) yield per recruit, (b) biomass per recruit, (c) stock-recruit and (d) yield from the SYM model for Georges Bank. The heavy red line is the mean of 50000 simulations, the blue line the median (yield only). 25 example plots from individual simulations are also shown.

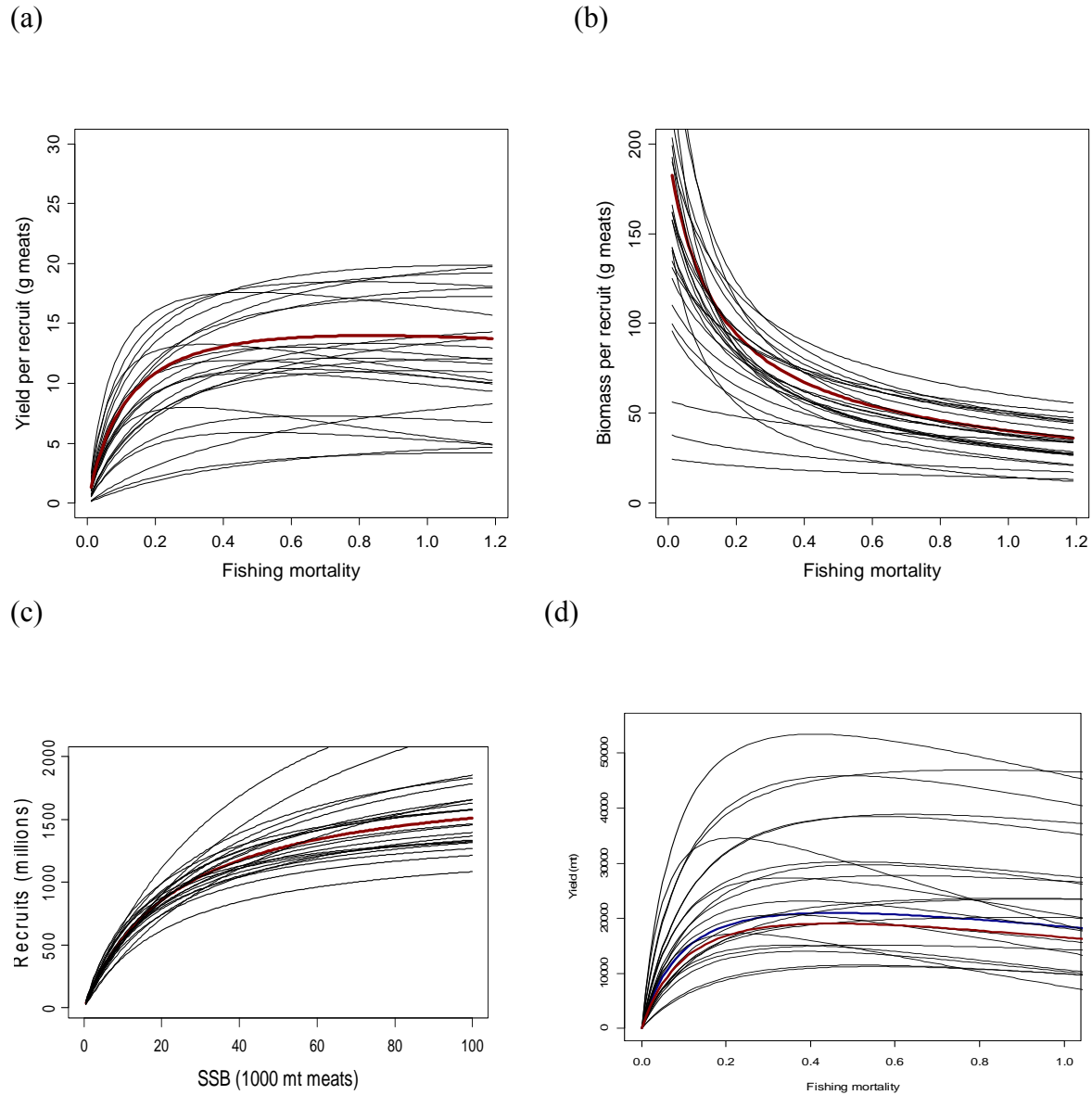
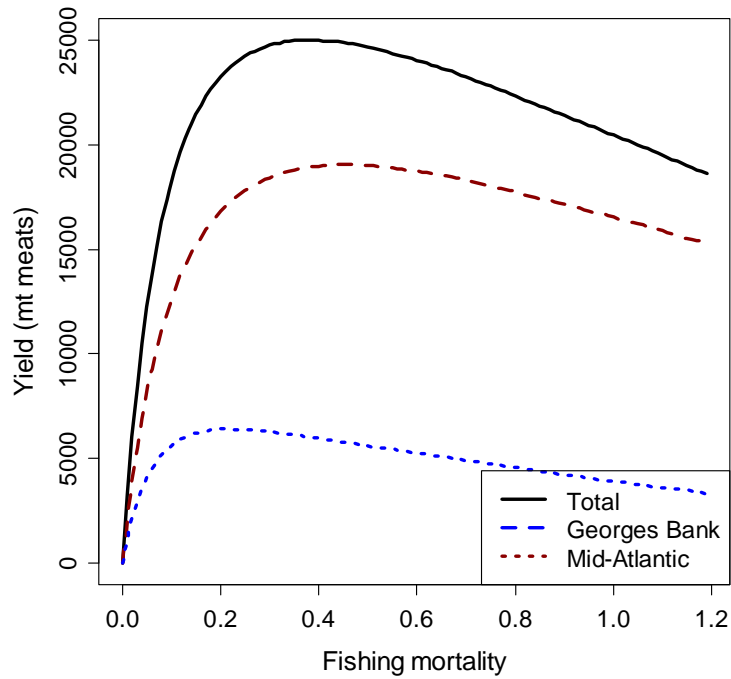
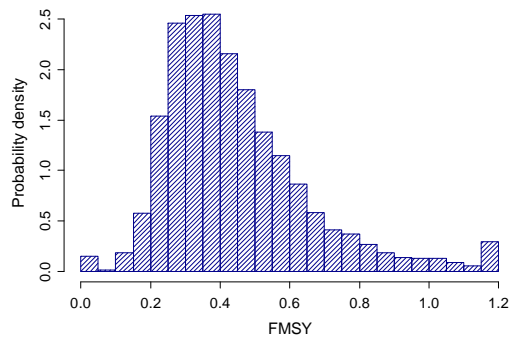


Figure B-58. Plots of (a) yield per recruit, (b) biomass per recruit, (c) stock-recruit and (d) yield from the SYM model for the Mid-Atlantic. The heavy red line is the mean of 50000 simulations, the blue line the median (yield only). 25 example plots from individual simulations are also shown.

(a)



(b)



(c)

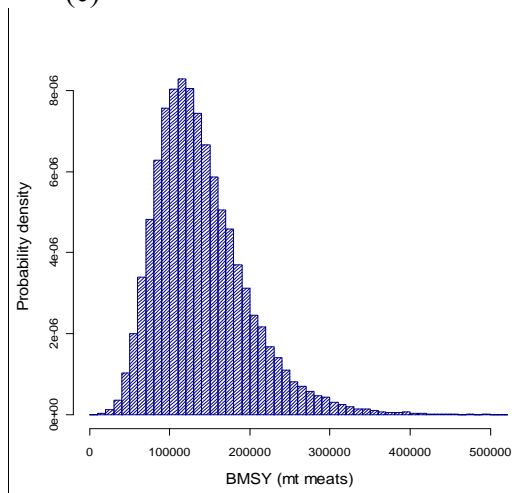


Figure B-59. (a) Median yield curves for Georges Bank, Mid-Atlantic, and overall yield. (b) Probability densities for whole-stock F_{MSY} and (c) probability densities for whole-stock B_{MSY} obtained from the SYM model.

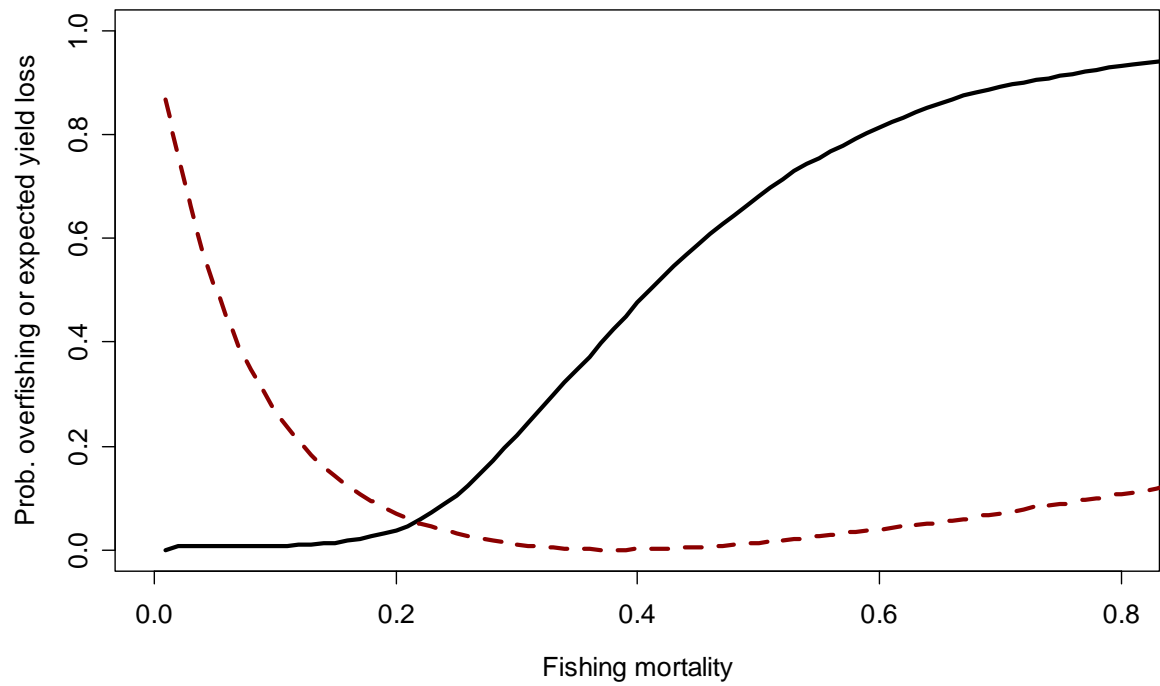


Figure B-60. The probability of overfishing as a function of realized fishing mortality (black solid line) and the loss of expected yield relative to that obtained at F_{MSY} .

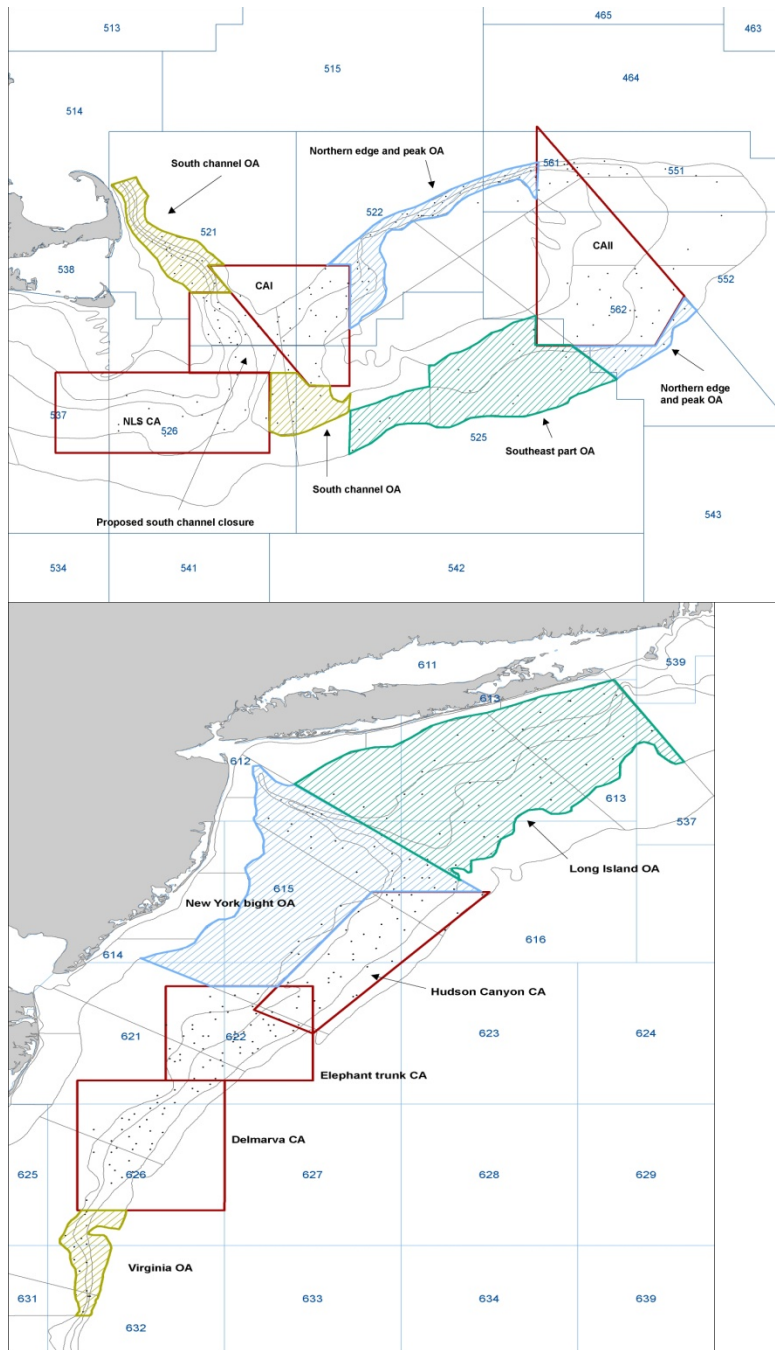
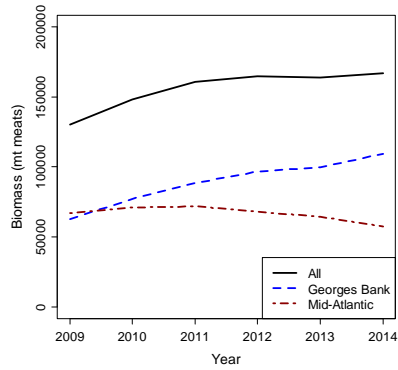
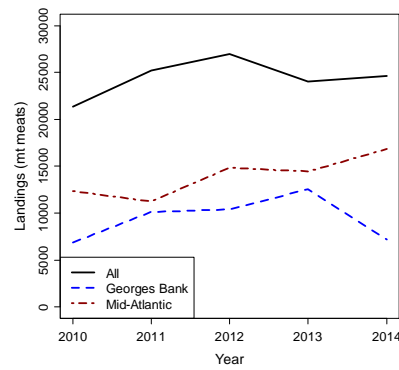


Figure B-61. Map of the 16 SAMS model areas. Each of the three Georges Bank closed areas are split into access and essential fish habitat areas, consistent with current management. Shellfish survey strata, NAFO statistical areas (rectangles), and 2009 NEFSC survey stations (dots) are also shown

(a)



(b)



(c)

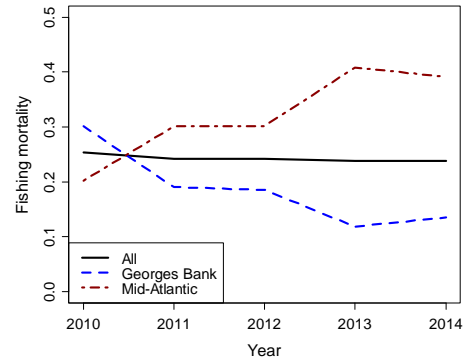
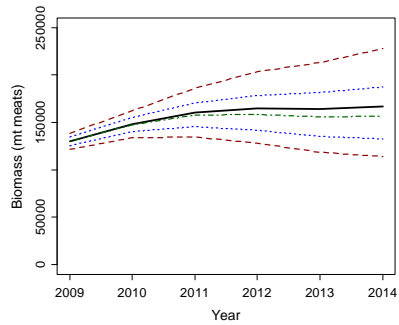


Figure B-62. Mean projected (a) biomass, (b) landings and (c) fishing mortality for Georges Bank (blue dashed line), Mid-Atlantic (red dot-dashed line) and overall (solid black line).

(a)



(b)

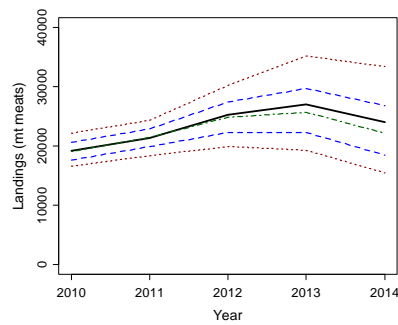


Figure B-63. The mean (black solid line), 10th and 90th percentiles (red dashed lines), 25th and 75th percentiles (dotted blue lines) and median (green dashed-dotted line) of projected overall (a) biomass and (b) landings.

Appendix B1: Invertebrate Subcommittee members

Invertebrate Subcommittee members who participated and contributed to the sea scallop assessment for SARC-50 at meetings during February-May, 2010. Participants are listed in alphabetical order by institution and then by last name.

Institution	Participants
Advanced Habitat Imaging Consortium (HabCam Group)	Karen Bolles, Patricia Keeting, Richard Taylor, Norman Vine
Department of Fisheries and Oceans, Halifax, N.S., Canada	Bob Mohn, Stephen Smith
Department of Fisheries and Oceans, Moncton, NB, Canada	Leslie-Anne Davidson
Fisheries Survival Fund	Ron Smolowitz
Maine Department of Marine Resources, Boothbay Harbour	Kevin Kelly
New England Fishery Management Council (NEFMC)	Andy Applegate, Deirdre Boelke, Jess Melgey
Northeast Fisheries Science Center, Woods Hole MA (NEFSC)	Jessica Blaylock, Larry Brady, Toni Chute, Dvora Hart (Assessment Lead), Daniel Hennen, Larry Jacobson (Invertebrate Subcommittee Chair), Chris Legault, Tim Miller, Victor Nordahl, Paul Rago, Alan Seaver, Jiashen Tang, Mark Terceiro
School for Marine Science and Technology, University of Massachusetts, Dartmouth (SMAST)	Jon Carey, Susan Inglis, Cate O'Keefe, Carly Mott, Kevin Stokesbury, Yuying Zhang
School of Marine Sciences, University of Maine, Orono	Sam Truesdell
Virginia Institute of Marine Science, College of William and Mary (VIMS)	Bill DuPaul, David Rudders
Woods Hole Oceanographic Institution (WHOI), Woods Hole, MA	Scott Gallager, Amber York

Appendix B2: Sea scallop discard estimates.

Jessica Blaylock, Northeast Fisheries Science Center, Woods Hole, MA.

Discard estimates for Atlantic sea scallop (*Placopecten magellanicus*) were calculated using the method described with the Standardized Bycatch Reporting Methodology (SBRM) (Wigley et al. 2007). This approach differs from that used in the previous assessment for this stock.

This paper presents updated sea scallop discard estimates for nine fleets, followed by a comparison of these values with the estimates presented at the previous assessment as part of the SAW 45 (NEFSC 2007).

Methods

Estimates of Atlantic sea scallop discards (mt meats) were derived for nine fleets: Georges Bank open and closed scallop dredge, and Mid-Atlantic Bight open and closed scallop dredge for the 1994 to 2009 time period, and Mid-Atlantic Bight scallop trawl, Georges Bank and Mid-Atlantic Bight small-mesh otter trawl, and Georges Bank and Mid-Atlantic Bight large-mesh otter trawl for the 1989 to 2008 time period.

In the scallop dredge analysis, observer and Vessel Trip Report (VTR) trips were partitioned into fleets using four classification variables: calendar quarter, gear type, area fished, and access area. In the scallop trawl and otter trawl analysis, observer and dealer trips were partitioned into fleets using the following four classification variables: calendar quarter, gear type, area fished, and mesh. Trips were not partitioned by trip category ('limited' versus 'general', for scallop dredge and scallop trawl) due to small sample size over the time series. Calendar quarter was based on landed date and used to capture seasonal variations in fishing activity. Gear type was based on Northeast gear codes (scallop dredge: negear 132; scallop trawl: negear 052; otter trawl: negear 050). Trips for which gear was unknown were excluded. Two broad geographical regions are defined for area fished based on statistical area: areas 520-562 constituted the Georges Bank (GBK) area, and areas 600 and above constituted the Mid-Atlantic Bight (MAB) area. For scallop dredge, two access area categories were used: 'open' and 'closed', where 'closed' includes all trips fishing in one of the scallop access areas (Closed Area I, Closed Area II and Nantucket Lightship in the GBK region; Hudson Canyon, Virginia Beach, Elephant Trunk, and Delmarva in the MAB region). Observer trips were assigned to the access area category based on program code, and VTR trips were assigned based on latitude and longitude. Finally, two mesh size groups were formed for otter trawl: small (mesh less than 5.5 inches) and large (5.5 inch mesh and greater).

Discards were estimated using a combined d/k_{all} ratio estimator (Cochran 1963), where d is discarded pounds of sea scallops and k_{all} is kept pounds of all species, calculated from Northeast Fishery Observer Program (NEFOP) data. Discard weight was derived by multiplying the d/k_{all} ratio of each fleet by the corresponding VTR or commercial landings (Wigley et al. 2007). Coefficients of variation (CV) were calculated as the ratio of the standard error of the discards divided by the discards.

In cases where limited observer data were available (i.e. two or less observed trips in a calendar quarter), an imputation approach was used to 'fill in' the missing (or incomplete) information using data from adjoining strata. In this imputation procedure, the temporal stratification (i.e., calendar quarter) was relaxed to entire year, recognizing that seasonal variations may occur that will thus not be accounted for. Numbers of annual observed trips by fleet are summarized in Table 1.

Comparison with previous discard estimates

Estimates of Atlantic sea scallop discards presented at SAW 45 were calculated for trips stratified by target species using the ratio of pounds of scallops caught for every pound of the target species landed (NEFSC 2007). Because of the different estimation method and stratification scheme, a direct comparison between these estimates and the current discard estimates was not possible.

To perform a more general comparison, sea scallop discard estimates from SAW 45 and current estimates were separated into two groups: estimated discards from trips using scallop gear (scallop dredge and scallop trawl), and estimated discards from trips using otter trawl gear. In the first group, scallop gear discard estimates from SAW 45 included the total 'estimated discards on directed scallop trips' (NEFSC 2007) for 1992-2006, which are assumed to be discards from trips that used mostly scallop dredge and scallop trawl gear. Scallop gear discard estimates from the current assessment included the sum of scallop dredge discard estimates across areas for the period 1994-2003, and the sum of scallop dredge and scallop trawl discard estimates across areas and gear types for the time period 2004-2006. For the second group, otter trawl discard estimates from SAW 45 included the total 'estimated discards in non-scallop otter trawl fisheries' (NEFSC 2007) for 1994-2006. Otter trawl discard estimates from the current assessment included the sum of otter trawl discard estimates across areas and mesh sizes for the period 1994-2006. For each group, a plot of SAW 45 sea scallop discard estimates and current estimates over time were produced. In addition, a third plot containing the sum of the SAW 45 estimates and the sum of current estimates described above was produced for illustrative purposes.

Discard to landings

To evaluate the proportion of estimated sea scallop discards to landings, the sum of the current discard estimates for scallop dredge was compared to the sum of estimated landings from Georges Bank, Southern New England, and Mid-Atlantic Bight (SAW 50) for the 1994 to 2009 time period.

Results and Discussion

Annual Atlantic sea scallop discard estimates by fleet are presented in Table 1 and Table 2. This analysis indicates that during the 1994 to 2008 time period, sea scallops were primarily discarded in the scallop dredge fleets with higher discarding in the 'open' category fleets. For 2008, estimated discards from the Mid-Atlantic Bight open and closed scallop dredge fleets were 201 and 52 mt meats, respectively. Estimated discards from the Georges Bank open and closed scallop dredge fleets were 214 and 96 mt meats, respectively. Discard estimates for the other five fleets for the same year ranged from less than 1 mt meats (Georges Bank small-mesh otter trawl) to 45 mt meats (Mid-Atlantic Bight large-mesh otter trawl).

The discard estimation presented here used a broad stratification approach. In addition, limitations are inherent in the use of VTR data for trip assignment to the 'access area' category because of missing or inaccurate position data. Consequently, these results should be considered as preliminary.

Comparison with previous discard estimates

Figure 1 shows updated sea scallop discard estimates compared with estimates presented at SAW 45. Accounting for missing estimates in some years (i.e. 2000, 2001), trends of discards are generally similar between the two sets of estimates. Values of discard estimates from trips using scallop gear are comparable between the two sets, while current estimate values from trips using otter

trawl gear are lower than those presented at SAW 45 in most years. Both sets of sea scallop discard estimates indicate that a majority of discarding occurred in trips using scallop gear for the 1994 to 2006 time period.

Figure 2 indicates that trends in SAW 45 and current estimates are similar and resemble those observed with estimated sea scallop discards from trips using scallop gear (Figure 1A). This was expected, given the relatively small magnitude of the estimated discards from trips using otter trawl gear (Figure 1B).

These results provide an approximate comparison of current sea scallop discard estimates with those presented at SAW 45 and should be considered with caution given the different approaches used to obtain each set of estimates, as well as the missing estimates in some years. In particular, Figure 2 is meant to provide a general perspective of sea scallop discard estimates over the 1994 to 2006 time period, and exact values should not be used to convey total scallop discarding.

Discard to landings

Current estimates of discards and landings from 1994 to 2009 are presented in Figure 3. Total catch (discards plus landings) averaged 6,739 mt meats between 1994 and 1998. Catch increased in the following six years to peak at 31,348 mt meats in 2004, and averaged 26,490 mt meats from 2005 to 2009. Discards generally represent a small portion of total catch, with discard-to-landing ratios ranging from 0.006 in 1997 to 0.099 in 2003.

These results represent estimated sea scallop discards and landings in weight (mt meats). It is likely that discard-to-landing ratios of numbers would be higher because of the different size distribution of discarded scallops compared to that of landed scallops.

Acknowledgements

I wish to thank all the NEFOP observers for their diligent efforts to collect the discard information used in this analysis.

References

- Cochran, W.L. 1963. *Sampling Techniques*. J. Wiley and Sons. New York.
- Northeast Fisheries Science Center (NEFSC). 2007. 45th Northeast Regional Stock Assessment Workshop (45th SAW): 45th SAW assessment report. US Dep. Commer., Northeast Fish. Sci. Cent. Ref.Doc. 07-16; 370 p. Available online: <http://www.nefsc.noaa.gov/publications/crd/crd0716/index.htm>
- Wigley, S.E., P.J. Rago, K.A. Sosebee, and D.L. Palka. 2007. *The Analytic Component to the Standardized Bycatch Reporting Methodology Omnibus Amendment: Sampling Design, and Estimation of Precision and Accuracy (2nd Edition)*. US Dep. Commer., Northeast Fish. Sci. Cent. Ref. Doc. 07-09; 156 p. Available online: <http://www.nefsc.noaa.gov/nefsc/publications/crd/crd0709/index.htm>

Appendix B2-Table 1A. Number of observed trips, sea scallop discards (mt meats) and coefficient of variation (CV) by the GBK open scallop dredge and GBK closed scallop dredge fleets, 1994-2009. Discards were not estimated for the GBK open scallop dredge fleet in 2000 and 2001 due to small sample size.

GBK open scallop dredge				GBK closed scallop dredge			
YEAR	Trips	Discards (mt meats)	CV	YEAR	Trips	Discards (mt meats)	CV
1994*	7	1	0.78	1994	n/a		
1995*	6	43	0.58	1995	n/a		
1996	15	103	0.37	1996	n/a		
1997*	11	26	0.67	1997	n/a		
1998*	9	6	0.46	1998	n/a		
1999*	8	51	0.68	1999*	15	53	0.26
2000	2			2000	226	246	0.03
2001	2			2001	16	28	0.16
2002*	11	100	0.39	2002	n/a		
2003*	14	177	0.45	2003	n/a		
2004*	16	34	0.32	2004	30	25	0.19
2005	41	372	0.36	2005	66	40	0.27
2006*	56	796	0.16	2006	79	41	0.26
2007	53	193	0.30	2007	127	41	0.26
2008	73	201	0.23	2008	140	52	0.12
2009	58	265	0.33	2009	23	24	0.30

* Imputed data were used for discard estimation for these years.

n/a: not applicable

Appendix B2-Table 1B. Number of observed trips, sea scallop discards (mt meats) and coefficient of variation (CV) by the MAB open scallop dredge and MAB closed scallop dredge, 1994-2009. Discards were not estimated for the MAB open scallop dredge fleet in 2001 due to small sample size.

MAB open scallop dredge				MAB closed scallop dredge			
YEAR	Trips	Discards (mt meats)	CV	YEAR	Trips	Discards (mt meats)	CV
1994	16	276	0.59	1994		n/a	
1995*	20	341	0.28	1995		n/a	
1996	23	22	0.72	1996		n/a	
1997*	18	8	1.15	1997		n/a	
1998*	16	42	0.66	1998		n/a	
1999*	8	7	0.56	1999		n/a	
2000	28	749	0.33	2000		n/a	
2001	3			2001	85	301	0.09
2002*	13	1,446	0.19	2002	74	150	0.10
2003	62	2,206	0.14	2003	46	119	0.12
2004	143	1,856	0.13	2004	92	503	0.10
2005	166	367	0.29	2005	54	38	0.21
2006*	87	71	0.39	2006*	6	3	0.49
2007	85	66	0.40	2007	93	63	0.22
2008	89	214	0.54	2008	337	96	0.14
2009	118	549	0.16	2009	233	199	0.16

* Imputed data were used for discard estimation for these years.

n/a: not applicable

Appendix B2-Table 1C. Number of observed trips, sea scallop discards (mt meats) and coefficient of variation (CV) by the MAB scallop trawl fleet, 1989-2008. Discards were not estimated prior to 2004 due to small sample size.

MAB scallop trawl			
YEAR	Discards		CV
	Trips	(mt meats)	
1989			
1990			
1991			
1992			
1993			
1994			
1995			
1996			
1997			
1998			
1999			
2000			
2001	4		
2002	1		
2003			
2004*	44	99	0.25
2005	137	61	0.13
2006*	30	150	0.33
2007	34	15	0.58
2008*	38	7	0.61

* Imputed data were used for discard estimation for these years.

Appendix B2-Table 1D. Number of observed trips, sea scallop discards (mt meats) and coefficient of variation (CV) by the GBK small-mesh otter trawl, and MAB small-mesh otter trawl fleets, 1989-2008.

GBK small-mesh otter trawl				MAB small-mesh otter trawl			
YEAR	Trips	Discards (mt meats)	CV	YEAR	Trips	Discards (mt meats)	CV
1989	64	2	0.53	1989	34	213	0.39
1990	31	<1	1.22	1990	47	8	0.44
1991	68	<1	0.80	1991	78	11	2.05
1992	42	<1	0.69	1992	47	6	0.53
1993*	15	<1	0.79	1993*	7	14	1.12
1994*	10	23	0.80	1994*	11	41	1.03
1995*	10	<1	1.40	1995	63	71	0.23
1996*	11	0	0.00	1996	78	15	1.62
1997*	19	<1	0.88	1997*	49	1	2.83
1998*	5	<1	1.61	1998*	26	5	1.43
1999*	8	<1	2.62	1999	33	21	1.07
2000*	17	<1	0.49	2000	34	2	0.95
2001*	14	<1	0.64	2001	54	<1	8.88
2002*	33	<1	0.81	2002	32	68	0.34
2003	54	<1	1.10	2003	72	18	0.75
2004	107	2	0.99	2004	246	6	0.38
2005	191	<1	0.47	2005	166	4	0.33
2006	59	<1	0.55	2006	144	14	2.50
2007	62	<1	1.54	2007	216	5	0.55
2008	49	<1	0.48	2008	149	10	0.54

* Imputed data were used for discard estimation for these years.

Appendix B2-Table 1E. Number of observed trips, sea scallop discards (mt meats) and coefficient of variation (CV) by the GBK large-mesh otter trawl, and MAB large-mesh otter trawl fleets, 1989-2008. Discards were not estimated for MAB large-mesh otter trawl prior to 1992 due to small sample size.

GBK large-mesh otter trawl				MAB large-mesh otter trawl			
YEAR	Trips	Discards (mt meats)	CV	YEAR	Trips	Discards (mt meats)	CV
1989	27	1	0.88	1989	1		
1990	33	1	0.72	1990			
1991	34	4	0.54	1991	4		
1992	35	<1	1.10	1992*	14	4	0.40
1993*	22	3	0.60	1993*	7	0	0.00
1994	27	<1	1.24	1994*	13	230	0.57
1995	60	<1	0.42	1995	52	107	0.80
1996	33	<1	0.78	1996*	16	<1	0.57
1997*	21	<1	1.00	1997*	5	0	0.00
1998*	7	<1	0.67	1998*	13	3	1.79
1999*	11	<1	1.36	1999*	5	0	0.00
2000	26	<1	0.54	2000	27	9	1.54
2001	51	<1	0.45	2001*	44	10	1.02
2002	77	2	0.60	2002*	37	8	2.37
2003	161	3	0.76	2003*	11	42	0.92
2004	314	42	0.35	2004	91	19	0.32
2005	952	10	0.18	2005	87	2	0.80
2006	457	30	0.37	2006	63	16	0.72
2007	463	5	0.25	2007	160	13	0.54
2008	562	6	0.21	2008	127	45	1.02

* Imputed data were used for discard estimation for these years.

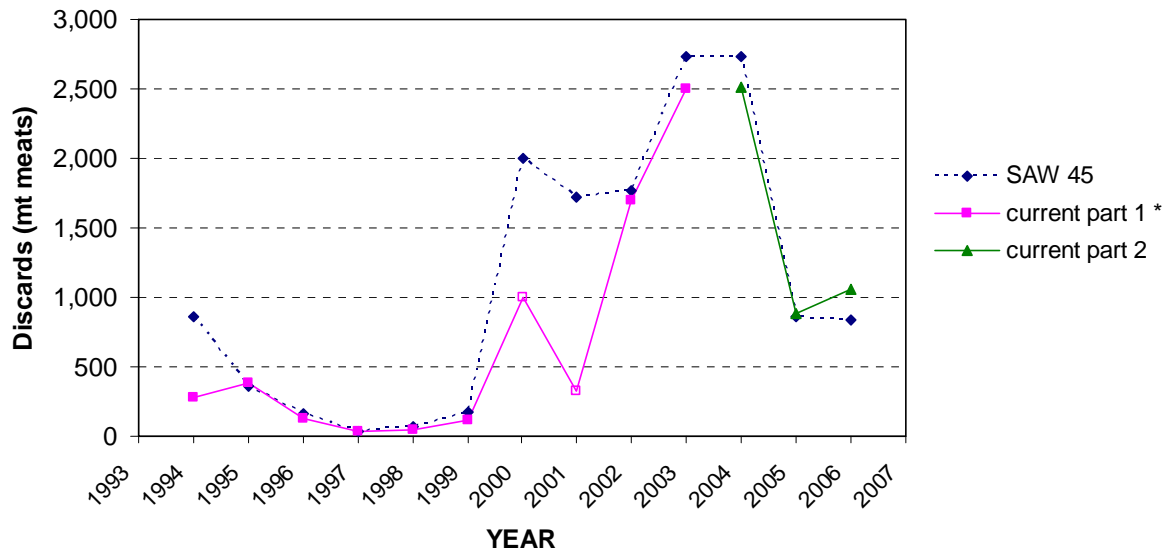
Appendix B2-Table 2. Summary of sea scallop discard estimates (mt meats) from Table 1 by region, 1994-2009.

Georges Bank (GBK)						Mid-Atlantic Bight (MAB)						
YEAR	open scallop dredge	closed scallop dredge	small-mesh otter trawl	large-mesh otter trawl	Total	YEAR	open scallop dredge	closed scallop dredge	scallop trawl	small-mesh otter trawl	large-mesh otter trawl	Total
1994	1	n/a	23	1	24	1994	276	n/a	*	41	230	547
1995	43	n/a	0	0	43	1995	341	n/a	*	71	107	519
1996	103	n/a	0	0	103	1996	22	n/a	*	15	1	38
1997	26	n/a	0	0	26	1997	8	n/a	*	1	0	9
1998	6	n/a	0	0	6	1998	42	n/a	*	5	3	50
1999	51	53	0	0	104	1999	7	n/a	*	21	0	28
2000	*	246	0	1	247	2000	749	n/a	*	2	9	760
2001	*	28	1	0	29	2001	*	301	*	1	10	312
2002	100	n/a	0	2	103	2002	1,446	150	*	68	8	1,673
2003	177	n/a	0	3	181	2003	2,206	119	*	18	42	2,386
2004	34	25	2	42	103	2004	1,856	503	99	6	19	2,482
2005	372	40	0	10	421	2005	367	38	61	4	2	473
2006	796	41	1	30	868	2006	71	3	150	14	16	254
2007	193	41	0	5	240	2007	66	63	15	5	13	162
2008	201	52	0	6	259	2008	214	96	7	10	45	372
2009	265	24	+	+	289	2009	549	199	+	+	+	748

* No discard estimate due to small sample size.

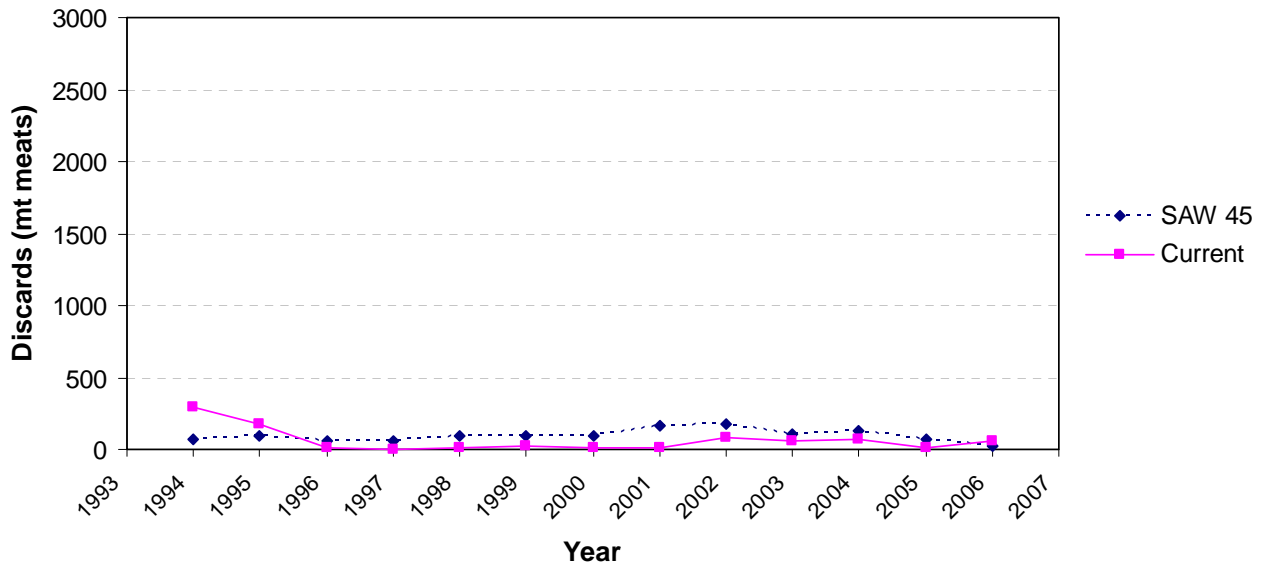
+ No discard estimate because 2009 data not yet available.

n/a: not applicable

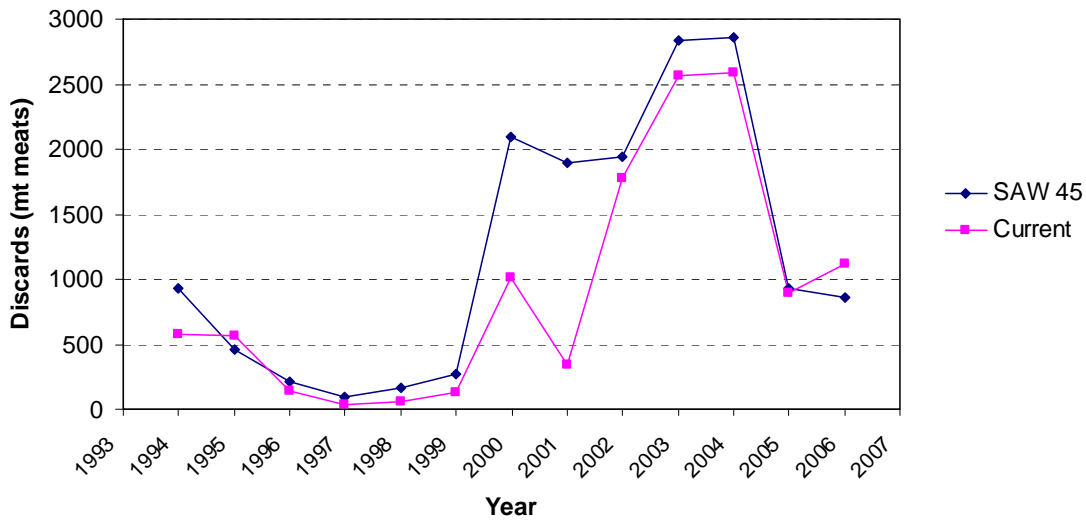


* Discards in 2000 and 2001 are underestimates because no discards were estimated for GBK open scallop dredge in 2000 and 2001, and MAB open scallop dredge in 2001 due to small sample size.

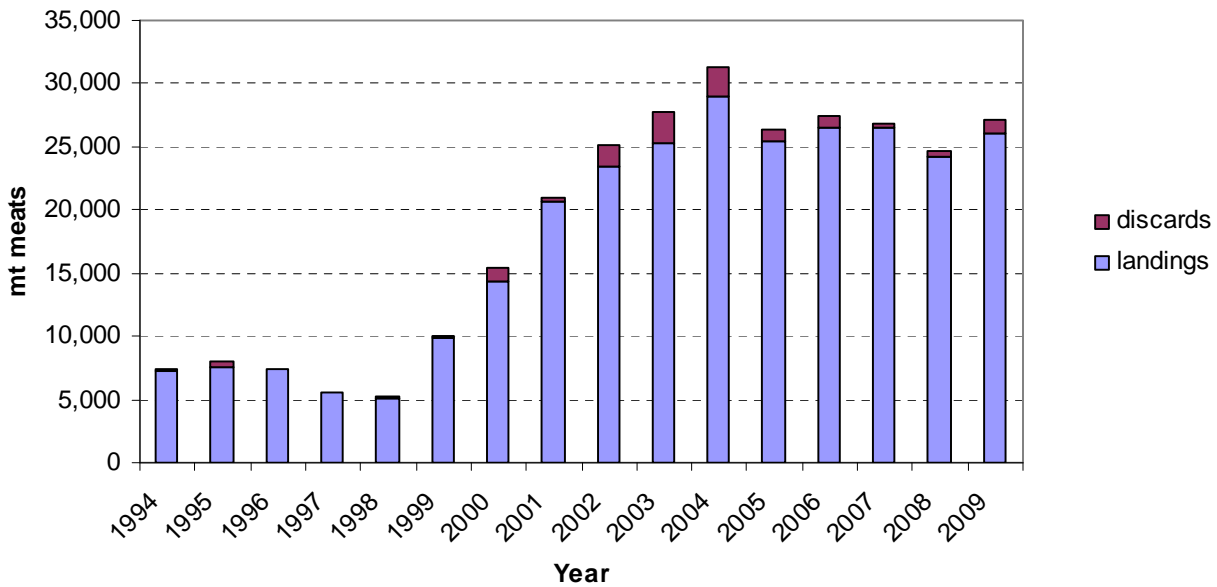
Appendix B2-Figure 1A. SAW 45 and current estimated sea scallop discards from trips using scallop gear (mt meats), 1994-2006. Current part 1 includes estimates from scallop dredge trips only, while part 2 includes estimates from scallop dredge and scallop trawl.



Appendix B2-Figure 1B. Estimated sea scallop discards from trips using otter trawl gear (mt meats), 1994-2006.



Appendix B2-Figure 2. Sum of the SAW 45 and current estimated sea scallop discards (mt meats) presented in Figure 1 (estimated discards from trips using scallop gear, and estimated discards from trips using other trawl gear), 1994-2006. This figure is for illustration purposes only and is not meant to convey exact total sea scallop discard estimates.



Appendix B2-Figure 3. Estimated scallop landings (SAW 50) and current estimated sea scallop discards from scallop dredge fleets (mt meats), 1994-2009.

Appendix B3: Comparison of scallop density estimates using the SMAST scallop video survey data with a reduced view field and reduced counts of individuals per image.

O'Keefe, Catherine E.¹, Jon D. Carey¹, Larry D. Jacobson², Deborah R. Hart² and Kevin D.E. Stokesbury¹

¹University of Massachusetts Dartmouth
School for Marine Science and Technology
200 Mill Road, Suite 325
Fairhaven, MA 02719

²National Marine Fisheries Service
Northeast Fisheries Science Center
166 Water Street
Woods Hole, MA 02543

Introduction

The University of Massachusetts Dartmouth School for Marine Science and Technology (SMAST) has conducted an annual continental shelf-wide video survey for scallops in the Mid-Atlantic and Georges Bank areas since 2003. The survey provides information about abundance, density, shell height distribution and spatial aggregation of scallops in the Mid Atlantic Bight (MAB) and Georges Bank (GBK) regions of the scallop resource.

In this analysis, we examined alternative methods for calculating scallop density from SMAST survey images. To address potential bias in density calculations resulting from scallops on an edge of the visible image, we compared different methods of counting scallops and different methods for expanding the image view area. For this assessment, the Invertebrate Subcommittee decided to calculate density using all scallops visible in images (as before) and an assumed view field equal to the area calculated from the dimensions of the sample frame plus $\frac{1}{2}$ of mean shell height in each area for each year. This increased density estimates by 1-3% in the MAB and GBK stock areas. In the future, densities will be calculated both by excluding scallops that lie on the top and right edges of the video images and using the area within the sampling frame and by including all visible scallops and adjusting the dimensions of the sample frame based on mean shell by area.

Methods

Original densities for the Mid Atlantic Bight and Georges Bank scallop stocks were calculated according to Stokesbury (2002) and Stokesbury et al. (2004). All scallops in each image were counted. The large camera view area of 2.84m² (1.986m x 1.430m) was expanded to account for scallops that were positioned on the edges of the image. The expansion of the view area was calculated based on a mean shell height of 112mm as observed in the 1999 Nantucket Lightship Closed Area video survey. We added half of the mean shell height to each edge of the camera view field to expand the area to 3.235m² ((1.986m + (2*56mm))*(1.430 + (2*56mm))), see Figure 1. Mean densities and standard errors are calculated according to Cochran (1977) for a two-stage sampling design. Density estimates represent the mean of the mean scallops per station, where there are 4 quadrats per station. The mean of the total sample is:

$$(1) \quad \bar{x} = \sum_{i=1}^n \left(\frac{\bar{x}_i}{n} \right)$$

where:

n = primary sample units (stations)

\bar{x}_i = sample mean per element (quadrat) in primary unit i (stations)

\bar{x} = the grand mean over the two stages of sampling.

The standard error of this mean is approximately:

$$(2) \quad S.E.(\bar{x}) = \sqrt{\frac{1}{n}(s^2)}$$

where:

$$s^2 = \sum_{i=1}^n (\bar{x}_i - \bar{x})^2 / (n - 1) = \text{variance among primary unit (stations) means.}$$

This simplified version of the two-stage variance is possible when the sampling fraction n/N is small, hundreds of m^2 are sampled compared with millions of m^2 in the area (Cochran, 1977; Krebs, 1999).

Experimental evaluation

We examined density estimates in a sample of images based on removing scallop counts from two edges of the image and not including an expansion adjustment to the image. By removing the counts from two edges of the image, the scallop counts are independent of scallop shell height. Counting scallops on only one vertical and one horizontal edge of each image reduces potential bias for inclusion of a greater number of small scallops than large scallops. We analyzed images from the Elephant Trunk Closed Area (ETCA) between 2003 and 2009 from our broad-scale 3 nm video survey. We counted scallops in the image with any portion of the animal along the top and right edges of the image. We subtracted the counts of the animals on these edges from the total count of animals in the image. We calculated density based on the actual camera view field without any expansion factor (2.84 m^2 ; Table 1). This method of calculation is consistent with land-based ecological methods (Krebs, 1999). Results showed that densities calculated in this manner were slightly higher than the original estimates. Interestingly, the decreases in numbers counted tends to be offset by the increases in area resulting in a slight increase in calculated density.

Ratio estimator approach for potential use in this assessment

We also used a ratio estimator (Cochran, 1977; Krebs, 1999) to determine the relative difference in densities between the original and reduced count density calculations. Again, we examined 2003-2009 ETCA scallop data (Table 1). The ratio estimator for the original densities and the densities that excluded scallop counts on two edges of the image is:

$$(3) \quad \hat{R} = \frac{y}{x}$$

where:

y = reduced mean density
 x = original mean density.

Historical density data might be adjusted approximately using the ratio estimate (i.e. adjusted density = dR). We calculated the variance in adjusted density estimates using an exact formula for the ratio of two independent variables (Goodman, 1960):

$$(4) \quad V(dR) = d^2V(R) + R^2V(d) + V(d)V(R)$$

where:

$V(x)$ = variance of x
 d = original density estimate
 R = ratio estimate

We also pooled the data for all years and calculated the ratio between the original scallop counts and the counts that excluded the top and right edges. We then applied this overall ratio to each year to calculate a new density for each year (Table 1). We calculated variance in the same way as the individual year variance estimates.

Expanded area approach for potential use in this assessment

Finally, we examined an alternative approach to density calculations that incorporated an image view expansion based on shell height by area. We determined the annual mean shell height for 2003 - 2009 in ETCA and recalculated density estimates by changing the camera view area adjustment. Instead of using the Nantucket Lightship Closed Area 1999 mean shell height (112mm) as a constant for expanding the camera view field, we used the mean shell height by area, by year (Figure 2). The camera view field expansion varied by year based on the equation:

$$(5) \quad ViewArea = (1.986m + (2 * (\frac{meanSH}{2}))) * (1.430m + (2 * (\frac{meanSH}{2})))$$

where:

meanSH = mean shell height.

For this analysis, we included all scallop counts and calculated the mean of the mean scallops per station, where each station had 4 quadrats (Table 1). The adjusted view field method did not include increases in variance so that uncertainty in the adjusted figures may be understated.

Comparison of methods applied to the same sample data

We applied the ratio and camera view field adjustments to the video survey data for the Mid Atlantic Bight (MAB) and Georges Bank (GBK) 3 nm survey estimates from 2003 through 2009. We compared the original density estimates with the overall ratio adjusted estimate and the mean shell height adjusted camera view area adjustment (Table 2).

Results

Table 1 and Figure 3 show a comparison of the original, yearly ratio adjusted, overall ratio adjusted and shell height adjusted density estimates for the ETCA from 2003-2009.

Tables 2 and 3 show the mean shell height adjusted density, abundance and biomass estimates for the MAB and GBK scallop resource areas from 2003-2009 for large and small cameras. On average, the density estimates increased by 1-3%.

Conclusion

It would have been ideal to reexamine all video images collected during 2003-2009 to exclude sea scallops along two edges of the view field from counts, and compute densities using the actual area of the sample frame, but this was not possible in time for the assessment. The only practical alternatives were to use either the ratio estimators or adjusted view field approach to correct the overall densities for each region and year.

The Invertebrate Subcommittee considered both approaches and decided to use the adjusted view field method because it accommodated differences among years in mean shell height, which may be important. For adjusting the stock assessment data, the adjusted view field approach was based on the average size of sea scallops in each area and year for the survey as a whole, rather than the average size in each image. The two types of adjustment factors were similar but no rigorous comparison of the two approaches was carried out.

Future research will include counting scallops that lie on the top and right edges of the image and subtracting those counts from the count of total scallops in the image. We will compare density estimates that include all counts with the reduced count estimates.

References

- Stokesbury, K.D.E., B.P. Harris, M.C. Marino II and J.I. Nogueira. 2004. Estimation of sea scallop abundance using a video survey in off-shore USA waters. *Journal of Shellfish Research* 23:33-44.
- Stokesbury, K.D.E. 2002. Estimation of sea scallop abundance in closed areas of Georges Bank, USA. *Transactions of the American Fisheries Society* 131:1081-1092.
- Cochran, W.G. 1977. *Sampling Techniques*, 3rd Edition. John Wiley & Sons. New York. 330pp.
- Krebs, C.J. 1999. *Ecological Methodology*, 2nd Edition. Addison-Wesley Educational Publishers, Inc. Menlo Park, CA. 620pp.
- Goodman, L.A. 1960. On the Exact Variance of Products. *Journal of the American Statistical Association* 55 (292):708-713.

Appendix B3-Table 1. ETCA 2003-2009 Large camera original density, reduced count density, ratio adjusted density (reduced count/original count), overall ratio adjusted density and mean shell height adjusted density.

Year	Mean SH	SH Adj Area	Original Density	Reduced Count Density	Ratio Adj Density (R/O)	Overall Ratio Adj Density	SH Adj Density
2003	60	3.049	2.1859	2.4463	2.4463	2.3848	2.3196
2004	81	3.123	0.8507	0.9426	0.9426	0.9281	0.8812
2005	94	3.170	0.7485	0.8156	0.8156	0.8166	0.7638
2006	98	3.184	0.6336	0.6656	0.6656	0.6913	0.6437
2007	98	3.183	0.5965	0.6438	0.6438	0.6508	0.6063
2008	101	3.194	0.4934	0.5288	0.5288	0.5383	0.4998
2009	99	3.187	0.1813	0.1986	0.1986	0.1978	0.1840

Appendix B3-Table 2. Large camera area surveyed, mean shell height (mm), shell height adjusted view field (m²), shell height adjusted density, abundance, biomass and 95% CI of the density for the MAB and GBK stock areas from 2003-2009.

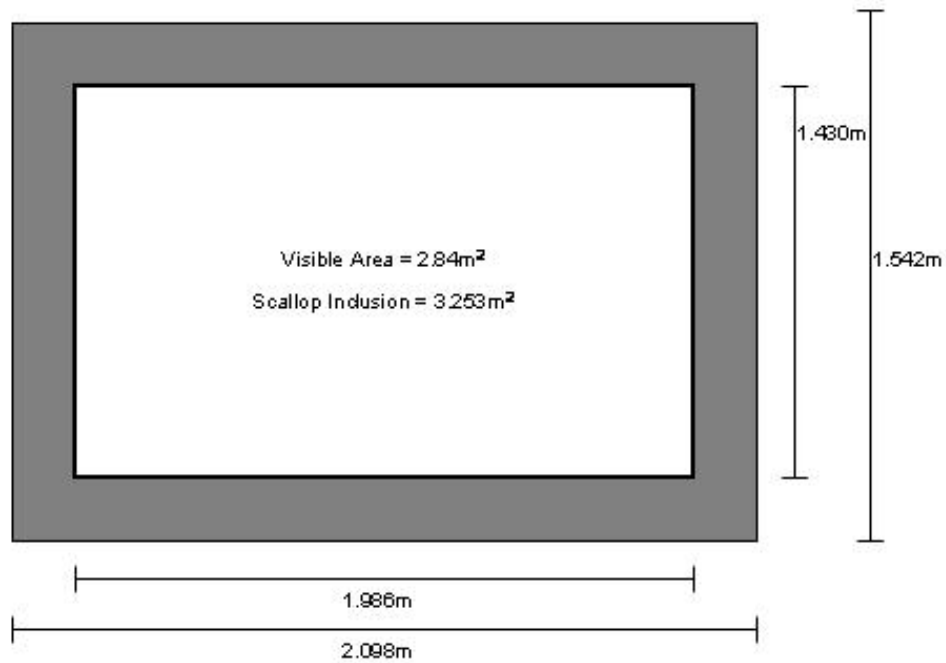
LARGE CAMERA

Year	Stations	Area Surveyed km ²	Mid Atlantic Bight					
			Mean SH mm	SH Adj Area m ²	SH Adj Density sc/m ²	Abundance	Biomass (mt)	95% CI
2003	804	24664	73.9	3.098	0.5047	12525017415.1	113401.8	0.16
2004	840	25591	90.4	3.157	0.2293	5945022074.1	80569.1	0.04
2005	864	26547	91.6	3.161	0.2148	5729979610.2	86770.8	0.05
2006	897	26918	92.0	3.163	0.1954	5411614262.4	78088.9	0.04
2007	941	28739	94.5	3.172	0.1826	5305430005.0	80333.9	0.03
2008	931	28184	91.4	3.161	0.1883	5412596845.3	85561.1	0.04
2009	928	28647	96.4	3.179	0.1366	3913262600.8	64727.5	0.02
Georges Bank								
2003	929	27906	102.1	3.199	0.1486	4260307453.6	89080.9	0.02
2004	935	28430	107.5	3.219	0.1223	3528997219.0	82852.3	0.03
2005	902	27844	106.6	3.215	0.1169	3254941556.5	76277.7	0.02
2006	939	28276	114.6	3.245	0.1093	3167772661.9	89942.1	0.02
2007	912	27813	99.0	3.188	0.1438	4047458860.7	87482.7	0.03
2008	910	27227	93.3	3.167	0.0998	2804734412.4	48591.2	0.02
2009	899	29079	92.2	3.164	0.1603	4448902027.8	72959.5	0.03

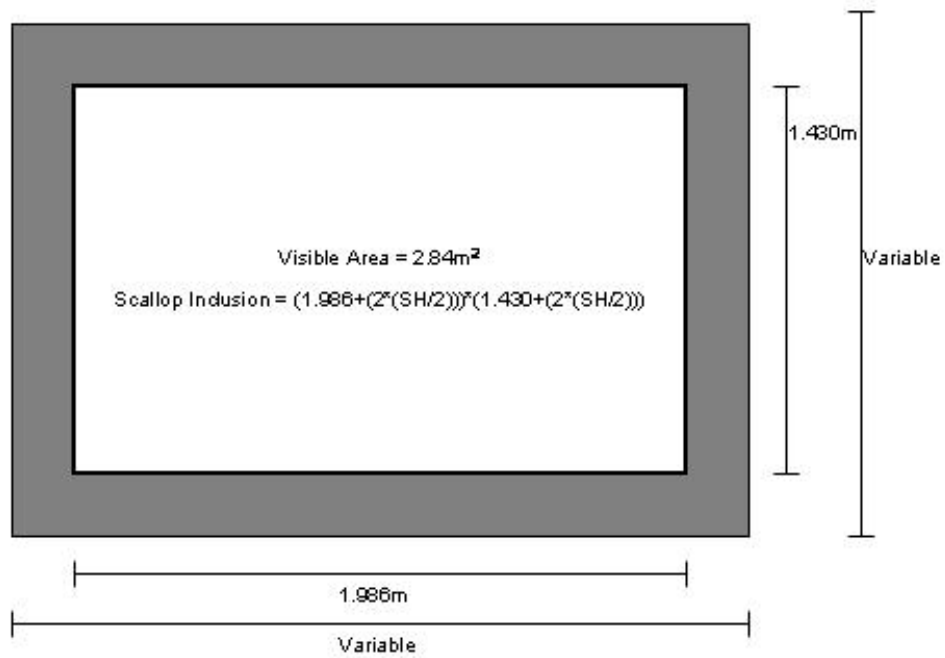
Appendix B3-Table 3. Small camera area surveyed, mean shell height (mm), shell height adjusted view field (m²), shell height adjusted density, abundance, biomass and 95% CI of the density for the MAB and GBK stock areas from 2003-2009.

SMALL CAMERA

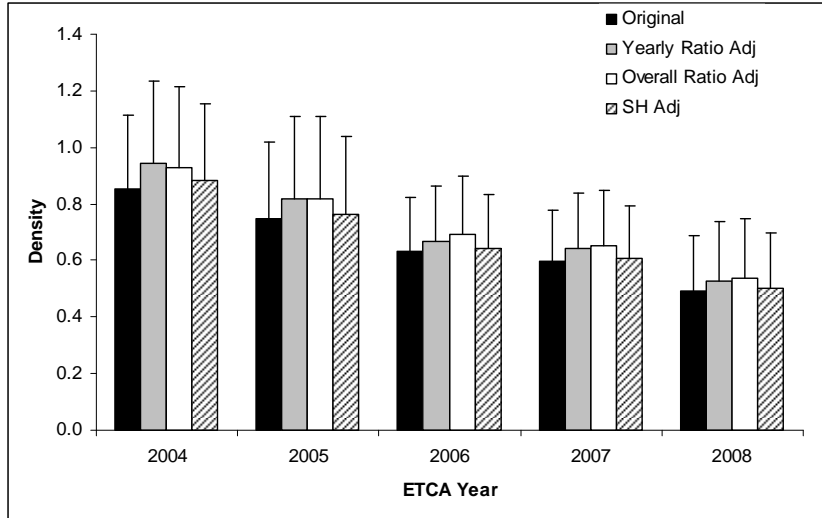
Year	Stations	Area Surveyed km ²	Mean SH mm	SH Adj Area m ²	SH Adj Density sc/m ²	Abundance	Biomass (mt)	95% CI
Mid-Atlantic Bight								
2003	799	24664	58.6	0.688	0.7063	17419973913	81353.3	0.28
2004	829	25591	84.7	0.732	0.2319	5935561328	69251.8	0.05
2005	860	26547	87.2	0.737	0.2181	5790580803	81756.4	0.05
2006	872	26918	93.4	0.747	0.2049	5516773301	88322.6	0.04
2007	931	28739	90.4	0.742	0.2204	6333997245	88940.8	0.04
2008	913	28184	90.7	0.743	0.2160	6086579306	103164.0	0.04
2009	928	28647	98.1	0.755	0.1260	3608213579	71935.6	0.02
Georges Bank								
2003	904	27906	88.3	0.738	0.1698	4737032049	66669.4	0.03
2004	921	28430	101.4	0.761	0.1256	3569624137	74431.9	0.03
2005	902	27844	111.2	0.778	0.1001	2787348077	77928.9	0.03
2006	916	28276	109.1	0.775	0.1412	3993072108	108804.7	0.03
2007	901	27813	80.0	0.724	0.1974	5489504503	77728.8	0.04
2008	882	27227	99.4	0.758	0.1526	4153894290	102841.8	0.04
2009	942	29079	96.1	0.752	0.1556	4525694473	94067.3	0.04



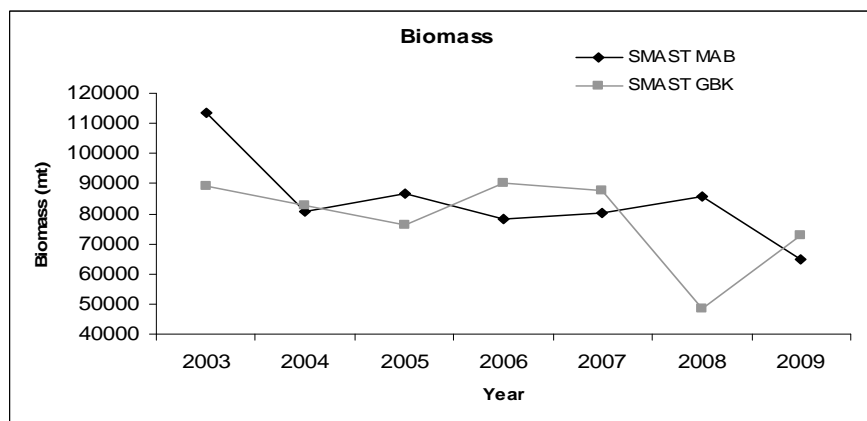
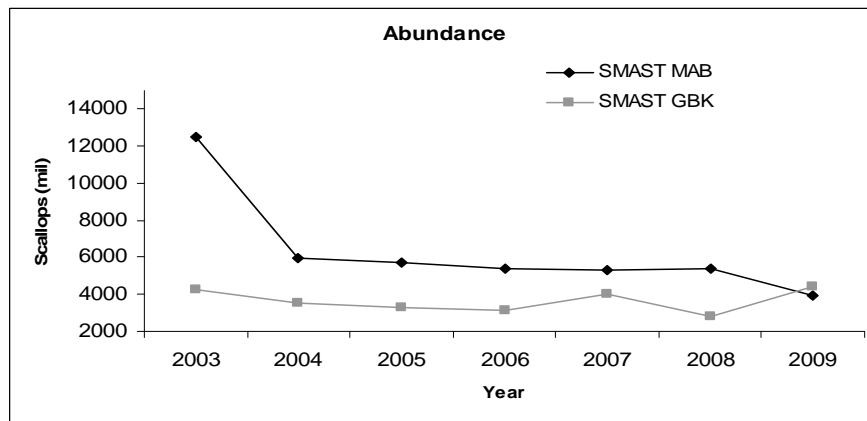
Appendix B3-Figure 1. Camera view field used in calculation of original density.



Appendix B3-Figure 2. Camera view field used in calculation of mean shell height adjusted density.



Appendix B3-Figure 3. Density estimates from ETCA 2004-2008 with associated 95% confidence intervals. Data for 2003 and 2009 are not included because the density was much higher (2003) and lower (2009) and muted the 95% CIs for the 2004-2008 data, not allowing comparison.



Appendix B3-Figure 4. Large camera abundance and biomass estimates for MAB and GBK for 2003-2009.

Appendix B4: Vessel calibrations for the NMFS sea scallop survey

In anticipation of the retirement of the R/V *Albatross IV*, the NOAA vessel that had conducted the annual synoptic sea scallop survey virtually uninterrupted since the 1970's, a series of paired tow calibration experiments were conducted to estimate fishing power correction factors. The objective of these experiments was to facilitate the transition of the NMFS sea scallop dredge survey time series from the R/V *Albatross IV* to a future survey platform. Due to some uncertainty in the subsequent survey platform, this information would facilitate the use of the calibrated vessel to either conduct the survey, or at least form a link from the R/V *Albatross IV* to any future survey platform. Ultimately, two calibration experiments were conducted in 2007 and 2009 with the calibration process being conducted in a stepwise fashion. We used a Generalized Linear Mixed Model (GLMM) to analyze the paired catch data to test for differences in both the pooled over length catch data as well as differences in the length composition of the catch. In 2007, the commercial scallop vessel, F/V *Nordic Pride* conducted a paired tow experiment with the R/V *Albatross IV*. Results indicate that while the R/V *Albatross IV* was slightly more efficient, the difference was small (~5%) and not statistically significant. Based on these results, the F/V *Nordic Pride* was considered to be equivalent with respect to fishing power to the R/V *Albatross IV*. In 2008, the R/V *Hugh Sharp* was selected as the replacement vessel for the R/V *Albatross IV* and during the 2009 survey an additional paired tow experiment was conducted between this vessel and the F/V *Nordic Pride*. Results indicate that the R/V *Hugh Sharp* was slightly more efficient (~10%) than the F/V *Nordic Pride*, however, this difference was not statistically significant. These results indicate that scallop dredge catches are robust to the effect of vessel and that any correction factor applied to this time series moving forward is small (~5%) or not justified.

Data collection and analysis

Experimental Design

The calibration experiments were conducted within the context of the NMFS annual sea scallop survey. This survey utilizes a stratified random design to sample throughout the entire U.S. range of the sea scallop. (Serchuk and Wigley 1986). For both paired tow experiments, the sampling occurred during the mid-Atlantic portion of the NMFS survey. For the first experiment, the standard NMFS sea scallop survey dredge that has been in service, virtually unmodified since the 1970's was used aboard both vessels. This dredge is 8 ft in width, with a dredge bag consisting of 2 inch rings. The twine top is comprised of 3.5 inch diamond mesh and there is a 1.5" liner throughout the dredge bag. For the second experiment, the F/V *Nordic Pride* used the standard dredge, while the R/V *Hugh Sharp* used a slightly modified version of the standard dredge referred to as the "prototype" dredge. The components of the prototype dredge are almost identical to the standard dredge (i.e. ring size, liner mesh size, twine top mesh size). Differences exist in relation to a slightly modified dredge frame, modifications to the ring bag and slight modifications to the mesh counts of the liner and twine top. A major difference between the standard and prototype dredge configurations is the addition of a wheel on the frame of the dredge as well as turtle/rock chains. In essence, the fishing power correction factor estimated for the second experiment attempts to calibrate the existing time series to a new entity that is represented by a unique vessel/gear combination.

While at sea, the sampling protocol included the re-occupation of sampling stations occupied by the R/V *Albatross IV*. Start/stop locations for each tow completed by the R/V *Albatross IV* were relayed to the commercial vessel via VHF radio. With the goal of re-occupying the stations as quickly as possible, a subset of stations was selected for re-sampling (the R/V *Albatross IV* conducts 24 hour operations, while the F/V's in this study sampled for roughly 16-18 hrs/day). During the execution of the tow, the captain of the F/V attempted to mirror the start/stop locations as close as possible. While it is safe to assume that there was some crossing of tow paths, it is unlikely that the tow path was duplicated precisely. For each comparative tow, the dredges were fished for 15 minutes with a towing speed of approximately 3.8-4.0 kts. High-resolution navigational logging equipment was used to accurately determine vessel position and speed over ground. Time stamps from the navigational log in conjunction with the tow level information recorded on the bridge were used to determine the location, duration and area fished by the dredges.

For each paired tow, the entire scallop catch was placed in baskets. A fraction of these baskets will be measured to estimate length frequency for the entire catch. The shell height of each scallop in the sampled fraction will be measured in 5 mm intervals. This protocol allowed for the determination of the size frequency of the entire catch by expanding the catch at each shell height by the fraction of total number of baskets sampled. Finfish and invertebrate bycatch was quantified, with finfish being sorted by species and measured to the nearest 1 cm. Sampling protocol was similar on the R/V *Albatross IV*.

Statistical Models

Scallop catch data from the paired tows provided the information to estimate differences in the fishing power of each vessel/gear combination tested and is based on the analytical approach included in Cadigan *et al.*, 2006. Assume that each vessel/gear combination tested in this experiment has a unique catchability. Let q_r equal the catchability of the R/V and q_f equal the catchability of the commercial vessel (F/V *Nordic Pride*) used in the study. The efficiency of the research vessel relative to the commercial vessel will be equivalent to the ratio of the two catchabilities.

$$\rho_l = \frac{q_r}{q_f} \quad (1)$$

The catchabilities of each the vessel/gear combination are not measured directly. However, within the context of the paired design, assuming that spatial heterogeneity in scallop density is minimized, observed differences in scallop catch for each vessel will reflect differences in the catchabilities of the vessel/gear combinations tested. Our analysis of the efficiency of the research vessel relative to the commercial vessels consisted of two levels of examination. The first analysis consisted of an examination of potential differences in the total scallop catch per tow. Subsequent analyses investigate whether scallop size was a significant factor affecting relative efficiency. Each analysis incorporates an approach to account for within-tow variation in the spatial heterogeneity of scallop density.

Let C_{iv} represent the scallop catch at station i by vessel v , where $v=r$ denotes the research vessel (R/V *Albatross IV* or R/V *Hugh Sharp*) and $v=f$ denotes the commercial vessel (F/V *Nordic Pride*). Let λ_{ir} represent the standardized scallop density for the i^{th} station by the R/V and λ_{if} the standardized scallop density encountered by the F/V. We assume that due to the tow paths taken by the respective vessels at tow i , the densities encountered by the two vessels may vary as a result of small-scale spatial heterogeneity as reflected by the relationship between scallop patch size and coverage by a standardized tow. The standardized unit of effort is a survey tow of 15 minutes at 3.8 kts. which covers a linear distance of approximately .95 nautical miles. The

probability that a scallop is captured during a standardized tow is given as q_r and q_f . These probabilities can be different for each vessel, but are expected to be constant across stations. Assuming that capture is a Poisson process with mean equal to variance, then the expected catch by the commercial vessel is given by:

$$E(C_{if}) = q_f \lambda_{if} = \mu_i \quad (2)$$

The catch by the R/V *Albatross IV* is also a Poisson random variable with:

$$E(C_{ir}) = q_r \lambda_{ir} = \rho \mu_i \exp(\delta_i) \quad (3)$$

Where $\delta_i = \log(\lambda_{ir} / \lambda_{if})$. For each station, if the standardized density of scallops encountered by both vessels is the same, then $\delta_i = 0$.

If the vessels encounter the same scallop density for a given tow, (i.e. $\lambda_{ir} = \lambda_{if}$), then ρ can be estimated via a Poisson generalized linear model (GLM). This approach, however, can be complicated especially if there are large numbers of stations and scallop lengths (Cadigan *et al.*, 2006). The preferred approach is to use the conditional distribution of the catch by the research vessel at station i , given the total non-zero catch of both vessels at that station. Let c_i represent the observed value of the total catch. The conditional distribution of C_{ir} given $C_i = c_i$ is binomial with:

$$\Pr(C_{ir} = x | C_i = c_i) = \binom{c_i}{x} p^x (1-p)^{c_i-x} \quad (4)$$

Where $p = \rho / (1 + \rho)$ is the probability a scallop is captured by the research vessel. In this approach, the only unknown parameters is ρ and the requirement to estimate μ for each station is eliminated as would be required in the direct GLM approach (equations 2 & 3). For the Binomial distribution $E(C_{ir}) = c_i p$ and $Var(C_{ir}) = c_i p (1-p)$. Therefore:

$$\log\left(\frac{p}{1-p}\right) = \log(\rho) = \beta \quad (5)$$

The model in equation 5, however does not account for spatial heterogeneity in the densities encountered by the two vessels for a given tow. If such heterogeneity does exist then the model becomes:

$$\log\left(\frac{p}{1-p}\right) = \beta + \delta_i \quad (6)$$

Where δ_i is assumed to be normally distributed with a mean=0 and variance= σ^2 . This model represent the formulation to estimate the vessel effect ($\exp(\beta_0)$) when scallop catch per tow is pooled over length.

Often, the replacement of a survey vessel presents an opportunity to make changes to the survey fishing gear. In those instances, the potential exists for the catchability of scallops at length, l to vary. Even in cases where the survey fishing gear remains the same, length effects are possible. Models to describe length effects are extensions of the models in the previous

section to describe the total scallop catch per tow. Again, assuming that between-pair differences in standardized scallop density exist, a binomial logistic regression GLMM model to reflect the situation where one vessel encounters more scallops, but they are of the same length distribution would be:

$$\log\left(\frac{p_i}{1-p_i}\right) = \beta_0 + \delta_i + \beta_1 l, \delta_i \sim N(0, \sigma^2), i = 1, \dots, n. \quad (7)$$

In this model, the intercept (β_0) is allowed to vary randomly with respect to station.

The potential exists, however, that there will be variability in both the number as well as the length distributions of scallops encountered within a tow pair. In this situation, a random effects model that allows both the intercepts (δ_0) and slopes (δ_1) to vary randomly between tows is appropriate (Cadigan and Dowden, 2009). This model is given below:

$$\log\left(\frac{p_i}{1-p_i}\right) = \beta_0 + \delta_{i0} + (\beta_1 + \delta_{i1})l, \delta_{ij} \sim N(0, \sigma_j^2), i = 1, \dots, n, j = 0, 1. \quad (8)$$

Adjustments for sub-sampling of the catch and differences in area swept

Additional adjustments to the models were required to account for sub-sampling of the catch as well as differences in the observed area swept by the two gears. In some instances, due to high volume, catches for particular tows were sub-sampled. Often this is accomplished by randomly selecting a subset of the total catch (in baskets) for length frequency analysis. One approach to accounting for this practice is to use the expanded catches. For example, if half of the total catch was measured for length frequency, multiplying the observed catch by two would result in an estimate of the total catch at length for the tow. This approach would artificially overinflate the sample size resulting in an underestimate of the variance, increasing the chances of spurious statistical inference (Millar *et. al.*, 2004; Holst and Revill, 2009). In our experiment, the proportion sub-sampled was consistent throughout each tow and did not vary with respect to scallop length. While experimental protocol dictates a standardized tow of roughly .95 nautical miles (3.8 kts. For 15 minutes), in practice variability exists in the actual tow distances covered by each vessel. These differences must be accounted for in the analysis to ensure that common units of effort are compared.

Let q_{ir} equal the sub-sampling fraction at station i for the vessel r and let d_{ir} be the areal coverage at station i , for vessel r . This adjustment results in a modification to the logistic regression model:

$$\log\left(\frac{p_i}{1+p_i}\right) = \beta_0 + \delta_{i0} + (\beta_1 + \delta_{i1})l_i + \log\left(\frac{q_{ir}d_{ir}}{q_{if}d_{if}}\right), \delta_{ij} \sim N(0, \sigma_j^2), i = 1, \dots, n, j = 0, 1. \quad (9)$$

The last term in the model represents an offset in the logistic regression (Littell, *et. al.*, 2006).

In some cases, we encountered difficulties with model convergence for the two parameter model. To simplify the computations in the optimization routine, scallop lengths were standardized to sum 0 based on the interquartile range. This reduced the magnitude of the steps between successive lengths and alleviated the convergence issues. We used SAS/STAT[®] PROC NLMIXED to fit the generalized linear mixed effects models.

Results and Discussion

Overall, roughly 100 paired tows were completed for each experiment. A visual representation of the spatial distribution of the relative catches for both experiments is shown in Figure 1. For the intercept only model (vessel effect only) a scatterplot of the catches from the paired tows are shown in Figure 2 and parameter estimates are shown in Table 1. For each experiment the R/V was slightly more efficient than the F/V *Nordic Pride* (correction factor is interpreted as $\exp(B_0)$). The calculated correction factors were 1.058 and 1.110 for the two experiments, respectively. In both cases, the logit of the estimated intercept was not significantly different than 0.

For the two parameter model (length effects) there was a significant difference detected in the length composition of catches from the two vessels (Figure 3 and Table 2). The direction of the difference was consistent between the two experiments and showed that the R/V was more efficient as a function of increasing scallop length. The increase in relative efficiency with respect to length for the first cruise may have resulted from measurement errors associated with different measuring devices between the two vessels. For the second experiment, an apparent pattern in the residuals at the small lengths was apparent, however the sum of the animals from lengths <60 mm only represented roughly 4% of the total catch and likely contributed little weight in the likelihood.

Literature Cited

- Cadigan, N.G., Walsh, S.J and W. Brodie. 2006. Relative efficiency of the *Wilfred Templeman* and *Alfred Needler* research vessels using a Campelen 1800 shrimp trawl in NAFO Subdivisions 3Ps and divisions 3LN. Can Sci Advis Secret Res Doc 2006/085; 59 pp.
- Cadigan, N.G. and J. J. Dowden. Statistical inference about relative efficiency from paired-tow survey calibration data. This work is not yet in press, but is expected to be at any time)
- Holst, R. and A. Revill. 2009. A simple statistical method for catch comparison studies. Fisheries Research. **95**: 254-259.
- Littell, R.C., Milliken, G.A., Stroup, W., Wolfinger, R., and W.O. Schabenberger. 2006. SAS for Mixed Models (2nd ed.). Cary, NC. SAS Institute Inc.
- Millar, R.B., M.K. Broadhurst, W.G. Macbeth. 2004. Modeling between-haul variability in the size selectivity of trawls. Fisheries Research. **67**:171-181.
- Serchuk, F.M. and S.E. Wigley. 1986. Evaluation of USA and Canadian research vessel survey for sea scallops (*Placopecten magellanicus*) on Georges Bank. Journal of Northwest Atlantic Fisheries Science. **7**:1-13.

The output and code for this paper was generated using the SAS/ STAT software, Version 9.2 of the SAS System for Windows Version 5.1.2600. Copyright © 2002-2008 by SAS Institute Inc.

SAS and all other SAS Institute Inc. products or services are registered trademarks or trademarks of SAS Institute Inc., Cary, NC, USA.

Table 1 Mixed effects model (vessel effect only) results including an offset term to account for the effect of differential tow lengths. Parameter estimates are on the logit scale and significant estimates are shown in bold.

Vessel/Gear	σ^2	Estimate (β_0)	Standard Error	Lower 95% CI	Upper 95% CI	t	p- value
F/V Nordic Pride vs. R/V <i>Albatross IV</i>	0.2386	0.0568	0.0501	-0.0427	0.1562	1.13	0.2602
F/V Nordic Pride vs. R/V <i>Hugh Sharp</i>	0.4827	0.1040	0.0707	-0.0364	0.2444	1.47	0.1448

Table 2 Two parameter mixed effects model results. Both comparisons model the logit of the proportion of the catch at length from the R/V relative to the total catch from both vessels. Parameter estimates reflect a model that includes an offset term in the model that accounted for both sub-sampling of the catch as well as differences in within-tow areal coverage. Confidence limits are Wald type confidence intervals. Parameter estimates are on the logit scale and significant parameter estimates are shown in bold.

Vessel	D F	σ^2 (intercept)	σ^2 (slope)		Estimate	Standard Error	Lower 95% CI	Upper 95% CI	t	p-value
F/V Nordic Pride vs. R/V Albatross IV	98	0.2744	0.5077	β_0	0.01199	0.05454	-0.09625	0.1202	0.22	0.8264
				β_1	0.4983	0.07964	0.3402	0.6563	6.26	<0.0001
F/V Nordic Pride vs. R/V Hugh Sharp	98	0.4887	0.3802	β_0	0.0908	0.07157	-0.05188	0.2329	1.27	0.2073
				β_1	0.1184	0.06879	0.05187	0.3249	2.74	0.0073

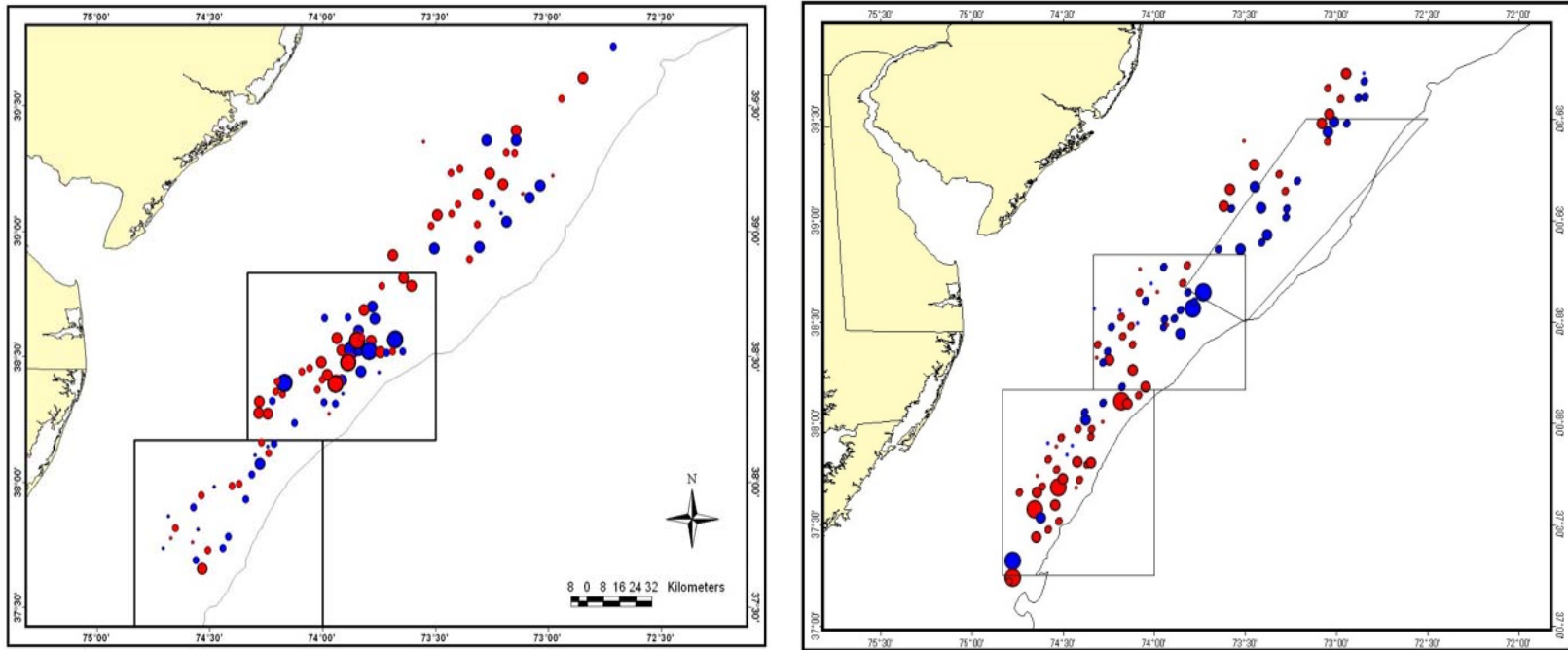


Figure 1 Catch differences between the F/V *Nordic Pride* (towing the standard NMFS dredge) and the R/V *Albatross IV* (left panel) or the R/V *Hugh Sharp* (right panel). Catches for each vessel are scaled to reflect both any sub-sampling of the catch as well as differences in areal coverage. Symbols are proportional to the magnitude of the observed differences in catch. Red dots represent higher levels of catch by the R/V. Blue dots represent higher levels of catch by the F/V *Nordic Pride*. Open circles represent zero difference between the two vessels. Polygons in both areas represent closed areas in existence at the time of the study, which are part of the spatial management strategy for the fishery. The dotted line represents the 50 fathom bathymetric contour.

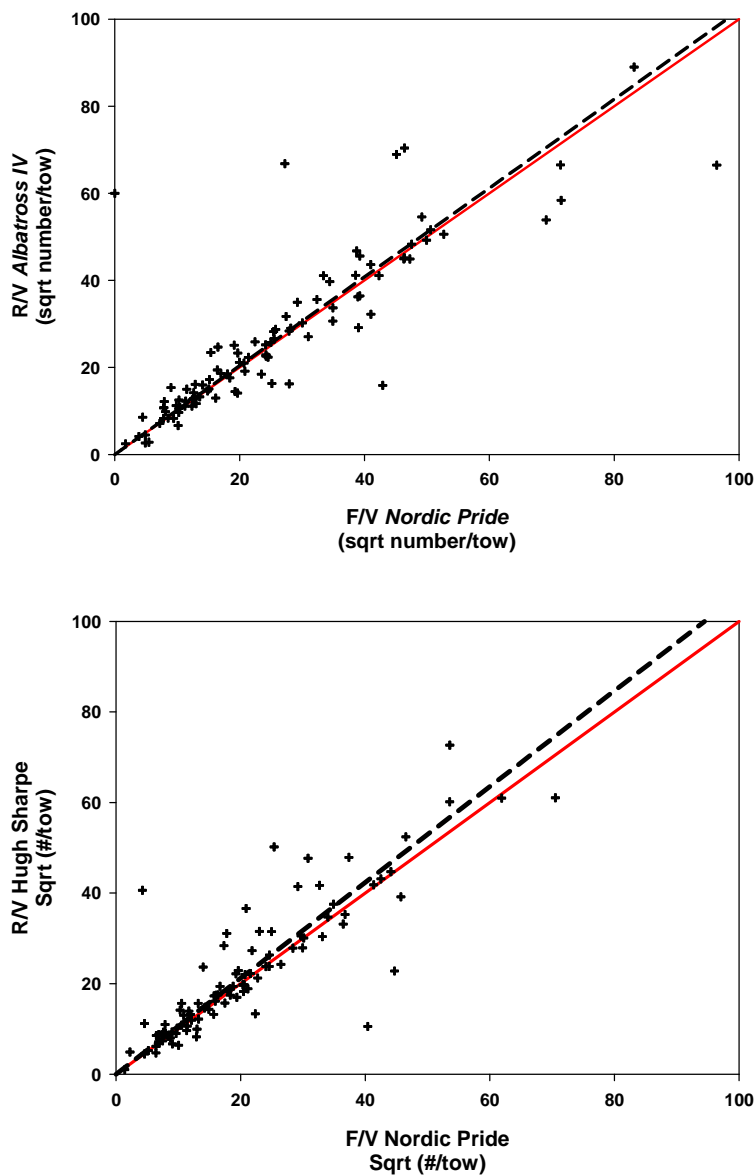


Figure 2 Top Panel: Total scaled catches for R/V *Albatross IV* vs. F/V *Nordic Pride* (top panel) and the R/V *Hugh Sharp* vs. the F/V *Nordic Pride* (bottom panel). The red line has a slope of one. The dashed line has a slope equal to the estimated relative efficiency (from the one parameter vessel effect only model).

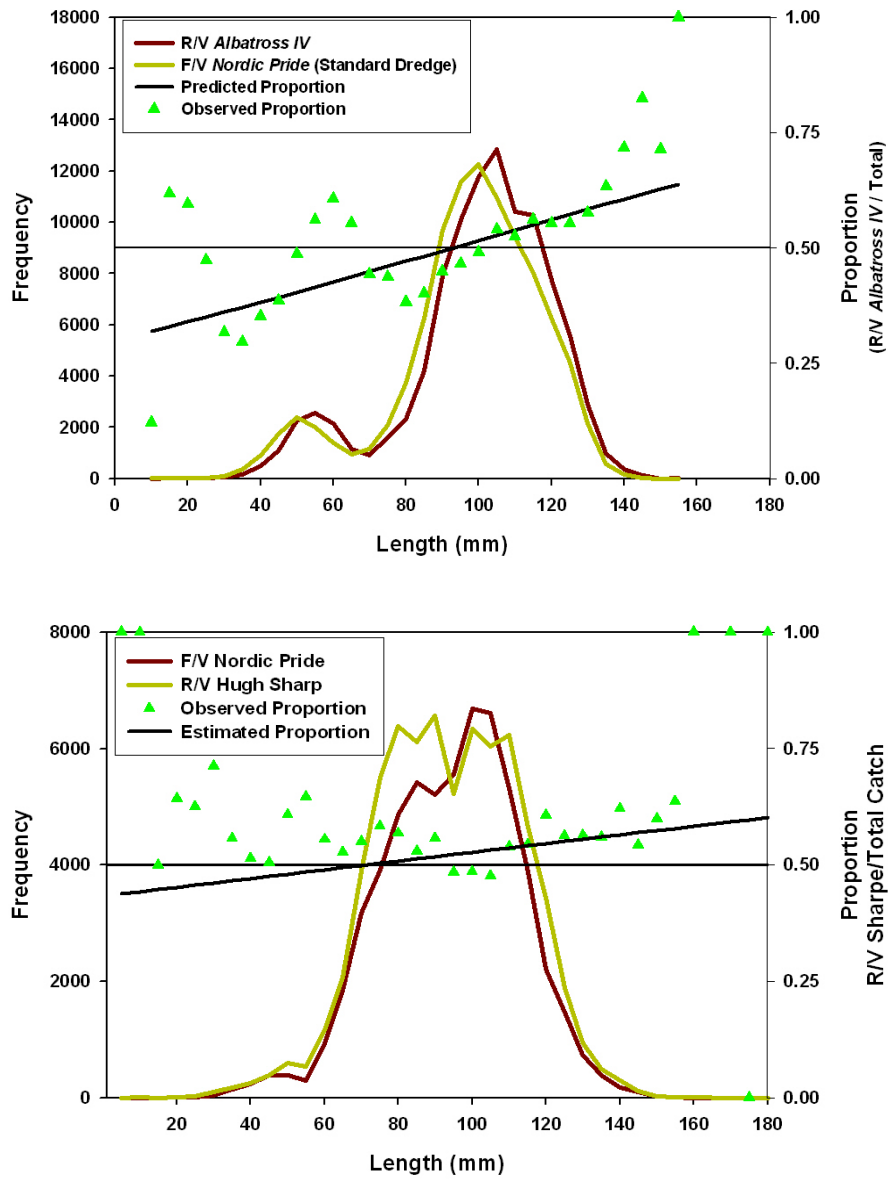


Figure 3 Observed scaled length frequency distributions for the R/V *Albatross IV* and the F/V *Nordic Pride* (top panel) and the R/V *Hugh Sharp* and F/V *Nordic Pride* (bottom panel). The green triangles represent the observed proportions ($Catch_{R/V} / (Catch_{F/V} + Catch_{R/V})$). The black line represents the length based relative efficiency as estimated by the two parameter (vessel and length effect model).

Appendix B5: Results from Maine sea scallop surveys, 2002-2008.

Kevin H. Kelly, Maine Department of Marine Resources, W. Boothbay Harbor, ME.

A dredge-based sea scallop (*Placopecten magellanicus*) survey of Maine state waters (≤ 3 nm from shore) has been conducted since 2002 (with the exception of 2004). This annual survey provides information on size distribution, the shell height-meat weight relationship, abundance, stock size and spatial distribution of scallops from near shore waters along the coast of Maine. For the first two years (2002-2003) the entire Maine coast was surveyed (Schick and Feindel 2005). During 2004-2008, at least one of three major sections of the coast has been surveyed each year on a rotating basis: 1) New Hampshire border to western Penobscot Bay (“Western Maine”); 2) eastern Penobscot Bay to Quoddy Head (“Eastern Maine”); and 3. Cobscook Bay). The following is a chronology of survey coverage by year:

<u>Year</u>	<u>Area surveyed</u>
2002	Coast-wide, including Cobscook Bay
2003	Coast-wide, including Cobscook Bay
2004	no survey
2005	New Hampshire border to western Penobscot Bay
2006	eastern Penobscot Bay to St. Croix River, including Cobscook Bay (<i>Higher intensity survey than '02 and '03</i>)
2007	Cobscook Bay
2008	Matinicus Island to Quoddy Head
2009	Cobscook Bay, St. Croix River and New Hampshire border to western Penobscot Bay (<i>data not yet analyzed</i>)

The purpose of the survey is to characterize and monitor the sea scallop resource within Maine’s coastal waters, and to compare results to previous years’ surveys in light of regulatory and environmental changes. It is necessary to monitor changes in abundance and stock size from year to year to evaluate effects of the fishery, document recruitment events and determine what is available for harvest. The survey provides information needed to evaluate potential management strategies such as rotational closures, harvest limits and area closures to protect spawning and enhance recruitment.

Methods

Each survey was conducted aboard a commercial scallop vessel equipped with a standardized survey drag. Vessels were selected by an RFP process where feasible (2005, 2006) but in some cases, particularly in the case of finding a vessel rigged to handle the survey gear and available in the location and time period necessary, there was an additional recruitment process used for vessel procurement.

In some years (2005-2006, and 2008) two vessels were used in order to broaden industry participation, to take advantage of local knowledge and to maximize survey efficiency (the survey was conducted over a broad geographic area with increased sampling intensity and within a fairly narrow time frame). Vessels used were: the *F/V North Star* from Portland (2005); *F/V Sea Ryder* from Spruce Head (2005); 45 ft. *F/V Foxy Lady II* from Stonington (2006, 2008, and

2009); 42 ft. *F/V Alyson J 4* from Cutler (2006, 2008); 40 ft. *F/V Bad Company* from Cutler (2007); and *F/V Kristin Lee* from Eastport (2009).

Surveys were carried out during October-November with the single exception of the fall 2005 survey which was carried over during Feb.-Apr. 2006). Surveys were done during this time to examine scallop size distribution and meat weight in and just prior to the commercial season which starts on December 1 (December 15 in 2009) and to help minimize conflict with lobster traps.

Gear

The survey dredge was a 7 ft. wide New Bedford-style chain sweep with 2½ in. rings in the ring bag to retain smaller scallops (Figure 1). Drag specifications were determined in consultation with several Maine scallop industry members in 2002 prior to the inaugural survey. The dredge was unlined and had rock chains. The twine top was double hung with 3½ in. mesh. The drag size and weight represented a compromise between being wide enough to cover a significant area per tow, heavy enough to sample deeper waters and of a size that can be transported by a large pickup truck (Schick and Feindel 2005).

Due to age and wear on the original drags made for the first state waters survey in 2002, survey dredge gear constructed for the 2009 Northern Gulf of Maine in federal waters survey replaced the original gear for the fall 2009 state survey (see Appendix B6). The new gear (Figure 2) was of a configuration largely consistent with that used in previous state surveys but had 2 in. rings to allow better retention of small scallops and a slightly larger pressure plate to facilitate towing in deeper waters.



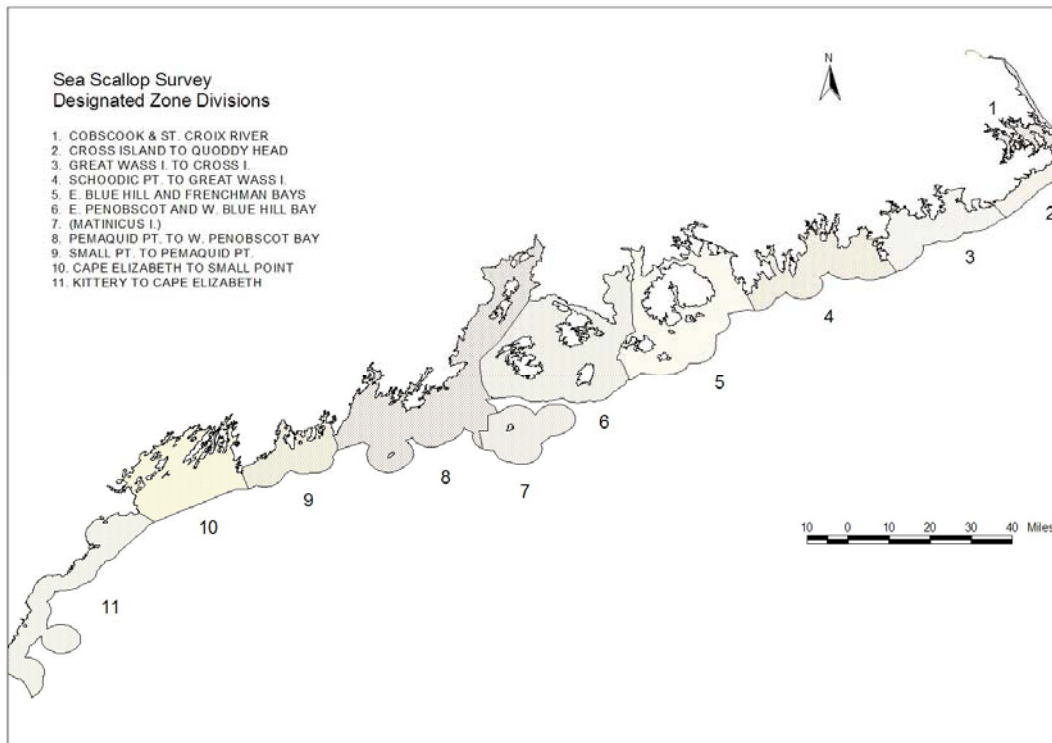
Appendix B5-Figure 1. View of survey drag used during 2005-2008 showing position of rock chains.



Appendix B5-Figure 2. View of survey drag constructed in 2009.

Survey design

A subset of the coastal zones (or “strata”) defined for the 2002-2003 surveys (Figure 3) were used in subsequent surveys during the report period with some modification.



Appendix B5-Figure 3. Survey strata and coastal zones in the Maine DMR scallop survey.

Strata were chosen to provide a manageable balance between area and sampling intensity. Scallop areas within the strata were mapped based on fisher information, prior survey data, sediment maps (<http://megisims.state.me.us/metadata/surf.htm>) and coastal wildlife inventory maps (<http://megisims.state.me.us/metadata/shell.htm>) (Schick and Feindel 2005).

Within each stratum except Stratum 1 (Cobscook Bay), survey stations within scallop areas were selected randomly using a 500 m grid (stratified random design). The number of stations assigned within each region was roughly proportional to the size of the strata. There were also a number of fixed stations located in some of the more historically important scallop areas such as Gouldsboro Bay and Libby Islands.

Cobscook Bay is one of 13 survey zones, or “strata”, used for the DMR scallop survey. Cobscook Bay is a large, strongly tidal estuary at the extreme eastern edge of the Maine coast near the U.S./Canada border. It has the most productive scallop fishery within Maine waters and is thus sampled with the most frequency and with the highest intensity of the survey zones. A direct assessment of scallop abundance for this stratum is made by using a systematic sampling design.

Six survey substrata (South Bay, Pennamaquan River, East Bay, Whiting Bay, Johnson Bay and area: other) within Cobscook Bay representing spatially contiguous fished areas were determined in consultation with fishing industry members prior to the 2002 survey and have been

repeated in subsequent surveys. The total number of stations sampled however was increased by 31% from previous surveys beginning in 2006.

Cobscook Bay tow locations were based on a 500 m grid overlaying each substratum. This grid accommodated an average tow length of approximately 300 m. There were 84 tows completed in the 2007 Cobscook Bay survey and 86 in 2009 (two stations added).

Sampling procedure

Stations to be sampled were plotted using Capn Voyager™ navigational software. A Garmin™ Map 76 GPS unit with Garmin™ GA 29 GPS antenna connected to a laptop computer displaying station location was used to position the vessel on station. Location and time were recorded at three points (dredge in, tow start and haul-back) for each tow. A Juniper Allegro™ ruggedized handheld computer was also connected to a GPS unit to record time/date/location information.

Tow times were 2.5-5 minutes (2.5 minutes in Cobscook Bay) depending on bottom conditions and presence of lobster traps. Stations were sampled by a straight line tow. Boat speed averaged 3.5-4 knots.

A ruggedized handheld computer with an RS232 serial port input for digital calipers was used to facilitate rapid entry of shell measurements and other information while sampling. Data entry screens for the sampling programs and survey were configured using Data Plus Professional™ software, which aided in standardizing data entry, providing error checks and minimizing subsequent data auditing and keying (Schick and Feindel 2005).

The following sampling protocol was employed for each tow:

- 1) Station information (location, time, depth) was entered from the wheelhouse.
- 2) Bottom type was recorded as combinations of mud, sand, rock, and gravel based on sounder information and dredge contents. For example “Sg” designated a primarily sand substratum with some gravel (after Kelley et. al.1998).
- 3) Once the drag was emptied, a digital picture of the haul was taken.
- 4) Scallops, sea cucumbers (*Cucumaria frondosa*) and ocean quahogs (*Arctica islandica*) were culled from the drag contents for subsequent measurement. Catches of the latter species were quantified because of their importance in other drag fisheries. While the survey gear is not suitable for formally sampling ocean quahogs their presence in the catch does suggest the existence of a bed below the sediment.
- 5) Bycatch (species other than sea scallops, sea cucumbers and ocean quahogs) was enumerated using a 0-5 qualitative abundance scale corresponding to “absent”, “present”, “rare”, “common”, “abundant”, and “very abundant”.
- 6) Total number of scallops was recorded. The total weight and volume of the scallop, sea cucumber, and ocean quahog catch was recorded.
- 7) The shell height (SH; distance from the umbo to the outer edge, perpendicular to the hinge line) of individual scallops was measured. All scallops from catches of 100 animals or less were measured for SH. If >100 scallops were present at least 100 were measured. Where n > 1,000 a subsample of 10% was measured.
- 8) On selected tows (normally every third or fourth tow) a subsample of 24 scallops, chosen to represent the catch of scallops $\geq 3\frac{1}{2}$ in. shell height, were measured (shell height, shell length and shell depth) and shucked for meat weight determination. Meats were placed in a

compartmentalized box in the order that the animals were measured and later individually weighed on shore (using an Ohaus Navigator™ balance connected to the ruggedized handheld computer) and matched to the corresponding shell measurements.

The following table summarizes data collected for each tow:

Data items collected – ME DMR Sea Scallop survey

COLLECTED DATA - FIELD SUMMARY

TRIP	STATION INFORMATION IDENTIFIERS	TOW LOCATION	TOW INFO	ENVIRON. DATA
Trip identifier	Tow identifier	Dredge in (Lat, Lo, Time stamp)	Tow time elapsed	Bottom type
Trip date	Zone	Tow start (Lat, Lo, Time stamp)	Depth	Bottom temperature
Port sailed from	Strata	Haulback (Lat, Lo, Time stamp)	Bearing	
Weather	Location (description)	Drag off-bottom (Lat, Lo, Time stamp)	Wire out	
Precipitation	Tow number	Distance towed	Tow speed	
Wind/sea stata	Sample type			
Return time	(random, exploratory, "fixed", other)			
Comments				

SCALLOP DATA				
CATCH	SIZE	STRUCTURE	BIOMETRICS	BYCATCH
Number scallops caught	Shell height		Shell height	Tow photo ID
Volume of catch (shellstock)			Shell length	Species
Weight of catch (shellstock)			Shell depth	Abundance (1-5 scale)
Proportion of tow sampled (100, 50, 25%)			Meat weight	Trash type
Number of clappers				Trash amount (1-5 scale)
Comments				Comments

AUXILLARY DATA		
QUAHOG CATCH	SEA CUCUMBER CATCH	CTD DATA
Number of quahogs	Number of cucumbers	Location (lat/ long)
Shell height	Catch weight	File identifier
Shell length	Catch volume	
Shell depth	Comments	
Shell (dead) abundance (1-5 scale)	Size index (SL x diam 1 x diam 2)	

from Schick and Feindel (2005)

Dredge efficiency

In November 2006, SCUBA transects were conducted in the South Bay substratum of Cobscook Bay in order to compare diver observations of scallop numbers with catch rates of the survey dredge in the same area. At each of three survey stations, five diver transects (covering 2 x 100=200 m²) were carried out. All scallops in each dive transect were measured for shell height and counted. These stations (SM1S39, SM1S46, and SM1S51) were located in areas of higher scallop density in South Bay. At each station two (2) replicate tows from each of the two (2) survey vessels (n = 4) were also performed to determine size-specific scallop density by dredge for comparison.

The diver transects indicated that the survey drag was 43.6% efficient at capturing scallops ≥ 95.25 mm (3 ¾ in) SH. (This shell height was chosen as it represented the minimum legal size of scallops in Maine in 2003 and dredge efficiency is of particular importance for estimating harvestable (minimum legal size and above) biomass. This efficiency estimate is less than previously reported for the survey dredge (68.0%; Schick and Feindel 2005) but compares favorably with the efficiency estimate for the NMFS survey dredge (45% in Closed Areas I and II on Georges Bank; NMFS/NEFSC 2004). Our estimate also compares well with efficiency

estimates from other New England-style commercial dredges (42.7%; Gedamke et al. 2004). For the cooperative survey of scallop abundance in Closed Area II using commercial-type gear (SMAST, VIMS, Fisheries Survival Fund, NMFS), commercial dredge efficiency was estimated to be 53.1 – 54.4% (Gedamke et al. 2005). The DMR dredge is unlined and therefore would be expected to have higher efficiency for legal scallops than a lined dredge (D. Hart, NMFS/NEFSC, pers. comm.). The particular bottom type of our dredge efficiency study sites was largely sandy gravel, typical of much of Cobscook Bay, which also likely increased gear efficiency compared to more rocky areas along much of the rest of coastal Maine. Given these considerations, the estimate of 43.6% efficiency is plausible.

Data analysis

Area swept per tow was determined from tow distance (tow start to haul-back) and drag width (7 ft. or 2.1 m). Tow distance was determined using Capn Voyager™ software. Based on this information, the scallop catch for each tow was standardized to density (number of scallops per square meter). Total abundance was calculated by multiplying density and area.

For analysis, total scallop catch was divided into the following size categories:

- “seed”: < 2½ in. (<63.5 mm) SH
- “sublegal”: 2½ in. to < 4 in. (63.5 – <101.6 mm) SH
- “harvestable”: ≥ 4 in. (≥101.6 mm) SH

Estimates of total abundance for each of the three size classes were calculated using Cochran’s (1977) standard approach for surveys. For each of the six survey substrata identified above, the average density was estimated as:

$$\bar{X} = \sum_{h=1}^H W_h \bar{X}_h$$

where \bar{X}_h the average density for substratum h , H is the total number of substrata, and W_h is proportion of the area of substratum h with respect to the survey area. The associated standard error was calculated:

$$std\ error(\bar{X}) = \sqrt{\sum_{h=1}^H W_h^2 \frac{1-f_h}{n_h} S_h^2}$$

where S_h^2 is the variance estimated for substratum h , $f_h = \frac{n_h}{N_h}$ is the finite population correction

for substratum h , and n_h and N are the number of stations sampled and the total number of stations available for sampling, respectively, in substratum h . The finite population correction factor was ignored since the proportion of area sampled was small compared to the total area of each substratum.

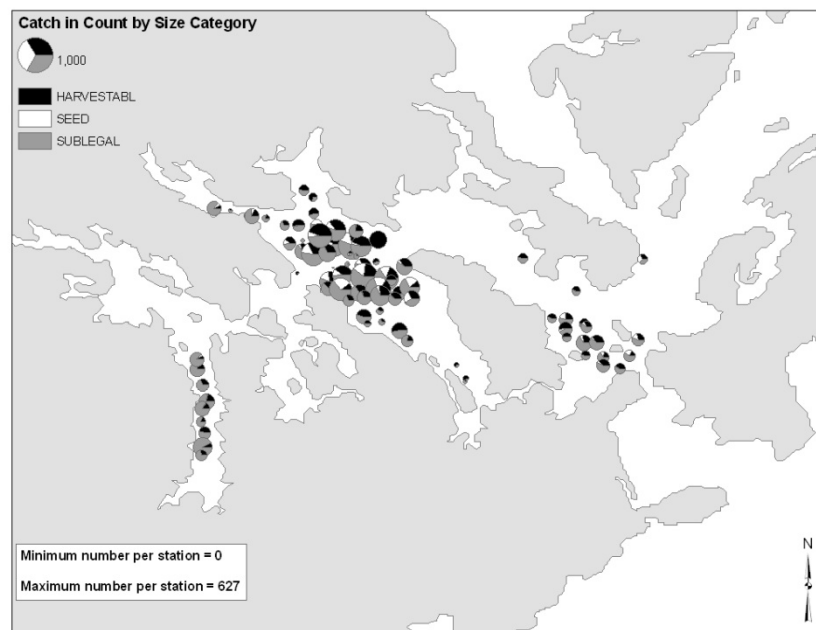
Harvestable biomass for Cobscook Bay was calculated by applying a calculated shell height-meat weight relationship to the numbers of harvestable scallops at shell height per substratum. Biomass was summed across substrata to determine total harvestable biomass for Cobscook Bay.

Results

Cobscook Bay was surveyed in 2003, 2006 and 2007. The survey indicated a large increase in abundance and biomass of harvestable (≥ 4 in. SH) scallops in Cobscook Bay between 2006 and 2007.

The abundance of harvestable scallops in 2007 was 96.2% greater than the previous high observed in 2003. This increase appears plausible because it followed the high abundance of sublegal (2.5 – 3.9 in. SH) scallops observed in 2006.

Although sublegal scallop abundance declined in 2007 from the high level of 2006 the density of seed (< 2.5 in. SH) was significantly ($p=0.008$) higher in South Bay in 2007 (0.064 m^{-2}) than 2006 (0.025 m^{-2}) (Table 1; Figure 8). Recruitment, although not as high as in 2006, appeared healthy in 2007 as considerable numbers of both seed and sublegal scallops were present in South Bay, the largest and most important fishing ground (Table 1; Figures 4-11).

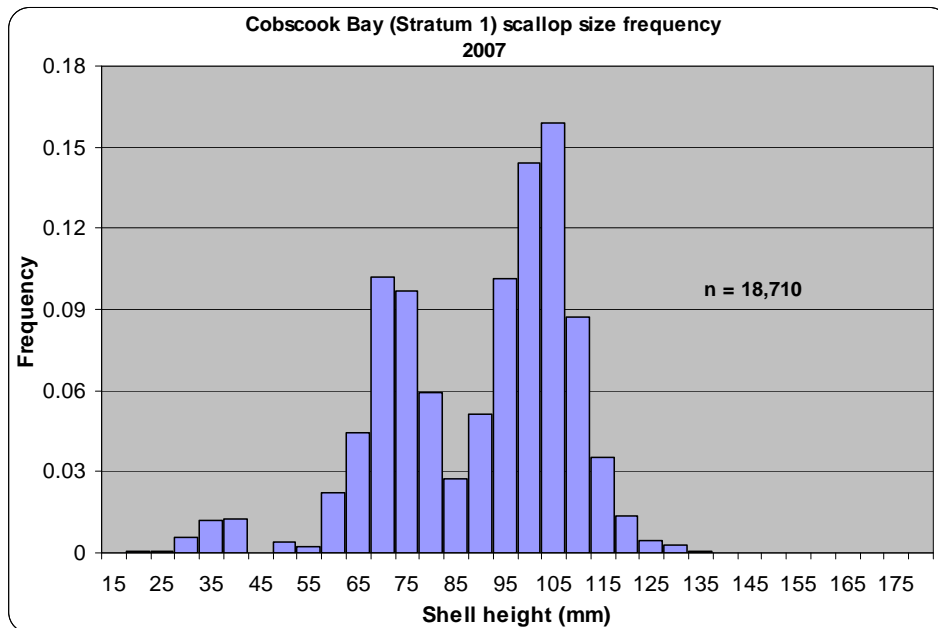


Appendix B5-Figure 4. Scallop size class composition and abundance (Cobscook Bay), 2007 survey.

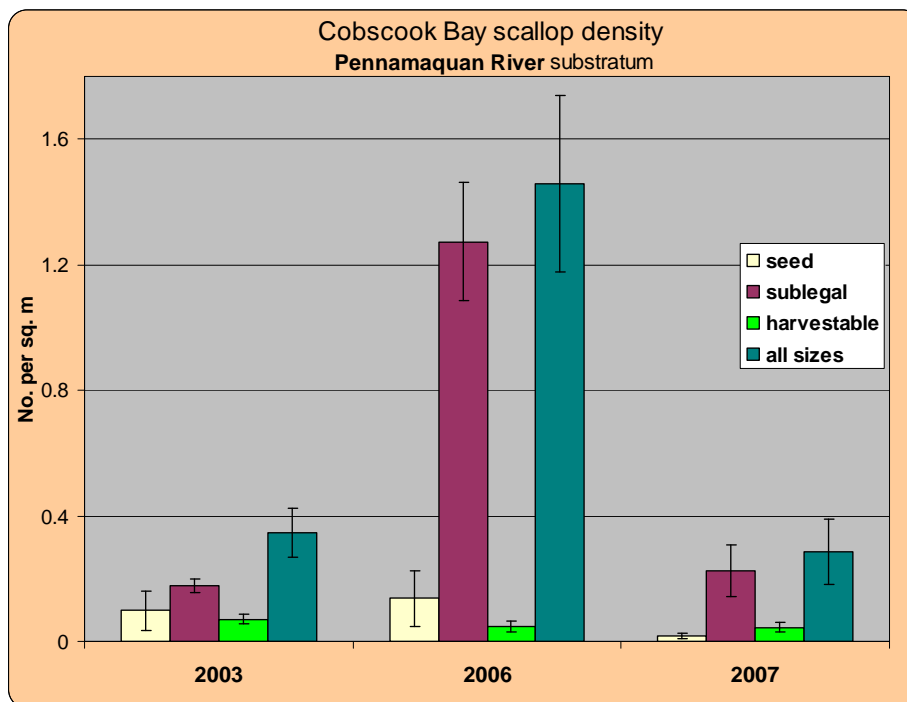
Appendix B5-Table 1. Survey summary statistics for Cobscook Bay (2007) by substratum and overall (mean +/- standard error).

Stratum 1 (Cobscook Bay) scallop survey - 2007

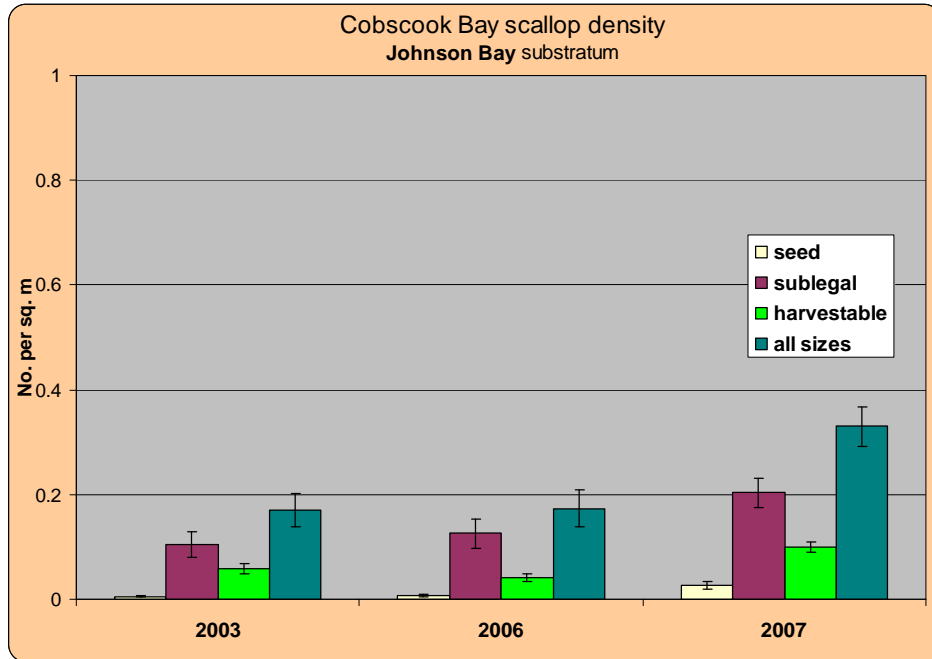
substratum	total	South Bay		East Bay		Penn. River		Whiting Bay		Johnson Bay		other		
area (hec)	2,158	1,182		92		64		135		401		284		
no. sites	83	48		3		5		9		15		3		
		<u>Density (scallops per sq m)</u>												
		density	S.E	density	S.E	density	S.E	density	S.E	density	S.E	density	S.E	
seed		0.064	0.013	0	0	0.017	0.009	0.004	0.002	0.027	0.006	0.029	0.027	
sublegal		0.345	0.042	0.108	0.031	0.225	0.083	0.338	0.062	0.203	0.028	0.107	0.011	
harvestable		0.147	0.018	0.144	0.008	0.045	0.017	0.060	0.009	0.099	0.010	0.089	0.010	
all sizes		0.556	0.066	0.252	0.037	0.287	0.103	0.402	0.063	0.330	0.038	0.224	0.037	
		<u>Abundance (no. scallops)</u>												
	abundance	abundance	S.E	abundance	S.E	abundance	S.E	abundance	S.E	abundance	S.E	abundance	S.E	
seed	964,714	757,544	147,935	0	0	10,792	5,531	5,655	2,487	108,018	25,975	82,706	76,000	
sublegal	5,891,034	4,073,386	500,090	99,133	28,358	143,899	53,111	455,899	83,118	815,680	111,276	303,037	31,850	
harvestable	2,635,277	1,741,962	210,599	132,439	7,599	28,885	10,665	81,462	12,449	398,798	39,610	251,731	27,170	
all sizes	9,491,025	6,572,892	785,229	231,572	33,669	183,576	66,200	543,016	84,968	1,322,495	153,474	637,474	105,264	
		<u>Harvestable biomass (kg) (unadjusted)</u>												
	biomass	S.E	biomass	S.E	biomass	S.E	biomass	S.E	biomass	S.E	biomass	S.E	biomass	S.E
	55,637	6,712	36,084	4,444	2,921	128	560	202	1,620	256	8,757	857	5,696	825



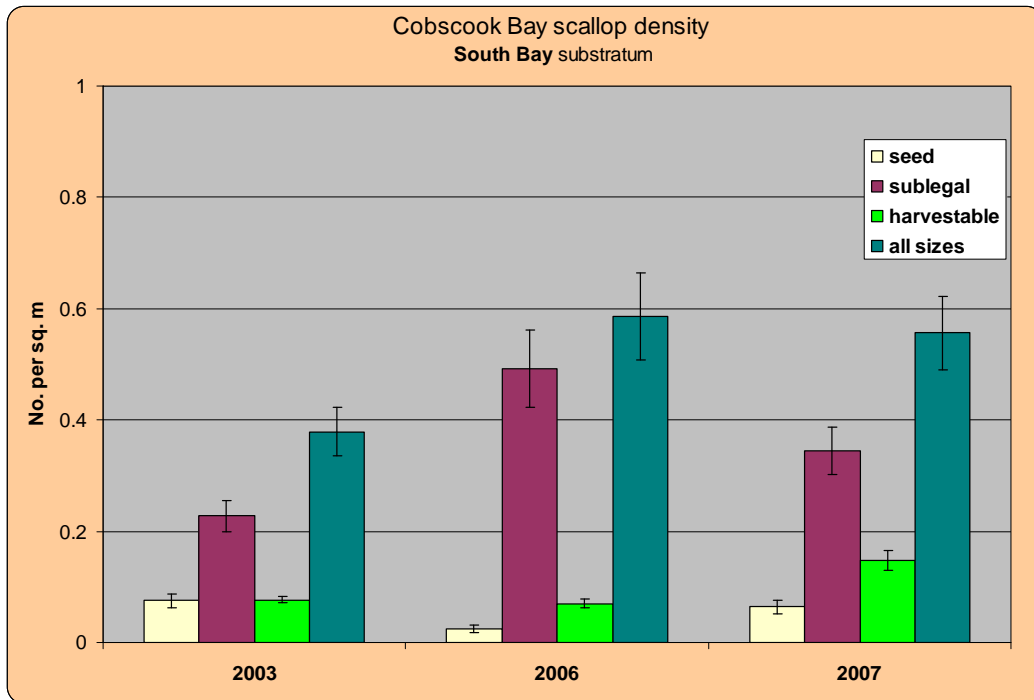
Appendix B5-Figure 5. Size frequency (5 mm increments) of scallops in Cobscook Bay, 2007.



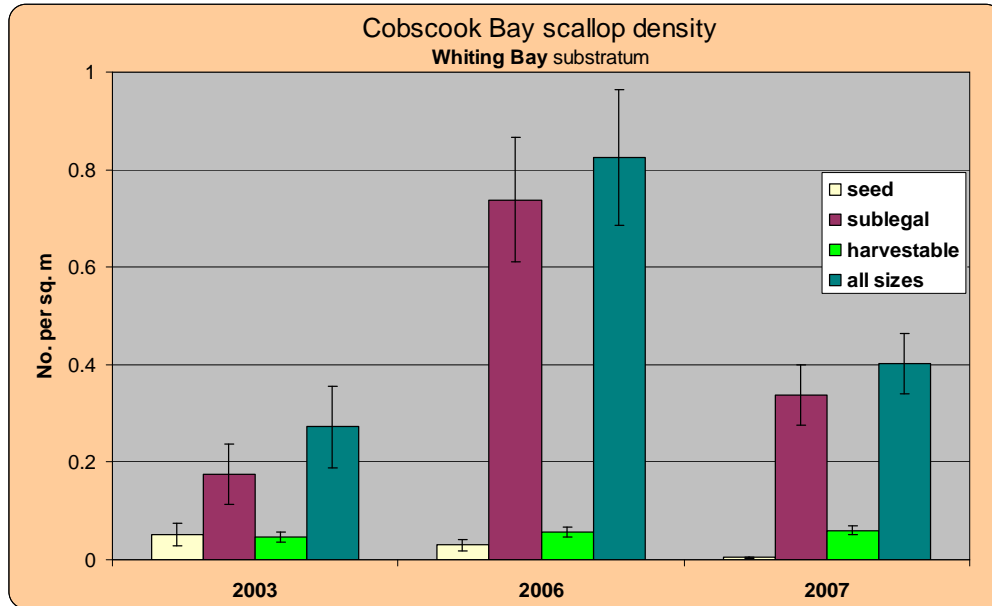
Appendix B5-Figure 6. Mean scallop density (+/- one standard error, unadjusted for dredge efficiency) by size class, Pennamaquan River substratum of Cobscook Bay.



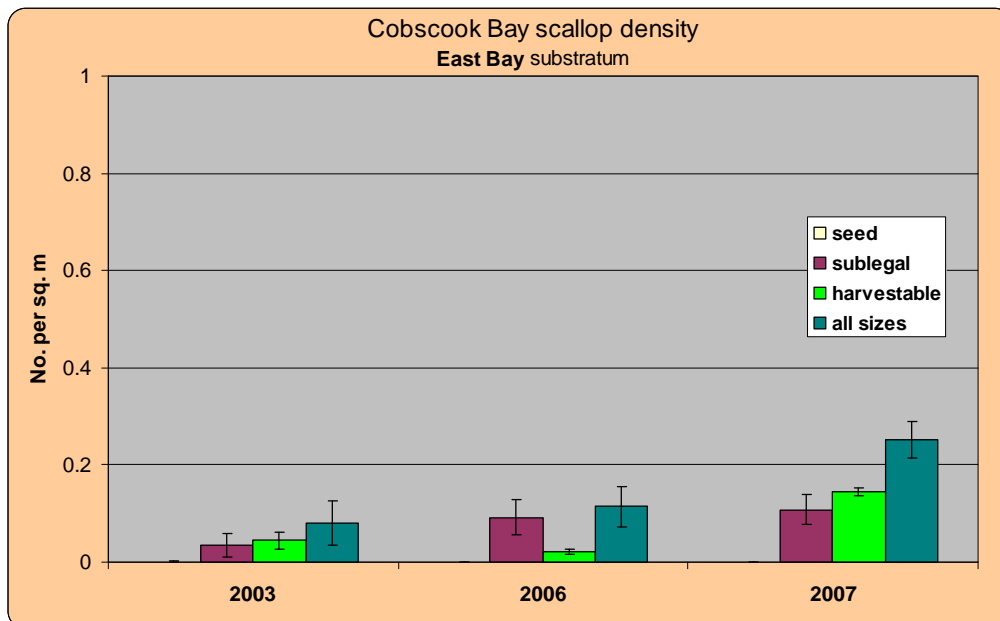
Appendix B5-Figure 7. Mean scallop density (+/- one standard error, unadjusted for dredge efficiency) by size class, Johnson Bay substratum of Cobscook Bay.



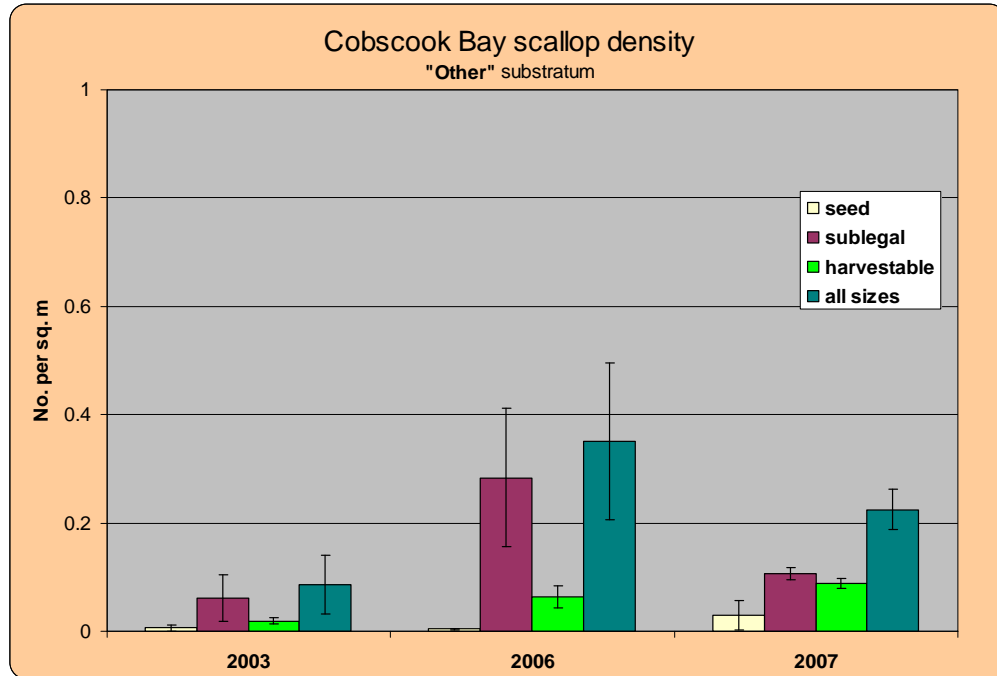
Appendix B5-Figure 8. Mean scallop density (+/- one standard error, unadjusted for dredge efficiency) by size class, South Bay substratum of Cobscook Bay.



Appendix B5-Figure 9. Mean scallop density (\pm 1 standard error, unadjusted for dredge efficiency) by size class, Whiting Bay substratum of Cobscook Bay.



Appendix B5-Figure 10. Mean scallop density (\pm one standard error, unadjusted for dredge efficiency) by size class, East Bay substratum of Cobscook Bay.

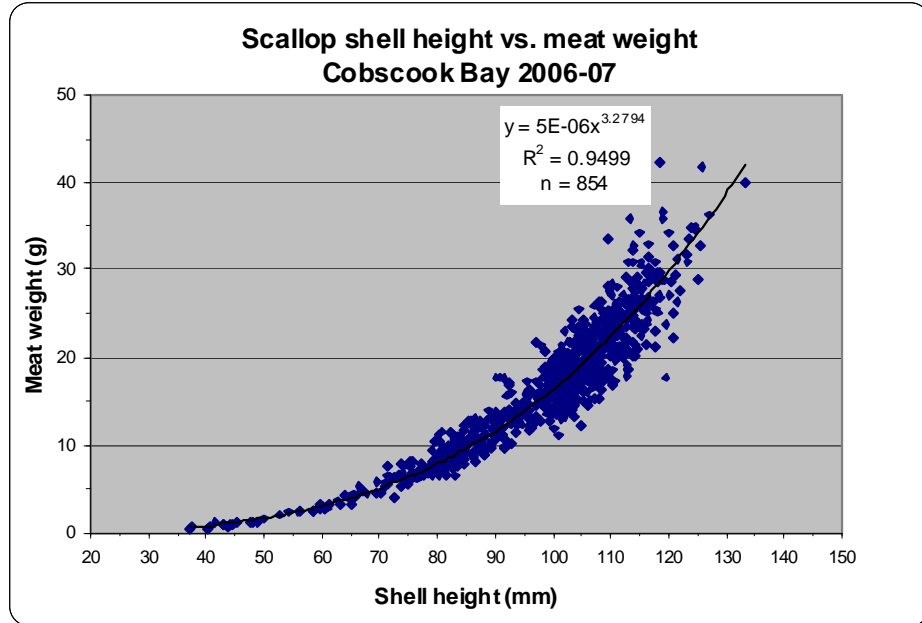


Appendix B5-Figure 11. Mean scallop density (with standard error, unadjusted for dredge efficiency) by size class, “other” substratum of Cobscook Bay.

Shell height-meat weight

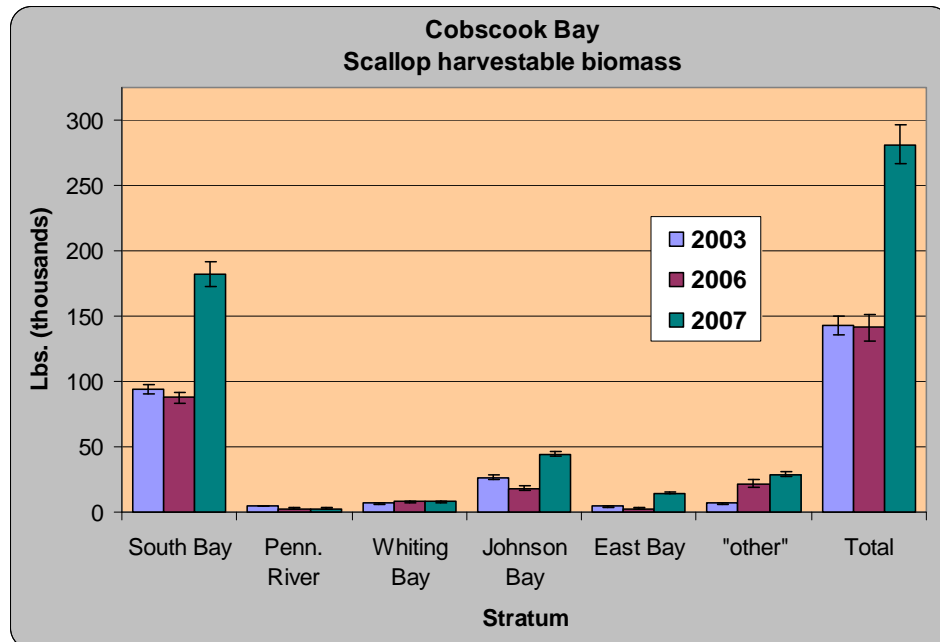
A shell height to meat weight relationship was calculated based on samples taken in 2006-2007 (Figure 12). Scallop meat weights from 2006-2007 were lower than those in 2002-2003 (18% less meat weight at 4 in. SH). The 2006-2007 relationship ($MW = 0.00000453 SH^{3.2794}$) differed significantly from the 2002-2003 equation ($MW = 0.000037 SH^{3.365}$) for Cobscook Bay (Schick and Feindel 2005).

Meat weights were greater in 2002-2003 than in 2006-2007. The 2006-2007 meat weights were larger however than those reported for 1987 and 1991 in an unpublished DMR study where the relation was $MW = 0.000005 SH^{3.2247}$. It should be noted that the 1987 and 1991 studies were based mainly on smaller (80-100 mm) scallops than those sampled in the more recent surveys (minimum legal size was 3.0 in. or 76.2 mm) until 1999). Thus predicted meat weights for scallops in the current legal size range (≥ 4 in.) from the 1987/1991 report may be less reliable than the more recent studies. Furthermore the 1987 and 1991 sample sizes were relatively small ($n = 296$). The 1987 and 1991 studies do provide some evidence that the 2006-2007 data are within a “normal” range for Cobscook Bay and still higher than overall meat weights for coast-wide Maine (Schick and Feindel 2005). The 2006-2007 commercial meat counts (26 per lb. at the 4 in. SH minimum size) also appeared well below the legal maximum commercial meat count (35 per lb.) for Cobscook Bay.



Appendix B5-Figure 12. Scallop meat weight (MW) as a function of shell height (SH) for Cobscook Bay, 2006-2007.

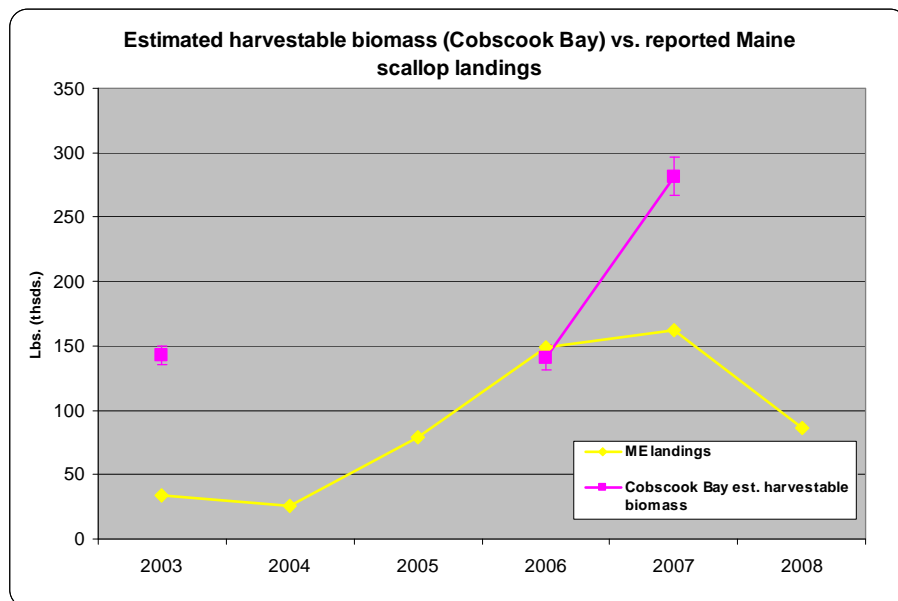
The 2007 estimate of harvestable biomass (128 mt or 281.3 thousand lbs of meats) was 99.4% higher than the previous year (Figure 13). South Bay had the largest proportion (65%) of harvestable biomass.



Appendix B5-Figure 13. Biomass (meat weight) of harvestable (legal-size) scallops in Cobscook Bay in 2003, 2006 and 2007.

An economic study (Athearn 2005) indicated that Cobscook Bay landings for the 2004-2005 season were 70.3 mt (155 thousand lbs) or meats. However, landings data for calculation of exploitation rates in Cobscook Bay were generally not available for years with surveys. Scallop harvesters in Maine were been required to report trip level information, including landings, beginning with the 2008-2009 season but there is too little information available from which to determine Cobscook Bay scallop landings for earlier years. Maine landings prior to 2008 were determined by a voluntary dealer reporting system which did not provide information on where the scallops were caught. Furthermore, many Cobscook Bay harvesters have traditionally “peddled” or retailed their scallops directly to consumers rather than sell to a dealer.

Based on industry input, observations from port sampling, the amount of resource available as observed on the dredge survey and the high level of fishing activity there, that a very large portion (perhaps 80-90%) of overall Maine scallop landings are from Cobscook Bay. A comparison of estimated harvestable biomass (Cobscook Bay) and reported Maine landings does not, however, show a high correlation (Figure 14), except for the slight trend upward in 2007 landings concurrent with the large increase in Cobscook Bay biomass. It is hoped that improved comparisons can be made beginning when 2009 survey data become available along with 2009-10 harvester reports.



Appendix B5-Figure 14. Cobscook Bay harvestable biomass as estimated by DMR survey in relation to reported Maine scallop landings, 2003-2008.

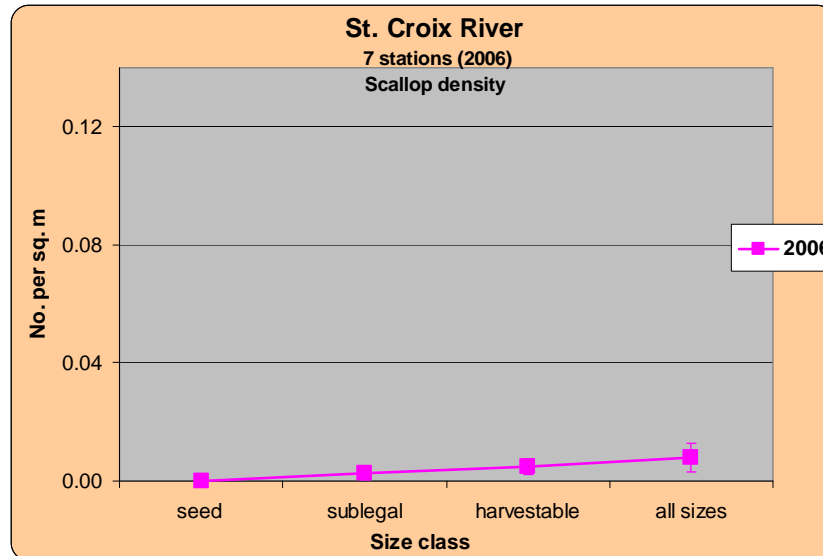
Cobscook Bay continued to exhibit relatively high scallop production during 2003-2008 despite the intense fishing effort which existed there. There are no official reports of fishing activity but it has been stated for example that 170 boats were operating there on opening day 1995 (Cobscook Bay Resource Center 2007). Maine Marine Patrol estimated that 90-100 vessels were fishing in Cobscook Bay in mid-December 2007 (Lt. A. Talbot, pers. comm.).

On the 2009 survey of Cobscook Bay/St. Croix River, approximately 20,400 scallops were caught and counted, 8,700 were measured for shell height and an additional 800 were sampled for shell size-meat weight determination. The new dredge with 2” rings seemed

particularly effective at sampling across the full size range of the resource. Data analysis and a report for this survey will be completed in 2010.

Stratum 1a (St. Croix River)

The St. Croix River was surveyed in 2002 and 2006. This stratum was characterized by relatively low scallop abundance (0.005 m^{-2}) in 2006 with harvestable sizes (0.003 m^{-2}) slightly more abundant than sublegals (0.002 m^{-2}) (Figure 15). Catch rates were also low in 2002 (Schick and Feindel 2005). The highest survey catch rate in 2006 was around Frost Island near Passamaquoddy Bay.



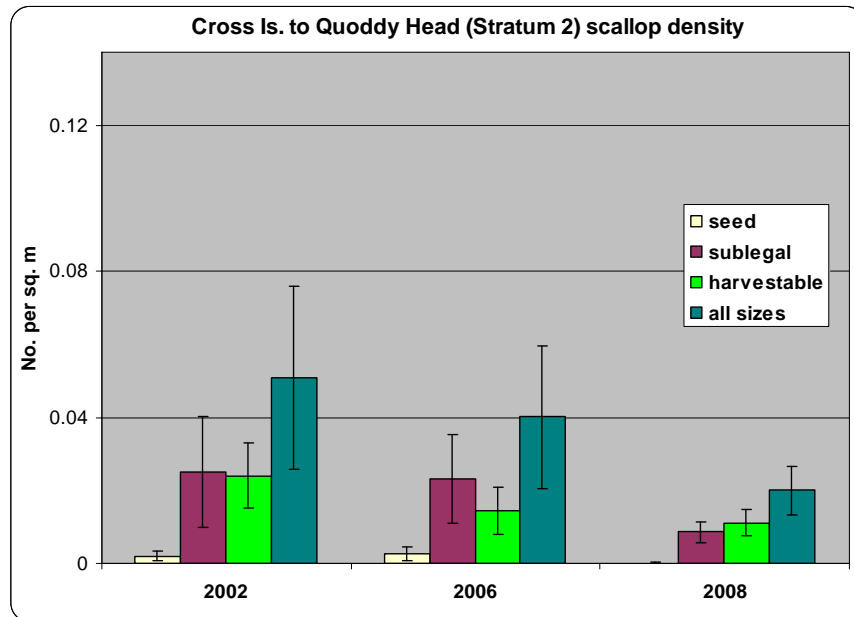
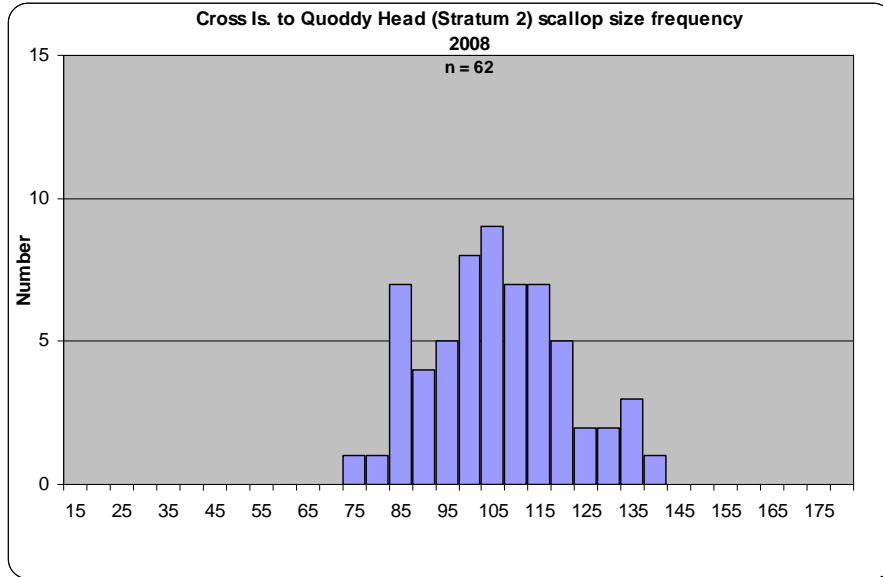
Appendix B5-Figure 15. Mean scallop density by size group, Stratum 1A.

Eastern Maine: Strata 2-7 (Quoddy Head to Matinicus Island)

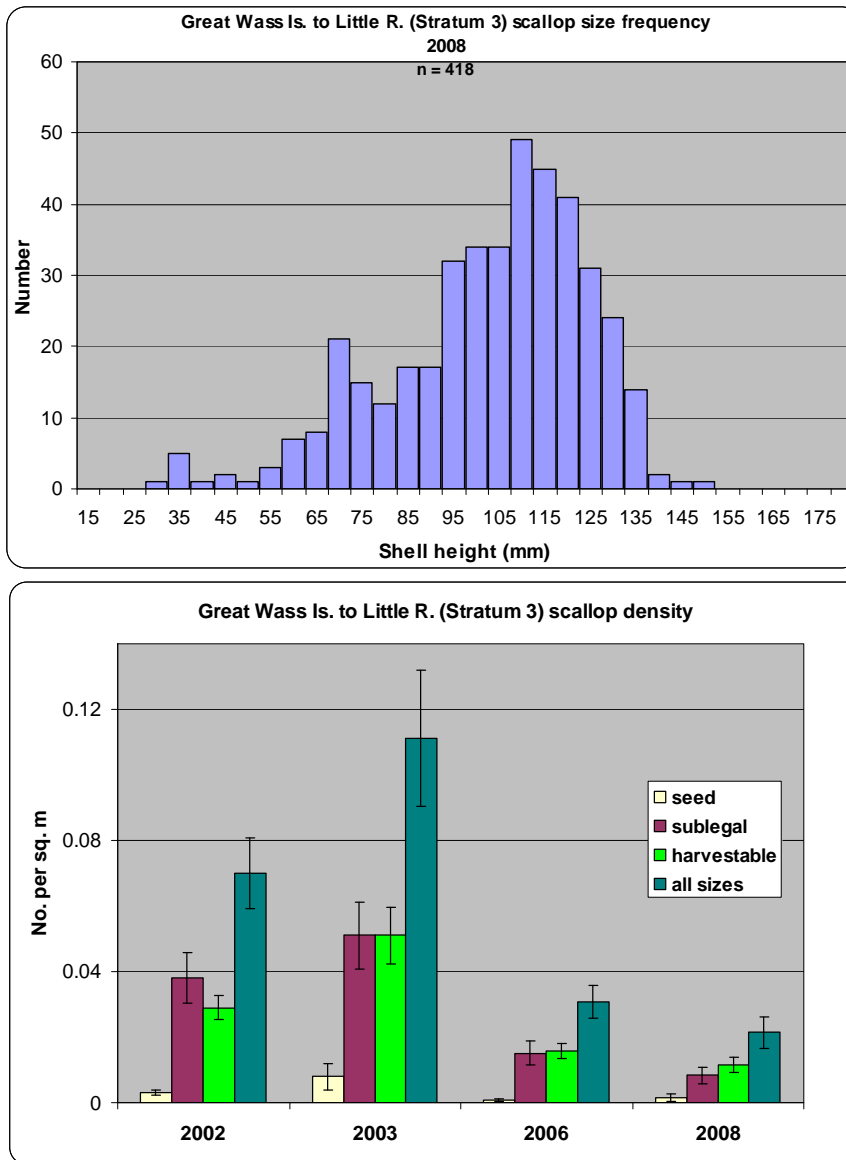
These strata were surveyed in 2005 (Stratum 7), 2006 (Strata 2-6) and 2008 (Strata 2-7). There were 183 tows completed in 2008. Most of the tow locations were randomly selected within the known scallop grounds of each stratum. The survey indicated that overall scallop abundance either declined slightly or remained unchanged at a low level of abundance for all areas except Stratum 6 (East Penobscot Bay and W. Blue Hill Bay). A slight increase was observed in the latter area (Figure 20). Although densities remained fairly low in this stratum, the size distribution indicated some successful recruitment.

Considerably higher densities had been observed in Stratum 3 (Great Wass Island to Little River), an area of relatively high fishing pressure. Densities were 0.111 m^{-2} in 2003, 0.031 m^{-2} during 2006 and 0.021 m^{-2} during 2008 (Figure 17). The size range in this stratum has shifted to older, larger scallops (similar to Stratum 4 in 2006) indicating reduced recruitment.

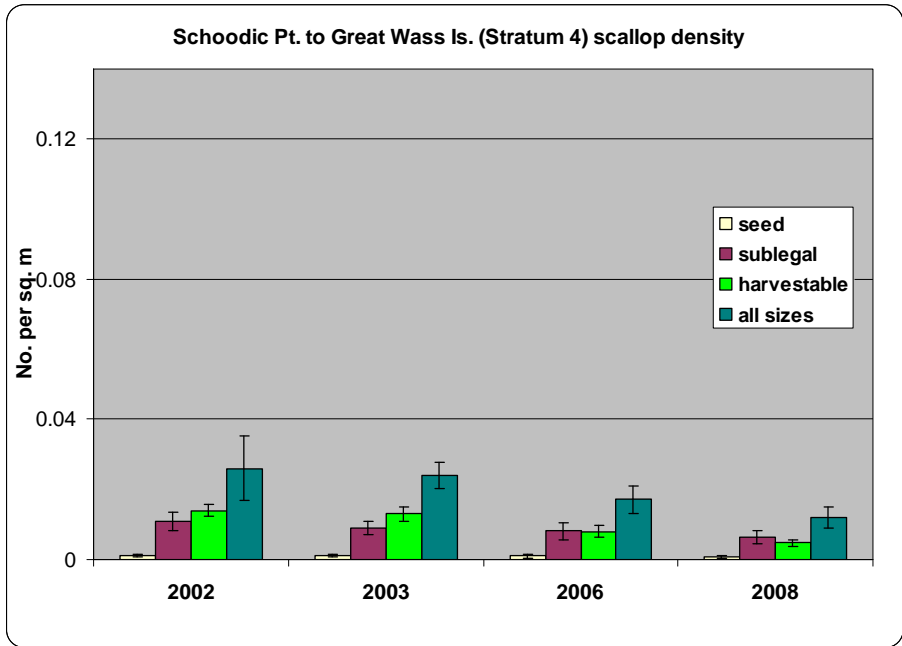
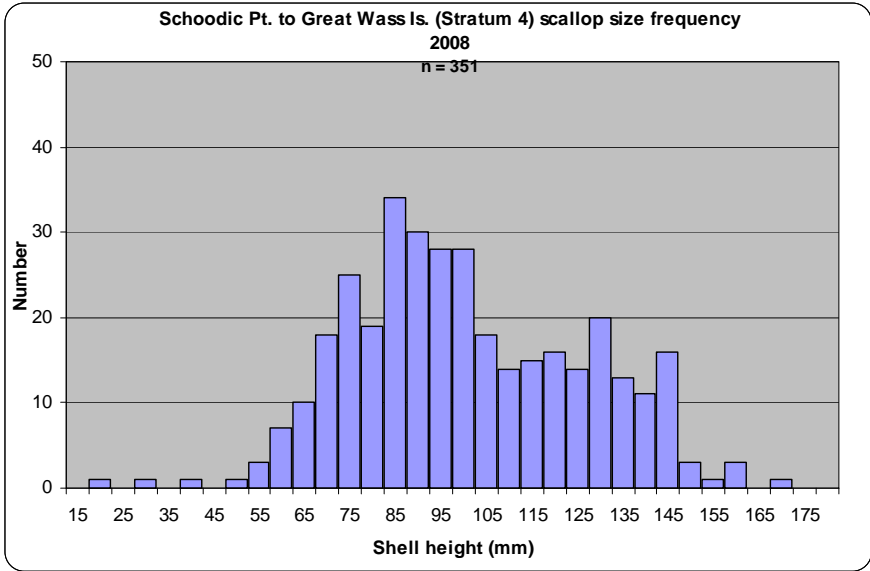
The presence of seed scallops (< 2½ in. shell height) was noted at six (6) locations in the overall eastern Maine area in 2008.



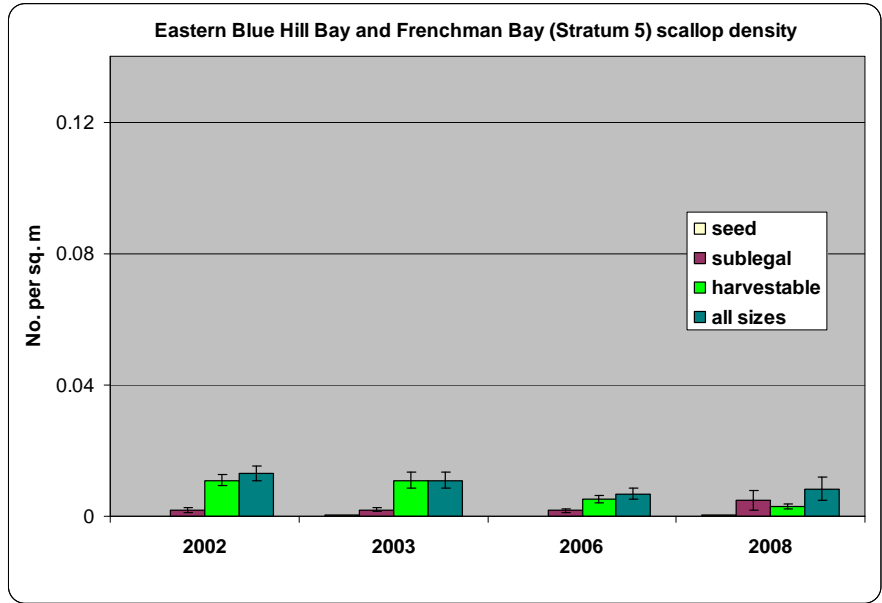
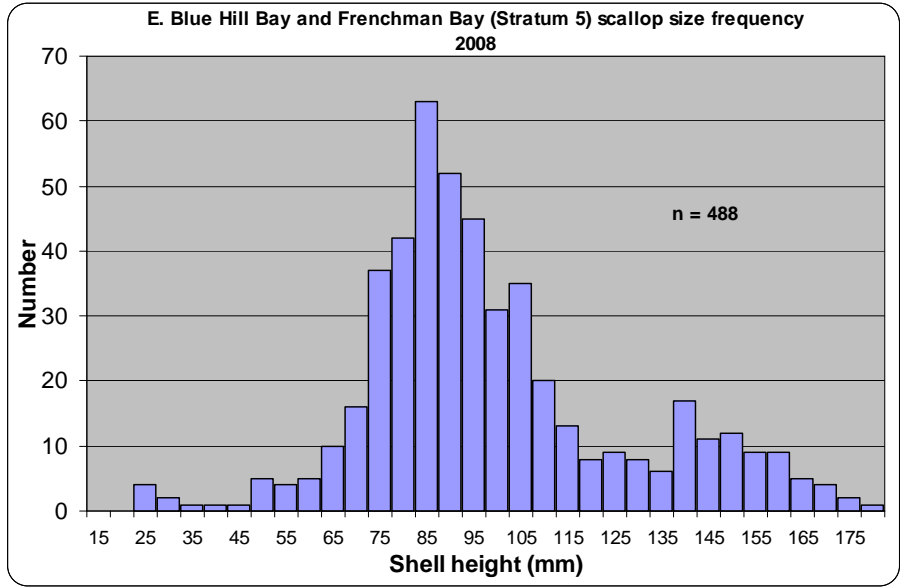
Appendix B5-Figure 16. Scallop size frequency (5 mm increments) (top) and mean density (+/- one standard error, unadjusted for dredge efficiency) by size class (bottom), Cross Island to Quoddy Head.



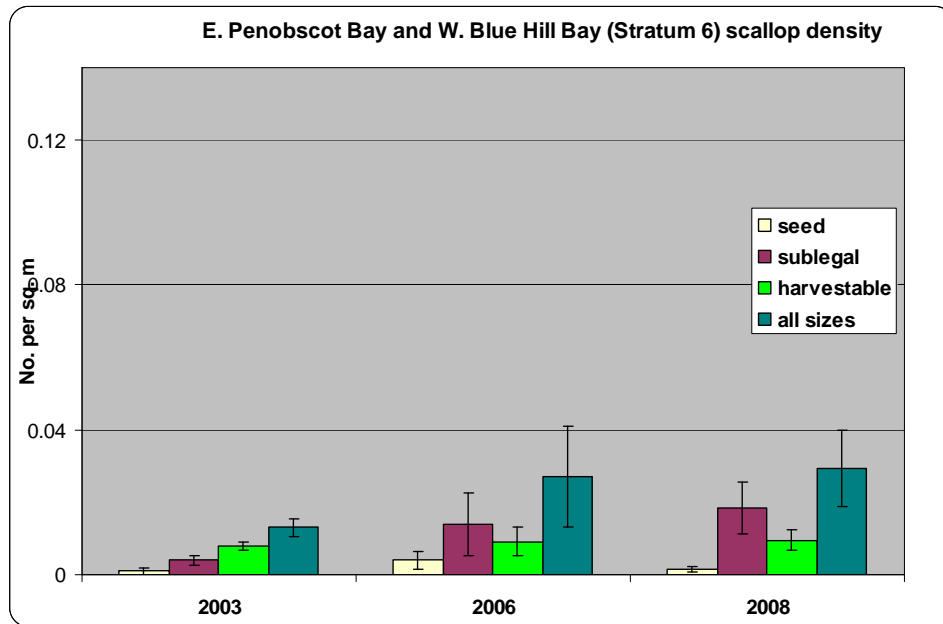
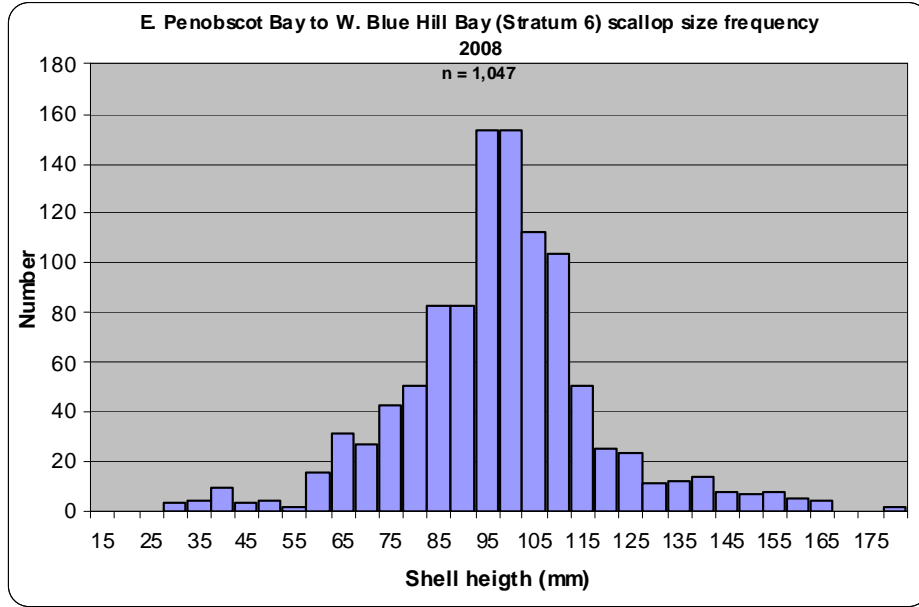
Appendix B5-Figure 17. Scallop size frequency (5 mm increments) (top) and mean density (+/- one standard error, unadjusted for dredge efficiency) by size class (bottom), Great Wass Island to Little River.



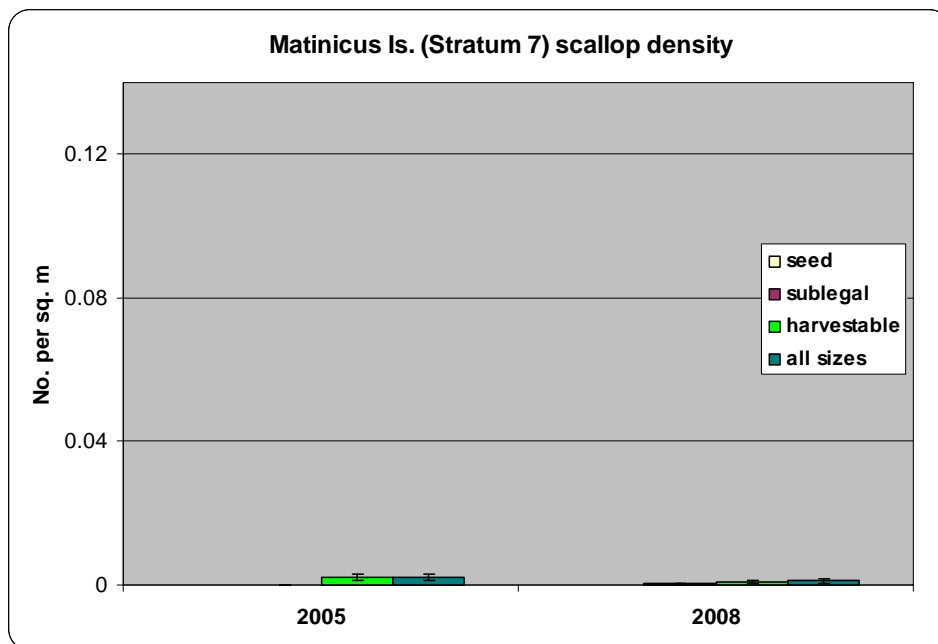
Appendix B5-Figure18. Scallop size frequency (5 mm increments) (top) and mean density (+/- one standard error, unadjusted for dredge efficiency) by size class (bottom), Schoodic Point to Great Wass Island



Appendix B5-Figure 19. Scallop size frequency (5 mm increments) (top) and mean density (+/- one standard error, unadjusted for dredge efficiency) by size class (bottom), East Blue Hill Bay and Frenchman Bay.



Appendix B5-Figure 20 . Scallop size frequency (5 mm increments) (top) and mean density (+/- one standard error, unadjusted for dredge efficiency) by size class (bottom), East Penobscot Bay and W. Blue Hill Bay.



Appendix 5-Figure 21. Scallop mean density (+/- one standard error, unadjusted for dredge efficiency) by size class, Matinicus Island

Results from the 2008 survey indicated that scallop abundance has remained low and in some areas slightly declined along the eastern Maine coast (Figures 6-21). These results are similar to reports for adjacent areas of the Canadian coast where landings and survey indices have either declined or remained unchanged since 2006 (Smith et al. 2008). The only region which showed slight improvement was between eastern Penobscot Bay and western Blue Hill Bay (Stratum 6) (Figure 20).

Some small recruitment signals were observed with the presence of seed around Libby Island, Gouldsboro Bay, Union River Bay, South Hancock, Blue Hill Harbor and Southeast Harbor. Three of the locations (Gouldsboro Bay, Blue Hill Harbor and Southeast Harbor) where seed were observed are currently being afforded protection by a series of 3-year area closures implemented by the state prior to the 2009 season. It is hoped the area closures could be particularly beneficial in areas such as these where some resource is present that could be allowed to grow to an optimal size for harvest.

Western Maine: Strata 8-11 (West Penobscot Bay to Kittery)

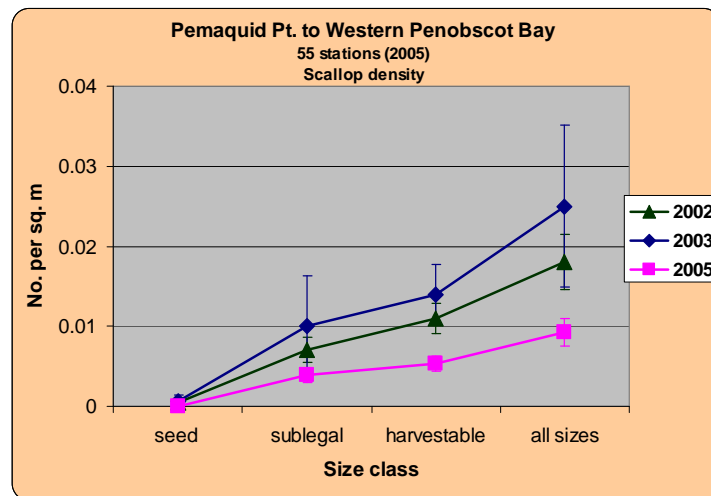
The survey covered these strata in 2005 and 2009. There were 109 tows completed in 2005 and 80 in 2009. The 2005 survey was carried out over 19 vessel days between Nov. 17, 2005 and April 25, 2006. The two contracted vessels were the *F/V North Star* from Portland and the *F/V Sea Ryder* from Spruce Head. The Portland vessel covered strata 10-11 during Nov.-Dec. 2005 and the Spruce Head vessel covered the remaining strata during Feb.-Apr. 2006.

The survey was intended to be performed during late fall, prior to the Dec. 1 opening of the scallop season and after most lobster traps had been removed from the water. For strata 10-11 however, vessel availability and an extended presence of lobster gear in the area precluded completion of the survey before Dec. 1, 2005. In strata 7-9, the survey vessel was not available until January and sampling personnel were not available until February.

Sampling in 2009 was also structured to monitor scallop abundance both inside and outside of the “closed” areas that went into effect in 2009. Tows were distributed to facilitate these areal comparisons. There were also several “fixed” stations sampled which were generally in areas that were considered especially important to monitor on a regular basis. The Piscataqua River area was added to the survey in Stratum 11. Lobster gear was still present in many areas, particularly Casco Bay. Highest 2009 catch rates appear to have been in western Casco Bay and Muscle Ridge Channel and data will be analyzed and a final report on this survey will be completed in 2010.

Results from the 2005 survey indicated that scallop abundance declined across all size categories and throughout all western coastal Maine strata. Overall scallop densities were 49-59% lower than in previous surveys done in 2002 and 2003. The survey zone which comprises Casco Bay had the largest decline.

Casco Bay had the highest density of harvestable scallops (0.006 m^{-2}) observed in the 2005 survey. By comparison the density of harvestable size sea scallops in South Bay (part of Cobscook Bay, the most productive scalloping area in Maine waters) was 0.070 m^{-2} when surveyed in 2006 (Kelly 2007). Highest harvestable density observed in the survey in western Maine was 0.019 m^{-2} in the Small Point to Pemaquid Point stratum in 2003. This survey zone declined to 0.003 m^{-2} in the 2005 survey.

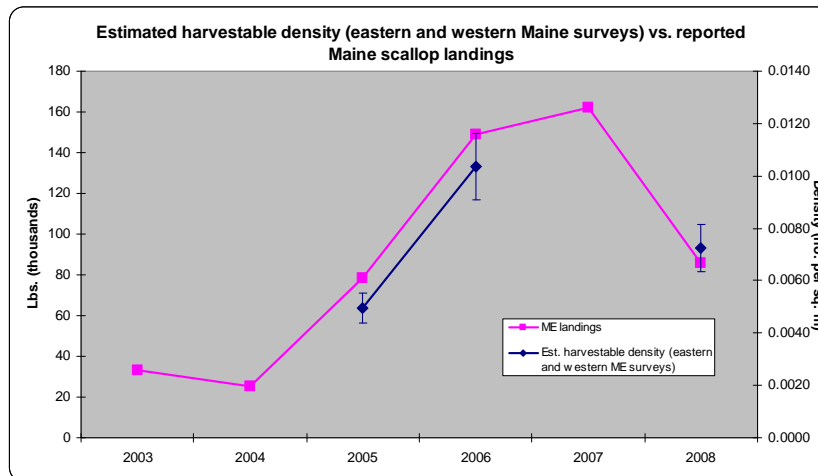


Appendix B5-Figure 22. Mean scallop density by size class, Pemaquid Point to West Penobscot Bay.

Interpretation of these results should be tempered by the fact that the 2005 survey was carried out between Small Point and Matinicus Island well after the commercial scallop season had begun. Although scallop fishing pressure is considered low throughout western Maine (perhaps the Damariscotta River being an exception) it is possible that 2005/2006 season fishing activity could have had an impact on the survey observations. This may account particularly for the size structure of scallops sampled in the Small Point to Pemaquid Point stratum in the 2005 survey. Although sublegal density was similar between 2003 and 2005, harvestable density was much lower in 2005. Fishing removals during 2005/2006 may account for some of the lower density of harvestable scallops observed in the Sheepscot and Damariscotta Rivers.

Eastern/Western Maine survey in relation to landings

As discussed above for Cobscook Bay, Maine scallop landings reports were not required from dealers (and harvesters) until 2008. Reports prior to 2008 were voluntary so landings may not be fully represented. Given those conditions, however, a strong correlation exists when comparing estimated mean harvestable scallop density from the scallop survey in either eastern or western Maine (depending on which area was surveyed in a particular year) and reported Maine landings (Figure 23). This relation is interesting and would not be expected based on the assumption that Maine scallop landings are largely a function of Cobscook Bay. One possible explanation is that the overall condition of the resource is better reflected by abundance within coastal strata rather than from within the rather unique situation of Cobscook Bay. This relation will be of interest to explore following future surveys.



Appendix 5-Figure 23. Mean scallop harvestable density (with standard error, unadjusted for dredge efficiency) estimated by DMR survey in western Maine (2005) and eastern Maine (2006, 2008) in relation to reported Maine landings.

Meat weight modeling

Meat weights were collected from 2,762 scallops during 2005-2008 surveys. Associated with each meat weight were the following parameters: shell height, shell length, shell depth, date, location (station) and depth. Generalized linear mixed models (GLMM) with a log link were used to predict scallop meat weight using the following fixed effects: shell height, shell depth, latitude and depth (Table 2). Random effects were grouped by a variable consisting of the

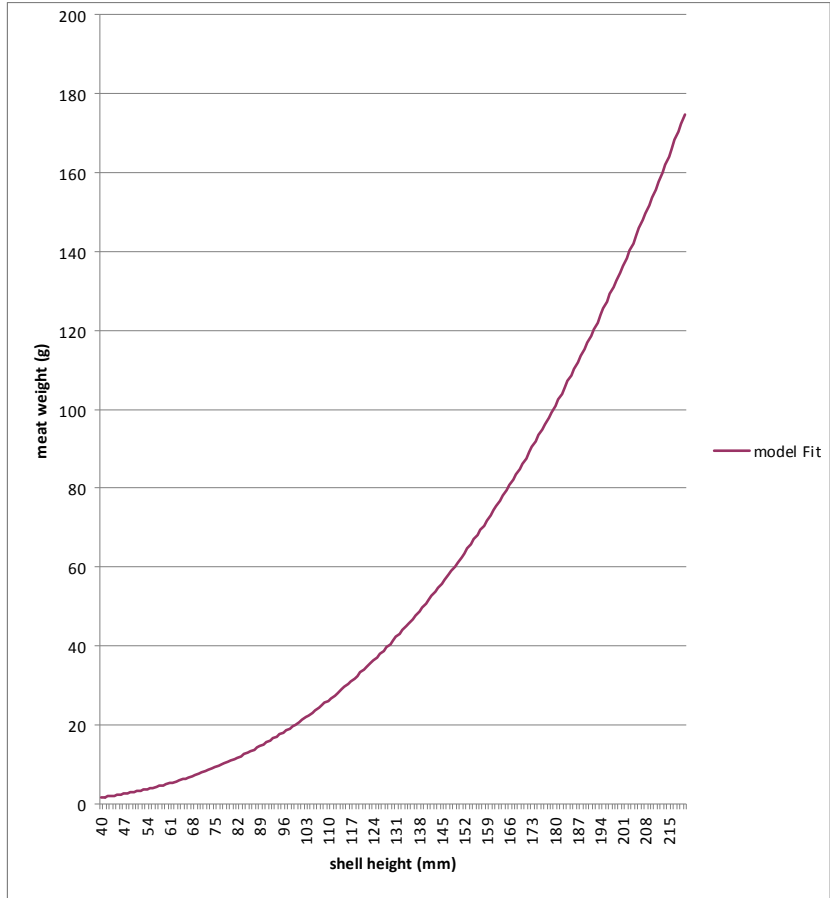
sampling station, or shell height and station. (Modeling courtesy of D. Hennen, Northeast Fisheries Science Center, Woods Hole, MA).

The following model for predicting meat weight had the lowest AIC value:

$$\text{meat_weight} \sim \text{height} + \text{depth} + \text{lat} + \text{s_depth} + (\text{height} + 1 \mid \text{station})$$

Appendix B5-Table 2. Mixed-effect model-building results for prediction of scallop meat weights in the state waters of Maine, 2005-2008.

Formula	AIC	BIC	logLik	deviance
Maine				
meat_weight ~ height + depth + lat + s_depth + (height + 1 station)	2083	2136	-1032	2065
meat_weight ~ height + depth + length + lat + (height + 1 station)	2184	2237	-1083	2166
meat_weight ~ height + depth + s_depth + (height + 1 station)	2189	2236	-1086	2173
meat_weight ~ height + depth + s_depth + height * depth + (height + 1 station)	2190	2244	-1086	2172
meat_weight ~ height + s_depth + height * depth + (height + 1 station)	2190	2244	-1086	2172
meat_weight ~ height + depth + lat + (height + 1 station)	2239	2286	-1112	2223
meat_weight ~ height + depth + lat + height * depth + (height + 1 station)	2241	2294	-1111	2223
meat_weight ~ height + depth + length + (height + 1 station)	2247	2295	-1116	2231
meat_weight ~ height + length + height * depth + (height + 1 station)	2249	2303	-1116	2231
meat_weight ~ height + depth + length + height * depth + (height + 1 station)	2249	2303	-1116	2231
meat_weight ~ height + depth + length + lat + (1 station)	2268	2309	-1127	2254
meat_weight ~ height + lat + (height + 1 station)	2275	2316	-1130	2261
meat_weight ~ height + length + (height + 1 station)	2281	2323	-1134	2267
meat_weight ~ height + depth + s_depth + (1 station)	2298	2333	-1143	2286
meat_weight ~ height + depth + (height + 1 station)	2305	2346	-1145	2291
meat_weight ~ height + height * depth + (height + 1 station)	2307	2354	-1145	2291
meat_weight ~ depth + height * depth + (height + 1 station)	2307	2354	-1145	2291
meat_weight ~ height + depth + length + (1 station)	2327	2363	-1158	2315
meat_weight ~ height + (height + 1 station)	2337	2372	-1162	2325
meat_weight ~ height + length + (1 station)	2363	2392	-1176	2353
meat_weight ~ height + depth + lat + (1 station)	2407	2443	-1197	2395
meat_weight ~ height + lat + (1 station)	2443	2473	-1217	2433
meat_weight ~ height + depth + (1 station)	2471	2500	-1230	2461
meat_weight ~ height + height * depth + (1 station)	2472	2508	-1230	2460
meat_weight ~ depth + height * depth + (1 station)	2472	2508	-1230	2460
meat_weight ~ height + (1 station)	2504	2528	-1248	2496
meat_weight ~ depth + (height + 1 station)	2729	2764	-1358	2717
meat_weight ~ depth + (1 station)	11467	11491	-5730	11459



Appendix B5-Figure 24. Scallop shell height vs. meat weight relationship based on Maine (2005-2008) data at 22 m (12 fathoms) in depth and 44°N latitude.

Conclusions

Results from the surveys of ME state eaters indicate that scallop abundance has remained low and in some areas has slightly declined along the eastern Maine coast. Some recruitment signals were observed, however, in the most recent eastern Maine survey (2008), particularly in the zone between eastern Penobscot Bay and western Blue Hill Bay. Cobscook Bay, at the far eastern end of the Maine coast, remains the most heavily fished and productive area in Maine waters. The 2007 estimate of harvestable biomass 128 mt (281.3 thousand lbs) of meats in Cobscook Bay was 99.4% higher than the previous year. Overall western Maine scallop densities were 49-59% lower in 2005 than in previous surveys done in 2002 and 2003. The survey zone which comprises Casco Bay had the largest decline in 2005.

References:

- Athearn, K. 2005. Cobscook Bay sea scallops: the fishery and the markets. Prepared for Cobscook Bay Resource Center, 59 p.
- Cochran, W.G. 1977. Sampling techniques, 3rd ed. John Wiley & Sons, New York. 428 p.
- Gedamke, T., W.D. DuPaul and J.M. Hoenig. 2004. A spatially explicit open-ocean DeLury analysis to estimate gear efficiency in the dredge fishery for sea scallop *Placopecten magellanicus*. *North American Journal of Fisheries Management* 24:335-351.
- Gedamke, T., W.D. DuPaul and J.M. Hoenig. 2005. Index-removal estimates of dredge efficiency for sea scallops on Georges Bank. *North American Journal of Fisheries Management* 25: 1122-1129.
- Kelley, J.T., W.A. Barnhardt, D.F. Belknap, S.M. Dickson and A.R. Kelley. 1998. The seafloor revealed: the geology of the northwestern Gulf of Maine inner continental shelf. Open-File 96-6 Maine Geological Survey Natural Resources Information and Mapping Center.
- Kelly, K.H. 2007. Results from the 2006 Maine sea scallop survey. Maine Department of Marine Resources, Research Reference Document, 34 p.
- National Marine Fisheries Service, Northeast Fisheries Science Center (NMFS/NEFSC). 2004. 39th Northeast Regional Stock Assessment Workshop (39th SAW) Assessment Summary Report & Assessment Report. *Northeast Fisheries Science Center Reference Doc.* 04-10.
- Schick, D.F. and S.C. Feindel. 2005. Maine scallop fishery: monitoring and enhancement. *Final Report to the Northeast Consortium (Sept. 1, 2005)*, 72 p.
- Smith, S.J., S. Rowe and M. Lundy. 2008. Scallop Production Areas in the Bay of Fundy: Stock Status for 2007 and Forecast for 2008. DFO Can. Sci. Advis. Sec. Res. Doc. 2008/002, 110 p.

Appendix B6: An assessment of the sea scallop resource in the Northern Gulf of Maine management area.

Samuel B. Truesdell (University of Maine, Orono), Kevin H. Kelly (Maine Department of Marine Resources, W. Boothbay Harbor, ME), Catherine E. O’Keefe (University of Massachusetts, Dartmouth), and Yong Chen (University of Maine, Orono).

The sea scallop fishery in the Northern Gulf of Maine (NGOM) occurs in federal waters and is managed by the New England Fishery Management Council. The NGOM resource and associated fishery are locally important but amount to a small portion of the total stock and landings. The fishery is managed by TAC independently of the rest of the EEZ sea scallop stock. In particular, management of the NGOM fishery does not involve biological reference points as targets or thresholds. A cooperative survey was carried out by the Maine Department of Marine Resources and the University of Maine in June-July, 2009. The best estimate based on survey results indicates that the biomass of NGOM sea scallops targeted by the fishery (102+ mm or 4+ in shell height) was approximately 103 mt of meats during 2009 with a 95% confidence interval ranging from about 53 to 186 mt. Landings during 2009 amounted to approximately 7 mt. The best estimate of exploitation rate (reported landings in weight / estimated biomass) in the NGOM during 2009 was 0.065, with a 95% confidence interval ranging from 0.035 to 0.12. These estimates are based on density estimates from the survey assuming a range of survey dredge capture efficiency of 40%. NGOM biomass was relatively low during 2009, although small (10-50 mm) “seed” scallops were abundant at two stations on Platts Bank.

Background

Sea scallops (*Placopecten magellanicus*) have been an important resource in the Gulf of Maine coastal region since before European settlement. Initially supplementing the diets of early European settlers and Native Americans (Bourne 1964), a commercial scallop fishery eventually developed in the 1880s (Dow 1956, Bourne 1964, Baird 1967). The Gulf of Maine fishery expanded after World War I (Dow 1971), although fishing effort remained mainly inshore until 1950, when some fishing began in more offshore areas (Dow 1956). Since then, the scallop fishery in the Gulf of Maine has undergone substantial fluctuations with landings ranging from hundreds of thousands to millions of pounds within as little as a three year period (Figure 1).

The recent Amendment 11 to the New England Fishery Management Council Sea Scallop Fishery Management Plan (New England Fishery Management Council 2008) created a separate limited entry program for general category fishing in the Northern Gulf of Maine (NGOM) management area (Figure 2). The program includes a yearly NGOM total allowable catch (TAC; currently 70,000 lbs.) and a daily possession limit of 200 lbs. (New England Fishery Management Council 2008). The effective date of the new management regime was June 1, 2008.

The 2008 NGOM TAC was set based on 2000-2006 landings from federal waters of the Gulf of Maine (New England Fishery Management Council 2008) because information on stock abundance in this area was minimal. In June-July 2009, the Maine Department of Marine Resources (DMR) and the University of Maine (UM) collaborated under the FY 2008 Scallop Research Set-Aside Program to survey this new management area, with the goal of estimating the harvestable scallop biomass and providing information that might be used in updating the

TAC. The survey was carried out aboard the F/V *Foxy Lady II* out of Stonington, ME under contract with the DMR.

Methods

The NGOM was divided into five areas for the purposes of this survey, referred to here (from east to west) as Machias Seal Island (Area 1), Mt. Desert Rock (Area 2), Platts Bank (Area 3), northern Stellwagen Bank (Area 4), and Cape Ann (Area 5; Figure 2). Selection of these areas was based on previous offshore Gulf of Maine scallop surveys (Spencer 1974, Serchuk and Rak 1983, Serchuk 1984, Serchuk and Wigley 1984); recent (2000-2008) vessel trip reports (VTR) indicating the location and magnitude of scallop catches by vessels fishing in federal portions of the Gulf of Maine; recent Maine/New Hampshire inshore trawl survey data (S. Sherman, DMR, pers. comm.); and input from two Maine-based federally-permitted scallop fishermen with experience fishing these areas. VTR data, in particular, indicate that most scallop catches by federally-permitted vessels during 2000-2008 were from Areas 4 and 5.

The survey followed an adaptive two-stage random stratified design (Francis 1984) in areas 4 and 5. These regions were delineated into high, medium, and low density sub-areas based on expected survey catch in order to increase sampling precision. The stratification was based on 2000-2008 VTR data and input from the survey captain and an experienced federally-permitted scallop fisherman. Forty tows were allocated to the first stage among the three sub-areas. After the first survey stage, the within sub-area variance was calculated. Using this variance in combination with the area size, the number of tows allocated to each sub-area in stage 2 was calculated according to the method used by Francis (1984).

Area 2 was stratified into high and low densities. However, because of its large size, the survey in this area was only a single stage. Areas 1 and 3 were not divided into subareas due to low expected scallop densities.

One hundred and ninety-six stations were occupied in total. Tows lasted either five or seven minutes depending on the bottom type and amount of fixed fishing gear in the area. The survey dredge was a 7 ft New Bedford style drag with 2 in rings, 1.75 in head bale, 3.5 in twine top, 10 in pressure plate and rock chains. The dredge had no liner.

At each tow location, all species were identified and counted. Excluding tows on Platts Bank where large numbers of scallop seed were caught, survey catches were low enough that approximately 98% of all scallops were measured for shell height (SH) and about 50% of measured scallops were also sampled for their meat weight (MW) for use in developing a SH to MW relationship.

Results

The most evident features of the NGOM survey length frequency distribution (Figure 3) are the dominance of scallops under 50 mm on Platts Bank and the size class distribution differences between the eastern and western NGOM.

Large numbers of scallop seed were found on Platts Bank, most of which were caught at two stations on the eastern side of the bank (estimated at over 15,000 individuals between the two tows). Some seed scallops were found in other areas but at substantially lower densities.

Another important finding regarding the length frequency distribution is the difference in breadth of size distribution between the eastern and western NGOM. The Cape Ann and Stellwagen Bank survey areas showed a broader size class distribution (approximately 50 – 150 mm) than those in the eastern NGOM (Platts Bank, Mt. Desert Rock and Machias Seal Is.;

Figure 3). This indicates that the western NGOM has had, in general, consistent recruitment and that scallops are able to settle and survive during most years. In contrast, the eastern NGOM tends toward episodic recruitment when conditions are favorable and the populations at these sites are composed primarily of a single size class. See Figure 4 for by-tow length frequency distribution.

Meat weights

The estimated meat weights used to determine the NGOM biomass estimates were based on area-specific shell height-meat weight (SHMW) relationships for the eastern and western NGOM. Meat weight was modeled as a function of shell height assuming multiplicative error structure as:

$$MW_i = \alpha SH_i^\beta e^{\epsilon_i}.$$

SHMT relationships varied considerably over the NGOM survey area (Figure 5). The largest meats were found on northern Stellwagen Bank, followed by Cape Ann and Mt. Desert Rock. The lowest meat weights were found on Platts Bank; however, this was based on a sample size of only 8 scallops. Low meat weights from some eastern Maine areas have been noted in previous reports (Serchuk and Rak 1983, Schick and Feindel 2005).

Biomass estimates

Bootstrapped biomass mean and 95% confidence interval estimates were calculated (1,000 replications) using the “NMFSSurvey” package version 1.0-2 written by Stephen Smith (Canada DFO) in R version 2.8.1. This package allows for various combinations of bootstrap mean and 95% confidence interval calculations. The available bootstrap mean methods are: naïve, rescaling and bootstrap-with-replacement (BWR) and the available confidence interval methods are: percentile (PCT), bias-corrected (BC), and bias-corrected-and-adjusted (BCa).

The bootstrap functions were run under each combination of bootstrap mean and 95% confidence interval calculations at assumed dredge capture efficiency estimates of 30%, 40%, and 50% (Figures 6 and 7). The middle estimate of 40% efficiency was selected as the best estimate because it is close to an estimate by the DMR of 43.6% measured in Cobscook Bay, Maine in 2006 (Kelly 2007). Figures 6-7 show that harvestable biomass was estimated at around 100 mt with absolute maximum confidence intervals from 39.7 (50% efficiency and BWR/PCT bootstrap approach) to 320 mt (30% efficiency and naïve/BCa bootstrap approach). Harvestable biomass was calculated assuming scallops under 4 in SH are too small for commercial boats to regularly target, so only scallops larger than 4 in SH were included in the estimates. The bootstrap means were stable for all efficiencies and all bootstrap methods, though there is some variation in confidence intervals among bootstrap approaches, especially at the upper bounds.

For ease of explanation, and because similar results were found under each combination of methods, the BWR/BC combination is used in the subsequent sections. This combination was found by Smith (1997) to be acceptable for estimating haddock numbers and 95% confidence intervals in a stratified random survey.

Regional biomass estimates

Figures 8 and 9 indicate that Area 1 has the highest mean biomass, though Area 3 has the largest upper confidence level bound (greater than 200,000 kg at 30% dredge efficiency) due to low sample size and high sample variability. Density calculations also show that scallops in Area 1 appear more abundant per unit area than in any of the other strata (although a substratum

in area 4 had the highest overall density). It is therefore surprising that federal vessel trip reports indicate low fishing effort in this region. Possible explanations include the high density of fixed gear in the region and poor meat quality. This area is an important lobster fishing ground and there are large numbers of lobster traps present. During the NGOM survey, alternate stations had to be used and tow durations had to be shortened in this region so that fixed gear was not damaged. Due to poor meat quality (Figure 5), more shucking effort is required to obtain the same amount of meat as in the more productive western NGOM.

Area 3 has the second highest bootstrapped mean biomass at 40% dredge efficiency (Figure 8), but because of limited time for sampling (16 tows) and high degree of variability in catch, the 95% confidence interval ranges from close to zero to over 150,000kg. This variability, along with the large year class of seed scallops, makes Platts Bank a high priority for subsequent NGOM surveys.

The Mt. Desert Rock area (Area 2) had few scallops. Historically there has been some fishing in this region and the Maine fishery has its origins in Mt. Desert Island inshore waters (Smith 1891), but little activity has been recorded in Area 2 in recent years.

The two western NGOM areas (4 and 5) exhibit relatively low biomass (Figure 8) but support most of the fishing activity. The limited fixed gear and good meat condition (Figure 5) are probably the two main contributors to the higher rate of fishing. The high sampling rate (60 tows in each of the two regions) increased precision over the other areas.

Exploitation rates

The 2009 estimated exploitation rate for the NGOM at 40% dredge efficiency was 0.065, with a 95% confidence interval ranging from 0.035 to 0.12 (based on the BWR/BC method; Figure 10). Landings are based on dealer and vessel reports and were retrieved from the NMFS Northeast Regional Office website.⁴

The exploitation estimates were somewhat sensitive to the assumed capture efficiency level. The mean exploitation rate for assumed efficiency of 30% is 0.049 and the mean for assumed efficiency of 50% is 0.080. The range in estimated confidence intervals (the lower bound of the 95% confidence interval at 30% efficiency and the upper bound of the 95% confidence interval at 50% efficiency) was from 0.027 to 0.15 (Figure 10).

The exploitation rate may be higher in some regions, particularly in Areas 4 and 5 in the western NGOM. However, these rates were not able to be estimated due to data confidentiality (VTR reports were for less than 3 vessels).

Platts Bank

The Platts Bank survey area (Area 3; Figure 11) deserves special consideration because two sample locations saw numbers of seed scallops in the thousands (see Figure 4 tows SM3C04 and SM3C10). These densities were much larger than elsewhere in state or federal waters of the Gulf of Maine. The DMR/UM survey had relatively few (16) tows in Platts Bank because. Although productive in the past, Platts Bank has seen little fishing in recent years so high densities were not anticipated.

The University of Massachusetts School for Marine Science and Technology (SMAST) also surveyed Platts Bank in 2009 (Figure 12). The SMAST survey used a drop pyramid with two different cameras which photographed the bottom at each sample location (see Stokesbury and Harris 2006 for details). Scallop densities and other individual and population statistics were

⁴ <http://www.nero.noaa.gov/ro/fso/Reports/ScallopProgram/NGOMReport%2020100223.pdf>

estimated from the photos. The DMR/UM survey occurred on July 28th and the SMAST survey on August 12 and 13, 2009. The two surveys complemented each other because the DMR/UM survey was able to cover a large area per station and the SMAST survey was able to sample a large number of stations distributed across the area.

As the survey areas were delineated differently between the two projects, biomass estimates are difficult to compare. Therefore, only densities and length frequency data are used in comparing results. Mean scallop densities from the two surveys were almost identical: SMAST estimated 1.87/m² and DMR/UM estimated 1.81/m² (table 1). The confidence intervals, however, were quite different. The SMAST confidence interval is symmetric and estimated assuming a normal distribution while the DMR/UM mean (assuming 40% dredge efficiency) was bootstrapped as described above. Despite the differences in computation of confidence intervals, the main reason the SMAST confidence interval is smaller is that the sampling design allowed for many more sampling locations. The two surveys generally agreed on the spatial distribution of scallop density (Figures 11 and 12) with highest densities on the eastern side of Platts Bank.

High scallop densities on Platts Bank were the result of a recruitment event. It is not known, however, whether this will result in increased fishing activity in the future. The scallops of harvestable size that were sampled on the DMR/UM survey had very low SHMW relationships but only 8 scallops larger than 4 inches were sampled (see Figure 5). Two reasons potentially explain this poor meat quality. One explanation is that Platts Bank is currently poor habitat for scallops. The other explanation is that the meats sampled were simply from older, poorer-condition scallops and that the new recruitment class will potentially have better meats.

The DMR/UM and SMAST shell height composition data are compared in Figures 13 and 14. Compared to the SH measurements from the SMAST large camera, the DMR/UM distribution is shifted somewhat to the left. However, compared to the SMAST digital still camera, the DMR/UM distribution is shifted only slightly to the left. This may be due to the timing of the surveys. The DMR/UM survey took place in late July 2009 and the SMAST survey in mid-August 2009, so the difference between the DMR/UM and SMAST digital still camera SH frequencies could be attributed to growth over the period between the surveys.

When the densities, length frequencies, and spatial distributions are considered, the two surveys compare well. It appears that the DMR/UM survey achieved a large enough sample size to well-characterize the Platts Bank population. Ideally, however, more tows will be included in the future to increase precision. In addition, the SMAST survey was able to estimate the length frequency distribution observed by the DMR/UM survey with their digital still camera without bringing animals to the surface, assuming the slight shift in the SMAST distribution is due to growth.

Recruitment dynamics are unclear in the NGOM. An interesting note is that little recent recruitment was observed in the southwestern NGOM (Cape Ann and Stellwagen Bank). It is possible that oceanographic conditions contributing to recruitment on Platts Bank also reduced larval input to southwestern NGOM.

Conclusions

The 2009 DMR/UM survey confirmed what recent landings data suggest: scallop biomass is currently low in the NGOM management area. NGOM scallops are not heavily fished as the exploitation rate (catch/biomass) is estimated at approximately 0.07. The survey found significant biomass in the Machias Seal Is. area (close to 50,000 kg), an area that is hardly fished probably due to the high concentration of fixed gear and poor meat quality. This area

contributes greatly to the low exploitation rate because of its size and lack of fishing. The western Gulf of Maine (Cape Ann and Stellwagen Bank areas) probably have higher exploitation rates. However, rates for these areas could not be estimated due to confidentiality constraints (VTR reports were for fewer than 3 vessels).

The high densities of scallop seed noted on Platts Bank by both the DMR/UM and SMAST surveys could prove important once those scallops recruit to the fishery. The poor meats encountered on Platts Bank by the DMR/UM survey also leave open the possibility that while densities on Platts Bank may be very high, meat quality may be low. Few samples were taken on Platts Bank, however, so the poor meats are not necessarily representative.

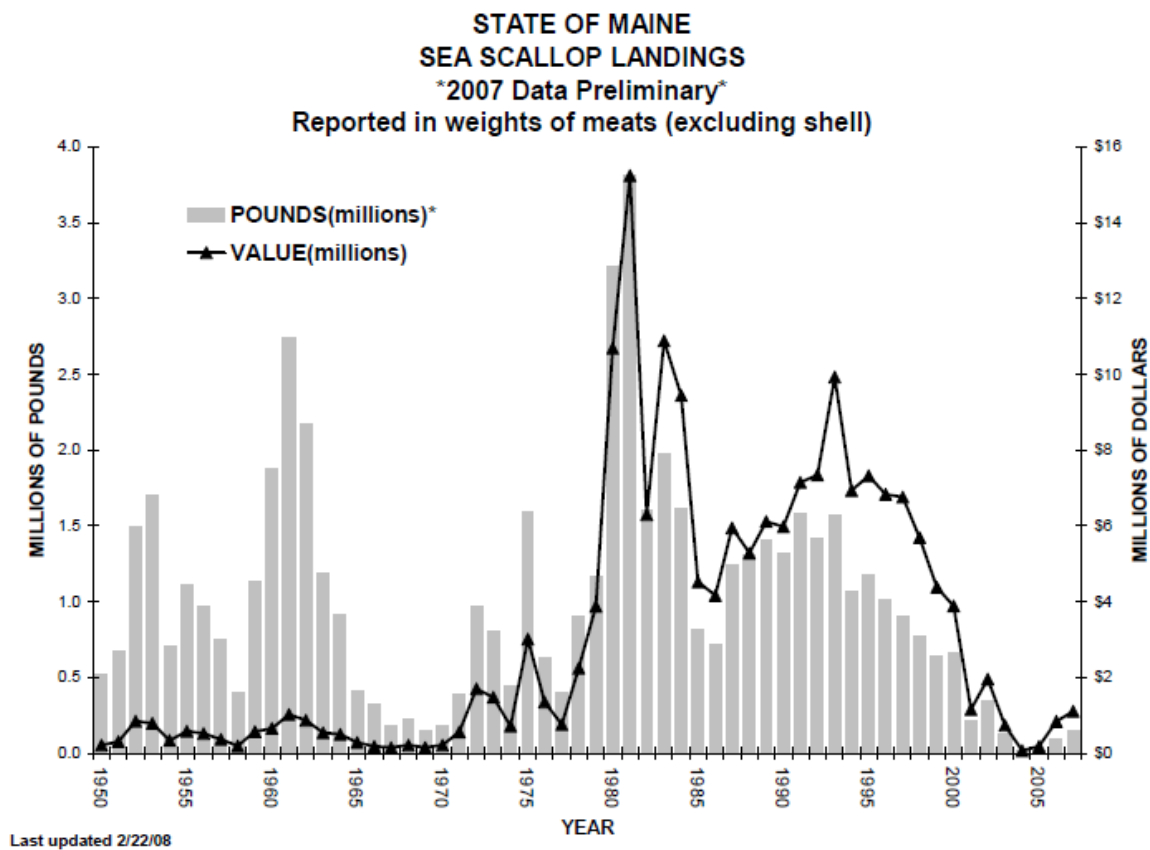
References

- Baird, F. T. J. 1967. Fisheries Education Series Unit No. 2: The Sea Scallop (*Pecten magellanicus*). Bulletin of the Department of Sea and Shore Fisheries.
- Bourne, N. 1964. Scallops and the Offshore Fishery of the Maritimes. Fisheries Research Board of Canada Bulletin 145.
- Dow, R. L. 1956. The Maine Sea Scallop Fishery. Bulletin of the Department of Sea and Shore Fisheries Fisheries Circular no. 19.
- Dow, R. L. 1971. Periodicity of Sea Scallop Abundance Fluctuations in the Northern Gulf of Maine. Bulletin of the Department of Sea and Shore Fisheries Research Bulletin No. 31.
- Francis, R. I. C. C. 1984. An adaptive strategy for stratified random trawl surveys. New Zealand Journal of Marine and Freshwater Research 18:59-71.
- Kelly, K. H. 2007. Results from the 2006 Maine Sea Scallop Survey. Maine Department of Marine Resources.
- New England Fishery Management Council. 2008. Fisheries of the Northeastern United States; Atlantic Sea Scallop Fishery; Amendment 11; Final Rule.
- Owen, E. F. 2008. Population structure of the Sea Scallop, *Placopecten magellanicus*, in coastal Maine. PhD thesis, University of Maine.
- Schick, D. F., and S. C. Feindel. 2005. Maine Scallop Fishery: Monitoring and enhancement. Final report to the Northeast Consortium.
- Serchuk, F. M. 1983. Results of the 1983 USA Sea Scallop research survey: distribution and abundance of Sea Scallops in the Georges Bank, Mid-Atlantic and Gulf of Maine Regions and biological characteristics of Iceland Scallops off the coast of Massachusetts. Northeast Fish. Cent., Woods Hole Lab. Ref. Doc. 83-37.
- Serchuk, F., and R. Rak. 1983. Biological characteristics of offshore Gulf of Maine sea scallop populations: size distributions, shell height meat weight relationships and relative fecundity patterns. Northeast Fish. Cent., Woods Hole Lab. Ref. Doc. 83-07. 42 p.
- Serchuk, F., and S. Wigley. 1984. Results of the 1984 USA sea scallop research vessel survey: status of sea scallop resources in the Georges Bank, Mid-Atlantic and Gulf of Maine regions and abundance and distribution of Iceland scallops off the southeastern coast of Cape Cod. U.S. Natl. Mar. Fish. Serv. Northeast Fish. Cent. Woods Hole Lab. Ref. Doc. 83-84. 74 p.
- Smith, H. M. 1891. The Giant Scallop Fishery of Maine; chapter 16 extracted from The Bulletin of the United States Fish Commission, Volume IX, for 1889. Pages 313-335. Government Printing Office, Washington

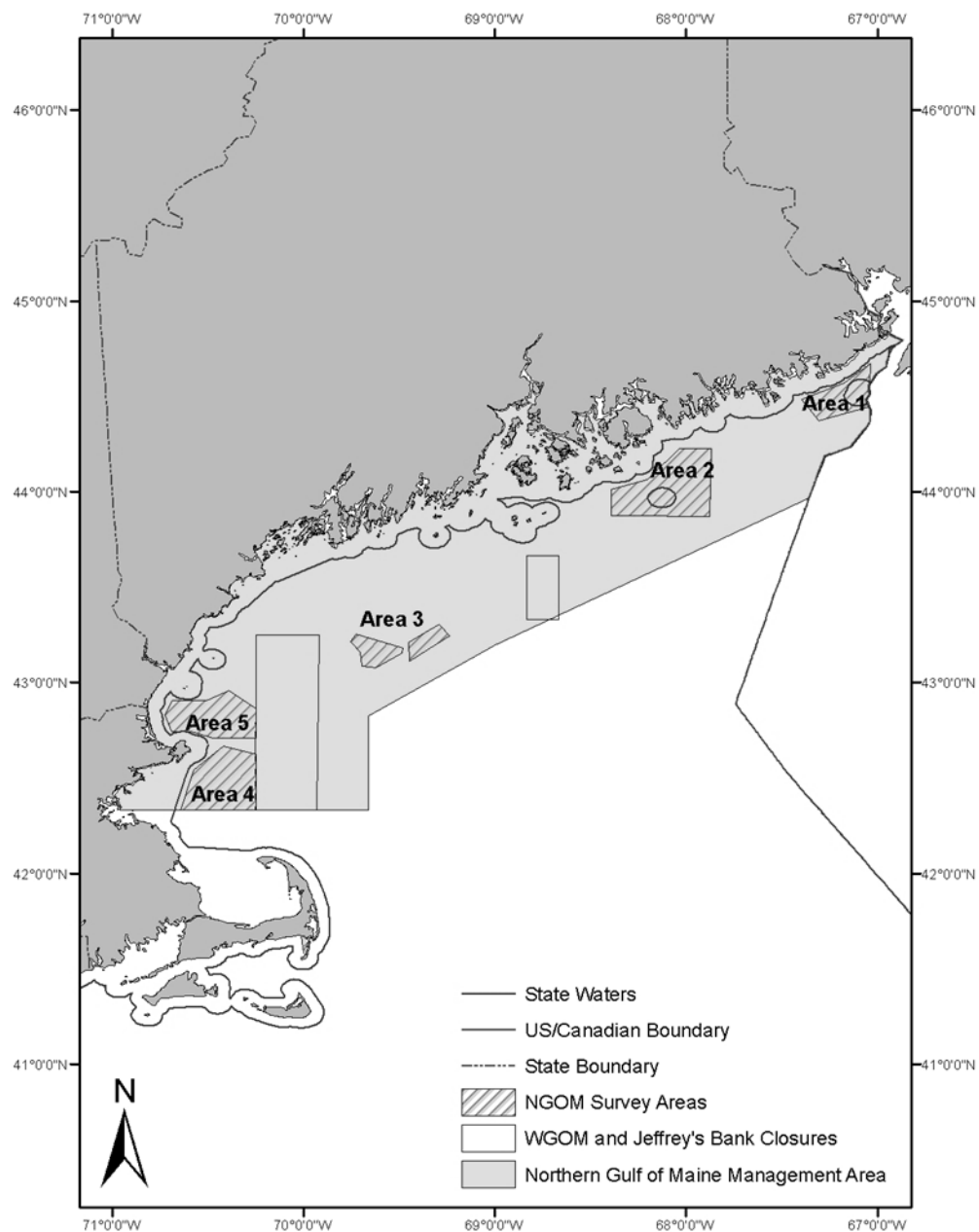
- Smith, S. J. 1997. Bootstrap confidence limits for groundfish trawl survey estimates of mean abundance. *Canadian Journal of Fisheries and Aquatic Sciences* 54:616-630.
- Spencer, F. 1974. Final report: offshore scallop survey - Cape Ann, Massachusetts to Maine-Canadian border. Maine Department of Marine Resources. 16p.
- Stokesbury, K. D. E., and B. P. Harris. 2006. Impact of limited short-term sea scallop fishery on epibenthic community of Georges Bank closed areas. *Marine Ecology Progress Series* 307:85-100.

Appendix 6-Table 1. Estimated scallop density (all size classes) on Platts bank for the DMR/UM and SMAST surveys in 2009.

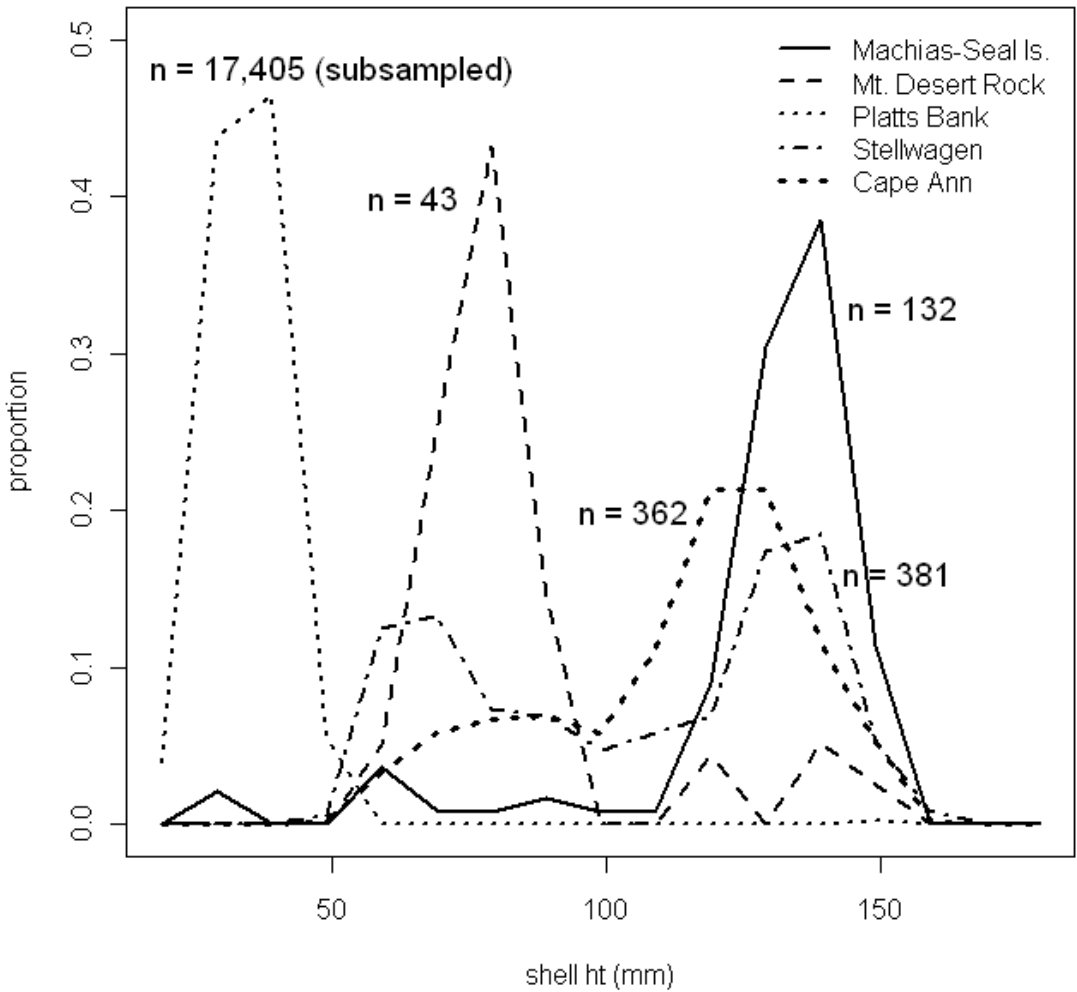
Survey	Mean Density	95% confidence interval
SMAST	1.87	(0.674 , 3.066)
DMR/UM	1.805	(0.014 , 5.071)



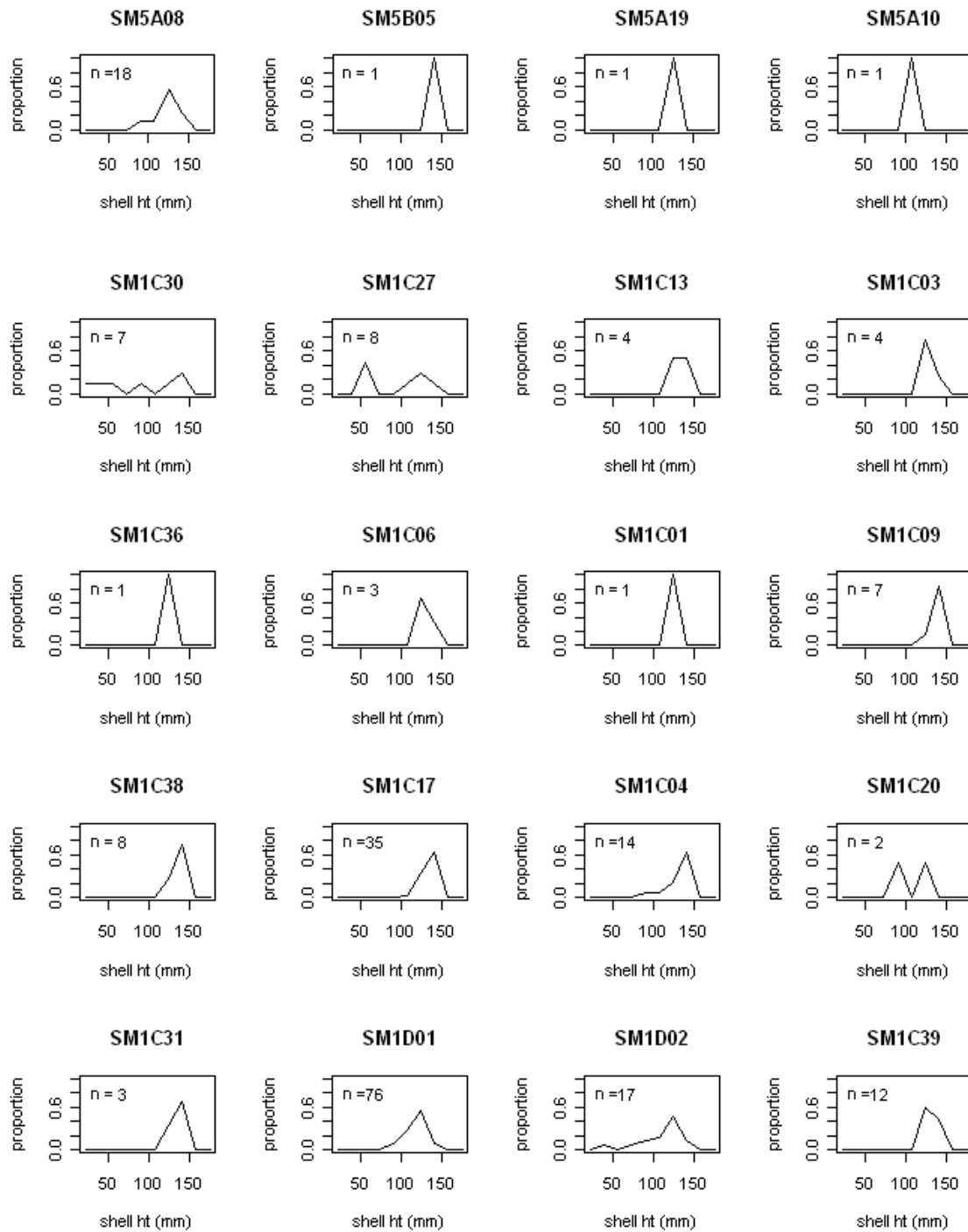
Appendix B6-Figure 1. Maine scallop landings (inshore and offshore) and ex-vessel revenues 1950 through 2007.

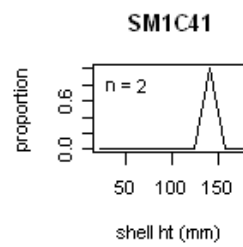
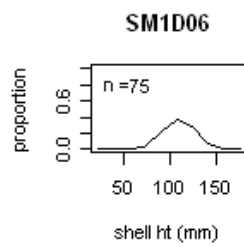
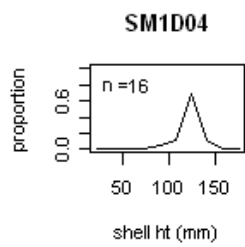
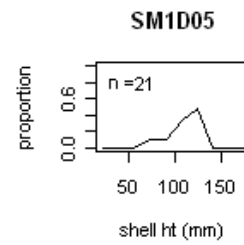
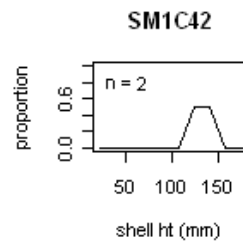
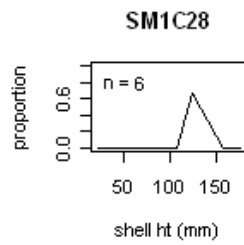
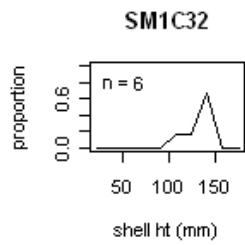


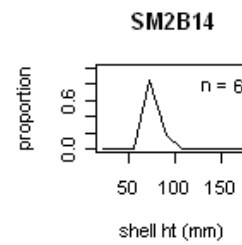
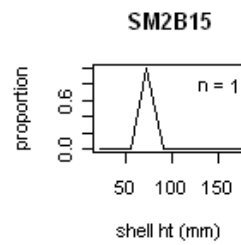
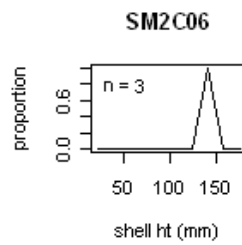
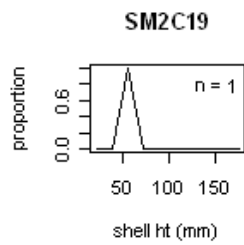
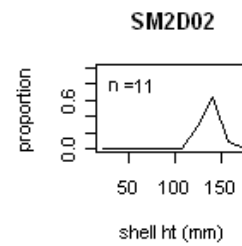
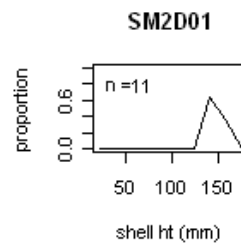
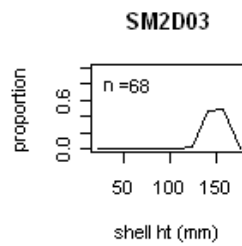
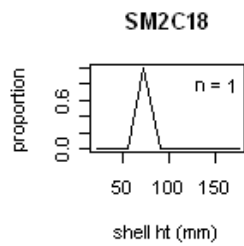
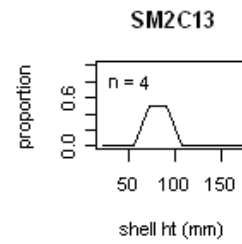
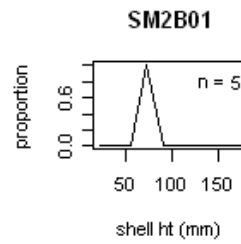
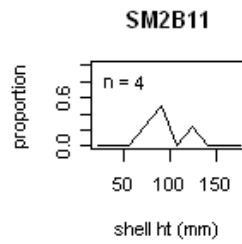
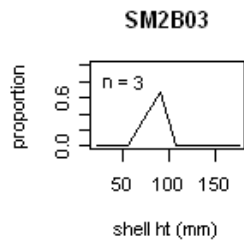
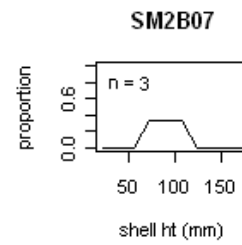
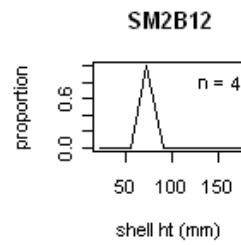
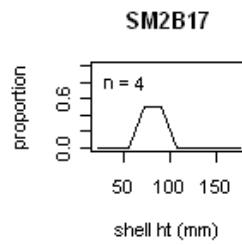
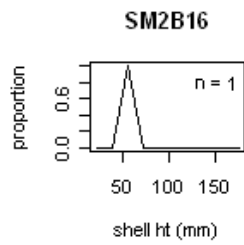
Appendix B6-Figure 2. The NGOM management area was divided into 5 regions for the DMR/UM 2009 survey. In numerical order the areas are: Machias Seal Island, Mt. Desert Rock, Platts Bank, Stellwagen Bank and Cape Ann.

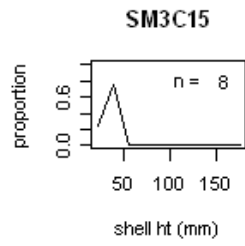
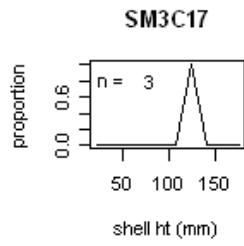
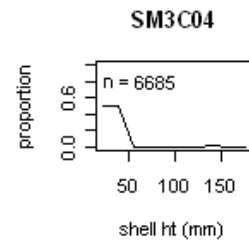
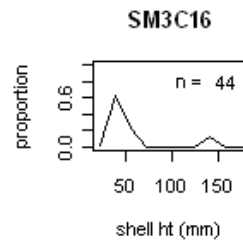
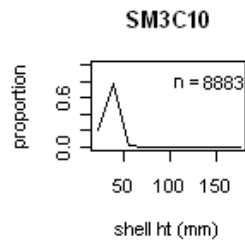
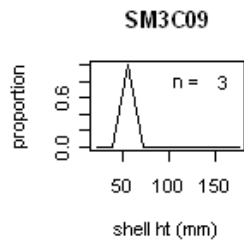


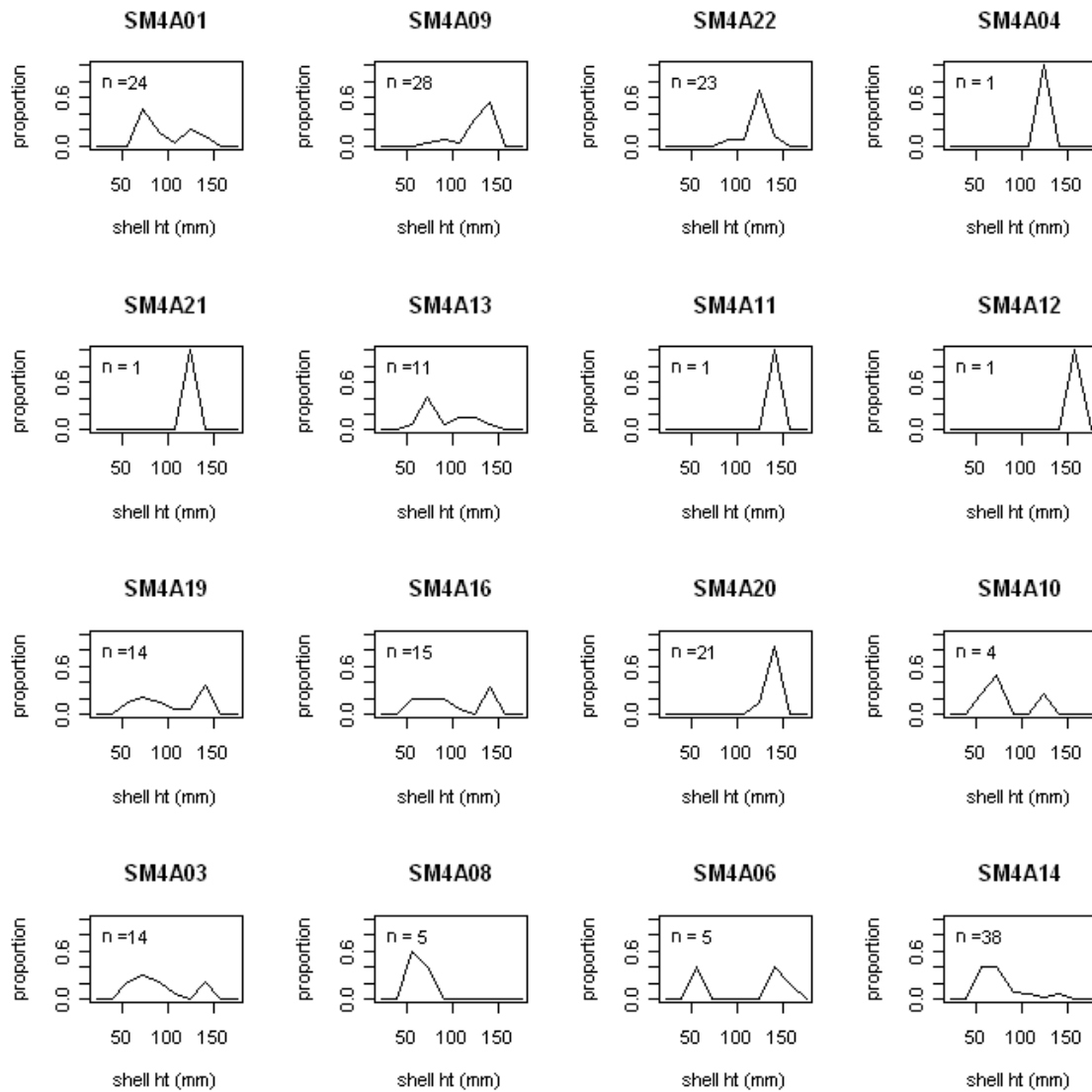
Appendix B6-Figure 3. The NGOM length frequency distribution estimated by the DMR/UM survey. The western Gulf of Maine (Stellwagen Bank and Cape Ann) has a much broader size class distribution. Large numbers of seed scallops were found on Platts Bank.

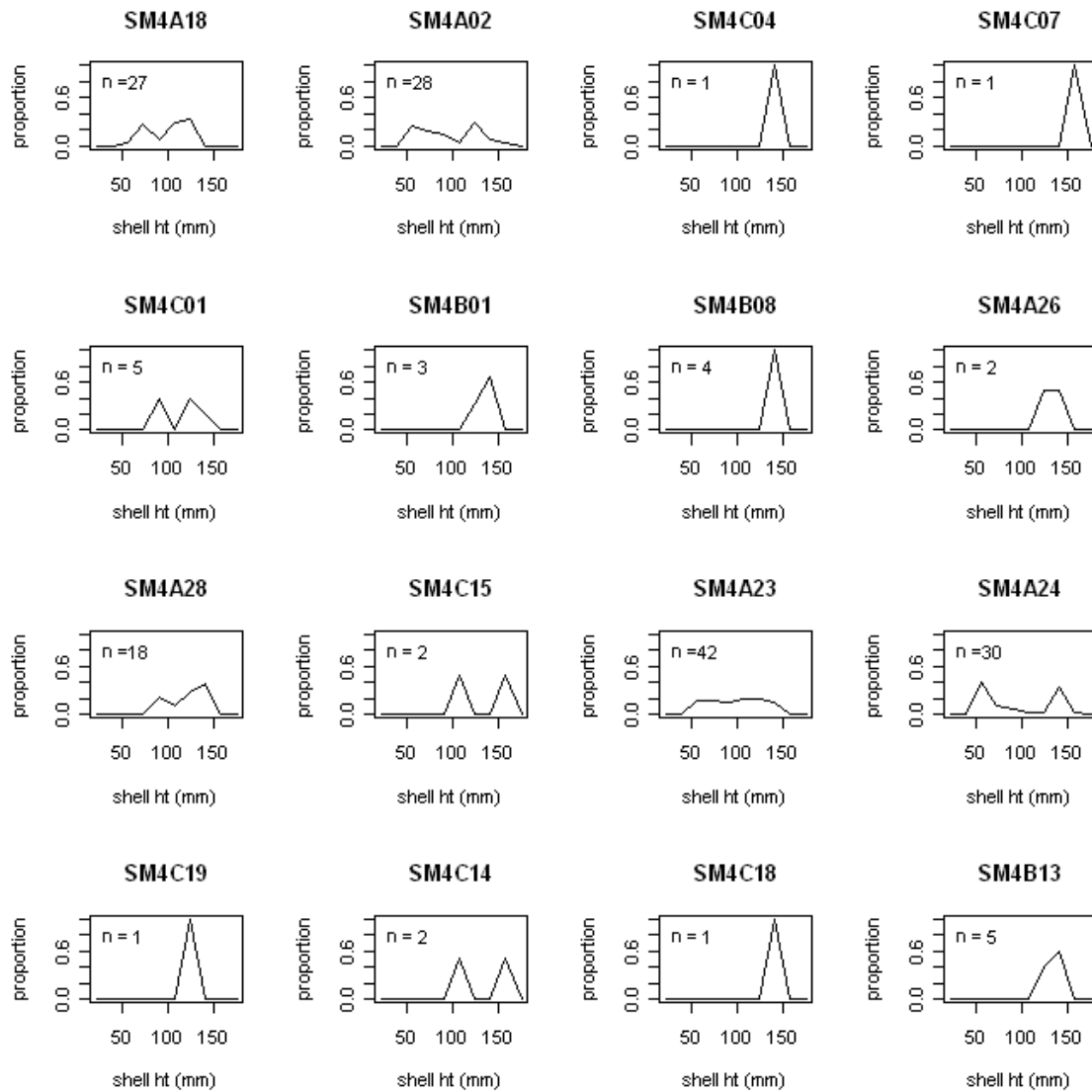


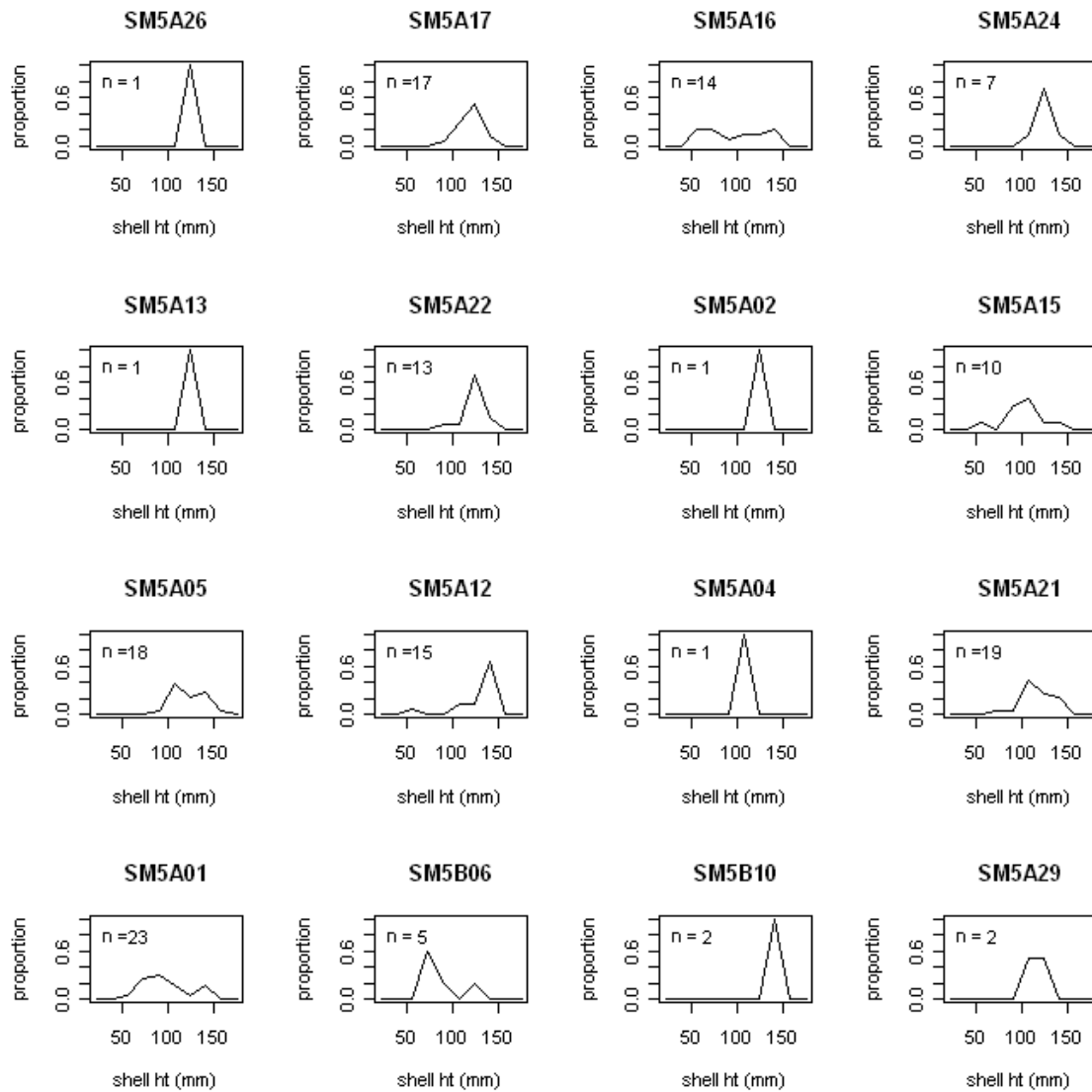


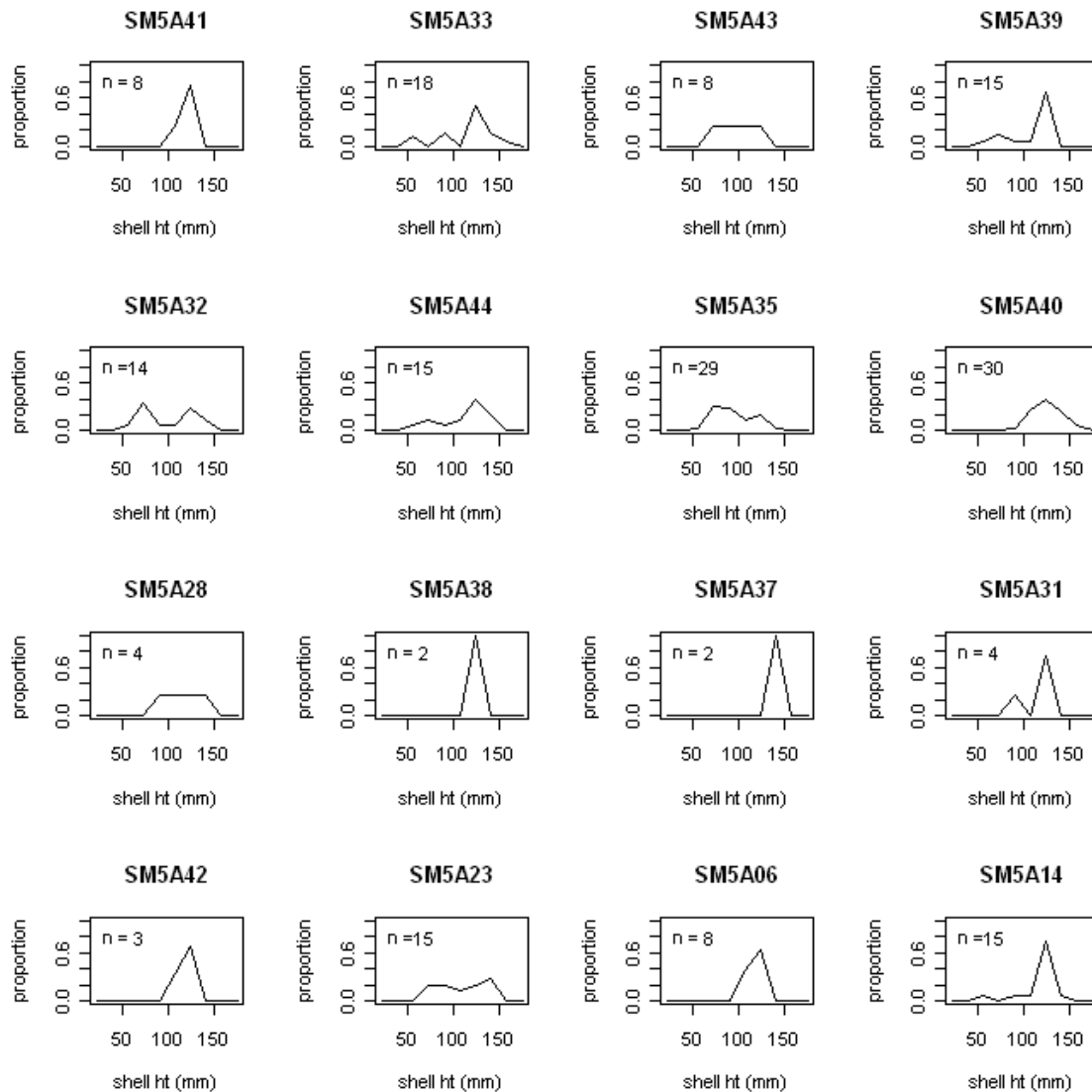






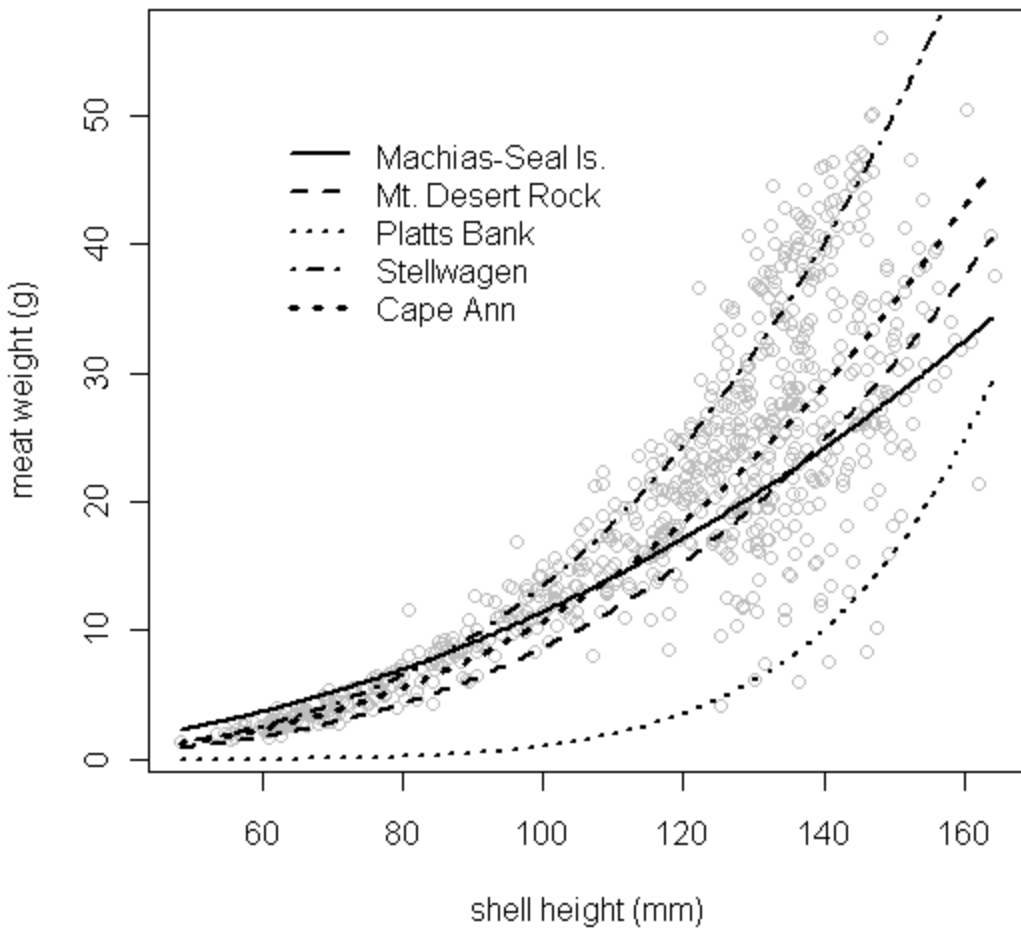






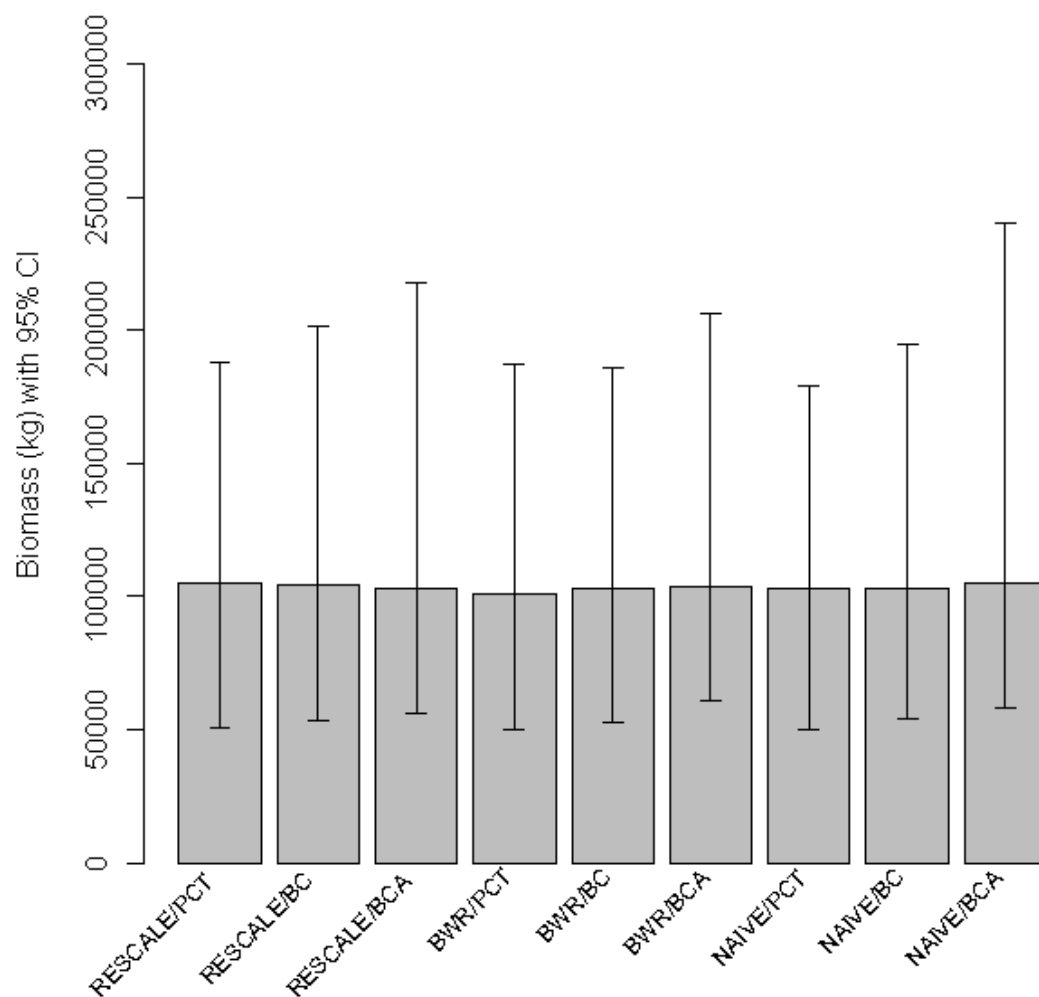
Appendix B6-Figure 4: Individual tow length frequency distributions. Example: SM5A14: 5 represents area 5; A represents subarea A (A is high density, B is medium density, C is low density, D is a tow in state waters); 14 indicates station number.

Meat Weight

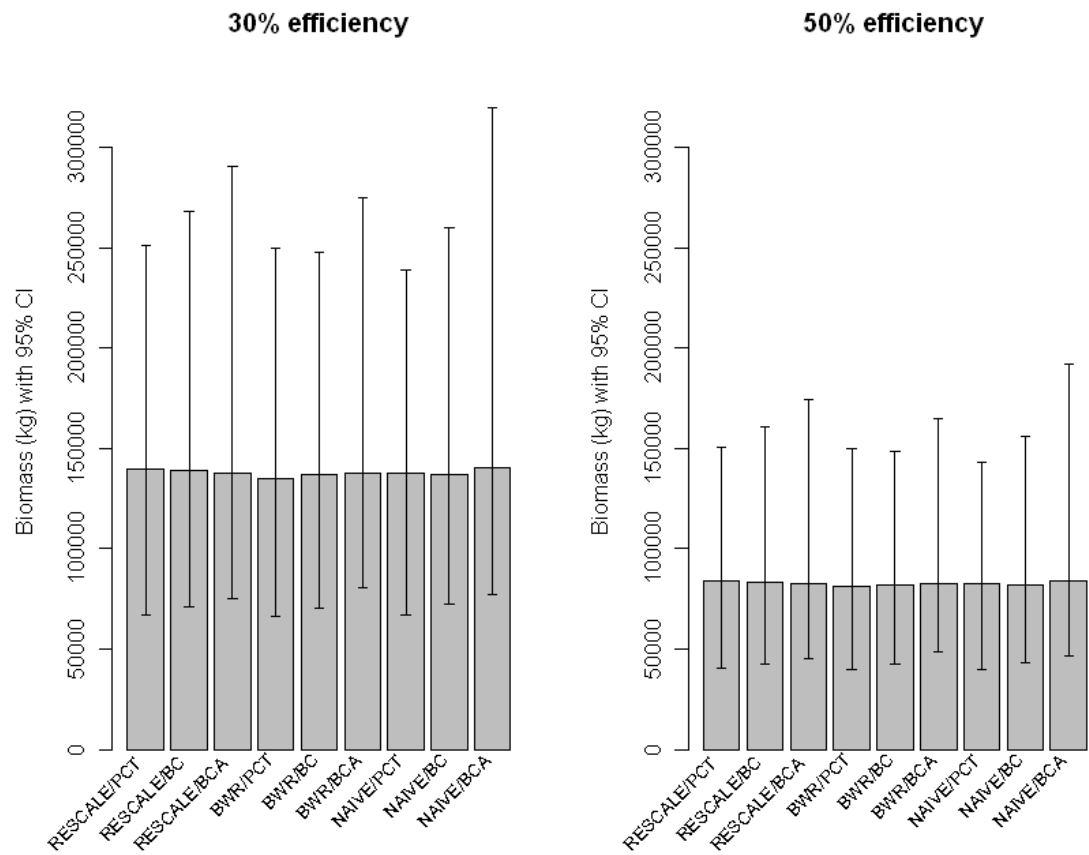


Appendix B6-Figure 5. SH-MW relationship observed for the NGOM survey. The largest meats relative to shell height were found on Stellwagen Bank. The model was $MW_i = \alpha SH_i^\beta e^{\epsilon_i}$. Platts Bank is based on sample size of 8 scallops.

40% efficiency

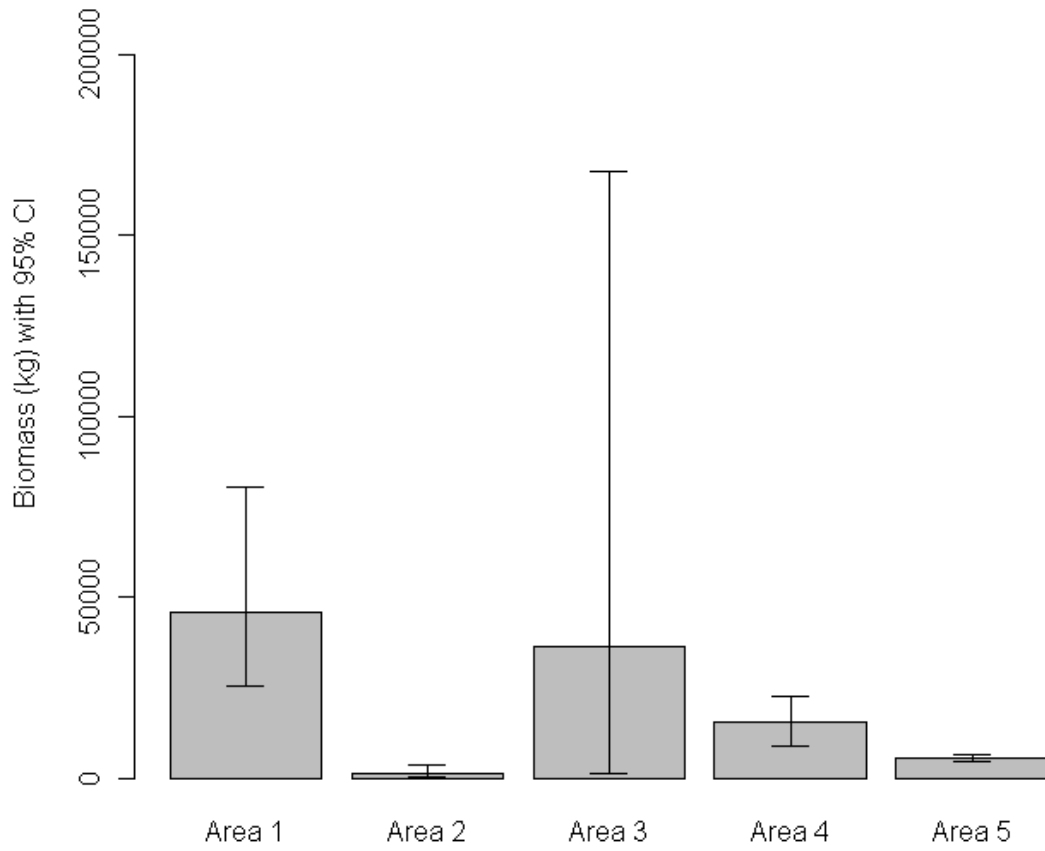


Appendix B6-Figure 6. Mean bootstrapped estimates of NGOM biomass and 95% confidence interval bounds assuming 40% dredge efficiency.

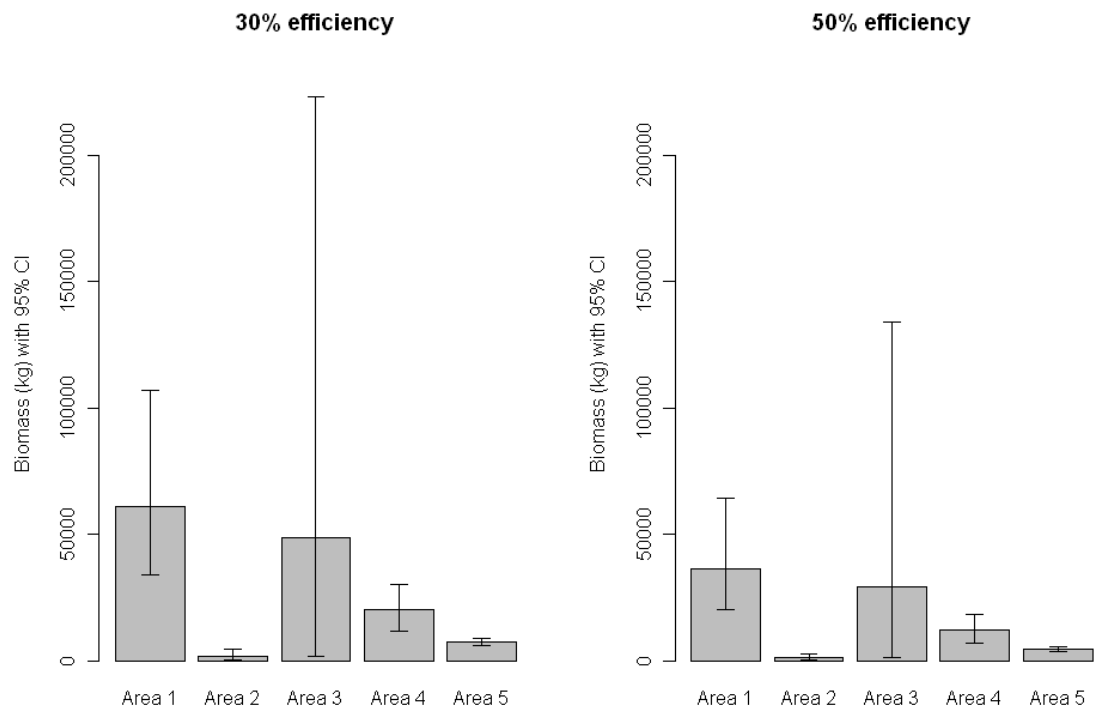


Appendix B6-Figure 7. Mean bootstrapped estimates of NGOM biomass and 95% confidence interval bounds assuming 30% and 50% dredge efficiency.

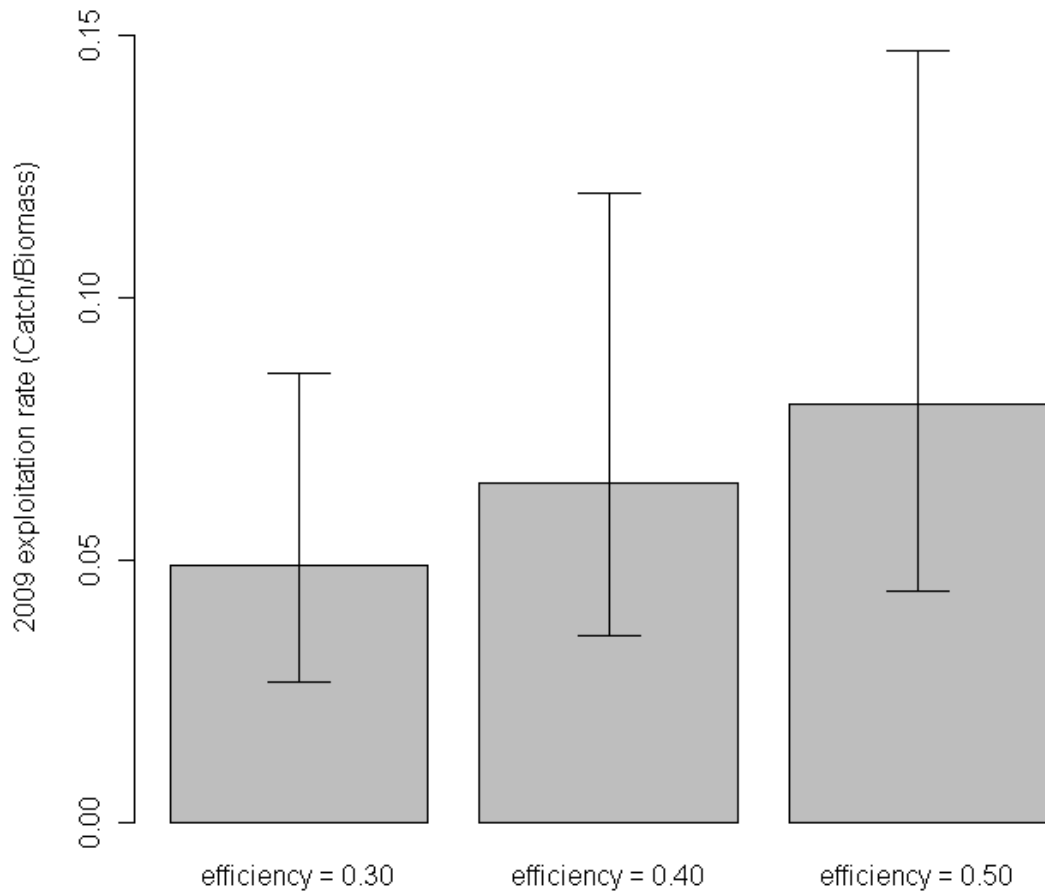
40% efficiency



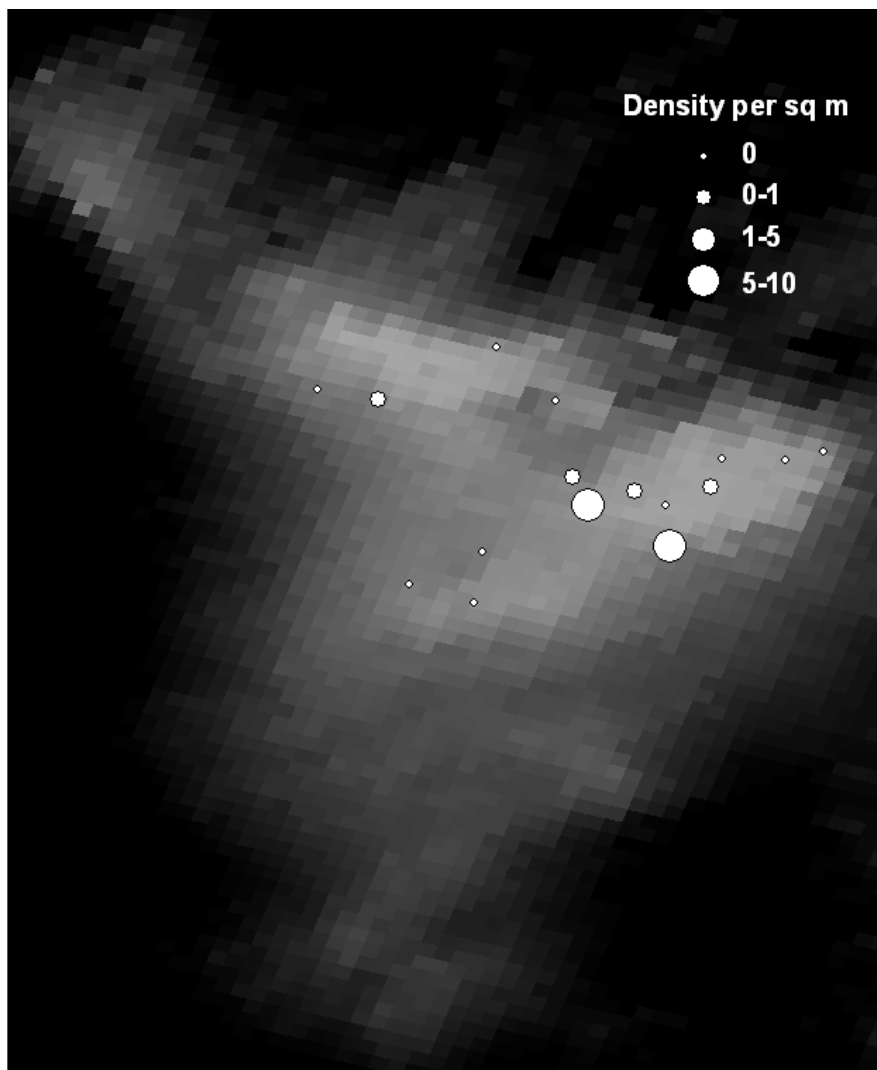
Appendix B6-Figure 8. Mean bootstrapped estimates of NGOM biomass by area and 95% confidence interval bounds using BWR/BC method and assuming 40% dredge efficiency.



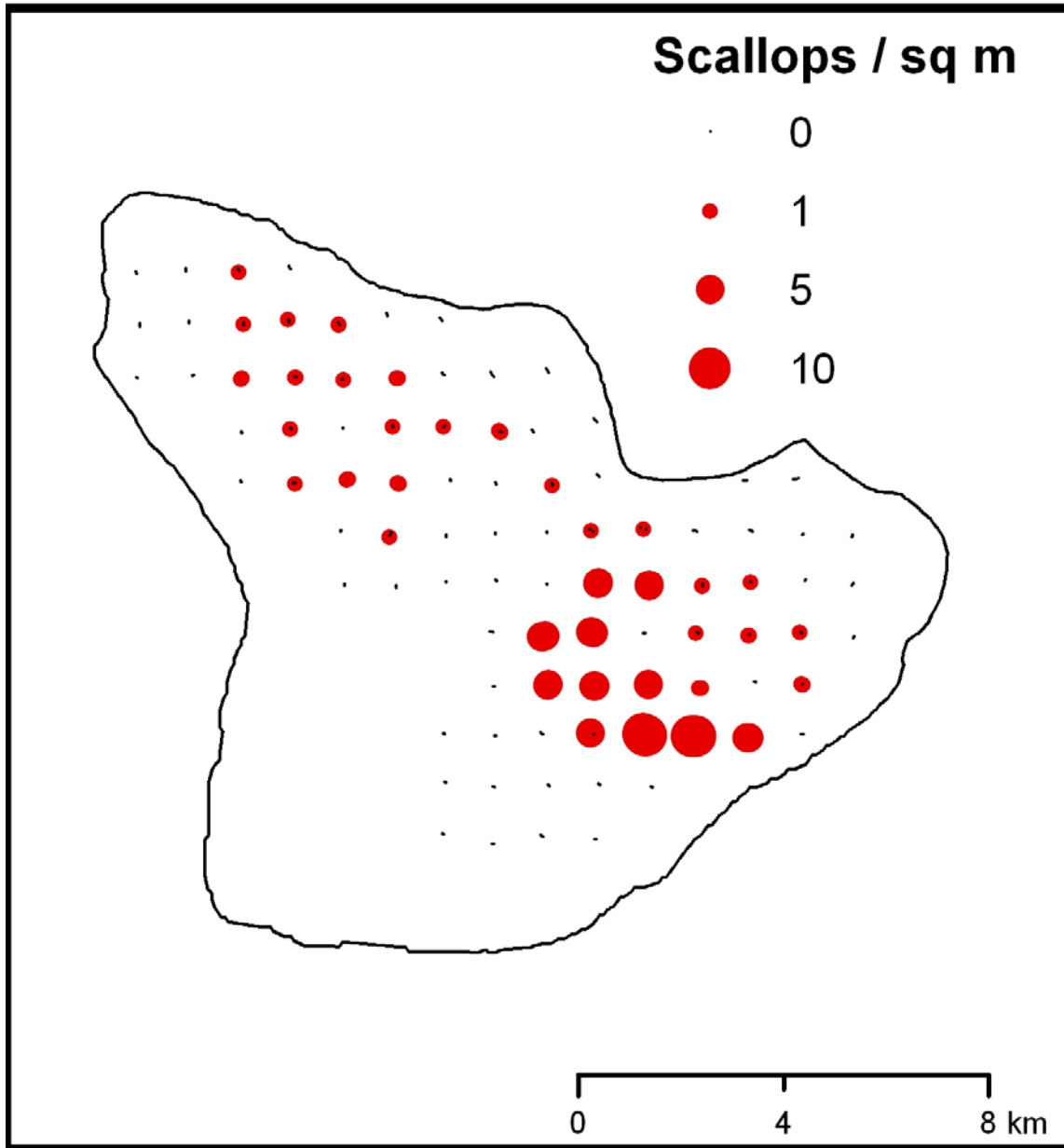
Appendix B6-Figure 9. Mean bootstrapped estimates of NGOM biomass by area and 95% confidence interval bounds using BWR/BC method and assuming 30% and 50% dredge efficiency.



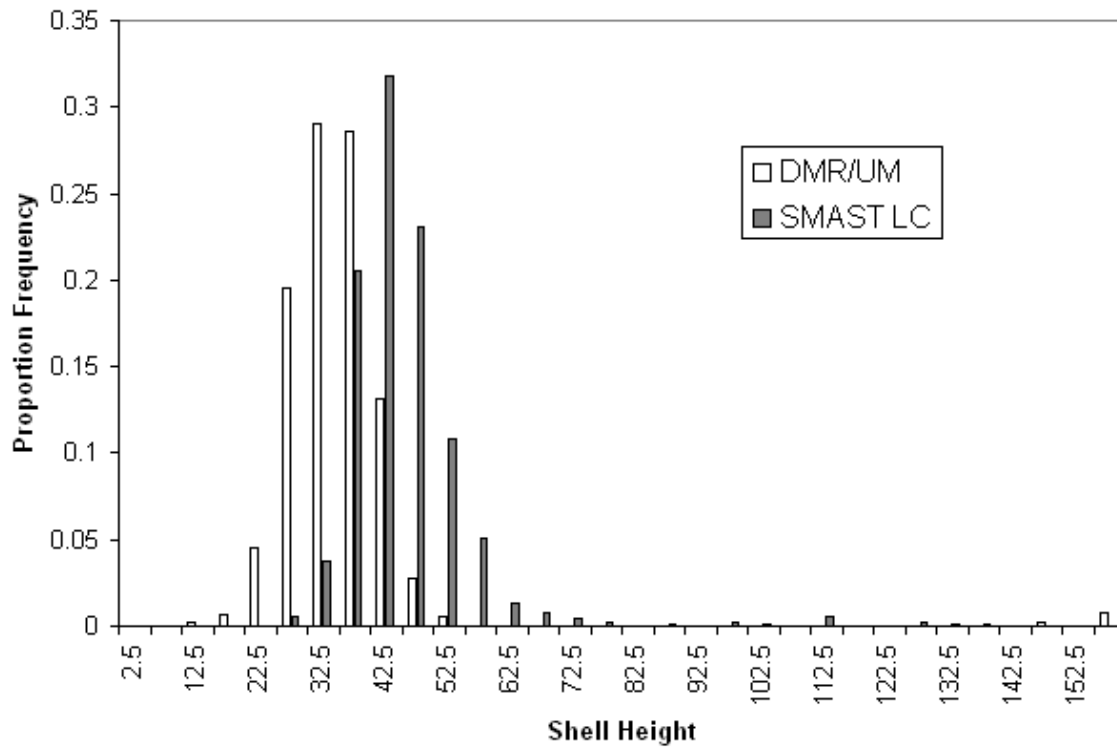
Appendix B6-Figure 10. Estimated NGOM exploitation rates at 30%, 40% and 50% dredge efficiencies with 95% confidence intervals based on BWR/BC method.



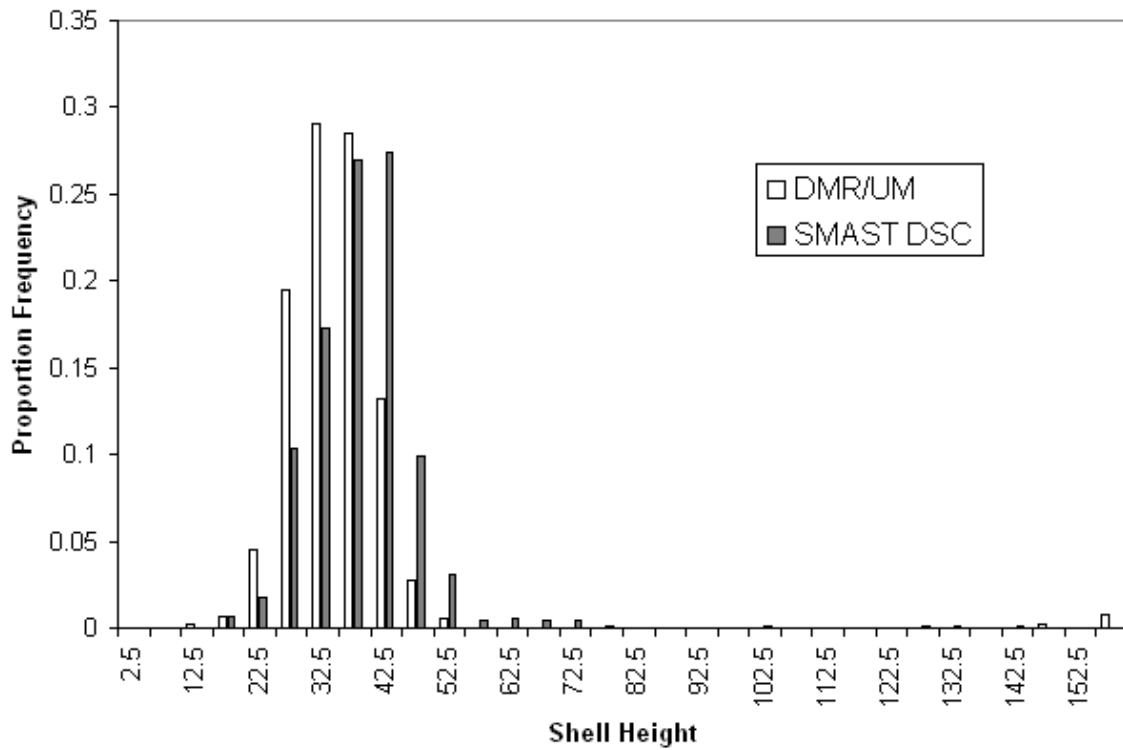
Appendix B6-Figure 11. DMR/UM Platts Bank survey locations indicating density per square meter.



Appendix B6-Figure 12. SMAST Platts Bank survey locations indicating density per square meter.



Appendix B6-Figure 13. Comparison of shell height distribution on Platts Bank between the DMR/UM survey and the SMAST survey (large camera). The DMR survey occurred on July 28th 2009 and the SMAST survey occurred August 12th and 13th 2009.



Appendix B6-Figure 14. Comparison of shell height distribution on Platts Bank between the DMR/UM survey and the SMAST survey (digital still camera). The DMR survey occurred on July 28th 2009 and the SMAST survey occurred August 12th and 13th 2009.

Appendix B7: Shell height-meat weight relationships from NEFSC survey data.

Dan Hennen and Dvora Hart, Northeast Fisheries Science Center, Woods Hole, MA.

New shell height and meat weight data were collected during 2007 – 2009 annual NMFS sea scallop surveys. This appendix updates shell height-meat weight relationships using these data.

Methods

Sea scallops (averaging about 6 per station) were collected for shell height-meat weight analysis at roughly half of all stations during 2001-2009 (717 stations in the Mid-Atlantic, 812 stations on Georges Bank). The scallops were measured to the nearest millimeter, carefully shucked, excess water was removed from the meat, and the meat was weighed to the nearest gram. Samples were collected in 2003, but there was partial data loss, so these data will not be used. During 2001-2009, whole and gonad weights were also recorded, but these data will not be presented here. The sampling protocol was altered slightly in 2009 to begin to account for seasonal shifts in scallop size. Since the data in 2009 were not collected at the same time of year as the data from earlier surveys, 2009 will generally be excluded from this analysis, though it is included in comparisons between years to illustrate the potential effects of shifts in the timing of the survey.

Preliminary analysis indicated a residual pattern for scallops with shell heights less than 70 mm. The small weights of these scallops (1-3 g) combined with the fact that meat weight could only be measured to the nearest gram resulted substantial measurement error. For this reason, the analysis was restricted to scallops that are at least 70 mm shell height. Scallops less than this height are below commercial size and have relatively little influence on CASA model calculations.

A generalized linear mixed model with a log link was used to predict meat weight using shell height, depth, density, latitude, and subarea (a finer scale regional division within each broad region). The GLM used a “quasi” likelihood with a log link, appropriate for data with “constant CV” error (McCullagh and Nelder 1989). This method avoids log-transforming the response variable (meat weight) which can lead to biased estimates when the results are back-transformed. The best model was chosen by AIC (Burnham and Anderson, 2002). The grouping variable for the random effects was a unique code formed by combination of survey station number and the year in which the survey took place. Survey stations were chosen randomly within NEFSC survey strata and generally in proportion to the size of the stratum. Survey stations numbers are assigned sequentially so that a survey station number in one year does not have any particular relationship to the same station number in the next year. Thus, a grouping variable based on a combination of survey station number and year incorporates random variation in the data that is due to both time (year) and fine scale spatial differences (station number).

Several analyses using simplified versions of the best model were employed to explore the effects of year, subarea, and fishing regulations.

All data analysis was conducted using the R statistical program (v2.9.2).

Results

In general, using mixed models appears to be very important in terms of AIC (Table 1). Accounting for the random effects of time and space measured as survey year and location absorbs much of the variation in the data.

Mid-Atlantic

The following model had the lowest AIC value (Table 1).

$$W = e^{(\alpha + a(St) + \beta \ln(H) + \gamma \ln(D) + \rho(\ln(L) * \ln(D))) + \epsilon} \quad (1)$$

Where W was meat weight (g), and St was the year-station grouping variable for the random effects. The random effects were always modeled as an intercept and sometimes as a slope coefficient. The fixed effects were: shell height (H) in mm, depth (D) in m, and an interaction between shell height and depth ($H*D$). A total of 4181 observations were sampled from 717 stations were used in the analysis (Figure 1). Parameters (Table 1) were well estimated with no evidence of residual patterns (Table 2, Figure 2-4). The estimates presented here were similar to most previous estimates (Table 3). Compared to the estimates used in previous assessments, with the exception of Lai and Helser (2004) (Figure 5), the new estimates predicted slightly heavier meats at small shell heights, but lighter meats at very large shell heights, though the differences were small. The relationship that includes a depth effect indicated that sea scallops have heavier meats at shallower depths (Figure 6).

Meat weights varied by year, with the heaviest meats during 2004 (Table 4, Figure 7). Meats were generally heavier in 2009 when the survey was conducted earlier in the year. Meat weights by subarea were less variable, though “New York Bight” did produce heavier meats at the larger shell heights, and particularly at deeper depths (60 and 70 m) than the other areas (Table 5, Figures 8-10). In general samples taken from the Mid-Atlantic tend to be from water shallower than 70 m (Figure 11).

Georges Bank

The following model had the lowest AIC value (Table 1).

$$W = e^{(\alpha + a(St) + \beta \ln(H) + \gamma \ln(D) + \delta \ln(lat) + \theta(sub) + b(L_{St})) + \epsilon} \quad (2)$$

Where W was meat weight (g), and survey station (St) was the grouping for the random effects. The random effects were modeled as an intercept (a), and as a slope parameter (b) for shell height (H). The fixed effects were in mm, D in m, latitude (lat) in decimal degrees, and subarea (sub) based on area management boundaries. Based on 6145 scallops from 812 stations, model fits appeared good with little or no residual pattern (Figures 12-15). Parameters were reasonably precise (Tables 1 and 2). They predict slightly heavier meat weights at small shell heights, and slightly lighter meat weights at large shell heights, than the model used in the previous assessment (Table 3, Figure 16). Meat weights were heavier at shallower depths (Figure 17).

Scallop shell height-meat weight relationships were generally consistent over time, although recent years (2007 and 2008) had heavier meats for large shell heights (Table 4, Figure 18). The 2009 survey which was conducted earlier in the year than previous surveys, collected meats that tended to be heavier at small shell heights, but did not otherwise differ from meats collected in other years. Results were dependent on subareas with “South East Part” and

“Closed Area 1” producing larger meats and “South Channel” and “Northern Edge and Peak” tending to produce lighter meats at all shell heights at the shallower depths (50 and 60 m) (Table 5, Figures 19 - 20). At 90 m depth, the heaviest meats were found in Northern Light Ship area at all shell heights and South East Channel produced some of the smallest meats at all shell heights. It should be noted however that samples from Northern Light Ship area were all taken from waters less than 90 m deep so the heavy weights found by the model fit could be an artifact of sampling (Figure 21). Areas that were closed to fishing tended to have larger meats (Figure 23).

Literature Cited

- Burnham and Anderson 2002. Model Selection and Multimodel Inference A Practical Information-Theoretic Approach. 2nd. Ed. Springer.
- Haynes EB. 1966. Length-weight relationship of the sea scallop *Placopecten magellanicus* (Gmelin). Res Bull Int Comm Northw Atl Fish. 3:32-48.
- Lai HL, Helser T. 2004. Linear mixed-effects models for weight-length relationships. Fish Res. 70:377-387.
- McCullagh and Nelder 1989. Generalized Linear Models 2nd. Ed. Chapman and Hall. New York.
- NEFSC. 2001. 32nd Northeast Regional Stock Assessment Workshop (32nd SAW). Stock Assessment Review Committee (SARC) consensus summary of assessments. NEFSC Ref Doc. 01-05; 289 p.
- NEFSC. 2007. 45th Northeast Regional Stock Assessment Workshop (45th SAW): 45th SAW assessment report. US Dep Commer, Northeast Fish Sci Cent Ref Doc 07-16; 370 p.
- Serchuk FM, Rak RS. 1983. Biological characteristics of offshore Gulf of Maine scallop populations: size distributions, shell height-meat weight relationships and relative fecundity patterns. NMFS Woods Hole Lab Ref Doc. 83-07; 42 p.

Appendix B7-Table 1. Model building results. The models with minimum AIC values are indicated by bold font. Random effects are shown as parameters inside parentheses. All random effects were grouped by year_station and each model included a random intercept represented by the 1 inside parentheses. Fixed effects are shown to the right of the ~ symbol which separates the response variable from the predictors. Interaction terms are represented as factor1 * factor2. The best model tested without random effects for each region is included for comparison.

Formula	AIC	BIC	logLik	deviance
Georges Bank				
<i>meat_weight</i> ~ <i>height</i> + <i>depth</i> + <i>lat</i> + <i>subarea</i> + (<i>height</i> + 1 <i>year_station</i>)	6636	6723	-3305	6610
<i>meat_weight</i> ~ <i>height</i> + <i>depth</i> + <i>subarea</i> + (<i>height</i> + 1 <i>year_station</i>)	6694	6774	-3335	6670
<i>meat_weight</i> ~ <i>height</i> + <i>depth</i> + <i>subarea</i> + <i>height</i> * <i>depth</i> + (<i>height</i> + 1 <i>year_station</i>)	6696	6783	-3335	6670
<i>meat_weight</i> ~ <i>height</i> + <i>subarea</i> + <i>height</i> * <i>depth</i> + (<i>height</i> + 1 <i>year_station</i>)	6696	6783	-3335	6670
<i>meat_weight</i> ~ <i>height</i> + <i>depth</i> + <i>lat</i> + (<i>height</i> + 1 <i>year_station</i>)	6707	6761	-3346	6691
<i>meat_weight</i> ~ <i>height</i> + <i>depth</i> + <i>density</i> + <i>lat</i> + (<i>height</i> + 1 <i>year_station</i>)	6708	6769	-3345	6690
<i>meat_weight</i> ~ <i>height</i> + <i>depth</i> + <i>lat</i> + <i>height</i> * <i>depth</i> + (<i>height</i> + 1 <i>year_station</i>)	6709	6770	-3346	6691
<i>meat_weight</i> ~ <i>height</i> + <i>depth</i> + <i>lat</i> + (1 <i>year_station</i>)	6761	6801	-3374	6749
<i>meat_weight</i> ~ <i>height</i> + <i>depth</i> + <i>subarea</i> + (1 <i>year_station</i>)	6761	6828	-3370	6741
<i>meat_weight</i> ~ <i>height</i> + <i>depth</i> + <i>density</i> + <i>lat</i> + (1 <i>year_station</i>)	6762	6809	-3374	6748
<i>meat_weight</i> ~ <i>height</i> + <i>depth</i> + (<i>height</i> + 1 <i>year_station</i>)	6786	6833	-3386	6772
<i>meat_weight</i> ~ <i>height</i> + <i>depth</i> + <i>density</i> + (<i>height</i> + 1 <i>year_station</i>)	6788	6841	-3386	6772
<i>meat_weight</i> ~ <i>depth</i> + <i>height</i> * <i>depth</i> + (<i>height</i> + 1 <i>year_station</i>)	6788	6842	-3386	6772
<i>meat_weight</i> ~ <i>height</i> + <i>height</i> * <i>depth</i> + (<i>height</i> + 1 <i>year_station</i>)	6788	6842	-3386	6772
<i>meat_weight</i> ~ <i>height</i> + <i>density</i> + <i>height</i> * <i>depth</i> + (<i>height</i> + 1 <i>year_station</i>)	6790	6850	-3386	6772
<i>meat_weight</i> ~ <i>height</i> + <i>depth</i> + <i>density</i> + <i>height</i> * <i>depth</i> + (<i>height</i> + 1 <i>year_station</i>)	6790	6850	-3386	6772
<i>meat_weight</i> ~ <i>height</i> + <i>depth</i> + (1 <i>year_station</i>)	6839	6873	-3414	6829
<i>meat_weight</i> ~ <i>height</i> + <i>depth</i> + <i>density</i> + (1 <i>year_station</i>)	6840	6881	-3414	6828
<i>meat_weight</i> ~ <i>depth</i> + <i>height</i> * <i>depth</i> + (1 <i>year_station</i>)	6841	6881	-3414	6829
<i>meat_weight</i> ~ <i>height</i> + <i>height</i> * <i>depth</i> + (1 <i>year_station</i>)	6841	6881	-3414	6829
<i>meat_weight</i> ~ <i>height</i> + <i>lat</i> + (<i>height</i> + 1 <i>year_station</i>)	6988	7035	-3487	6974
<i>meat_weight</i> ~ <i>height</i> + (<i>height</i> + 1 <i>year_station</i>)	7040	7081	-3514	7028
<i>meat_weight</i> ~ <i>height</i> + <i>lat</i> + (1 <i>year_station</i>)	7041	7075	-3515	7031
<i>meat_weight</i> ~ <i>height</i> + <i>density</i> + (<i>height</i> + 1 <i>year_station</i>)	7042	7090	-3514	7028
<i>meat_weight</i> ~ <i>height</i> + (1 <i>year_station</i>)	7093	7120	-3542	7085
<i>meat_weight</i> ~ <i>height</i> + <i>density</i> + (1 <i>year_station</i>)	7095	7128	-3542	7085
<i>meat_weight</i> ~ <i>depth</i> + (<i>height</i> + 1 <i>year_station</i>)	9074	9115	-4531	9062
<i>meat_weight</i> ~ <i>depth</i> + (1 <i>year_station</i>)	29295	29322	-14643	29287
<i>meat_weight</i> ~ <i>height</i> + <i>depth</i> + <i>height</i> * <i>depth</i> + <i>lat</i> + <i>subarea</i>	42747		-6107	376871

Mid-Atlantic Bight				
<i>meat_weight</i> ~ <i>depth</i> + <i>height</i> * <i>depth</i> + (1 <i>year_station</i>)	3626	3664	-1807	3614
<i>meat_weight</i> ~ <i>height</i> + <i>height</i> * <i>depth</i> + (1 <i>year_station</i>)	3626	3664	-1807	3614
<i>meat_weight</i> ~ <i>height</i> + <i>depth</i> + <i>density</i> + <i>height</i> * <i>depth</i> + (<i>height</i> + 1 <i>year_station</i>)	3629	3686	-1806	3611
<i>meat_weight</i> ~ <i>height</i> + <i>density</i> + <i>height</i> * <i>depth</i> + (<i>height</i> + 1 <i>year_station</i>)	3629	3686	-1806	3611
<i>meat_weight</i> ~ <i>height</i> + <i>height</i> * <i>depth</i> + (<i>height</i> + 1 <i>year_station</i>)	3630	3681	-1807	3614
<i>meat_weight</i> ~ <i>depth</i> + <i>height</i> * <i>depth</i> + (<i>height</i> + 1 <i>year_station</i>)	3630	3681	-1807	3614
<i>meat_weight</i> ~ <i>height</i> + <i>depth</i> + <i>lat</i> + <i>height</i> * <i>depth</i> + (<i>height</i> + 1 <i>year_station</i>)	3631	3688	-1807	3613
<i>meat_weight</i> ~ <i>height</i> + <i>depth</i> + <i>subarea</i> + <i>height</i> * <i>depth</i> + (<i>height</i> + 1 <i>year_station</i>)	3632	3708	-1804	3608
<i>meat_weight</i> ~ <i>height</i> + <i>subarea</i> + <i>height</i> * <i>depth</i> + (<i>height</i> + 1 <i>year_station</i>)	3632	3708	-1804	3608
<i>meat_weight</i> ~ <i>height</i> + <i>depth</i> + <i>density</i> + (1 <i>year_station</i>)	3634	3672	-1811	3622
<i>meat_weight</i> ~ <i>height</i> + <i>depth</i> + (1 <i>year_station</i>)	3635	3667	-1813	3625
<i>meat_weight</i> ~ <i>height</i> + <i>depth</i> + <i>subarea</i> + (1 <i>year_station</i>)	3636	3693	-1809	3618
<i>meat_weight</i> ~ <i>height</i> + <i>depth</i> + <i>density</i> + <i>lat</i> + (1 <i>year_station</i>)	3636	3681	-1811	3622
<i>meat_weight</i> ~ <i>height</i> + <i>depth</i> + <i>density</i> + (<i>height</i> + 1 <i>year_station</i>)	3637	3687	-1810	3621
<i>meat_weight</i> ~ <i>height</i> + <i>depth</i> + <i>lat</i> + (1 <i>year_station</i>)	3637	3675	-1812	3625
<i>meat_weight</i> ~ <i>height</i> + <i>depth</i> + (<i>height</i> + 1 <i>year_station</i>)	3638	3682	-1812	3624
<i>meat_weight</i> ~ <i>height</i> + <i>depth</i> + <i>subarea</i> + (<i>height</i> + 1 <i>year_station</i>)	3638	3708	-1808	3616
<i>meat_weight</i> ~ <i>height</i> + <i>depth</i> + <i>density</i> + <i>lat</i> + (<i>height</i> + 1 <i>year_station</i>)	3638	3696	-1810	3620
<i>meat_weight</i> ~ <i>height</i> + <i>depth</i> + <i>lat</i> + (<i>height</i> + 1 <i>year_station</i>)	3639	3690	-1812	3623
<i>meat_weight</i> ~ <i>height</i> + <i>depth</i> + <i>lat</i> + <i>subarea</i> + (<i>height</i> + 1 <i>year_station</i>)	3640	3716	-1808	3616
<i>meat_weight</i> ~ <i>height</i> + <i>lat</i> + (1 <i>year_station</i>)	3838	3870	-1914	3828
<i>meat_weight</i> ~ <i>height</i> + <i>lat</i> + (<i>height</i> + 1 <i>year_station</i>)	3841	3886	-1914	3827
<i>meat_weight</i> ~ <i>height</i> + (1 <i>year_station</i>)	3848	3873	-1920	3840
<i>meat_weight</i> ~ <i>height</i> + <i>density</i> + (1 <i>year_station</i>)	3848	3880	-1919	3838
<i>meat_weight</i> ~ <i>height</i> + (<i>height</i> + 1 <i>year_station</i>)	3851	3889	-1919	3839
<i>meat_weight</i> ~ <i>height</i> + <i>density</i> + (<i>height</i> + 1 <i>year_station</i>)	3851	3895	-1918	3837
<i>meat_weight</i> ~ <i>depth</i> + (<i>height</i> + 1 <i>year_station</i>)	5644	5682	-2816	5632
<i>meat_weight</i> ~ <i>depth</i> + (1 <i>year_station</i>)	15340	15365	-7666	15332
<i>meat_weight</i> ~ <i>height</i> + <i>depth</i>	26144		-8715	126965

Appendix B7-Table 2. The standard errors for the parameter estimates in Table 1. The parameters estimated are: the intercept (α), the shell height coefficient (β), the depth coefficient (γ), the latitude coefficient (δ), and (ρ) the shell height by depth interaction in MAB, and the subarea coefficient in GBK.

	α	β	γ	δ	ρ	resid.
Mid-Atlantic Bight						
NEFSC (2007)	0.150	0.050				
NEFSC (2007) with Depth effect	0.390	0.050	0.080			
NEFSC (2010)	0.024	0.096				3.61 ^a
NEFSC (2010) with Depth effect	0.021	0.093	0.104			3.61 ^a
NEFSC (2010) with Depth effect and interaction	0.021	0.095	0.106		0.472	3.61 ^a
Georges Bank						
NEFSC (2007)	0.270	0.060				
NEFSC (2007) with Depth effect	0.170	0.050	0.050			
NEFSC (2010)	0.034	0.090				4.57 ^a
NEFSC (2010) with Depth and Latitude effect	0.028	0.102	0.131			4.46 ^a
NEFSC (2010) with Depth, Latitude and subarea effect	0.061	0.104	0.129	3.286	0.098 ^b	4.46 ^a

a - these are standard deviations

b - averaged across all subarea levels

Appendix B7-Table 3. Current shell height/meat weight parameters, compared with those from other studies. The parameters estimated are: the intercept (α), the shell height coefficient (β), the depth coefficient (γ), the latitude coefficient (δ), and (ρ) the shell height by depth interaction in MAB, and the average subarea coefficient in GBK.

	α	β	γ	δ	ρ
Mid-Atlantic Bight					
Haynes (1966)	-11.09	3.04			
Serchuk and Rak (1983)	-12.16	3.25			
NEFSC (2001)	-12.25	3.26			
Lai and Helser (2004)	-12.34	3.28			
NEFSC (2007)	-12.01	3.22			
NEFSC (2007) with Depth effect	-9.18	3.18	-0.65		
NEFSC (2010)	-10.80	2.97			
NEFSC (2010) with Depth effect	-8.94	2.94	-0.43		
NEFSC (2010) with Depth effect and interaction	-16.88	4.64	1.57	-	-0.43
Georges Bank					
Haynes (1966)	-10.84	2.95			
Serchuk and Rak (1983)	-11.77	3.17			
NEFSC (2001)	-11.60	3.12			
Lai and Helser (2004)	-11.44	3.07			
NEFSC (2007)	-10.70	2.94			
NEFSC (2007) with Depth effect	-8.62	2.95	-0.51		
NEFSC (2010)	-10.25	2.85			
NEFSC (2010) with Depth effect	-8.05	2.84	-0.51		
NEFSC (2010) with Depth, Latitude and subarea effect	14.380	2.826	0.529	5.980	0.051 ^b

b - averaged across all subarea levels

Appendix B7-Table 4. Current shell height/meat weight parameters, compared across years. The parameters estimated are: the intercept (α), the shell height coefficient (β), the depth coefficient (γ). The numbers of stations used in each year are also shown.

	α	β	γ	$n_{(\text{stations})}$
Mid-Atlantic Bight ^b				
2001	-10.40	2.97	-0.1007	69
2002	-8.54	2.86	-0.4601	54
2003 ^a				
2004	-9.70	2.98	-0.2592	124
2005	-8.60	3.12	-0.7516	130
2006	-8.75	3.05	-0.6331	111
2007	-8.83	2.77	-0.2365	120
2008	-8.03	2.80	-0.4744	109
2009	-8.44	2.75	-0.303	101
Georges Bank ^b				
2001	-7.7695	2.8203	-0.5614	52
2002	-7.3727	2.72	-0.5394	90
2003 ^a				
2004	-7.9818	2.7536	-0.4313	154
2005	-8.3563	2.8691	-0.477	137
2006	-7.0069	2.728	-0.6328	135
2007	-7.6659	2.9681	-0.7194	155
2008	-9.247	2.9165	-0.3091	89
2009	-7.1515	2.5507	-0.3874	110

a - estimates using 2003 survey data were excluded from the model

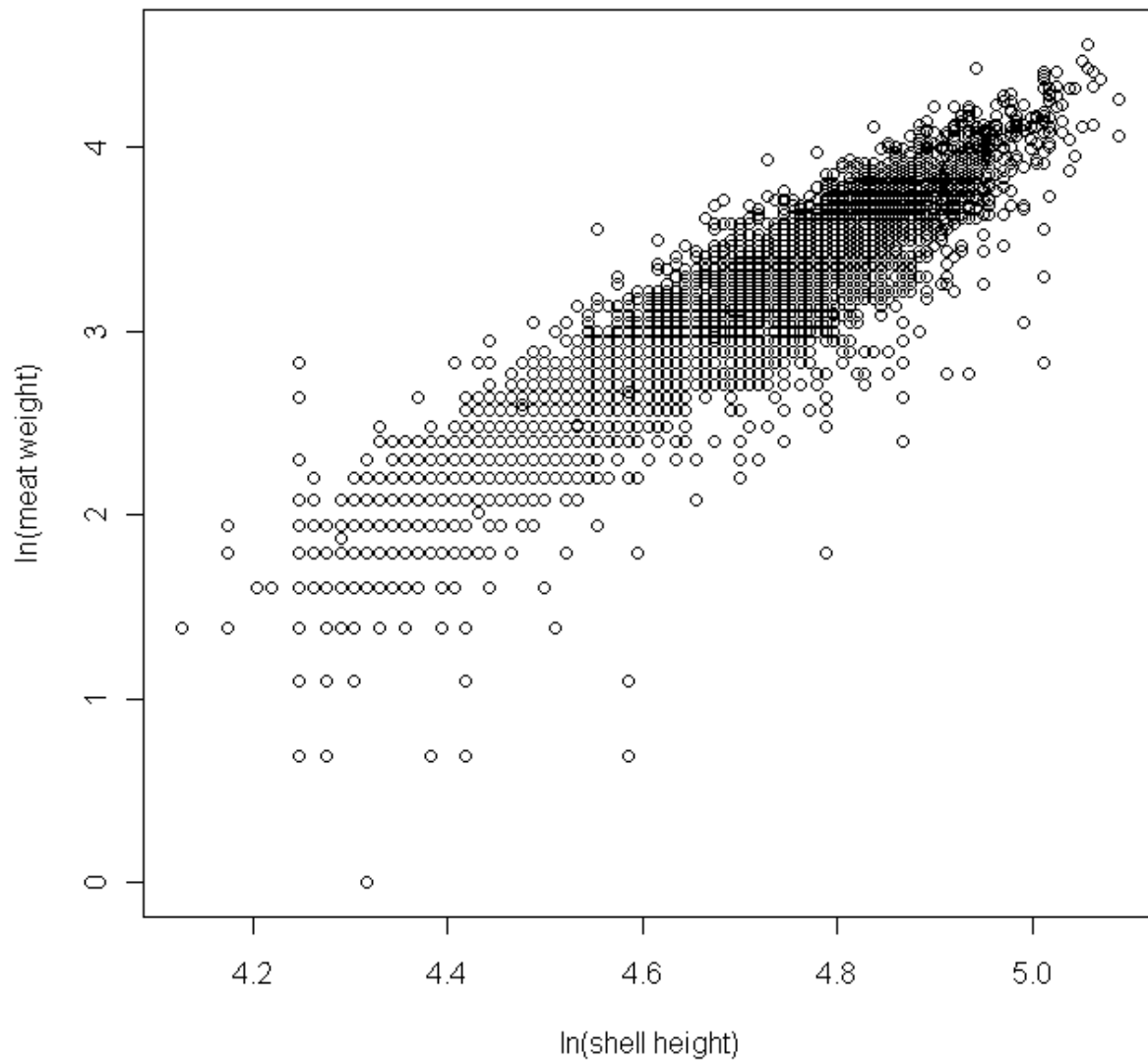
b - model = $\text{meat_weight} \sim \text{height} + \text{depth} + (1 | \text{year_station})$

Appendix B7-Table 5. Current shell height/meat weight parameters, compared across subareas within each region. The parameters estimated are: the intercept (α), the shell height coefficient (β), the depth coefficient (γ). The numbers of stations used in each year are also shown.

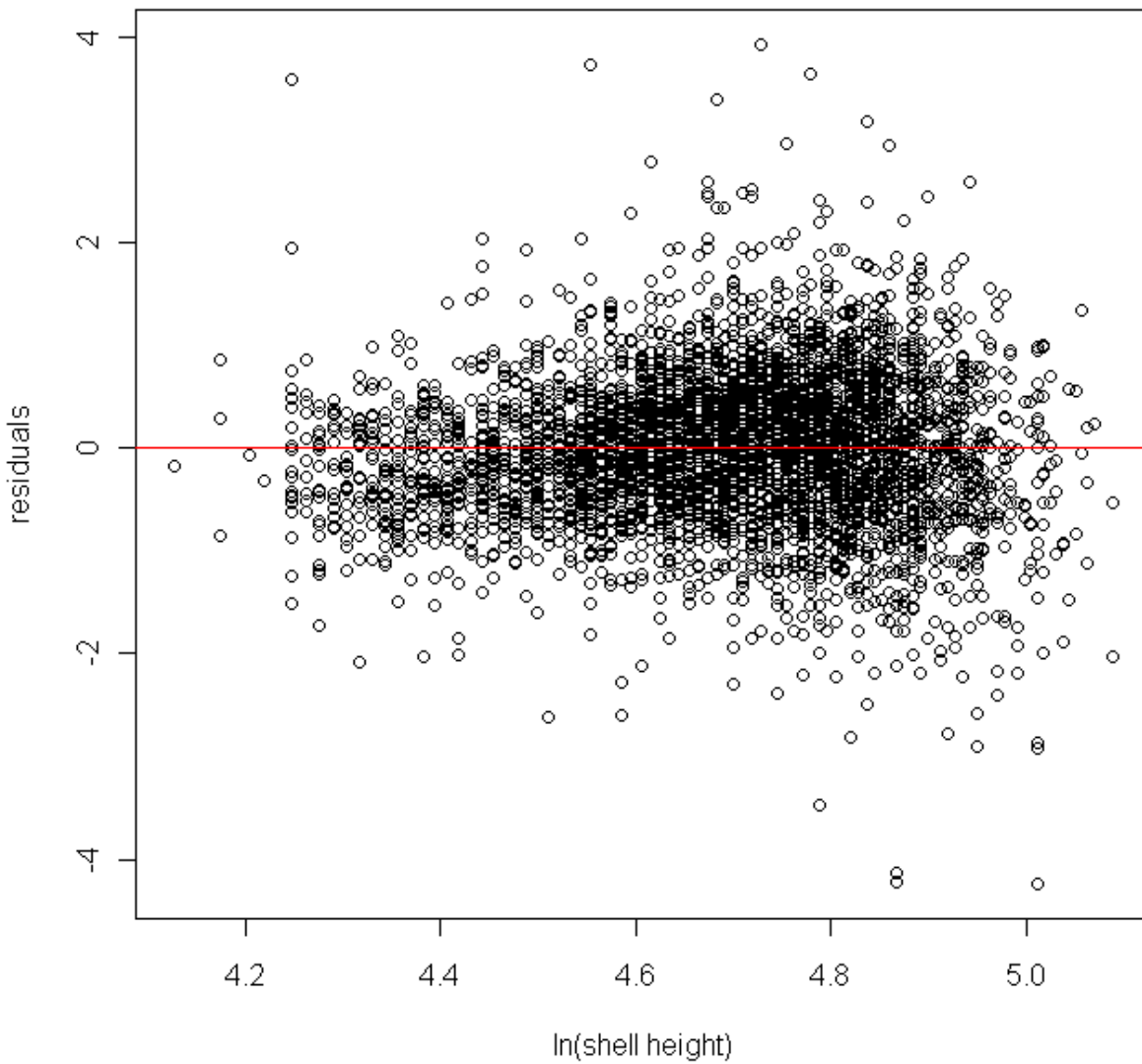
	α	β	γ	n(stations)
Mid-Atlantic Bight ^a				
DMV-VB	-8.0407	2.8249	-0.5194	125
ET	-7.0358	2.9036	-0.861	194
HC	-7.305	2.9066	-0.7863	139
LI	-9.7815	2.9439	-0.224	150
NYB	10.3701	3.0698	-0.213	109
Georges Bank ^b				
CL-1	-6.3757	2.7999	-0.8405	148
CL-2	-8.7026	2.8338	-0.3354	205
NEP	-7.9355	2.8325	-0.5477	152
NLS	-8.1709	2.6454	-0.2298	92
Sch	-9.5245	2.9359	-0.2808	146
SEP	-4.3756	2.6291	-1.1166	69

a - model = $meat_weight \sim height + depth + (1 | year_station)$

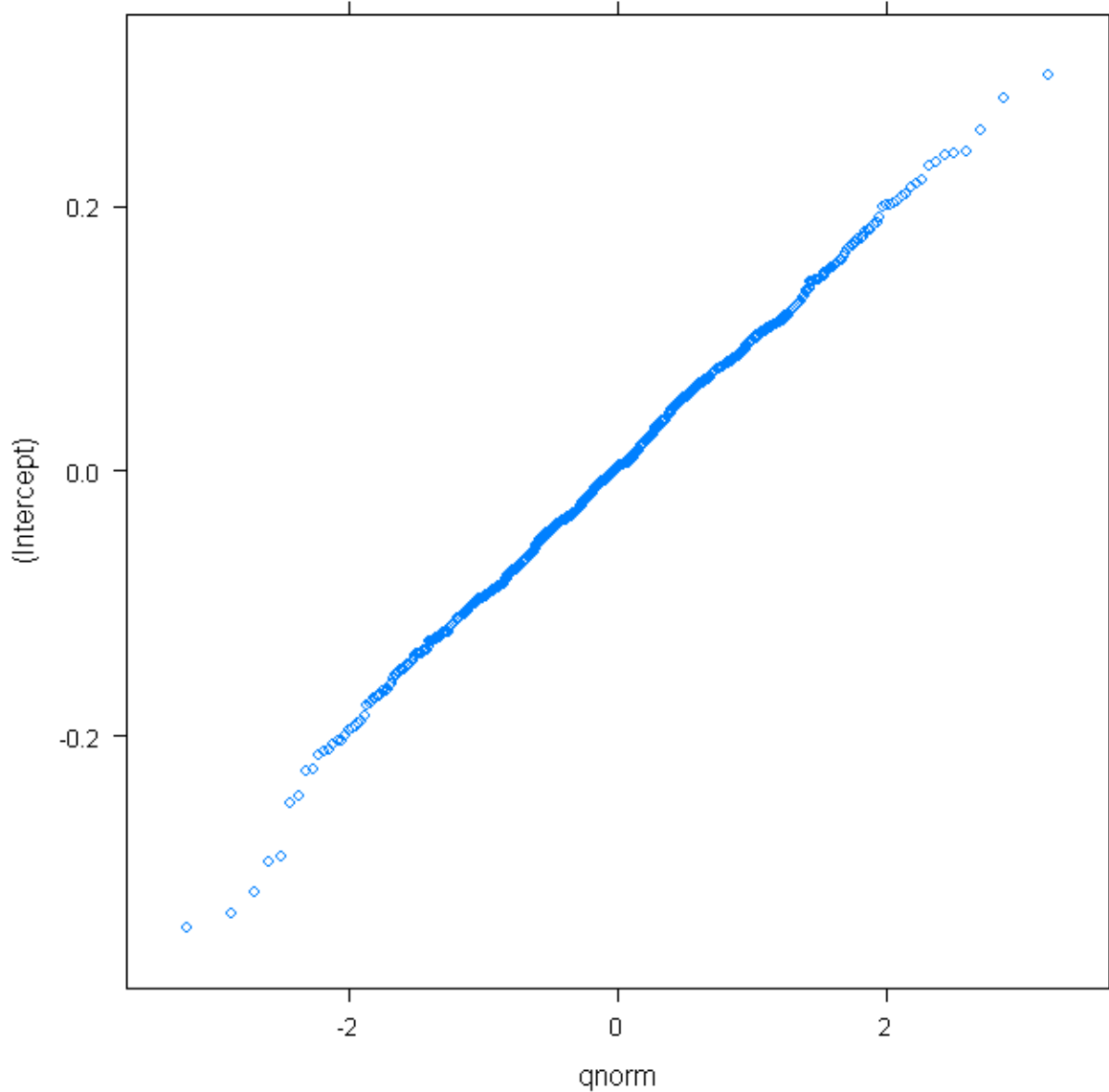
b - model = $meat_weight \sim height + depth + (height + 1 | year_station)$



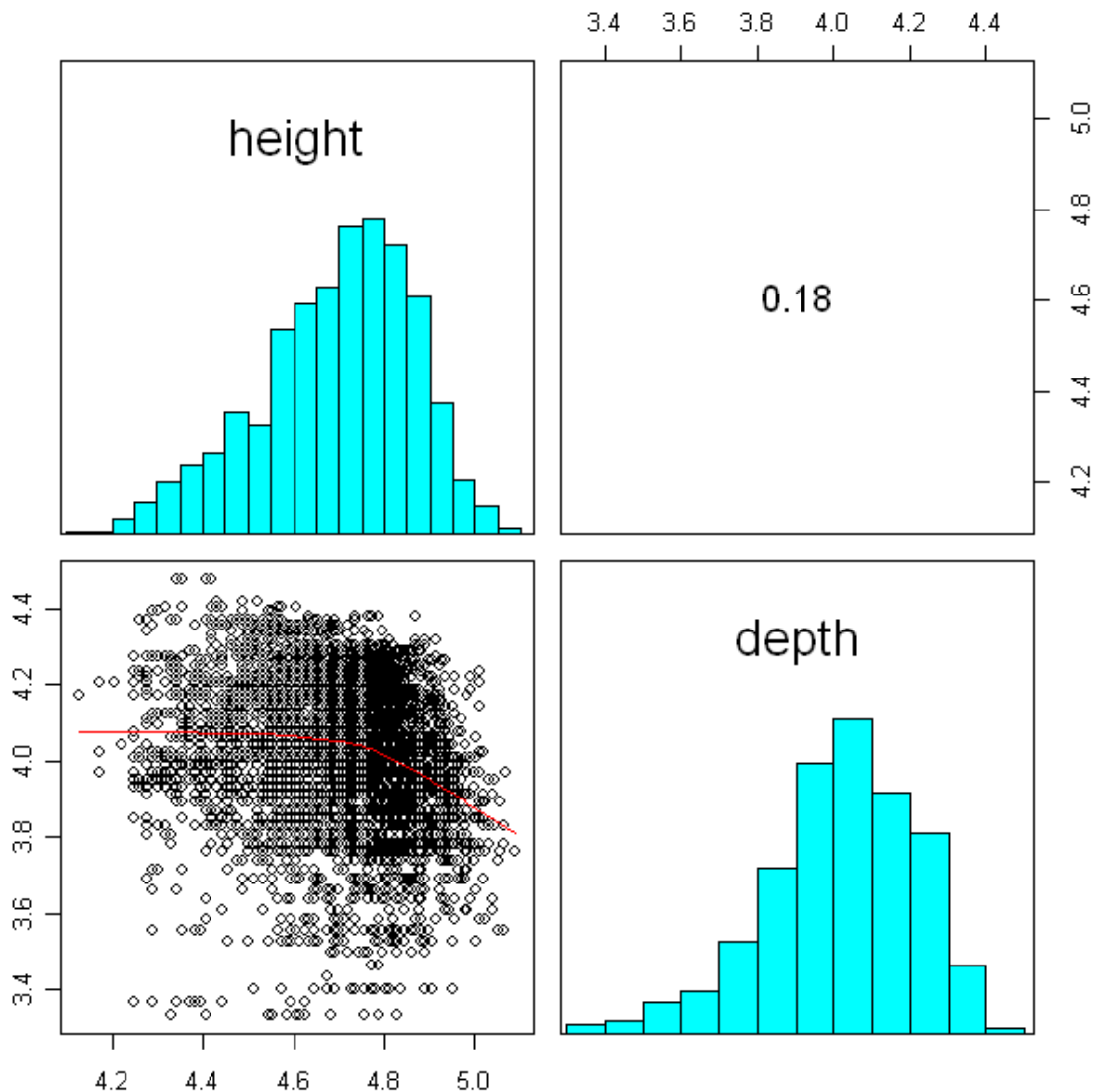
Appendix B7-Figure 1. Mid-Atlantic shell height/meat weight data



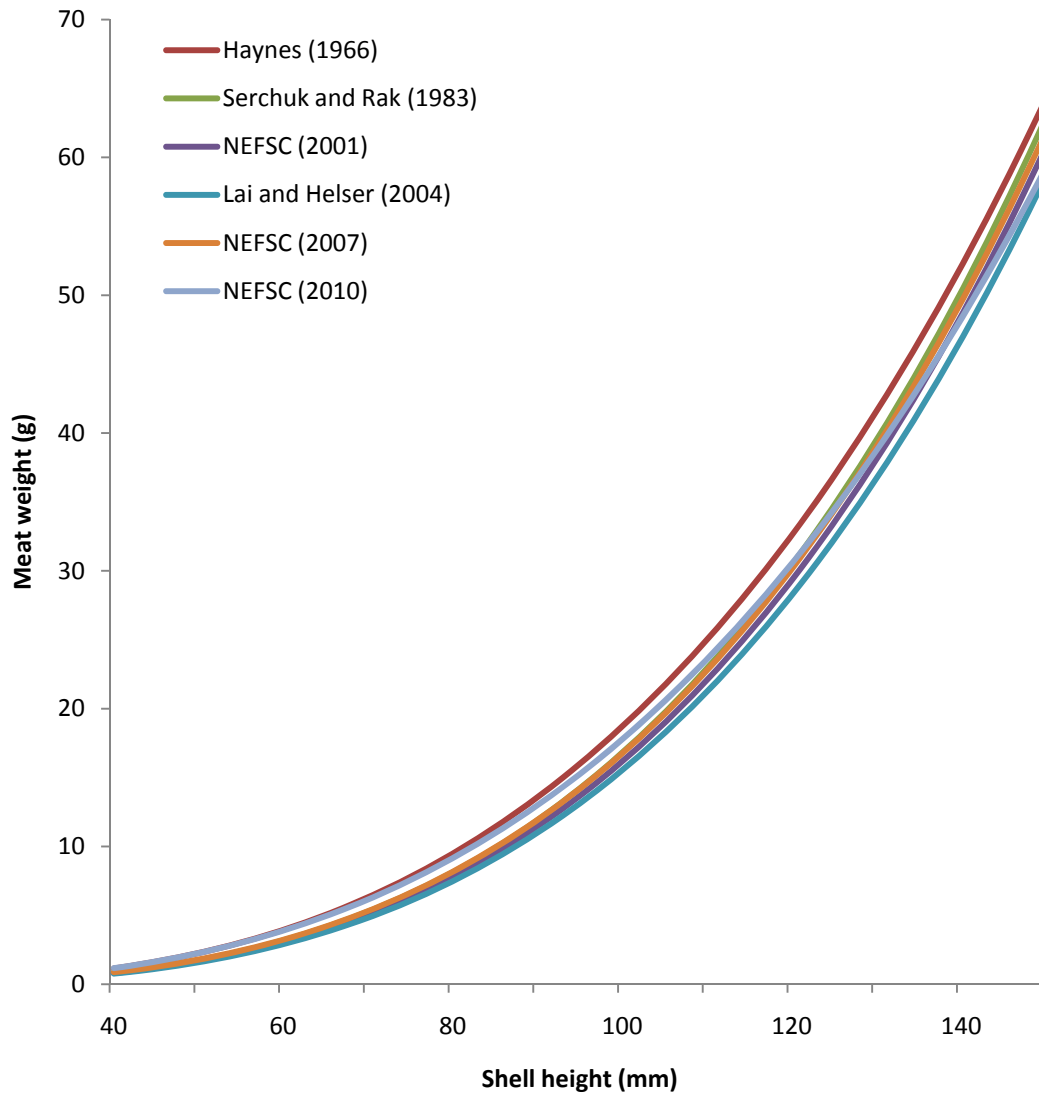
Appendix B7-Figure 2. Residual plot of Mid-Atlantic shell height/meat weight data



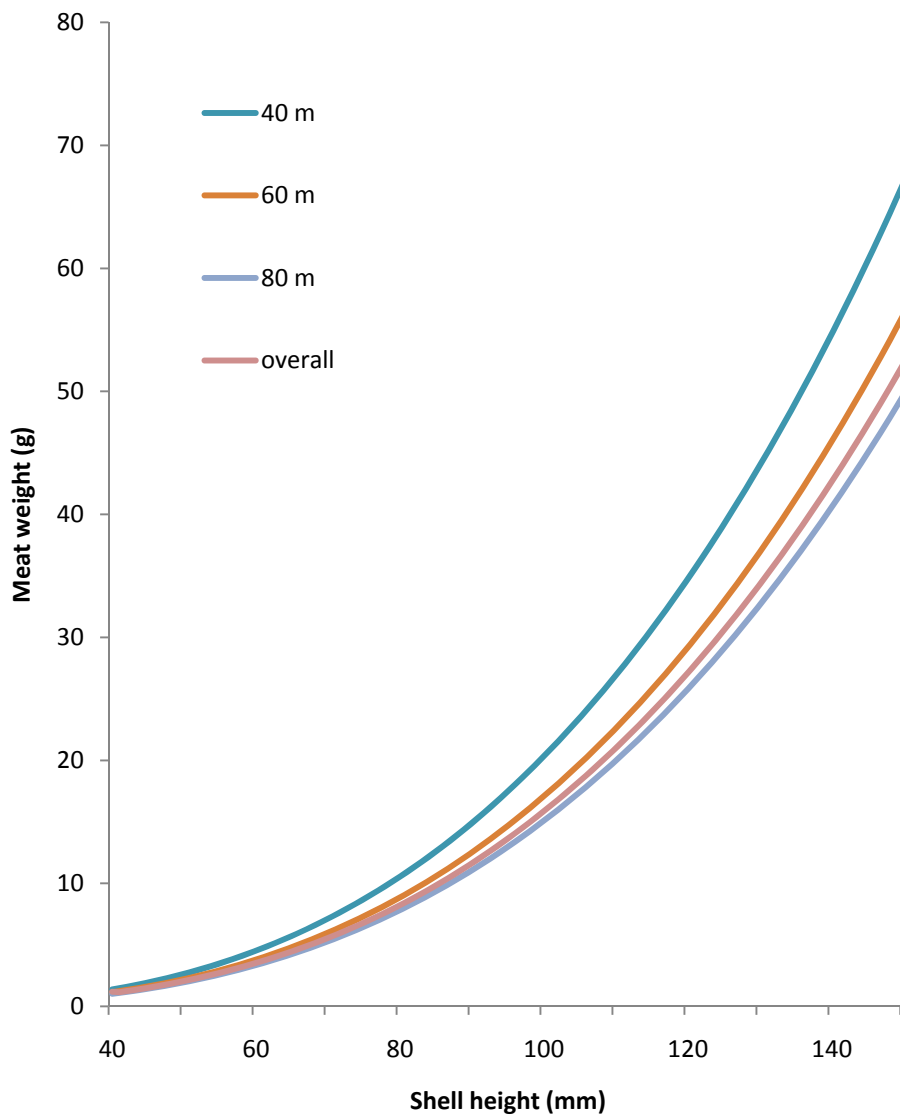
Appendix B7-Figure 3. Normality plot of the BLUPs (Best Linear Unbiased Predictions of the random effects) from the best model (Eq. 1) for the Mid-Atlantic Bight. The only random effect is an intercept, grouped by station (where station is a unique identifier that incorporates spatial – survey station, and temporal – year, variability).



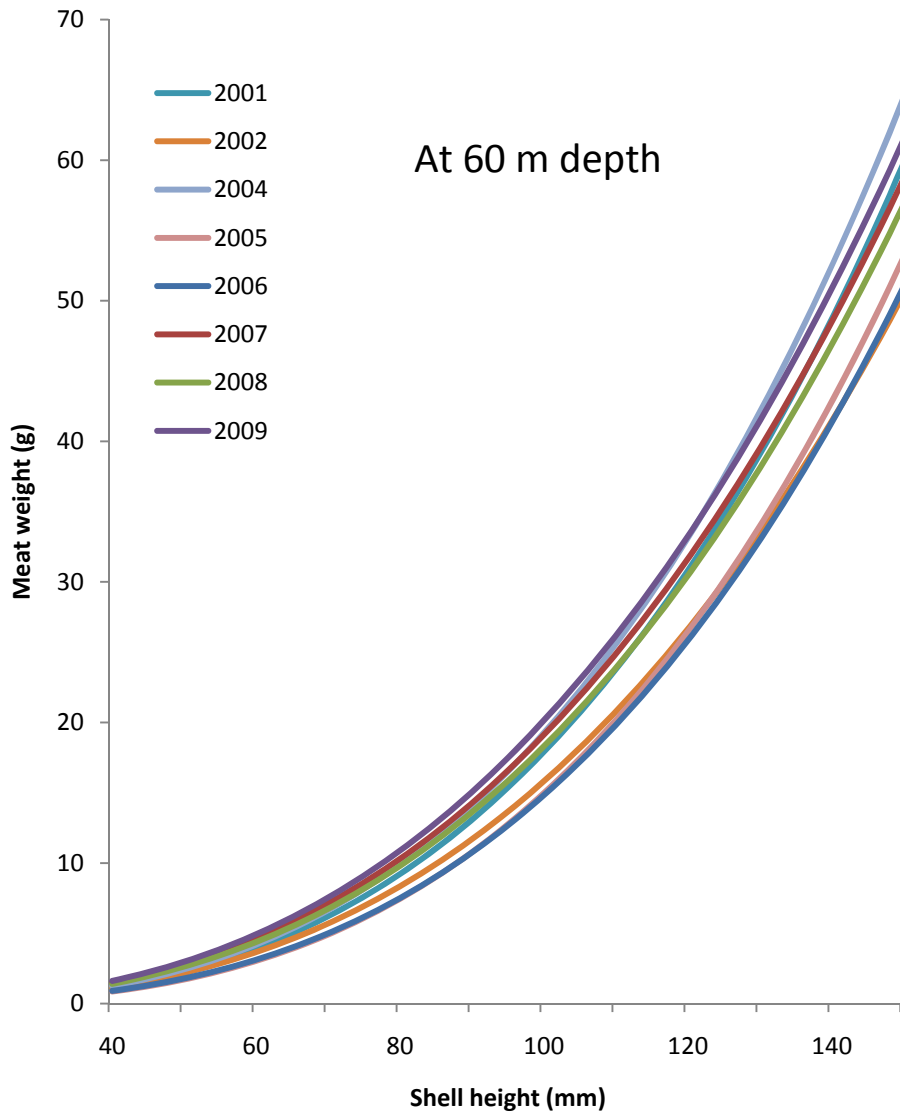
Appendix B7-Figure 4. The correlation plot of the fixed effects from the best model (Eq. 1) for the Mid-Atlantic Bight. The values of the correlation coefficients for each comparison are shown in the upper diagonal. The main diagonal shows the frequency histogram of each effect and the scatter plot in the lower diagonal includes a smooth curve meant only to aid visual interpretation.



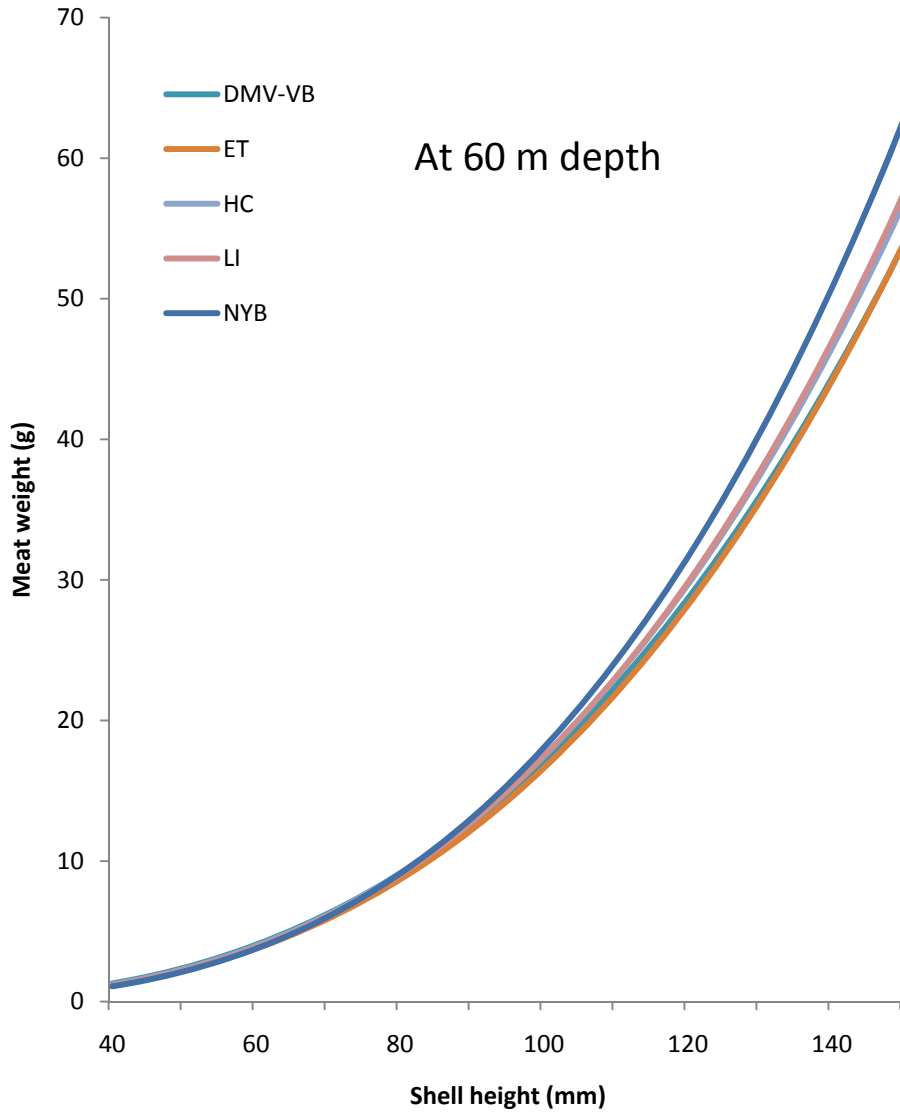
Appendix B7-Figure 5. Comparison of historical shell height/meat weight parameter estimates in the Mid-Atlantic (directly comparable models only, i.e. of the form $W = e^{(\alpha+a(St)+\beta)+\epsilon}$).



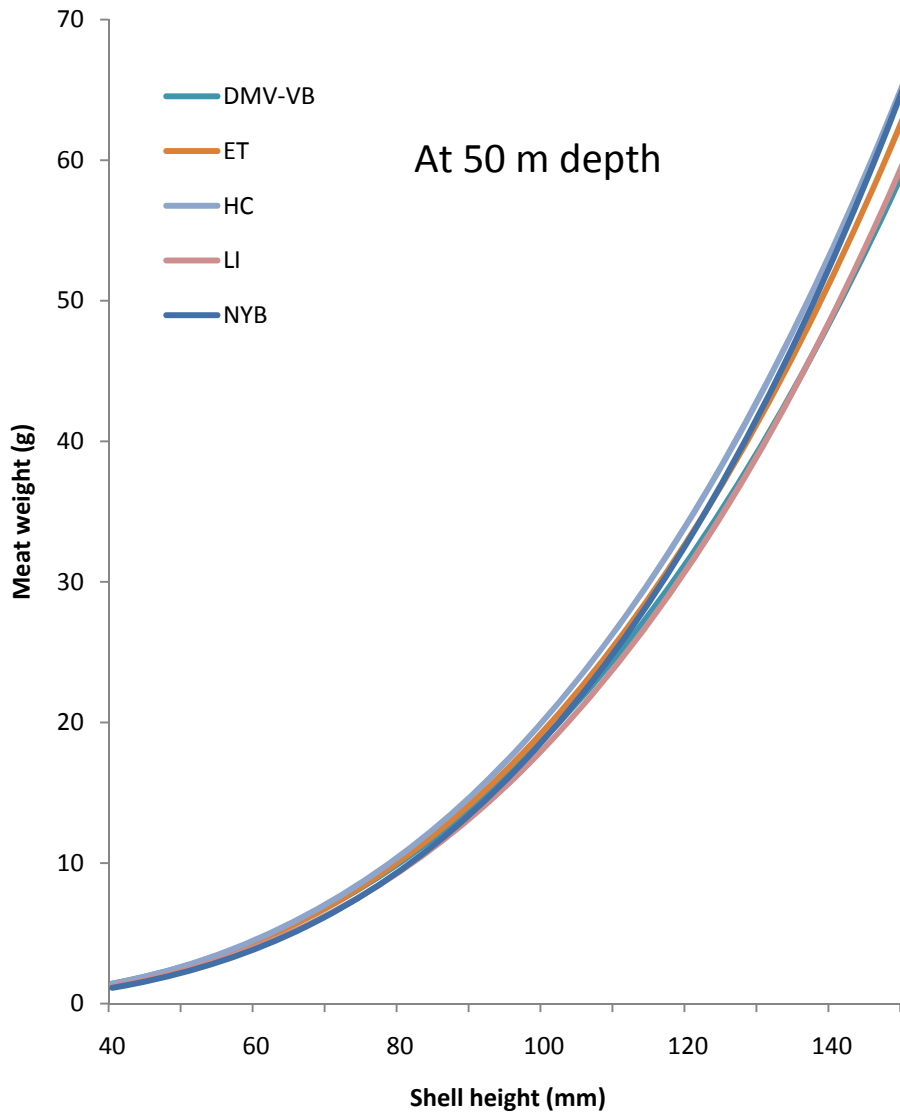
Appendix B7-Figure 6. Shell height/meat weight relationships at relationships 40, 60, 80 m depth, and overall in the Mid-Atlantic ($W = e^{(\alpha+a(St)+\beta \ln(L)+\gamma \ln(D))+\epsilon}$).



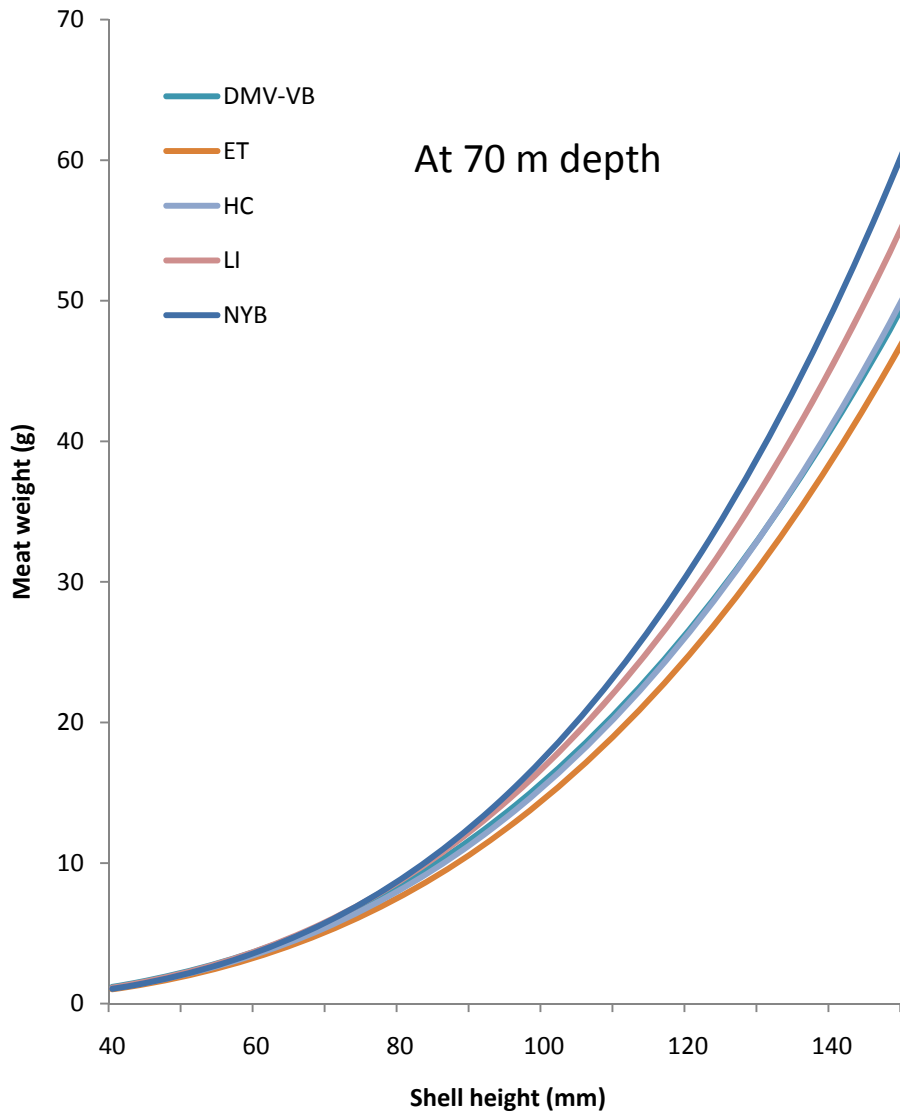
Appendix B7-Figure 7. Shell height/meat weight relationships for each survey year at 60 m depth in the Mid-Atlantic Bight ($W = e^{(\alpha+a(St)+\beta \ln(L)+\gamma \ln(D))+\epsilon}$).



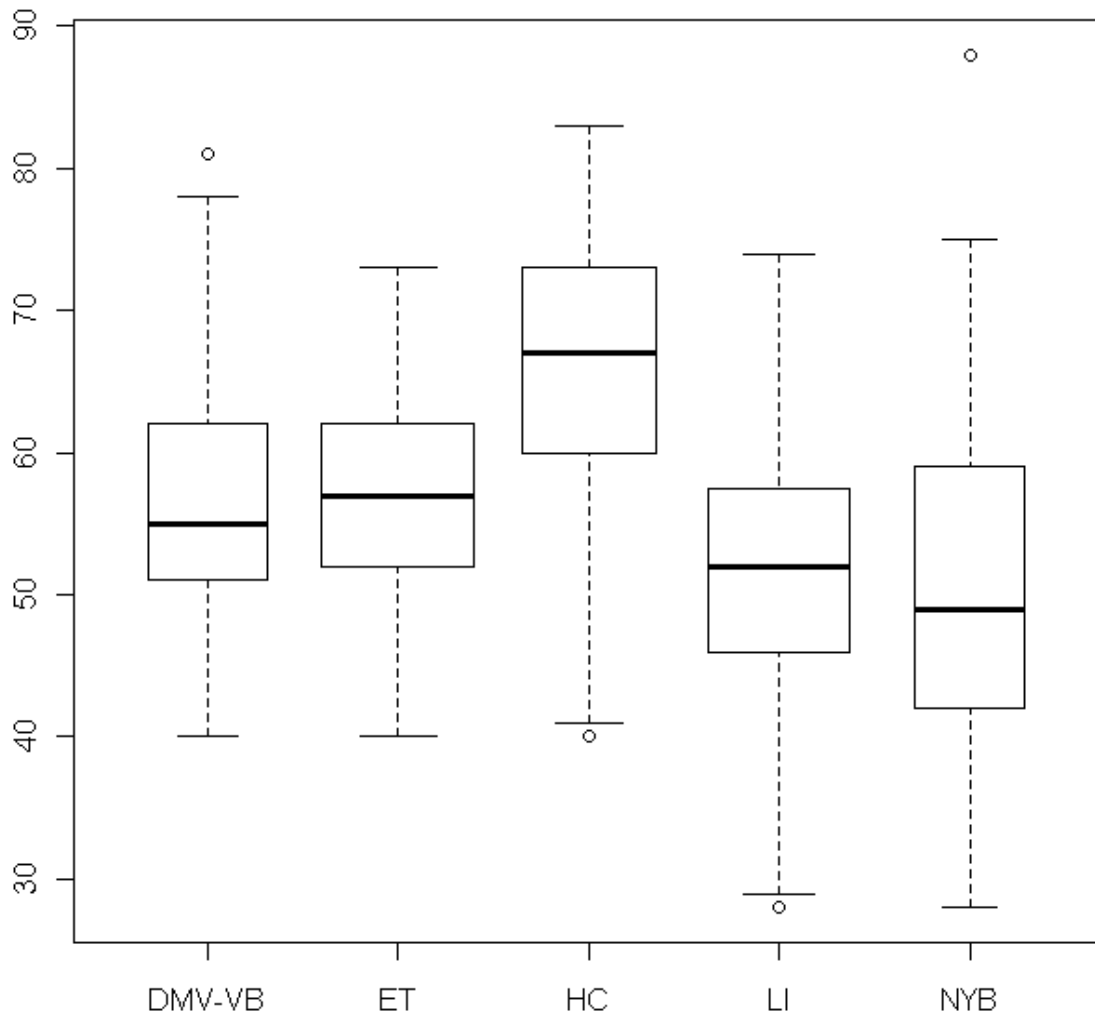
Appendix B7-Figure 8. Shell height/meat weight relationships for each subarea at 60 m depth in the Mid-Atlantic Bight ($W = e^{(\alpha+a(St)+\beta \ln(L)+\gamma \ln(D))+\epsilon}$).



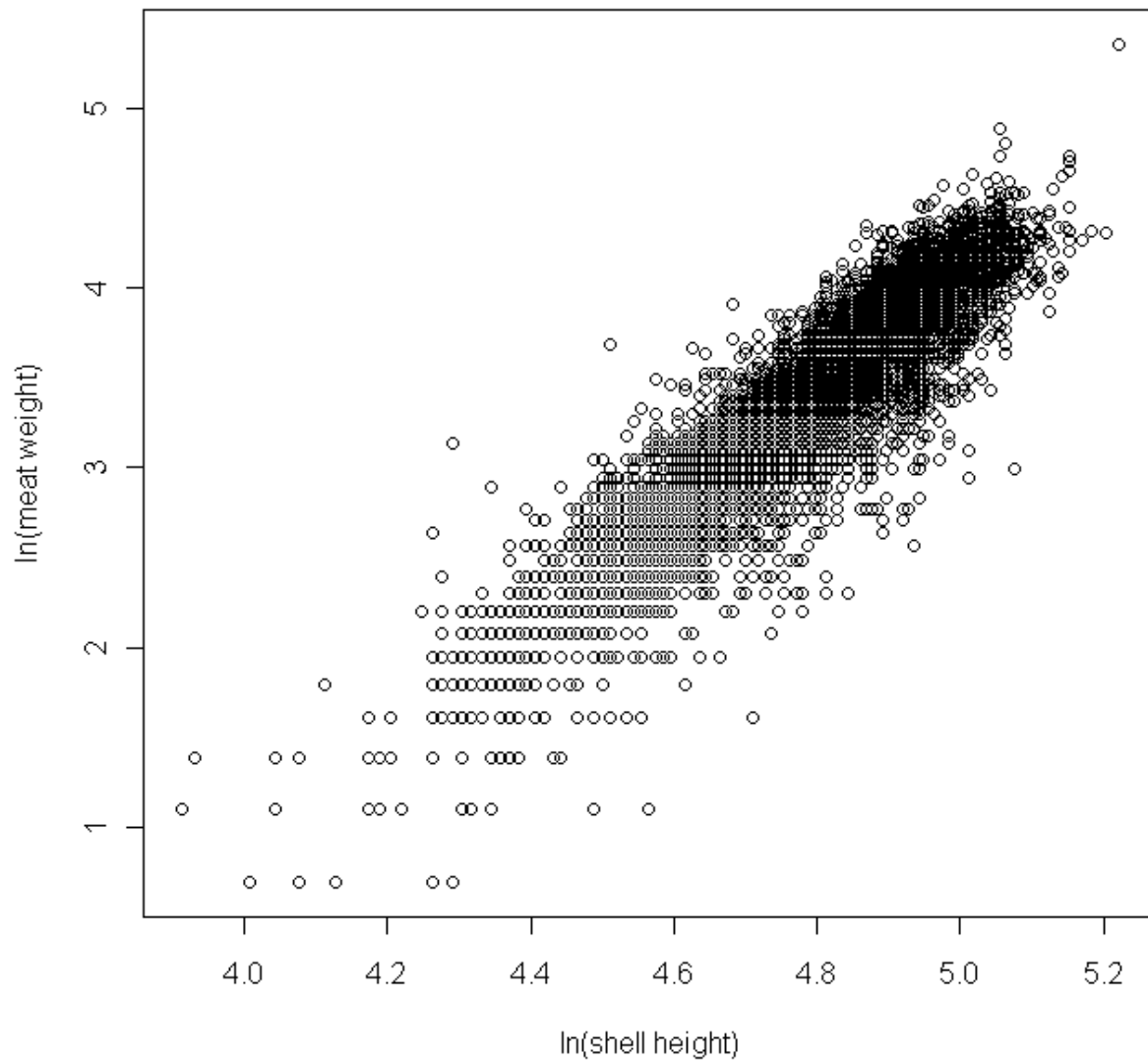
Appendix B7-Figure 9. Shell height/meat weight relationships for each subarea at 50 m depth in the Mid-Atlantic Bight ($W = e^{(\alpha+a(St)+\beta \ln(L)+\gamma \ln(D))+\epsilon}$).



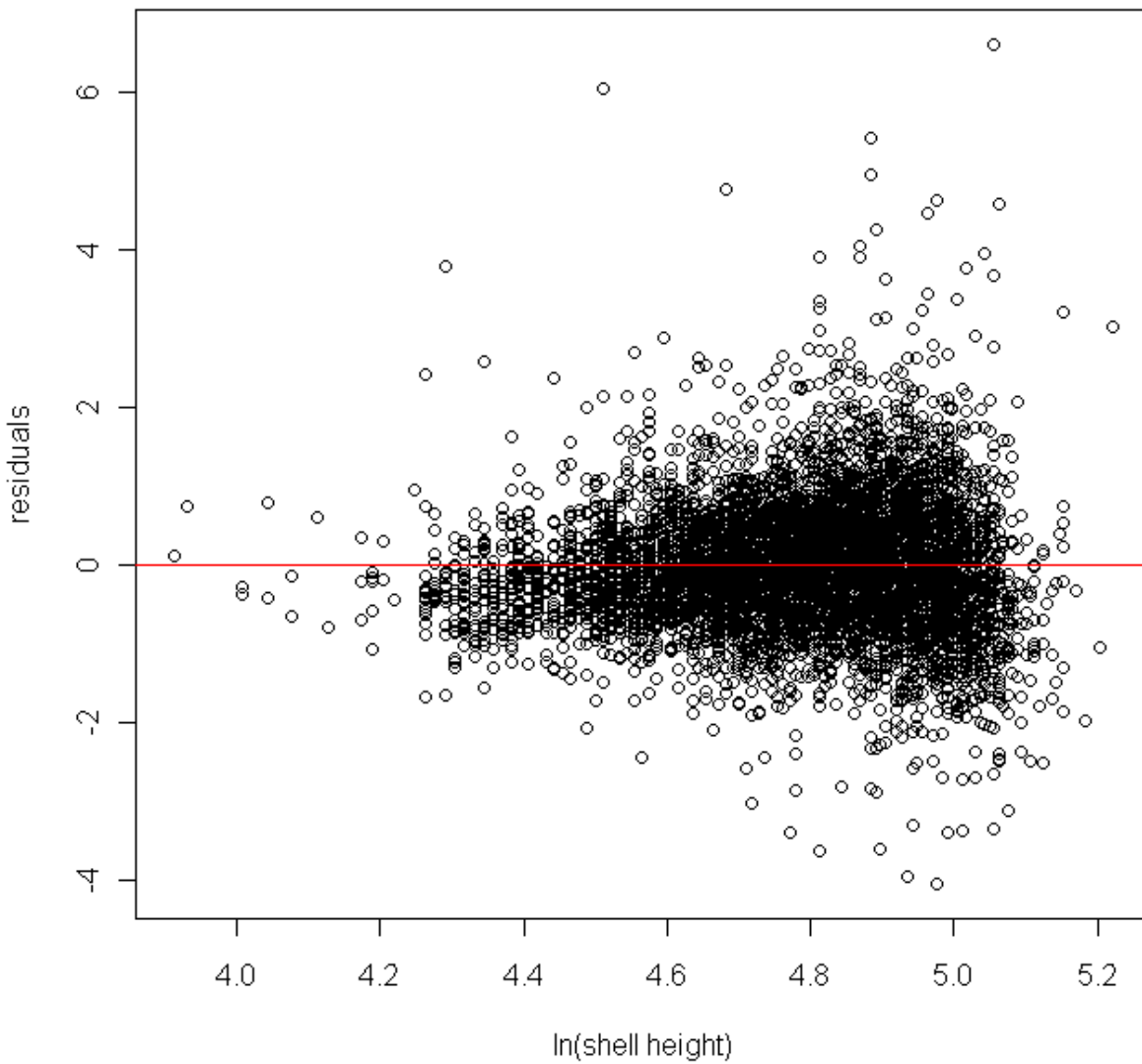
Appendix B7-Figure 10. Shell height/meat weight relationships for each subarea at 70 m depth in the Mid-Atlantic Bight ($W = e^{(\alpha+a(St)+\beta \ln(L)+\gamma \ln(D))+\epsilon}$).



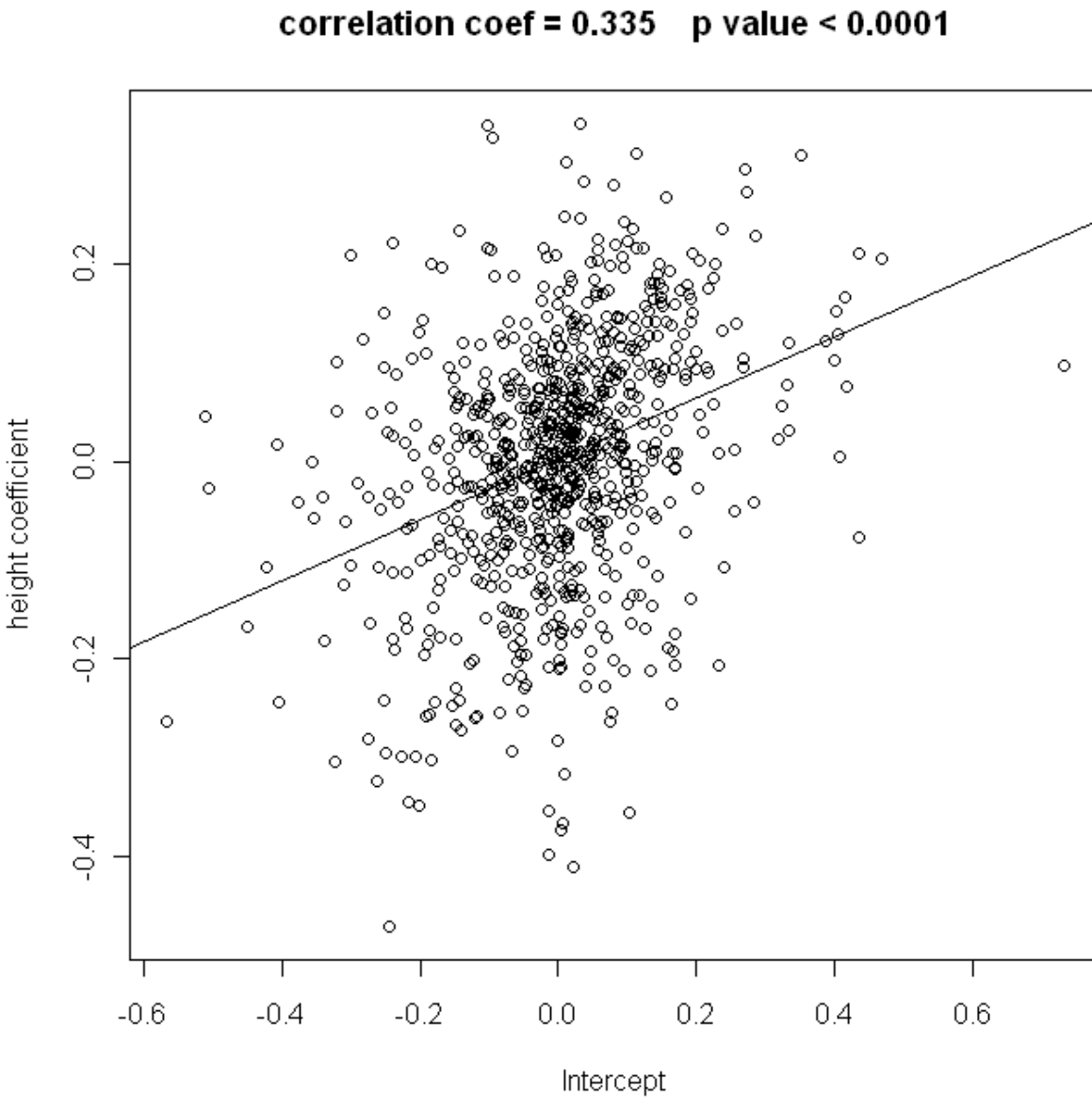
Appendix B7-Figure 11. Box plots of the depths of samples taken from each of the subareas in the Mid-Atlantic Bight.



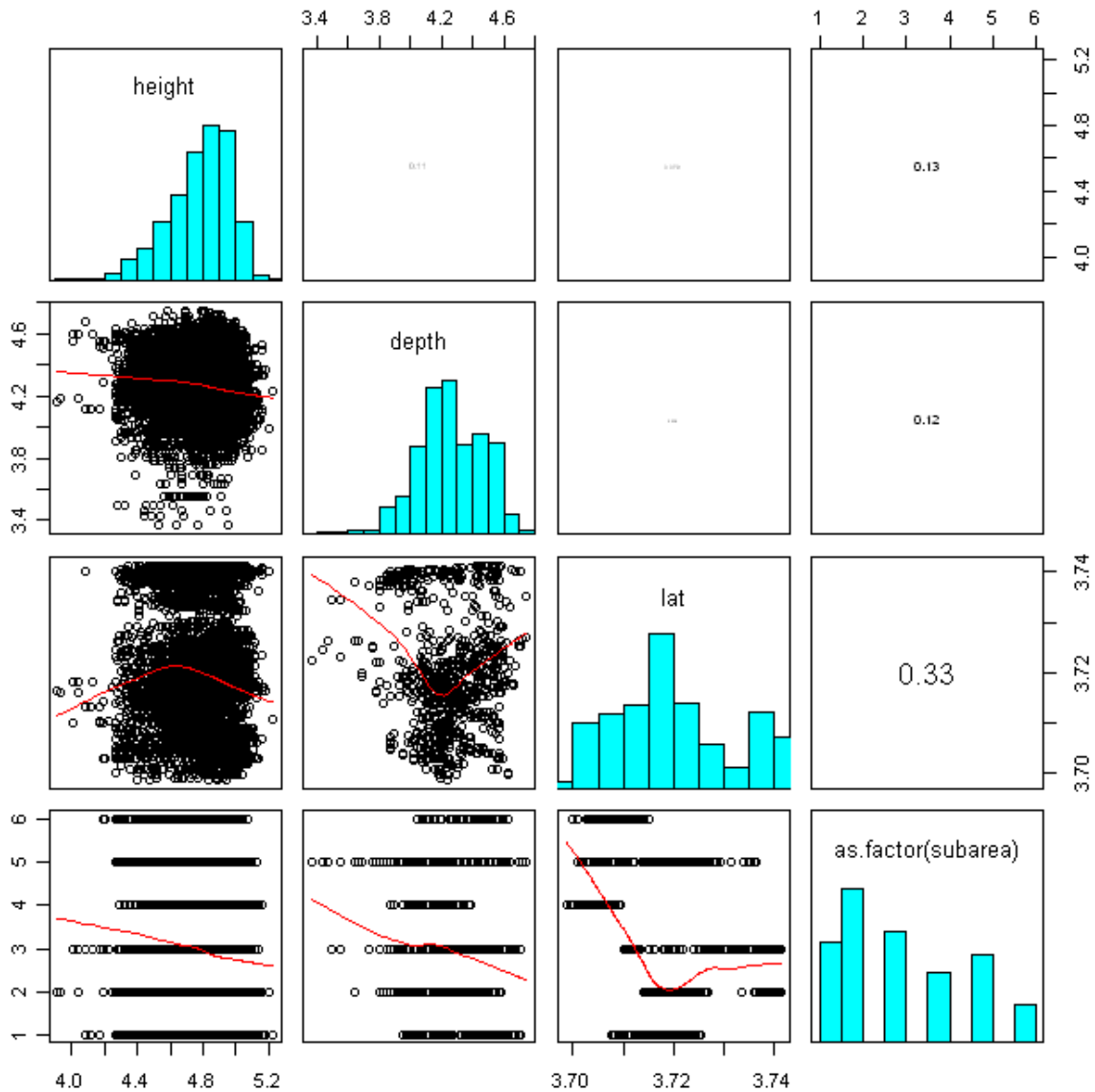
Appendix B7-Figure 12. Georges Bank shell height/meat weight data.



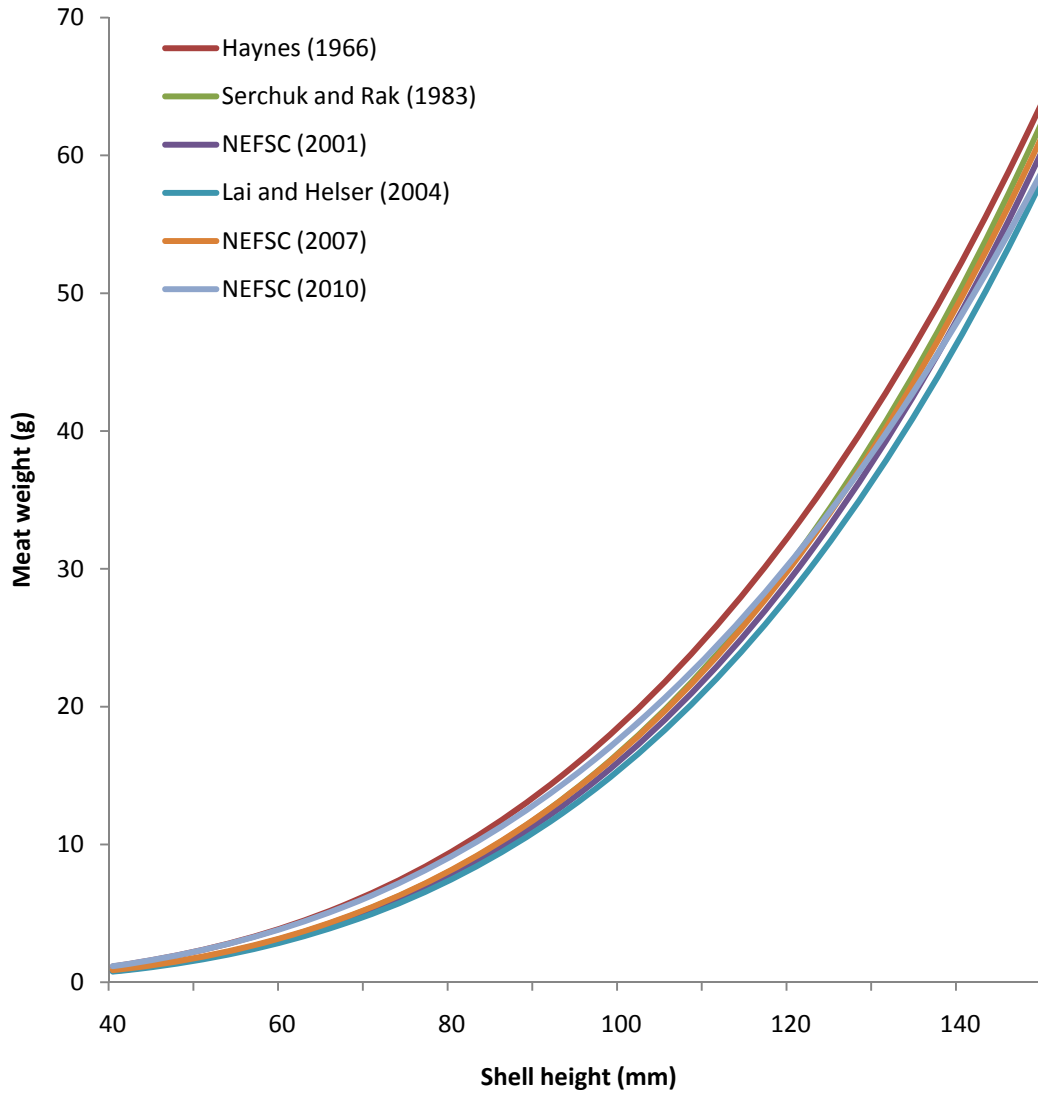
Appendix B7-Figure 13. Residual plot of Georges Bank shell height/meat weight data.



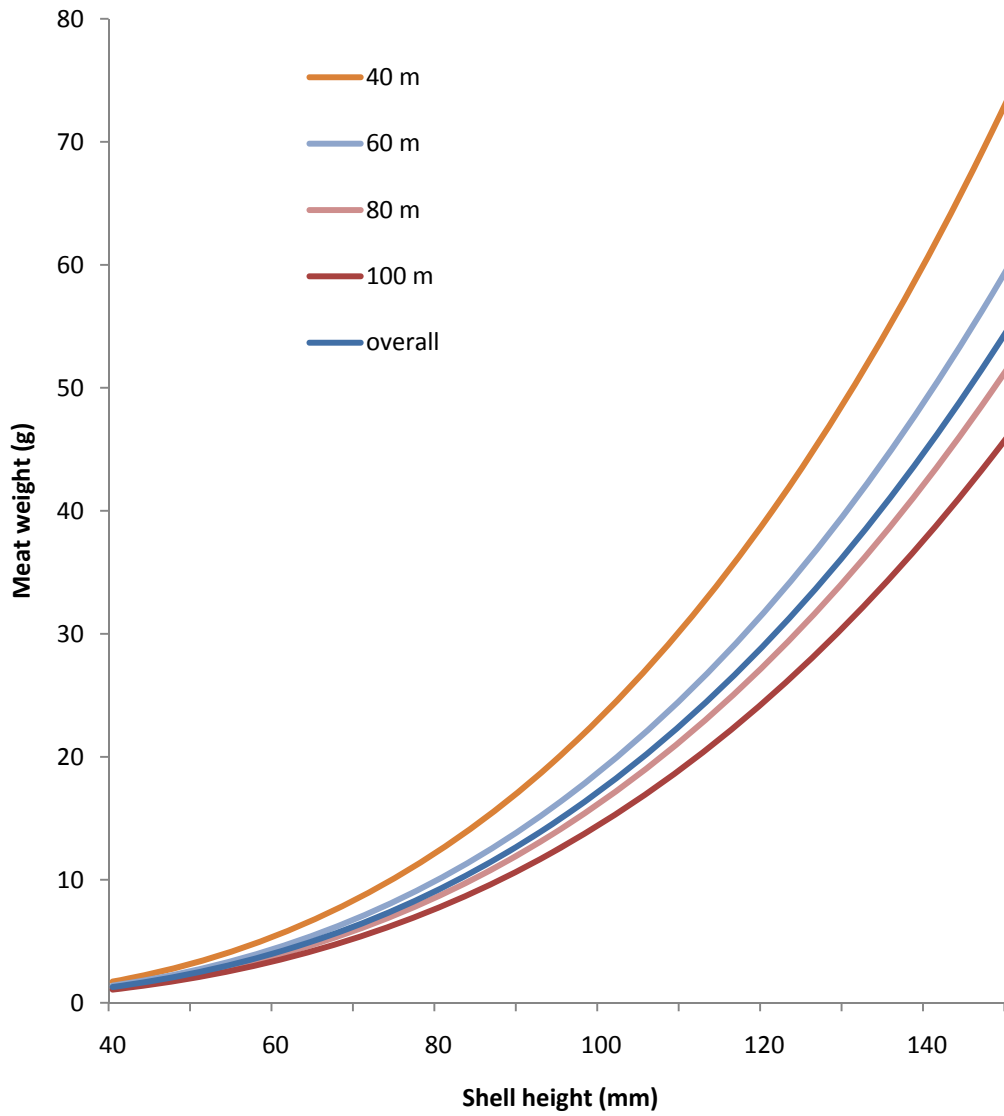
Appendix B7-Figure 14. The correlation between BLUPs (Best Linear Unbiased Predictions of random effects) from the best model (2) for Georges Bank. These are a random slope coefficient (on shell height) and a random intercept, both grouped by station (where station is a unique identifier that incorporates spatial – survey station, and temporal – year, variability).



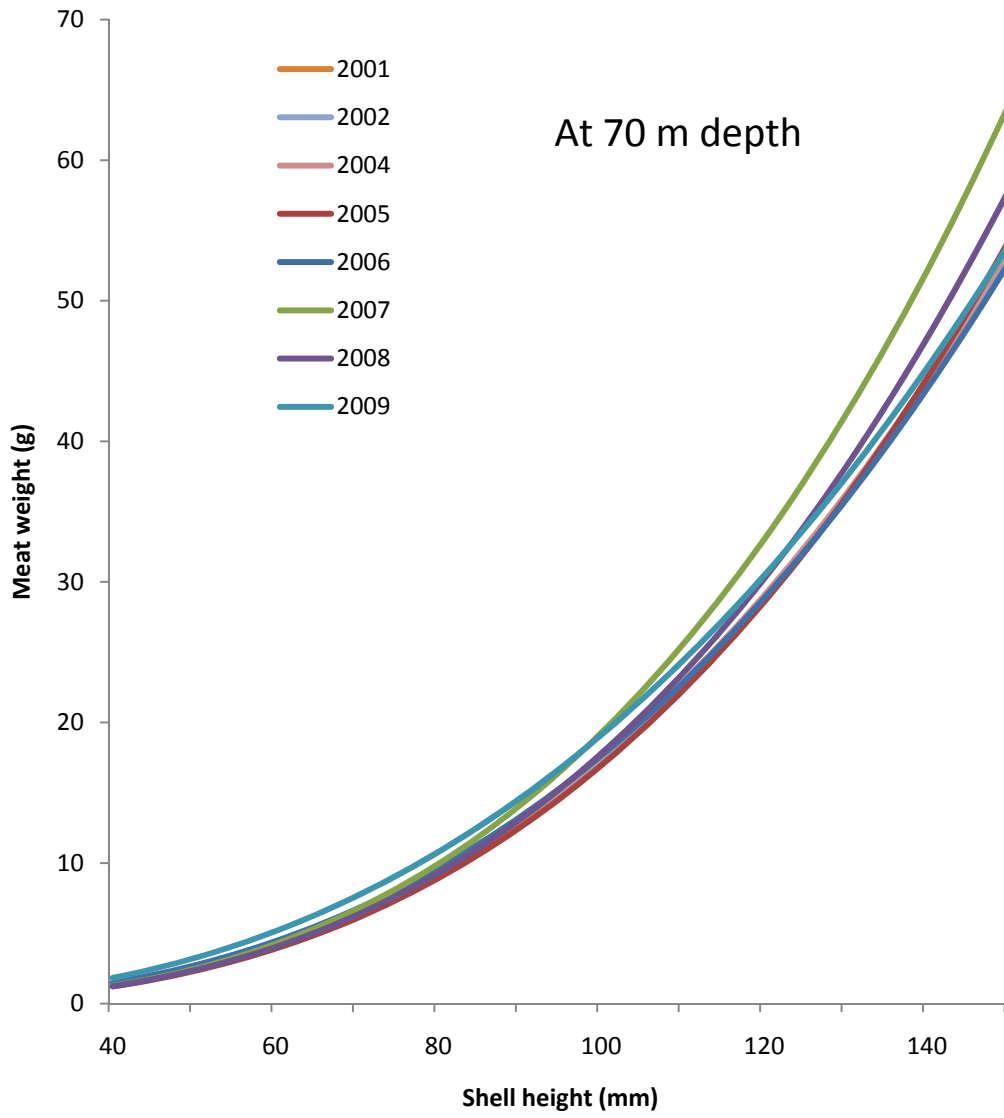
Appendix B7-Figure 15. Correlation of Fixed effects from the best model (2) for Georges Bank. The values of the correlation coefficients for each comparison are shown in the upper diagonal and the text font is scaled relative to the significance of the correlation. The main diagonal shows the frequency histogram of each effect and the scatter plots in the lower diagonal include a smooth line meant only to aid visual inspection.



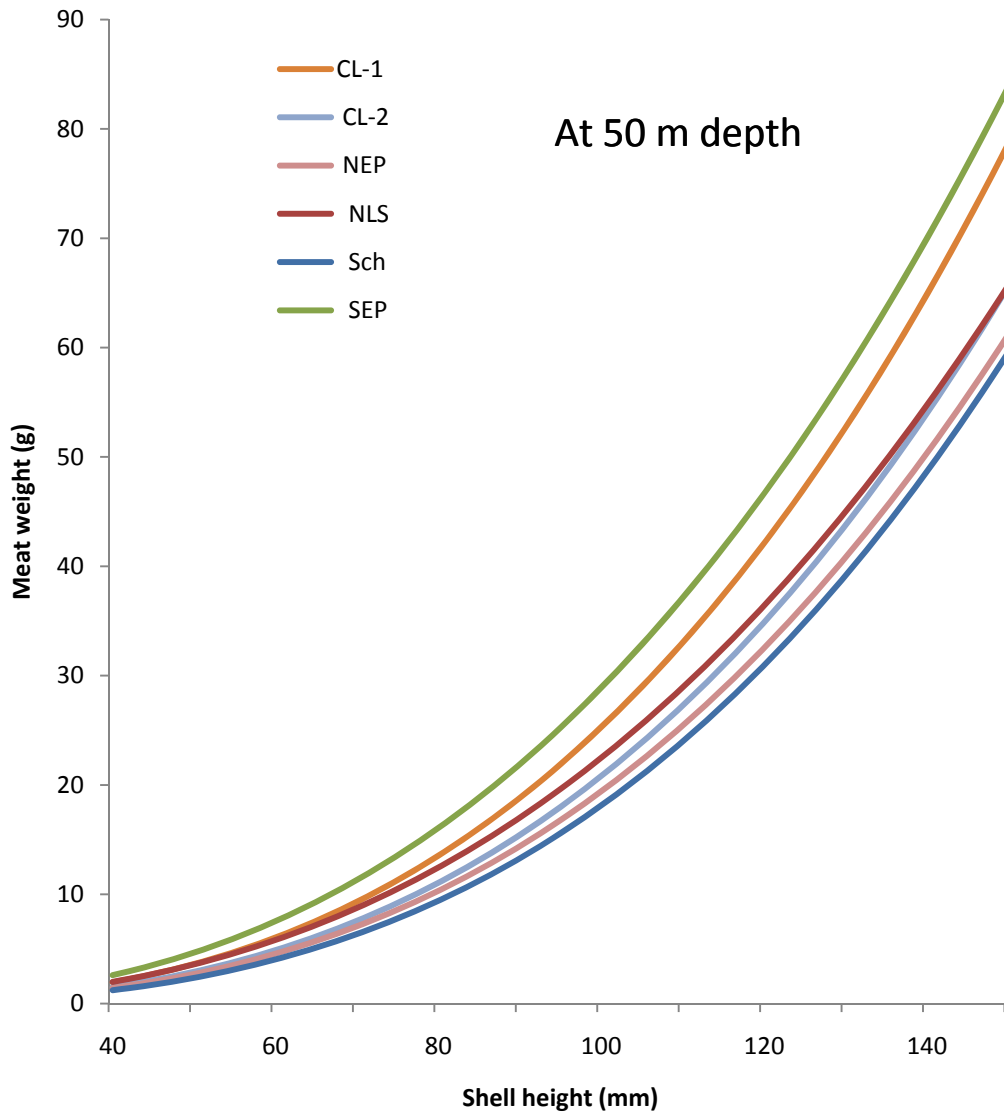
Appendix B7-Figure 16. Comparison of shell height/meat weight parameter estimates in the Georges Bank (directly comparable models only, i.e. of the form $= e^{(\alpha+a(St)+\beta)+\epsilon}$).



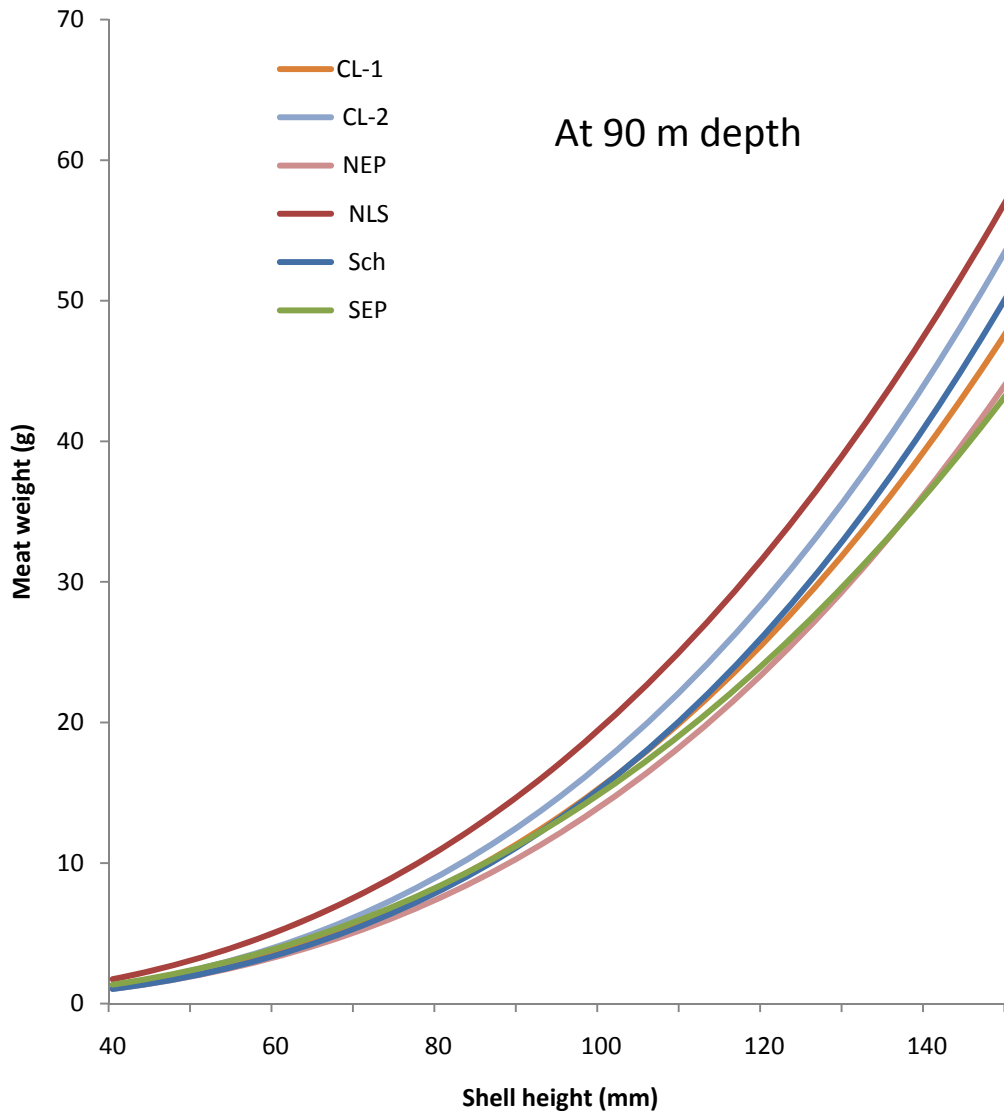
Appendix B7-Figure 17. Shell height/meat weight relationships at relationships 40, 60, 80, 100 m depth, and overall in Georges Bank ($W = e^{(\alpha+a(St)+\beta \ln(L)+\gamma \ln(D)+b(L_{St}))+\epsilon}$).



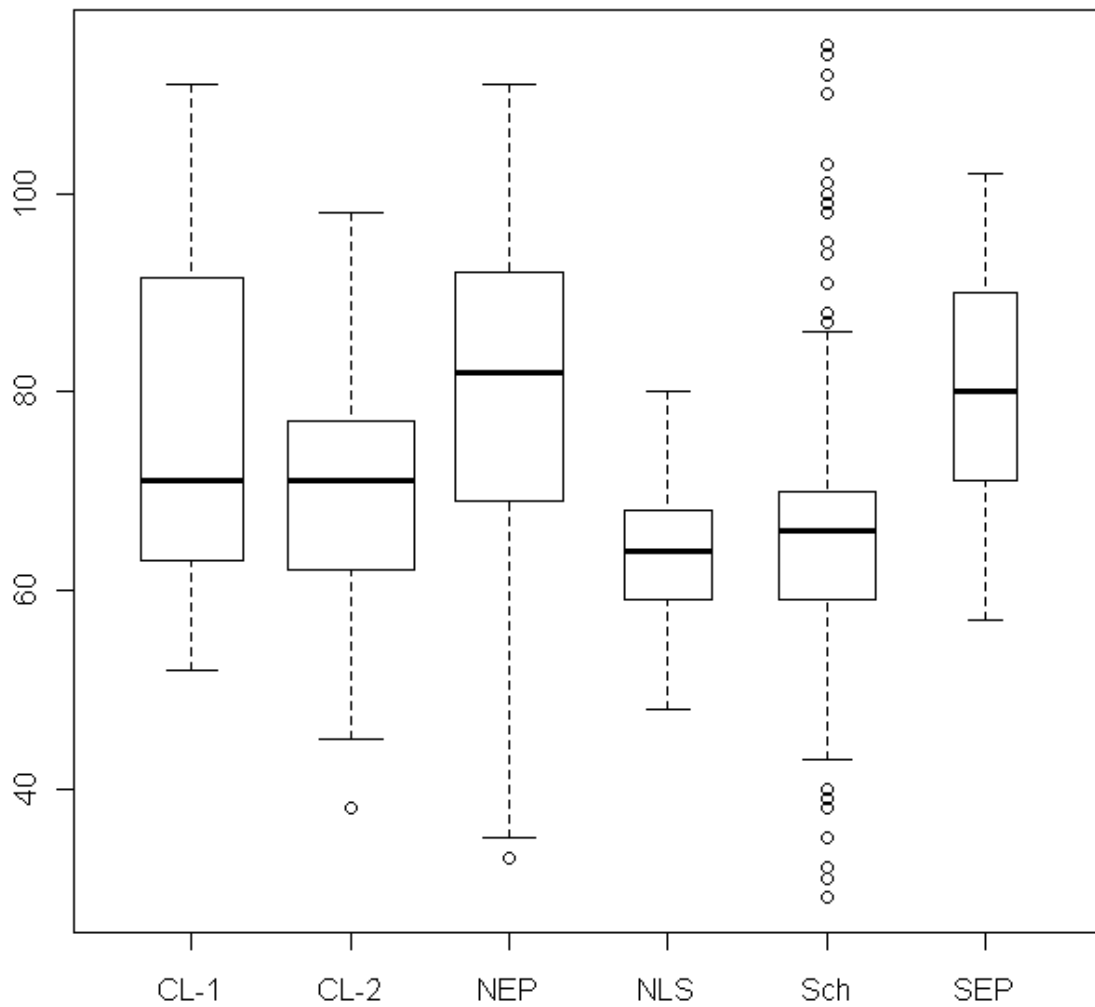
Appendix B7-Figure 18. Shell height/meat weight relationships for each survey year at 70 m depth on Georges Bank ($W = e^{(\alpha+a(S_t)+\beta \ln(L)+\gamma \ln(D)+b(L_{St}))+\epsilon}$).



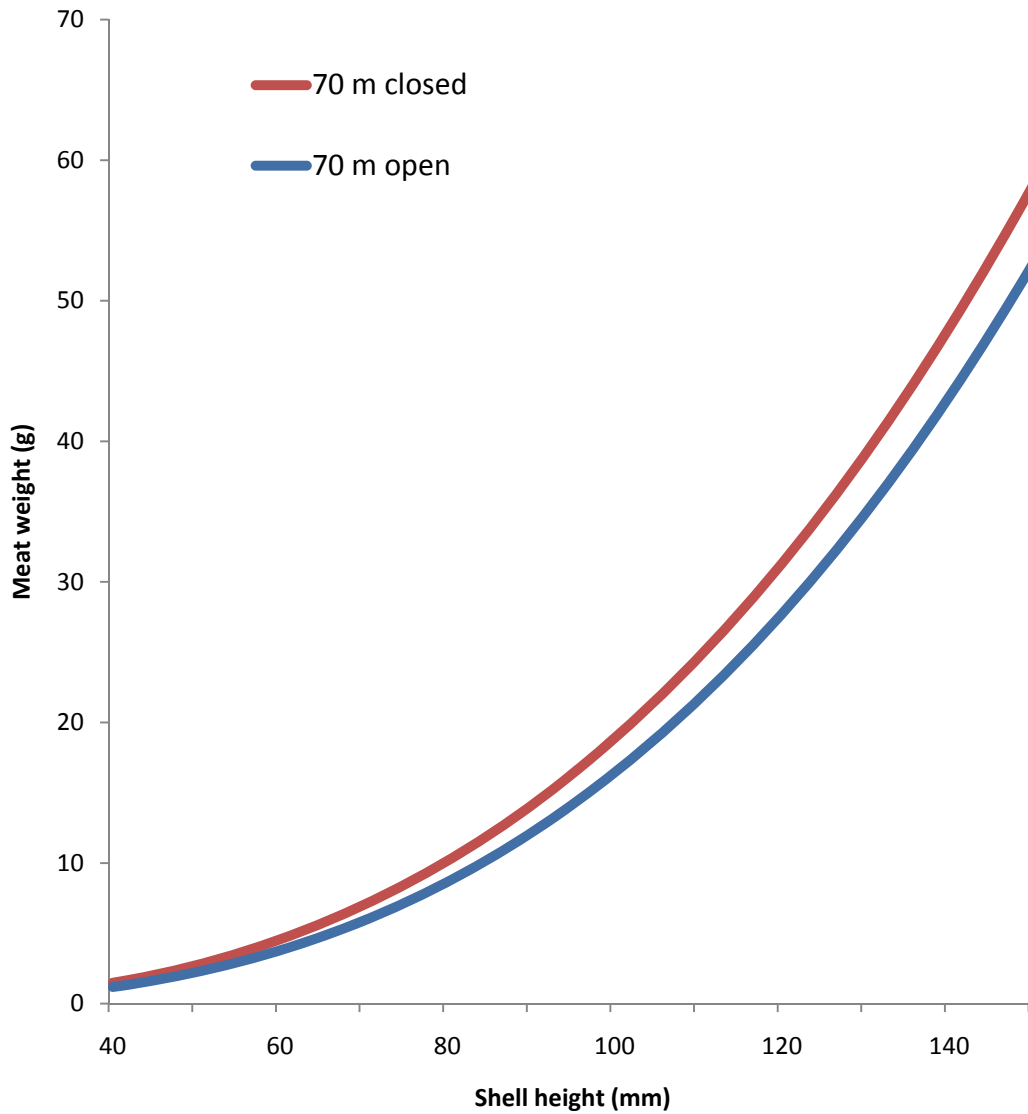
Appendix B7-Figure 19. Shell height/meat weight relationships for each survey year at 50 m depth on Georges Bank ($W = e^{(\alpha+a(S_t)+\beta \ln(L)+\gamma \ln(D)+b(L_{St}))+\epsilon}$).



Appendix B7-Figure 20. Shell height/meat weight relationships for each survey year at 90 m depth on Georges Bank ($W = e^{(\alpha+a(S_t)+\beta \ln(L)+\gamma \ln(D)+b(L_{St}))+\epsilon}$).



Appendix B7-Figure 21. Box plots of the depths of samples taken from each of the subareas on Georges Bank.



Appendix B7--Figure 22. Shell height/meat weight relationships at relationships for open and closed to fishing areas at 60 m depth on Georges Bank ($W = e^{(\alpha+a(St)+\beta \ln(L)+\gamma \ln(D)+b(L_{St}))+\epsilon}$).

Appendix B8: Seasonal patterns in commercial meat weight and meat weight anomalies.

Dan Hennen and Dvora Hart, Northeast Fisheries Science Center, Woods Hole, MA.

This appendix describes updated estimates of seasonal patterns in mean commercial meat weights and updated annual commercial meat weight anomalies. The anomalies are used in the CASA model (Appendix 11) in calculating predicted catch weight to account for differences in shell-height meat weight relationships between the NEFSC scallop survey and commercial fishery. Relationships from the NEFSC scallop survey are used to calculate mid-year biomass for the population. Anomalies for the commercial fishery are calculated on an annual basis to account for overall and seasonal differences in survey and commercial meat weight, and changes over time in the seasonal distribution of catches.

Methods

The NMFS Observer program provided meat weight estimates from commercial catches that occurred throughout the year. These meat weights are for sea scallops in samples that are shucked by fishermen after the observer measures shell height. Meats from the observer program are not weighed individually. They are packed into a graduated cylinder and a volume for a sample (typically ~100 scallops) is recorded. The meat weight for a sample is calculated assuming a density estimate of 1.05 g/ml³ (Caddy and Radley-Walters 1972; Smolowitz et al. 1989). Shell height data from the observer program for individual scallops are binned by 5 mm increments.

Predicted meat weights for the Mid-Atlantic Bight (MAB) and Georges Bank (GBK) were based on the models

$$W = e^{(\alpha + \beta \ln(H) + \gamma \ln(D) + \rho(\ln(L) * \ln(D))) + \epsilon} \quad (\text{MAB}) \quad (1)$$

$$W = e^{(\alpha + \beta \ln(H) + \gamma \ln(D) + \rho \ln(L)) + \epsilon} \quad (\text{GBK}) \quad (2)$$

where W is meat weight (g), H is shell height in mm, D is depth in m, and L is latitude measured in decimal degrees. This model was fit using NMFS scallop survey data from 2001 – 2008 (Appendix B7). As described in NEFSC (2007), the surveys for scallops occur in the summer when meat weights are typically high. The estimated coefficients from (1) and (2) were applied to the shell heights and depths recorded from observer samples from 2001 – 2009. Observer data for 2006 is incomplete and was not used in this analysis. Monthly anomalies were

computed using median predicted meat weights and median meat weights derived from observer data:

$$\frac{(pred.-obs.)}{pred.} \quad (3)$$

Median meat weights were used instead of mean meat weights to reduce the influence of outliers in the data. In general, the observed meat weights (from observed volumes) should be less than the survey-based, predicted meat weights because the commercially shucked scallops leave some meat on the shell, and because the surveys occur in mid to late summer, a time of typically high meat weight. For both the Mid-Atlantic and Georges Bank, however, there were months of the year where the observed scallop meats were heavier than the predicted meats. In the Mid-Atlantic, peak meat weight occurred in April through August (Figure 1), while on Georges Bank peak meat weight occurred in June (Figure 2).

There are differences in the month in which peak meat weight occurs over the years of the study (Figures 3 and 4). Peak meat weight appears to have occurred earlier during recent years, though the time series is too short and there are too few observations to provide precise estimates of seasonal patterns on an annual basis. The typical seasonal pattern is therefore used in calculating anomalies for all years.

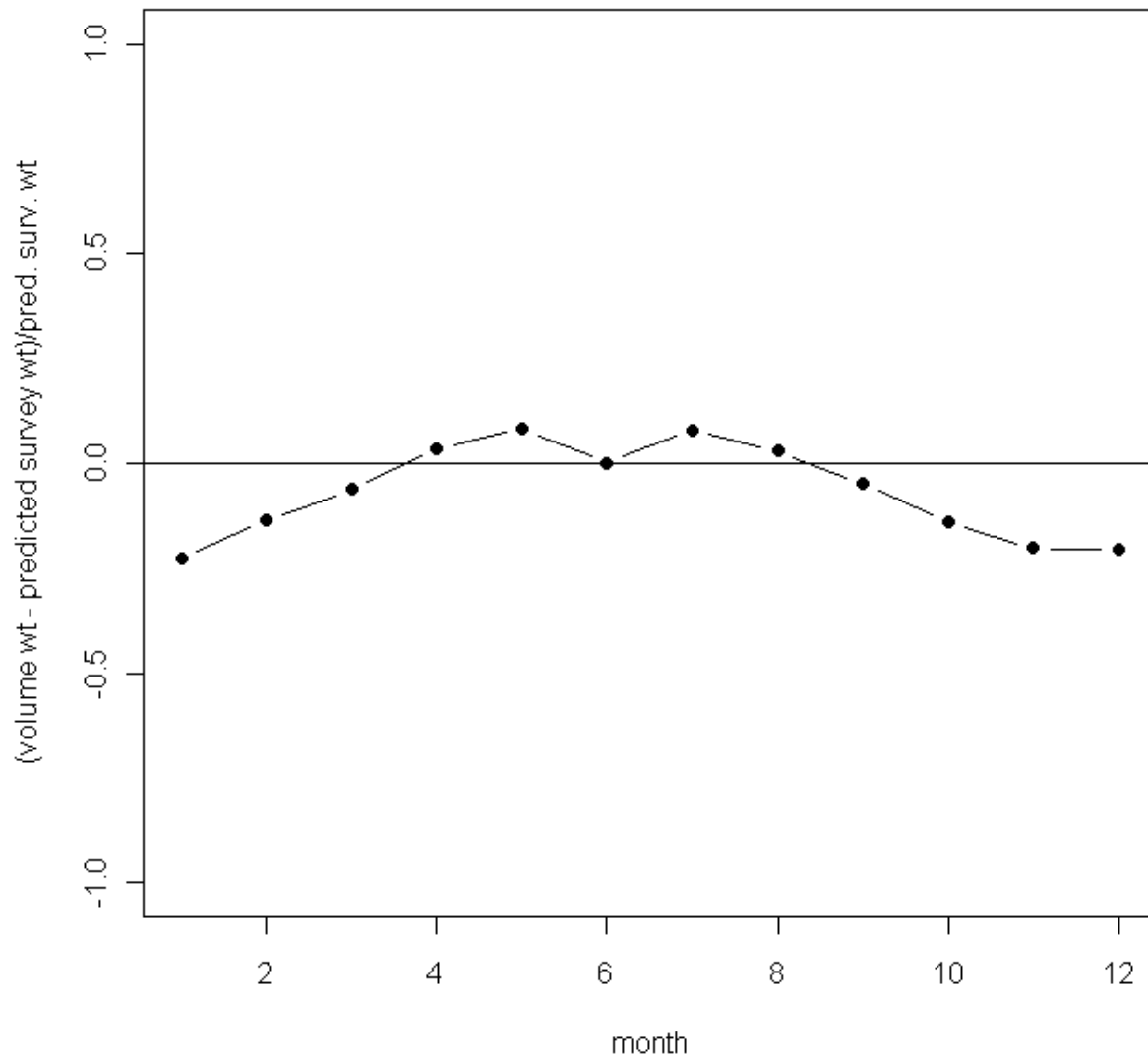
Median meat weight anomalies for 2003-2008 were smoothed by a second order polynomial loess function with a span of 0.25 (months). This short smoothing span provided a modest smooth that allowed the data to strongly influence the model fit (Figures 5 and 6). The smooth was applied to a duplicated annual cycle (i.e. 24 months were fit, using identical data in each 12 month period) and the middle 12 months were selected and reordered so that January was the first month in the resulting model fit. This manipulation guaranteed that December and January produced linking estimates. The smoothed monthly anomalies were then weighted by the landings in each month in each year for which we have landings data (1975 – 2008) and annual median values were calculated.

Updated annual meat weight anomalies differ from those in the last assessment (Figures 7 and 8). The updated anomalies are generally higher in the MAB (~7% higher on average) and lower in the GBK (~8% lower on average). In MAB the differences are due to new observer data which reflect an increase in meat weights during 2007-2008 (Figure 9). In GBK, 2007 and 2008 had relatively heavy survey meat weights (Figure 11). These two years are 40% of the years considered in this analysis. Therefore the meat weight trends in recent survey years are influential.

Literature Cited

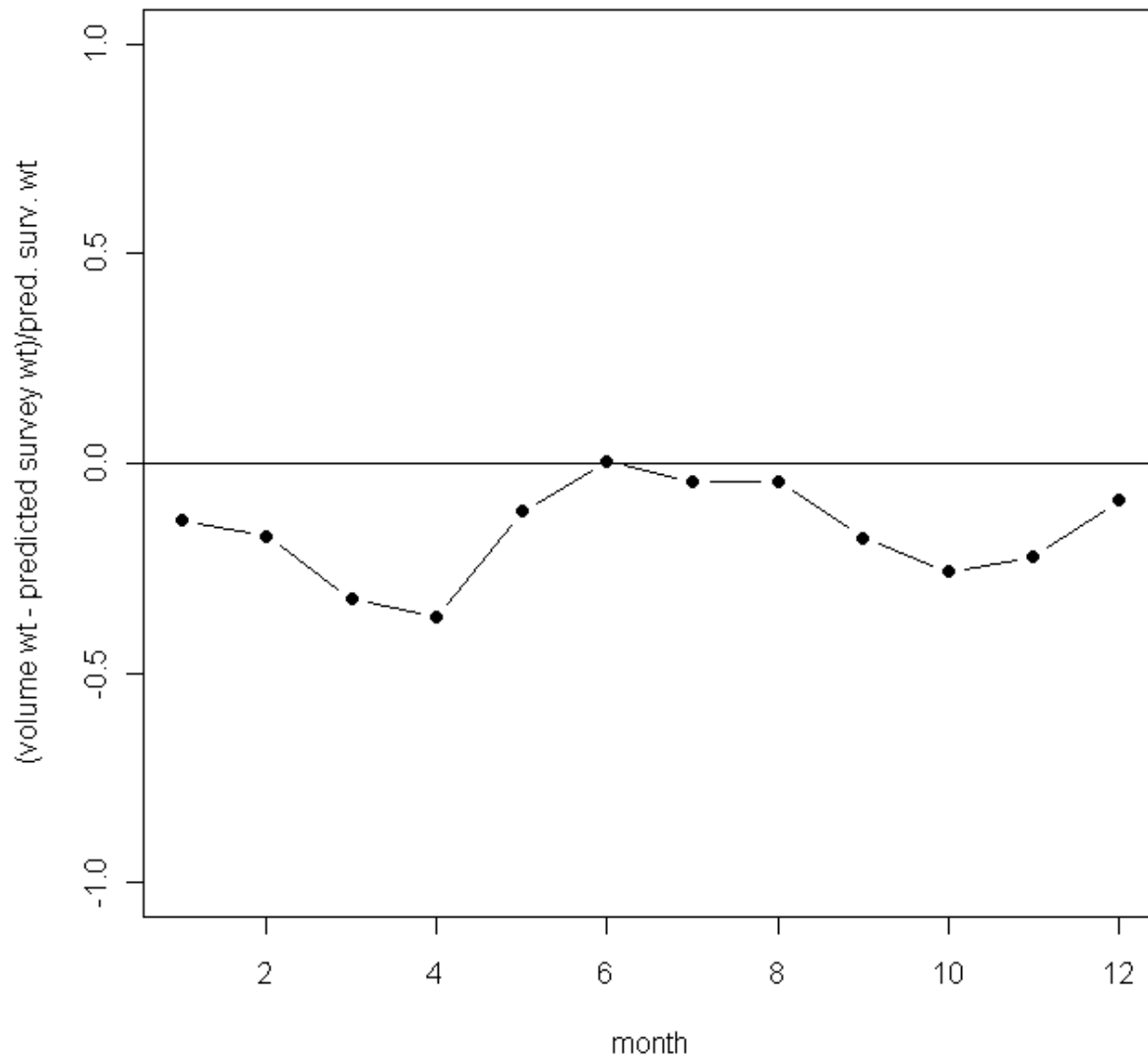
- Caddy, J.F. and C. Radley-Walters. 1972. Estimating count per pound of scallop meats by volumetric measurement. Fish. Res. Brd. Can. Man. Rep. Ser. 1202.
- Smolowitz, R.J., F.M. Serchuk and R.J. Reidman. 1989. The use of a volumetric measure for determining sea scallop meat count. NOAA Tech. Mem. F/NER-1.

Median proportional difference in survey to obs. meat weights



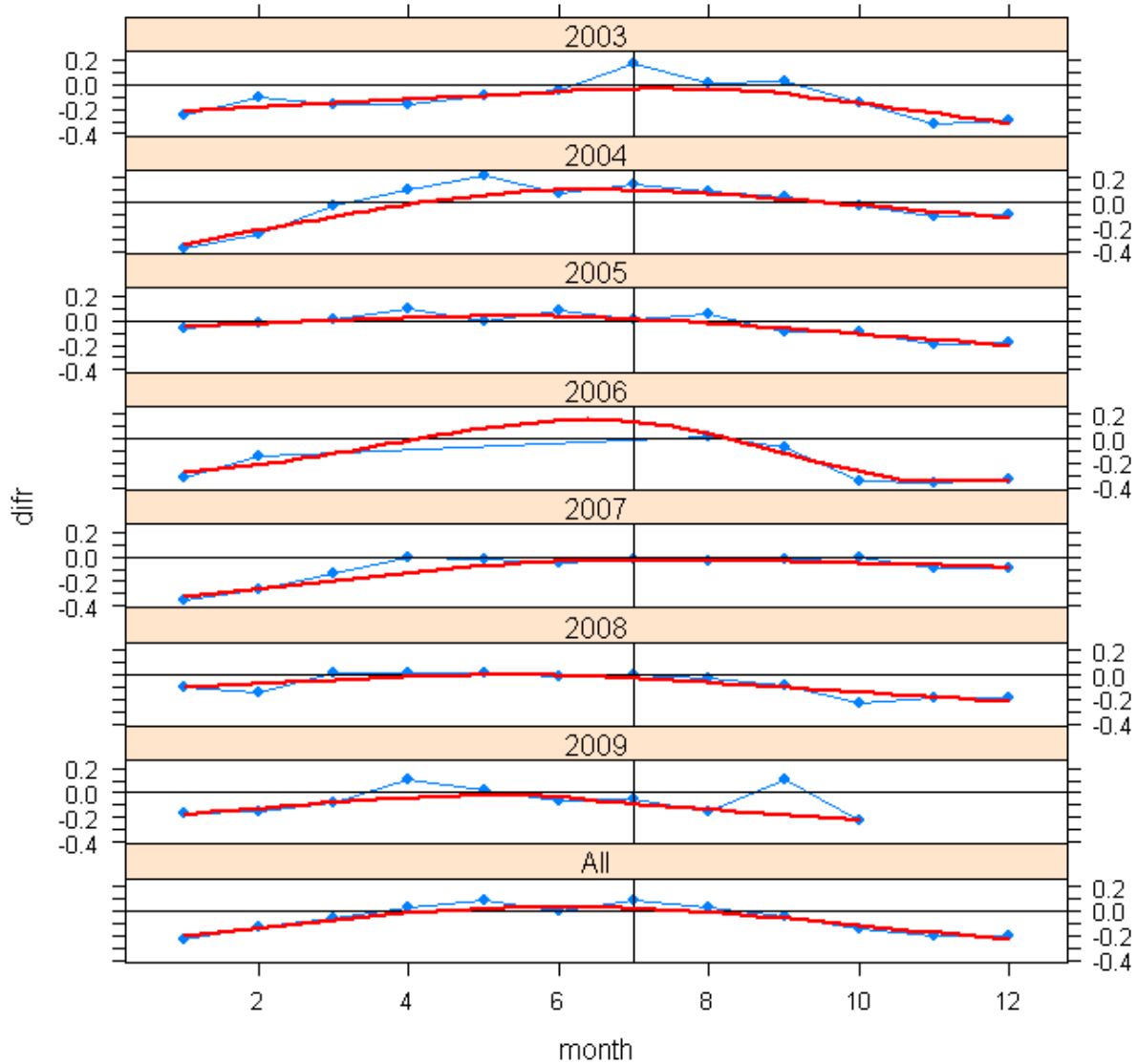
Appendix B8-Figure 1. Meat weight anomalies by month for the Mid-Atlantic Bight.

Median proportional difference in survey to obs. meat weights



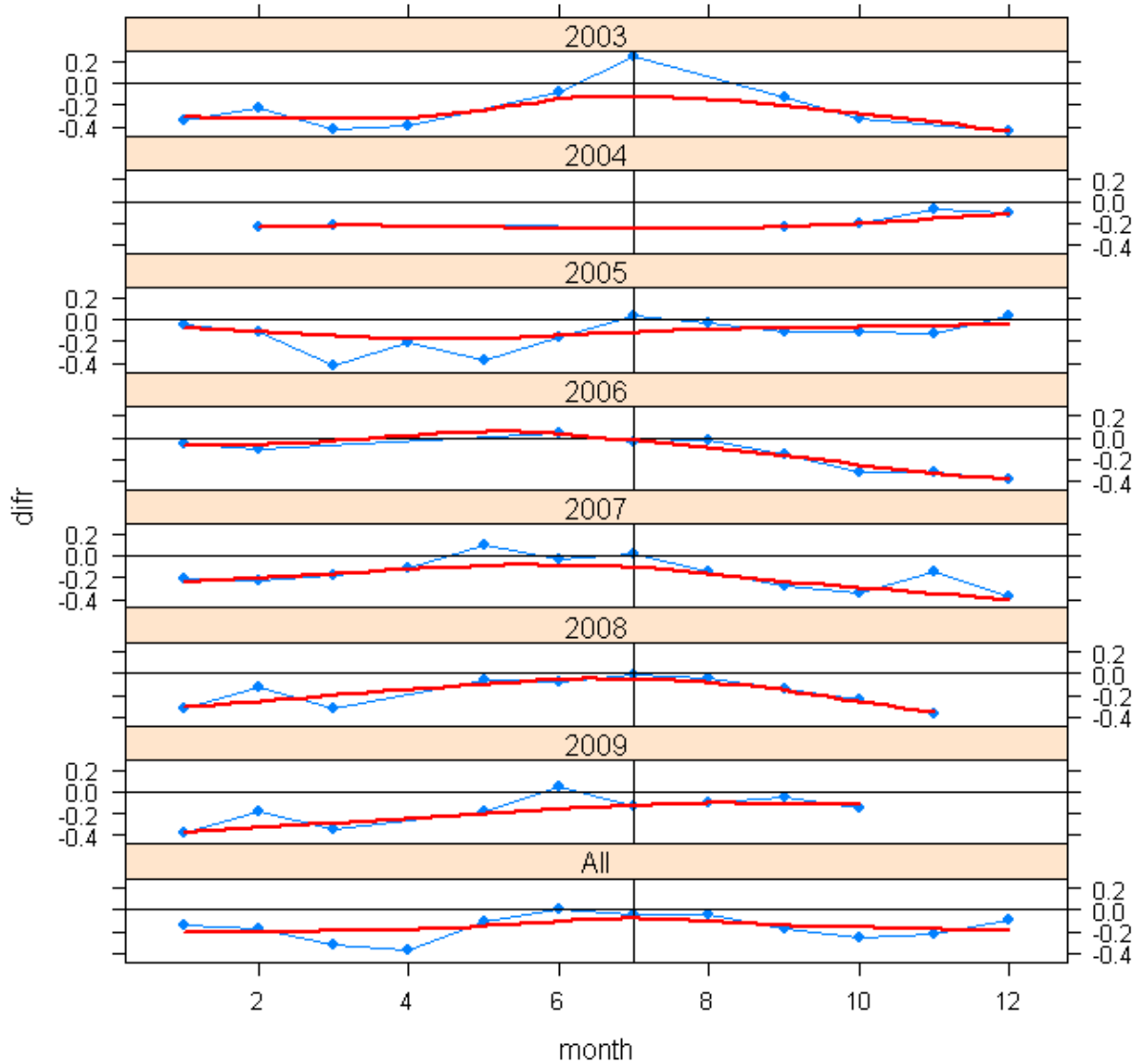
Appendix B8-Figure 2. Meat weight anomalies by month for Georges Bank.

Med. proportional diff. in surv. to obs. meat wt. by year

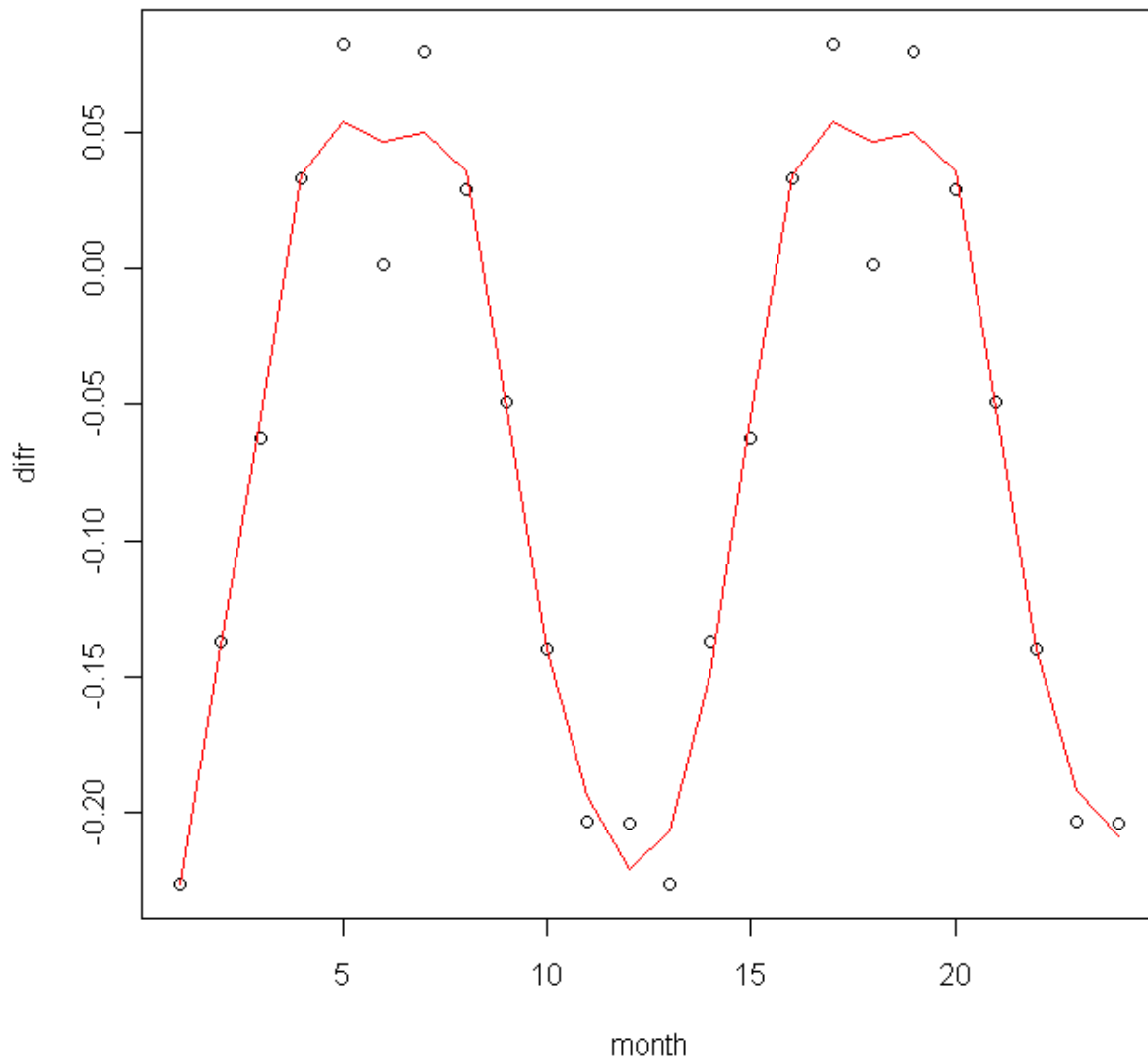


Appendix B8-Figure 3. Observer predicted meat weights (based on volume) compared to meat weights predicted by a model based survey data, by month, year, and overall, from the Mid-Atlantic. The red line is a loess regression and is used only to illustrate seasonal trends.

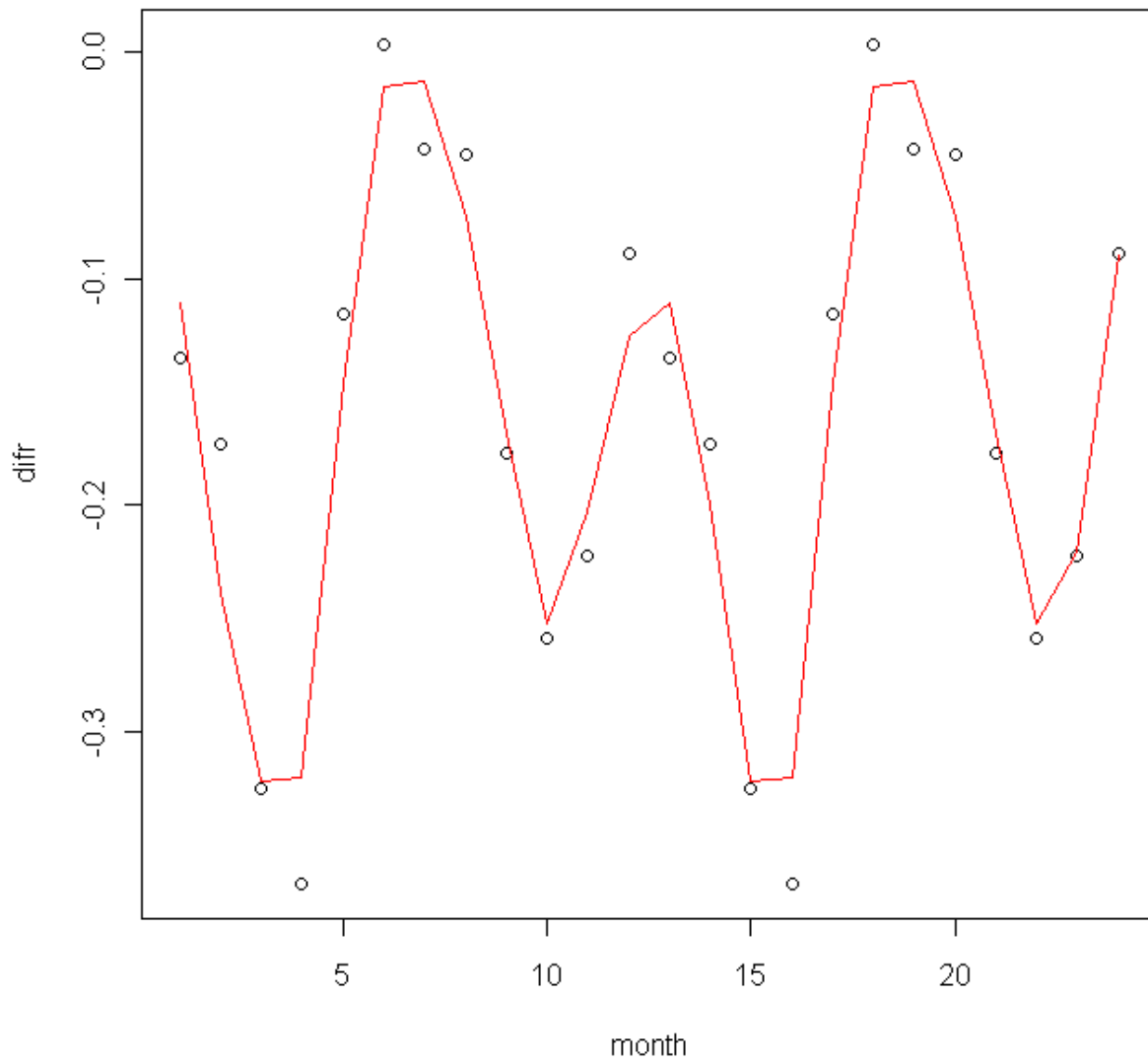
Med. proportional diff. in surv. to obs. meat wt. by year



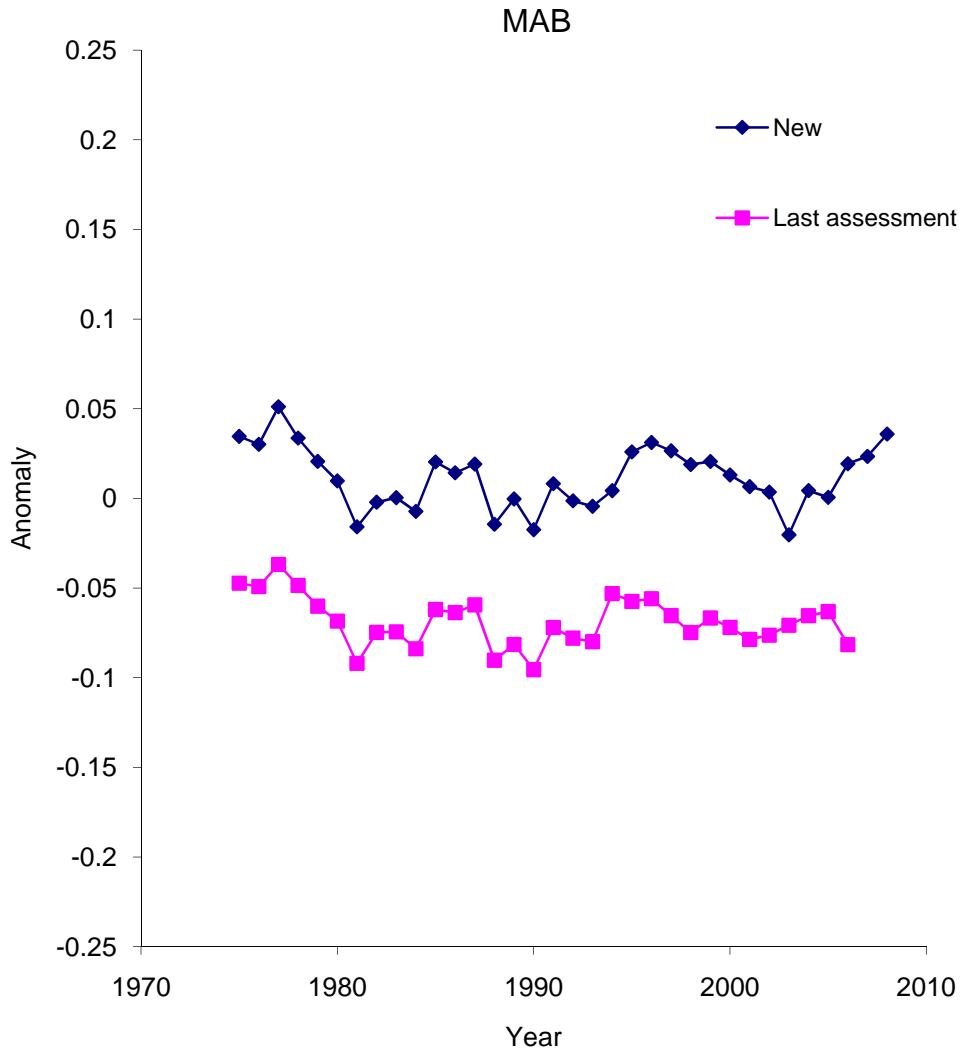
Appendix B8-Figure 4. Observer predicted meat weights (based on volume) compared to meat weights predicted by a model based on survey data, by month, in each year, and overall, from Georges Bank. The red line is a loess regression and is used only to illustrate seasonal trends.



Appendix B8-Figure 5. Smoothed meat weight anomalies by month in the MAB.

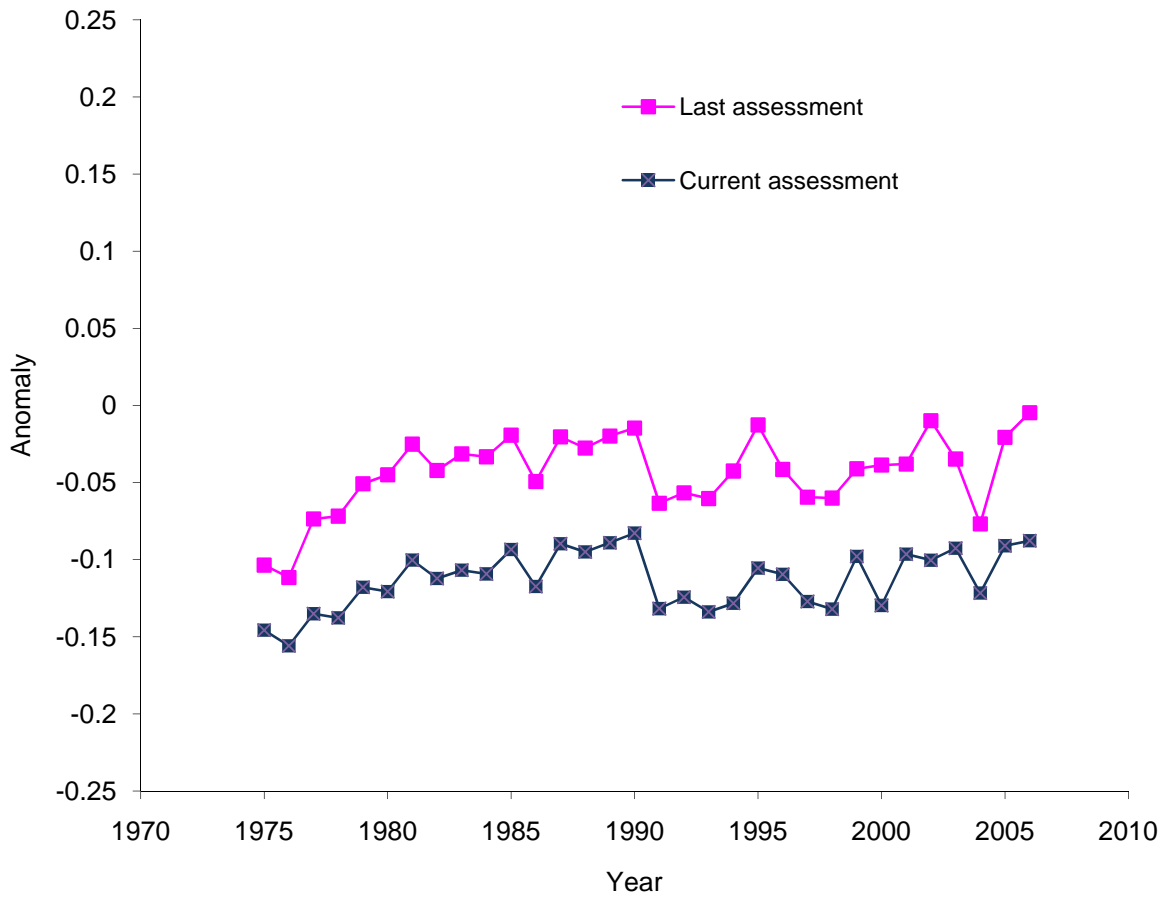


Appendix B8-Figure 6. Smoothed meat weight anomalies by month in the MAB.



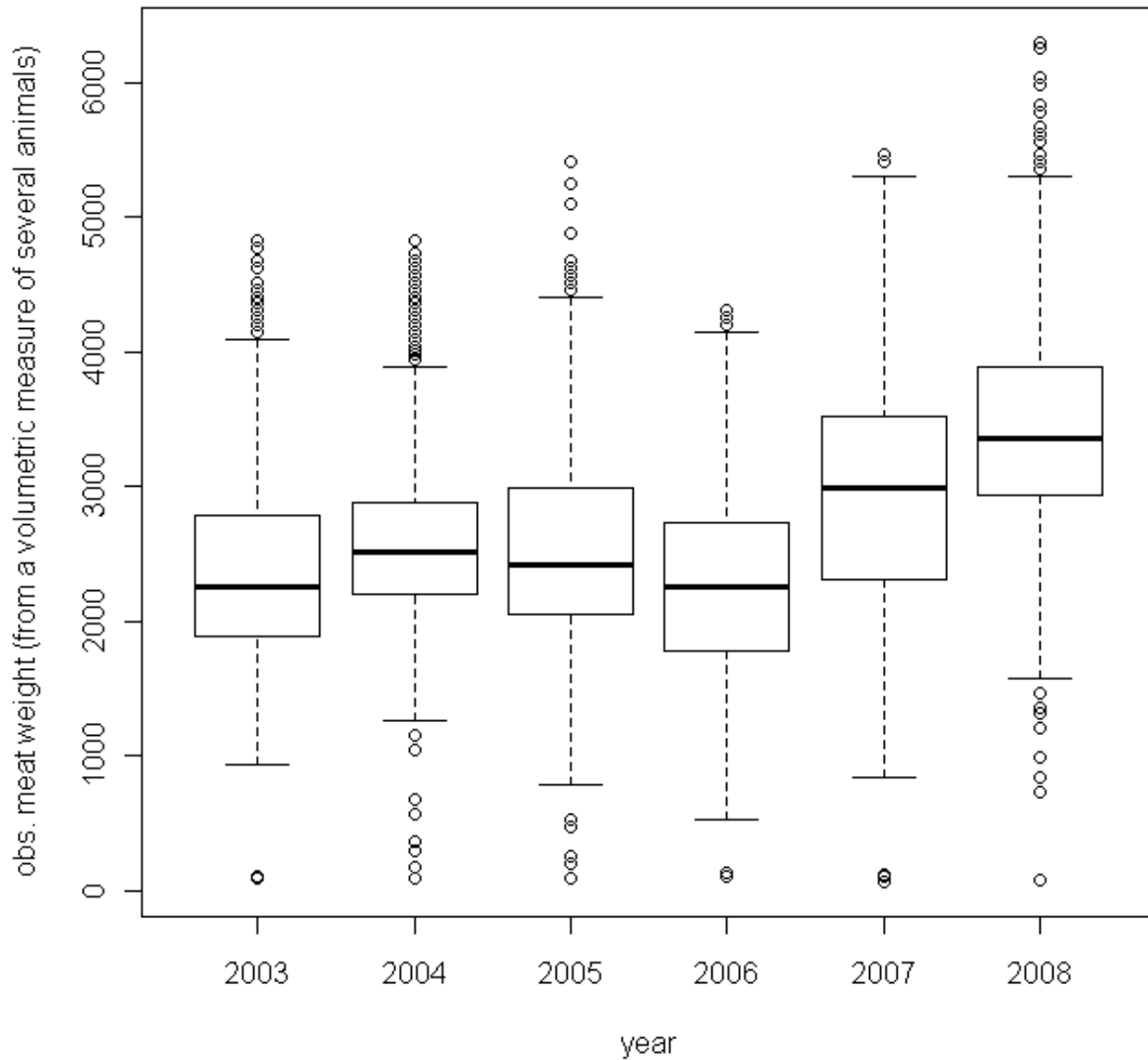
Appendix B8-Figure 7. A comparison between the meat weight anomaly (smoothed and weighted by landings in each month) by year, as calculated in the last assessment and the current meat weight anomaly in the MAB.

GBK

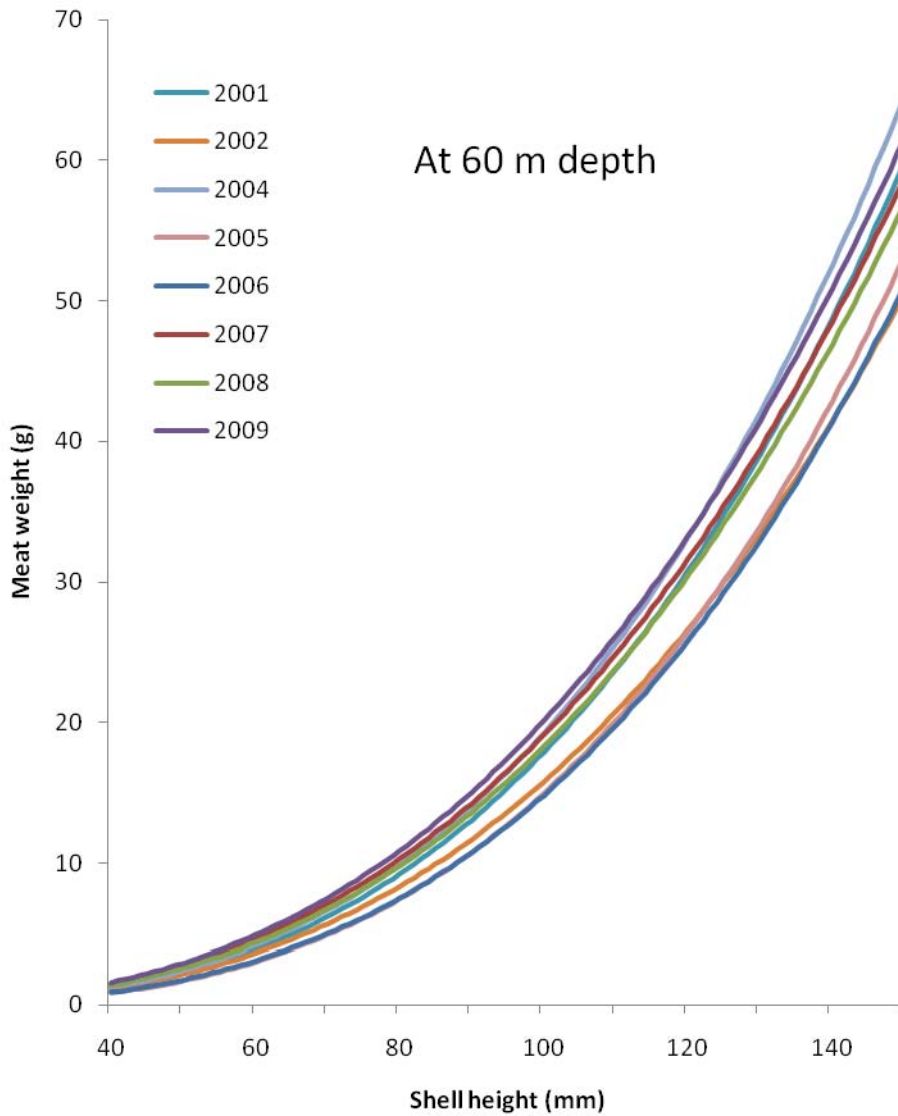


Appendix B8-Figure 8. A comparison between the meat weight anomaly (smoothed and weighted by landings in each month) by year, as calculated in the last assessment and the current meat weight anomaly in the GBK.

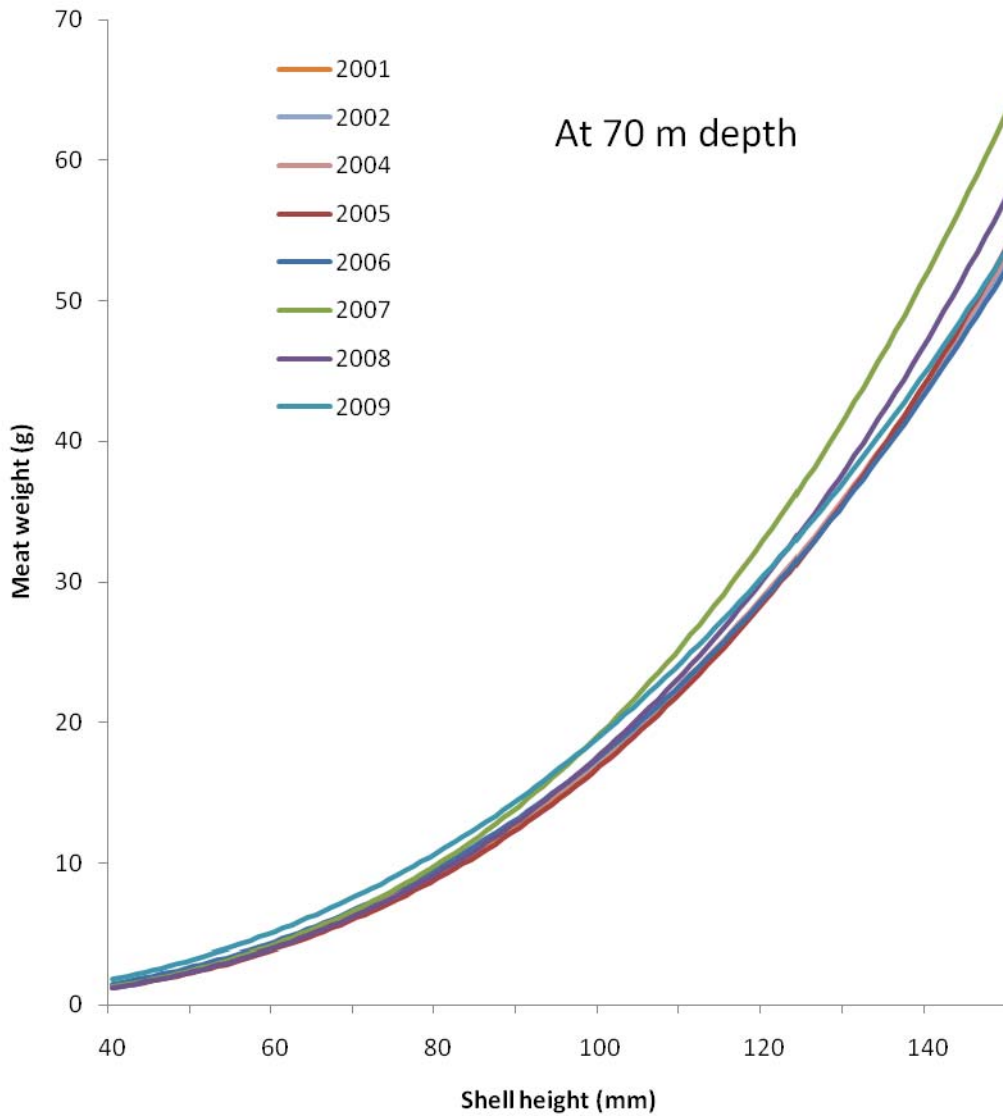
Median meat weight by year



Appendix B8-Figure 9. The observed meat weight in the commercial catch by year. Observed meat weights are based on a simple density conversion of the volume of approximately 100 commercially shucked meats.



Appendix B8-Figure 10. Shell height/meat weight relationships for each survey year at 60 m depth in the Mid-Atlantic Bight ($W = e^{(\alpha+a(St)+\beta \ln(L)+\gamma \ln(D))+\epsilon}$).



Appendix B8-Figure 11. Shell height-meat weight relationships by survey year at 70 m depth on Georges Bank ($W=e^{(\alpha+a(St)+\beta \ln(L)+\gamma \ln(D)+b(L_{St}))+\epsilon}$).

Appendix B9: Summary of HabCam survey results for sea scallops and yellowtail flounder in the Nantucket Lightship Closed Area during 2009

The HabCam Group

Scott M. Gallager^{1, 2}, Amber D. York^{1, 2}

Richard Taylor^{2, 3}, Norman Vine²

Jonathan Howland¹, Steve Lerner¹

Karen Bolles^{3, 4}

(1) Woods Hole Oceanographic Institution

(2) Advanced Habitat Imaging Consortium

(3) Arnie's Fisheries, New Bedford, MA

(4) Ocean Explorium, New Bedford, MA

Conclusions

HabCam is a cabled optical and acoustic imaging system that is “flown” from a ship traveling at 5 kn at an altitude of 1 to 3 meters off the bottom while collecting high resolution still images at a rate of six images per second. Imaging rate provides ~50% overlap to allow for construction of image mosaics of the seafloor. A track approximately 100 nautical miles in length and 259,200 m² in area is imaged each 24 hour day while at sea. When operating continuously, HabCam samples nearly 2.5 times the area covered by a survey dredge.

Manual classification of the images provides the following information: 1) counts and measurements on sea scallops and groundfish (i.e. cod, haddock, flounders), epibenthic megafauna and many benthic infaunal species; 2) characterization of substrate; 3) observations on animal behaviors, inter- and intra-species interactions, biodiversity and community structure; 4) the ability to assess and monitor invasive species; 5) the tools to characterize oceanic properties (salinity, temperature, nutrients); and 6) the means to “map” the location of lost fishing gear (e.g. trawl and gillnets, lobster pots, and other miscellaneous fishing gear and parts). Automated methods for target classification are currently under development and will provide tools to reprocess archived results of image surveys as new technologies are developed.

Here we report on use of the HabCam camera system to: (1) conduct sea scallop surveys in the Nantucket Lightship Closed Area (NLSCA) as part of an effort to compare sampling technologies, (2) conduct dredge calibration with NOAA/NMFS vessels, and (3) conduct an analysis of inherent errors in camera calibration, scallop abundance estimates, and shell height measurements.

The objectives of the 2009 NLSCA survey were to estimate scallop abundance, shell height frequency distribution and biomass, and to estimate the distribution and abundance of yellowtail flounder in relation to substrate. A survey track line was designed as a modified spiral with track spacing from 2.6 to 1.3 nm. Total track line length was 348 nm with 1,235,251 images collected. Every 10th image was processed for a total of 123,000 images resulting in a total area covered of 0.187 nm² or 0.57% of the NLSCA. The density of scallops along survey tracks ranged between 0 and 23 scallops/m² with dense aggregations occurring at patch scales of about 400 and 900m. The raw values for scallop abundance on a per image basis were interpolated across the closed area using ordinary kriging. Total number of scallops in the NLSCA was 197,545,580. The overall mean for the closed area was 0.187 scallops/m² with a CV of 0.04.

Variance between cells ranged between 0.5, where the sampling density was highest, to over 0.7 where the sampling density was lower. A simple, alternative method to kriging for calculating total scallop counts is to multiply the mean abundance by the area. Our results using this approach is $0.187 \text{ scallops/m}^2 \times 1,142,280,000 \text{ m}^2 = 213,606,360$ scallops with a CV of 0.034, which is similar to the value estimated by kriging. Mean biomass per scallop was 32.9 g. Scallop meat biomass estimated by kriging in the closed area was 6,782 MT.

The HabCam system may be useful for mobile demersal fish, such as yellowtail flounder, in addition to sessile organisms. In the NLSCA, 124 observations of yellowtail flounder were made with the densest concentration in the central region. This region was also characterized by being mostly sand with patches of gravel. The most abundant aggregations of yellowtail were observed in the Southeast Part of CLAI and on the Canadian side with densities exceeding 0.14 fish/m^2 .

Since 2007, joint tows between the NMFS annual dredge survey and HabCam have been designed to compare scallop abundances and size estimates from the standard federal dredge survey with those derived from HabCam. HabCam estimates of scallop abundance were consistently greater than those for the dredge. Mean shell height measurements were similar between dredge and HabCam but the tails of the frequency distribution for HabCam are higher than those for the dredge indicating some inherent measurement error.

In June 2009, in addition to shadowing the Sharp with the Kathy Marie during Legs 1 and 2 of the annual scallop survey, HabCam was towed from the A-frame of the Sharp as part of routine dredge operations on Leg 3. Regression slopes between dredge and HabCam scallop abundances were 0.34 for Georges Bank stations and 0.46 for Mid Atlantic Bight stations. When the data are broken out by substrate regardless of region, the regression slope for sand was 0.35. For sand plus other substrate types such as shell hash the slope was 0.40 and on gravel it was 0.35. These results are a simple measure of the sampling efficiency of the dredge relative to HabCam but are biased low: see Appendix X for an unbiased approach. Results (dredge sampling efficiencies for sea scallops ~ 0.3 to 0.45) are similar to results from other studies. Moreover, they illustrate the potential for use of HabCam in directly estimating the sampling efficiency of other types of survey and fishing gear.

Errors associated with camera calibration and manual measurement of scallop shells on the computer screen were assessed. Camera resolution depends on altitude off the bottom and ranges between $0.37 - 0.89 \text{ mm/pixel}$. Following camera calibration intrinsic pixel error was ± 1.59 pixels resulting in a real-world error of $0.58 - 1.41 \text{ mm}$. Extrinsic errors associated with geometric projection of the image plane on the seafloor, taking into account of vehicle roll, pitch, and changes in altitude, produces real-world errors of $1.11 - 1.78 \text{ mm}$ under optimal water quality conditions in a test tank.

To estimate the level of error associated with manual screen measurement of scallops both within and between a given technician, we assigned four identical 4.2 nm long image transects containing 4,432 images from Western Great South Channel to four technicians. In most cases, the mean shell height within technician measurements were either accurate to the same number of pixels or within one pixel suggesting that within technician variability was extremely low. However, between technician variability was greater with an overall error ranging ± 4 pixels, which represents a real-world error of 3.0 to 7.1 mm . Therefore, measurement errors of scallop shell height are dominated by human extraction of data from the images.

Introduction

There is a great need in fisheries science to develop and utilize new tools and technologies that could help improve the assessment and management of our national marine resources. Coupled with this is a major change in approach from single species to ecosystem based management. The HabCam system was developed to move toward these goals.

HabCam is a seafloor imaging camera system mounted in a ten foot steel frame, and towed at about five knots 1 to 3 m off the ocean floor. HabCam is normally towed behind the F/V Kathy Marie, a New Bedford sea scallop vessel and can operate over the range of the continental shelf, 20 to 250 m depth. The HabCam Group consists of independent researchers, Woods Hole Oceanographic Institution engineers and scientists, and fishermen. HabCam was initially designed and constructed with funding from the Northeast Consortium with major improvements made with funding from the Scallop Research Set Aside Program. The initial goal of the HabCam project was to help improve sea scallop stock assessments by increasing the accuracy of scallop biomass estimates. Additional funding from the NOAA Integrated Ocean Observing Systems (IOOS) Program to support the Northeast Benthic-pelagic Observatory (NEBO) has greatly expanded the range of uses of the HabCam instrument. For example, small study areas have been revisited seasonally providing the baseline of an ecological time series.

Attributes of the HabCam system include: 1) acquisition of optical and acoustic imagery which can be viewed in “real time”, 2) the ability to count and measure scallops and groundfish (i.e. cod, haddock, flounders), 3) measurement of biodiversity and community structure, 4) the means to “map” where there are lost fishing gears (e.g. trawl and gillnets, lobster pots, and other miscellaneous fishing gear and parts), 5) characterization of substrate 6) measurement of oceanic properties (salinity, temperature, nutrients) 7) availability of data and data products online, and 8) relatively inexpensive operating costs. The HabCam system also has the ability to observe animal behaviors including inter- and intraspecies interactions as well as assess and monitor invasive species such as *Didemnum vexillum* and other epibenthic megafauna, and benthic infaunal species.

A historic record of images will be beneficial to understanding patterns, particularly in the implementation of ecosystem management schema. Further, because of direct industry participation, it may help to raise the confidence of the industry in stock assessment methods, monitoring capabilities, and management of our fisheries resources. The Habcam Group has also developed education activities and participated in various outreach projects. The group is currently collaborating with The Ocean Explorium, an education center and aquarium located in New Bedford, Massachusetts and local science teachers and educators.

Methods and Results

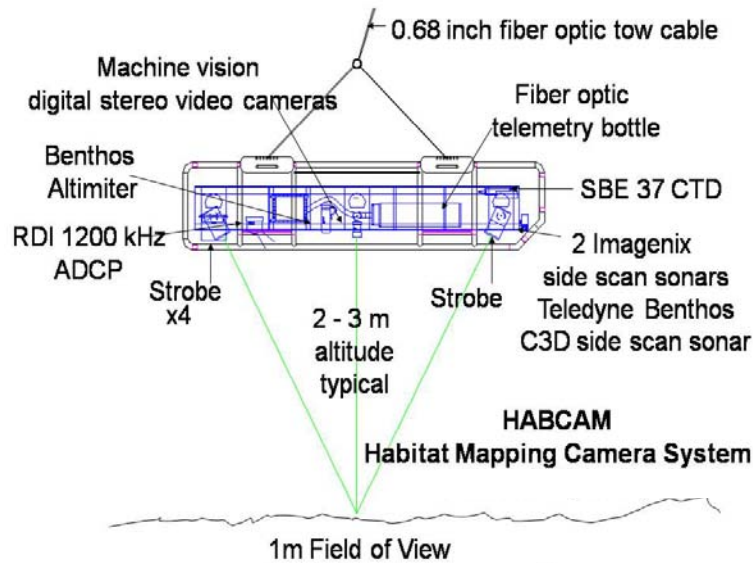
Onboard sensors include a high resolution machine vision GigE color camera, four xenon strobes, side scan sonar, CTD with temperature, salinity, chlorophyll, turbidity, and pH, and a variety of engineering sensors including vehicle roll, pitch, and heading (Fig. 1). All sensors are networked subsea and data transferred via a GigE network to the surface so that data are collected and sent to the ship in real-time where they are recorded, time stamped, and stored.

The HabCam imaging system is “flown” by an operator who controls the winch keeping the vehicle 1.5 to 3 meters off bottom while being towed at 4 to 5 knots (~2.5 m/sec). A track approximately 100 nautical miles is imaged each 24 hour day while at sea. Optical imagery is

collected at a width of approximately 1 to 1.25 meters (total ~200,000 m² /24 hr day). Images (1280x1024 pixels, 16 Bit) are acquired at 5-6 Hz providing a minimum of 50% overlap between images. Images are processed in real-time on the ship by color correcting raw 16 bit tiff images and converting them to 24 bit jpegs (Fig 2). Figure 2 represents a combination of existing data structures and what we envision as fully operational database.

The current NEFSC survey dredge is 8' wide dredge makes approximately 24, 15 min tows at 3.8 kt per day, covering about 4,500 m² per tow and 106,704 m²/day. Continuous operations with HabCam towing at 5 kt and producing 5 images per second with 50% overlap covers 259,200 m²/day. Thus, the spatial coverage of HabCam is nearly 2.5 times the area covered by the survey dredge.

We have implemented two simultaneous and complementary forms of image informatics

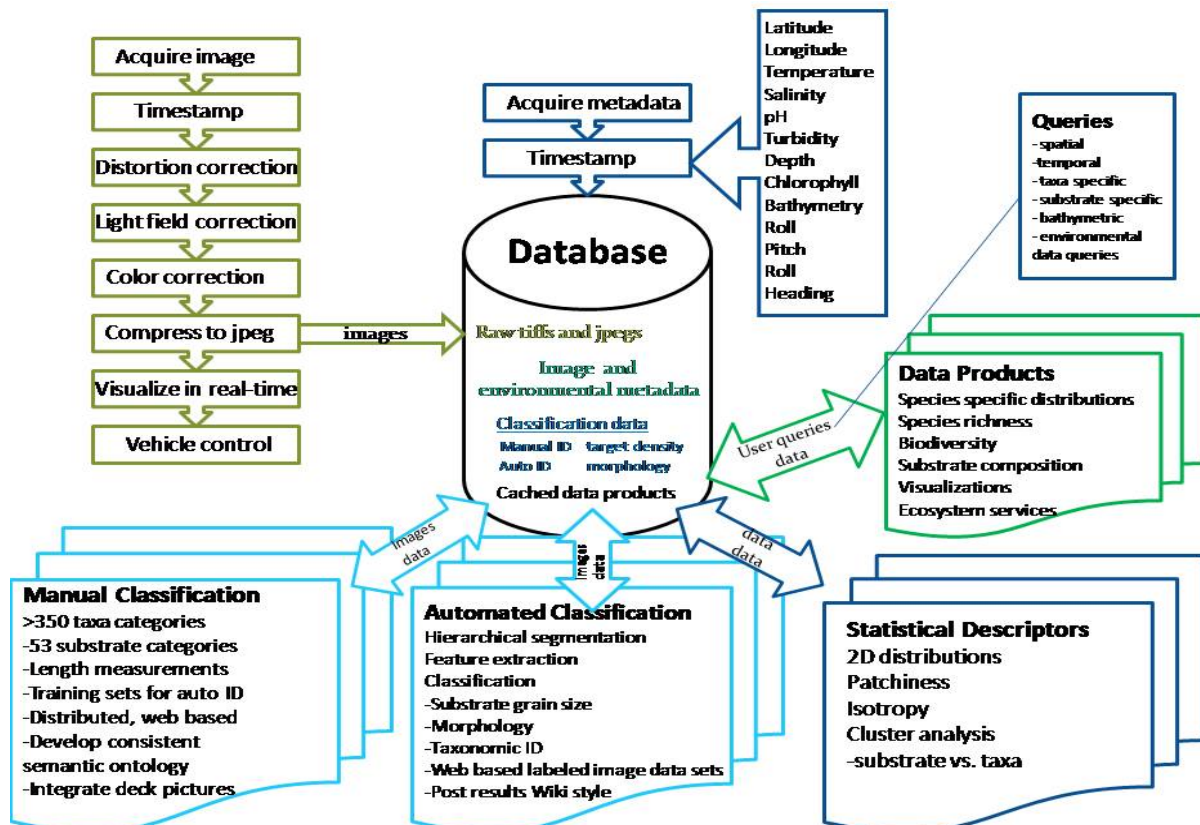


Appendix B9-Figure 1. The HabCam vehicle is towed on 0.68" fiber optic cable ~ 1.5-3 m from the bottom. The camera provides a field of view of 0.5-2 m². Four strobes flash synchronously with each image. Ancillary sensors include side scan acoustics, CTD, chlorophyll fluorometer, and CDOM fluorometer.

(i.e., extracting information from images): manual and automated classification. Manual

classification proceeds by having one or more operators review individual, or sets of, images to identify and measure target species using a GUI with point and click functionality. This allows about 60 to 200 images per hour per operator to be processed depending on image complexity and number of individual species being identified.

More than 460 taxa or taxonomic groups ranging in size between ~1 mm to 2 m have been observed and identified with HabCam. While taxonomic definitions used in image analysis are based on epibenthic organisms, a variety of infauna can typically be observed and quantified such as bivalve siphons, turbularian worms, burrowing shrimp, and some vertebrates (e.g., tilefish and their burrows). During manual operations, the operator also evaluates the substrate type in each image and categorizes it into one of 43 groups ranging from silt, sand, gravel, shell, cobble, boulder, and a variety of combinations. Development of approaches for automated



Appendix B9-Figure 2. Future iterations of the HabCam data workflow environment. Images and associated metadata enter the processing path from the left. Following preliminary image processing steps conducted in real-time (e.g., color correction), images are viewed and classified by scientists onboard. Results are entered into the database and used as training sets for automated classifiers. The database may be queried both spatially and temporally to build a set of data products shown on the right.

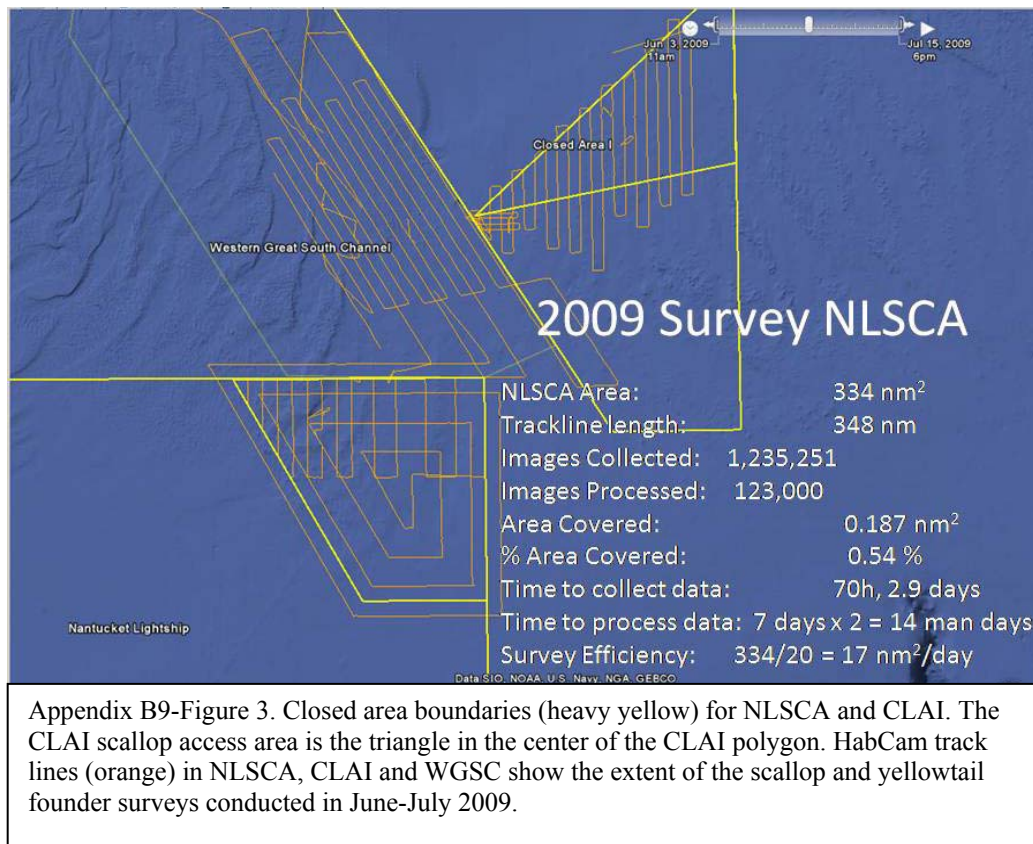
classification of targets and substrate is proceeding using the manually classified images as training sets. This is an area of ongoing research.

For the purpose of the scallop surveys reported here, images were classified manually by several technicians, who characterized substrate into the categories noted above and measured all scallops and groundfish, including yellowtail flounder. To speed the process, every 10th image was analyzed. Rationale for this strategy is discussed in the following sections.

2009 Nantucket Lightship Closed Area (NLSCA)

The objectives were to estimate scallop abundance, biomass, and shell height composition in the NLSCA using the data collected. A secondary objective was to estimate the distribution and abundance of yellowtail flounder in relation to substrate. The area of NLSCA is 334 nm². Total track line length was 348 nm with 1,235,251 images collected. A total of 123,000 images were processed for a total area covered of 0.187 nm². Total area sampled by HabCam was 0.57% of the NLSCA. The survey required 72 hours of continuous towing and approximately 27 person days to process the data, assuming 12 hour shifts.

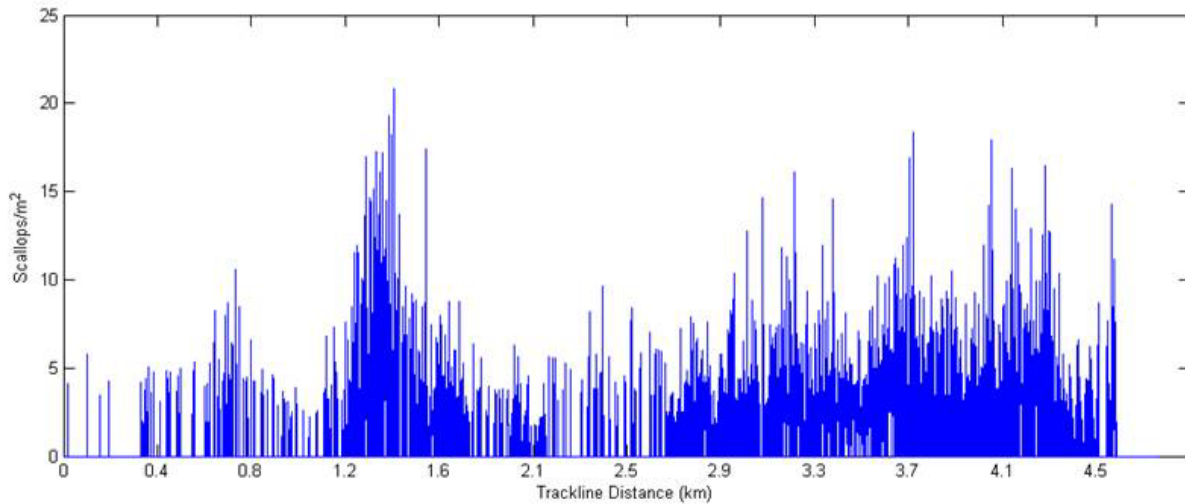
The survey track line was a modified spiral which started 1.3 nm outside the boundary of the closed area to allow interpolation of the final abundances without boundary influences (Fig. 3). The spiral was conducted around the border then continued at an interval of 2.6 nm.



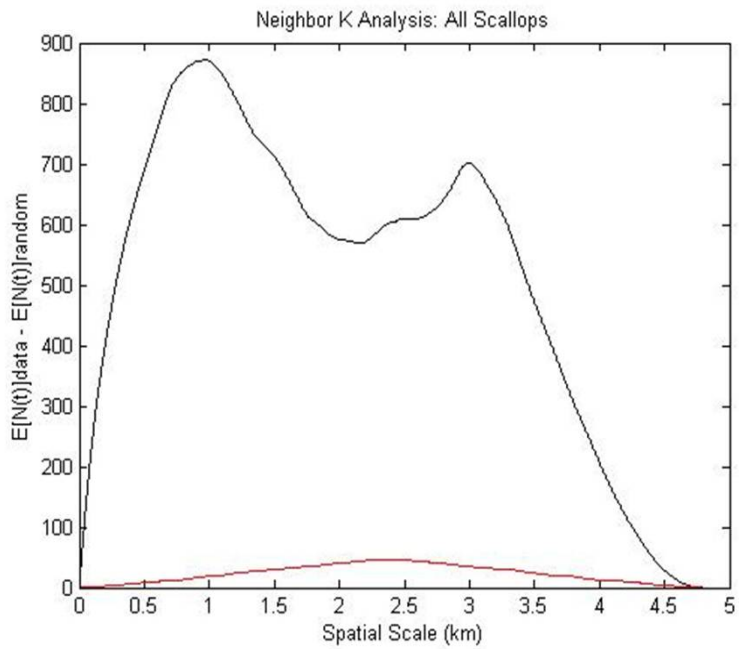
Following completion of the spiral, the vessel steamed to the northeastern corner and began a finer grid extending from the northern edge to the center of the closed area. This finer grid pattern began at an interval of 2.6 nm but compressed to 1.3 nm as the vessel approached the north-central section of the closed area. This was to provide higher resolution where prior knowledge indicated dense scallop abundance.

To assess multi-scale patchiness and to determine how many images should be processed, a preliminary transect from east to west 2 nm in length was processed by manually counting and measuring every other image. This provided information for calculating the appropriate image subsampling rate for processing the remainder of the spiral and for calculating a patchiness index for use in setting appropriate interpolation scales. Images were subsampled for the sake of efficient and fast data processing.

The density of scallops along survey tracks ranged between 0 and 23 scallops/m² (Fig. 4). It appeared that aggregations of scallops at densities between 5 and 20 /m² occurred in clumps at a spatial scale of 400m. Therefore, a Nearest Neighbor-k analysis was performed to establish the dominant spatial scales of patchiness. The Neighbor-k showed strong patchiness ranging from 400 to 900m and again at 3000m (Fig. 5).



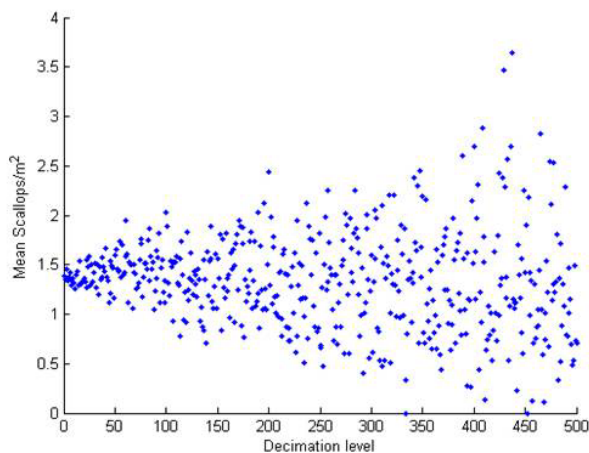
Appendix B9-Figure 4. Scallop abundance in the northern section of the NLSCA survey along a 4.5 km (2 nm) track. Every other image was classified manually to establish a baseline for subsampling and to estimate patchiness. Note the very patchy distribution ranging from 0 to >20 scallops per m².



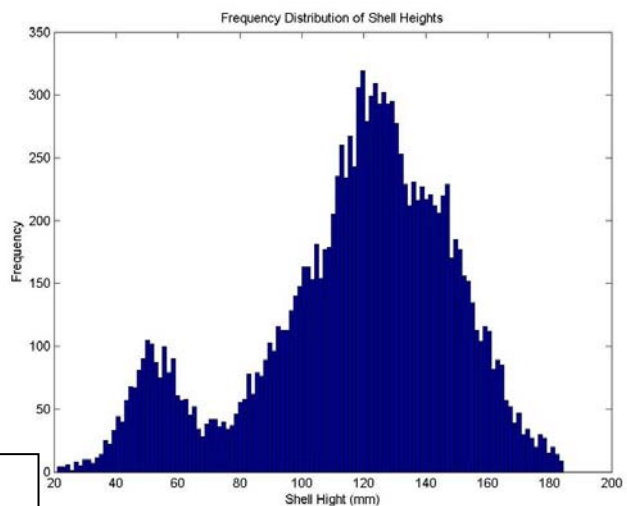
Appendix B9-Figure 5. Ripley's Neighbor-k analysis for one-dimensional patchiness was applied to scallop densities measured along the track (every other image was processed for this analysis). Spatial scale is on the x axis while the residual between observed and predicted nearest neighbor distance under randomness (1000 Monte Carlo simulations) is on the y axis. The first mode indicating a characteristic patch size is located at 700-900 m, and a second at 3.2 km. Both modes are well above the red line under randomness indicating these patch dimensions to be statistically significant at the 95% confidence level.

To determine an optimal image subsampling rate, data from every other image along the track was processed by extracting abundances and calculating the CV for density at sampling intervals ranging from every 4th, 8th, 10th, 12th etc. out to every 500th image. The mean and CV remained stable up to a subsample level of every 10th image. Therefore, the remaining spiral was processed at a rate of every 10th image (Fig. 6).

Over 12,900 scallop shell heights were counted and measured using MIP (Manual Identification Program developed by A.D. York), which allows users to quickly point and click on scallops to extract measurements and select substrate type from a menu. The shell height distribution was strongly bimodal with modes at 53 and 125 mm (Fig. 7). A third, less prominent mode was located at 142 mm.



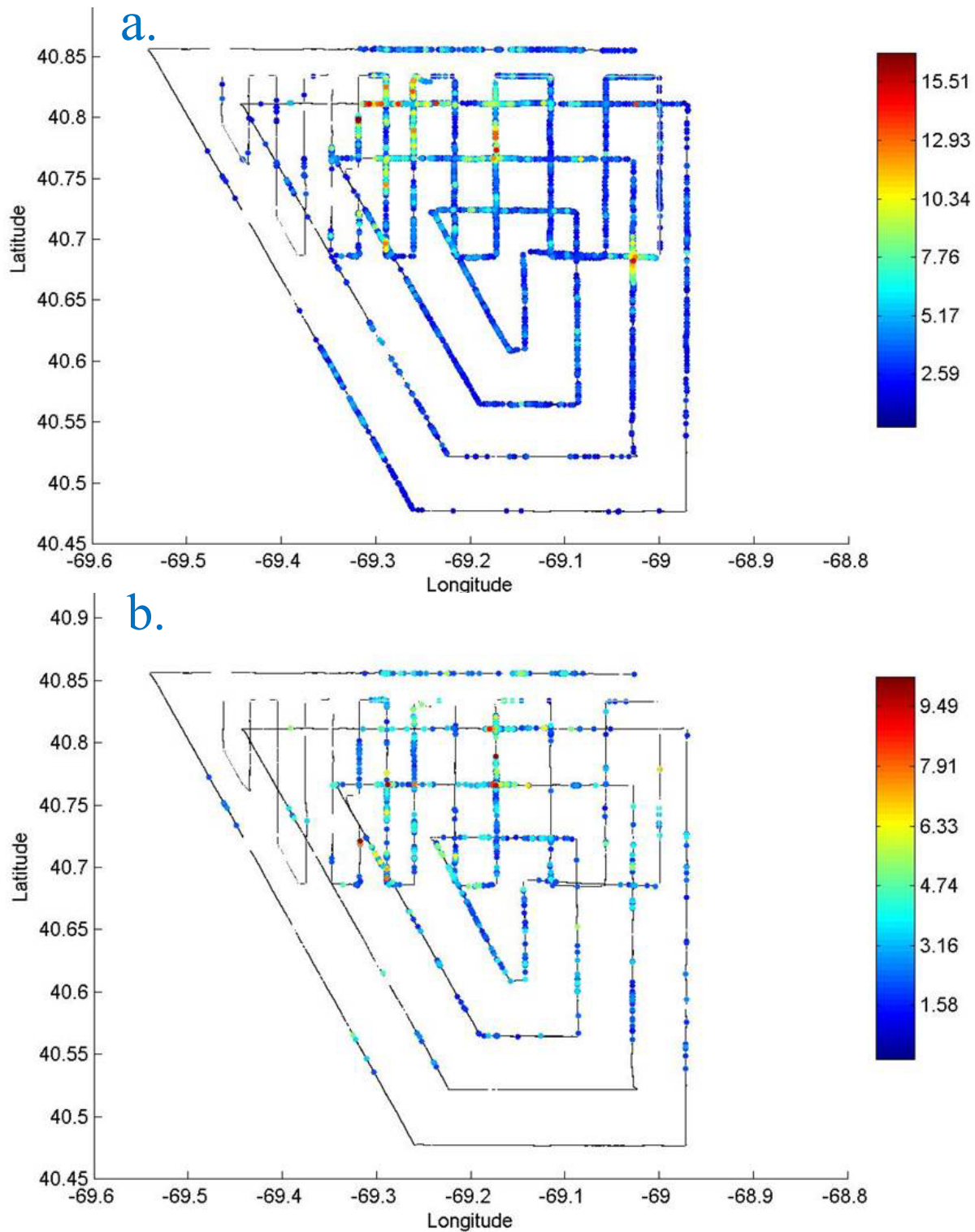
Appendix B9-Figure 6. The effect of subsampling (decimation) the continuous record of scallop abundance along the track line in Figure 3. Images were analyzed at subsampling rates of every 4th, 8th, 10th, 12th... out to 500 and the scallop abundance recalculated. Mean abundance is stable out to a subsampling rate of greater than 20 so a conservative level of processing every 10 image was chosen for the remainder of the analysis.



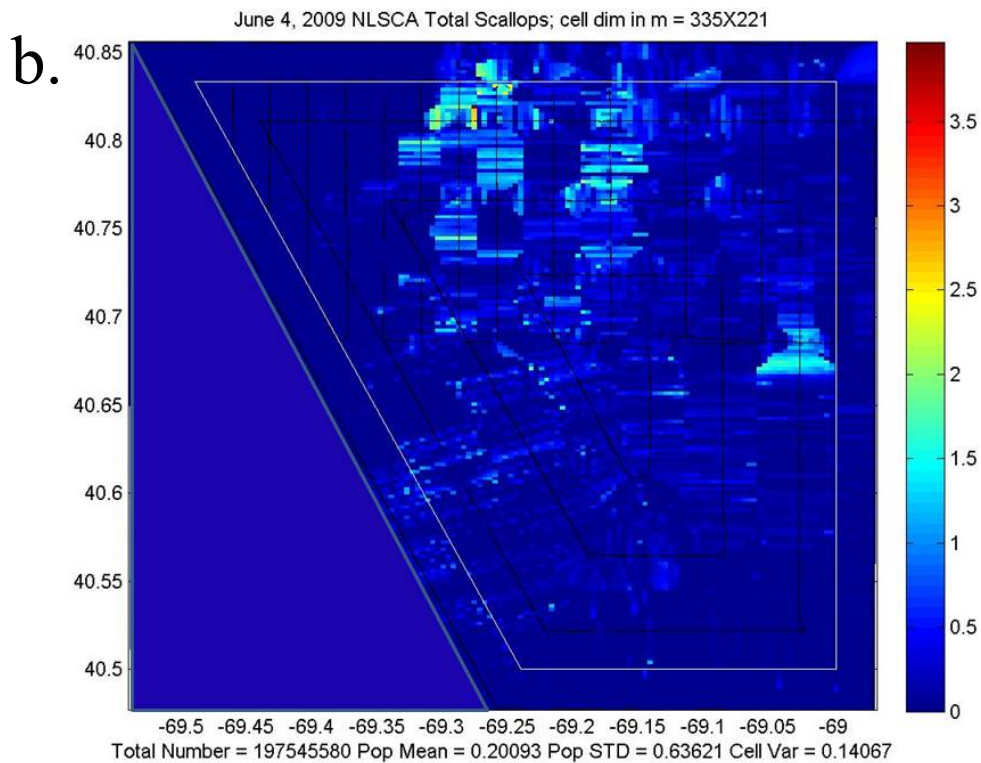
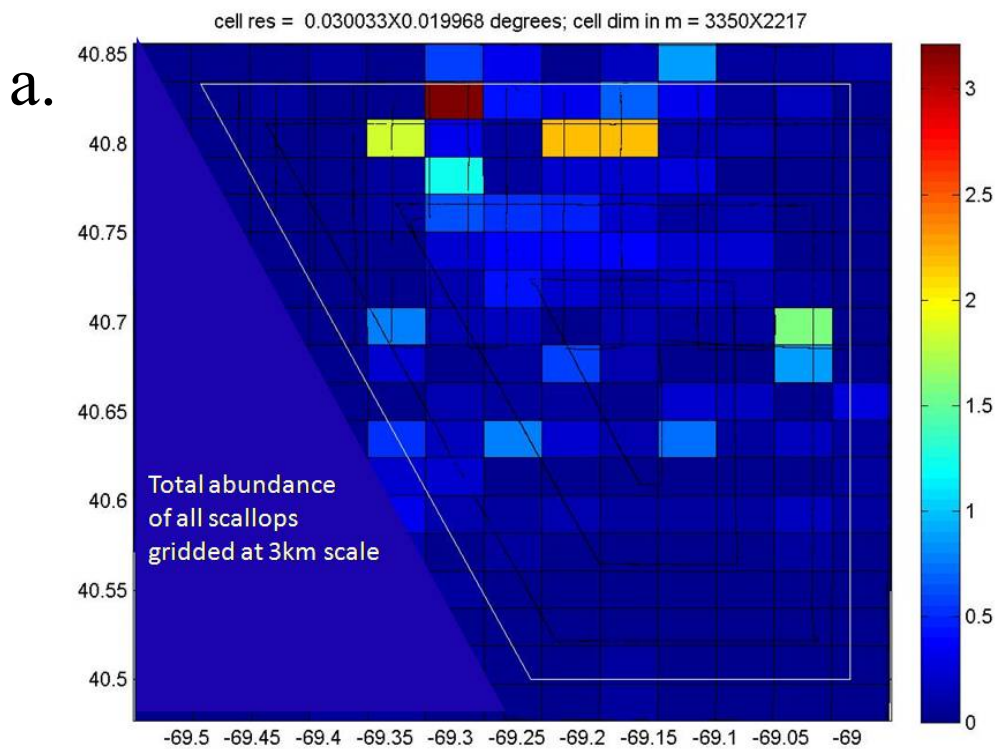
Appendix B9-Figure 7. Shell height frequency distribution for all scallops measured from the NLSCA survey. N=129,237. The shell height distribution was strongly bimodal with modes at 53 and 125 mm with a third, less prominent mode located at 142 mm.

The scallop density from every 10th image plotted as color coded dots for all scallops showed highest aggregations in the central upper third and in the central eastern region of the closed area (Fig. 8a). Scallops were sparse in the northwestern corner and southern regions. A similar plot for just those scallops with shell height between 20 and 65mm showed that small scallops were most abundant in the east central region of the closed area (Fig. 8b).

The raw scallop density per image was interpolated into rectangular grids at two scales using ordinary kriging based on cells of 3350x2217m and 335x221m. First, a semi-variogram was constructed to evaluate autocorrelation of the data. For the coarse and fine scales, the mean for each grid cell was color coded (Fig. 9a, b). Total abundance, mean, and variance for each grid cell were calculated. An overall CV was calculated by bootstrapping the standard error divided by the mean for each grid cell. Data were collected and kriged beyond the location of the closed area boundary, but results presented are only for the area within the NLSCA boundaries. The highest mean value was 4 and 6 scallops/m² for the coarse and fine scale grids, respectively.



Appendix B9-Figure 8. Raw abundance ($\#/m^2$) estimates on a per image basis for all scallops regardless of shell height. Each dot represents a single image with the abundance indicated by color. Where no dots exist, no scallops were observed. a) All Scallops ($\#/m^2$). b) Scallops with shell height less than 60mm.



Appendix B9-Figure 9. a) Kriged scallop densities at a scale of 3350x2217 m . Mean densities represented by color referenced to the color bar on the right. b) Kriged scallop densities at a scale of 335x221 m showing considerable patchiness at this fine

Total abundance within the closed area boundary was calculated by summing each of the grid cells that fell within the boundary. Those cells that were partially within the boundary were evaluated by including only the proportion of the cell falling within the boundary. Total scallops in the coarse and fine scale grids were 174,966,666 and 197,545,580 scallops, respectively. The discrepancy in total abundance between grid scales probably lies in the fact that the scallops were patchy at scales of 400-900 m as shown from the Nearest Neighbor-k analysis. The courser grid scale smoothes high density patch values over a larger area than the higher resolution grid. The finer grid, therefore, is providing a more representative view of the scallop distribution and also the most accurate estimate. The overall mean for the fine scale grid was 0.187 scallops/m² with a CV of 0.04. Variance between cells ranged from 0.5 where sampling density was greatest to over 0.7 where sample density was low (Fig. 10).



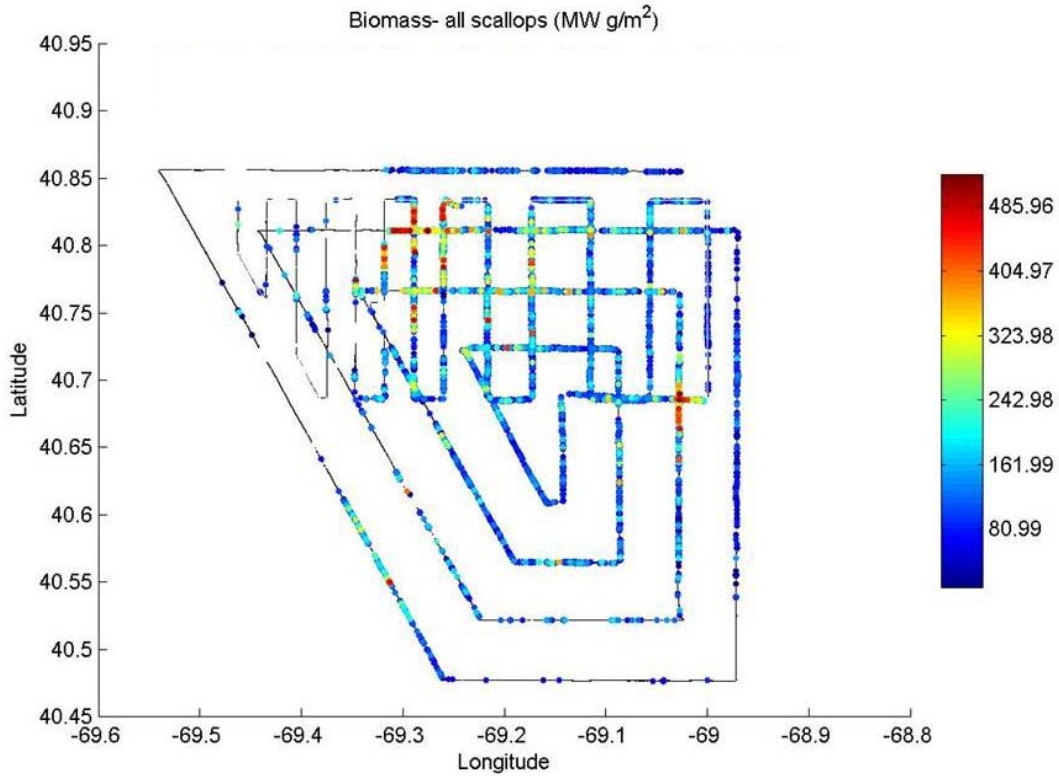
Appendix B9-Figure 10. Variance per cell for kriged scallop densities at the fine scale.

The weight of individual scallops used to estimate biomass was calculated using a shell height-meat weight relationship that included depth:

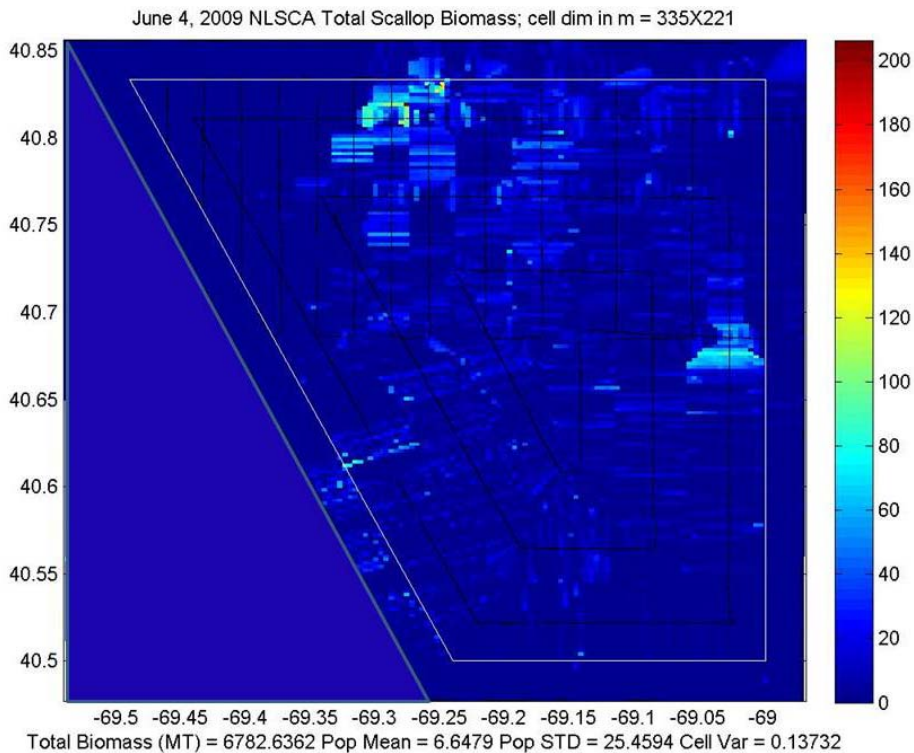
$$W = \exp(a+b \log(\text{SH}) + c \log(\text{depth}))$$

where W is weight (g), SH is shell height (mm), depth is in meters and the parameters a = -8.62, b = 2.95, and c = -0.51 (D. Hart, NEFSC, pers. comm.).

Mean biomass per scallop was 32.9 g. The basic pattern of distribution followed that of scallop abundance with dense scallop areas in the central northern region and in the central eastern region (Fig. 11). Biomass estimated by kriging at the fine scale 6,782 MT meats (Fig. 12).

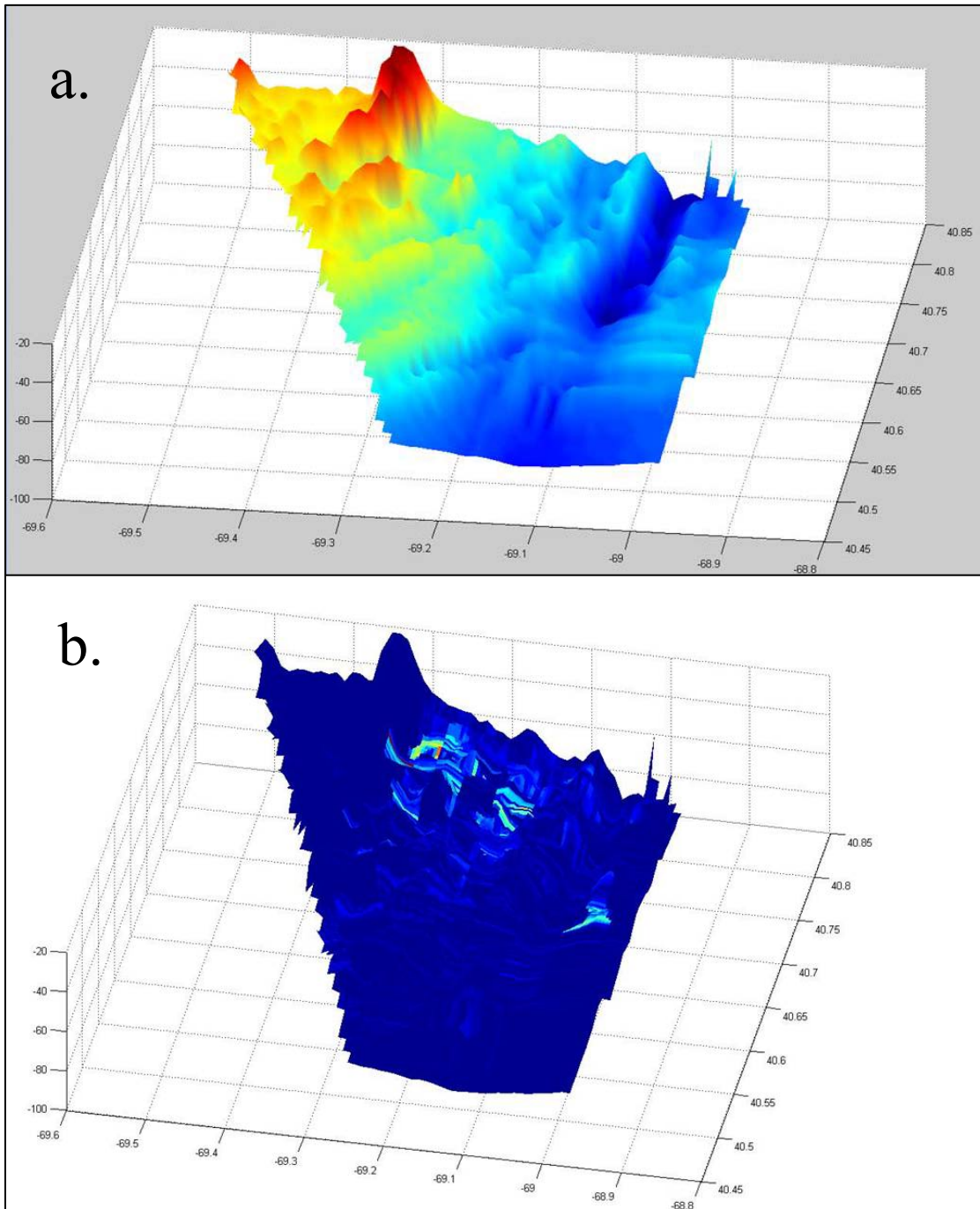


Appendix B9-Figure 11. Scallop biomass densities along the track line for all scallops of all sizes.

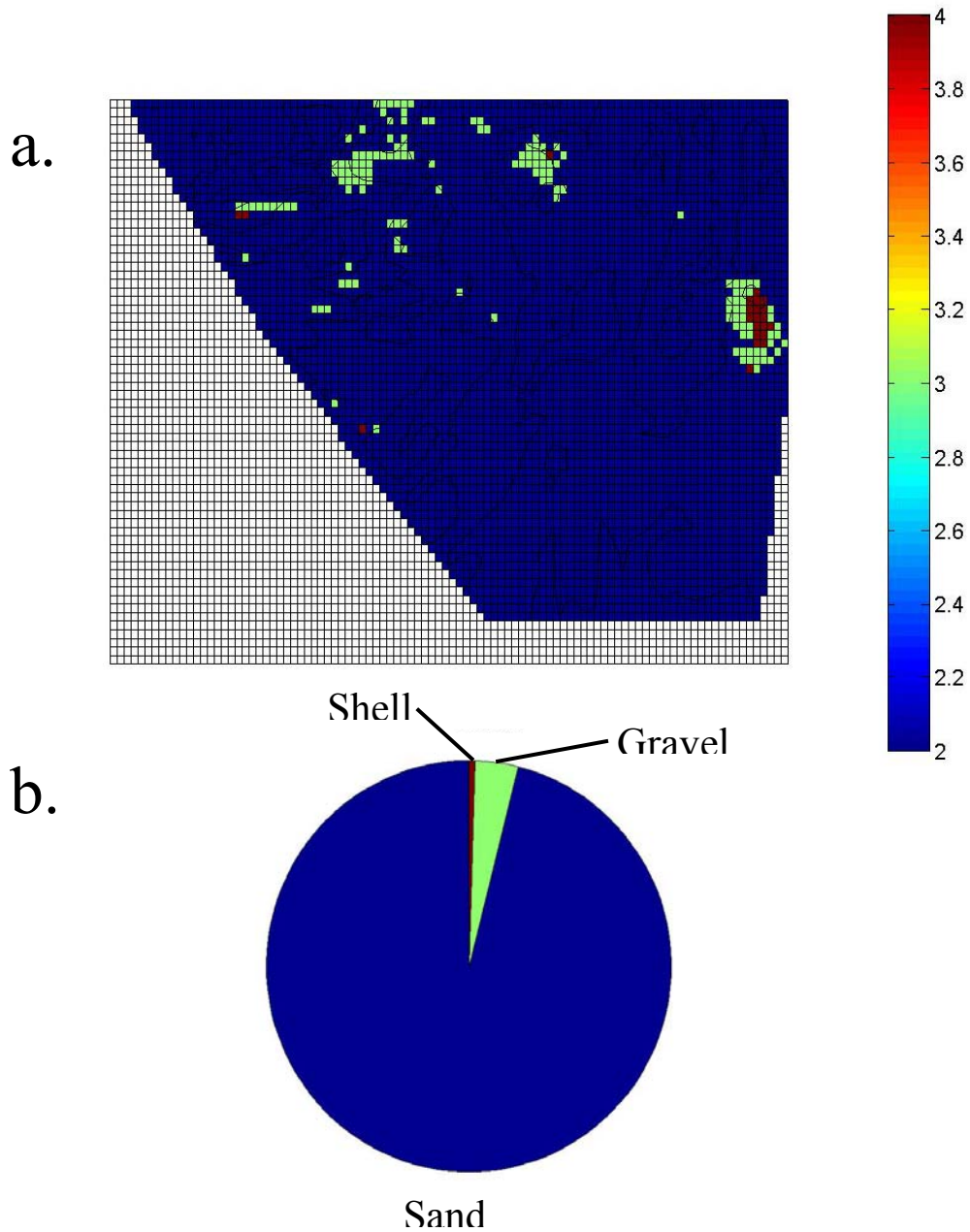


Appendix B9-Figure 12. Kriged biomass estimates generated at the fine scale for scallops of all sizes.

To examine relationships between density of scallops, depth, and substrate type, the depth from the ship's echosounder was linearly interpolated onto a uniform grid and colored as a function of depth (Fig. 13a). Sand waves in the northern central region and a trough in the central eastern region are notable. When scallop density was plotted as a color map over the interpolated depth data, it was clear that greatest densities were at the eastern base of the sand waves and just eastward of the trough, but not in the trough (Fig. 13b).

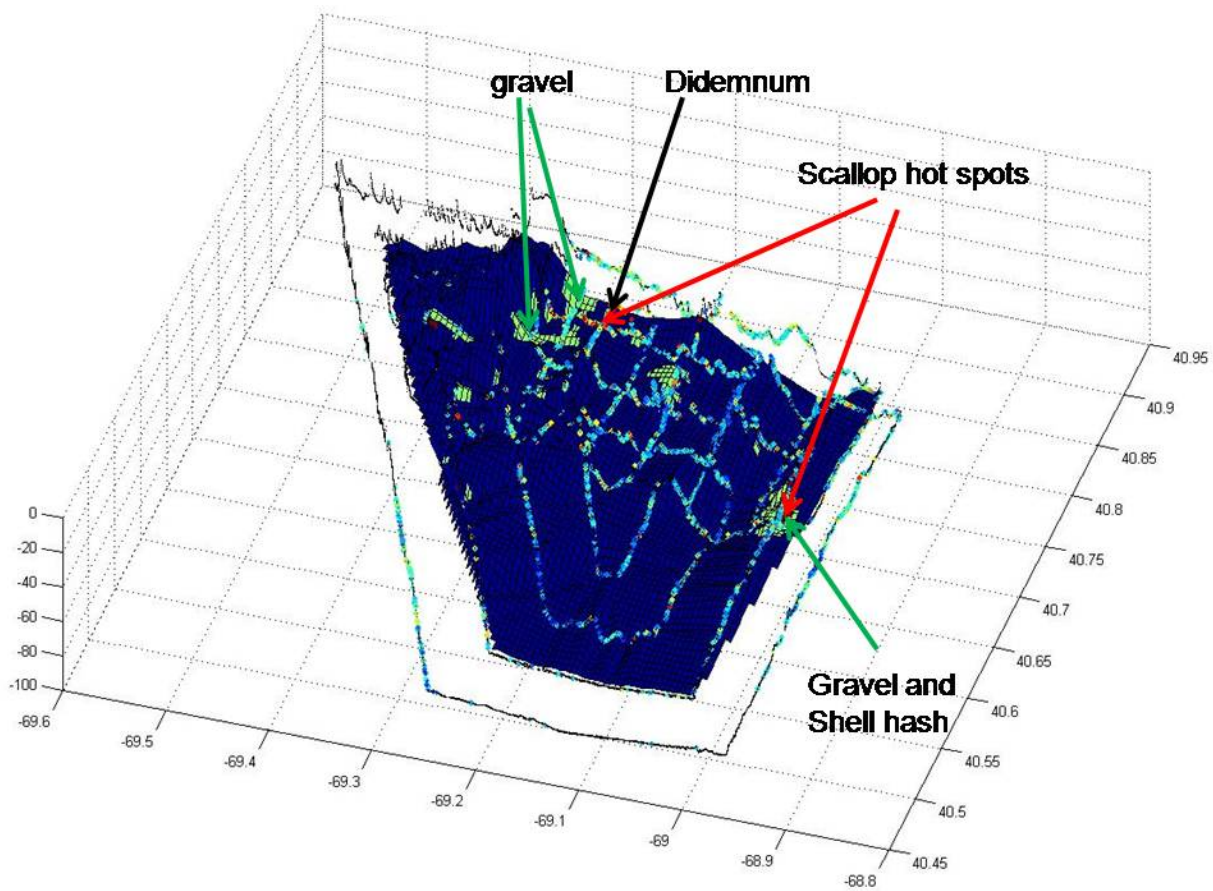


Appendix B9-Figure 13. a) Depth from the ship's sonar interpolated to a uniform grid.
b) Depth with overlaid scallop abundance on the same color scale as in Fig. 12.
Z axis is exaggerated for visualization purposes.

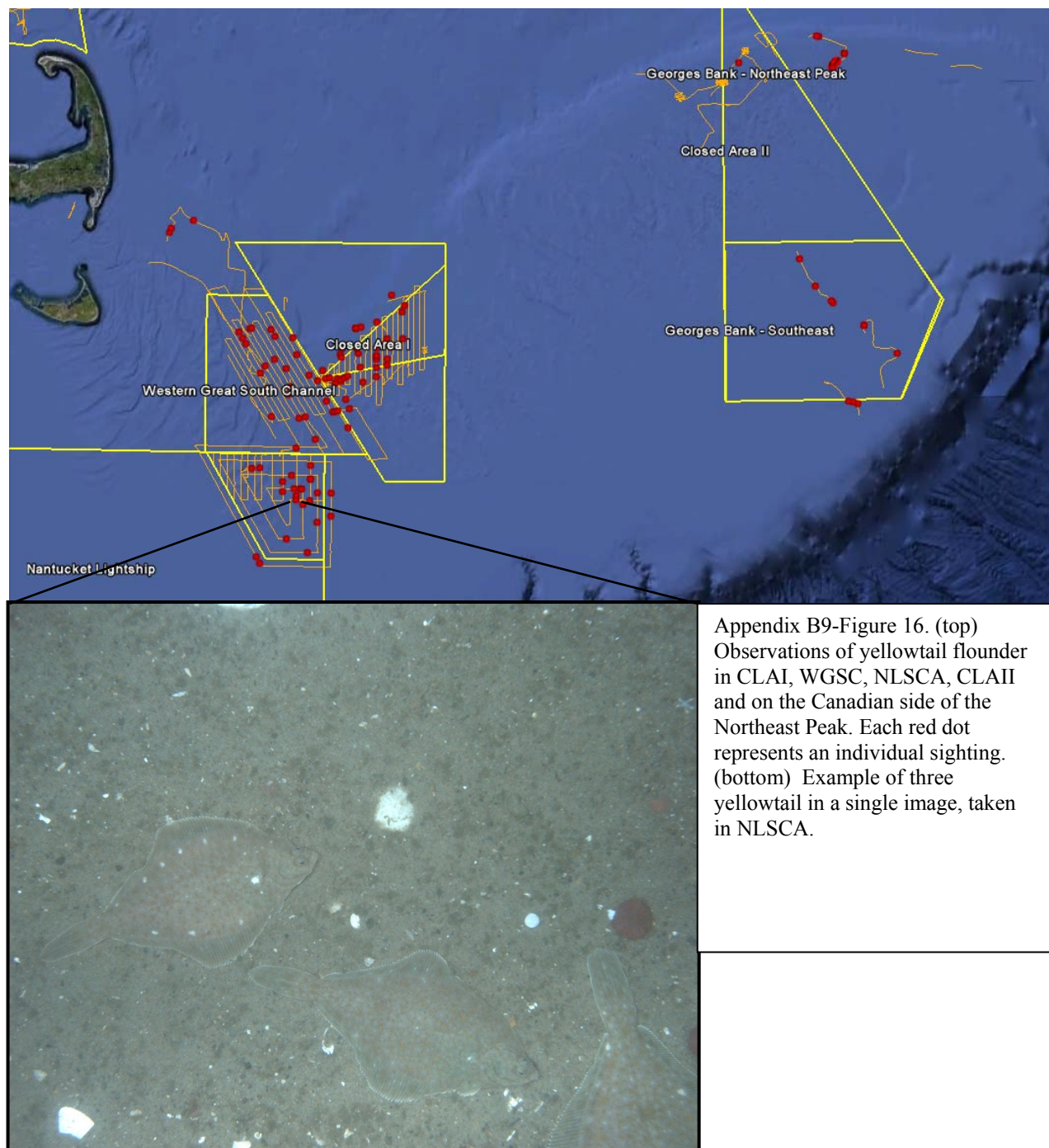


Appendix B9-Figure 14. a) Dominant substrate binned numerically into three categories (2) sand, (3) gravel, (4) shell. b) Sand dominated pie chart of substrate in NLSCA.

Substrate classifications were re-categorized into three numeric bins of dominant substrate: (2) sand, (3) gravel, and (4) shell. Dominant substrate categories include mixed substrate types, for example, “gravel” contains mixed substrate images such as gravel/sand and gravel/shell. Interpolation of these substrate categories across the NLSCA grid showed the entire area to be mostly sand (Fig. 14a,b). The greatest accumulation of sand/shell hash corresponded to areas of high scallop densities. The region to the central eastern side of the trough had notable sections of gravel, which is also where scallops were most abundant, particularly scallops less than 60mm in height. The combination of all three variables, scallop density, depth, and substrate (Fig. 15) provides a visualization of how scallop distribution is affected by these variables. HabCam data for the invasive tunicate *Didemnum vexillum* collected simultaneously with sea scallop data during the survey, illustrate spatial relationships of two species and substrate type and demonstrate the potential for use of data in ecological studies (Fig. 15).



Appendix B9-Figure 15. Depth overlaid with scallop abundance and substrate. Note location of invasive tunicate *Didemnum vexillum* in relation to high scallop densities.



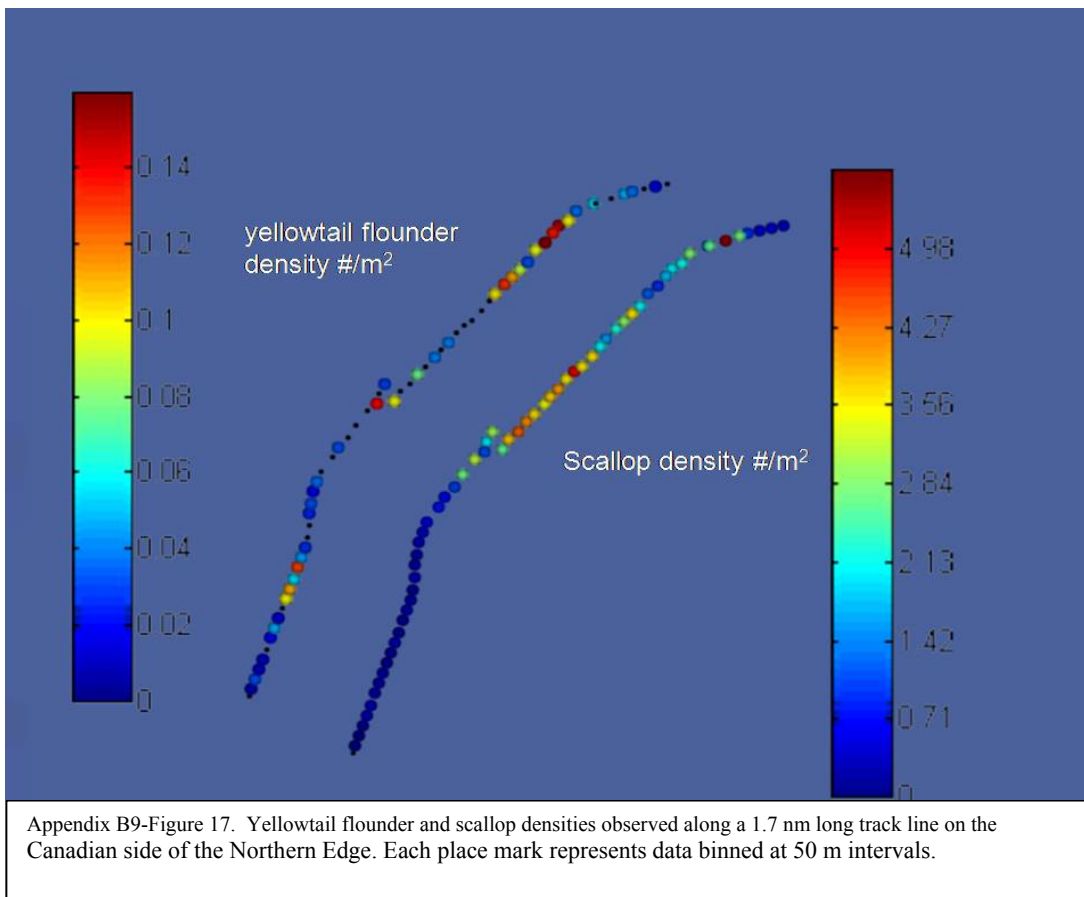
Appendix B9-Figure 16. (top) Observations of yellowtail flounder in CLAI, WGSC, NLSCA, CLAI and on the Canadian side of the Northeast Peak. Each red dot represents an individual sighting. (bottom) Example of three yellowtail in a single image, taken in NLSCA.

As an alternative method for calculating total population abundance of scallops without kriging or interpolating, one may simply use the overall mean observed in images multiplied by the total area. Our results using this approach is $0.187 \text{ scallops/m}^2 \times 1,142,280,000 \text{ m}^2 = 213,606,360$ scallops with a CV of 0.034.

In addition to sessile organisms, the HabCam system may be useful for imaging mobile demersal fishes. Yellowtail flounder were observed in NLSCA and other regions during our survey at relatively low densities (Fig. 16). In NLSCA, 124 observations were made with the densest concentration in the central region. This region was also characterized by being mostly

sand with patches of gravel. The most abundant aggregations of yellowtail were observed in the Southeast Part of CLAI and on the Canadian side with densities exceeding 0.14 fish/m². In some cases two or three fish were observed in a single image. Images from CLAI show yellowtail to be found on mostly sandy bottom with shell hash and occasionally on gravel.

An interesting relationship between scallop and yellowtail density was observed on the Canadian side of the Northern Edge. Data for yellowtail and scallops for the same track line are plotted alongside each other in Figure 17. Note that yellowtail appeared to be at highest densities where the abundance of scallops were low. This seemingly inverse relationship only holds for this track line at that point in time and is probably related more to substrate, food supply, reproduction, or environmental variables, than a true relationship between scallops and yellowtail. These results indicate the potential of HabCam data for use in fisheries management where, for example, the goal is to reduce bycatch of yellowtail during scallop fishing.



Joint ship operations

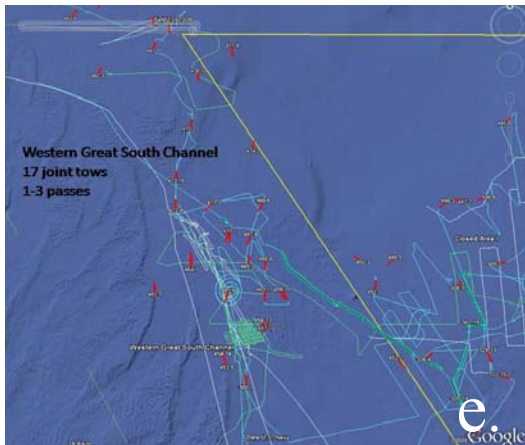
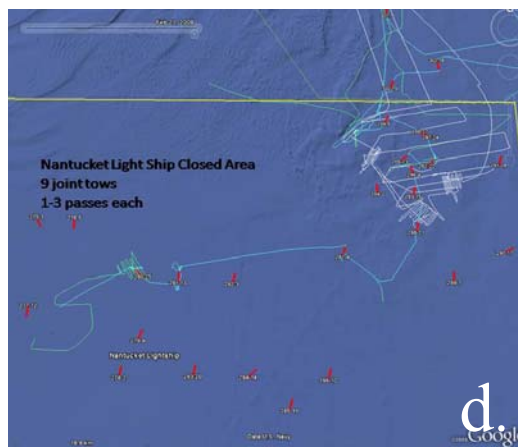
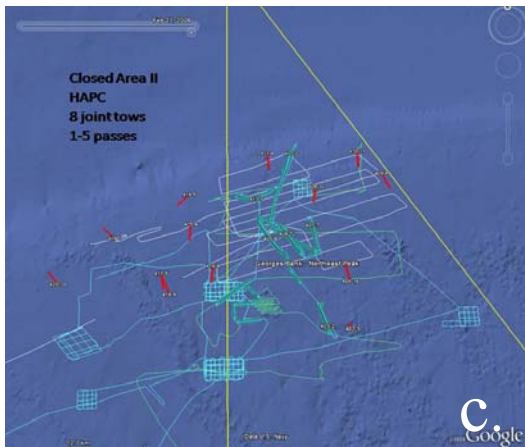
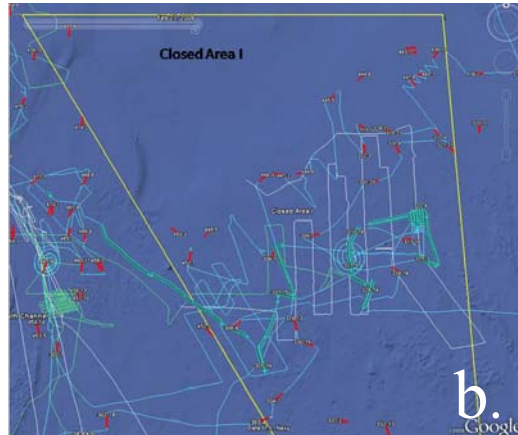
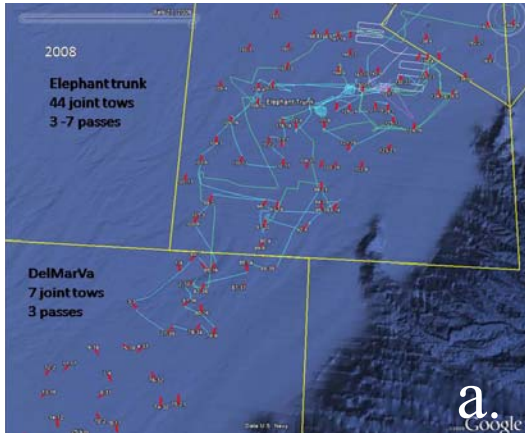
Since 2007, The HabCam Group has been collaborating with the NMFS in their annual scallop surveys by conducting paired tow experiments. These joint tows were designed to compare scallop abundances and size estimates from the standard federal dredge survey with those derived from HabCam imagery. Data will be presented here for 2008 and 2009.

In June and July 2008, The F/V Kathy Marie ‘shadowed’ the R/V Sharp on 113 total tows with 44 in the Elephant Trunk, 35 in CLAI, 8 in CLAI HAPC, 9 in NLSCA, and 17 in the proposed WGSC HAPC (Fig. 18). HabCam made at least three passes at over 50% of the NMFS stations, and in a few cases made up to seven. These multiple passes were designed to assess the variability of scallop density along each track and between multiple passes. Images from all passes were processed at a subsampled rate of every 10th image. This translates into processing about 1 m² for every 5 m of track line.

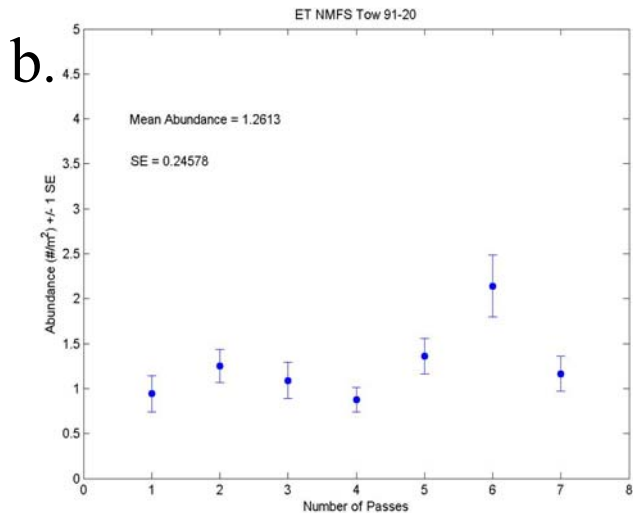
Within hours of conducting a dredge tow, the beginning and end points for the tow were communicated at sea via radio from the Sharp to the Kathy Marie. This allowed the captain of the Kathy Marie to line the vessel up on the dredge tow and follow a straight line from one end to the other. Because the absolute position of neither the dredge nor the HabCam vehicle was precisely known, our best efforts were to make multiple passes that coincided within about 50m of the dredge tow line and between each pass of HabCam. As an example, data for seven passes along the dredge tow for one station in Elephant Trunk (91) shows within and between variability of scallop densities observed by HabCam (Fig. 19). Although Pass 6 appears to be an outlier, results of a one-way ANOVA suggest that there is no significant difference between all 7 passes ($p < 0.001$).

HabCam estimates of scallop abundance were consistently greater than dredge counts, indicating that dredge efficiency is well less than 1. Mean shell height measurements were similar between dredge and HabCam (Fig. 20), but as will be discussed in the section under error analysis, the tails of the frequency distribution for HabCam are higher than those for the dredge indicating some inherent error in the measurement of shell heights. Count data tend to be accurate in optical surveys but some degree of body size measurement error is typical (Jacobson et al., 2010). This is an area of ongoing research.

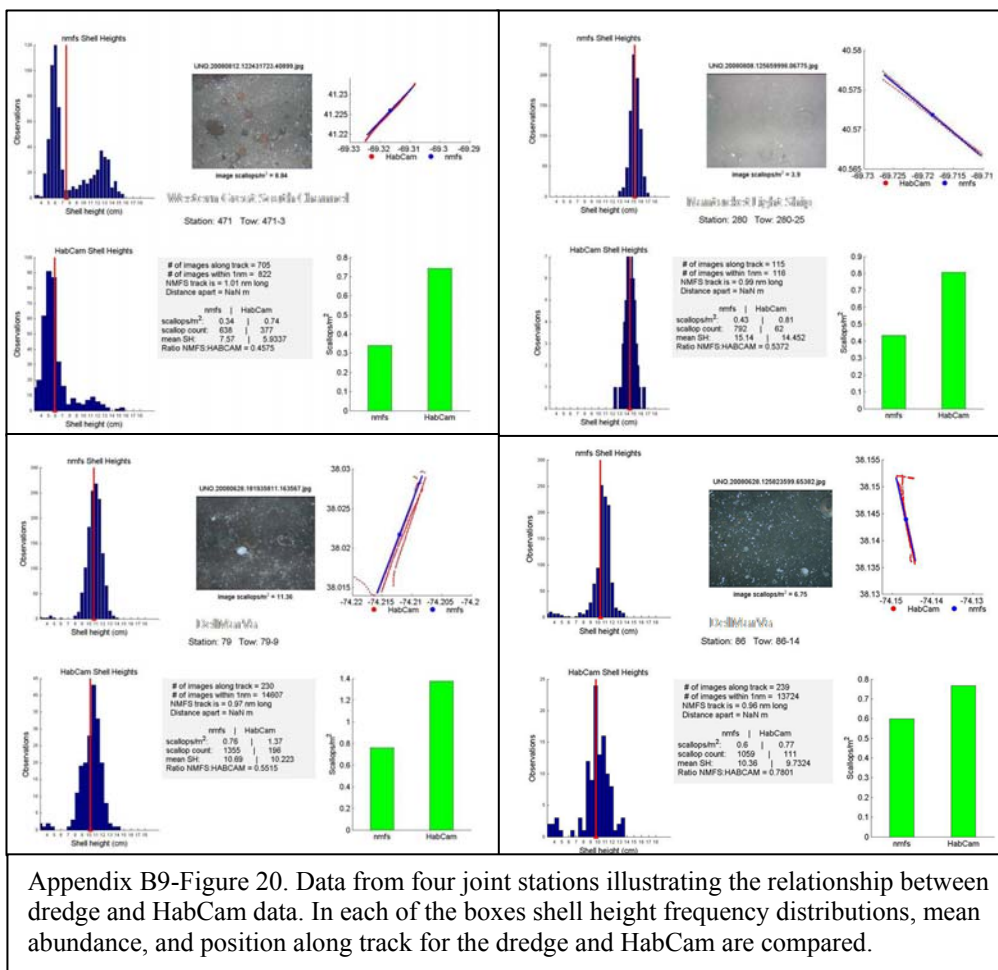
In June 2009, in addition to shadowing the Sharp with the Kathy Marie during Legs 1 and 2 of the annual scallop survey, HabCam was towed from the A-frame of the R/V Hugh R Sharp as part of routine dredge operations on Leg 3. This project was designed for comparison of HabCam data for sea scallops and yellowtail flounder with data from the standard dredge tows during Leg 3 of the 2009 NMFS Scallop Survey. Because of sea state and time considerations, HabCam was towed at and between 23 stations. HabCam collected a total of 787,832 images with a footprint of about 1 m² each. By area, 85,572 images were collected in CLAI, 216,809 images in CLAI, 183,070 images on the Canadian side of the Northern Edge of Georges Bank, and 302,381 images between stations. A final report has been filed with the NOAA CINAR office and Russell Brown at the NEFSC (HabCam Group, 2010).



Appendix B9-Figure 18. 44 Joint tows between R/V Sharp and HabCam on the F/V Kathy Marie in the (a) Elephant Trunk, (b) CLAI, (c) CLAII HAPC, (d) NLSCA, and (e) WGSC. Red lines are dredge tows, blue lines are HabCam track lines.



Appendix B9-Figure 19. (a) Federal dredge station 91 in ET with 1 nm tow shown in red. Seven passes by HabCam shown in blue. Multiple passes of HabCam were within 50m of each other. (b) Mean +/- SE of scallop abundance ($\#/m^2$) from each of the seven passes at station 91.



Appendix B9-Figure 20. Data from four joint stations illustrating the relationship between dredge and HabCam data. In each of the boxes shell height frequency distributions, mean abundance, and position along track for the dredge and HabCam are compared.

As each image represents about 1 m² and there is approximately 50% overlap, an area of about 242,000 m² was imaged. In an area on the Canadian side called the ‘seed box’, the density of small (50-60 mm) scallops was extremely high, upwards of 50 to 90 scallops per image (e.g. Fig. 21).

Shell height measurements from HabCam showed a strongly skewed distribution to the left with a mode of 55 mm and a mean of 79 mm (Fig. 22), indicating that this area was dominated by two year old scallops with relatively few older individuals.

Along track abundance of scallops at Station 404 ranged from 0 to well over 60/m² (Fig. 23). A Neighbor-k analysis of scallop distributions along the track in Fig. 4 showed that patchiness was significant at several spatial scales from 600 to 1000m (Fig. 24).

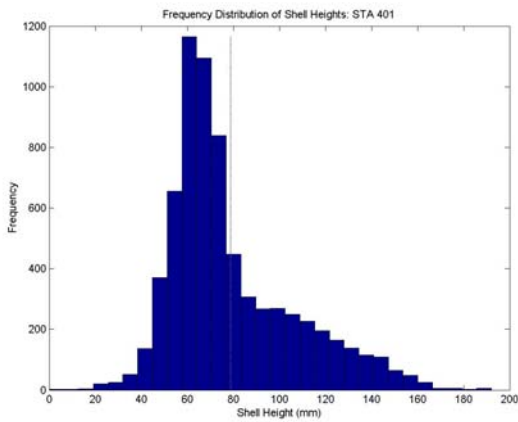
Yellowtail flounder were sparse but most abundant in the Southeast Part of CLAI and on the Canadian side of the Northern Edge (Fig. 25). Images show yellowtail to be found on mostly sandy bottom with shell hash and occasionally on gravel (Fig. 26).

Survey dredge capture efficiency is low relative to optical surveys and might be variable due to tow direction in relation to tidal currents, substrate composition, wire out, tow speed, and tow duration. To compare scallop abundances estimated by the NMFS dredge and HabCam, plots were generated by region and by substrate and include data for both 2008 and 2009 (Fig. 27). Georges Bank includes NLSCA, WGSC, CLAI and CLAI. Mid Atlantic Bight includes Elephant Trunk, Delmarva, and Hudson Canyon. Regression slopes were 0.34 for Georges and 0.46 for Mid Atlantic Bight. When the data are broken out by substrate regardless of region, the regression slope for sand was 0.35, for sand plus other substrate types such as shell hash it was 0.40, and on gravel it was 0.35. These slopes should modestly underestimate the sampling efficiency of the dredge relative to HabCam (due to errors in variables, i.e., that the x coordinates in the regression are uncertain since HabCam does not go over the exact same ground as the dredge). Results (dredge sampling efficiencies for sea scallops ~ 0.3 to 0.45) are similar to results from other studies. Moreover, they illustrate the potential for use of HabCam in directly estimating the sampling efficiency of other types of survey and fishing gear. Estimates from simple regressions are biased low because of errors in variables: see Appendix X for unbiased methodology.

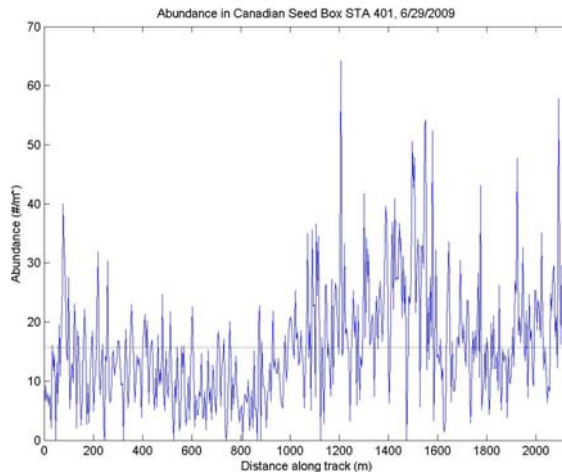
Bland-Altman plots are used to assess the correspondence between two forms of measurement for the same data and are constructed by plotting the differences between paired observations from two data sets against their mean. It was necessary to normalize the residuals for the sum of both dredge and HabCam samples. The mean residual for all data for 2008 and 2009 was 0.37 (Fig. 28), which is consistent with the regression analyses presented in Figure 27. The residuals are normally distributed between the limits of agreement suggesting that while there is a strong systematic bias, neither measurement approach is affected by abundance of scallops being measured.



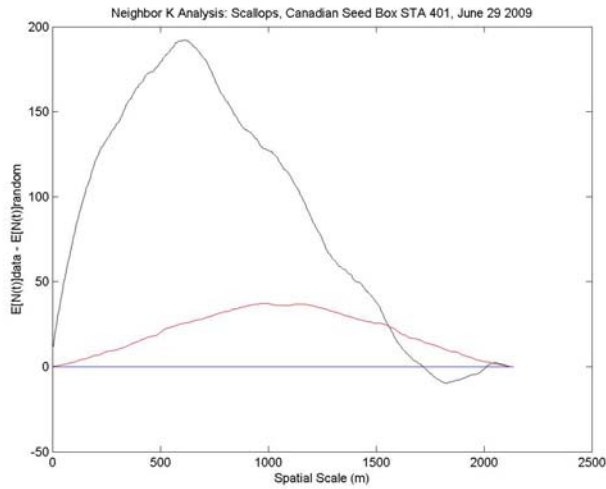
Appendix B9-Figure 21. The HabCam Manual Identification Program (MIP) while processing an image collected on the Canadian side near station 404 where 90 scallops were counted and measured in a single



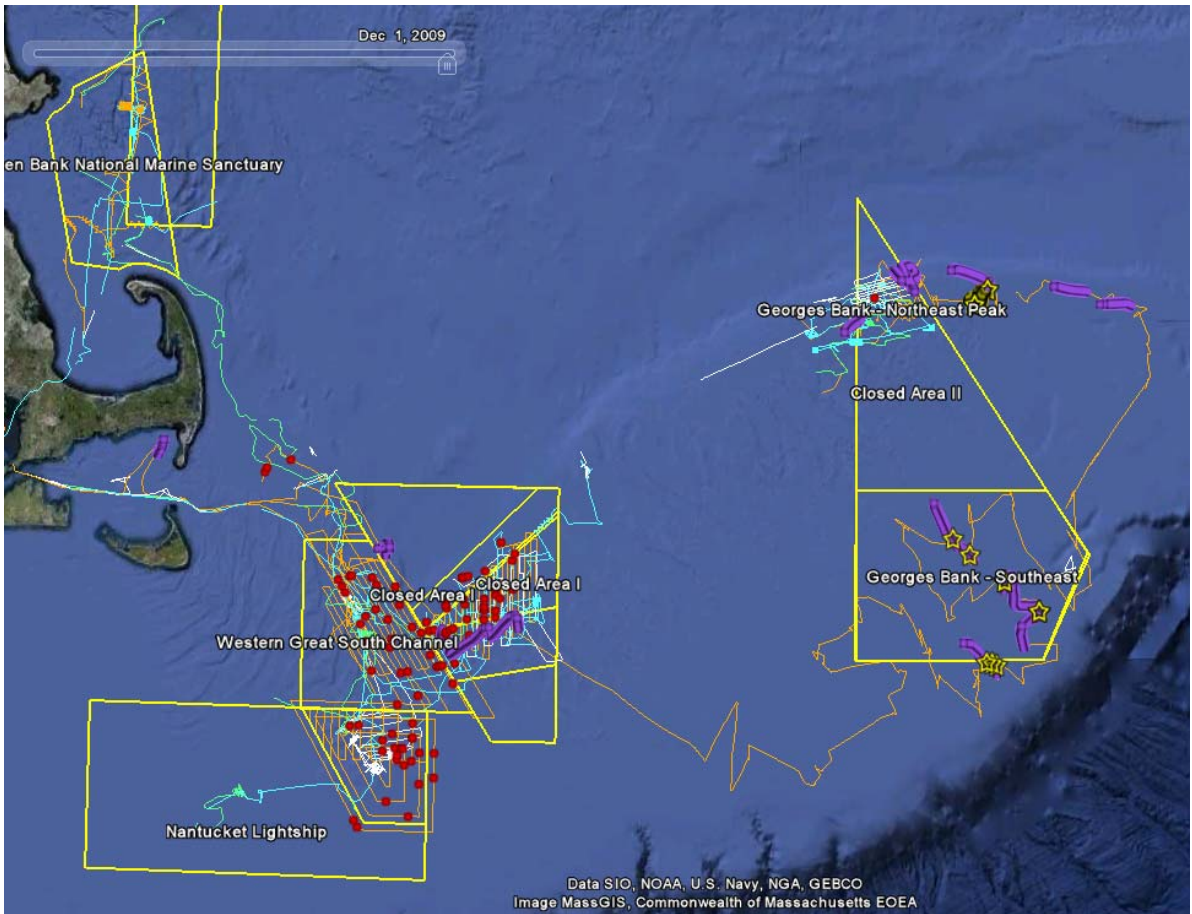
Appendix B9-Figure 22. Frequency distribution of scallop shell heights from HabCam images at Station 401 in the seed box.



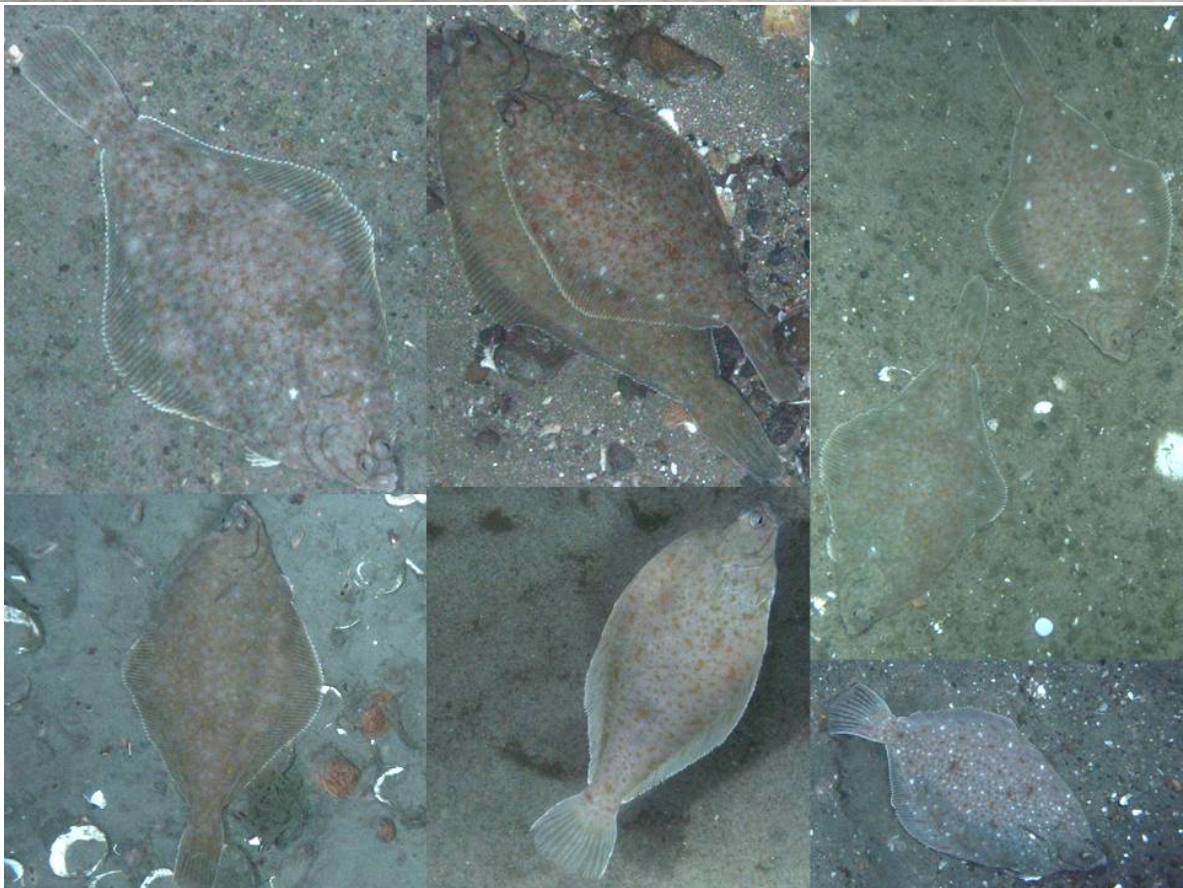
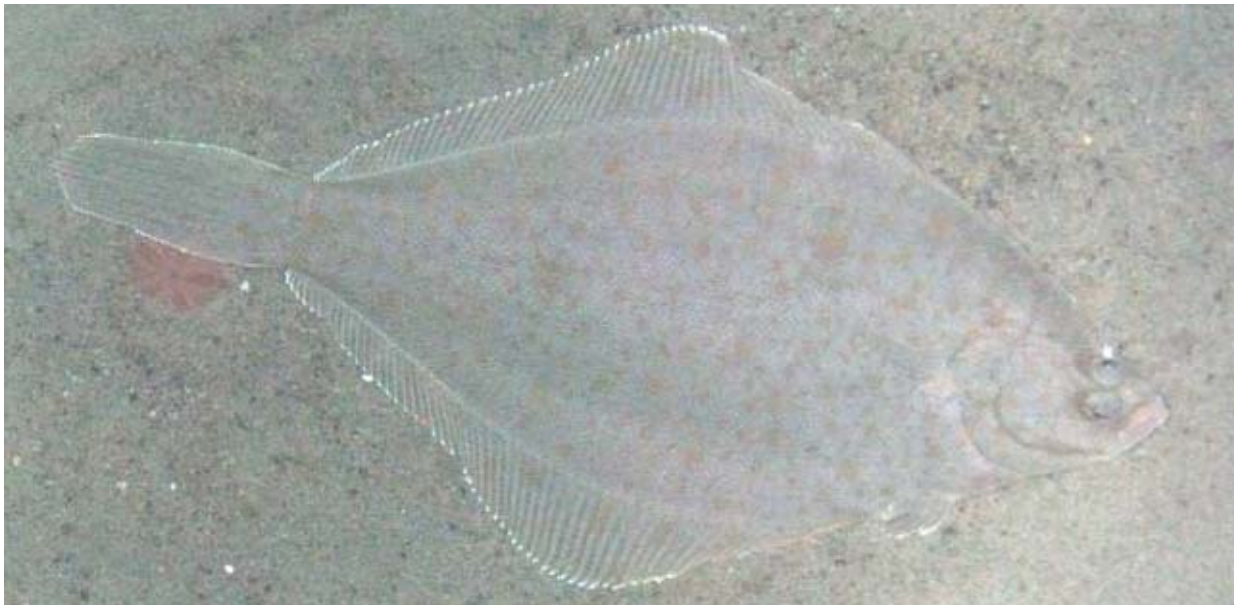
Appendix B9-Figure 23. Along track abundance of scallops at Station 401 in the 'seed box' on the Canadian side. Mean abundance was 16 scallops/m².



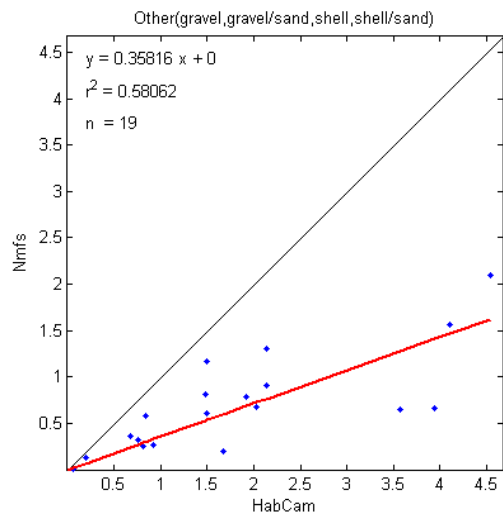
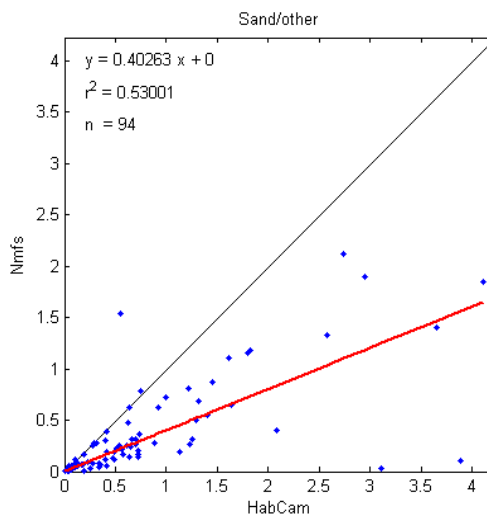
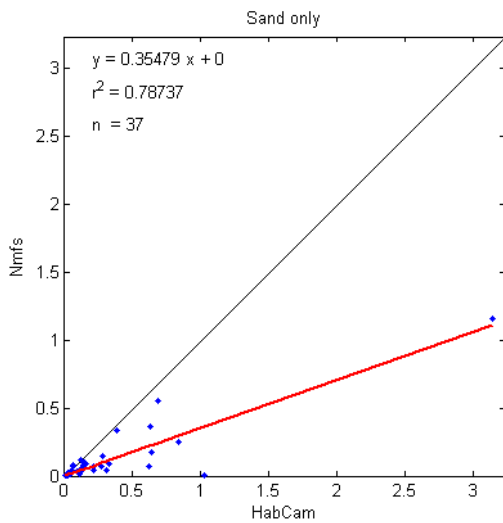
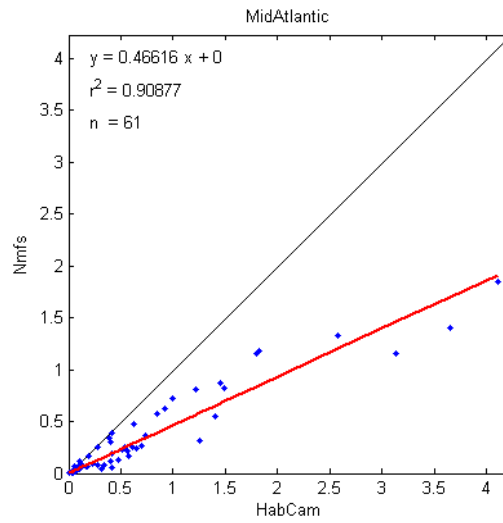
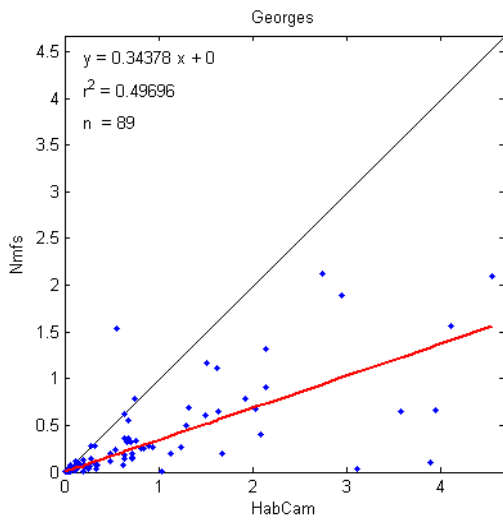
Appendix B9-Figure 24. Neighbor-k analysis of the distribution of scallops at Station 404. Note significant



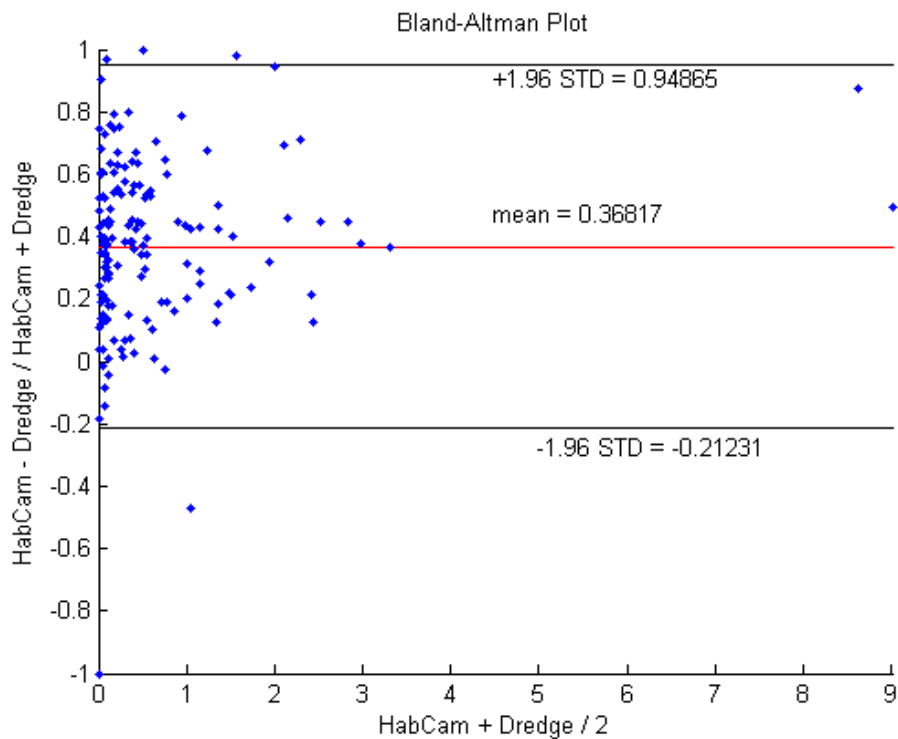
Appendix B9-Figure 25. Georges Bank and track lines of the R/V Hugh Sharp Leg 3 of the NMFS scallop survey (orange) and the regions where HabCam was deployed and collecting images (purple). Red dots and yellow stars are yellowtail flounder sightings



Appendix B9-Figure 26. Composite of example images of yellowtail flounder from Georges Bank.



Appendix B9-Figure 27. Regressions of dredge survey estimates against HabCam estimates of scallop densities for both Years 2008 and 2009. Each point represents a single 1nm tow in the Georges Bank (a) or Mid Atlantic Bight (b) areas. Data broken out by substrate type in sand (c), sand plus shell hash (d), and gravel (e). The one to one correspondence line is plotted in black.



Appendix B9-Figure 28. Bland-Altman plot of the residuals for all joint tows in 2008 and 2009. The y axis represents $(\text{Dredge}-\text{HabCam})/(\text{Dredge}+\text{HabCam})$ and the x axis is the mean of the two observations. The mean difference and the limits of agreement are also plotted.

Assessment of Real and Potential Errors Associated with HabCam Image Data

The sources of error to be assessed in this section are:

- a) Border rules for measuring and counting scallops
- b) Engineering Error
 - Calibration of Field of View (FOV), complete camera model for intrinsic parameters, estimation of in-water, focal length, principle point, and pixel error
 - Incorporation of extrinsic parameters for each image into calculation of FOV (area swept)- roll, pitch, heading, altitude
- c) Human Error
 - Analysis of measurement error both between individuals and within individuals using Intra Class Correlation
- d) Imaging Error
 - Scallop shells not orthogonal to camera axis
- e) Total Measurement Error
 - Analysis of shell height measurement error relative to NMFS dredge survey in NLSCA

- f) Errors in interpolation of 1D data into 2D
- Kriging correlograms and variograms
 - Variance within and between gridded cells
 - Non-model based assessment of biomass

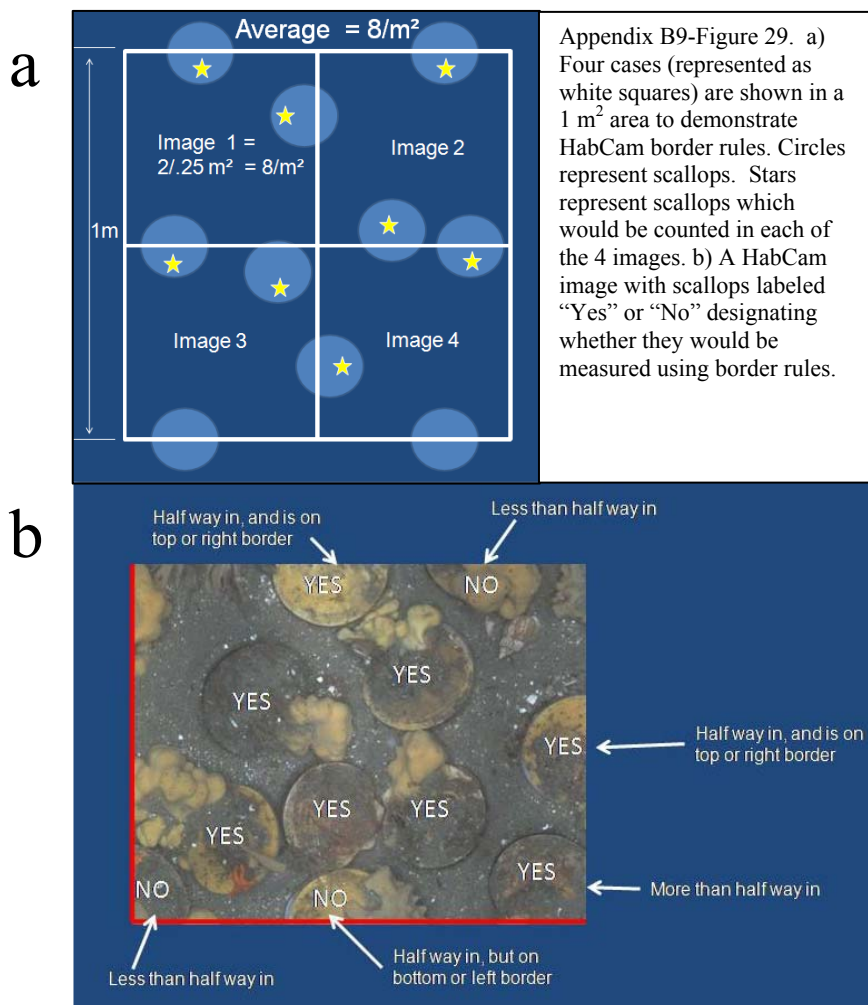
Each of these sources of potential error is discussed below.

HabCam border rules

The purpose of the HabCam rules for border effects is to reduce undercounting or over counting due to animals being on the edge of images. The desired outcome is to count scallops on the edge of images exactly half the time. To achieve this, the following rules, which result in counting only scallops that have their centroid in the image, are followed (Fig. 29):

Primary Rule: Count all organisms that are more than half way in the image.

Secondary Rule: If the organism is exactly half way in the image, count only the organisms that are half way in the top and right sides. This process is identical to that described for counting blood cells on a Spears-Levy Hemacytometer and eliminates the need for altering the field of view (FOV) on an image to account for image basis.



Engineering errors-Calibration of Field of View (FOV)

Calibration of an optical system must include a complete camera model for intrinsic parameters, estimation of in-water focal length, principle point, and pixel error, followed by image correction by employing extrinsic parameters collected for each image.

The intrinsic parameters for the HabCam camera were calculated using images of a 1m² target marked off at 10cm intervals in a 4 m deep seawater tank. The HabCam vehicle was positioned above the target at various altitudes (1-3m), roll, and pitch (0 and 20 degrees). Twenty eight images representing a range of positions were used for calibration of the camera with the Calibration Toolbox in Matlab.

Engineering errors-Intrinsic parameters

(based on 28 images of target at different altitudes and orientations)

Focal Length: $fc = [2773.25504 \ 2764.28859] \pm [7.18117 \ 7.13362]$

Principal point: $cc = [778.19667 \ 509.00401] \pm [4.13012 \ 3.80811]$

Skew: $\alpha_c = [0.00000] \pm [0.00000] \Rightarrow$ angle of pixel axes = 90.00000 ± 0.00000 degrees

Distortion: $kc = [-0.31591 \ 0.14388 \ 0.00070 \ 0.00138 \ 0.00000] \pm [0.00702 \ 0.02649 \ 0.00038 \ 0.00056 \ 0.00000]$

Pixel error: $err = [0.53035 \ 0.50489]$

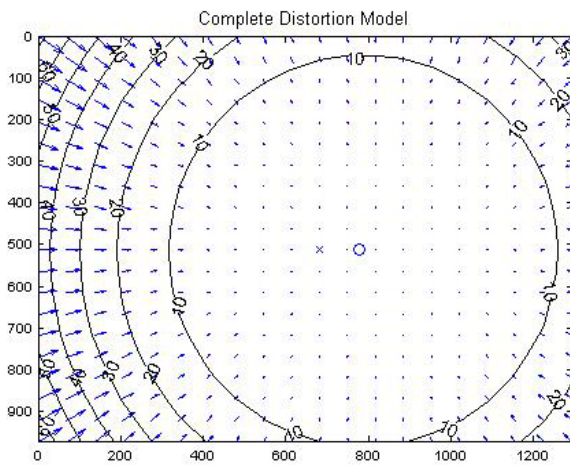
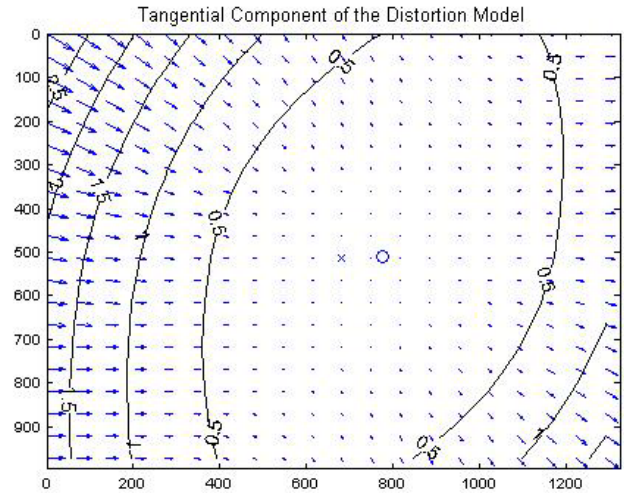
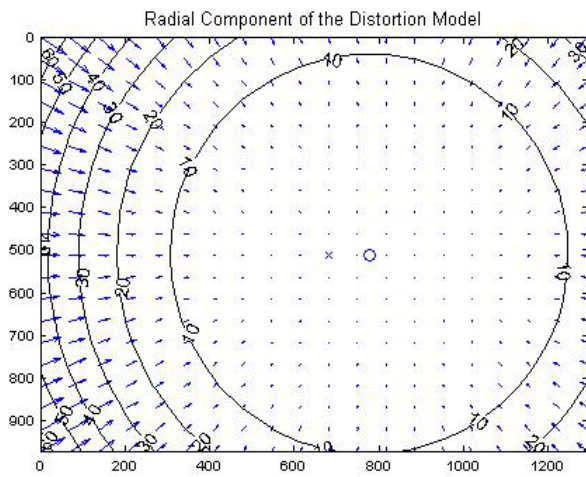
The numerical errors are approximately three times the standard deviations

Intrinsic pixel error = +/- 1.59 pixels

Resolution range f (FOV): 0.37 – 0.89 mm/pixel

Intrinsic real-world error : 0.58 – 1.41 mm

These values provide error bounds on the resolution and accuracy of the camera system in water. Plots of the relative errors show that the camera CCD chip, lens and housing window are slightly out of alignment in both radial and tangential attitudes (Fig. 30). The pixel resolution is a function of FOV, which in turn is a function of altitude off the bottom. In calibrated screen measurement space, the overall measurement error is between 0.58 and 1.41 mm.



Appendix B9-Figure 30. Radial, tangential, and complete distortion model for the HabCam camera.

Distortion in each image is first corrected using the intrinsic parameters given above (Fig. 31).
 $KK = [fc(1) \alpha_c * fc(1) cc(1); 0 fc(2) cc(2); 0 0 1];$
where the KK matrix is the uncorrected image matrix.

$r2_extreme = (nx^2/(4*fc(1)^2) + ny^2/(4*fc(2)^2));$

$dist_amount = 1; \% (1+kc(1)*r2_extreme + kc(2)*r2_extreme^2);$

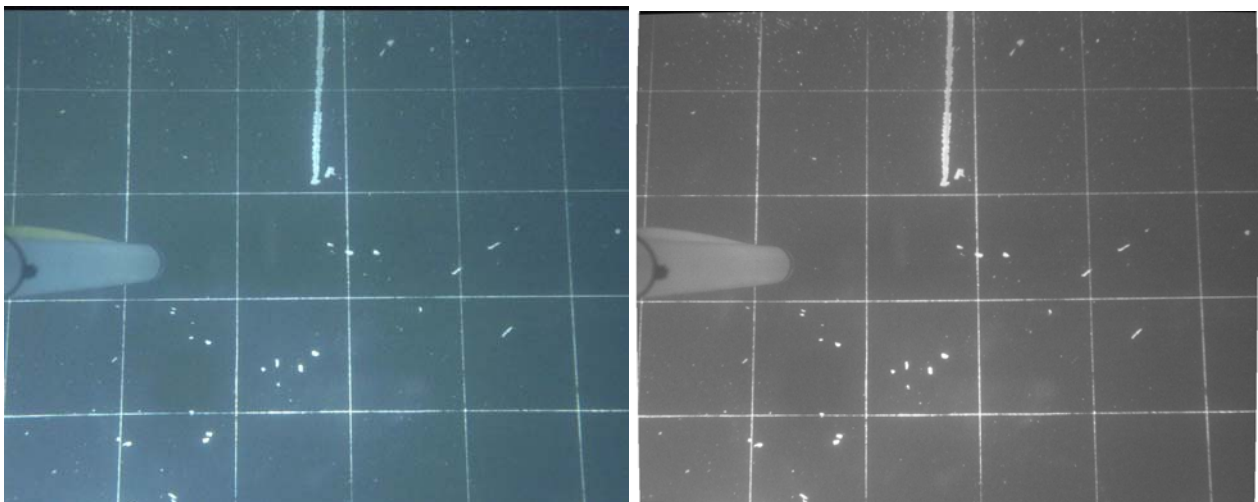
$fc_new = dist_amount * fc;$

$KK_new = [fc_new(1) \alpha_c * fc_new(1) cc(1); 0 fc_new(2) cc(2); 0 0 1];$

KK_new is the corrected image matrix.

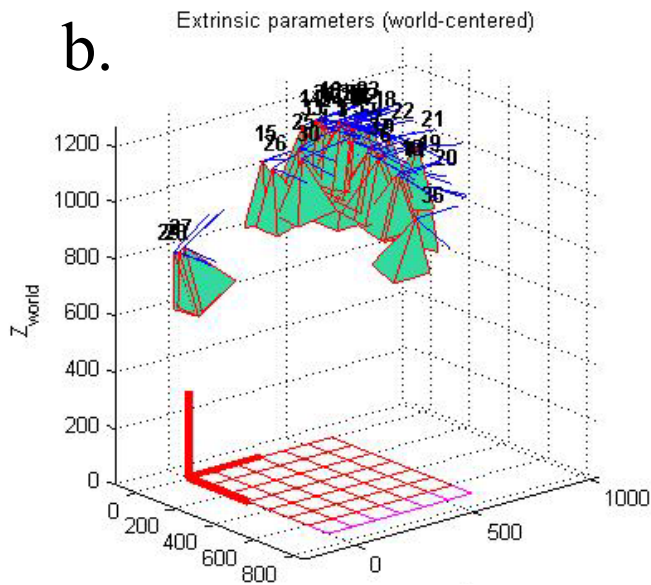
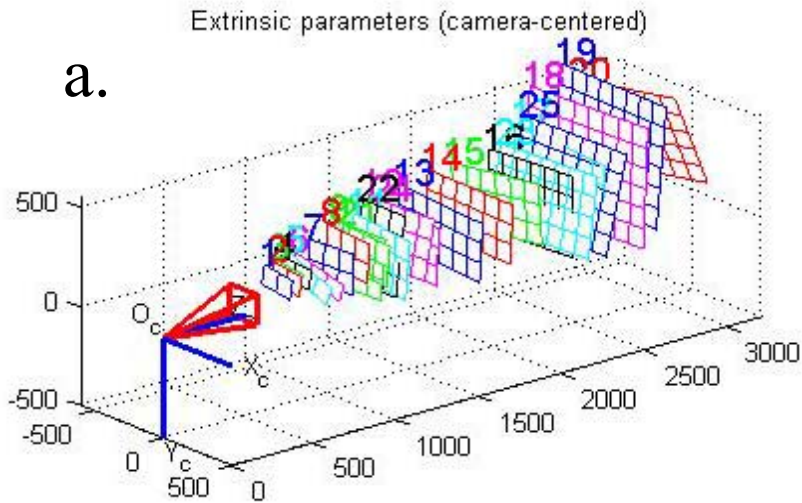
$[I2] = rect(I, eye(3), fc, cc, kc, KK_new);$

Where I is the distorted image and I2 is the undistorted image



Appendix B9-Figure 31. Correction of a distorted image of the calibration target in water (left) using intrinsic camera parameters. The corrected image (right) shows straight rather than curved lines particularly towards the corners of the image.

Extrinsic parameters relate to the combination of intrinsic parameters plus the orientation of the camera relative to the image plane. The calibration matrix is built up from the 28 views indicated in Figure 32.



Appendix B9-Figure 32.

- a) Camera centric views of 28 orientations and altitudes to build extrinsic parameter list.
- b) World centric views of 28 orientations and altitudes.

Engineering errors-Calculation of extrinsic parameters

Cross over points in the calibration chart are automatically detected and their locations in pixel space extracted before calculation of extrinsic parameters (Fig. 33).

The extrinsic parameters are encoded in the form of a rotation matrix (**Rc_ext**) and a translation vector (**Tc_ext**). The rotation vector **omc_ext** is related to the rotation matrix (**Rc_ext**) through the Rodrigues formula: **Rc_ext** = **rodrigues(omc_ext)**.

Let **P** be a point space of coordinate vector **XX** = [**X**;**Y**;**Z**] in the grid reference frame (**O,X,Y,Z**).

Let **XX_c** = [**X_c**;**Y_c**;**Z_c**] be the coordinate vector of **P** in the camera reference frame (**O_c,X_c,Y_c,Z_c**). Then **XX** and **XX_c** are related to each other through the following rigid motion equation:
XX_c = **Rc_ext** * **XX** + **Tc_ext**

In addition to the rigid motion transformation parameters, the coordinates of the grid points in the grid reference frame are also stored in the matrix **X_ext**.

Each image taken by HabCam has its own unique set of extrinsic parameters.

Extrinsic parameters for an example image:

Translation vector:

$$Tc_ext = [-225.840216 \quad -130.369514 \quad 608.628548]$$

Rotation vector:

$$omc_ext = [-2.148393 \quad -2.284790 \quad -0.123388]$$

Rotation matrix:

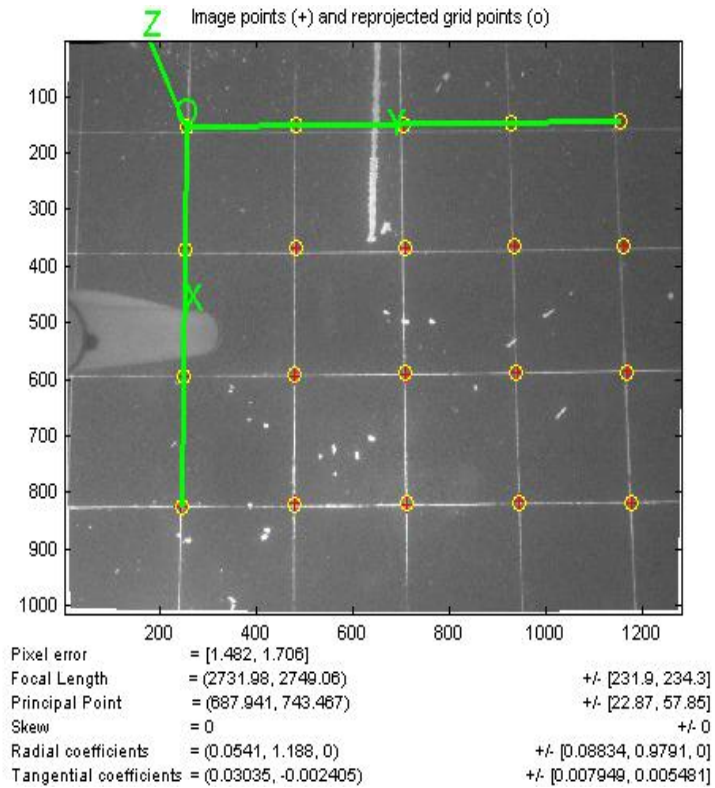
$$Rc_ext = [-0.062925 \quad 0.996680 \quad 0.051672 \\ 0.996448 \quad 0.059838 \quad 0.059254 \\ 0.055966 \quad 0.055217 \quad -0.996905]$$

$$\text{Reprojection Pixel Error:} \quad err = [2.00116 \quad 1.26492]$$

Extrinsic pixel error = +/- 2 pixels

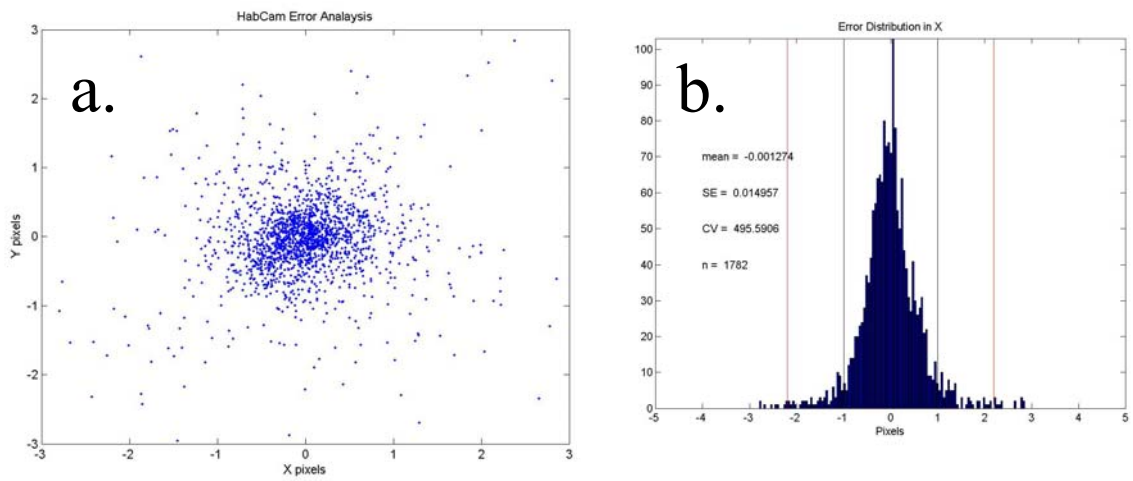
Resolution range (FOV): 0.37 – 0.89 mm/pixel

The extrinsic real-world error becomes: 1.11 – 1.78 mm (under best optical conditions)



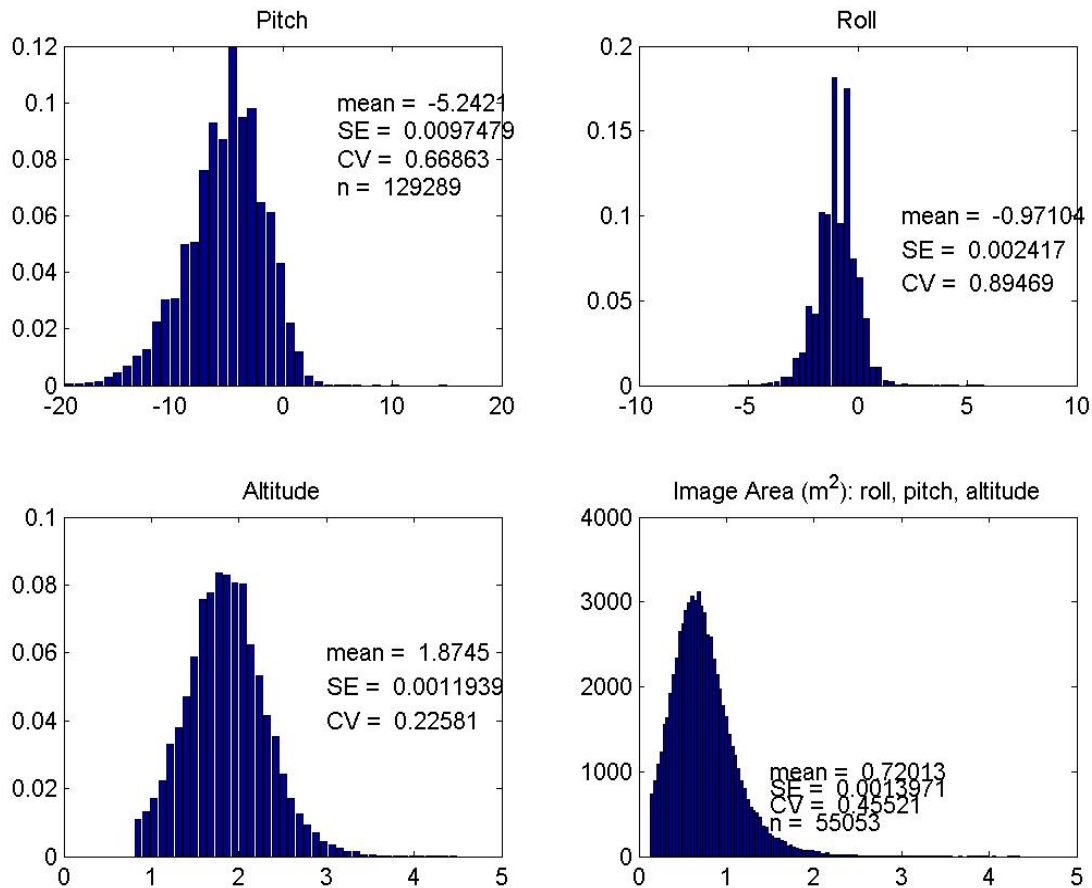
Appendix B9-Figure 33. Extrinsic parameters for image 24 above, as an example.

Pixel error in X and Y can be visualized as a scatter plot and frequency distribution (Fig. 34). Note that 99% of values are less than 2.2 pixels.



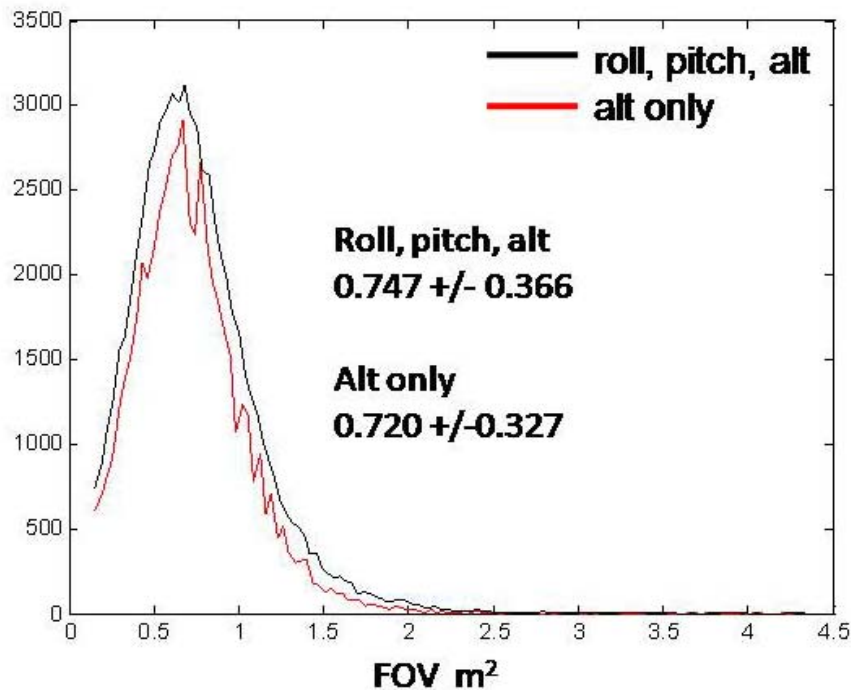
Appendix B9-Figure 34. (a) Scatter plot of pixel error around the origin. (b) Frequency distribution of pixel error along x axis.

Frequency distributions of pitch, roll, altitude, and image area (FOV) for the NLSCA 2009 survey based on 129,289 images are shown in Figure 35. The mean pitch was -5.24 degrees indicating that, on average, the nose of the vehicle pointed down slightly. Downward pitch is part of the system design and tends to stabilize the vehicle while underway. Mean roll was -0.97 with very little variation indicating the vehicle is quite stable, laterally. Altitude measurement varied from <1 to 4.5 m off the bottom with a mean of 1.87m. Images below 1 m were out of focus and removed from the image database. Images taken higher than 3 m were typically not sufficiently clear, due to turbidity, to be useful and were also not used. Taking roll and pitch into account using the extrinsic equations present above, the FOV ranged from 0.2 to >4m² with a mean of 0.72 m². 95% of the calculations for FOV fell between 0.4 and 1.5 m². Figure 36 shows a comparison between FOV calculated with and without the use of roll and pitch, i.e., directly from the altitude, only. Incorporation of roll and pitch into the geometric projection of the FOV has an effect of broadening and smoothing the frequency distribution of values without changing the mean.



Appendix B9-Figure 35. Frequency distributions of pitch, roll, altitude, and image area (FOV) for the NLSCA 2009 survey.

**Distribution of Image Area m² (FOV)
NLSCA 2009 Survey**

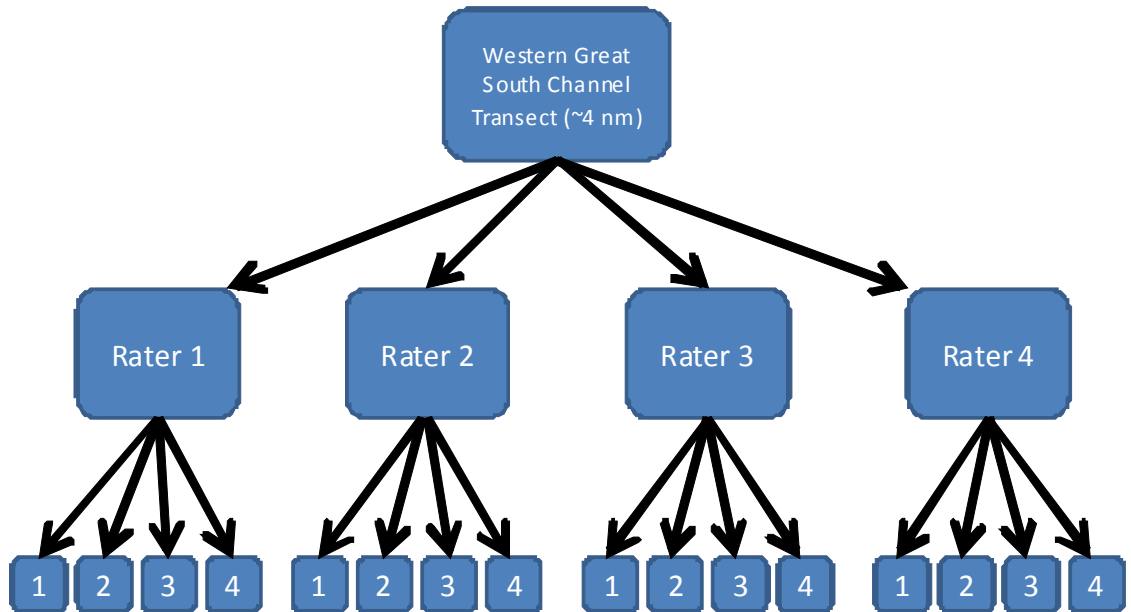


Appendix B9-Figure 36. Comparison between calculations of FOV with and without the effect of roll and pitch on geometric projection of FOV. Note broadening and smoothing of the distribution without a significant change in the mean, when projected geometry is used in conjunction with altitude.

Human errors: Analysis of measurement error both between individuals and within individuals
It was desired to estimate the level of error associated with the manual screen measurement of scallops both within a given technician and between technicians. The former would provide insight into measurement repeatability and the latter into systematic bias between individuals.

To accomplish this, we assigned four identical 4.2 m long image transects containing 4,432 images from Western Great South Channel to six individuals (raters) (Fig. 37). Raters measured scallops using MIP under the same measurement rules as would be used under normal conditions (edge effects, height vs. width, etc).

ICC Intra Class Correlation Analysis



Two-way mixed effects model

$$X_{ij} = \mu + r_i + c_j = \mu_{ij} + e_{ij}$$

μ : population mean, r : row effects, c : column effects, e : residual effects

281 scallops x 4 raters x 4 passes = 4,496 measurements

Appendix B8-Figure 37. Inter Class Correlation analysis of scallop shell height measurements. Four individuals measured scallops from one transect four times.

Appendix B9-Table 1. Summary statistics in pixels. N = 277 for each run. A total of 4,432 scallops were measured. KLB, ADY, PK, and DPF are initials of the four raters.

rater	KLB				
	run1	run2	run3	run4	mean
mean	132.41	132.21	132.58	132.28	132
STD	31.61	31.61	31.44	31.69	
SE	1.89	1.91	1.88	1.9	
rater	ADY				
	run1	run2	run3	run4	mean
mean	128.48	128.46	128.41	128.75	128
STD	31.42	31.55	31.44	31.78	
SE	1.88	1.89	1.88	1.9	
rater	PK				
	run1	run2	run3	run4	mean
mean	135.57	135.88	134.95	134.28	135
STD	31.86	31.94	31.81	31.63	
SE	1.91	1.91	1.91	1.9	
rater	DPF				
	run1	run2	run3	run4	mean
mean	128.36	127.39	127.48	127.56	127
STD	31.74	31.63	31.45	31.57	
SE	1.9	1.9	1.89	1.89	

In most cases, mean within rater measurements were either accurate to the same number of pixels or within one pixel suggesting that within rater variability was extremely low (Table 1). Between rater variability was greater than within rater variability with mean values of 132, 128, 135, 127, providing a range of 135 to 127, or 8 pixels. Given the resolution range for varying FOV presented above (i.e., 0.37 – 0.89 mm/pixel), an error of 8 pixels represents a real-world error of 3.0 to 7.1 mm.

Inter and intra-Class correlations were analyzed using ICC, Intra Class Correlation analysis (McGraw and Wong, 1996). A two-way mixed effect model

$$X_{ij} = \mu + r_i + c_j = \mu_{ij} + e_{ij}$$

μ : population mean, r : row effects, c : column effects, e : residual effects

was used to test the hypotheses that there is no difference between scallop measurements made by the same rater four times, and that there is no difference between individual raters.

ICC Type C-1: Tests the degree of consistency among measurements

$$r = (\text{MSR} - \text{MSE}) / (\text{MSR} + (k-1)*\text{MSE});$$

$$F = (\text{MSR}/\text{MSE}) * (1-r^2)/(1+(k-1)*r^2);$$

$$df1 = n - 1;$$

$$df2 = (n-1)*(k-1);$$

$$p = 1 - \text{fcdf}(F, df1, df2);$$

ANOVA Table					
Source	SS	df	MS	F	Prob>F
Time	143.5	3	47.8	6.28	0.0003
Group	40170.4	3	13390.1	3.36	0.0182
Ineratcion	480.6	9	53.4	7.01	0
Subjects (matching)	4398738.9	1104	3984.4	522.79	0
Error	25241.8	3312	7.6		
Total	4464775.2	4431			

$$r = 0.9842$$

$$LB = 0.9827$$

$$UB = 0.9857$$

$$p = 0$$

ICC Type A-1: Test the degree of absolute agreement among measurements.

$$r = (MSR - MSE) / (MSR + (k-1)*MSE + k*(MSC-MSE)/n);$$

$$a = (k*r0) / (n*(1-r0));$$

$$b = 1 + (k*r0*(n-1))/(n*(1-r0));$$

$$F = MSR / (a*MSC + b*MSE);$$

$$df1 = n - 1;$$

$$df2 = (a*MSC + b*MSE)^2 / ((a*MSC)^2 / (k-1) + (b*MSE)^2 / ((n-1)*(k-1)));$$

$$p = 1 - \text{fcdf}(F, df1, df2);$$

ANOVA Table					
Source	SS	df	MS	F	Prob>F
Time	143.5	3	47.8	6.28	0.0003
Group	40170.4	3	13390.1	3.36	0.0182
Ineratcion	480.6	9	53.4	7.01	0
Subjects (matching)	4398738.9	1104	3984.4	522.79	0
Error	25241.8	3312	7.6		
Total	4464775.2	4431			

$$r = 0.9796$$

$$LB = 0.9695$$

$$UB = 0.9856$$

$$p = 0$$

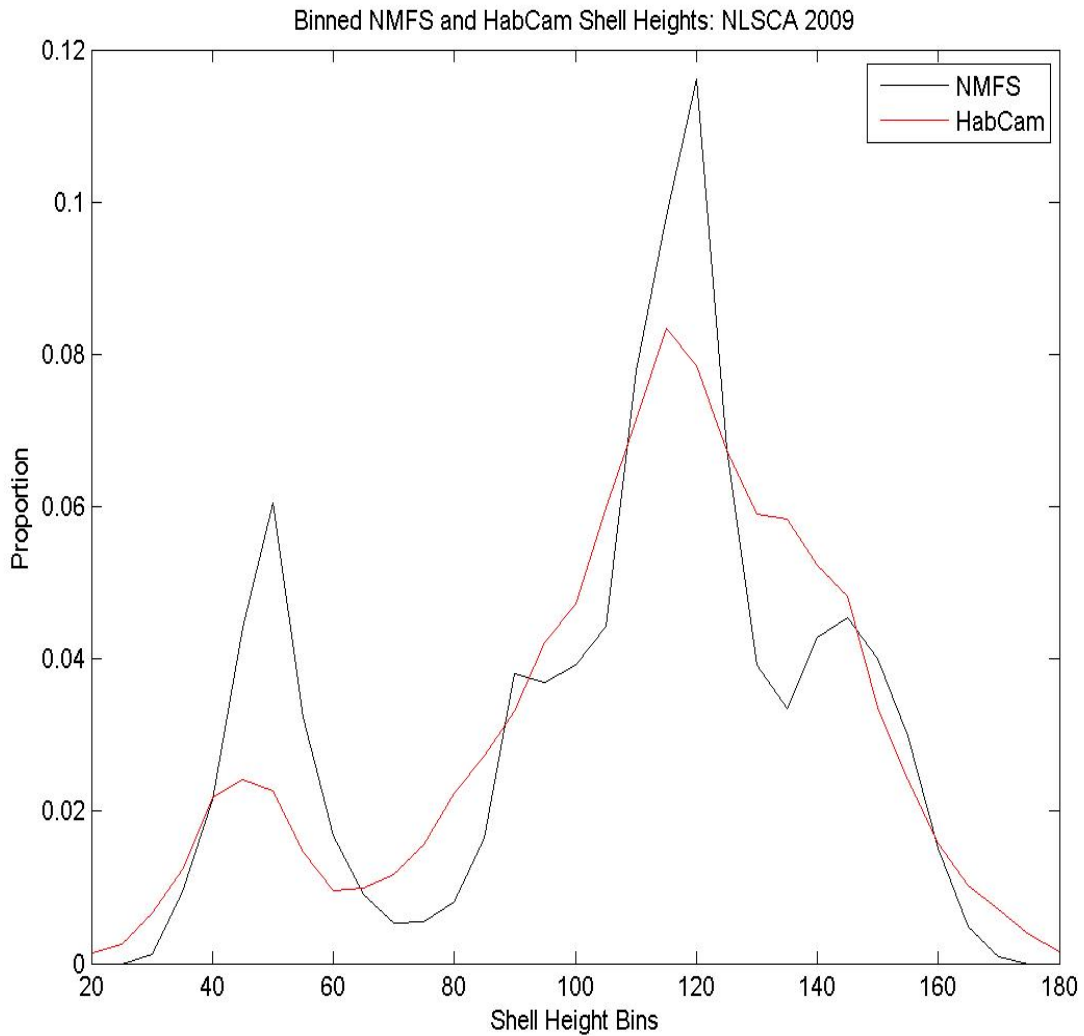
Summary

There is no difference in measurements made by the same individual raters or between individual raters.

Human errors-Analysis of shell height measurement error

Shell height measurements from HabCam images taken during the 2009 Nantucket Lightship survey were compared with shell height measurements made from 12 dredge tows on 2009 Leg 2 of the R/V Hugh Sharp during normal survey operations. The HabCam survey was conducted in early June 2009 while the NMFS survey was conducted in min July, 2009.

Frequency distribution for shell height measurements for HabCam and NMFS dredge survey show surprising similarity in overall pattern (Fig. 38). Since the NMFS survey was conducted about five weeks following the HabCam survey, the shift in mode of the NMFS data for small scallops can be accounted for by growth. The tails of the distribution for HabCam data are spread out more than for the NMFS data suggesting a source of measurement error. There is no indication of selectivity by either sampling approach.



Appendix B9-Figure 38. Shell height size frequency distributions for NMFS (black) and HabCam (red) measurements in the NLSCA. HabCam surveyed in early June while NMFS surveyed in mid July. Note a shift to the right of the mode for small scallops in NMFS data relative to that for HabCam probably due to growth.

Shell heights made from HabCam and NMFS dredge survey were analyzed using the approach described by Jacobson et al. 2010). Accuracy (RMSE, root mean square error) , bias (HabCam-Dredge), and precision (STD) were calculated.

HabCam measurements were positively biased relative to NMFS data by 3.7%. Percentage square root of the mean square error was 3.70%. Both NMFS and HabCam distributions were negatively skewed and more peaked relative to normal distributions.

stat		NMFS		HabCam
n		4,178		13,576
bias		NA		3.8
min		30		20
max		170		180
avg		106.4		110.3
%bias		NA		3.70%
STD		33.4		32.2
CV		31.4		27.90%
RMSE		NA		3.8
% RMSE		NA		3.70%
skewness (g1)		-0.59		-0.66
kurtosis (g2)		2.41		2.98

Summary of error analysis

Measurement error can come from a number of sources including intrinsic error in camera calibration, extrinsic error due to camera orientation and altitude relative to geometric projection on the image plane, and errors associated with human operators measuring scallops on the computer screen. Given the resolution range for varying FOV presented above (i.e., 0.37 – 0.89 mm/pixel), a real world for each source may identified.

Source	+/- mm error
Intrinsic	0.58 – 1.41
Extrinsic	1.11 – 1.78
Within operator	0.5
Between operator	3.0 – 7.1

Clearly, the magnitude of between operator errors dominates the overall potential for measurement error. However, once this source of variability is identified and characterized for each individual technician measuring scallops, a correction factor could be applied for each individual to normalize the results. In addition, automated counting and sizing of scallops and other targets is improving and will eventually be used in conjunction with manual measurements to produce more accurate results.

Appendix B10: Estimation of survey dredge efficiency relative to HabCam.

Tim Miller and Dvora Hart, Northeast Fisheries Science Center, Woods Hole, MA.

Introduction

Using data from a paired-tow calibration experiment, the goal is to estimate the efficiency of the NMFS scallop survey dredge relative to that of the HabCam. The HabCam survey instrument is usually assumed to be 100% efficient so that the absolute efficiency of the survey dredge can be estimated. However, the relative efficiency of the NMFS survey dredge can be estimated without this assumption.

Methods

The data we have to work are for both HabCam and survey dredge at over 140 stations. For the HabCam, we have a number of images of the substrate along a track at each station. For each image, we have the numbers of scallops as well as the estimated area covered by the image. The HabCam captures images continuously along each track, but a thinned subset are used in our analyses. Thinning is intended to make serial correlation of the images within a station negligible. For the dredge, we have the total number of scallops captured at each station as well as an estimate of the swept area.

Statistical models

For these analyses, we consider different probability models for the HabCam and dredge data, but common to all models is our assumption that the expected catch in numbers of the dredge at station i is

$$E(N_{Di} | \delta_{Di}, A_{Di}) = q_D \delta_{Di} A_{Di} \quad (1)$$

and that of the HabCam for photo j at station i is

$$E(N_{Hij} | \delta_{Hij}, A_{Hij}) = q_H \delta_{Hij} A_{Hij} \quad (2)$$

where δ_{Di} and δ_{Hij} are the average density available to the dredge over the entire tow and the average density in the HabCam for image j at station i , and q_D and q_H are the catchabilities for the dredge and HabCam. The respective areas swept by the dredge and in the image j from the HabCam are A_{Di} and A_{Hij} which are assumed known.

The simplest probability model for count data is the Poisson distribution and in gear comparison studies it is common to make use of binomial models which are conditional on the total catch at a given station (e.g., Millar 1992, Lewy et al. 2004). If the density was constant across all of the HabCam images and the dredge, the binomial model would be useful for these data (Appendix B9). However, densities may vary within a station and the numerous HabCam observations at each station allow us to investigate the plausibility of this assumption.

Suppose that each datum for the HabCam and the dredge arises from a Poisson distribution with mean (and variance) given by eqs. 1 and 2, respectively. If we assume the densities for the HabCam photos at station i to be independently and identically distributed as

$$\delta_{Hij} \sim \text{Gamma}(\Delta_i, \tau_{li})$$

where $E(\delta_{Hij}) = \Delta_i$ is the mean density and the variance is $V(\delta_{Hij}) = \Delta_i^2 / \tau_{1i}$, then the catches in each photo arise marginally from a negative binomial distribution with mean and variance

$$E(N_{Hij} | A_{Hij}) = q_H \Delta_i A_{Hij} = \mu_{Hi} A_{Hij}$$

$$V(N_{Hij} | A_{Hij}) = E(N_{Hij}) + E(N_{Hij})^2 / \tau_{1i}$$

where $\mu_{Hi} = q_H \Delta_i$. As the dispersion parameter τ_{1i} increases, the variability in densities within a station decreases and the observed number in the image approaches the Poisson in distribution.

We can also model variability in densities for the dredge,

$$\delta_{Di} \sim \text{Gamma}(\Delta_i, \tau_{2i})$$

so that the marginal distribution of the number caught in the dredge is negative binomial with

$$E(N_{Di}) = q_D \Delta_i A_{Di} = \rho \mu_{Hi} A_{Di}$$

and

$$V(N_{Di}) = E(N_{Di}) + E(N_{Di})^2 / \tau_{2i}.$$

The dispersion parameter for the dredge is distinguishable from that of the HabCam data which allows the variability among the observed average densities in HabCam images to differ from that of the dredge. This model is estimable when there is only a single observation from the dredge at each station because the mean is related to that of the HabCam images by the relative catchability parameter, ρ , which is informed by data from all stations, and because the mean catch per unit area of HabCam images μ_{Hi} is informed by all of the HabCam images at the station. Therefore, the single observation by the dredge can inform the dispersion parameter τ_{2i} .

Note that simpler models where $\Delta_i = \Delta$, $\tau_{1i} = \tau_1$, or $\tau_{2i} = \tau_2$ are special cases.

The relative efficiency of the dredge to the HabCam may differ by substrate type. We observe the substrate in each HabCam image, but the dredge track may cover various substrates which are not directly observed. The lack of these observations for the dredge makes estimation of relative efficiency for specific substrates impossible, but because certain substrates are known to be more prevalent in particular strata, we may consider using these broader regions as proxies that can be used as covariates. As such, we defined three regional indicators for the stations in this study depending on the strata where they occur. Sandy bottom is predominant in the Mid-Atlantic region which includes strata 6130, 6140, 6150, 6180, and 6190 and Georges Bank strata 6460, 6470, 6530, 6540, 6550, 6610, 6621, and 6670 whereas rock and gravel substrates are common in Georges Bank strata 6490, 6500, 6510, 6520, 6651, 6652, 6661, 6662, and 6710. We also formed an alternative set of two regional indicators where the two regions with predominantly sandy bottom were combined.

Model fitting

We fit models using programs in AD Model Builder (ADMB 2009). The likelihood function depends on the assumptions about the parameters and distributions and the parameters were estimated in log-space to avoid boundary conditions.

We restricted the data used for model fitting to stations where there was more than 1 scallop observed in the HabCam images because estimating a positive mean catch per image area at the station is impossible when no scallops are observed. We also removed data for stations where there were less than 2 non-zero counts on HabCam images because fitting negative

binomial models for these data at each station requires a sufficient number of positive observations to provide estimates of uncertainty. Ultimately, we used data from 140 of the 146 stations in the original data set.

During the analyses, we discovered that fitted models where the negative binomial assumption was made at all stations for the HabCam data converged in the parameter space where the Hessian matrix was not positive definite. Upon inspection, several of the station-specific dispersion parameters were estimated at extremely large values which implied that the data at these stations were better treated with a Poisson model. We fit both negative binomial and Poisson models to the HabCam data at each station and compared the fits by AIC_c (Burnham and Andersen 2002) to determine which stations we could assume were Poisson distributed. These results were corroborated by inspection of the magnitude of the estimated quasi-likelihood dispersion parameters and negative binomial dispersion parameters at each station.

The full set of models that we fit to estimate relative efficiency of the dredge is provided in Table 1. In the first, most basic, set of models (P/P), we assume the Poisson distribution for all of the data for the HabCam and the dredge. In the second set of models (P/NBP), the dredge data are Poisson distributed and the HabCam data from each station arise from either a Poisson or negative binomial distribution depending on the AIC_c values of those models at each station. For the third set of models (NBP/NBP), both the dredge and HabCam data at each station are either Poisson or negative binomial distributed based on the AIC_c values of the model fits to the HabCam data. In the last set of models (NB/NBP), all of the dredge data are negative binomial distributed.

Within each set of models we allow different parameterization assumptions for specific models (Table 1). The marginal scallop density at a given station may either be constant or station-specific. The relative efficiency may either be constant, region-specific (substrate proxy), or station-specific. For models with negative binomial assumptions, dispersion parameters for the HabCam data may either be constant or station-specific.

One last model in the NB/NBP set was fit where the negative binomial dispersion parameter for the dredge was allowed to be station-specific, but similar to the HabCam data, there were stations where the dispersion parameter was estimated extremely high and variance estimation was not possible. We assigned Poisson distributions to stations where the dispersion parameter estimates were greater than 1000.

Results

As one would expect, the use of AIC_c to determine whether the Poisson is preferred by station corresponds well to the magnitude of the estimated quasi-likelihood dispersion parameter for the corresponding stations (Figure 1). When the quasi-likelihood dispersion parameter is equal to one, the variance is equal to the mean which is an implicit assumption for the Poisson model. Because the variance is always greater than the mean for the negative binomial model, the Poisson model which is more parsimonious is expected to have a lower AIC_c value if the quasi-likelihood dispersion parameter is approximately equal or less than one. The AIC_c criterion also corresponds well with magnitude of the estimated negative binomial dispersion parameter when that model is fitted (Figure 2). When the negative binomial dispersion parameter is large the data approach Poisson in distribution.

That the negative binomial assumption is better for many stations is also reflected in lower AIC_c values (over all stations) for fitted models that allow it (Table 2). The models where the Poisson distribution is assumed for both the dredge and HabCam observations at all stations had the poorest fits based on AIC_c . The lowest AIC_c value for any P/P model was approximately 10,000 units greater than the best fits among other classes of models that we considered.

Fits for two of the models converged but the Hessian was not positive definite and variance estimation was not possible (NBP/NBP M_5 and NB/NBP M_5). These models were among the best fits with regard to AIC_c , but a model with the Poisson assumption for the dredge data and negative binomial or Poisson assumptions for the HabCam data provided the same maximized log-likelihood with fewer parameters and a positive-definite hessian matrix (P/NBP M_5). Although P/NBP M_5 provided the best fit, it is parameterized with station-specific relative efficiencies which cannot be used to infer the efficiency of the dredge in previous years.

The model with the lowest AIC_c that can be used to infer efficiency of the dredge throughout the time series is NB/NBP M_6 which allowed different relative efficiencies for the regions predominant in gravel and sand. The estimated relative efficiency of the dredge is 0.462 (0.006 SE) in the sandy regions and 0.401 (0.011 SE) in the gravel regions.

Discussion

We found that among the fitted models the best fit was provided by allowing the calibration factors to be station-specific. This was not practical for the uses here in the scallop assessment, but these results imply that there is substantial heterogeneity in the relative efficiency of the dredge. A better model would allow a further hierarchy to describe the variation in the relative efficiency, which is an important avenue of analyses in the future.

Of the applicable models that we fit, the best model allowed different relative efficiencies for the regions with predominantly sandy and gravel substrates. The higher relative efficiency of the dredge in the sandy region is expected because the dredge is intended to operate optimally in finer substrates rather than coarse substrates such as gravel and rock.

Finally, it should be noted that these analyses were carried out with swept areas for the dredge based on nominal tow path estimates. Work carried out concurrent to this study suggests that the true tow path is about 4-10% more than those used here. An additional adjustment to our estimates of survey dredge sampling efficiency may be required in some applications.

References

- ADMB Project. 2009. AD Model Builder: automatic differentiation model builder. Developed by David Fournier and freely available at admb-project.org.
- Burnham, K. P. and Anderson, D. R. 2002. Model selection and multimodel inference: a practical information-theoretic approach. Springer-Verlag, New York.
- Lewy, P., Nielsen, J. R., and Hovgård, H. 2004. Survey gear calibration independent of spatial fish distribution. *Can. J. Fish. Aquat. Sci.* 61: 636–647.
- Millar, R. B. 1992. Estimating the size-selectivity of fishing gear by conditioning on the total catch. *J. Stat. Assoc. Am.* 87: 962-968.

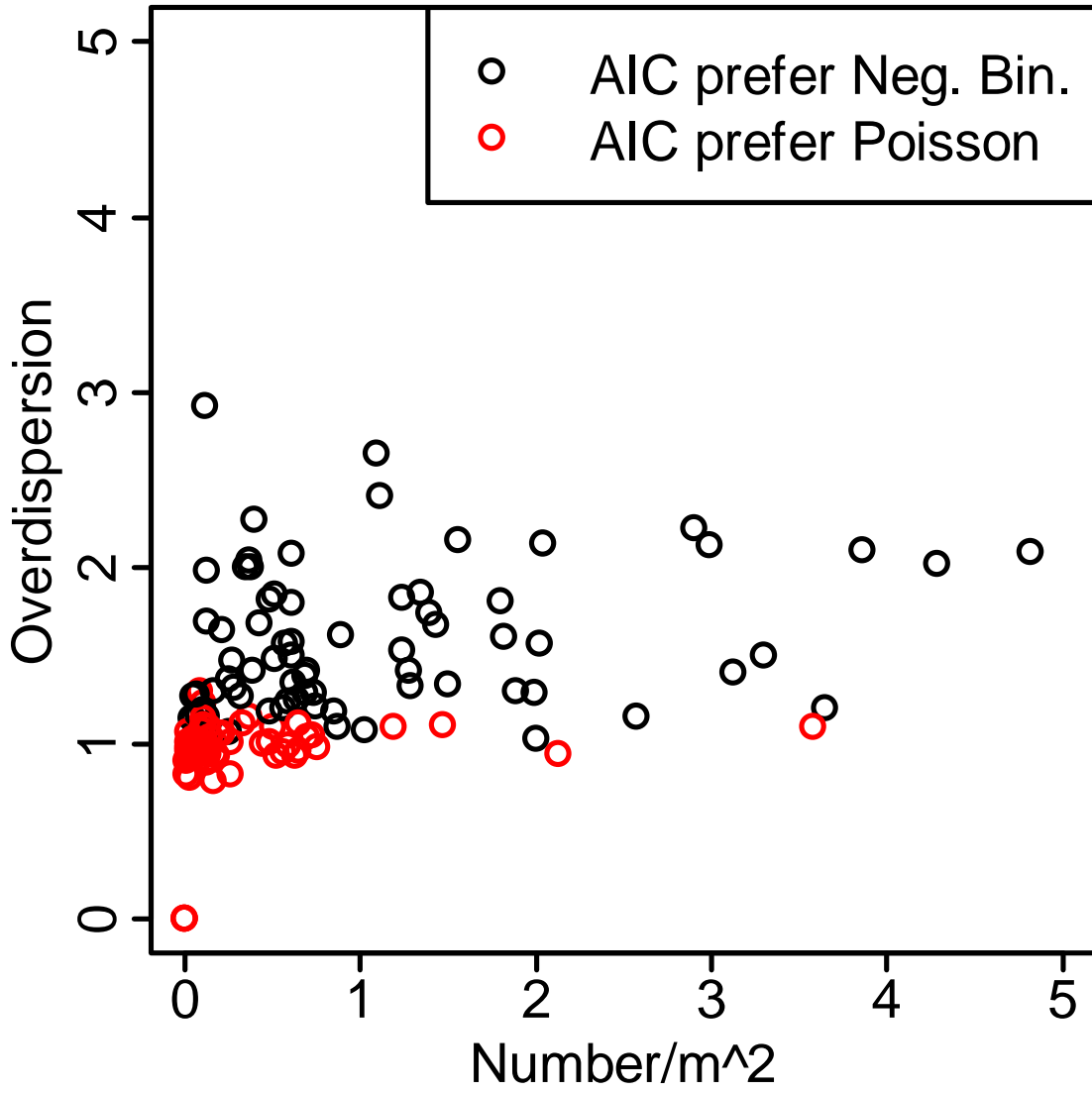
Appendix B10-Table 1. Models fitted to the HabCam and dredge data.

Model	Description	Parameters
P/P M_0	Dredge data and HabCam data are Poisson distributed. Density is constant, relative catchability is constant.	ρ and μ_H
P/P M_1	Dredge data and HabCam data are Poisson distributed. Density is station-specific, relative catchability is constant.	ρ and μ_{Hi}
P/P M_2	Dredge data and HabCam data are Poisson distributed. Density is station-specific, relative catchability is region-specific (Gravel/Sand).	ρ_s and μ_{Hi}
P/P M_3	Dredge data and HabCam data are Poisson distributed. Density is station-specific, relative catchability is region-specific (GB Gravel/GB Sand/MA Sand).	ρ_r and μ_{Hi}
P/P M_4	Dredge data and HabCam data are Poisson distributed. Density is station-specific, relative catchability is station-specific.	ρ_i and μ_{Hi}
P/NBP M_0	Dredge data are Poisson distributed and HabCam data are either Poisson or negative binomial distributed. Density is constant, relative catchability is constant, dispersion is constant	ρ , μ_H , τ_1
P/NBP M_1	Dredge data are Poisson distributed and HabCam data are either Poisson or negative binomial distributed. Density is station-specific, relative catchability is constant, dispersion is constant.	ρ , μ_{Hi} , and τ_1
P/NBP M_2	Dredge data are Poisson distributed and HabCam data are either Poisson or negative binomial distributed. Density is station-specific, relative catchability is constant, dispersion is station-specific.	ρ , μ_{Hi} , and τ_{li}
P/NBP M_3	Dredge data are Poisson distributed and HabCam data are either Poisson or negative binomial distributed. Density is station-specific, relative catchability is region-specific (Gravel/Sand), dispersion is station-specific.	ρ_s , μ_{Hi} , and τ_{li}
P/NBP M_4	Dredge data are Poisson distributed and HabCam data are either Poisson or negative binomial distributed. Density is station-specific, relative catchability is region-specific (GB Gravel/GB Sand/MA Sand), dispersion is station-specific.	ρ_r , μ_{Hi} , and τ_{li}
P/NBP M_5	Dredge data are Poisson distributed and HabCam data are either Poisson or negative binomial distributed. Density is station-specific, relative catchability is station-specific, dispersion is station-specific.	ρ_i , μ_{Hi} , and τ_{li}
NBP/NBP M_0	Dredge data and HabCam data at each station are either Poisson or negative binomial distributed. Density is constant, relative catchability is constant, dispersion parameters are constant.	ρ , μ_H , τ_1 , and τ_2
NBP/NBP M_1	Dredge data and HabCam data at each station are either Poisson or negative binomial distributed. Density is station-specific, relative catchability is constant, dispersion parameters are constant.	ρ , μ_{Hi} , τ_1 , and τ_2
NBP/NBP M_2	Dredge data and HabCam data at each station are either Poisson or negative binomial distributed. Density is station-specific, relative catchability is constant, HabCam dispersion is station-specific, dredge dispersion parameter is constant.	ρ , μ_{Hi} , τ_{li} , and τ_2
NBP/NBP M_3	Dredge data and HabCam data at each station are either Poisson or negative binomial distributed with a common dispersion parameter. Density is station-specific, relative catchability is region-specific (Gravel/Sand), HabCam dispersion is station-specific, dredge dispersion parameter is constant.	ρ_s , μ_{Hi} , τ_{li} , and τ_2
NBP/NBP M_4	Dredge data and HabCam data at each station are either Poisson or negative binomial distributed with a common dispersion parameter. Density is station-specific, relative catchability is region-specific (GB Gravel/GB Sand/MA Sand), HabCam dispersion is station-specific,	ρ_r , μ_{Hi} , τ_{li} , and τ_2

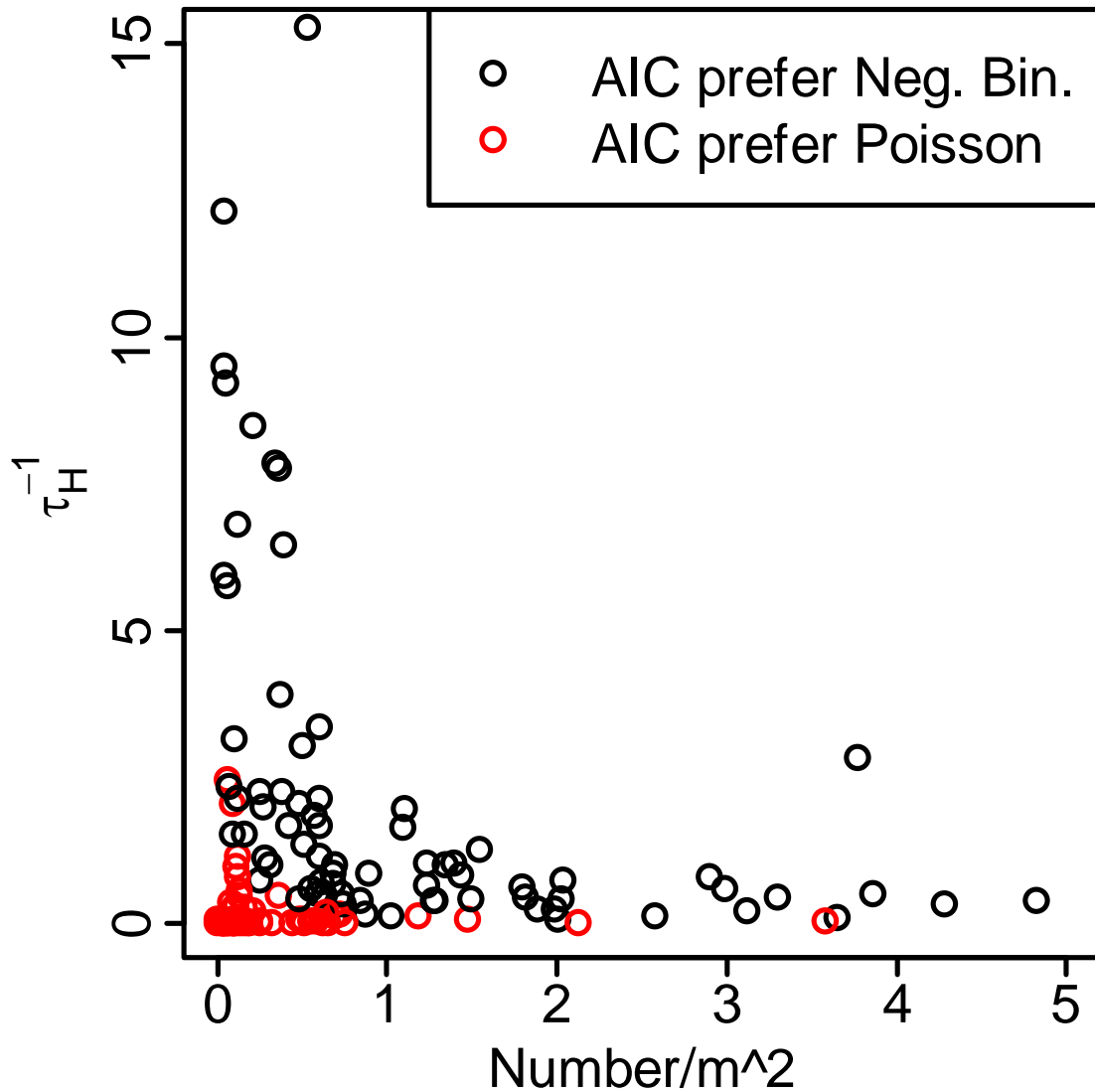
	dredge dispersion parameter is constant.	
NBP/NBP M_5	Dredge data and HabCam data at each station are either Poisson or negative binomial distributed. Density is station-specific, relative catchability is station-specific, HabCam dispersion is station-specific, dredge dispersion parameter is constant.	ρ_i , μ_{Hi} , τ_{li} , and τ_2
NB/NBP M_0	Dredge data are negative binomial distributed and HabCam data are either Poisson or negative binomial distributed. Density is constant, relative catchability is constant, dispersion parameters are constant	ρ , μ_H , τ_1 , and τ_2
NB/NBP M_1	Dredge data are negative binomial distributed and HabCam data are either Poisson or negative binomial distributed. Density is station-specific, relative catchability is constant, dispersion parameters are constant.	ρ , μ_{Hi} , τ_1 , and τ_2
NB/NBP M_2	Dredge data are negative binomial distributed and HabCam data are either Poisson or negative binomial distributed. Density is station-specific, relative catchability is constant, HabCam dispersion is station-specific, dredge dispersion parameter is constant.	ρ , μ_{Hi} , τ_{li} , and τ_2
NB/NBP M_3	Dredge data are negative binomial distributed and HabCam data are either Poisson or negative binomial distributed. Density is station-specific, relative catchability is region-specific (Gravel/Sand), HabCam dispersion is station-specific, dredge dispersion parameter is constant.	ρ_s , μ_{Hi} , τ_{li} , and τ_2
NB/NBP M_4	Dredge data are negative binomial distributed and HabCam data are either Poisson or negative binomial distributed. Density is station-specific, relative catchability is region-specific (GB Gravel/GB Sand/MA Sand), HabCam dispersion is station-specific, dredge dispersion parameter is constant.	ρ_r , μ_{Hi} , τ_{li} , and τ_2
NB/NBP M_5	Dredge data are negative binomial distributed and HabCam data are either Poisson or negative binomial distributed. Density is station-specific, relative catchability is station-specific, HabCam dispersion is station-specific, dredge dispersion parameter is constant.	ρ_i , μ_{Hi} , τ_{li} , and τ_2
NB/NBP M_6	Dredge data are either Poisson or negative binomial distributed and HabCam data are either Poisson or negative binomial distributed. Density is station-specific, relative catchability is region-specific (Gravel/Sand), HabCam dispersion is station-specific, dredge dispersion parameter is station-specific.	ρ_s , μ_{Hi} , τ_{li} , and τ_{2i}

Appendix B10-Table 2. Number of parameters, maximized log-likelihood value and AIC_c for each fitted model. Log-likelihood and AIC_c values are in parentheses for models without invertible hessian matrices.

Model	No. Parameters	Log-Likelihood	AIC_c
P/P M_0	2	-278,850.0	557,704.0
P/P M_1	141	-72,019.1	144,320.8
P/P M_2	142	-71,581.8	143,448.2
P/P M_3	143	-71,578.9	143,444.4
P/P M_4	280	-62,693.0	125,948.5
P/NBP M_0	3	-250,341.0	500,688.0
P/NBP M_1	142	-63,288.6	126,861.8
P/NBP M_2	242	-60,667.5	121,820.8
P/NBP M_3	243	-60,511.4	121,510.7
P/NBP M_4	244	-60,503.0	121,495.9
P/NBP M_5	381	-57,444.1	115,654.8
NBP/NBP M_0	4	-94,524.7	189,057.4
NBP/NBP M_1	143	-58,743.3	117,773.2
NBP/NBP M_2	243	-57,932.3	116,352.5
NBP/NBP M_3	244	-57,924.1	116,338.1
NBP/NBP M_4	245	-57,918.5	116,328.9
NBP/NBP M_5	382	(-57,444.1)	(115,656.8)
NB/NBP M_0	4	-78,974.0	157,956.0
NB/NBP M_1	143	-58,706.5	117,699.6
NB/NBP M_2	243	-57,895.1	116,278.1
NB/NBP M_3	244	-57,893.8	116,277.5
NB/NBP M_4	245	-57,893.7	116,279.3
NB/NBP M_5	382	(-57,444.1)	(115,656.8)
NB/NBP M_6	315	-57,730.5	116,094.1



Appendix B10-Figure 1. Estimated overdispersion and mean observed number/m² from fitted quasi-likelihood model for HabCam count data at each station with log link. Red points indicate that the Poisson model was preferred based on AIC_c.



Appendix B10-Figure 2. Estimated (inverse) negative binomial dispersion parameter and mean observed number/m² for HabCam count data at each station. Red points indicate that the Poisson model was preferred based on AIC_c.

Appendix B11: Technical documentation for the CASA length structured stock assessment model.

Larry Jacobson, Northeast Fisheries Science Center, Woods Hole, MA.

[This technical description is current through CASA version nc238 used for the SARC50 sea scallop assessment.]

The stock assessment model described here is based on Sullivan et al.'s (1990) CASA model.⁵ CASA is entirely length-based with population dynamic calculations in terms of the number of individuals in each length group during each year. Age is almost completely irrelevant in model calculations. Unlike many other length-based stock assessment approaches, CASA is a dynamic, non-equilibrium model based on a forward simulation approach. CASA incorporates a very wide range of data with parameter estimation based on maximum likelihood. CASA can incorporate prior information about parameters such as survey catchability and natural mortality in a quasi-Bayesian fashion and MCMC evaluations are practical. The implementation described here was programmed in AD-Model Builder (Otter Research Ltd).⁶

Population dynamics

Time steps in the model are years, which are also used to tabulate catch and other data. Recruitment occurs at the beginning of each time step. All instantaneous rates in model calculations are annual (y^{-1}). The number of years in the model n_y is flexible and can be changed easily (e.g. for retrospective analyses) by making a single change to the input data file. Millimeters are used to measure body size (e.g. sea scallop shell heights). Length-weight relationships should generally convert millimeters to grams. Model input data include a scalar that is used to convert the units for length-weight parameters (e.g. grams) to the units of the biomass estimates and landings data (e.g. mt). The units for catch and biomass are usually metric tons.

The definition of length groups (or length “bins”) is a key element in the CASA model and length-structured stock assessment modeling in general. Length bins are identified in CASA output by their lower bound and internally by their ordinal number. Calculations requiring information about length (e.g. length-weight) use the mid-length ℓ_j of each bin. The user specifies the first length (L_{min}) and the size of length bins (L_{bin}). Based on these specifications, the model determines the number of length bins to be used in modeling as $n_L = 1 + \text{int}[(L_\infty - L_{min})/L_{bin}]$, where L_∞ is maximum asymptotic size based on a von Bertalanffy growth curve supplied by the user, and $\text{int}[x]$ is the integer part of x . The last length bin in the model is always a “plus-group” containing individuals L_∞ and larger. Specifications for length data used in tuning the model are separate (see below).

⁵ Original programming in AD-Model Builder by G. Scott Boomer and Patrick J. Sullivan (Cornell University), who bear no responsibility for errors in the current implementation.

⁶ AD-Model Builder can be used to calculate variances for any estimated or calculated quantity in a stock assessment model, based on the Hessian matrix with “exact” derivatives and the delta method.

Growth

Growth is modeled in CASA using annual and/or monthly growth transition matrices supplied by the user. There are three options. Under option 1, the model ignores seasonal growth and calculated annual growth based on an annual growth transition matrix. Option 2 is similar but the annual growth matrix is constructed internally based on raw growth increments in the input file. Under option 3, monthly growth transition matrices from the input files are used in a variety of calculations (e.g. in tuning to body size composition data). Options 1 or 2 (annual growth only) are recommended at this time because of unresolved problems in using Option 3 with seasonal growth).

In population dynamics calculations, individuals in each size group grow (or not) at the beginning of the year, based on the annual growth transition matrix $P_0(b,a)$ which measures the probability that a survivor in size bin a at the beginning of the previous year will grow to bin b at the beginning of the current year (columns index initial size and rows index subsequent size).⁷ Growth probabilities do not include any adjustments for mortality and are applied to surviving scallops based on their original size in the preceding year.

Seasonal growth patterns are accommodated in some calculations under Option 3 (see above). Each CASA model data file contains 13 growth matrices: one matrix for annual growth (January 1 to December 31) and one matrix for growth to the middle of each month (e.g. January 1 to mid-February, January 1 to mid-March, etc.). Growth matrices are identified using the subscripts 0 to 12, where 0 is for the annual growth matrix, 1 for growth between January 1 and mid-February, 2 is for growth between January 1 and mid-March, etc. Under Option 3, in fitting to survey size composition data as an example, the program decides which growth matrix to use based on the Julian date of the survey. The monthly growth matrices are ignored under growth Options 1. All input growth matrices are ignored under Option 2 when the annual growth matrix is calculated internally based on raw shell increment data. Under Option 2:

$$P_0(b,a) = \frac{n(b|a)}{\sum_{j=a}^{n_t} n(j|a)}$$

where $n(b|a)$ is the number of individuals that started at size a and grew to size b after one year in the raw size increment data.

Age is not considered in model calculations, although age may be inferred during output calculations assuming an underlying von Bertalanffy growth curve. Two von Bertalanffy growth parameters (L_∞ and K) are included in model input. The growth parameter L_∞ is not estimable in the current model because it is used in defining length bins prior to the parameter estimation phase.⁸ The von Bertalanffy growth parameter K is implemented as an estimable parameter but should not be estimated because it has no effect on the objective function in the model.

The input file contains information equivalent to the von Bertalanffy growth parameter t_0 (hypothetical size at age zero) but this information does not affect the objective function in the model. Instead of entering t_0 , the user enters the size at some specified age. In other words, the

⁷ For clarity in bookkeeping, mortality and annual growth calculations are always based on the size on January 1.

⁸ “Estimable” means a potentially estimable parameter that is specified as a variable that may be estimated in the CASA computer program. In practice, estimability depends on the available data and other factors. It may be necessary to fix certain parameters at assumed fix values or to use constraints of prior distributions for parameters that are difficult to estimate, particularly if data are limited.

user should input any age $a \geq 0$ and the corresponding a at age a on January 1. The conventional von Bertalanffy t_0 parameter is then calculated:

$$t_0 = \ln(1 - L/L_\infty) / K + a$$

Note that the calculated $t_0 = t_0$ if $a=0$ and $L=t_0$.

Abundance, recruitment and mortality

Population abundance in each length bin during the first year of the model is:

$$N_{1,L} = N_1 \pi_{1,L}$$

where L is the size bin, and $\pi_{1,L}$ is the initial population length composition expressed as

proportions so that $\sum_{L=1}^{n_L} \pi_L = 1$. $N_1 = e^\eta$ is total abundance at the beginning of the first modeled

year and η is an estimable parameter. It is not necessary to estimate recruitment in the first year because recruitment is implicit in the product of N_1 and π_L . The current implementation of CASA takes the initial population length composition as data supplied by the user, typically based on survey size composition data and a preliminary estimate of survey size-selectivity.

Abundance at length in years after the first is calculated:

$$\vec{N}_{y+1} = P_0 (\vec{N}_y \circ \vec{S}_y) + \vec{R}_{y+1}$$

where \vec{N}_y is a vector (length n_L) of abundance in each length bin during year y , P_0 is the matrix ($n_L \times n_L$) of annual growth probabilities $P_0(\mathbf{b}, \mathbf{a})$, \vec{S}_y is a vector of length-specific survival fractions for year y , \circ is the operator for an element-wise product, and \vec{R}_y is a vector holding length-specific abundance of new recruits at the beginning of year y .

Survival fractions are:

$$S_{y,L} = e^{-Z_{y,L}} = e^{-(M_{y,L} + F_{y,L} + I_{y,L})}$$

where $Z_{y,L}$ is the total instantaneous mortality rate and $M_{y,L}$ is the instantaneous rate for natural mortality (see below). Length-specific fishing mortality rates are $F_{y,L} = F_y s_{y,L}$ where $s_{y,L}$ is the size-specific selectivity⁹ for fishing in year y (scaled to a maximum of one at fully recruited size groups), F_y is the fishing mortality rate on fully selected individuals. Fully recruited fishing mortality rates are $F_y = e^{\phi + \delta_y}$ where ϕ is an estimable parameter for the log of the geometric mean of fishing mortality in all years, and δ_y is an estimable “dev” parameter.¹⁰ The instantaneous rate for “incidental” mortality ($I_{y,L}$) accounts for mortality due to contact with the fishing gear that does not result in any catch on deck (see below).¹¹ The degree of variability in dev parameters for fishing mortality, natural mortality and for other variables can be controlled by specifying variances or likelihood weights $\neq 1$, as described below.

⁹ In this context, “selectivity” describes the combined effects of all factors that affect length composition of catch or landings. These factors include gear selectivity, spatial overlap of the fishery and population, size-specific targeting, size-specific discard, etc.

¹⁰ Dev parameters are a special data type for estimable parameters in AD-Model Builder. Each set of dev parameters (e.g. for all recruitments in the model) is constrained to sum to zero. Because of the constraint, the sums $\phi + \delta_y$ involving $n_y + 1$ terms amount to only n_y parameters.

¹¹ See the section on per recruit modeling below for formulas used to relate catch, landings and incidental mortality.

Natural mortality rates $M_{y,L} = u_L e^{\zeta + \xi_y}$ may vary from year to year and by length.

Variability among length groups is based on a user-specified vector \bar{u} that describes the relative natural mortality rate for each length group in the model. The user supplies a value for each length group which the model rescales so that the average of all of the values is one (i.e. \bar{u} is set by the user and cannot be estimated). Temporal variability in natural mortality rates are modeled in the same manner as temporal variability in fishing mortality. In particular, ζ is an estimable parameter measuring the mean log natural mortality rate during all years and ξ_y is an estimable year-specific dev parameter. Several approaches are available for estimating natural mortality parameters (i.e. natural mortality covariates and surveys that measure numbers of dead individuals, see below).

Incidental mortality $I_{y,L} = F_y u_L i$ is the product of fully recruited fishing mortality (F_y , a proxy for effective fishing effort, although nominal fishing effort might be a better predictor of incidental mortality), relative incidental mortality at length (u_L) and a scaling parameter i , both of which are supplied by the user and not estimable in the model. Incidental mortality at length is supplied by the user as a vector (\bar{u}) containing a value for each length group in the model. The model rescales the relative mortality vector so that the mean of the series is one.

Given abundance in each length group, natural mortality, and fishing mortality, predicted fishery catch-at-length in numbers is:

$$C_{y,L} = \frac{F_{y,L} (1 - e^{-Z_{y,L}}) N_{L,y}}{Z_{y,L}}$$

Total catch number during each year is $C_y = \sum_{j=1}^{n_L} C_{y,L}$. Catch data (in weight, numbers or as

length composition data) are understood to include landings (L_y) and discards (d_y) but to exclude losses to incidental mortality (i.e. $C_y = L_y + d_y$).

Discard data are supplied by the user in the form of discarded biomass in each year or a discard rate for each year (or a combination of biomass levels and rates). In the current model, discards have the same selectivity as landed catch and size composition data for discards are not included in the input file.¹² It is important to remember that discard rates in CASA are defined the ratio of discards to landings (d/L). The user may also specify a mortal discard fraction between zero and one if some discards survive. If the discard fraction is less than one, then the discarded biomass and discard rates in the model are reduced correspondingly. See the section on per recruit modeling below for formulas used to relate catch, landings and incidental mortality.

Recruitment (the sum of new recruits in all length bins) at the beginning of each year after the first is calculated:

$$Ry = e^{\rho + \gamma_y}$$

where ρ is an estimable parameter that measures the geometric mean recruitment and the γ_y are estimable dev parameters that measure inter-annual variability in recruitment. As with natural mortality devs, the user specified variance or likelihood weight $\neq 1$ can be used to help estimate recruitment deviations (see below).

¹² The model will be modified in future to model discards and landing separately, and to use size composition data for discards.

Proportions of recruits in each length group are calculated based on a beta distribution $B(w,r)$ over the first n_r length bins that is constrained to be concave down.¹³ Proportions of new recruits in each size group are the same from year to year. Beta distribution coefficients must be larger than one for the shape of the distribution to be unimodal. Therefore, $w=1+e^\omega$ and $r=1+e^\rho$, where ω and ρ are estimable parameters. It is presumably better to calculate the parameters in this manner than as bounded parameters because there is likely to be less distortion of the Hessian for w and r values close to one and parameter estimation is likely to be more efficient.

Surplus production during each year of the model can be computed approximately from biomass and catch estimates (Jacobson et al., 2002):

$$P_t = B_{t+1} - B_t + C_t$$

In future versions of the CASA model, surplus production will be more accurately calculated by projecting the population at the beginning of the year forward one year assuming only natural mortality.

Weight at length¹⁴

The assumed body weight for size bins except the last is calculated using user-specified length-weight parameters and the middle of the size group. Different length-weight parameters are used for the population and for the commercial fishery. Mean body weight in the last size bin is read from the input file and can vary from year to year. Typically, mean weight in the last size bin for the population would be computed based on survey length composition data for large individuals and the population length-weight relationship. Mean weight in the last size bin for the fishery would be computed in the same manner based on fishery size composition data.

In principle, these calculations could be carried out in the model itself because all of the required information is available. In practice, it seems better to do the calculations externally and supply them to the model as inputs because of decisions that typically have to be made about smoothing the estimates and years with missing data.

Population summary variables

Total abundance at the beginning of the year is the sum of abundance at length $N_{y,L}$ at the beginning of the year. Average annual abundance for a particular length group is:

$$\bar{N}_{y,L} = N_{y,L} \frac{1 - e^{-Z_{y,L}}}{Z_{y,L}}$$

The current implementation of the assessment model assumes different weight-at-length relationships for the stock and the fishery. Average stock biomass is computed using the population weight at length information.

Total stock biomass is:

$$B_y = \sum_{L=1}^{n_L} N_{y,L} w_L$$

¹³ Standard beta distributions used to describe recruit size distributions and in priors are often constrained to be unimodal in the CASA model. Beta distributions $B(w,r)$ with mean $\mu = w/(w+r)$ and variance

$\sigma^2 = wr/[(w+r)^2(w+r+1)]$ are unimodal when $w > 1$ and $r > 1$. See

http://en.wikipedia.org/wiki/Beta_distribution for more information.

¹⁴ Model input data include a scalar that is used to convert the units for length-weight parameters (e.g. grams) to the units of the biomass estimates and landings data (e.g. mt).

where w_L is weight at length for the population on January 1. Total catch weight is:

$$W_y = \sum_{L=1}^{n_L} C_{y,L} w'_L$$

where w'_L is weight at length in the fishery.

F_y estimates for two years are comparable only when the fishery selectivity in the model was the same in both years. A simpler exploitation index is calculated for use when fishery selectivity changes over time:

$$U_y = \frac{C_y}{\sum_{j=x}^{n_L} N_{y,L}}$$

where x is a user-specified length bin (usually at or below the first bin that is fully selected during all fishery selectivity periods). U_y exploitation indices from years with different selectivity patterns may be relatively comparable if x is chosen carefully.

Spawner abundance in each year is (T_y) is computed:

$$T_y = \sum_{L=1}^{n_L} N_{y,L} e^{-\tau z_y} g_L$$

Where $0 \leq \tau \leq 1$ is the fraction of the year elapsed before spawning occurs (supplied by the user). Maturity at length (g_L) is from an ascending logistic curve:

$$g_L = \frac{1}{1 + e^{a-bL}}$$

with parameters a and b supplied by the user. Spawner biomass is computed using the population length-weight values.

Egg production (S_y) in each year is computed:

$$S_y = \sum_{L=1}^{n_L} N_{y,L} e^{-\tau z_y} g_L x_L$$

where:

$$x_L = cL^v$$

Where the fecundity parameters (c and v) for fecundity are supplied by the user. Fecundity parameters per se include no adjustments for maturity or survival. They should represent reproductive output for a spawner of given size.

Fishery and survey selectivity

The current implementation of CASA includes six options for calculating fishery and survey selectivity patterns. Fishery selectivity may differ among “fishery periods” defined by the user. Selectivity patterns that depend on length are calculated using lengths at the mid-point of each bin (ℓ). After initial calculations (described below), selectivity curves are rescaled to a maximum value of one.

Option 1 is a flat with $s_L=1$ for all length bins. Option 2 is an ascending logistic curve:

$$s_{y,\ell} = \frac{1}{1 + e^{A_y - B_y \ell}}$$

Option 3 is an ascending logistic curve with a minimum asymptotic minimum size for small size bins on the left.

$$s_{y,\ell} = \left(\frac{1}{1 + e^{A_Y - B_Y \ell}} \right) (1 - D_y) + D_y$$

Option 4 is a descending logistic curve:

$$s_{y,\ell} = 1 - \frac{1}{1 + e^{A_Y - B_Y \ell}}$$

Option 5 is a descending logistic curve with a minimum asymptotic minimum size for large size bins on the right:

$$s_{y,\ell} = \left(1 - \frac{1}{1 + e^{A_Y - B_Y \ell}} \right) (1 - D_y) + D_y$$

Option 6 is a double logistic curve used to represent “domed-shape” selectivity patterns with highest selectivity on intermediate size groups:

$$s_{y,\ell} = \left(\frac{1}{1 + e^{A_Y - B_Y \ell}} \right) \left(1 - \frac{1}{1 + e^{D_Y - G_Y \ell}} \right)$$

The coefficients for selectivity curves A_Y , B_Y , D_Y and G_Y carry subscripts for time because they may vary between fishery selectivity periods defined by the user. All options are parameterized so that the coefficients A_Y , B_Y , D_Y and G_Y are positive. Under options 3 and 5, D_Y is a proportion that must lie between 0 and 1.

Depending on the option, estimable selectivity parameters may include α , β , δ and γ . For options 2, 4 and 6, $A_Y = e^{\alpha_Y}$, $B_Y = e^{\beta_Y}$, $D_Y = e^{\delta_Y}$ and $G_Y = e^{\gamma_Y}$. Options 3 and 5 use the same conventions for A_Y and B_Y , however, the coefficient D_Y is a proportion estimated as a logit-transformed parameter (i.e. $\delta_Y = \ln[D_Y/(1-D_Y)]$) so that:

$$D_Y = \frac{e^{\delta_Y}}{1 + e^{\delta_Y}}$$

The user can choose, independently of all other parameters, to either estimate each fishery selectivity parameter or to keep it at its initial value. Under Option 2, for example, the user can estimate the intercept α_Y , while keep the slope β_Y at its initial value.

Per recruit modeling

The per recruit model in CASA uses the same population model as in other model calculations under conditions identical to the last year in the model. It is a standard length-based approach except that discard and incidental mortality are accommodated in all calculations. In per recruit calculations, fishing mortality rates and associated yield estimates are understood to include landings and discard mortality, but to exclude incidental mortality. Thus, landings per recruit L are:

$$L = \frac{C}{(1 + \Delta)}$$

where C is total catch (yield) per recruit and Δ is the ratio of discards D to landings in the last year of the model. Discards per recruit are calculated:

$$D = \Delta L$$

Losses due to incidental mortality (G) are calculated:

$$G = \frac{I(1 - e^{-Z})B}{Z}$$

$$= IK$$

where $I = Fu$ is the incidental mortality rate, u is a user-specified multiplier (see above) and B is stock biomass per recruit. Note that $C = FK$ so that $K = C/F$. Then,

$$G = \frac{FuC}{F}$$

$$G = uC$$

The model will estimate a wide variety ($F_{\%SBR}$, F_{max} and $F_{0.1}$) of per recruit model reference points as parameters. For example,

$$F_{\%SBR} = e^{\theta_j}$$

where $F_{\%SBR}$ is the fishing mortality reference point that provides a user specified percentage of maximum SBR. θ_j is the model parameter for the j^{th} reference point.

A complete per recruit output table is generated in all model runs that can be used for evaluating the shape of YPR and SBR curves, including the existence of particular reference points. Per recruit reference points are time consuming to estimate and it is usually better to estimate them after other more important population dynamics parameters are estimated. Phase of estimation can be controlled individually for %SBR, F_{MAX} and $F_{0.1}$ so that per recruit calculations can be delayed as long as possible. If the phase is set to zero or a negative integer, then the reference point will not be estimated. As described below, estimation of F_{max} always entails an additional phase of estimation. For example, if the phase specified for F_{max} is 2, then the parameter will be estimated initially in phase 2 and finalized the last phase (phase ≥ 3). This is done so that the estimate from phase 2 can be used as an initial value in a slightly different goodness of fit calculation during the latter phase.

Per recruit reference points should have no effect on other model estimates. Residuals (calculated – target) for %SBR, $F_{0.1}$ and F_{max} reference points should always be very close to zero. Problems may arise, however, if reference points (particularly F_{max}) fall on the upper bound for fishing mortality. In such cases, the model will warn the user and advise that the offending reference points should not be estimated. *It is good practice to run CASA with reference point calculations turned on and then off to see if biomass and fishing mortality estimates change.*

The user specifies the number of estimates required and the target %SBR level for each. For example, the target levels for four %SBR reference points might be 0.2, 0.3, 0.4 and 0.5 to estimate $F_{20\%}$, $F_{30\%}$, $F_{40\%}$ and $F_{50\%}$. The user has the option of estimating F_{max} and/or $F_{0.1}$ as model parameters also but it is not necessary to supply target values.

Tuning and goodness of fit

There are two steps in calculating the negative log likelihood (NLL) used to measure how well the model fits each type of data. The first step is to calculate the predicted values for data. The second step is to calculate the NLL of the data given the predicted value. The overall goodness of fit measure for the model is the weighted sum of NLL values for each type of data and each constraint:

$$\Lambda = \sum \lambda_j L_j$$

where λ_j is a weighting factor for data set j (usually $\lambda_j=1$, see below), and L_j is the NLL for the data set. The NLL for a particular data is itself is usually a weighted sum:

$$L_j = \sum_{i=1}^{n_j} \psi_{j,i} L_{j,i}$$

where n_j is the number of observations, $\psi_{j,i}$ is an observation-specific weight (usually $\psi_{j,i}=1$, see below), and $L_{j,i}$ is the NLL for a single observation.

Maximum likelihood approaches reduce the need to specify *ad-hoc* weighting factors (λ and ϕ) for data sets or single observations, because weights can often be taken from the data (e.g. using CVs routinely calculated for bottom trawl survey abundance indices) or estimated internally along with other parameters. In addition, robust maximum likelihood approaches (see below) may be preferable to simply down-weighting an observation or data set. However, despite subjectivity and theoretical arguments against use of *ad-hoc* weights, it is often useful in practical work to manipulate weighting factors, if only for sensitivity analysis or to turn an observation off entirely. Observation specific weighting factors are available for most types of data in the CASA model.

Missing data

Availability of data is an important consideration in deciding how to structure a stock assessment model. The possibility of obtaining reliable estimates will depend on the availability of sufficient data. However, NLL calculations and the general structure of the CASA model are such that missing data can usually be accommodated automatically. With the exception of catch data (which must be supplied for each year, even if catch was zero), the model calculates that NLL for each datum that is available. No NLL calculations are made for data that are not available and missing data do not generally hinder model calculations.

Likelihood kernels

Log likelihood calculations in the current implementation of the CASA model use log likelihood “kernels” or “concentrated likelihoods” that omit constants. The constants can be omitted because they do not affect slope of the NLL surface, final point estimates for parameters or asymptotic variance estimates.

For data with normally distributed measurement errors, the complete NLL for one observation is:

$$L = \ln(\sigma) + \ln(\sqrt{2\pi}) + 0.5 \left(\frac{x - u}{\sigma} \right)^2$$

The constant $\ln(\sqrt{2\pi})$ can always be omitted. If the standard deviation is known or assumed known, then $\ln(\sigma)$ can be omitted as well because it is a constant that does not affect derivatives. In such cases, the concentrated NLL is:

$$L = 0.5 \left(\frac{x - \mu}{\sigma} \right)^2$$

If there are N observations with possible different variances (known or assumed known) and possibly different expected values:

$$L = 0.5 \sum_{i=1}^N \left(\frac{x_i - \mu_i}{\sigma_i} \right)^2$$

If the standard deviation for a normally distributed quantity is not known and is estimated (implicitly or explicitly) by the model, then one of two equivalent calculations is used. Both approaches

assume that all observations have the same variance and standard deviation. The first approach is used when all observations have the same weight in the NLL:

$$L = 0.5N \ln \left[\sum_{i=1}^N (x_i - u)^2 \right]$$

The second approach is equivalent but used when the weights for each observation (w_i) may differ:

$$L = \sum_{i=1}^N w_i \left[\ln(\sigma) + 0.5 \left(\frac{x_i - u}{\sigma} \right)^2 \right]$$

In the latter case, the maximum likelihood estimator:

$$\hat{\sigma} = \sqrt{\frac{\sum_{i=1}^N (x_i - \hat{x})^2}{N}}$$

(where \hat{x} is the average or predicted value from the model) is used explicitly for σ . The maximum likelihood estimator is biased by $N/(N-d_f)$ where d_f is degrees of freedom for the model. The bias may be significant for small sample sizes, which are common in stock assessment modeling, but d_f is usually unknown.

If data x have lognormal measurement errors, then $\ln(x)$ is normal and L is calculated as above. In some cases it is necessary to correct for bias in converting arithmetic scale means to log scale means (and *vice-versa*) because $\bar{x} = e^{\bar{\chi} + \sigma^2/2}$ where $\chi = \ln(x)$. It is often convenient to convert arithmetic scale CVs for lognormal variables to log scale standard deviations using $\sigma = \sqrt{\ln(1 + CV^2)}$.

For data with multinomial measurement errors, the likelihood kernel is:

$$L = n \sum_{i=1}^n p_i \ln(\theta_i) - K$$

where n is the known or assumed number of observations (the “effective” sample size), p_i is the proportion of observations in bin i , and θ_i is the model’s estimate of the probability of an observation in the bin. For surveys, θ_i is adjusted for mortality up to the date of the survey and for growth up to the mid-point of the month in which the survey occurs. For fisheries, θ_i accommodates all of the mortality during the current year and is adjusted for growth during January 1 to mid-July. The constant K is used for convenience to make L easier to interpret. It measures the lowest value of L that could be achieved if the data fit matched the model’s expectations exactly:

$$K = n \sum_{i=1}^n p_i \ln(p_i)$$

For data x that have measurement errors with expected values of zero from a gamma distribution:

$$L = (\gamma - 1) \ln \left(\frac{x}{\beta} \right) - \frac{x}{\beta} - \ln(\beta)$$

where $\beta > 0$ and $\gamma > 0$ are gamma distribution parameters in the model. For data that lie between zero and one with measurement errors from a beta distribution:

$$L = (p - 1) \ln(x) + (q - 1) \ln(1 - x)$$

where $p > 0$ and $q > 0$ are parameters in the model.

In CASA model calculations, distributions are usually described in terms of the mean and CV. Normal, gamma and beta distribution parameters can be calculated mean and CV by the method of moments.¹⁵ Means, CV's and distributional parameters may, depending on the situation, be estimated in the model or specified by the user.

The NLL for a datum x from gamma distribution is:

$$L = (1 - k) * \ln(x) + \frac{x}{\theta} + \ln[\Gamma(k)] + k \ln(\theta)$$

where k is the shape parameter and θ is the scale parameter. The last two terms on the right are constants and can be omitted if k and θ are not estimated. Under these circumstances,

$$L = (1 - k) * \ln(x) + \frac{x}{\theta}$$

Robust methods

Goodness of fit for survey data may be calculated using a “robust” maximum likelihood method instead of the standard method that assumes lognormal measurement errors. The robust method may be useful when survey data are noisy or include outliers.

Robust likelihood calculations in CASA assume that measurement errors are from a Student's t distribution with user-specified degrees of freedom d_f . Degrees of freedom are specified independently for each observation so that robust calculations can be carried out for as many (or as few) cases as required. The t distribution is similar to the normal distribution for $d_f \geq 30$. As d_f is reduced, the tails of the t distribution become fatter so that outliers have higher probability and less effect on model estimates. If $d_f = 0$, then measurement errors are assumed in the model to be normally distributed.

The first step in robust NLL calculations is to standardize the measurement error residual $t = (x - \bar{x})/\sigma$ based on the mean and standard deviation. Then:

$$L = \ln \left(1 + \frac{t^2}{d_f} \right) \left(1 - \frac{1 - d_f}{2} \right) - \frac{\ln(d_f)}{2}$$

Catch weight data

Catch data (landings plus discards) are assumed to have normally distributed measurement errors with a user specified CV. The standard deviation for catch weight in a particular year is $\sigma_y = \kappa \hat{C}_y$, where “^” indicates that the variable is a model estimate and errors in catch are assumed to be normally distributed. The standardized residual used in computing NLL for a single catch observation and in making residual plots is $r_y = (C_y - \hat{C}_y) / \sigma_y$.

¹⁵ Parameters for standard beta distributions $B(w,r)$ with mean $\mu = w/(w+r)$ and variance

$\sigma^2 = wr / [(w+r)^2(w+r+1)]$ are calculated from user-specified means and variances by the method of moments. In particular, $w = \mu[\mu(1-\mu)/\sigma^2 - 1]$ and $r = (1-\mu)[\mu(1-\mu)/\sigma^2 - 1]$. Not all combinations of μ and σ^2 are feasible. In general, a beta distribution exists for combinations of μ and σ^2 if $0 < \mu < 1$ and $0 < \sigma^2 < \mu(1-\mu)$. Thus, for a user-specified mean μ between zero and one, the largest feasible variance is $\sigma^2 < \mu(1-\mu)$. These conditions are used in the model to check user-specified values for μ and σ^2 . See http://en.wikipedia.org/wiki/Beta_distribution for more information.

Specification of landings, discards, catch

Landings, discard and catch data are in units of weight and are for a single or “composite” fishery in the current version of the CASA model. The estimated fishery selectivity is assumed to apply to the discards so that, in effect, the length composition of catch, landings and discards are the same.

Discards are from external estimates (d_t) supplied by the user. If $d_t \geq 0$, then the data are used as the ratio of discard to landed catch so that:

$$D_t = L_t \Delta_t$$

where $\Delta_t = D_t/L_t$ is the ratio of discard and landings (a.k.a. d/K ratios) for each year. If $d_t < 0$ then the data are treated as discard in units of weight:

$$D_t = \text{abs}(d_t).$$

In either case, total catch is the sum of discards and landed catch ($C_t = L_t + D_t$). It is possible to use discards in weight $d_t < 0$ for some years and discard as proportions $d_t > 0$ for other years in the same model run.

If catches are estimated (see below) so that the estimated catch \hat{C}_t does not necessarily equal observed landings plus discard, then estimated landings are computed:

$$\hat{L}_t = \frac{\hat{C}_t}{1 + \Delta_t}$$

Estimated discards are:

$$\hat{D}_t = \Delta_t \hat{L}_t.$$

Note that $\hat{C}_t = \hat{L}_t + \hat{D}_t$ as would be expected.

Fishery length composition data

Data describing numbers or relative numbers of individuals at length in catch data (fishery catch-at-length) are modeled as multinomial proportions $c_{y,L}$:

$$c_{y,L} = \frac{C_{y,L}}{\sum_{j=1}^{n_L} C_{y,j}}$$

The NLL for the observed proportions in each year is computed based on the kernel for the multinomial distribution, the model’s estimate of proportional catch-at-length (\hat{c}_y) and an estimate of effective sample size ${}^c N_y$ supplied by the user. Care is required in specifying effective sample sizes, because catch-at-length data typically carry substantially less information than would be expected based on the number of individuals measured. Typical conventions make ${}^c N_y \leq 200$ (Fournier and Archibald, 1982) or set ${}^c N_y$ equal to the number of trips or tows sampled (Pennington et al., 2002). Effective sample sizes are sometimes chosen based on goodness of fits in preliminary model runs (Methot, 2000; Butler et al., 2003).

Standardized residuals are not used in computing NLL fishery length composition data. However, approximate standardized residuals $r_y = (c_{y,L} - \hat{c}_{y,L})/\sigma_{y,L}$ with standard deviations

$\sigma_{y,L} = \sqrt{\hat{c}_{y,L}(1 - \hat{c}_{y,L})/{}^c N_y}$ based on the theoretical variance for proportions are computed for use in making residual plots.

Survey index data

In CASA model calculations, “survey indices” are data from any source that reflect relative proportional changes in an underlying population state variable. In the current version, surveys may measure stock abundance at a particular point in time (e.g. when a survey was carried out), stock biomass at a particular point in time, or numbers of animals that dies of natural mortality during a user-specified period. For example, the first option is useful for bottom trawl surveys that record numbers of individuals, the second option is useful for bottom trawl surveys that record total weight, and the third option is useful for survey data that track trends in numbers of animals that died due to natural mortality (e.g. survey data for sea scallop “clappers”). Survey data that measure trends in numbers dead due to natural mortality can be useful in modeling time trends in natural mortality. In principle, the model will estimate model natural mortality and other parameters so that predicted numbers dead and the index data match in either relative or absolute terms.

In the current implementation of the CASA model, survey indices are assumed to be linear indices of abundance or biomass so that changes in the index (apart from measurement error) are assumed due to proportional changes in the population. Nonlinear commercial catch rate data are handled separately (see below). Survey index and fishery length composition data are handled separately from trend data (see below). Survey data may or may not have corresponding length composition information.

In general, survey index data give one number that summarizes some aspect of the population over a wide range of length bins. Selectivity parameters measure the relative contribution of each length bin to the index. Options and procedures for estimating survey selectivity patterns are the same as for fishery selectivity patterns, but survey selectivity patterns are not allowed to change over time.

NLL calculations for survey indices use predicted values calculated:

$$\hat{I}_{k,y} = q_k A_{k,y}$$

where q_k is a scaling factor for survey index k , and $A_{k,y}$ is stock available to the survey. The scaling factor is computed using the maximum likelihood estimator:

$$q_k = e^{\frac{\sum_{i=1}^{N_k} \left[\frac{\ln\left(\frac{I_{k,i}}{A_{k,i}}\right)}{\sigma_{k,i}^2} \right]}{\sum_{j=1}^{N_k} \left(\frac{1}{\sigma_{k,j}^2} \right)}}$$

where N_k and $\sigma_{k,j}^2$ is the log scale variance corresponding to the assumed CV for the survey observation.¹⁶

Available stock for surveys measuring trends in abundance or biomass is calculated:

$$A_{k,y} = \sum_{L=1}^{n_L} s_{k,L} N_{y,L} e^{-Z_{y,L} \tau_{k,y}}$$

¹⁶ Scaling factors in previous versions were calculated $q_s = e^{\varpi_s}$ where ϖ_s is an estimable and survey-specific parameter. However, prior distributions were shown to have a strong effect on the parameters such that the relationship $N=qA$ did not hold. The approach in the current model avoids this problem.

where $s_{k,L}$ is size-specific selectivity of the survey, $\tau_{k,y}=J_{k,y}/365$, $J_{k,y}$ is the Julian date of the survey in year y , and $e^{-Z_y\tau_{k,y}}$ is a correction for mortality prior to the survey. Available biomass is calculated in the same way except that body weights w_L are included in the product on the right hand side.

Available stock for indices that track numbers dead by natural mortality is:

$$A_{k,y} = \sum_{L=1}^{n_L} s_{k,L} \tilde{M}_{y,L} \bar{N}_{y,L}$$

where $\bar{N}_{y,L}$ is average abundance during the user-specified period of availability and $\tilde{M}_{y,L}$ is the instantaneous rate of natural mortality for the period of availability. Average abundance during the period of availability is:

$$\bar{N}_{y,L} = \frac{\tilde{N}_{y,L} (1 - e^{-\tilde{Z}_{y,L}})}{\tilde{Z}_{y,L}}$$

where $\tilde{N}_{y,L} = N_{y,L} e^{-Z\Delta}$ is abundance at elapsed time of year $\Delta = \tau_{k,y} - \nu_k$, $\nu_k = j_k / 365$, and j_k is the user-specified duration in days for the period of availability. The instantaneous rates for total $\tilde{Z}_{y,L} = Z_{y,L} (\tau_{k,y} - \nu_k)$ and natural $\tilde{M}_{y,L} = M_{y,L} (\tau_{k,y} - \nu_k)$ mortality are also adjusted to correspond to the period of availability. In using this approach, the user should be aware that the length based selectivity estimated by the model for the dead animal survey ($s_{k,L}$) is conditional on the assumed pattern of length-specific natural mortality (\bar{u}) which was specified as data in the input file.

NLL calculations for survey index data assume that log scale measurement errors are either normally distributed (default approach) or from a t distribution (robust estimation approach). In either case, log scale measurement errors are assumed to have mean zero and log scale standard errors either estimated internally by the model or calculated from the arithmetic CVs supplied with the survey data.

The standardized residual used in computing NLL for one survey index observation is $r_{k,y} = \ln(I_{k,y} / \hat{I}_{k,y}) / \sigma_{k,y}$ where $I_{k,y}$ is the observation. The standard deviations $\sigma_{k,y}$ will vary among surveys and years if CVs are used to specify the variance of measurement errors. Otherwise a single standard deviation is estimated internally for the survey as a whole.

Survey length composition data

Length bins for fishery and survey length composition data are flexible and the flexibility affects goodness of fit calculations in ways that may be important to consider in some applications. The user specifies the starting size (bottom of first bin) and number of bins used for each type of fishery and survey length composition. The input data for each length composition record identifies the first/last length bins to be used and whether they are plus groups that should include all smaller/larger length groups in the data and population model when calculating goodness of fit. Goodness of fit calculations are carried out over the range of lengths specified by the user. Thus length data in the input file may contain large or small size bins that are ignored in goodness of fit calculations. As described above, the starting size and bin size for the population model are specified separately. In the ideal and simplest case, the

minimum size and same length bins are used for the population and for all length data. However, as described below, length specifications in data and the population model may differ.

For example, the implicit definitions of plus groups in the model and data may differ. If the first bin used for length data is a plus group, then the first bin will contain the sum of length data from the corresponding and smaller bins of the original length composition record. However, the first bin in the population model is never a plus group. Thus, predicted values for a plus group will contain the sum of the corresponding and smaller bins in the population. The observed and predicted values will not be perfectly comparable if the starting sizes for the data and population model differ. Similarly, if the last bin in the length data is a plus group, it will contain original length composition data for the corresponding and all larger bins. Predicted values for a plus group in the population will be the sum for the corresponding bin and all larger size groups in the population, implicitly including sizes $> L_{\infty}$. The two definitions of the plus group will differ and goodness of fit calculation may be impaired if the original length composition data does not include all of the large individuals in samples.

In the current version of the CASA model, the size of length composition bins must be $\geq L_{bin}$ in the population model (this constraint will be removed in later versions). Ideally, the size of data length bins is the same or a multiple of the size of length bins in the population. However, this is not required and the model will prorate the predicted population composition for each bin into adjacent data bins when calculating goodness of fit. With a 30-34 mm population bin and 22-31 and 32-41 mm population bins, for example, the predicted proportion in the population bin would be prorated so that 2/5 was assigned to the first data bin and 3/5 was assigned to the second data bin. This proration approach is problematic when it is used to prorate the plus group in the population model into two data bins because it assumes that abundance is uniform over lengths within the population group. The distribution of lengths in a real population might be far from uniform between the assumed upper and lower bounds of the plus group.

The first bin in each length composition data record must be $\geq L_{min}$ which is the smallest size group in the population model. If the last data bin is a plus group, then the *lower* bound of the last data bin must be \leq the upper bound of the last population bin. Otherwise, if the last data bin is not a plus group, the *upper* bound of the last data bin must be \leq the upper bound of the population bin.

NLL calculations for survey length composition data are similar to calculations for fishery length composition data. Surveys index data may measure trends in stock abundance or biomass but survey length composition data are always for numbers (not weight) of individuals in each length group. Survey length composition data represent a sample from the true stock which is modified by survey selectivity, sampling errors and, if applicable, errors in recording length data. For example, with errors in length measurements, individuals belonging to length bin j , are mistakenly assigned to adjacent length bins $j-2, j-1, j+1$ or $j+2$ with some specified probability. Well-tested methods for dealing with errors in length data can be applied if some information about the distribution of the errors is available (e.g. Methot 2000).

Prior to any other calculations, observed survey length composition data are converted to multinomial proportions:

$$i_{k,y,L} = \frac{n_{k,y,L}}{\sum_{j=L_{k,y}^{first}}^{L_{k,y}^{last}} n_{k,y,j}}$$

where $n_{k,y,j}$ is an original datum and $i_{k,y,L}$ is the corresponding proportion. As described above, the user specifies the first $L_{k,y}^{first}$ and last $L_{k,y}^{last}$ length groups to be used in calculating goodness of fit for each length composition and specifies whether the largest and smallest groups should be treated as “plus” groups that contain all smaller or larger individuals.

Using notation for goodness of fit survey index data (see above), predicted length compositions for surveys that track abundance or biomass are calculated:

$$A_{k,y,L} = \frac{s_{k,L} N_{y,L} e^{-Z_{y,j} \tau_{k,y}}}{\sum_{L=L_{k,y}^{first}}^{L_{k,y}^{last}} s_{k,L} N_{y,L} e^{-Z_{y,j} \tau_{k,y}}}$$

Predicted length compositions for surveys that track numbers of individuals killed by natural mortality are calculated:

$$A_{k,y} = \frac{s_{k,L} \tilde{M}_{y,L} \bar{N}_{y,L}}{\sum_{L=L_{k,y}^{first}}^{L_{k,y}^{last}} s_{k,L} \tilde{M}_{y,L} \bar{N}_{y,L}}$$

Considering the possibility of structured measurement errors, the expected length composition $\bar{A}'_{k,y}$ for survey catches is:

$$\bar{A}'_{k,y} = \bar{A}_{k,y} \mathbf{E}_k$$

where \mathbf{E}_k is an error matrix that simulates errors in collecting length data by mapping true length bins in the model to observed length bins in the data.

The error matrix \mathbf{E}_k has n_L rows (one for each true length bin) and n_L columns (one for each possible observed length bin). For example, row k and column j of the error matrix gives the conditional probability $P(k|j)$ of being assigned to bin k , given that an individual actually belongs to bin j . More generally, column j gives the probabilities that an individual actually belonging to length bin j will be recorded as being in length bins $j-2, j-1, j, j+1, j+2$ and so on. The columns of \mathbf{E}_k add to one to account for all possible outcomes in assigning individuals to observed length bins. \mathbf{E}_k is the identity matrix if there are no structured measurement errors. In CASA, the probabilities in the error matrix are computed from a normal distribution with mean zero and $CV = e^{\pi_k}$, where π_k is an estimable parameter. The normal distribution is truncated to cover a user-specified number of observed bins (e.g. 3 bins on either side of the true length bin).

The NLL for observed proportions at length in each survey and year is computed with the kernel for a multinomial distribution, the model's estimate of proportional survey catch-at-length ($\hat{i}_{k,y,L}$) and THE effective sample size ${}^L N_y$ supplied by the user. Standardized residuals for residual plots are computed as for fishery length composition data.

Effective sample size for length composition data

Effective sample sizes that are specified by the user are used in goodness of fit calculations for survey and fishery length composition data. A post-hoc estimate of effective sample size can be calculated based on goodness of fit in a model run (Methot 1989). Consider the variance of residuals for a single set of length composition data with N bins used in calculations. The variance of the sum based on the multinomial distribution is:

$$\sigma^2 = \sum_{j=1}^N \left[\frac{\hat{p}_j(1 - \hat{p}_j)}{\varphi} \right]$$

where φ is the effective sample size for the multinomial and \bar{p}_j is the predicted proportion in the j^{th} bin from the model run. Solve for φ to get:

$$\varphi = \frac{\sum_{j=1}^N [\hat{p}_j(1 - \hat{p}_j)]}{\sigma^2}$$

The variance of the sum of residuals can also be calculated:

$$\sigma^2 = \sum_{j=1}^N (p_j - \hat{p}_j)^2$$

This formula is approximate because it ignores the traditional correction for bias. Substitute the third expression into the second to get:

$$\varphi = \frac{\sum_{j=1}^N [\hat{p}_j(1 - \hat{p}_j)]}{\sum_{k=1}^N (p_j - \hat{p}_j)^2}$$

which can be calculated based on model outputs. The assumed and effective sample sizes will be similar in a reasonable model when the assumed sample sizes are approximately correct. Effective sample size calculations can be used iteratively to manually adjust input values to reasonable levels (Methot 1989).

Variance constraints on dev parameters

Variability in dev parameters (e.g. for natural mortality, recruitment or fishing mortality) can be limited using variance constraints that assume the deviations are either independent or that they are autocorrelated and follow a random walk. When a variance constraint for independent

deviations is activated, the model calculates the NLL for each log scale residual γ_y / σ_γ , where γ_y

is a dev parameter and σ is a log-scale standard deviation. If the user supplies a positive value for the arithmetic scale CV, then the NLL is calculated assuming the variance is known.

Otherwise, the user-supplied CV is ignored and the NLL is calculated with the standard deviation estimated internally. Calculations for autocorrelated deviations are the same except

that the residuals are $(\gamma_y - \gamma_{y-1}) / \sigma_\gamma$ and the number of residuals is one less than the number of dev parameters.

LPUE data

Commercial landings per unit of fishing effort (LPUE) data are modeled in the current implementation of the CASA model as a linear function of average biomass available to the fishery, and as a nonlinear function of average available abundance. The nonlinear relationship with abundance is meant to reflect limitations in “shucking” capacity for sea scallops.¹⁷ Briefly, tows with large numbers of scallops require more time to sort and shuck and therefore reduce LPUE from fishing trips when abundance is high. The effect is exaggerated when the catch is composed of relatively small individuals. In other words, at any given level of stock biomass, LPUE is reduced as the number of individuals in the catch increases or, equivalently, as the mean size of individuals in the catch is reduced.

Average available abundance in LPUE calculations is:

$${}^a\bar{N}_y = \sum_{L=1}^{n_L} s_{y,L} \bar{N}_{y,L}$$

and average available biomass is:

$${}^a\bar{B}_y = \sum_{L=1}^{n_L} s_{y,L} w_L^f \bar{N}_{y,L}$$

where the weights at length w_L^f are for the fishery rather than the population. Predicted values for LPUE data are calculated:

$$\hat{L}_y = \frac{{}^a\bar{B}_y \eta}{\sqrt{\phi^2 + {}^a\bar{N}_y^2}}$$

Measurement errors in LPUE data are assumed normally distributed with standard deviations $\sigma_y = CV_y \hat{L}_y$. Standardized residuals are $r_y = (L_y - \hat{L}_y) / \sigma_y$.

Per recruit (SBR and YPR) reference points¹⁸

The user specifies a target %SBR value for each reference point that is estimated. Goodness of fit is calculated as the sum of squared differences between the target %SBR and %SBR calculated based on the reference point parameter. Except in pathological situations, it is always possible to estimate %SBR reference point parameters so that the target and calculated %SBR levels match exactly. Reference point parameters should have no effect on other model estimates and the residual (calculated – target %SBR) should always be very close to zero. Goodness of fit for $F_{0.1}$ estimates is calculated in a manner similar to %SBR reference points. Goodness of fit is calculated as the squared difference between the slope of the yield curve at the estimate and one-tenth of the slope at the origin. Slopes are computed numerically using central differences if possible or one-sided (right hand) differences if necessary.

¹⁷ D. Hart, National Marine Fisheries Service, Northeast Fisheries Science Center, Woods Hole, MA, pers. comm.

¹⁸ This approach is not currently estimated because of performance problems. The user can, however, estimate per recruit reference point from a detailed table written in the main output file (nc.rep). However, variances are not available in the table.

F_{max} is estimated differently in preliminary and final phases. In preliminary phases, goodness of fit for F_{max} is calculated as $(1/Y)^2$, where Y is yield per recruit at the current estimate of F_{max} . In other words, yield per recruit is maximized by finding the parameter estimate that minimizes its inverse. This preliminary approach is very robust and will find F_{max} if it exists. However, it involves a non-zero residual $(1/Y)$ that interferes with calculation of variances and might affect other model estimates. In final phases, goodness of fit for F_{max} is calculated as (d^2) where d is the slope of the yield per recruit curve at F_{max} . The two approaches give the same estimates of F_{MAX} but the goodness of fit approach used in the final phases has a residual of zero (so that other model estimates are not affected) and gives more reasonable variance estimates. The latter goodness of fit calculation is not used during initial phases because the estimates of F_{MAX} tend to “drift down” the right hand side of the yield curve in the direction of decreasing slope. Thus, the goodness of fit calculation used in final phases works well only when the initial estimate of F_{MAX} is very close to the best estimate.

Per recruit reference points should have little or no effect on other model estimates. Problems may arise, however, if reference points (particularly F_{max}) fall on the upper bound for fishing mortality. In such cases, the model will warn the user and advise that the offending reference points should not be estimated. *It is good practice to run CASA with and without reference point calculations to ensure that reference points do not affect other model estimates including abundance, recruitments and fishing mortality rates.*

Growth data

Growth data in CASA consist of records giving initial length, length after one year of growth, and number of corresponding observations. Growth data may be used to help estimate growth parameters that determine the growth matrix P . The first step is to convert the data for each starting length to proportions:

$$P(b,a) = \frac{n(b,a)}{\sum_{j=n_L-b+1}^{n_L} n(j,a)}$$

where $n(b,a)$ is the number of individuals starting at size a that grew to size b after one year. The NLL is computed assuming that observed proportions $p(a|b)$ at each starting size are a sample from a multinomial distribution with probabilities given by the corresponding column in the models estimated growth matrix P . The user must specify an effective sample size ${}^P N_j$ based, for example, on the number of observations in each bin or the number of individuals contributing data to each bin. Observations outside bin ranges specified by the user are ignored. Standardized residuals for plotting are computed based on the variance for proportions.

Survey gear efficiency data

Survey gear efficiency for towed trawls and dredges is the probability of capture for individuals anywhere in the water column or sediments along the path swept by the trawl. Ideally, the area surveyed and the distribution of the stock coincides so that:

$$I_{k,y} = q_k B_{k,y}$$

$$q_k = \frac{a_k e_k u_k}{A}$$

$$e_k = \frac{A q_k}{a_k u_k}$$

$$K_t = \frac{A}{a_k u_k}$$

$$e_k = K_t q_t$$

Where $I_{k,y}$ is a survey observation in units equivalent to biomass (or numerical) density (e.g. kg per standard tow), $B_{k,y}$ is the biomass (or abundance) available to the survey, A is the area of the stock, a_k is the area swept during one tow, $0 < e_k \leq 1$ is efficiency of the survey gear, and u_k is a constant that adjusts for different units.

Efficiency estimates from studies outside the CASA model may be used as prior information in CASA. The user supplies the mean and CV for the prior estimate of efficiency, along with estimates of A_k , a_k and u_k . At each iteration if the model, the gear efficiency implied by the current estimate of q_k is computed. The model then calculates the NLL of the implied efficiency estimate assuming it was sampled from a unimodal beta distribution with the user-specified mean and CV.

If efficiency estimates are used as prior information (if the likelihood weight $\lambda > 0$), then it is very important to make sure that units and values for the survey data (I), biomass or abundance (B), stock area (A), area per tow (a), and adjustments for units (u) are correct (see Example 1). The units for biomass are generally the same as the units for catch data. In some cases, incorrect specifications will lead to implied efficiency estimates that are ≤ 0 or ≥ 1 which have zero probability based on a standard beta distribution used in the prior. The program will terminate if $e \leq 0$. If $e \geq 1$ during an iteration, then e is set to a value slightly less than one and a penalty is added to the objective function. In some cases, incorrect specifications will generate a cryptic error that may have a substantial impact on estimates.

Implied efficiency estimates are useful as a model diagnostic even if very little prior information is available because some model fits may imply unrealistic levels of implied efficiency. The trick is to down weight the prior information (e.g. $\lambda = 1e^{-6}$) so that the implied efficiency estimate has very little effect on model results as long as $0 < e < 1$. Depending on the situation, model runs with e near a bound indicate that estimates may be implausible. In addition, it may be useful to use a beta distribution for the prior that is nearly a uniform distribution by specifying a prior mean of 0.5 and variance slightly less than $1/12 = 0.083333$.

Care should be taken in using prior information from field studies designed to estimate survey gear efficiency. Field studies usually estimate efficiency with respect to individuals on the same ground (e.g. by sampling the same grounds exhaustively or with two types of gear). It seems reasonable to use an independent efficiency estimate and the corresponding survey index to estimate abundance in the area surveyed. However, stock assessment models are usually applied to the entire stock, which is probably distributed over a larger area than the area covered by the survey. Thus the simple abundance calculation based on efficiency and the survey index will be biased low for the stock as a whole. In effect, efficiency estimates from field studies tend to be biased high as estimates of efficiency relative to the entire stock.

Maximum fishing mortality rate

Stock assessment models occasionally estimate absurdly high fishing mortality rates because abundance estimates are too small. The NLL component used to prevent this potential problem is:

$$L = \lambda \sum_{t=0}^N (d_t^2 + q^2)$$

where:

$$d_t = \begin{cases} Ft - \Phi & \text{if } Ft > \Phi \\ 0 & \text{otherwise} \end{cases}$$

and

$$q_t = \begin{cases} \ln(Ft / \Phi) & \text{if } Ft > \Phi \\ 0 & \text{otherwise} \end{cases}$$

with the user-specified threshold value Φ set larger than the largest value of F_t that might possibly be expected (e.g. $\Phi=3$). The weighting factor λ is normally set to a large value (e.g. 1000).

References

- J.L. Butler, L.D. Jacobson, J.T. Barnes, and H.G. Moser. 2003. Biology and population dynamics of cowcod (*Sebastes levis*) in the southern California Bight. Fish. Bull. 101: 260-280.
- Fournier, D., and Archibald, CP. 1982. General theory for analyzing catch at age data. Can. J. Fish. Aquat. Sci. 39: 1195-1207.
- Jacobson, L.D., Cadrin, S.X., and J.R. Weinberg. 2002. Tools for estimating surplus production and F_{MSY} in any stock assessment model. N. Am. J. Fish. Mgmt. 22: 326-338.
- Methot, R. D. 2000. Technical description of the stock synthesis assessment program. NOAA Tech. Memo. NMFS-NWFSC-43: 1-46.
- Pennington, M., Burmeister, L-M., and Hjellvik, V. 2002. Assessing the precision of frequency distributions estimated from trawl-survey samples. Fish. Bull. 100: 74-80.
- Press, W.H., Flannery, B.P., S.A. Teukolsky, and W.T. Vetterling. 1990. Numerical recipes. Cambridge Univ. Press, NY.
- Sullivan, P.J., Lai, H.L., and Gallucci, V.F. 1990. A catch-at-length analysis that incorporates a stochastic model of growth. Can. J. Fish. Aquat. Sci. 47: 184-198.

Appendix B12: Forecasting methodology (SAMS model).

Dvora Hart, Northeast Fisheries Science Center, Woods Hole, MA.

The model presented here is a version of the SAMS (Scallop Area Management Simulator) model used to project sea scallop abundance and landings as an aid to managers since 1999. Subareas were chosen to coincide with current management. In particular, Georges Bank was divided into four open areas (two portions of the South Channel, Northern Edge and Peak, and Southeast Part), the three access portions of the groundfish closures, and the three no access portions of these areas. The Mid-Atlantic was subdivided into six areas: Virginia Beach, Delmarva, the Elephant Trunk Closed Area, the Hudson Canyon South Access Area, New York Bight, and Long Island.

Methods

The model tracks population vectors $\mathbf{p}(i,t) = (p_1, p_2, \dots, p_n)$, where $p_j(i,t)$ represents the density of scallops in the j th size class in area i at time t . The model uses a difference equation approach, where time is partitioned into discrete time steps t_1, t_2, \dots , with a time step of length $\Delta t = t_{k+1} - t_k$. The landings vector $\mathbf{h}(i,t_k)$ represents the catch at each size class in the i th region and k th time step. It is calculated as:

$$h(i,t_k) = [I - \exp(\Delta t H(i,t_k))] p(i,t_k),$$

where I is the identity matrix and H is a diagonal matrix whose j th diagonal entry h_{jj} is given by:

$$h_{jj} = 1/(1 + \exp(s_0 - s_1 * s))$$

where s is the shell height of the mid-point of the size-class.

The landings $L(i,t_k)$ for the i th region and k th time step are calculated using the dot product of landings vector $\mathbf{h}(i,t_k)$ with the vector $\mathbf{m}(i)$ representing the vector of meat weights at shell height for the i th region:

$$L(i,t_k) = A_i \mathbf{h}(i,t_k) \bullet \mathbf{m}(i) / (w e_i)$$

where e_i represents the dredge efficiency in the i th region, and w is the tow path area of the survey dredge (estimated as $8/6076 \text{ nm}^2$).

Even in the areas not under special area management, fishing mortalities tend not to be spatially uniform due to the sessile nature of sea scallops (Hart 2001). Fishing mortalities in open areas were determined by a simple “fleet dynamics model” that estimates fishing mortalities in open areas based on area-specific exploitable biomasses, and so that the overall DAS or open-area F matches the target. Based on these ideas, the fishing mortality F_i in the i th region is modeled as:

$$F_i = \mathbf{k} * \mathbf{f}_i * \mathbf{B}_i$$

where B_i is the exploitable biomass in the i th region, f_i is an area-specific adjustment factor to take into account preferences for certain fishing grounds (due to lower costs, shorter steam times, ease of fishing, habitual preferences, etc.), and k is a constant adjusted so that the total DAS or fishing mortality meets its target. For these simulations, $f_i = 1$ for all areas.

Scallops of shell height less than a minimum size s_d are assumed to be discarded, and suffer a discard mortality rate of d . Discard mortality was estimated in NEFSC (2004) to be 20%. There is also evidence that some scallops not actually landed may suffer mortality due to incidental damage from the dredge. Let F_L be the landed fishing mortality rate and F_I be the rate of incidental mortality. For Georges Bank, which is a mix of sandy and hard bottom, we used $F_I = 0.2F_L$. For the Mid-Atlantic (almost all sand), we used $F_I = 0.1F_L$.

Growth in each subarea was specified by a growth transition matrix G , based on area-specific growth increment data. Recruitment was modeled stochastically, and was assumed to be log-normal in each subarea. The mean, variance and covariance of the recruitment in a subarea was set to be equal to that observed in the historical time-series between 1979-2008. New recruits enter the first size bin at each time step at a rate r_i depending on the subarea i , and stochastically on the year. These simulations assume that recruitment is a stationary process, i.e., no stock-recruitment relationship is assumed. This may underestimate recruitment in the Mid-Atlantic if the recent strong recruitment there are due to a stock-recruit relationship.

The population dynamics of the scallops in the present model can be summarized in the equation:

$$p(i, t_{k+1}) = \rho_i + G \exp(-M\Delta t H) p(i, t_k),$$

where ρ_i is a random variable representing recruitment in the i th area. The model was run with 10 time steps per year. The population and harvest vectors are converted into biomass by using the shell-height meat-weight relationship:

$$W = \exp[a + b \ln(s)],$$

where W is the meat weight of a scallop of shell height s . For calculating biomass, the shell height of a size class was taken as its midpoint.

Commercial landing rates (LPUE, landed meat weight per day) were estimated using an empirical function based on the observed relationship between annual landing rates, expressed as number caught per day (NLPUE) and survey exploitable numbers per tow. At low biomass levels, NLPUE increases roughly linearly with survey abundance. However, at high abundance levels, the catch rate of the gear will exceed that which can be shucked by a seven-man crew. This is similar to the situation in predator/prey theory, where a predator's consumption rate is limited by the time required to handle and consume its prey (Holling 1959). The original Holling Type-II predator-prey model assumes that handling and foraging occur sequentially. It predicts that the per-capita predation rate R will be a function of prey abundance N according to a Monod functional response:

$$R = \frac{\alpha N}{\beta + N},$$

where α and β are constants. In the scallop fishery, however, some handling (shucking) can occur while foraging (fishing), though at a reduced rate because the captain and one or two crew members need to break off shucking to steer the vessel during towing and to handle the gear during haulback.

The fact that a considerable amount of handling can occur at the same time as foraging means that the functional response of a scallop vessel will saturate quicker than predicted by the above equation. To account for this, a modified Holling Type-II model was used, so that the landings (in numbers of scallops) per unit effort (DAS) L (the predation rate, i.e., NLPUE) will depend on scallop (prey) exploitable numbers N according to the formula:

$$L = \frac{\alpha N}{\sqrt{\beta^2 + N^2}}.$$

The parameters α and β to this model were fit to the observed fleet-wide LPUE vs. exploitable biomass relationship during the years 1994-2004 (previous years were not used because of the change from port interviews to logbook reporting). The number of scallops that can be shucked should be nearly independent of size provided that the scallops being shucked are smaller than about a 20 count. The time to shuck a large scallop will go up modestly with size. To model this, if the mean meat weight of the scallops caught, g , in an area is more than 20 g, the parameters α and β in the above equation are reduced by a factor $\sqrt{20/g}$. This means, for example, that a crew could shuck fewer 10 count scallops per hour than 20 count scallops in terms of numbers, but more in terms of weight.

An estimate of the fishing mortality imposed in an area by a single DAS of fishing in that area can be obtained from the formula $F_{DAS} = L_a/N_a$, where L_a is the NLPUE in that area obtained as above, and N_a is the exploitable abundance (expressed as absolute numbers of scallops) in that area. This allows for conversion between units of DAS and fishing mortality.

Initial conditions for the population vector $\mathbf{p}(i,t)$ were estimated using the 2009 NMFS research vessel sea scallop survey, with dredge efficiency chosen so as to match the 2009 CASA biomass estimates. The initial conditions from the 2009 surveys were bootstrapped using the bootstrap model of Smith (1997), so that each simulation run had both its own stochastically determined bootstrapped initial conditions, as well as stochastic recruitment stream.

Appendix B13: Modifications to the NEFSC sea scallop survey database.

Larry Jacobson and Dvora Hart, Northeast Fisheries Science Center, Woods Hole, MA.

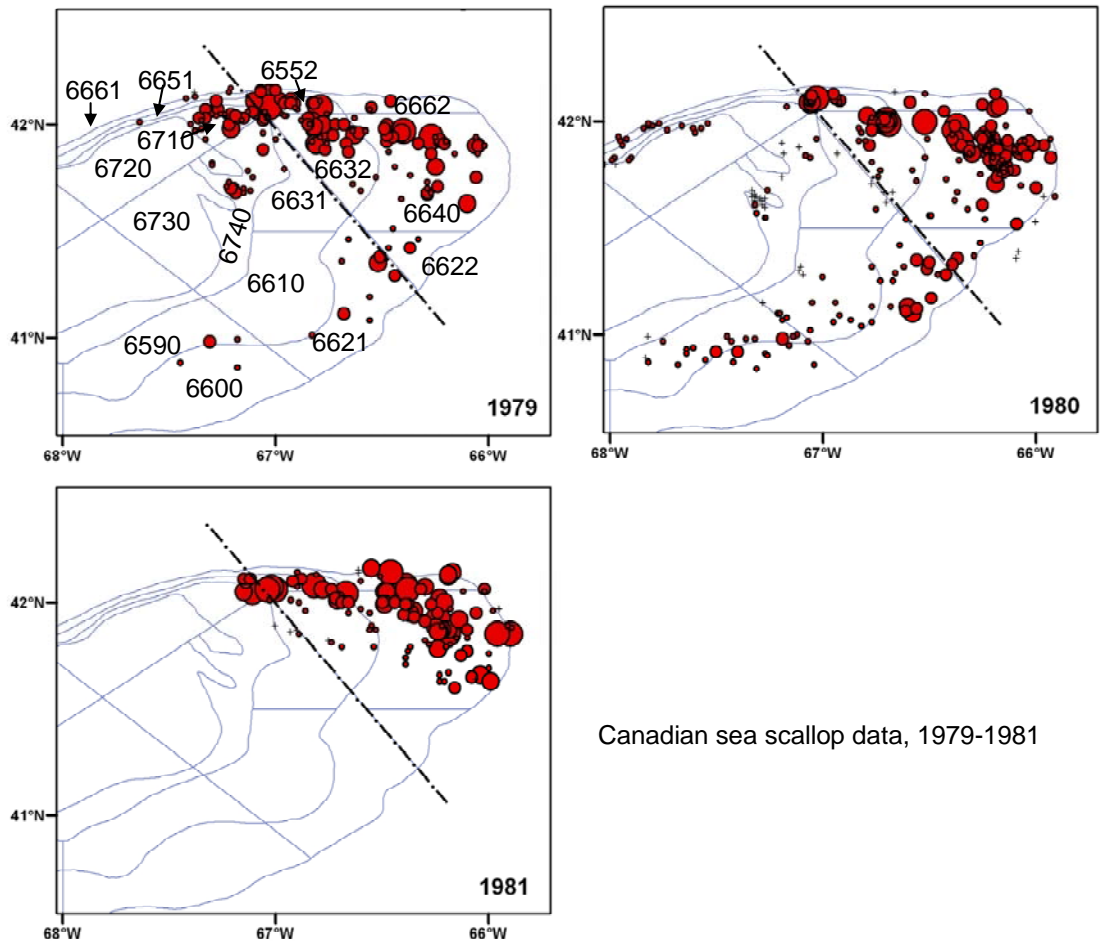
Two modifications were made to the scallop survey database for this assessment. The first modification accommodated a change in the survey vessel and survey dredge. Beginning in 2007, the NEFSC scallop survey was carried out using the *R/V Hugh Sharp* in place of the *R/V Albatross IV*, new survey protocols and a modified survey dredge. In the database, the catch in each tow can be adjusted to account for differences in tow distance and potential differences in survey dredge efficiency. Specifically, the adjusted catch in tow t for surveys during 2008-2009 is $C_t^* = \phi C_t$ where C_t was the original catch and ϕ is the adjustment factor that converts survey catches during 2008-2009 surveys to *R/V Albatross IV* equivalent units. Variances for adjusted strata means were computed using Goodman's (1960) exact formula for the variance of the product of two random variables. Based on experimental work described in this assessment, $\phi=1/1.05=0.9524$ to accommodate a 5% increase in tow distance for the new research vessel. For lack of information, the CV for the adjustment was assumed to be zero.

The second modification made it possible to compute survey abundance and biomass trends for GBK sea scallops back to 1979 instead of 1982. The years 1979-1982 were not used for GBK in the previous assessment because survey strata 6610, 6621, 6631, 6651, 6661, 6710, 6720 and 6740 were usually not sampled. In this assessment, Canadian data were used to fill these holes and Canadian data for other GBK strata were included as well (Figure 1). The Canadian survey also uses an 8' New Bedford style dredge with a liner. However the Canadians survey has a shorter tow distance (0.667 nm vs. 0.875 nm) and stratification is based on commercial LPUE in the preceding season rather than NEFSC shellfish strata. The Canadian data were adjusted for differences in tow distance based on the ratio of tow distances

$C_s^* = \frac{0.667}{0.875} C_s$. Serchuk and Wigley (1986) showed that Canadian and US data from the same strata are similar after adjustment for differences in tow distance. Differences in stratification were therefore ignored. Canadian data were also used in the statistical model used to fill holes (strata not sampled in some survey years). Imputation procedures are described in NEFSC (2007).

References

- Goodman, L.A. 1960. On the Exact Variance of Products. J. Am. Stat. Assoc. 55: 708-713
Northeast Fisheries Science Center. 2007. NEFSC. 2007. 45th Northeast Regional Stock Assessment Workshop (45th SAW): 45th SAW assessment report. Northeast Fish. Sci. Cent. Ref. Doc. 07-16.



Canadian sea scallop data, 1979-1981

Appendix B13-Figure 1. Location of Canadian sea scallop survey data for 1979-1981, which were used in this assessment. The size of the symbol in each plot indicates relative catch size.

Appendix B14: Comparison of surveys in the Nantucket Lightship Access Area during 2009.

Dvora Hart, Northeast Fisheries Science Center, Woods Hole, MA.

In 2009, three projects were funded by the sea scallop research set-aside program to intensively survey the Nantucket Lightship Access Area. One goal was to allow an effective comparison of density and shell height composition estimates. The three surveys were conducted by the Virginia Institute of Marine Science (VIMS), SMAST, and the HabCam team. The NEFSC lined dredge and SMAST drop camera “broad-scale” surveys, which are routinely carried out over the entire stock area, also covered the Nantucket Lightship Access Area, albeit less intensely. This analysis compares size-frequencies and abundance estimates from each survey.

Methods

The VIMS survey used two dredges towed side by side: a lined (38 mm) survey dredge (which is also used on the NEFSC survey) and a commercial dredge with 4” rings. The SMAST survey used the drop camera system used on their broad-scale survey including the primary “large” and secondary “small” cameras. The small camera gives better resolution because it is closer to the sea floor but covers less area (~0.8 sqm/drop). The HabCam survey used a towed digital camera system, towed at ~5 kts, taking overlapping digital images, each covering about 1 m² and with overlap between adjacent frames (Appendix B9). Table 1 gives more details on each survey.

The Nantucket Lightship Access Area was closed to scallop fishing in December 1994. It was reopened to fishing during portions of 2000 and 2004-2008. Previous surveys have observed three recent strong year classes: 1999, 2001, and 2004. The 1999 and 2001 year classes have been heavily fished. The remaining scallops from these year classes were expected to be around 150 mm shell height in 2009 (near their asymptotic size). The 2004 year class was lightly fished in 2008 only, and would be expected to be around 120+ mm shell height. All surveys were conducted in late spring or early summer in 2009, when the area was closed to fishing.

Results

Estimated shell height size-frequency (> 40 mm SH) from each survey were normalized to sum to one prior to the analysis. The VIMS survey dredge catches are used as a baseline for the size-frequencies analysis because the survey dredge is an important standard and shell height data collected by dredge surveys are relatively accurate (Jacobson et al. 2010).

The VIMS survey dredge showed the expected year class peaks at 120 and 150 mm SH, plus an incoming recruitment peak at 50 mm SH (Figure 1). The commercial dredge showed a similar size distribution for large scallops, but had reduced catchability for scallops less than 100 mm SH.

HabCam shell-height distributions were wider than the survey dredge shell height composition, probably due to less precise shell height measurements from photographs (Jacobson et al. 2010). Nonetheless, HabCam and the survey dredge are in reasonable agreement with no indication of dredge size-selectivity. The HabCam survey was conducted before the

VIMS survey, and the difference in timing may explain the differences between HabCam and VIMS in shell height distributions for smaller scallops that grow quickly.

The large drop camera survey suggests there is a much higher fraction of scallops in the 70-90 mm range than either the survey dredge or HabCam. The large camera size-frequencies are relatively noisy, with some evidence of reduced size-selectivity for small scallops. The divergence between the surveys may be due to the low sample size of the drop camera (315 scallops measured) and imprecision in shell height measurements (Jacobson et al. 2010). The small camera is intended to allow full detectability of small scallops, and indeed a higher proportion of small scallops were detected than with the large camera. However, the small camera data are noisier than the large camera data, due to the small number of scallops measured (76).

The NEFSC broad-scale survey had only 14 tows in the area. It found similar modes as the VIMS survey dredge, but in different proportions, likely due to the small sample size. The SMAST broad-scale large camera survey had a noisy shell height distribution, likely because of the small number of scallops measured (87).

Estimates of abundances are compared in Table 2. The dredge surveys were assumed to have an efficiency of 0.44 (see Appendix B4), whereas the optical surveys were assumed to have an efficiency of one. The individual 95% confidence intervals for each survey contain the inverse-variance weighted mean calculated for the abundance estimates from all of the surveys (205 million scallops). The three intensive dedicated surveys all had lower coefficients of determination (CV) than the broad-scale surveys.

Discussion and Conclusions

This study demonstrates the utility of fine-scale surveys for rotational area management in areas of relatively small size. Both abundance and the shell height composition data from the broad scale surveys are too imprecise because of the small sample sizes. It appears that the VIMS survey dredge gave the best estimate of shell height composition, as was assumed in the analysis. Both optical surveys showed evidence of shell height measurement errors. The SMAST survey did not measure sufficient scallops to estimate size-frequencies precisely. On the other hand, the optical surveys (SMAST and HabCam) had the lowest CVs for abundance. The HabCam survey had a remarkably low CV, due to its large sample sizes. Optical and dredge sampling have complementary attributes, and the ideal survey would probably include both types of sampling.

References

Jacobson, L.D., Stokesbury, K.D.E., Allard, M.A., Chute, A., Harris, B.P., Hart, D., Jaffarian, T., Marino, M.C., Nogueira, J.I., and Rago, P. 2010. Measurement errors in body size of sea scallops (*Placopecten magellanicus*) and their effects on stock assessment models. Fish. Bull. 108: 237-247.

Appendix B14-Table 1. Basic characteristics of the surveys.

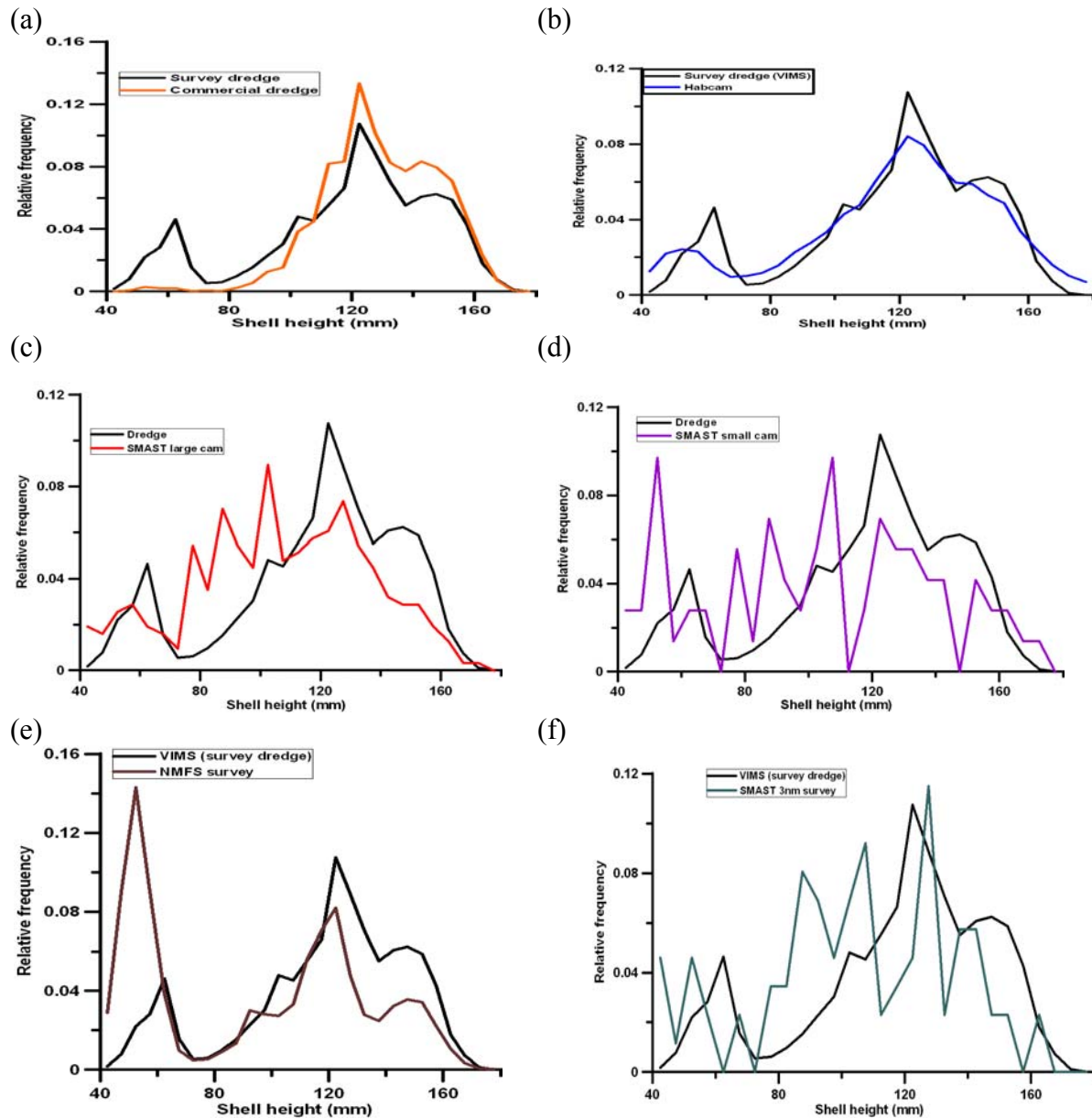
Survey	Gear	Design	Number of stations	Area swept (m ²)	Sea days	Number of scallops measured	Post-processing resources required
VIMS	Survey dredge	Systematic grid	91	409,500	4	13149	Low
VIMS	Commercial dredge	Systematic grid	91	767,813	4	16300	Low
SMAST	Large drop video camera	Systematic grid	164	1,940	2	315	Moderate
SMAST	Small drop video camera	Systematic grid	164	510	2	76	Moderate
Habcam	Towed digital still camera	Continuous transect	N/A*	123,500**	3	13644	High

*1.235 million images were collected, of which 1/10th were processed

**Processed images only

Appendix B14-Table 2. Abundance and biomass estimates from the surveys

Survey	Method	Assumed efficiency	Estimated abundance (millions)	CV	95% CI (millions)	Mean meat weight (g)	Estimated biomass (mt)
VIMS	survey dredge	0.44	259	0.14	192 to 334	34.0	10752
SMAST	large drop camera	1	240	0.13	183 to 305	25.0	5991
SMAST	small drop camera	1	234	0.16	166 to 313	24.6	5749
Habcam	towed camera	1	198	0.04	182 to 214	32.9	6782
NMFS broad-scale	survey dredge	0.44	100	0.45	32 to 206	32.5	3965
SMAST broad-scale	large drop camera	1	241	0.24	141 to 367	24.5	5902
Grand mean (inverse-variance weighted)		NA	207	0.035	193 to 231	34	7038
Broad-scale combo mean (inverse-variance weighted, NMFS and SMAST broad-scale surveys only)		NA	178	0.22	110 to 263	32.5	5798



Appendix B14-Figure 1. Plots of observed normalized shell heights for each survey. The VIMS survey dredge size-frequencies (black line) are included for reference on each plot. (a) VIMS commercial dredge. (b) HabCam. (c) SMAST large camera. (d) SMAST small camera. (e) Lined survey dredge. (f) SMAST broad-scale large camera survey. The NEFSC broad-scale survey data are not shown.